



Final Report SPR-FY22(011)

WBS Report #
26-1107-0202-001

Truck Platooning Effects on Girder Bridges: Phase II - Service

Joshua S. Steelman, PhD, PE

Associate Professor
Department of Civil and
Environmental Engineering
University of Nebraska-Lincoln

Jay A. Puckett, PhD, PE

Professor
Durham School of Architectural Engineering
and Construction
University of Nebraska-Lincoln

Daniel G. Linzell, PhD, PE

Associate Dean for Graduate and
International Programs
Leslie D. Martin Professor, Department of
Civil and Environmental Engineering
University of Nebraska-Lincoln

Bowen Yang, MS

Doctoral Graduate Student
Department of Civil and
Environmental Engineering
University of Nebraska-Lincoln

Nebraska Department of Transportation Research

Headquarters Address (402) 479-4697
1400 Nebraska Parkway [https://dot.nebraska.gov/
Lincoln, NE 68509 business-center/research/
ndot.research@nebraska.gov](https://dot.nebraska.gov/business-center/research/)

Nebraska Transportation Center

262 Prem S. Paul Research Lincoln, NE 68583-0851
Center at Whittier School (402) 472-1932
2200 Vine Street <http://ntc.unl.edu>

This report was funded in part through grant from the U.S. Department of Transportation Federal Highway Administration. The views and opinions of the authors expressed herein do not necessarily state or reflect those of the U.S. Department of Transportation.

Truck Platooning Effects on Girder Bridges: Phase II-Service

Joshua S. Steelman, PhD, PE
Associate Professor
Department of Civil and Environmental
Engineering
University of Nebraska-Lincoln

Jay A. Puckett, PhD, PE
Professor
Durham School of Architectural
Engineering and Construction
University of Nebraska-Lincoln

Daniel G. Linzell, PhD, PE
Associate Dean for Graduate and
International Programs
Leslie D. Martin Professor, Department of
Civil and Environmental Engineering
University of Nebraska-Lincoln

Bowen Yang, MS
Doctoral Graduate Student
Department of Civil and Environmental
Engineering
University of Nebraska-Lincoln

Sponsored By

Nebraska Department of Transportation and US Department of Transportation Federal Highway
Administration

August 11, 2023

TECHNICAL REPORT DOCUMENTATION PAGE

1. Report No. SPR-FY22(011)	2. Government Accession No.	3. Recipient's Catalog No.	
4. Title and Subtitle Truck Platooning Effects on Girder Bridges: Phase II-Service		5. Report Date August 11, 2023	
		6. Performing Organization Code	
7. Author(s) Joshua S. Steelman, Jay A. Puckett, Daniel G. Linzell, Bowen Yang		8. Performing Organization Report No. WBS 26-1107-0202-001	
9. Performing Organization Name and Address Department of Civil and Environmental Engineering University of Nebraska-Lincoln 900 N. 16th Street Nebraska Hall W181 PO Box 880531 Lincoln, NE 68588-0531		10. Work Unit No.	
		11. Contract SPR-FY22(011)	
12. Sponsoring Agency Name and Address Nebraska Department of Transportation Research Section 1400 Hwy 2 Lincoln, NE 68502		13. Type of Report and Period Covered Final Report July 2021-May 2023	
		14. Sponsoring Agency Code	
15. Supplementary Notes			
16. Abstract <p>Truck platooning—wirelessly linking two or more trucks to travel in a closely spaced convoy—is federally promoted to save fuel, improve the environment, and improve traffic operations. Platooning places trucks much closer than current design codes anticipate. While this strategy can provide higher fuel efficiency, it also can potentially overload structures. Previous reliability-based studies (Steelman et al., 2021; Yang et al., 2021) have focused on the Strength I limit state and have shown that trucks can operate at weights exceeding standard legal load limits even with short headways at operating-level reliability. However, service limit states in the AASHTO LRFD <i>Bridge Design Specifications</i> (2020) were not originally calibrated to produce uniform safety through reliability theory. Currently, no target implicit reliability index ($\beta_{Implicit}$) nor reliability-based evaluation guidance for the service limit states is stated in the AASHTO <i>Manual for Bridge Evaluation</i> (2018). In addition, a reliability-based service limit state evaluation protocol for bridges subjected to platoons does not currently exist.</p> <p>A parametric study considered different girder spacings, span lengths, span numbers, structure types, truck configurations, truck numbers, and adjacent-lane loading scenarios. Using Monte Carlo Simulation (MCS), target $\beta_{Implicit}$ values were identified based on current design loads to calibrate heavy-load limits for the service limit state (e.g., permit vehicles and platoons). LRFR live load factors were developed for service over a range of coefficients of variation (<i>CoV</i>s) and were presented in association with a potential new permit load, i.e., a platoon permit. The framework for explicitly aggregating live load uncertainties based on truck weight, dynamic amplification, and girder distribution factors was developed and proposed. Four representative steel and prestressed concrete girder bridges from the Nebraska inventory were load rated for strength and service. The study also preliminarily evaluated the fatigue performance of welded cross-frame connections to girder flanges and shear studs for the steel bridges and determined cracking probabilities ($\beta_{Cracking}$) for prestressed concrete bridges. As an illustration of possible operational strategies, headway guidance information and a summary of guidelines were developed for platoon loads, including varying truck weights.</p>			
17. Key Words Platooning, Structural Reliability, Load Rating, Permitting, LRFR, Girder Bridges, Service II, Service III		18. Distribution Statement No restrictions.	
19. Security Classification (of this report) Unclassified	20. Security Classification (of this page) Unclassified	21. No. of Pages 195	22. Price N/A

Disclaimer

The contents of this report reflect the views of the authors, who are responsible for the facts and the accuracy of the information presented herein. The contents do not necessarily reflect the official views or policies neither of the Nebraska Department of Transportations nor the University of Nebraska-Lincoln. This report does not constitute a standard, specification, or regulation. Trade or manufacturers' names, which may appear in this report, are cited only because they are considered essential to the objectives of the report.

The United States (U.S.) government and the State of Nebraska do not endorse products or manufacturers. This material is based upon work supported by the Federal Highway Administration under SPR-FY22(011). Any opinions, findings and conclusions or recommendations expressed in this publication are those of the author(s) and do not necessarily reflect the views of the Federal Highway Administration.

This report has been reviewed by the Nebraska Transportation Center for grammar and context, formatting, and 508 compliance.

Table of Contents

Disclaimer	iii
Table of Contents	iv
List of Figures	viii
List of Tables	xi
Symbols.....	xiii
Abbreviations	xviii
Abstract	xx
Chapter 1 Introduction	1
1.1 Background	1
1.2 Research Objectives.....	5
1.3 Research Scope	6
1.4 Report Organization.....	7
Chapter 2 Literature Review	8
2.1 Overview.....	8
2.2 Structural Reliability.....	8
2.3 Strength I Limit State Reliability.....	10
2.4 Service III Limit State Reliability.....	18
2.5 Service II Limit State Reliability	23
2.6 Steel Bridge Fatigue.....	26
2.7 Summary	31
Chapter 3 Research Methodology.....	32
3.1 Overview.....	32
3.2 Platoon Parameters.....	33
3.2.1 Truck Type and Number of Platoon Trucks	33
3.2.2 Headway	34
3.2.3 Lane Loading Scenarios.....	35
3.3 Bridge Parameters.....	36
3.4 Reliability Analysis for Service III.....	37
3.4.1 General Reliability Analysis Procedure.....	37
3.4.2 Nominal Resistance	40
3.4.3 Bridge Details	43
3.4.4 Prestress Loss Method Parameters.....	45
3.4.5 Nominal Dead Loads	47
3.4.6 Nominal Design Live Loads	47
3.4.7 Statistical Parameters	48
3.4.8 Limit State Function for Service III.....	50
3.5 Reliability Analysis for Service II	51
3.5.1 General Reliability Analysis Procedure.....	51
3.5.2 Nominal Resistance	53
3.5.3 Bridge Design Parameters and Assumptions.....	56
3.5.4 Nominal Dead and Live Loads	61
3.5.5 Statistical Parameters	61

3.5.6 Limit State Function for Service II	62
3.6 Monte Carlo Simulation.....	63
3.7 Summary	70
Chapter 4 Optimal Design and Target Reliability Results	71
4.1 Overview.....	71
4.2 Nominal Live Load Positive Moments.....	71
4.3 Service III Optimal Design and Target Reliability Results	74
4.3.1 Service III Optimal Design Results	74
4.3.2 Service III Target Reliability Results	80
4.3.3 Effects of Parameter Uncertainty on Service III.....	90
4.4 Service II Optimal Design and Target Reliability Results.....	91
4.4.1 Service II Optimal Design Results.....	91
4.4.2 Service II Target Reliability Results.....	93
4.4.3 Effects of Parameter Uncertainty on Service II.....	95
4.5 Summary	96
Chapter 5 LRFR Live Load Factor Calibration	97
5.1 Overview.....	97
5.2 Service III Calibration Procedure	97
5.3 Service III Calibration Results.....	99
5.3.1 Single-Lane Loaded Service III Results	99
5.3.2 Platoon with Routine Traffic in Adjacent Lane Service III Results	101
5.4 Service II Calibration Procedure.....	102
5.5 Service II Calibration Results	104
5.5.1 Single-Lane Loaded Service II Results.....	104
5.5.2 Platoon with Routine Traffic in Adjacent Lane Service II Results	106
5.6 Proposed LRFR Factors.....	107
5.7 Summary	110
Chapter 6 Serviceable Combinations of Truck Weight and Headway	111
6.1 Overview.....	111
6.2 Prestressed Concrete Bridges Service III.....	111
6.2.1 Single-Lane Platoon Without Adjacent Traffic	115
6.2.2 Single-Lane Platoon, Routine Traffic in Adjacent Lane	117
6.3 Steel Bridges Service II	118
6.3.1 Single-Lane Platoon Without Adjacent Traffic	119
6.3.2 Single-Lane Platoon, Routine Traffic in Adjacent Lane	121
6.4 Preliminary Operational Guidance	122
6.5 Summary	125
Chapter 7 Framework for Aggregating Live Load Uncertainties	127
7.1 Overview.....	127
7.2 Live Load Statistical Model.....	127
7.3 Truck Weight Uncertainty Framework.....	128
7.4 Dynamic Amplification Uncertainty Framework	132
7.5 Girder Distribution Factor Uncertainty Framework	137
7.6 Sensitivity Analysis for Platoon Uncertainty.....	140

7.7 Summary	141
Chapter 8 Illustrative Examples for Platoon Evaluation.....	142
8.1 Overview.....	142
8.2 Prestressed Concrete Simple-Span Bridge (S080 41653).....	142
8.2.1 Bridge Details	143
8.2.2 Vehicle Details.....	146
8.2.3 Moment and Shear Rating Check Locations	147
8.2.4 Moment and Shear Rating Check Results	148
8.3 Prestressed Concrete Continuous Span Bridge.....	149
8.3.1 Bridge Details	150
8.3.2 Vehicle Details.....	153
8.3.3 Moment and Shear Rating Check Locations	154
8.3.4 Moment and Shear Rating Check Results	155
8.4 Steel Simple-Span Bridge.....	155
8.4.1 Bridge Details	156
8.4.2 Vehicle Details.....	159
8.4.3 Fatigue Damage Assessment	159
8.4.4 Moment and Shear Rating Check Locations	160
8.4.5 Moment and Shear Rating Check Results	161
8.5 Steel Continuous Span Bridge	163
8.5.1 Bridge Details	164
8.5.2 Vehicle Details.....	167
8.5.3 Fatigue Damage Assessment	167
8.5.4 Moment and Shear Rating Check Locations	168
8.5.5 Moment and Shear Rating Check Results	168
8.6 Summary.....	170
Chapter 9 Cracking Reliability and Probability for Prestressed Girder Bridges	171
9.1 Overview.....	171
9.2 Service III Cracking Reliability and Probability Results.....	171
9.3 Summary	178
Chapter 10 Summary and Conclusions.....	179
10.1 Summary.....	179
10.2 Conclusions for Prestressed Concrete Bridges	181
10.3 Conclusions for Steel Bridges.....	183
10.4 Recommended Future Research	185
10.5 Implementation and Technology Transfer.....	185
References.....	189
Appendices.....	196
Appendix A.....	A-0
Appendix B.....	B-0
Appendix C.....	C-0
Appendix D.....	D-0
Appendix E.....	E-0
Appendix F.....	F-0

Appendix G..... G-0

List of Figures

Figure 2.1 PDFs of Load, Resistance, and Margin of Safety for Strength	10
Figure 2.2 Safe Platoon Headways with Adjacent Traffic, 120-ft, Simple-Span Steel Bridge (Yang et al., 2021)	17
Figure 2.3 Reliability Indices for Bridges at Maximum Allowable Tensile Stress Limit State (ADTT = 5,000, and $f_t = 0.0948\sqrt{f'_c}$). (Wassef et al., 2014)	21
Figure 2.4 Service III Positive Moment Reliability vs Span Length (Optimized In-Service Bridges) (Barker et al., 2020)	23
Figure 2.5 Service II Positive Moment Reliability vs Span Length (Optimized In-Service Bridges) (Barker et al., 2020)	26
Figure 2.6 Stress Range Versus Number of Cycles (<i>LRFD BDS</i> , 2020)	28
Figure 3.1 Notional Rating Load (AASHTO, 2020)	34
Figure 3.2 Typical Two-Truck Configuration and Headway Definition (Steelman et al. 2021)..	35
Figure 3.3 Platoon with Adjacent Routine Traffic Load Case (90 – 200 ft Two-span Bridges) (Steelman et al. 2021)	36
Figure 3.4 Service III Research Methodology	39
Figure 3.5 Pretensioned Nebraska University I-Girder with Strand Layout (Hanna et al., 2010)	45
Figure 3.6. Service II Research Methodology	52
Figure 3.7 Monte Carlo Simulation Flowchart	65
Figure 4.1 Loading Scenarios for Comparison of Nominal LL Moments.....	73
Figure 4.2 <i>LL</i> Moments for Platoons and HL-93 Loadings on Prestressed Girder Bridges	73
Figure 4.3 Tensile Stresses Due to Factored Dead and Live Loads, and Optimal A_{ps} for f_t ($\kappa =$ 0.0948) for Various Design Scenarios	76
Figure 4.4 Prestress Loss and Elastic Gains for Design and Evaluation at f_t ($\kappa = 0.0948$)	78
Figure 4.5 Effective Prestress Force and Resistance for Design and Evaluation at f_t ($\kappa = 0.0948$)	80
Figure 4.6 Probability Density Functions for Evaluating Service III at f_t ($\kappa = 0.0948$) for 120-ft Simple-Span Bridges Designed by using <i>Post-1.0-Gains</i>	81
Figure 4.7 Reliability Index β and Corresponding Probabilities of Exceeding Tension Limits for Simple-span Bridges Designed using <i>Post-1.0-Gains</i> Method, Similar Design and Evaluation f_t (κ)	83
Figure 4.8 Reliability Index $\beta_{Implicit}$ and Corresponding Probabilities of Exceeding Tension Limits for Simple-span Bridges Designed using <i>Post-0.8-No-gains</i> Method, Similar Design and Evaluation f_t (κ)	84
Figure 4.9 Reliability Index $\beta_{Implicit}$ and Corresponding Probabilities of Exceeding Tension Limits for Simple-span Bridges Designed using <i>Approx-0.8-No-gains</i> Method, Similar Design and Evaluation f_t (κ)	85
Figure 4.10 Reliability Index $\beta_{Implicit}$ and Corresponding Probabilities of Exceeding Tension Limits for Simple-span Bridges Designed using <i>Post-0.8-Gains</i> and <i>Approx-0.8-Gains</i> Methods, Similar Design and Evaluation f_t (κ)	87
Figure 4.11 Reliability Index β and Corresponding Probabilities of Exceeding Tension Limits for Simple-span Bridges Designed using <i>Pre-1.0-No-gains</i> , Similar Design and Evaluation f_t (κ) ...	89

Figure 4.12 Normal Probably Plots for 120-ft Prestressed Concrete Bridges Designed by <i>Post-I.0-Gains</i> with f_t ($\kappa_{des} = 0.0948$).....	91
Figure 4.13 Performance Ratios for Simple-, and Two-span Positive Moment at Strength I and Service II.....	92
Figure 4.14 Performance Ratios for Two-span Negative Moment at Strength I and Service II... 93	93
Figure 4.15 Probability Density Functions for Evaluating Service II for 120-ft Simple-Span Bridges Positive Moment Region.....	94
Figure 4.16 Reliability Index β for Simple-span and Two-span Bridges at Service II.....	95
Figure 4.17 Normal Probably Plots for 120-ft Simple-span Steel Bridges Positive Moment at the Mid.....	96
Figure 6.1 Single-lane Loaded Four-truck NRL Platoon without Routine Traffic on a Simple-Span Bridge Scenario for Developing Headway Tables.....	113
Figure 6.2 Single-lane Loaded Four-truck NRL Platoon with Routine Traffic on a Simple-Span Bridge Scenario for Developing Headway Table.....	114
Figure 6.3 Legal Load Platoon Headway Restrictions for Steel and Prestressed Bridges.....	123
Figure 6.4 Headway Restrictions for Prestressed Concrete and Steel Girder Bridges ($CoV = 0.18$).....	124
Figure 7.1 Normal Distribution with Mean = 1.0 (95% Compliance).....	130
Figure 7.2 Truck Weight Uncertainty Framework.....	132
Figure 7.3 Two-truck Platoon on a Simple-span Bridge.....	134
Figure 7.4 Dynamic Allowance Uncertainty Framework.....	137
Figure 7.5 Girder Distribution Factor Uncertainty Framework.....	140
Figure 8.1 Prestressed Concrete Simple-Span Bridge (S080 41653) (Google Map, 2023).....	143
Figure 8.2 Bridge Plan View for S080 41653 (AASHTOWare™ BrR, 2023).....	144
Figure 8.3 Bridge Cross Section for S080 41653 (AASHTOWare™ BrR, 2023).....	144
Figure 8.4 Bridge Girder Details for S080 41653 (AASHTOWare™ BrR, 2023).....	145
Figure 8.5 Vertical Shear Reinforcement Ranges (AASHTOWare™ BrR, 2023).....	146
Figure 8.6 Moment and Shear Rating Check Locations.....	148
Figure 8.7 Prestressed Concrete Continuous Span Bridge (S080 41465) (Google Map, 2023). 150	150
Figure 8.8 Bridge Plan View for S080 41465 (AASHTOWare™ BrR, 2023).....	150
Figure 8.9 Bridge Cross Section for S080 41465 (AASHTOWare™ BrR, 2023).....	151
Figure 8.10 Bridge Girder Details for S080 41465 (AASHTOWare™ BrR, 2023).....	152
Figure 8.11 Vertical Shear Reinforcement Ranges (AASHTOWare™ BrR, 2023).....	153
Figure 8.12 Moment and Shear Rating Check Locations.....	154
Figure 8.13 Steel Welded Plate Girder Simple-Span Bridge (S080 00526) (Google Map, 2023).....	156
Figure 8.14 Bridge Plan View for S080 00526 (AASHTOWare™ BrR, 2023).....	157
Figure 8.15 Bridge Cross Section for S080 00526 (AASHTOWare™ BrR, 2023).....	157
Figure 8.16 Bridge Girder Details for S080 00526 (AASHTOWare™ BrR, 2023).....	158
Figure 8.17 Moment and Shear Rating Check Locations.....	161
Figure 8.18 Steel Rolled Beam Three-Span Bridge (S080 40375) (Google Map, 2023).....	164
Figure 8.19 Bridge Plan View for S080 40375 (AASHTOWare™ BrR, 2023).....	165
Figure 8.20 Bridge Cross Section for S080 40375 (AASHTOWare™ BrR, 2023).....	165
Figure 8.21 Bridge Girder Details for S080 40375 (AASHTOWare™ BrR, 2023).....	166

Figure 8.22 Moment and Shear Rating Check Locations	168
Figure 9.1 Probability Density Functions for evaluating cracking at f_r ($\kappa = 0.24$) for 120-ft Simple-Span Bridges Designed by using <i>Post-1.0-Gains</i>	172
Figure 9.2 $\beta_{Cracking}$ and Cracking Probability for Simple-span Bridges Designed using <i>Post-1.0-Gains</i> , <i>Post-0.8-No-gains</i> , and <i>Approx-0.8-No-gains</i> Methods, Different f_r ($\kappa = 0.24$, 0.30, and 0.37)	175
Figure 9.3 $\beta_{Cracking}$ and Cracking Probability for Simple-span Bridges Designed using <i>Post-0.8-Gains</i> and <i>Approx-0.8-Gains</i> Methods, Different f_r ($\kappa = 0.24$, 0.30, and 0.37).....	176
Figure 9.4 $\beta_{Cracking}$ and Cracking Probability for Simple-span Bridges Designed using <i>Pre-1.0-No-gains</i> , <i>Post-0.8-No-gains</i> Method, and <i>Approx-0.8-No-gains</i> Methods, Different f_r ($\kappa = 0.24$, 0.30, and 0.37)	177
Figure 10.1 Potential Workflow Process for Permitting Platoons on Girder Bridges in Nebraska	188

List of Tables

Table 2.1 Expected Maximum Adjacent Live Load and CoV for Simple-Span Bridges (Steelman et al., 2021)	13
Table 2.2 Proposed Calibrated LL Factors for the Target $\beta = 2.5$ (Steelman et al., 2021).....	15
Table 2.3 Safe Simple-Span Bridge Platoon Headways (ft) With Adjacent Traffic ($CoV=0.18$) (Yang et al., 2021)	18
Table 2.4 Reliability Indices for Existing and Simulated Bridges with a Return Period of One Year and ADTT 5,000 (Wassef et al., 2014)	20
Table 2.5 Load Factor for LL for Service III Load Combination, γ_{LL} (<i>LRFD BDS</i> , 2020).....	21
Table 3.1 Design Scenarios.....	46
Table 3.2 Statistical Parameters for Variables.....	50
Table 3.3 Girder Size Design Guidance	57
Table 3.4 Optimal Design Girder Sections for Simple-span Positive Moment at the Midspan ...	60
Table 3.5 Optimal Design Girder Sections for Two-span Positive Moment at the 0.4L of End Spans.....	60
Table 3.6 Optimal Design Girder Sections for Two-span Negative Moment at the Interior Support.....	61
Table 3.7 Statistical Parameters for Variables.....	62
Table 5.1 Single-Lane Platoon (Without Adjacent Traffic) Positive Moment Critical Amplification Factor, α	100
Table 5.2 Single-Lane Platoon (Without Adjacent Traffic) Positive Moment Calibrated LL Factors, γ_{LL}	101
Table 5.3 Single-Lane Platoon (With Adjacent Traffic) Positive Moment Critical Amplification Factor, α	102
Table 5.4 Single-Lane Platoon (With Adjacent Traffic) Positive Moment Calibrated LL Factors, γ_{LL}	102
Table 5.5 Single-Lane Platoon (Without Adjacent Traffic) Positive Moment Critical Amplification Factor, α	105
Table 5.6 Single-Lane Platoon (Without Adjacent Traffic) Positive Moment Calibrated LL Factors, γ_{LL}	105
Table 5.7 Single-Lane Platoon (With Adjacent Traffic) Positive Moment Critical Amplification Factor, α	106
Table 5.8 Single-Lane Platoon (With Adjacent Traffic) Positive Moment Calibrated LL Factors, γ_{LL}	107
Table 5.9 Proposed Moment Calibrated LL Factors for Service III	109
Table 5.10 Proposed Moment Calibrated LL Factors for Service II.....	109
Table 6.1 Acceptable Simple-Span Bridge Platoon Headways (ft) Without Adjacent Routine Traffic ($CoV = 0.18$)	116
Table 6.2 Acceptable Simple-Span Bridge Platoon Headways (ft) With Adjacent Routine Traffic (100 Crossings, and ADTT = 5000) ($CoV = 0.18$)	118
Table 6.3 Acceptable Simple-Span Bridge Platoon Headways (ft) Without Adjacent Routine Traffic ($CoV = 0.18$)	120

Table 6.4 Acceptable Simple-Span Bridge Platoon Headways (ft) With Adjacent Routine Traffic (100 Crossings, and ADTT = 5000) ($CoV = 0.18$)	122
Table 7.1 ASTM 1318E-09 Functional Performance Requirements for WIM Systems (Reproduced Based on ASTM, 2017).....	130
Table 7.2 Comparison of Field-Measured GDF to <i>LRFD BDS</i> GDF (Reproduced Based on Ghosn, 2019 and Puckett et al., 2007)	138
Table 7.3 Sensitivity Analysis for Different Terms in Determining Platoon Uncertainty	141
Table 8.1 Rating Factors for Different Limit States	149
Table 8.2 Rating Factors for Different Limit States	155
Table 8.3 Cumulative Fatigue Damage Assessment.....	160
Table 8.4 Rating Factors for Strength and Service Limit States.....	162
Table 8.5 Rating Factors for Fatigue Limit States for Welded Cross-frame Connection Plate..	163
Table 8.6 Rating Factors for Fatigue Limit States for Shear Stud.....	163
Table 8.7 Cumulative Fatigue Damage Assessment.....	167
Table 8.8 Rating Factors for Strength and Service Limit States.....	169
Table 8.9 Rating Factors for Fatigue Limit States for Welded Cross-frame Connection Plate..	169
Table 8.10 Rating Factors for Fatigue Limit States for Shear Stud.....	170

Symbols

A : constant defined for each detail category given in *LRFD BDS* Table 6.6.1.2.5-1
 $(ADTT)_{SL}$: single-lane *ADTT* as specified in *LRFD BDS* Article 3.6.1.4.
 A_g : nominal gross section area
Approx-0.8-Gains: Approximate loss method, $\gamma_L = 0.8$, with elastic gain
Approx-0.8-No-gains: Approximate loss method, $\gamma_L = 0.8$, without elastic gain
 A_{ps} : nominal total area of prestressing reinforcement
 C : capacity
 C_b : moment gradient modifier
CFD: Cumulative Fatigue Damage
 CoV : coefficient of variation
 CoV_{adj} : adjacent lane live load effect coefficient of variation
 CoV_{GDF} : girder distribution factor coefficient of variation
 CoV_{IM} : dynamic impact factor coefficient of variation
 CoV_L : static live load coefficient of variation
 CoV_{L_GDF+IM} : dynamic live load and girder distribution factor coefficient of variation
 CoV_{max} : Extreme Type I coefficient of variation
 d : distance between the two trucks
 D : nominal dead load effect
 D_c : nominal composite dead load moment
 D_{gw} : nominal girder dead load moment
 D_n : nominal dead load
 D_{nc} : nominal noncomposite dead load moment
 D_c : nominal composite dead load moment
 D_w : nominal wearing dead load moment
 e_{nc} : nominal eccentricity from the noncomposite centroid to prestress strand centroid
 f'_{c_deck} : final concrete deck strength
 f'_{c_girder} : final concrete girder strength
 f'_{c_deck} : initial concrete deck strength

f'_{ci_girder} : initial concrete girder strength
 f_1 : natural frequency of the bridge
 f_{DC} : nominal stress due to dead loads from components
 f_{DW} : nominal stress due to wearing surfaces
 f_{des} : design bottom tension stress
 f_l : nominal flange lateral bending stress in *LRFD BDS* Article 6.10.1.6
 f_{LL+IM} : nominal tensile stress due to live loads including impact
 f_{pi} : nominal initial prestressing
 f_{pu} : ultimate tensile strength
 f_r : concrete modulus of rupture
 f_R : nominal flexure resistance
 f_{req} : required effective stress
 f_{Reval} : available resistance to tension stress for evaluation
 f_t : nominal design allowable tensile stress
 f_{truck} : excitation frequency of the truck
 F_y : yield stress
 F_{yf} : nominal flange yield stress
 g : limit state function
 GDF : girder distribution factor
 GDF_m : multiple-lanes loaded girder distribution factor
 $GDF_{platoon}$: girder distribution factor for a platoon
 GDF_s : single-lane loaded girder distribution factor
 H : platooning truck headway
 IM : impact factor
 $IM_{desired}$: desired impact factor for load rating
 IM_{HL-93} : impact factor associated with AASHTO LRFD/R HL-93 load
 $IM_{platoon}$: impact factor applied to platoon static live load
 K_g : longitudinal stiffness parameter (in.⁴)
 L_{adj} : adjacent lane live load effect
 L_b : unbraced length

LL : total live load effect, or nominal static live load effect
 LL_{HL-93} : HL-93 design live load effect
 $LL_{platoon}$: platoon nominal static live load effect
 L_n : nominal live load effect
 L_{PL} : static platoon nominal load effect
 m : slope constant of the $S-N$ curve
 M_y : Yield moment
 N : number of cycles to failure, or total number of data
 n : number of stress range cycles per truck passage in *LRFD BDS* Table 6.6.1.2.5-2
 n_i : actual number of stress cycles experienced
 N_i : fatigue life corresponding to the i_{th} stress-range bin S_i
 N_m : number of maximum stress range caused by an individual truck passage
 Num : number of truck passages during the given time
 P : Permanent loads other than dead loads
 P_e : nominal effective prestress force after losses
 P_{eval} : effective prestress force for the evaluation
 P_f : probability of failure
 $Post-0.8-Gains$: Post-2005 loss method, $\gamma_L = 0.8$, with elastic gain
 $Post-0.8-No-gains$: Post-2005 loss method, $\gamma_L = 0.8$, without elastic gain
 $Post-1.0-Gains$: Post-2005 loss method, $\gamma_L = 1.0$, with elastic gain
 $Post2005$: AASHTO *LRFD BDS* 5.9.3.4 prestress loss method
 $Pre-1.0-No-gains$: Pre-2005 loss method, $\gamma_L = 1.0$, without elastic gain
 $Pre2005$: Standard Specifications 9.16.2.1 prestress loss method
 P_{req} : required effective force
 Q : load
 R : resistance
 RF : Rating Factor
 R_h : hybrid factor shown in *LRFD BDS* Article 6.10.1.10.1
 R_n : nominal resistance
 $R_{n_Service}$: minimum required nominal moment resistance for Service II

$R_{n_Strength}$: minimum required nominal resistance for Strength I
 S_{cb} : nominal composite section modulus for the bottom fiber
 S_{LT} : nominal long-term composite section modulus
 S_{max} : the maximum stress range
 S_{NC} : nominal noncomposite elastic section modulus
 S_{ncb} : nominal noncomposite section modulus for the bottom fiber
 S_{ri} : higher-order stress range
 S_{rp} : maximum stress range
 S_{ST} : nominal short-term composite section modulus
 t : time it takes for each truck to pass the same point
 v : speed of the trucks
 $v_{critical}$: critical speeds that will cause resonance effects
 α : amplification factor
 β : reliability index
 $\beta_{Cracking}$: cracking reliability provided by code-compliant bridge designs
 $\beta_{implicit}$: target implicit reliability index that provided by code-compliant bridge designs
 β_{target} : target reliability index
 γ : load factor
 γ_D : dead load factor
 γ_{DC} : dead load factor for components
 γ_{DW} : dead load factor for wearing surfaces
 γ_L : live load factor
 γ_{LL} : live load factor
 γ_P : load factor for permanent loads other than dead loads
 $\gamma_{platoon}$: platoon live load factor
 Δf : live load stress range due to the fatigue truck in *LRFD BDS* Article 3.6.1.4
 Δf_{pES} : elastic shortening loss
 $\Delta f_{pGainDL}$: elastic gain from dead loads
 $\Delta f_{pGainLL}$: elastic gain from live loads
 $\Delta f_{platoon}$: live load stress range due to platoons

Δf_{pLT} : long-term prestress loss

Δf_s : nominal prestress losses

Δf_s (w/o LL gain): the prestress loss without accounting for elastic gains

Δf_{Seval} : prestress loss for the evaluation

$(\Delta F)_n$: nominal fatigue resistance provided in LRFD BDS Article 6.6.1.2.5

κ : coefficient before $\sqrt{f'_c}$ (ksi) in the f_t

κ_{des} : coefficient before $\sqrt{f'_c}$ (ksi) in the design f_t

κ_{eva} : coefficient before $\sqrt{f'_c}$ (ksi) in the evaluation f_t

λ : bias factor

λ_{GDF} : girder distribution factor bias factor

λ_{max} : maximum mean live load effect bias for adjacent lane loading

$\lambda_{platoon}$: platoon live load bias factor

μ : mean value

μ_{IM} : mean dynamic amplification

σ : standard deviation

ϕ : resistance factor

Φ : standard normal cumulative density function

Abbreviations

AASHO	American Association of State Highway Officials
AASHTO	American Association of State Highway and Transportation Officials
ADTT	Average Daily Truck Traffic
ASD	Allowable Stress Design
AV	Autonomous Vehicles
BDS	Bridge Design Specifications
BOPP	Bridge Office Policies and Procedures
CAFT	Constant-Amplitude Fatigue Threshold
CoV	Coefficient of Variation
CV	Connected Vehicles
ENSC	Equivalent Number of Stress Cycles
FBF	Federal Bridge Formula
FEM	Finite Element Method
GDF	Girder Distribution Factor
GVW	Gross Vehicle Weight
ILDS	Inductive Loops
LFD	Load Factor Design
LFR	Load Factor Rating
LLF	Live Load Factor
LRFD	Load and Resistance Factor Design
LRFR	Load and Resistance Factor Rating
MBE	Manual for Bridge Evaluation
MCFT	Modified Compression Field Theory
MCS	Monte Carlo Simulation
MPF	Multiple Presence Factor
NBI	National Bridge Inventory
NCHRP	National Cooperative Highway Research Program
NDOT	Nebraska Department of Transportation

NFSP	National Freight Strategic Plan
NRL	Notional Rating Load
NSBACSS	National Steel Bridge Alliance Continuous Span Standards
PDF	Probability Distribution Function
PPSBD	Preferred Practices for Steel Bridge Design
RF	Rating Factor
VBI	Vehicle-Bridge Interaction
WIM	Weigh-in-Motion
WWF	Welded wire fabric

Abstract

Truck platooning—wirelessly linking two or more trucks to travel in a closely spaced convoy—is federally promoted to save fuel, improve the environment, and improve traffic operations. Platooning places trucks much closer than current design codes anticipate. While this strategy can provide higher fuel efficiency, it also can potentially overload structures. Previous reliability-based studies (Steelman et al., 2021; Yang et al., 2021) have focused on the Strength I limit state and have shown that trucks can operate at weights exceeding standard legal load limits even with short headways at operating-level reliability. However, service limit states in the AASHTO LRFD *Bridge Design Specifications* (2020) were not originally calibrated to produce uniform safety through reliability theory. Currently, no target implicit reliability index ($\beta_{Implicit}$) nor reliability-based evaluation guidance for the service limit states is stated in the AASHTO *Manual for Bridge Evaluation* (2018). In addition, a reliability-based service limit state evaluation protocol for bridges subjected to platoons does not currently exist.

A parametric study considered different girder spacings, span lengths, span numbers, structure types, truck configurations, truck numbers, and adjacent-lane loading scenarios. Using Monte Carlo Simulation (MCS), target $\beta_{Implicit}$ values were identified based on current design loads to calibrate heavy-load limits for the service limit state (e.g., permit vehicles and platoons). LRFR live load factors were developed for service over a range of coefficients of variation (CoV s) and were presented in association with a potential new permit load, i.e., a platoon permit. The framework for explicitly aggregating live load uncertainties based on truck weight, dynamic amplification, and girder distribution factors was developed and proposed. Four representative steel and prestressed concrete girder bridges from the Nebraska inventory were load rated for

strength and service. The study also preliminarily evaluated the fatigue performance of welded cross-frame connections to girder flanges and shear studs for the steel bridges and determined cracking probabilities ($\beta_{Cracking}$) for prestressed concrete bridges. As an illustration of possible operational strategies, headway guidance information and a summary of guidelines were developed for platoon loads, including varying truck weights.

Chapter 1 Introduction

1.1 Background

Platoons constitute a portion of an emerging population of Connected and Automated Driving System (C/ADS)—equipped vehicles, which are expected to become increasingly common in the United States and industrialized countries globally. Effective platooning can save fuel (e.g., Tsugawa et al., 2011; Lammert et al., 2014), improve the environment (Bibeka et al., 2019), and improve traffic operations (Hassan et al., 2020). In the US Department of Transportation's National Freight Strategic Plan (NFSP) released in early September 2020, platooning was mentioned as a revolutionary technology that can improve safety and efficiency for long-haul freight operations. Consolidating freight into heavy truck platoons could provide enhanced cost-effectiveness from the perspective of transportation costs. However, doing so may impose greater structural demands than current design and evaluation procedures anticipate under normal traffic conditions. At the same time, optimal computer control of closely spaced heavy trucks traveling at high speeds likely requires greater certainty of individual truck weights. Bridge owners must responsibly manage traffic operations, and accordingly need to correlate platoon characteristics to safe and sustainable bridge loading limits and facilitate load ratings for platoons.

Studies of platooning effects have focused on the American Association of State and Highway Transportation Officials (AASHTO) *Load and Resistance Factor Design (LRFD) Bridge Design Specifications (BDS)* (2020) Strength I limit state. Using a line-girder analysis, Yarnold and Weidner (2019) evaluated the effects of platoons with varying headways and truck numbers on steel bridge behavior. Their study concentrated on the Florida C5 truck configuration

that satisfied the Federal Bridge Formula B (FBF B) legal limit. According to their results, the HL-93 design live load (LL) generally envelopes moment and shear effects for platoons, except for some long-span bridges with closely spaced platoons. Using the same bridge and platoon parameters as Yarnold and Weidner (2019), Tohme and Yarnold (2020) assessed the effect of platoons on moment load ratings using a benchmark steel bridge. The moment load rating results indicated that platoons passing over long bridges with small headways exceeded the Strength I limit state. Wassef et al. (2021) studied platooning headways of 30, 50, and 70 ft and found that four-truck platoons with 30-ft headways produced higher load effects for long bridges (200 - 300 ft). Ibrahim et al. (2022) examined the effects of up to 20 combined HS-20 loadings with 10 to 30 ft headways on load ratings. These studies, however, were based on nominal LL comparisons rather than reliability analyses.

Platooning with CV technologies potentially places trucks much closer than current design codes anticipate to realize aerodynamic benefits. Truck weights must be known with greater certainty than currently assumed in *LRFD BDS* to ensure safe platooning operations while facilitating maximum benefits with close headways. Yang et al. (2021) and Steelman et al. (2021) demonstrated that trucks can carry unusually heavy loads without compromising safety if LL uncertainties are reduced, headways are controlled, and multiple presence scenarios are controlled. It is still possible to maintain the Strength I operating level reliability index $\beta = 2.5$ specified by the *Manual for Bridge Evaluation (MBE)* (2018). Sajid et al. (2022) further parameterized bias and coefficient of variation (CoV) and determined that two-lane bridges can reliably accommodate platoons to achieve an inventory level reliability index $\beta = 3.5$ for strength. Yang et al. (2021) and Steelman et al. (2021) considered a range of CoV s for platoon

LL calibrations between 0 and 0.2 without explicitly aggregating *LL* uncertainties resulting from the truck weight, dynamic allowance (*IM*), and girder distribution factors (*GDF*). Wassef et al. (2021) began exploring the effects of platooning on service limit states by comparing platoons directly with the effects of the HL-93 design load. However, reliability-based evaluations of the effects of platoons on service limit state performance are still lacking.

Target reliability indices, β , for service limit states are needed to evaluate platoon effects on girder bridge performance in a reliability-based framework. However, reliability-based evaluation criteria for service are not specified by AASHTO. Few recent studies have investigated the target reliability index β for service. Wassef et al. (2014) evaluated Service II based on one or two loaded lanes using Weigh-in-Motion (WIM) data from sites with an average daily truck traffic (ADTT) of 5000. Barker et al. (2020) evaluated Service II for Wyoming bridges under two-lanes loaded with heavy truck traffic caused by extended interstate closures. They assumed the bridges designed by the current *LRFD BDS* perform satisfactorily on Service II. These two studies provided a similar target reliability index of approximately 1.60 for Service II based on multiple-lane loaded WIM data. Wassef et al. (2014) proposed a higher target reliability for Service III than Barker et al. (2020) based on a single-lane loaded evaluation. Barker et al. (2020) found that using two lanes of I-80 WIM load data after extended road closures resulted in negative operational reliability indices for Service III, which indicated that prestressed concrete beams may crack in tension under service loads, despite Service III's nominal intention to limit tensile stresses to below the modulus of rupture. These inconsistencies between the intention of Service III and the outcome of these reliability-based evaluations motivated the investigation of prestressed concrete bridge cracking probability.

Increasing platoon weights and reducing headways may accelerate bridge fatigue damage. Each passage of a platoon with different headways may produce multiple load cycles over a short time duration, which may reduce fatigue life. As a result, fatigue-induced damage caused by heavy platoons should be examined. Fatigue effects from permit loads have been studied widely, but not for platoons. Braguim et al. (2021) investigated platooning fatigue effects on simple-span and two-equal span continuous steel bridges. They observed that, depending on the number of trucks and their headways, platoons reduced fatigue damage more effectively than individual truck passages. Deng and Yan (2018) proposed a method for determining truck weight limits and overload permits based on cumulative fatigue damage. Stawska et al. (2022) established an incremental consumption equation based on cumulative fatigue damage from the AASHTO Fatigue Truck and permit loads. Although Yang et al. (2021) and Steelman et al. (2021) demonstrated that platoons with five-ft headways can still be considered safe for strength, such short headways may not be acceptable for fatigue.

Platoon deployments are imminent according to the timeline provided by Trimble et al. (2018e). Strength rating LL factors may be reduced if smart systems are deployed to regulate truck traffic and enable platooning with less uncertainty than typical design traffic. However, reduced uncertainty may not decrease calibrated LL factors for service limit states. In addition, platoons could have negative impacts for fatigue. Platoons of heavy trucks will be economically advantageous for freight operators in the near future. However, information currently available is insufficient for bridge owners to establish platoon operation limitations and guidelines, ensuring safe and serviceable loading demands in girder bridge structures in terms of truck weights, LL uncertainties, and headways.

1.2 Research Objectives

The main objectives of this project are to:

1. Calibrate appropriate *LL* factors for use with platoons to address the Service III limit state for prestressed concrete girder bridges, the most common girder type supporting interstate live loads in Nebraska;
2. Calibrate appropriate *LL* factors for use with platoons to address the Service II limit state for steel girder bridges;
3. Propose an uncertainty characterization framework to enable reductions in uncertainties for components of live load – static weight, dynamic amplification, and girder load distribution – to be combined into aggregate platoon LL uncertainty;
4. Facilitate adoption of platoon permitting protocols through demonstration of sample implementation in illustrative examples; and
5. Preliminarily assess the significance of platoon-induced fatigue.

1.3 Research Scope

The research considered:

- one and two lanes loaded,
- simple- and two-span continuous bridges,
- span lengths ranging from 60 to 200 ft,
- simple- and two-span continuous bridges,
- steel and prestressed composite I-girders,
- girder spacing ranging from 8 to 12 ft,
- truck types: legal load trucks at 80 kips GVW,
- headways ranging 5 – 50 ft,
- Live loading:
 - single-lane platoon loaded in one lane,
 - two identical platoons in adjacent lanes,
 - platoon with routine traffic in an adjacent lane,
- AASHTO limit states:
 - Service III, positive moment regions for prestressed concrete bridges,
 - Service II, positive and negative moment regions for steel bridges,
 - Fatigue I and II for steel bridges (welded cross-frame-to-girder connections and shear stud).

1.4 Report Organization

This document is long and, in some places, quite complex. The description below outlines the Chapter content to provide a context for how various topics are laid out.

Chapter 2 contains a summary of related literature reviewed during the execution of the project, focusing on previous platooning studies and bridge reliability assessments.

Chapter 3 outlines a detailed reliability analysis research methodology for service.

Chapter 4 provides the target reliability indices for service.

Chapter 5 and Chapter 6 present *LL* factors and safe headway spacing tables, respectively, for platoons with a *CoV* range of 0 to 0.2.

Chapter 7 proposes a framework for quantifying *LL CoV*, explicitly aggregating *LL* uncertainty relating to static weight, dynamic allowance, and girder distribution factors, to facilitate optimal selection of *LL* factors for strength and service evaluations.

Chapter 8 presents four case study examples illustrating platoon permitting evaluations.

Chapter 9 addresses the apparent intent of Service III to prevent cracks at the bottom of prestressed concrete girders between supports under routine traffic loads.

Chapter 10 provides summary and conclusions for the research.

Appendices provide comprehensive rating example computations for simple- and continuous-span steel and prestressed concrete bridges, calibrated *LL* factors and acceptable headways with respect to *LL CoV* for steel bridges, as well as suggestions for AASHTOWare™ BrR implementation for platoon load ratings.

Chapter 2 Literature Review

2.1 Overview

The literature review focuses on general structural reliability and the effects of platoons or heavy loads. Reliability analyses have been conducted to evaluate platoon effects for Strength I (Steelman et al., 2021; Yang et al., 2021; Sajid et al., 2022). This study analyzes Service II and Service III limit state reliability for platoon loads. Previous studies were reviewed to identify target service reliability indices for design and rating. In addition, an abbreviated literature review that examined available fatigue assessment methods for heavy loads was completed.

2.2 Structural Reliability

Structural reliability analysis establishes probabilities of exceeding limit state criteria. Such limit state criteria are established based on past performance, previous design methodologies, and judgment. According to Nowak and Collins (2012), Equation 2.1 represents a general limit state function,

$$g(R, Q) = R - Q \tag{2.1}$$

where R and Q are random variables representing resistance and load effects, respectively.

Monte Carlo Simulation (MCS) was used to conduct the reliability analysis. MCS is performed by randomly generating N load and resistance samples, counting the number of instances in which the limit state is violated (i.e., g in Equation 2.1 is less than zero), and assessing the probability of failure, P_f , as a ratio of the number of failure samples, F , to the total number of samples, N . g is typically assumed to follow a normal distribution, so that β can be

determined as shown in Equation 2.2,

$$\beta = -\Phi^{-1}(P_f) \quad 2.2$$

where $-\Phi^{-1}$ is the inverse of the standard normal cumulative distribution function. The index is routinely used in structural reliability frameworks to characterize structural safety (i.e., strength limit states). Figure 2.1 presents typical probability density functions (PDFs) for a sample bridge's loads, resistance, and limit state function evaluations. The reliability index, β , represents the number of standard deviations the mean value of g is from zero. At the strength level, design and inventory load ratings target $\beta = 3.5$, whereas operating load ratings relax the target β to 2.5. For service limit states, operating load rating or inventory load rating target β 's are not specified in AASHTO. Therefore, necessary information is unavailable to determine reliability-calibrated platooning load limits for service.

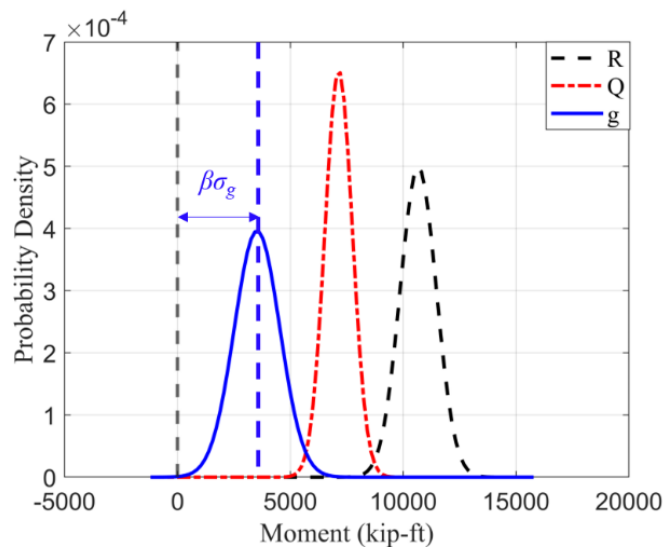


Figure 2.1 PDFs of Load, Resistance, and Margin of Safety for Strength

2.3 Strength I Limit State Reliability

According to the *LRFD BDS* (2020), the Strength I limit state has been calibrated for a target reliability index of 3.5 based on 75 years of HL-93 design loads. The reliability index for LRFD-designed bridges was calibrated by Nowak (1999) based on two weeks of WIM data obtained in Canada to satisfy a β of 3.5. Moses (2001) calibrated permit vehicle *LL* factors using the same WIM data. Using a database of 124 representative bridges, Kulicki et al. (2007) further updated *LRFD BDS* Strength I limit state calibration. A more detailed discussion of the calibration of the Strength I limit state can be found in Steelman et al. (2021).

Previous research has illustrated the negative impact of platooning at the Strength I limit state. A recent study by Yarnold and Weidner (2019) evaluated potential effects of platooning and identified conditions for which past and current design specifications may not be adequate. Their study focused on total bridge cross-sectional moment and neglected transverse distribution of live loads. Different spans and platoon configurations were analyzed and compared with

AASHTO *Standard Specifications* (2002) and *LRFD BDS* (2020) design specifications. Yarnold and Weidner determined that bridges designed using load factor design (LFD) according to the *Standard Specifications* (2002) were more vulnerable to platooning than identical, LRFD-designed bridges.

Tohme and Yarnold (2020) extended the work by Yarnold and Weidner to evaluate platoon effects on multi-girder steel bridge load ratings. Their study used a general bridge cross-section consistent with *MBE* (2018) load rating Example A1. A1 girders were redesigned for alternate span lengths and continuity conditions to maintain a legal load rating of at least 1.0. According to their assumptions, they found that bridges may exceed the *Load and Resistance Factor Rating (LRFR)* Strength I limit state for positive bending at 20 ft headways, the smallest headways studied, on longer spans. It should be noted that Tohme and Yarnold (2020) and Yarnold and Weidner (2019) focused primarily on comparing nominal platoon loads in conjunction with design or legal trucks rather than reliability analysis to evaluate bridge safety.

A reliability-based analysis of platoon effects was recently conducted by Steelman et al. (2021). A parametric study that incorporated different girder spacings, span lengths, numbers of spans, bridge types, truck configurations, truck numbers, and adjacent lane loading scenarios was completed. WIM data from Barker and Puckett (2016) was used to characterize adjacent lane loading and assumed up to 100 platoon crossings per day. Steelman et al. (2021) adopted multiple presence probabilities for platoons loaded with adjacent routine traffic from Ghosn et al. (2011) to characterize adjacent lane loading statistical parameters. Expected maximum adjacent *LL* bias (λ_{max}) with respect to HL-93 loading, adjacent lane traffic *CoV* (CoV_{max}), and platoon total *CoV* were determined for simple-span (Table 2.1) and two-span bridges with different

platoon crossings per day and bridge span lengths. Note that λ_{max} in Table 2.1 is defined as the expected maximum adjacent lane LL divided by the HL-93 LL . The CoV_{max} in Table 2.1 is defined as the standard deviation of the expected maximum adjacent LL divided by the mean of the expected maximum adjacent LL . The Total CoV in Table 2.1 is determined by incorporating the $CoVs$ from the impact factor, girder distribution factor, and static LL and the mean of the impact factor. Steelman et al. (2021) provide more details on adjacent lane load characteristics.

Table 2.1 Expected Maximum Adjacent Live Load and *CoV* for Simple-Span Bridges (Steelman et al., 2021)

Number of crossings per day	ADTT	30 ft			60 ft			90 ft		
		λ_{max}	CoV _{max}	Total COV	λ_{max}	CoV _{max}	Total COV	λ_{max}	CoV _{max}	Total COV
10	100	1.060	0.041	0.147	0.965	0.039	0.146	0.953	0.038	0.146
	1000	1.091	0.036	0.145	0.992	0.035	0.145	0.980	0.034	0.145
	5000	1.106	0.035	0.145	1.005	0.033	0.144	0.992	0.032	0.144
100	100	1.134	0.031	0.144	1.029	0.030	0.144	1.015	0.029	0.144
	1000	1.160	0.029	0.144	1.051	0.027	0.143	1.037	0.027	0.143
	5000	1.172	0.028	0.143	1.062	0.026	0.143	1.047	0.026	0.143

Number of crossings per day	ADTT	120 ft			150 ft			200 ft		
		λ_{max}	CoV _{max}	Total COV	λ_{max}	CoV _{max}	Total COV	λ_{max}	CoV _{max}	Total COV
10	100	0.964	0.039	0.146	0.985	0.039	0.146	0.960	0.041	0.147
	1000	0.990	0.034	0.145	1.013	0.035	0.145	0.988	0.036	0.145
	5000	1.003	0.033	0.144	1.026	0.033	0.145	1.002	0.034	0.145
100	100	1.027	0.030	0.144	1.051	0.030	0.144	1.026	0.031	0.144
	1000	1.049	0.027	0.143	1.073	0.028	0.143	1.050	0.029	0.144
	5000	1.059	0.026	0.143	1.085	0.027	0.143	1.061	0.028	0.143

Steelman et al. (2021) calculated reliability indices based on MCS for platoons with different headways, weights, and CoV . Results indicated that loads significantly higher than legal are acceptable for platoons with lower uncertainties while maintaining a traditional operating target $\beta = 2.5$, consistent with MBE permit loadings. In addition, Steelman et al. (2021) proposed LL factors for platoons with different CoV s based on inventory or operating rating targets of $\beta = 3.5$ or 2.5 . Table 2.2 reproduces calibrated LL factors for $\beta = 2.5$, with load factors for platoons calibrated using $IM_{platoon} = 0.33$ (see table footnote). Proposed LL factors decrease with decreasing CoV . It should be noted that Steelman et al. (2021) did not explicitly calculate platoon CoV s based on the proposed statistical model but discretely determined them for values between 0 and 0.20 at 0.01 intervals.

Table 2.2 Proposed Calibrated *LL* Factors for the Target $\beta = 2.5$ (Steelman et al., 2021)

Truck Platoon	Frequency	Loading Condition	DF	ADTT (One direction)	Live load factors by <i>CoV</i> of total live load				
					$COV_{LL} = 0$	$COV_{LL} = 0.05$	$COV_{LL} = 0.1$	$COV_{LL} = 0.15$	$COV_{LL} = 0.2$
Multiple Trucks in Platoon	Single-trip	No other vehicles on the bridge	One lane	N/A	1.00	1.05	1.10	1.20	1.25
	Single-trip	Two identical platoons loaded on two lanes	Two or more lanes	N/A	1.00	1.05	1.10	1.20	1.25
	10 Crossings	Mixed with routine traffic in the adjacent lane	One lane	> 5000	1.35	1.35	1.40	1.45	1.55
				1000	1.35	1.35	1.40	1.45	1.50
				< 100	1.35	1.35	1.40	1.45	1.50
	100 Crossings	Mixed with routine traffic in the adjacent lane	One lane	> 5000	1.35	1.40	1.45	1.50	1.60
				1000	1.35	1.40	1.45	1.45	1.55
				< 100	1.35	1.35	1.45	1.45	1.55

a. DF is the *LRFD BDS* approximate GDF, with the multiple presence factor (MPF=1.2) removed for one-lane GDFs.

b. To use with a different IM factor, scale tabulated values by $1.33 / (1 + IM_{desired})$.

Based on the results of Steelman et al. (2021), Yang et al. (2021) developed safe headway guidance to illustrate potential safe operational strategies for varying truck weights and platoon LL effect uncertainties to achieve a target $\beta = 2.5$. They found that safe headways were insensitive to whether a bridge was constructed of steel or prestressed concrete girders. By reducing platoon CoV , Yang et al. (2021) found that maximum safe amplification factors (α) scaling platooning vehicle GVW may be increased, depending on headway, as shown for an example case of a 120-ft, simple-span, two-lane steel bridge with routine traffic in the lane adjacent to a platoon in Figure 2.2. Figure 2.2a is a three-dimensional (3D) surface depicting safe headways accounting for both moment and shear as a function of α and CoV . Similarly, Figure 2.2b is a 2D contour map of safe headways as a function of α and CoV . As shown in Figure 2.2, safe headways, α , and CoV are related, and the strength-based operational limit of one parameter can be determined if the other two are specified. Similar results are available for other conditions. Yang et al. (2021) developed safe headway guidance for simple- and two-span bridges using 75 years of design HL-93 loadings provided by Nowak (1999) and Kulicki et al. (2007) and different loading scenarios, bridge span lengths, and amplification factors. An example of safe simple-span bridge headways for platoons with adjacent traffic is provided in Table 2.3. “Fail” in Table 2.3 indicates that either the required headway is greater than 50 ft or the bridge has reached its limit regardless of headway, as mentioned in Yang et al. (2021).

Stelman et al. (2021) and Yang et al. (2021) conducted reliability analyses for Strength I and observed that LL could be higher using a reduced CoV . Platoon rating LL factors for Strength I were proposed by Steelman et al. (2021) and safe headway guidance for Strength I was provided by Yang et al. (2021). However, reliability-based evaluations and subsequent

rating *LL* factors and safe headway guidance for platoons at bridge Service III and Service II limit states were not developed at that time.

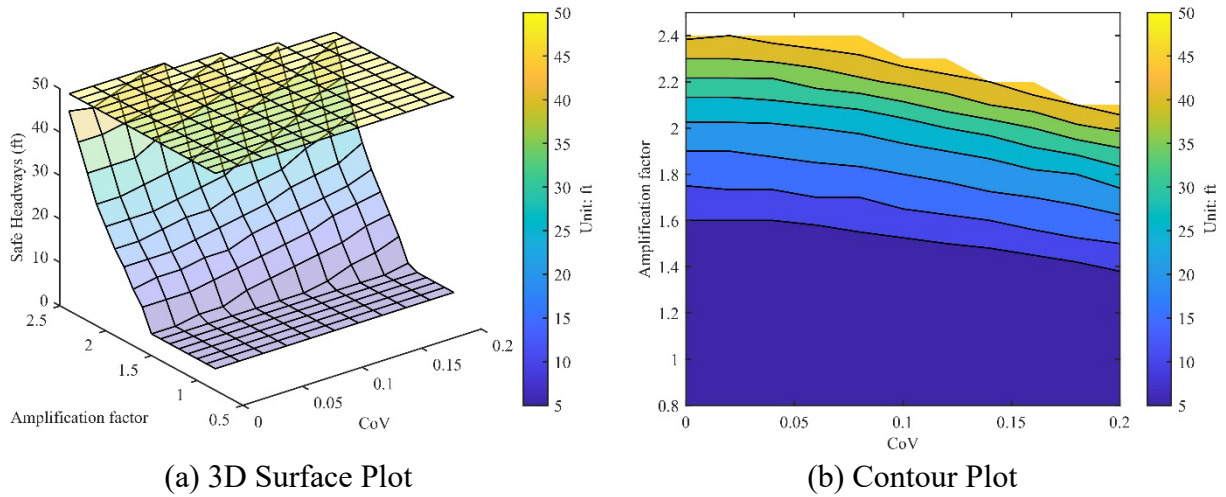


Figure 2.2 Safe Platoon Headways with Adjacent Traffic, 120-ft, Simple-Span Steel Bridge (Yang et al., 2021)

Table 2.3 Safe Simple-Span Bridge Platoon Headways (ft) With Adjacent Traffic ($CoV=0.18$)
(Yang et al., 2021)

Amplification factor α	L (ft)					
	30 ft	60 ft	90 ft	120 ft	150 ft	200 ft
0.8	5	5	5	5	5	5
0.9	5	5	5	5	5	5
1.0	5	5	5	5	5	5
1.1	5	5	5	5	5	5
1.2	5	5	5	5	5	5
1.3	5	5	5	5	6	5
1.4	5	5	5	9	14	13
1.5	5	5	7	14	20	23
1.6	5	5	10	18	25	32
1.7	5	5	12	21	31	39
1.8	5	7	17	25	34	46
1.9	5	10	23	31	39	Fail
2.0	5	13	27	39	47	Fail
2.1	Fail	15	32	45	Fail	Fail
2.2	Fail	18	36	Fail	Fail	Fail
2.3	Fail	Fail	40	Fail	Fail	Fail
2.4	Fail	Fail	45	Fail	Fail	Fail
2.5	Fail	Fail	Fail	Fail	Fail	Fail

Note: The α is the amplification factor, and the L is the span length.

2.4 Service III Limit State Reliability

AASHTO *LRFD BDS* (2020) notes that the Service III limit state is not calibrated based on reliability but on past practice and experience. The 8th Edition of the *Standard Specifications* (1961) first established the maximum allowable tensile stress limit for prestressed concrete bridges under service loads. The allowable tensile limit was revised in the 11th Edition (2014), but additional, significant modifications have not occurred for approximately a half-century. According to the current *BDS* (2020), the allowable Service III tensile stress for bridges under severe corrosion conditions should be the smaller of $0.0948\sqrt{f'_c}$ (ksi) or 0.3 ksi. Under no

worse than moderate corrosion conditions, the allowable tensile stress is relaxed to be the smaller of $0.19\sqrt{f'_c}$ (ksi) or 0.6 ksi. The tensile stress limits in prestressed concrete at Service III after losses can be found in *LRFD BDS* (2020) Table 5.9.2.3.2b-1.

Literature on platoon effects on Service III performance is limited. Wassef et al. (2021) directly compared effects of platooning on Service III limit states to the effects of the HL-93 design load. Findings indicated that, except in a small number of cases, platoons generally do not produce higher load effects than heavy vehicles currently running on highways. It was preliminarily concluded that more than two trucks in a platoon at small headways might adversely affect long-span prestressed concrete bridges for Service III.

Wassef et al. (2014) calibrated the Service III limit state using WIM data collected over one year at 32 sites across the United States. They used a *LL* model based on single-lane loading with MPF = 1.2 removed from AASHTO LRFD approximate GDFs. The *LL* model was based on an ADTT of 5000 and a return period of one year. They conservatively increased calculated mean maximum *LL* by 1.5 standard deviations to account for possible bias in WIM data due to data collection locations. Wassef et al. (2014) assumed that bridges designed in accordance with the *Standard Specifications* (2002) performed well in service. They adopted dead and live loads, and statistical resistance parameters from previous studies (Siriaksorn and Naaman, 1980; Nowak et al., 2008; Gross and Burns, 2000; Tadros et al., 2003; Nowak 1999; and Kulicki et al., 2007). They created a “simulated” bridge database by designing simple-span prestressed concrete bridges with girder spacing of 8 to 12 ft using AASHTO I-girder sections. For simulated bridges, they considered the "Pre2005" loss method (consistent with prestress loss method in *Standard Specifications* 9.16.2.1) and the "Post2005" loss method (consistent with

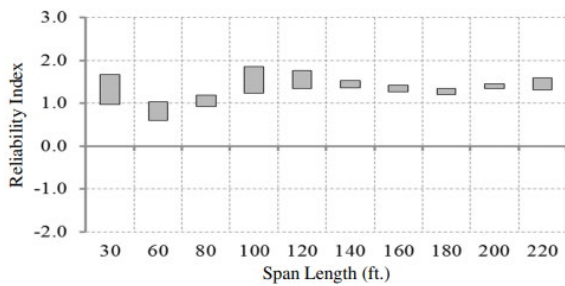
prestress loss method in *LRFD BDS* 5.9.3.4). The designs were approximately optimal, with prestress strand quantities rounded up to even integers. Additionally, they compiled an existing bridge database by selecting 30 I- and bulb-T girder, 31 adjacent box girder, and 36 spread box girder bridges from Mlynarski et al. (2011). Target reliability indices, reproduced in Table 2.4, were proposed based on simulated bridges designed with the “Pre2005” loss method with tension limits of $0.0948\sqrt{f'_c}$ or $0.19\sqrt{f'_c}$ and based on existing bridges from Mlynarski et al. (2011). As shown in Table 2.4, the target β for bridges based on different performance levels (e.g., decompression, maximum tensile stress, and maximum crack width of 0.016 in) was always positive.

Table 2.4 Reliability Indices for Existing and Simulated Bridges with a Return Period of One Year and ADTT 5,000 (Wassef et al., 2014)

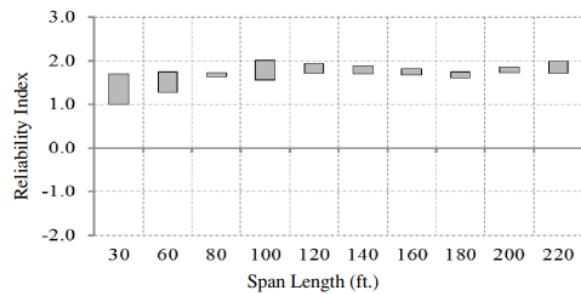
Performance Level	Average β for			Proposed Target β for	
	Existing Bridges in NCHRP 12-78	Simulated Bridges Designed for $f_t = 0.0948\sqrt{f'_c}$ and Pre-2005 Loss Method	Simulated Bridges Designed for $f_t = 0.19\sqrt{f'_c}$ and Pre-2005 Loss Method	Bridges in Severe Environment	Bridges in Normal Environment
Decompression	0.74	1.44	1.07	1.20	1.00
Maximum allowable tensile stress of $f_t = 0.19\sqrt{f'_c}$	1.05	1.80	1.43	1.50	1.25
Maximum allowable crack width of 0.016 in.	2.69	3.68	3.15	3.30	3.10

Wassef et al. (2014) then determined reliability indices for bridges designed using the prestress loss method (“Post2005”) proposed by Tadros et al. (2003), which was adopted in *LRFD BDS*. In Wassef et al. (2014), the “Post2005” loss method considered elastic gains and used gross section properties. Wassef et al. observed that the reliability index for bridges

designed using the “Post2005” loss method with a LL factor of 0.8 (Figure 2.3a) was lower than the target reliability in Table 2.4 and less uniform across span lengths compared to Figure 2.3b. Therefore, they proposed increasing the design LL factor to 1.0 to meet the target reliability index in Table 2.4 (Figure 2.3b). The recommendation was adopted in the current *LRFD BDS* Table 3.4.1.4, reproduced in Table 2.5.



(a) Reliability Indices for Bridges Designed with “Post2005” Loss Method ($\gamma_L = 0.8$)



(b) Reliability Indices for Bridges Designed with “Post2005” Loss Method ($\gamma_L = 1.0$)

Figure 2.3 Reliability Indices for Bridges at Maximum Allowable Tensile Stress Limit State (ADTT = 5,000, and $f_t = 0.0948\sqrt{f'_c}$). (Wassef et al., 2014)

Table 2.5 Load Factor for LL for Service III Load Combination, γ_{LL} (*LRFD BDS*, 2020)

Component	γ_{LL}
Prestressed concrete components designed using the refined estimates of time-dependent losses as specified in Article 5.9.5.4 in conjunction with taking advantage of the elastic gain	1.0
All other prestressed concrete components	0.8

Wassef et al. (2014) determined target reliabilities using single-lane loaded WIM data. However, multiple loaded lanes HL-93 are typically used when considering Service III. As a result, target reliability indices presented in Table 2.4 may be higher than those based on multiple HL-93 loaded lanes.

Barker et al. (2020) evaluated Service III for Wyoming I-80 bridges under heavy truck traffic due to extended roadway closures that would produce long trains of trucks loading both lanes. They considered the performance of bridges designed and evaluated under current LRFD BDS Service III criteria as satisfactory and computed target reliability indices on that basis. Barker et al. used the same load and resistance statistics as Kulicki et al. (2007), and they validated their process by independently reproducing example bridge results.

See Figure 2.4 where Barker et al. used the notation "NCHRP: LLF = 0.8" as they estimated the maximum truck load effects based on truck raw data upper-tail statistics similar to the NCHRP projects (Nowak, 1999; Kulicki et al., 2007). "NCHRP: LLF = 0.8" represents the reliability index for bridges designed with LRFD BDS Service III with a design *LL* factor equal to 0.8 and evaluated using multiple lanes loaded HL-93 loading.

Reliability indices (I-80 WIM: LLF = 0.8 in Figure 2.4) were also determined using I-80 WIM data records, i.e., where I-80 WIM: LLF = 0.8 represents the reliability index for bridges designed with LRFD BDS Service III with a design *LL* factor equal to 0.8, and evaluated using multiple lanes loaded with I-80 WIM data. They plotted reliability indices against the dead-to-live ratios, as shown in Figure 2.4. To more closely match target reliability indices (NCHRP: LLF = 0.8); they recommended that design *LL* factors for Service III be increased to 1.00 from 0.80 (I-80 WIM: LLF = 1.0 in Figure 2.4). Note that multiple loaded HL-93 lanes produced a lower target reliability index (NCHRP: LLF = 0.8) in Figure 2.4 than the proposed target reliability index based on single lane-loaded WIM data from Wassef et al. (2014). Using I-80 WIM vehicle load characteristics, load effects resulted in negative reliability indices for Service

III. This finding indicates that some reliability concerns may exist for heavy-load, truck-train situations (Barker et al., 2020).

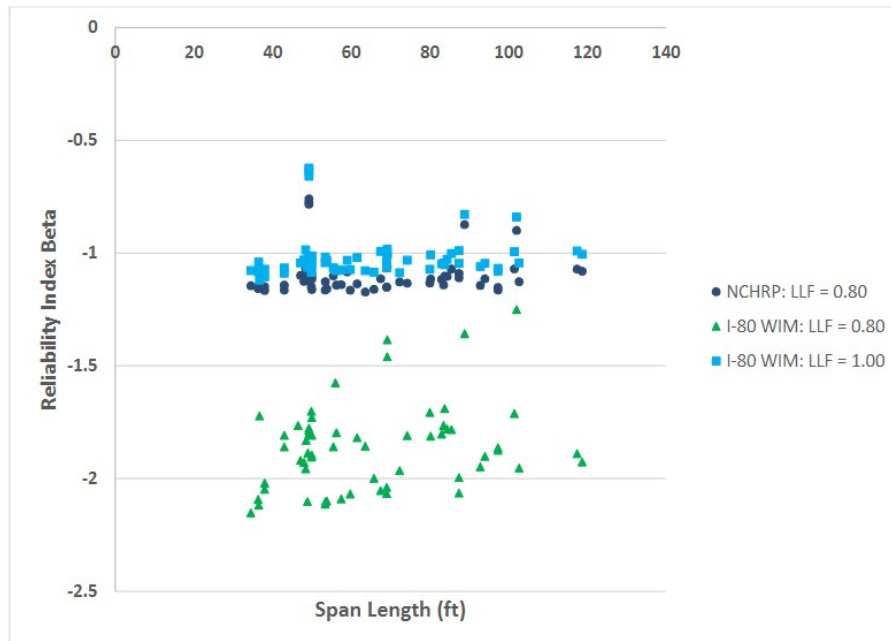


Figure 2.4 Service III Positive Moment Reliability vs Span Length (Optimized In-Service Bridges) (Barker et al., 2020)

2.5 Service II Limit State Reliability

The AASHTO *Standard Specifications* (1996) specify a Service II Limit State, which was based on limited experimental results obtained from the *American Association of State Highway Officials* (AASHTO) 1960 Road Test (Highway Research Board, 1962). All the bridges in the Road Test were 50-ft slab-on-steel beam simple-span bridges. Three types of rolled steel beams were used: noncomposite with cover plates, noncomposite without cover plates, and composite with cover plates. Maximum yield stresses of 27 ksi and 35 ksi were selected for design. The AASHTO Road Test experiments demonstrated that permanent midspan beam

deformations could occur at stresses lower than the nominal yield point. In most cases, permanent set was accumulated early during the repetitive load tests. Results for composite and noncomposite structures were extrapolated to anticipate an accumulated displacement of 1" at 95% and 80% of theoretical yield, respectively. These criteria are currently included in *LRFD BDS* (2020) as the Service II limit state. This limit state is not calibrated, and *LRFD BDS* C6.10.4.2.2 states that limits are intended to prevent objectionable permanent deflections caused by severe traffic loads. However, "objectionable permanent deflections" and "rideability" are not clearly defined and, as a result, the Service II limit state has been questioned in several studies (Mertz, 2000; Connell et al., 2007).

Literature studying Service II platoon effects on steel bridges is limited. Wassef et al. (2021) preliminarily concluded that more than two trucks in a platoon with small headways might adversely affect long-span prestressed concrete bridges based on comparing platoon effects to the HL-93 design load.

Wassef et al. (2014) proposed a target reliability index for simple-span steel bridges at the Service II limit state. Wassef et al. mentioned that although the Service II limit state is typically evaluated assuming multiple lanes are loaded, WIM data records suggest that the Service II *LL* does not occur often enough to warrant design for multiple lanes. Their study extracted flexural resistances for interior girders from 41 simple-span composite steel girder bridges from Mlynarski et al. (2011). Using single-lane HL-93 loading from the *LRFD BDS*, Wassef et al. (2014) performed MCS to determine mean and *CoV* of reliability indices of 1.8 and 0.32, respectively, for these bridges. They also determined mean and *CoV* of reliability indices of 1.6 and 0.92, respectively, using multiple lanes of HL-93 loading.

Barker et al. (2020) also evaluated Service II for Wyoming I-80 bridges under heavy truck traffic due to extended roadway closures that would produce long trains of trucks loading both lanes. They considered the performance of bridges designed and evaluated under current *LRFD BDS* Service II criteria was considered satisfactory and computed target reliability indices on that basis. Barker et al. converted the Service II limit state function from a stress format to a moment format.

See Figure 2.5 where Barker et al. used the notation "NCHRP: LLF = 1.30" as they estimated the maximum truck load effects based on truck raw data *upper-tail* statistics similar to the NCHRP projects (Nowak, 1999; Kulicki et al., 2007). "NCHRP: LLF = 1.30" represents the reliability index for bridges designed with *LRFD BDS* Service II with a design *LL* factor equal to 1.30 and evaluated using multiple lanes loaded with HL-93 loading.

Reliability indices (I-80 WIM: LLF = 1.30 in Figure 2.5) were also determined using I-80 WIM data records, i.e., where I-80 WIM: LLF = 1.30 represents the reliability index for bridges designed with *LRFD BDS* Service II with a design *LL* factor equal to 1.30, and evaluated using multiple lanes loaded with I-80 WIM data. They plotted reliability indices against the span length, as shown in Figure 2.5. To more closely match target reliability indices (NCHRP: LLF = 1.30), they recommended that design *LL* factors for Service II be increased to 1.45 from 1.30 (I-80 WIM: LLF = 1.45 in Figure 2.5). Barker et al. (2020) and Wassef et al. (2014) proposed similar target reliability indices of approximately 1.60 using multiple lanes of HL-93 design loads.

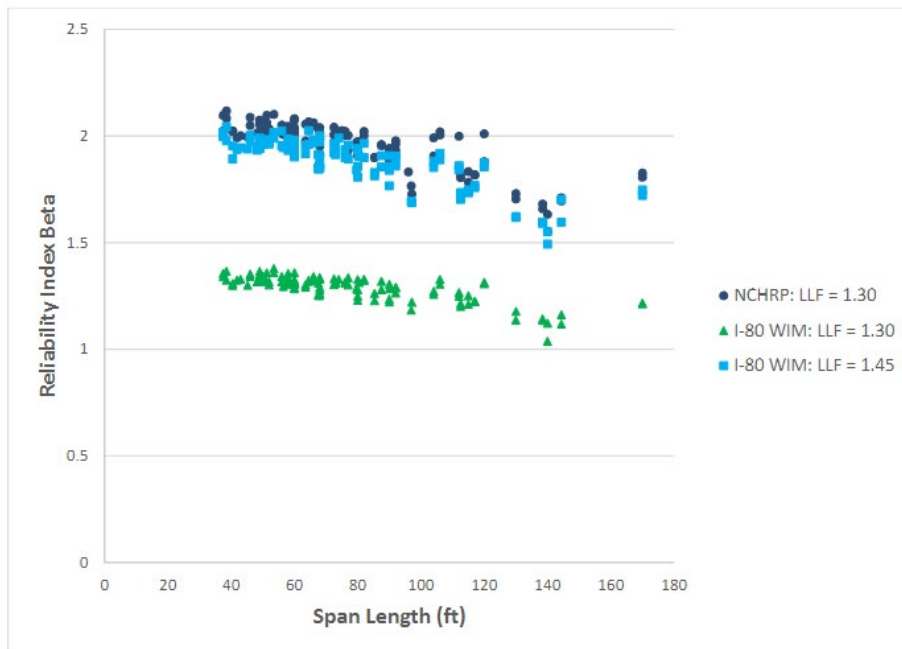


Figure 2.5 Service II Positive Moment Reliability vs Span Length (Optimized In-Service Bridges) (Barker et al., 2020)

In summary, Barker et al. (2020) and Wassef et al. (2014) target or implicit reliability indices were comparable for Service II; however, they significantly differed for Service III where different loading assumptions were used. The former used HL-93 loads for a 75-year service life with multiple loaded lanes, and the latter used a reduced, one-year-return live load model with one loaded lane. The present study used HL-93 loads and a 75-year service life with multiple loaded lanes for to establish target reliability indices, which is consistent with design loads.

2.6 Steel Bridge Fatigue

A fatigue limit state restricts the stress range caused by a single fatigue truck with respect to an expected number of stress range cycles (AASHTO, 2020). The fatigue load is based on the HS20 design truck in the *Standard Specifications*, but with a fixed rear-axle spacing of 30 ft. As *LRFD BDS* Article 3.6.1.4 specifies, the fatigue truck is single-lane loaded with a 15% dynamic

allowance. The *LRFD BDS* provides two limit states for load-induced fatigue: Fatigue I, which relates to infinite load-induced fatigue life; and Fatigue II, which relates to finite load-induced fatigue life. *LRFD BDS* Article 6.6.1.2.2 provides the following load-induced steel stress check:

$$\gamma(\Delta f) \leq (\Delta F)_n \tag{2.3}$$

where γ is the load factor provided in *LRFD BDS* Table 3.4.1-1, Δf is the *LL* stress range due to the passage of the Fatigue Truck, and $(\Delta F)_n$ is the nominal fatigue resistance provided in *LRFD BDS* Article 6.6.1.2.5.

Components and details susceptible to load-induced fatigue are grouped into eight categories, and the fatigue resistance for each category is provided in *LRFD BDS* Article 6.6.1.2.3. Keating and Fisher (1986) summarized mean finite-life fatigue resistance curves for fatigue detail categories A through E'. Figure 2.6 illustrates nominal finite-life resistance curves (*LRFD BDS* Figure C6.6.1.2.5-1). The requirement that the maximum stress range experienced by a detail be less than the constant-amplitude fatigue threshold (CAFT) theoretically provides an infinite fatigue life. *LRFD BDS* Table 6.6.1.2.5-3 specifies CAFTs for the Fatigue I limit state used as $(\Delta F)_n$ in Equation 2.3.

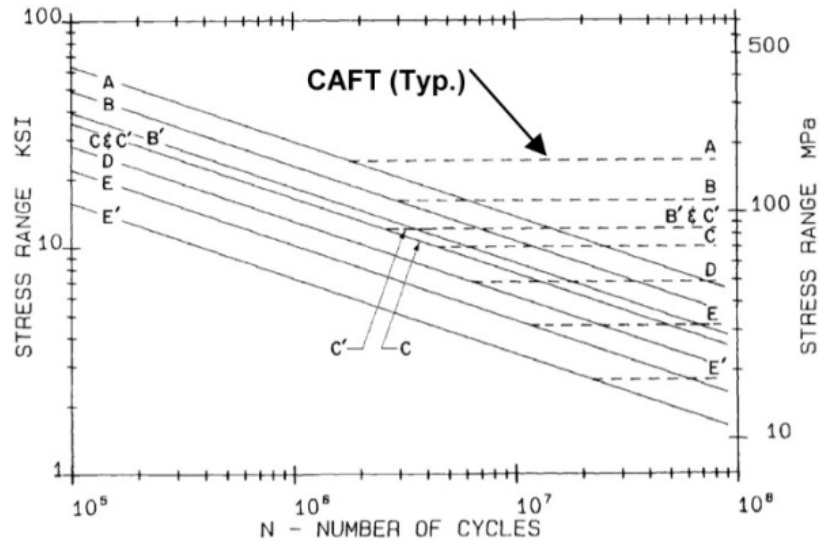


Figure 2.6 Stress Range Versus Number of Cycles (*LRFD BDS*, 2020)

For Fatigue II, finite life, $(\Delta F)_n$ is defined in the *LRFD BDS* Equation 6.6.1.2.5-2 as,

$$(\Delta F)_n = \left(\frac{A}{N} \right)^{\frac{1}{3}} \quad 2.4$$

$$N = (365)(75)n(ADTT)_{SL} \quad 2.5$$

where A is a constant defined for each detail category given in *LRFD BDS* Table 6.6.1.2.5-1, N is the number of cycles to failure, n is the number of stress range cycles per truck passage in *LRFD BDS* Table 6.6.1.2.5-2, and $(ADTT)_{SL}$ is the single-lane $ADTT$ as specified in *LRFD BDS* Article 3.6.1.4. Fatigue I and Fatigue II limit states for a welded cross-frame connection plate in steel bridges subjected to platoons were evaluated.

Each truck passage can result in one or more load cycles, which may reduce bridge fatigue life. Schilling (1984) proposed a formula for calculating effective stress cycles associated with a single truck passage to determine fatigue damage resulting from a maximum stress range with an equivalent number of stress cycles (ENSC). Deng and Yan (2018) used this ENSC equation to determine the number of stress cycles for permit vehicles. This ENSC relationship can be determined using:

$$ENSC = N_m + \left(\frac{S_{r1}}{S_{rp}}\right)^m + \left(\frac{S_{r2}}{S_{rp}}\right)^m + \dots + \left(\frac{S_{ri}}{S_{rp}}\right)^m \quad 2.6$$

where m is the slope constant of the S - N curve; N_m is the number of maximum stress ranges caused by an individual truck passage; S_{ri} is the higher-order stress range; and S_{rp} is the maximum stress range, which can be calculated as the algebraic difference between the maximum and minimum stress.

Permit load fatigue evaluation has been studied widely, but not for platoons. Deng and Yan (2018) proposed a method for determining vehicle weight limits and overload permits based on cumulative fatigue damage where cumulative fatigue damage due to vehicle loads was calculated based on stress history. The linear accumulative fatigue damage model for a given time ($CFD(t)$) used in Deng and Yan (2018) is:

$$CFD(t) = \sum_i \frac{n_i}{N_i} \quad 2.7$$

$$N_i = \frac{A}{S_i^m} \quad 2.8$$

$$CFD(t) = Num \times \frac{ENSC \times S_{max}^m}{A} \quad 2.9$$

where n_i is the actual number of stress cycles experienced; S_{max} is the maximum stress range, which can be calculated as the algebraic difference between the maximum and minimum stress; N_i is the fatigue life corresponding to the i_{th} stress-range bin S_i ; m is the slope constant of the $S-N$ curve ($m = 3$ based on *LRFD BDS*); and Num is the number of truck passages during a given time. Generally, this linear accumulative fatigue damage model applies to this study. The parameters A and Num can be easily determined, and then time-dependent analysis can be used to calculate the ENSC, and *LL* analysis can be used to determine the stress range for platoons.

Stawska et al. (2022) established an incremental consumption equation based on cumulative fatigue damage from the AASHTO fatigue truck and permit loads in order to estimate bridge life. They calculated the cost of one permit for the permit vehicle by estimating the damage ratio between a permit vehicle and a fatigue truck caused by one crossing assuming a bridge life of 75 years based on single lane AASHTO fatigue truck crossings as specified in *LRFD BDS* 6.6.1.2.5-3, and assuming that girders would need to be replaced immediately after exhausting their code-specified fatigue life.

Recently, Braguim et al. (2021) started investigating platoon load-induced fatigue in steel girder bridges. The rainflow counting method was used to determine stress ranges and cycles, and Miner's rule was used to quantify fatigue damage for platoons with headways ranging from 20 to 40 ft. When calculating fatigue damage on simple- and two-span bridges, up to four legal

loads per platoon were considered. Accumulative fatigue damage from each truck in the platoon was compared to the fatigue truck to a single platoon truck traveling alone. Braguim et al. observed that platoons could reduce fatigue damage when compared to individual trucks, depending on the number of trucks and their headways.

According to Steelman et al. (2021), closely spaced platoons could produce higher shear loads than HL-93 design loading. Higher shear loading may lead to fatigue damage of shear connectors or other fatigue-prone details. *LRFD BDS* Article 6.10.10 specifies shear stud Fatigue I and Fatigue II limit states based on a nominal fatigue truck, but reliability calibration would be required similar to other limit states discussed herein in order to evaluate implications with respect to fatigue.

2.7 Summary

Bridge reliability analyses for platoon loads at strength limit states have been conducted; however, service reliability analyses are lacking. It is necessary to determine target reliability indices for Service III and Service II limit states to ensure such that target bridge performance is maintained under platoon loading. Fatigue limit state reliability calibration is also necessary, but was beyond the scope of this study.

Chapter 3 Research Methodology

3.1 Overview

This research investigated potential platooning operations to ensure service-based structural reliability. General platoon and bridge characteristics and configurations were selected for a parametric study used to conduct a reliability analysis. Probabilistic representations of uncertain dead loads, live loads, and resistances are well understood from previous work and used in the reliability analysis. To address the first two objectives of the project, which were the calibration of *LL* factors and development of acceptable platoon headways for service, the range of total *CoV* for a platoon was taken from Steelman et al. (2021).

Based on frameworks presented in this chapter, target implicit reliability indices (β implicit) for Service II and III were calculated using Monte Carlo Simulation (MCS), which were then used to calibrate *LFR LL* factors. Platoons were parametrically investigated by varying the:

- type of platoon truck,
- headway between trucks,
- weight of individual trucks, and
- degree of uncertainty associated with *LL*.

Bridges were parameterized based on span length, span type (simple and continuous), construction material (steel and prestressed concrete), and girder spacing. The nominal dead loads of prestressed concrete and steel girder bridges were estimated. The resistances of prestressed concrete girder bridges were determined based on Service III combinations for the nominal dead loads, HL-93, and HS20-44 design *LL*. For steel bridges, resistances were

determined using Service II and Strength I combinations to support estimated nominal dead loads and HL-93 design *live load*. Finally, nominal loads and resistances were converted to probability distributions with characteristic means and deviations, and the probability of failure for each parametric combination was calculated using MCS.

The three primary *LL* scenarios were the same as in Steelman et al. (2021):

- a platoon in a single bridge lane,
- two identical platoons operating in adjacent lanes, and
- a combination of a platoon in one lane and routine traffic in the adjacent lane.

3.2 Platoon Parameters

Several platoon parameters are discussed in this section. They include truck type, headways between platoons, the number of trucks in a platoon, and platoon loading scenarios.

3.2.1 Truck Type and Number of Platoon Trucks

The present study adopted similar vehicles to those from Steelman et al. (2021) and Yang et al. (2022). The Notional Rating Load (NRL) (see Figure 3.1), with 6-ft axle spacing between the first and second axle enveloped load effects of all routine legal vehicle configurations for considered, critical, single- and two-span positive moment locations. Envelope platoon load effects for the two-span negative moment region were taken from Steelman et al. (2021).

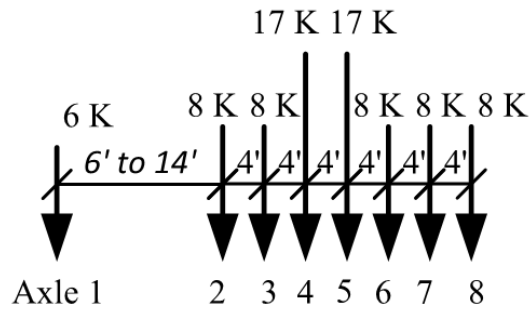


Figure 3.1 Notional Rating Load (AASHTO, 2020)

Steelman et al. (2021) found that demands for three trucks in a platoon are not significantly different from those for four trucks in a platoon for single-span bridges less than 150 ft. This study considered four-truck platoons crossing single-span bridges and continuous two-span bridges.

3.2.2 Headway

Figure 3.2 illustrates the definition of headway used in the current study. Headway is the distance between the leading truck's last axle and the following truck's first axle. This study considered headways between 5 ft and 50 ft, similar to Steelman et al. (2021). The upper limit was set at 50 ft because it corresponds to a traffic spacing that provides negligible aerodynamic efficiency benefits (Lammert et al., 2020). All distances were parametrically incremented at one-ft intervals.

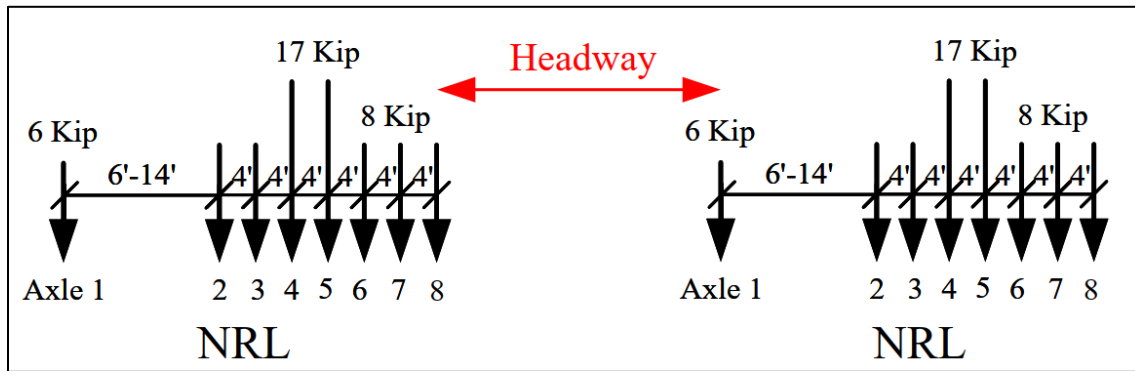
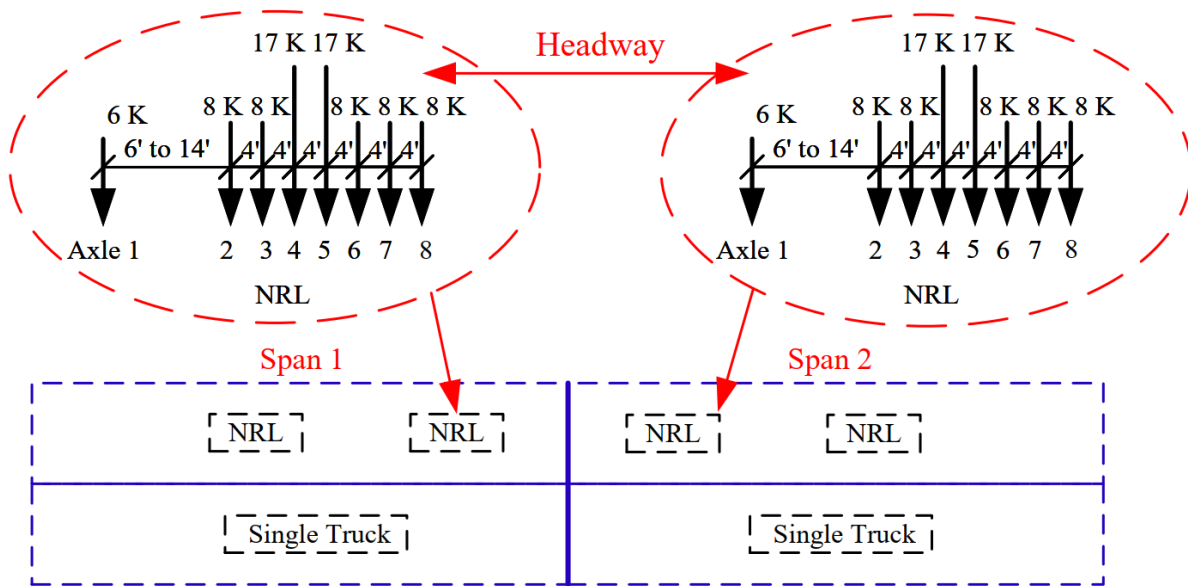


Figure 3.2 Typical Two-Truck Configuration and Headway Definition (Steelman et al. 2021)

3.2.3 Lane Loading Scenarios

One- and two-lane loading scenarios were the same as those used by Steelman et al. (2021). These scenarios included a single platoon in one lane, two identical platoons in adjacent lanes, and a platoon operating with routine traffic in an adjacent lane to formulate operational guidelines. Statistical parameters for adjacent lane loads (bias and CoV) were adopted from Section 3.5.5 of Steelman et al. (2021) and were based on WIM data from Interstate I-80 for a single truck event recorded from Barker and Puckett (2016). Due to a lack of WIM data, two-span positive moment regions were assumed to be equal to simple-span positive moment statistical parameters. Data from Barker and Puckett (2016) represents single-truck events. As span length increases, critical effects may be governed by more than one truck in an adjacent, routine traffic lane. To determine critical negative moments, the routine traffic lane adjacent to a platoon was assumed to contain two trucks, one truck positioned in each span, for two-span, 90- to 200-ft bridges, as shown in Figure 3.3. Truck-to-truck variability was assumed to be random and uncorrelated.



Platoon with Adjacent Routine Traffic (90- 200 ft Two-span Bridges)

Figure 3.3 Platoon with Adjacent Routine Traffic Load Case (90 – 200 ft Two-span Bridges) (Steelman et al. 2021)

As presented by Steelman et al. (2021), the platoon was assumed to cross the bridge 100 times per day and the bridge was routinely loaded with truck traffic at a 5,000 ADTT. Multiple presence probabilities for platoons having adjacent routine traffic were taken from Ghosn et al. (2011). Ghosn et al. (2011) collected WIM data in New York and observed side-by-side probabilities of 2% for 5,000 ADTT (heavy truck volumes), 1.25% for 1,000 ADTT (average truck volumes), and 0.5% for 100 ADTT (light truck volumes).

3.3 Bridge Parameters

The present study included the following bridge types:

- simple-span steel composite girders,
- two equal-span continuous steel composite girders,
- simple-span prestressed I-girders, and

- two equal-span continuous prestressed I-girders.

Steel girder bridges had span lengths between 60 and 200 ft and were assumed to carry two lanes of traffic. The upper span length for prestressed concrete girders was set at 150 ft. Typical girder spacings for Nebraska interstate bridges range between 8 ft and 12 ft, and the scope of this study initially spanned this representative range. A typical 10-ft spacing was ultimately selected because results indicated that reliability indices were insensitive to girder spacing. Interior girders were expected to be critical load-carrying elements. In summary, parameter ranges for the one- and two-span bridge analyses were:

- prestressed composite concrete I-girder bridges with spans of 60, 90, 120, and 150 ft;
- composite steel girders with spans of 60, 90, 120, 150, and 200 ft; and
- girder spacing of 10 ft.

3.4 Reliability Analysis for Service III

This section presents nominal values, statistical parameters, and procedures for conducting reliability analyses for the Service III limit state for a critical girder. A limit state function is presented for evaluating bridges optimally designed for Service III and Strength I under the *LRFD BDS*.

3.4.1 General Reliability Analysis Procedure

The following reliability indices are defined:

- Implicit reliability (index), $\beta_{Implicit}$, is reliability provided by code-compliant bridge designs, i.e., β is inferred from designs produced from historical practice.
- Cracking reliability, $\beta_{Cracking}$, is reliability against mechanical cracking limits provided by code-compliant bridge designs.

This research examined implicit reliabilities for different design scenarios and evaluated cracking probability for prestressed concrete bridges optimally designed according to service criteria in the *LRFD BDS* or the *Standard Specifications*. Bridges were also designed based on appropriate live loads, load distributions, dynamic amplifications, and service load combinations from the *Standard Specifications* to evaluate the influence of applying prestress losses according to *Standard Specifications* criteria. However, all designs were evaluated using HL-93 loading for consistent comparisons. Figure 3.4 provides a research framework overview where shaded cells illustrate the pathway used to complete optimal bridge designs and reliability analyses.

Three inputs are required for reliability analyses: (1) nominal values, (2) bias factors (i.e., ratio of mean to nominal value), and (3) *CoV*s (i.e., ratio of standard deviation to mean). A parametric study was conducted that varied allowable tensile stresses, prestress loss methods, girder spacings, and span numbers and lengths to investigate the effects of these parameters on service implicit reliability. Optimal design resistances were determined by incorporating nominal dead with nominal HL-93 and HS20-44 live load. “Optimal design” refers to a bridge for which capacity exactly satisfied service load requirements according to LRFD BDS and Allowable Stress Design (ASD) criteria.

This study assumed that the implicit β based on current and past design criteria would provide satisfactory in-service performance, similar to Wassef et al. (2014) and Barker and Puckett (2020). Nominal demands, live loads, and resistances were mapped onto probabilistic distributions with characteristic means and *CoV*s. The probability of failure for each parametric combination was calculated using MCS and $N = 1,000,000$ samples to determine β . The selected number of samples corresponded to a maximum perceptible reliability index of approximately β

= 4.75.

This process was repeated to conduct reliability analyses for different design scenarios, identify an implicit β , and investigate cracking reliability for optimally designed prestressed concrete bridges for service. Cracking reliability was evaluated for bridges designed using an allowable stress limit ($0.0948\sqrt{f'_c}$ (ksi)), and considering rupture moduli between $0.24\sqrt{f'_c}$ and $0.37\sqrt{f'_c}$ (ksi) as specified in *LRFD BDS C5.4.2.6*. Cracking probability is discussed in Chapter 9.

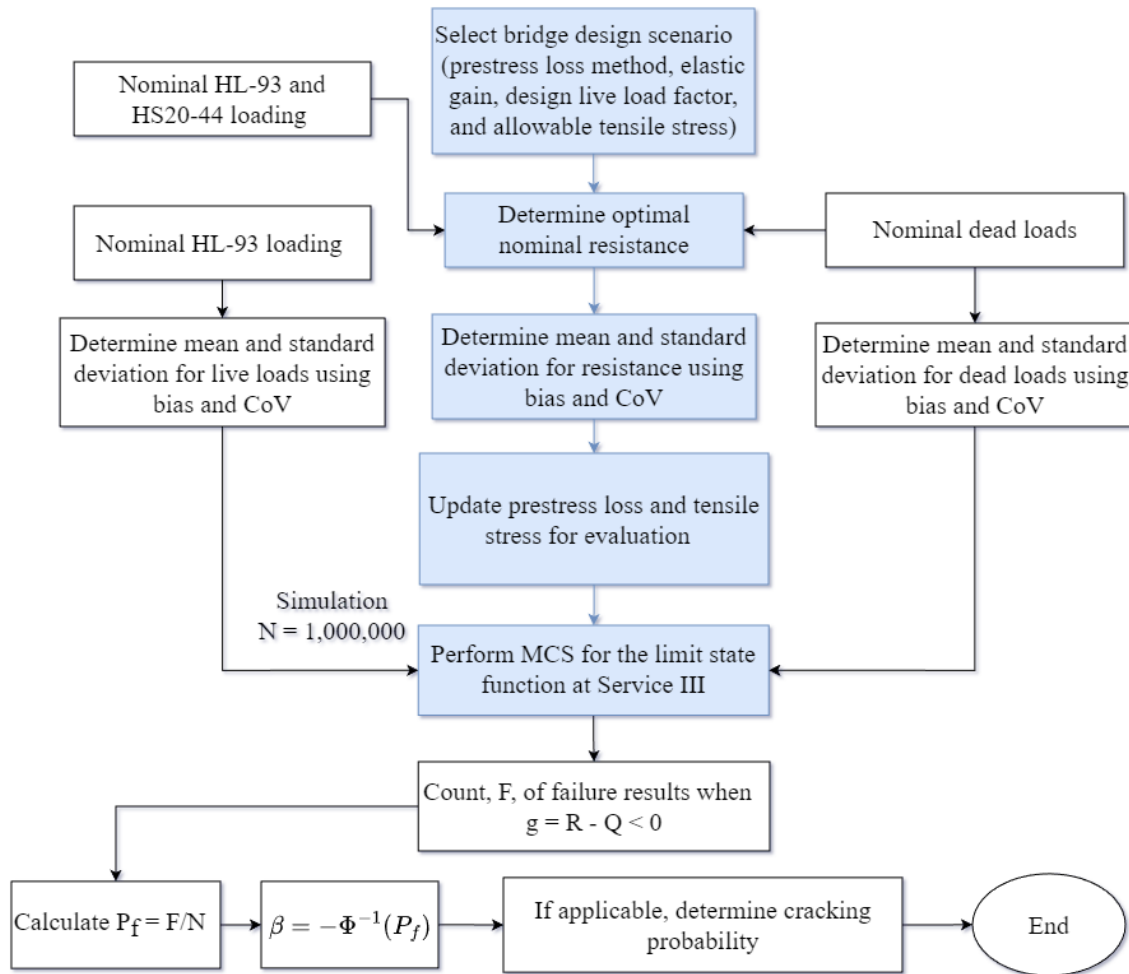


Figure 3.4 Service III Research Methodology

3.4.2 Nominal Resistance

MBE Equation 6A.5.4.1 is used for LRFD rating (LRFR) for Service III:

$$RF = \frac{f_R - (\gamma_D)(f_D)}{(\gamma_L)(f_{LL+IM})} \quad 3.1$$

where RF is the rating factor, γ_D the dead load factor for rating, and γ_L the rating LL factor.

Remaining load and resistance terms in Equation 3.1 for composite prestressed concrete girder bridges are based on gross section properties and are calculated as shown in Equations -

$$f_R = f_t + \frac{P_e}{A_g} + \frac{P_e e_{nc}}{S_{ncb}} \quad 3.2$$

$$P_e = A_{ps} (f_{pi} - \Delta f_s) \quad 3.3$$

$$f_D = \frac{(D_{gw} + D_{nc})}{S_{ncb}} + \frac{(D_c + D_w)}{S_{cb}} \quad 3.4$$

$$f_{LL+IM} = \frac{LL(1+IM)GDF_m}{S_{cb}} \quad 3.5$$

where:

f_R = nominal flexure resistance,

f_D = nominal tensile stress due to dead loads,

f_{LL+IM} = nominal tensile stress due to LL including impact,

f_t = nominal design allowable tensile stress,

f_{pi} = nominal initial prestressing,

P_e = nominal effective prestress force after losses,

Δf_s = nominal prestress losses,

A_{ps} = nominal total area of prestressing reinforcement,

A_g = nominal gross section area,

e_{nc} = nominal eccentricity from the noncomposite centroid to prestress strand centroid,

D_{gw} = nominal girder dead load moment,

D_{nc} = nominal noncomposite dead load moment,

D_c = nominal composite dead load moment,

D_w = nominal wearing dead load moment,

LL = nominal HL-93 design loading (LRFD bridges), or HS20-44 design loading (LFD/ASD bridges),

IM = nominal impact factor; LRFD BDS Article 3.6.2 (LRFD bridges); Standard Specifications Equation 3-1 (LFD/ASD bridges),

GDF_m = nominal LRFD BDS moment Girder Distribution Factor (GDF) (LRFD bridges), or nominal GDF in Standard Specifications (LFD/ASD bridges),

S_{ncb} = nominal noncomposite section modulus for the bottom fiber, and

S_{cb} = nominal composite section modulus for the bottom fiber.

The nominal optimal resistance based on *LRFD BDS* at Service III is determined by setting $RF = 1.0$. Bridges designed based on the *Standard Specifications* follow the same procedure using appropriate live loads, *GDFs*, and *IMs*. The nominal resistance is calculated by

reforming Equation 3.1 as follows,

$$f_t + \frac{P_e}{A_g} + \frac{P_e e_{nc}}{S_{ncb}} = \frac{\gamma_D(D_{gw} + D_{nc})}{S_{ncb}} + \frac{\gamma_D(D_c + D_w)}{S_{cb}} + \frac{\gamma_L LL(1+IM)GDF_m}{S_{cb}} \quad 3.6$$

The design tension stress at the bottom of the girder, f_{des} , was calculated as the right side of Equation 3.6. For a given f_t , the required effective stress, f_{req} , in the prestressing strands after losses was calculated using Equations 3.7-3.9. The required effective prestress force based on f_{req} was then determined as follows,

$$f_{des} = \frac{\gamma_D(D_{gw} + D_{nc})}{S_{ncb}} + \frac{\gamma_D(D_c + D_w)}{S_{cb}} + \frac{\gamma_L LL(1+IM)GDF_m}{S_{cb}} \quad 3.7$$

$$f_{req} = f_{des} - f_t \quad 3.8$$

$$f_{req} = \frac{P_e}{A_g} + \frac{P_e e_{nc}}{S_{ncb}} \quad 3.9$$

$$P_{req} = \frac{f_{req}}{\frac{1}{A_g} + \frac{e_{nc}}{S_{ncb}}} \quad 3.10$$

Based on calculated f_{req} and corresponding P_{req} , for the initial iteration the required number of strands was calculated and used to determine A_{ps} , e_{nc} , and Δf_s , which included or neglected elastic gains depending on the design scenario under consideration. The number of strands was iterated until Equation 3.10 was satisfied, which meant P_e equaled P_{req} in Equation 3.3. This study aimed to investigate theoretically optimal reliability indices and implicit β 's,

preferably without step functions and discontinuities that may occur due to providing even integers of strands as is typical for physically constructed girders. Accordingly, optimal designs were configured with decimal fractions of strands.

3.4.3 Bridge Details

The *LRFD BDS*, *Standard Specifications*, and *MBE* require the Service III limit state to be evaluated in positive moment regions. Accordingly, this study only considered positive moments at the midspan of simple-span prestressed composite girder bridges and at 40% of the span length ($0.4L$) from the supporting abutments for two equal-span, continuous, prestressed composite girder bridges. Consistent use of $0.4L$ was deemed reasonably representative of critical positive moments in continuous spans, although exact critical positive moment locations were typically around $0.43 - 0.45L$, at which exact critical moment values differed from those at $0.4L$ by about 2%. The bridges were assumed to carry two lanes of traffic, and internal girders were designed using NU-I girders according to Hanna et al. (2010). Design details were:

- 60-, 90-, 120-, and 150-ft spans,
- Five NU 900 (60 ft), NU 1100 (90 ft), NU 1600 (120 ft), and NU 2000 (150 ft) girders,
- 3.5-ft overhangs,
- 10-ft girder spacings,
- Composite 8.5-in. deck with 0.5-in. sacrificial and 2-in. asphalt wearing surfaces,
- 1-in. deck haunch,
- 17-in. wide barrier that produced a weight of 0.124 k/ft per girder, and
- Simple and equal continuous spans.

Four tension stress limit values (hereafter f_t) were considered for service. The maximum considered design f_t was the modulus of rupture (f_r), $0.24\sqrt{f'_c}$ (ksi), which is larger than the 0.6 ksi upper bound for f_t in the *LRFD BDS*. A minimum design f_t of zero was used, commonly called the decompression limit. The two most common design-allowable tensile stresses, $0.0948\sqrt{f'_c}$ (ksi) and $0.19\sqrt{f'_c}$ (ksi), were also included in the study. For simplicity, the coefficient before $\sqrt{f'_c}$ (ksi) in the design f_t is referred to herein as κ . Preliminary analyses indicated that service reliability results for optimally designed bridges were insensitive to final and initial concrete strength parameters. Initial concrete strength was used to calculate prestress loss based on the refined time-dependent loss method in the *LRFD BDS*, derived initially from Tadros et al. (2001). Parameters considered for κ , f_t , f'_c , and f'_{ci} included:

- $f_t = \kappa\sqrt{f'_c}$ ksi, where $\kappa = 0, 0.0948, 0.19$, and 0.24 ,
- $f'_{c_girder} = 8$ ksi,
- $f'_{ci_girder} = 5$ ksi,
- $f'_{c_deck} = 4$ ksi, and
- $f'_{ci_deck} = 3.2$ ksi.

Grade 270 0.6 in. low-relaxation strands with modulus of elasticity of 28,500 ksi were used. The initial stress at transfer (f_{pi}) was 75% of the ultimate tensile strength (f_{pu}). Following girder details provided by Hanna et al. (2010) (see Figure 3.5), the maximum number of strands was set to 60 with those strands placed in up to seven layers (18 strands per layer in the flange, reduced to two strands per layer in the web). Bottom concrete cover was assumed to be 2 in., and the distance between prestressing layers was also two in. Participation of any mild reinforcing

steel in cross-sectional resistance was ignored.

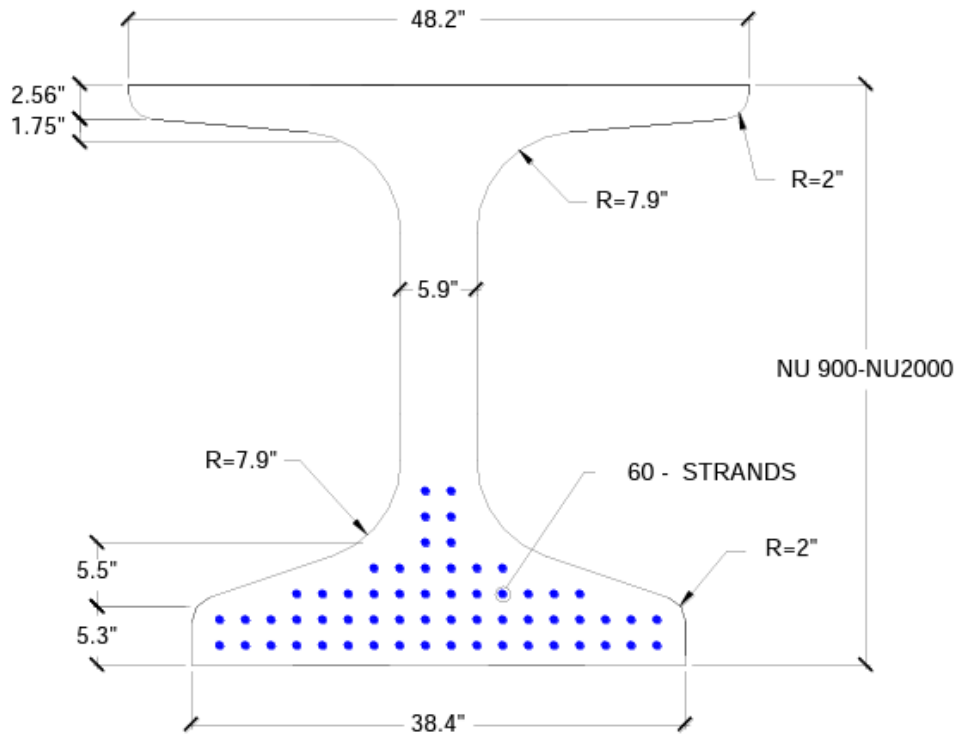


Figure 3.5 Pretensioned Nebraska University I-Girder with Strand Layout (Hanna et al., 2010)

3.4.4 Prestress Loss Method Parameters

Prestress loss calculations were based on gross section properties (A_g , S_{ncb} , and S_{cb}). Bridges having a 47-ft width and a travelway width of 40 ft-2 in. were subjected to HL-93 load in two lanes. Gross deck area was transformed using the modular ratio when determining S_{cb} . *LFRD BDS* Equation C5.4.2.4-2 was used to calculate the modulus of elasticity. S_{cb} was determined after reducing the nominal bridge deck thickness by 0.5 in. to account for future wearing surface degradation. Three loss methods and six design scenarios were considered, as summarized in Table 3.1.

Table 3.1 Design Scenarios

ID	Loss Computation	Design Live Load Factor (γ_L)	Elastic gains (Y/N)	Comment
<i>Post-1.0-Gains</i>	Post-2005 loss method (LRFD BDS 5.9.3.4)	1.0	Y	LRFD Table 3.4.1-4: Prestressed concrete components designed using refined estimates for time-dependent losses in Article 5.9.3.4 in conjunction with elastic gains
<i>Post-0.8-Gains</i>	Post-2005 loss method (LRFD BDS 5.9.3.4)	0.8	Y	Same as Scenario <i>Post-1.0-Gains</i> with a lower live load
<i>Post-0.8-No-gains</i>	Post-2005 loss method (LRFD BDS 5.9.3.4)	0.8	N	LRFD Table 3.4.1-4: All other prestressed concrete components
<i>Approx-0.8-Gains</i>	Approximate loss method (LRFD BDS 5.9.3.3)	0.8	Y	LRFD Table 3.4.1-4: All other prestressed concrete components
<i>Approx-0.8-No-gains</i>	Approximate loss method (LRFD BDS 5.9.3.3)	0.8	N	LRFD Table 3.4.1-4: All other prestressed concrete components
<i>Pre-1.0-No-gains</i>	Pre-2005 loss method	1.0	N	<i>Standard Specifications</i> 9.16.2.1

According to *LRFD BDS* Tables 3.4.1-1 and 3.4.1-4, and *Standard Specifications* Table 3.22.1A, the design dead load factor (design γ_D) for service is 1.0. However, design *LL* factors (design γ_L) vary according to the selected prestress loss method and the decision to include or neglect elastic gains in the effective prestress force.

The *Post-1.0-Gains* case was treated as a baseline, consistent with Wassef et al. (2014). The study also considered *Post-0.8-Gains*, representing how some bridges might have been designed between when post-2005 losses were included in the *LRFD BDS* and when the required design γ_L was increased to 1.0. *Post-0.8-No-gains* is technically consistent with *LRFD BDS* Table 3.4.1-4. Using approximate loss methods with or without elastic gain was interpreted as an instance of ambiguity or subtlety within the *LRFD BDS*, and Commentary C5.9.3.3 in the *LRFD BDS* explains that elastic gains “should” be included unless transformed section properties are used. Due to higher prestress loss predictions and a design *LL* factor of 1.0, bridges designed using *Pre-1.0-No-gains* typically required the most strands.

Sensitivity analyses were conducted using information from bridges designed in Nebraska to examine effects of concrete age and average relative humidity on reliability. Analysis results negligibly influenced the factors and, as a result, the following parameters were used:

- Prestress transfer: 1 day,
- Deck placement: 30 days,
- Final analysis time: 3650 days, and
- Average Relative Humidity: $H = 65\%$.

3.4.5 Nominal Dead Loads

Realistic estimates for nominal dead loads were calculated for various bridge types and span lengths. As shown in Equation 3.6, dead load moment had four components (D_{gw} , D_{nc} , D_c , and D_w). All concrete was assumed to be normal weight and 145 pcf (150 pcf with reinforcement). Designs produced the same optimal NU sections for both simple- and two-span bridges having similar spans. Preliminary analyses verified that this assumption had negligible effects on implicit reliability analysis results.

3.4.6 Nominal Design Live Loads

The HL-93 load model from *LRFD BDS* and the HS20-44 model from the *Standard Specifications* were the nominal design live loads. The HL-93 *LL* consisted of axle loads from a truck or tandem combined with a uniform distributed lane load. A constant *IM* of 0.33 was applied to truck and tandem loads in accordance with the *LRFD BDS*. The interior girder GDF for multiple lane loading (GDF_m) in Equation 3.6 was determined using *LRFD BDS* Table 4.6.2.2.2b-1. The longitudinal stiffness (K_g) term was calculated based on optimally designed

girder cross-sectional geometry when determining GDF_m . The HS20-44 load effect was determined by combining the larger load effect from a truck, or from a lane load with a concentrated load as specified in the *Standard Specifications*. For GDF_m , Equation 3.6 used an equivalent lane-based GDF for the *Standard Specifications*, taken as $S/11$, where S is the girder spacing, for prestressed concrete bridges. IM was taken as a function of span length, with a maximum value of 0.30, according to *Standard Specifications* Equation 3-1.

3.4.7 Statistical Parameters

Statistical parameters were implemented in the reliability analyses, as shown in Figure 3.4. Selected statistical parameters and their sources for dead loads (D_{gw} , D_{nc} , D_c , and D_w), live loads (LL_{HL-93} , $LL_{Platoon}$), and selected variables affecting resistance (e_{nc} , e_c , A_{ps} , f_{pi} , Δf_s (w/o LL gain), f_t ($\kappa = 0, 0.095$, and 0.19), and f_r) are summarized in Table 3.2.

The total HL-93 CoV represented combined uncertainty contributions from truck weight, dynamic amplification, and load distribution (Kulicki et al., 2007). Δf_s (w/o LL gain) bias and CoV applied to the prestress loss considered elastic shortening loss, long-term loss, and the dead load elastic gains. The LL elastic gain was not included in these statistical parameters as its variability was included based on LL statistics, and its bias was assumed to be 1.0. The statistical uncertainty for f_r was from Holombo and Tadros (2010), who determined that the mean and CoV of the modulus of rupture were $7.02\sqrt{f'_c}$ (psi) and 0.24, respectively. The typical nominal modulus of rupture was $7.5\sqrt{f'_c}$ (psi), and the bias for f_r was the ratio of 7.02 to 7.5. The modulus of rupture for the $0.30\sqrt{f'_c}$ and $0.37\sqrt{f'_c}$ cracking limits were uncertain and assumed to have the same bias and CoV as $0.24\sqrt{f'_c}$. Allowable tension limits (f_t) for κ ranged between 0 and

0.19 and were considered deterministic values because these limits were historically specified based on engineering judgment. Results were insensitive to variations of gross sectional area, section modulus, and prestressing steel and concrete moduli. Accordingly, these parameters were also treated as having biases of 1.0. The probabilistic mean for dynamic amplification due to impact, IM , was set to 10% as presented in Kulicki et al. (2007). The platoon bias was assumed to be 1.0, and platoon LL CoV ranged from 0 to 0.20, consistent with Steelman et al. (2021). A bias of 1.0 indicates that nominal and mean values for platoons are the same, so that the assumed weight used in calculations and the actual weight of the permit vehicle are equal. The upper CoV bound of 0.20 is slightly higher than 0.18 used in the AASHTO LRFD BDS Strength I calibration for 75 years of HL-93 loading from Nowak (1999). The lower CoV bound of 0 reflects the potential for IM , GDF , and truck weight uncertainties to approach zero in the future. Chapter 7 formulates protocols for evaluating and incorporating reduced operational uncertainties to estimate more reasonable CoV bounds for platoons.

Table 3.2 Statistical Parameters for Variables

Variables	Distribution	Bias	CoV	References
D_{gw}	Normal	1.03	0.08	Kulicki et al. (2007)
D_{nc}	Normal	1.05	0.1	Kulicki et al. (2007)
D_c	Normal	1.05	0.1	Kulicki et al. (2007)
D_w	Normal	1	0.25	Kulicki et al. (2007)
LL_{HL-93}	Normal	1.18	0.18	Kulicki et al. (2007)
$LL_{Platoon}$	Normal	1.00	0-0.20	Steelman et al. (2021)
e_{nc}, e_c	Normal	1	0.04	Siriaksorn and Naaman (1980)
A_{ps}	Normal	1.01176	0.0125	Siriaksorn and Naaman (1980)
f_{pi}	Normal	0.97	0.08	Wassef et al. (2014), and Gross and Burns (2000)
Δf_s (w/o LL_{gain})	Normal	1.05	0.1	Wassef et al. (2014) and Tadros et al. (2001)
f_r	Normal	0.936	0.24	Holombo and Tadros (2010)
f_t ($\kappa = 0-0.19$)	Deterministic	1	0	Assumption

Note: e_c = eccentricity between the gross composite centroid and prestressing strand centroid

3.4.8 Limit State Function for Service III

Reliability analyses were implemented by progressing through the middle, shaded portion of Figure 3.4 using defined nominal values and statistical parameters, recognizing that effective prestress force for evaluation may have differed from effective prestress force used in design. HL-93 loading, GDF_m , and IM in *LRFD BDS* were applied in all reliability evaluations for single- and two-span bridges designed based on either the *LRFD BDS* or *Standard Specifications*. Equation 3.11 represents the limit state function for determining target implicit reliability for Service III. The limit state functions for evaluating platoon load scenarios were varied as described in Section 3.6.

$$g = R - Q = \left(f_t + \frac{P_{eval}}{A_g} + \frac{P_{eval} e_{nc}}{S_{ncb}} \right) - \left(\frac{(D_{gw} + D_{nc})}{S_{ncb}} + \frac{(D_c + D_w)}{S_{cb}} + \frac{LL_{HL-93}(1 + IM)GDF_m}{S_{cb}} \right) \quad 3.11$$

$$P_{eval} = A_{ps} (f_{pi} - \Delta f_{S_{eval}}) = A_{ps} (f_{pi} - (\Delta f_{pES} + \Delta f_{pLT} - \Delta f_{GainDL} - \Delta f_{GainLL})) \quad 3.12$$

$$f_{Reval} = f_t + \frac{P_{eval}}{A_g} + \frac{P_{eval} e_{nc}}{S_{ncb}} \quad 3.13$$

where the P_{eval} is the effective prestress force for the evaluation, $\Delta f_{S_{eval}}$ is the prestress loss for the evaluation, Δf_{pES} is the elastic shortening loss, Δf_{pLT} is the long-term prestress loss, $\Delta f_{pGainDL}$ is the elastic gain from dead loads, and $\Delta f_{pGainLL}$ is the elastic gain from *LL. Post-1.0-Gains* defined in Table 3.1 and consistent with Wassef et al. (2014) was used to determine prestress losses in all cases when evaluating bridge performance, regardless of the loss method used for design. f_{Reval} is the available resistance to tension stress for evaluation and can be determined using Equation 3.13.

3.5 Reliability Analysis for Service II

This section presents nominal values, statistical parameters, and procedures for conducting reliability analyses for the Service II limit state. A limit state function is presented for evaluating bridges optimally designed for Service II and Strength I under the *LRFD BDS*.

3.5.1 General Reliability Analysis Procedure

This research examined target implicit reliability for steel girder bridges designed according to Service II and Strength I criteria in the *LRFD BDS*. Based on *LRFD BDS* criteria, optimal steel bridge girder sections were designed to meet both Service II and Strength I load requirements. In this study, the bottom flange was varied to arrive at optimal designs with a maximum performance ratio (i.e., ratio of capacity to demand) of 1.0 for Service II and Strength I. Nominal dead loads, live loads, and resistances were then combined with statistical parameters

to conduct reliability analyses based on the limit state function for Service II. The framework in Figure 3.6 illustrates how steel bridge designs and reliability analyses were conducted. A parametric study was conducted varying girder spacings and span numbers. For simple and two-span bridges, positive moment regions were considered as well as negative moment regions for two-span bridges. By incorporating nominal dead loads with nominal HL-93 live loads, the optimal design resistance that meets both Service II and Strength I were determined. Biases and $CoVs$ were then incorporated into reliability analyses. β was calculated from nominal demands, live loads, and resistances with corresponding biases and uncertainties using MCS with $N = 1,000,000$ samples.

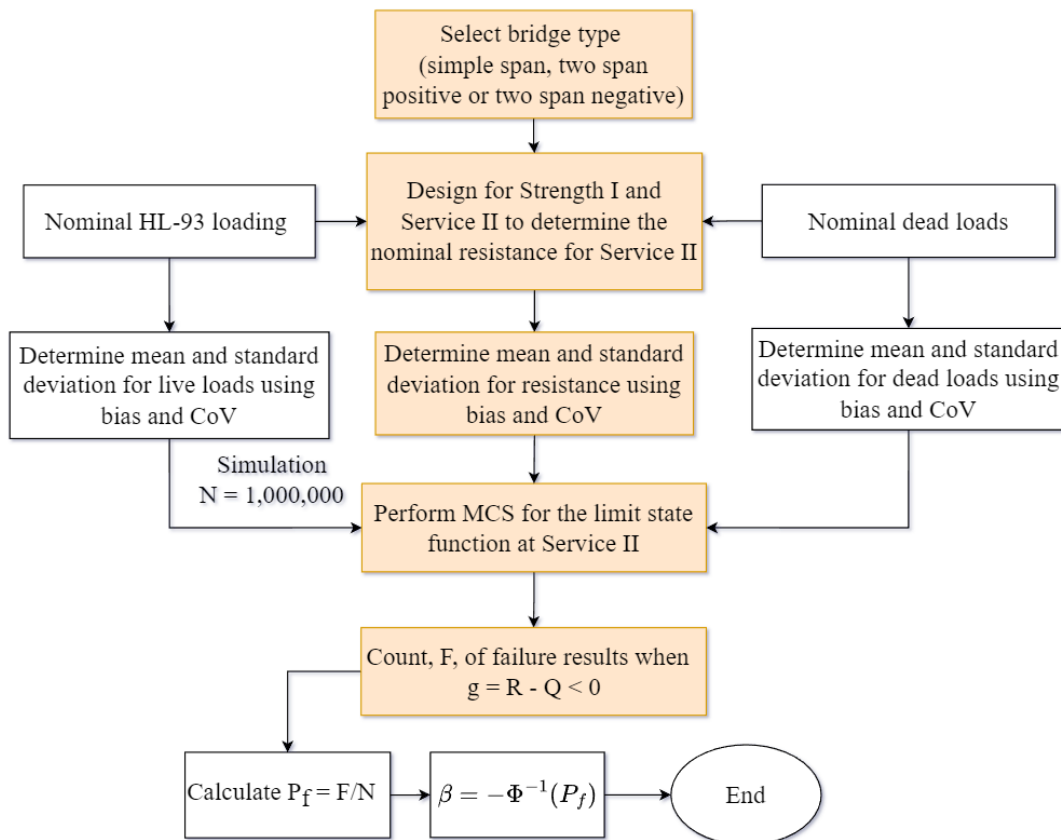


Figure 3.6. Service II Research Methodology

3.5.2 Nominal Resistance

Recall the Load and Resistance Factor Rating equation in the MBE 6A 4.2.1-1:

$$RF = \frac{C - (\gamma_{DC})DC - (\gamma_{DW})DW - (\gamma_P)P}{(\gamma_{LL})(LL + IM)} \quad 3.14$$

The *MBE* considers dead load effects from components, *DC*, wearing surfaces *DW*, and permanent loads other than dead loads, *P*. *LL* is the nominal static live load effect. *IM* is dynamic impact amplification. γ_{LL} is the live load factor, γ_{DC} is the dead load factor for dead load effects from components, γ_{DW} is the dead load factor for wearing surfaces, and γ_P is the factor for permanent loads other than dead loads. Permanent loads other than dead loads were not considered in the research. *C* represents capacity, and can be factored moment, shear, or other capacity values. A minimum value of *C* corresponds to an implicit $RF = 1$. *MBE* Equation 6.A.4.2.2-1 (Equation 3.14) shows that when the rating factor for Strength I equals 1.0, the optimal resistance with Strength I load factors in *MBE* Table 6.A.4.2.2-1 becomes:

$$R_{n_Strength} = \frac{1.25DC + 1.5DW + 1.75L_n(1 + IM)GDF_m}{\phi} \quad 3.15$$

where $R_{n_Strength}$ is the minimum required nominal resistance (demand) for Strength I, ϕ is the resistance factor corresponding to the material and limit state under consideration (equal to 1.0 for steel bridges), *IM* is the *LRFD BDS* Article 3.6.2 nominal impact factor, GDF_m is the nominal moment GDF, and L_n is the nominal effect due to HL-93 loading.

For the service limit state, *C* represents the resistance in a stress format, as shown in *MBE* Equation 6A.4.2.1-4. Rearranging Equation 3.14 in a stress format for an *LRFR* Service II rating

becomes:

$$RF = \frac{f_R - (\gamma_{DC})(f_{DC}) - (\gamma_{DW})(f_{DW})}{(\gamma_{LL})(f_{LL+IM})} \quad 3.16$$

where RF is the load rating factor, γ_{DC} , γ_{DW} and γ_{LL} definitions remain the same as above.

However, the values for load factors are for Service II in *MBE* Table 6.A.4.2.2-1. The terms in Equation 3.16 for dead load, live load, and resistance are shown below:

$$f_R = 0.95R_h F_{yf} \quad (f_l = 0) \quad 3.17$$

$$f_{DC} = \frac{(D_{gw} + D_{nc})}{S_{NC}} + \frac{(D_c)}{S_{LT}} \quad 3.18$$

$$f_{DW} = \frac{(D_w)}{S_{LT}} \quad 3.19$$

$$f_{LL+IM} = \frac{LL(1+IM)GDF_m}{S_{ST}} \quad 3.20$$

where:

RF = rating factor,

f_R = nominal flexure resistance (considered the composite section),

R_h = hybrid factor shown in LRFD BDS Article 6.10.1.10.1 (assumed to be 1),

F_{yf} = nominal flange yield stress,

f_{DC} = nominal stress due to dead loads from components,

f_{DW} = nominal stress due to wearing surfaces,

f_l = nominal flange lateral bending stress in LRFD BDS Article 6.10.1.6 (assumed to be zero),

f_{LL+IM} = nominal stress due to LL including impact,

γ_{DC} = dead load factor for dead load effects from components,

γ_{DW} = dead load factor for wearing surfaces,

γ_{LL} = live dead load factor,

D_{gw} = nominal girder dead load moment,

D_{nc} = nominal noncomposite dead load moment,

D_c = nominal composite dead load moment,

D_w = nominal wearing dead load moment,

LL = nominal HL-93 design loading,

IM = nominal impact factor; LRFD BDS Article 3.6.2,

GDF_m = nominal moment GDF,

S_{NC} = nominal noncomposite elastic section modulus,

S_{ST} = nominal short-term composite section modulus, and

S_{LT} = nominal long-term composite section modulus.

Service II design limits are checked using stresses. By setting $RF = 1.0$ and multiplying both sides of Equation 3.16 by S_{ST} , Barker and Puckett (2020) determined nominal optimal resistance for Service II using moments. According to Barker and Puckett (2020), the required nominal resistance to satisfy Service II is as follows:

$$R_{n_Service} = 0.95S_{ST}F_{yf} = \frac{S_{ST}}{S_{NC}}(D_{gw} + D_{nc}) + \frac{S_{ST}}{S_{LT}}(D_c + D_w) + LL(1 + IM)GDF_m \quad 3.21$$

where $R_{n_Service}$ is the minimum required nominal moment resistance (demand) for Service II.

Optimally designed girder sections achieved a maximum performance ratio equal to 1.0 considering both Service II and Strength I. When Service II governed the design, the nominal resistance was optimized for Service II (rating factor = 1.0 for Equation 3.16). In contrast, if Strength I governed the design, Service II had an oversized nominal resistance (rating factor > 1.0 for Equation 3.16).

3.5.3 Bridge Design Parameters and Assumptions

The *LRFD BDS* and *MBE* address Service II and Strength I limit states in both positive and negative moment regions. This study considered simple-span positive moments at midspan, two-span positive moments at 0.4L from the interior support, and two-span negative moments at the interior support for steel composite girder bridges. Two traffic lanes were assumed, and interior girders were sized (except for the bottom flange width for optimal design) according to guidance provided by the Nebraska Department of Transportation (NDOT) *Bridge Office Policies and Procedures (BOPP)* (2016), *Preferred Practices for Steel Bridge Design (PPSBD)* (2021), and *National Steel Bridge Alliance Continuous Span Standards (NSBACSS)* (2015).

This study used *LRFD BDS* Article 2.5.2.6.3. as a starting point for determining the web depth, which suggests that the minimum overall depth for I-beams is 0.033L for simple spans and 0.027L for continuous spans. Based on the dimensions of thirty-three homogeneous bridges from *NSBACSS* (2015), the web was approximately 0.035L. For consistency, the web depth was

conservatively assumed to be $0.035L$ for both simple- and two-span bridges. As a result of this assumption, there was no significant difference in reliability results, and this assumption was also reasonable because web depths were typically greater than the recommended minimum depth. The minimum flange thickness was assumed to be 0.75 in. to prevent thinner plates from cupping excessively when welded to the web. Flange thicknesses ranged from 1 to 3 in. in 0.25 in. increments. The minimum web thickness was assumed to be 0.5 in. to avoid excessive welding distortion (PPSBD, 2021).

The *BOPP* (2016) requires two design thicknesses for the web; this study used the unstiffened web design. The minimum flange width considered was 12 in. based on the *BOPP* (2016). Table 3.3 provides more information about the girder dimensions.

Table 3.3 Girder Size Design Guidance

Parameters	BOPP (2016)	PPSBD (2021)	NSBACSS (2015)
Web depth	Increments: 2 in.	Composite girder height: 0.033L to 0.04L	<i>In average: 0.035L</i>
Flange thickness	Minimum thickness: 0.75 in. Increments: 0.125 in.	<i>Minimum thickness: 0.75 in. Increments: 0.25 in. for thickness from 1 to 3 in.</i>	Minimum thickness: 0.75 in.
Web thickness	Two thickness designs needed (stiffened and <i>unstiffened web</i>)	<i>Minimum thickness: 0.5 in.</i>	Minimum thickness: 0.4375 in.
Flange width	Increments: 2 in. <i>Minimum width: 12 in.</i>	Minimum width: 15 in.	Minimum width: 16 in.

Note: For steel bridges, the red italicized text in the table was used to configure optimal designs.

Assumptions used for the girder designs are as follows:

- 3.5-ft overhang length,
- five girders,

- 10-ft girder spacings (results indicated insensitivity of β with 6-, 8-, 10-, and 12-ft spacing),
- homogenous plate girders ($F_y = 50$ ksi),
- steel modulus of 29000 ksi,
- composite 8-in deck thickness with sacrificial 0.5-in and 2-in. asphalt wearing surfaces,
- 2-in. deck haunch (from top of the girder to bottom of deck),
- miscellaneous and cross frames of 0.015 klf,
- 17-in. wide barrier, weight of 0.124 k/ft per girder, and
- A girder unit weight of 0.49 kcf.

Design resistance specifications used were:

- For simple- and two-span positive moment regions:
 1. *LRFD BDS* Article 6.10.2 proportion limits,
 2. *LRFD BDS* Article 6.10.4.2.2 Service II limit, and
 3. *LRFD BDS* Article 6.10.7 Strength I limit.
- For two-span negative moment region:
 1. *LRFD BDS* Article 6.10.2 proportion limits,
 2. *LRFD BDS* Article 6.10.4.2.2 Service II limit (also used web requirement based on Equation 6.10.4.2.2-4), and
 3. *LRFD BDS* Article 6.10.8 Strength I limit.

Design assumptions included:

- ignoring participation of mild reinforcing steel in girder cross-sectional resistance,

- having the total area of the longitudinal reinforcement provided in negative bending regions being no less than 1% of the total cross-sectional area of the concrete deck based on *LRFD BDS* Article 6.10.1.7,
- setting the lateral bending stress $f_l = 0$,
- using unshored construction for compact composite sections in positive moment regions to avoid checking longitudinal compressive stress caused by Service II loads in the concrete deck based on *LRFD BDS* Article 6.10.4.2.2,
- setting the hybrid factor $R_h = 1$,
- ensuring the nominal moment resistance for the case of two-span positive moment regions satisfied *LRFD BDS* Equation 6.10.7.1.2-3,
- setting the unbraced length (L_b) to 25 ft, and the moment gradient modifier (C_b) to 1.0 to estimate lateral torsional buckling resistance in *LRFD BDS* Article 6.10.8.2.3,
- assuming the deck was not effective for the negative moment region at Service II, and
- assuming there was no inelastic moment redistribution.

For Strength I, the deck is typically ineffective in the negative moment region. The deck may be considered effective for Service II if it meets requirements outlined in *LRFD BDS* Article 6.10.4.2.1. A reliability analysis was performed to evaluate deck effectiveness for two-span bridge negative moment regions at Service II. The optimal design performance ratios described in Chapter 4 indicated that Strength I, not Service II, governed negative moment designs. Therefore, this study focused on positive moment regions for Service II. The concrete deck was assumed ineffective for negative moment regions for Service II. Yield moment (M_y) corresponded to first yield in the bottom (tension) flange for positive moment regions. Yield

moment at negative moment regions was determined as the lesser moment that first caused yield in the bottom flange, the top flange, or the steel reinforcement, in accordance with *LRFD BDS* D6.2.3.

Optimally designed girder section component dimensions and section moduli ratios that satisfy Service II and Strength I designs for simple- and two-span bridges are given in Table 3.4 through Table 3.6. For negative moment regions assuming a cracked deck, S_{ST} and S_{LT} were the same for Service II and Strength I.

Table 3.4 Optimal Design Girder Sections for Simple-span Positive Moment at the Midspan

Span (ft)	D (in)	t_w (in)	b_{tf} (in)	t_{tf} (in)	b_{bf} (in)	t_{bf} (in)	S_{ST}/S_{NC}	S_{ST}/S_{LT}
60	26	0.500	12	0.750	13.02	1.000	1.603	1.084
90	38	0.500	12	0.750	15.77	1.250	1.494	1.077
120	51	0.500	13	0.750	20.09	1.250	1.436	1.080
150	64	0.500	16	1.000	19.87	1.500	1.336	1.081
200	85	0.625	22	1.250	24.60	1.500	1.265	1.088

Table 3.5 Optimal Design Girder Sections for Two-span Positive Moment at the 0.4L of End Spans

Span (ft)	D (in)	t_w (in)	b_{tf} (in)	t_{tf} (in)	b_{bf} (in)	t_{bf} (in)	S_{ST}/S_{NC}	S_{ST}/S_{LT}
60	26	0.500	9	0.750	9.49	0.750	1.741	1.092
90	38	0.500	12	0.750	13.99	0.750	1.536	1.084
120	51	0.500	12	0.750	13.16	1.000	1.491	1.086
150	64	0.500	13	0.750	15.60	1.000	1.454	1.090
200	85	0.625	17	1.000	17.09	1.000	1.380	1.107

Note: The minimum flange width for the 60-ft two-span bridge positive moment region was initially 12 in. but the girder was overdesigned. Therefore, the minimum flange width was reduced to 9 in.

Table 3.6 Optimal Design Girder Sections for Two-span Negative Moment at the Interior Support

Span (ft)	D (in)	t_w (in)	b_{tf} (in)	t_{tf} (in)	b_{bf} (in)	t_{bf} (in)	S_{ST}/S_{NC}	S_{ST}/S_{LT}
60	26	0.500	12	1.500	12.81	2.000	1.625	1.000
90	38	0.500	16	1.500	17.07	2.000	1.541	1.000
120	51	0.500	19	1.500	19.58	2.000	1.400	1.000
150	64	0.500	21	1.500	21.96	2.000	1.329	1.000
200	85	0.625	22	2.000	22.47	2.500	1.213	1.000

3.5.4 Nominal Dead and Live Loads

The four dead load components (D_{gw} , D_{nc} , D_c , and D_w) were determined using section properties and other previously noted assumptions. All concrete was assumed to be normal weight (i.e., 150 pcf).

The HL-93 load model from the LRFD BDS was the nominal design LL. A constant IM = 0.33 was applied to live loads in accordance with the *LRFD BDS*. The interior girder GDF_m for multiple lanes in Equation 3.20 was determined using *LRFD BDS* Table 4.6.2.2.2b-1.

Longitudinal stiffness (K_g) was calculated based on girder cross-sectional geometry when determining GDF_m .

3.5.5 Statistical Parameters

Statistical parameters were implemented in reliability analyses as shown in Figure 3.6. Statistical parameters and their sources for dead loads (D_{gw} , D_{nc} , D_c , and D_w), live loads (LL_{HL-93} and $LL_{Platoon}$), and resistance (R) are summarized in Table 3.7. Statistical parameters for dead loads and resistance were adopted from Kulicki et al. (2007). The bias and CoV for two-lane HL-93 design loads were also obtained from Kulicki et al. (2007). It was assumed that platoon bias was 1.0, and that the range of CoV was 0 to 0.20, as presented in Steelman et al. (2021), to

calibrate the *LL* factors. The probabilistic mean for the dynamic amplification due to impact was taken as 10% (Kulicki et al., 2007).

Table 3.7 Statistical Parameters for Variables

Variables	Distribution	Bias	CoV	References
D_{gw}	Normal	1.03	0.08	Kulicki et al. (2007)
D_{nc}	Normal	1.05	0.10	Kulicki et al. (2007)
D_c	Normal	1.05	0.10	Kulicki et al. (2007)
D_w	Normal	1.00	0.25	Kulicki et al. (2007)
LL_{HL-93}	Normal	1.18	0.18	Kulicki et al. (2007)
$LL_{Platoon}$	Normal	1.00	0-0.20	Steelman et al. (2021)
R	Lognormal	1.12	0.10	Kulicki et al. (2007)

3.5.6 Limit State Function for Service II

As shown in Figure 3.6, reliability analyses were performed using previously defined nominal values and statistical parameters. In this study, the limit state function for determining target implicit reliability for Service II was adopted from Barker and Puckett (2020) for simple- and two-span bridges designed based on *LRFD BDS*.

$$g = R - Q = 0.95S_{ST}F_{yf} - \frac{S_{ST}}{S_{NC}}(D_{gw} + D_{nc}) - \frac{S_{ST}}{S_{LT}}(D_c + D_w) - LL_{HL-93}(1 + IM)GDF_m \quad 3.22$$

where S_{ST}/S_{LT} was 1.0 for the two-span negative moment cases. Limit state functions for evaluating platoon load scenarios varied and are described in Section 3.6.

3.6 Monte Carlo Simulation

MATLAB was used to perform MCS to calculate reliability indices, β , for parametric combinations of bridge and platoon configurations and scenarios outlined in Sections 3.2 and 3.3. The general procedure was to randomly generate dead load effects, live load effects, and resistances N times, where N is a sufficiently large number to verify a target probability of failure, then to evaluate the limit-state function as shown in Figure 3.7. The outcome was recorded as a failure if the limit state evaluation result was negative. Failure probability, P_f , was determined as the ratio of the total number of failure instances, F , to the total number of simulations, N .

The total CoV of the platoon was parameterized from 0 to 0.2, with platoon truck headways primarily between 5 and 50 ft. The platoon load effect mean was systematically adjusted by an amplification factor, α , to scale the platoon load effect to a maximum permissible limit conforming to targeted reliabilities, β . Bridges were initially evaluated using legal loads scaled by $\alpha = 0.6$, and then α was increased incrementally until the target β was reached.

The selection of the target β is a key point when calibrating LL factors. For Strength I, bridges are generally evaluated at the inventory or operating levels, with corresponding β targets of 3.5 and 2.5, respectively. In the *LRFD BDS* and *MBE*, such reliability indices for Service II and Service III have not yet been established, hindering platoon optimal use. This study proposes target implicit reliability ($\beta_{Implicit}$) indices for Service II and Service III platoons based on bridge designs developed using historical practice. Equation 3.11 was used for Service III, and Equation 3.22 was used for Service II to determine target implicit reliability. After determining implicit reliability indices for service, LL factors were calibrated, and acceptable headway tables were

developed. A flow chart of the MCS procedure is shown in Figure 3.7. Descriptions of MCS procedures used to evaluate each of the three platoon loading cases are provided below.

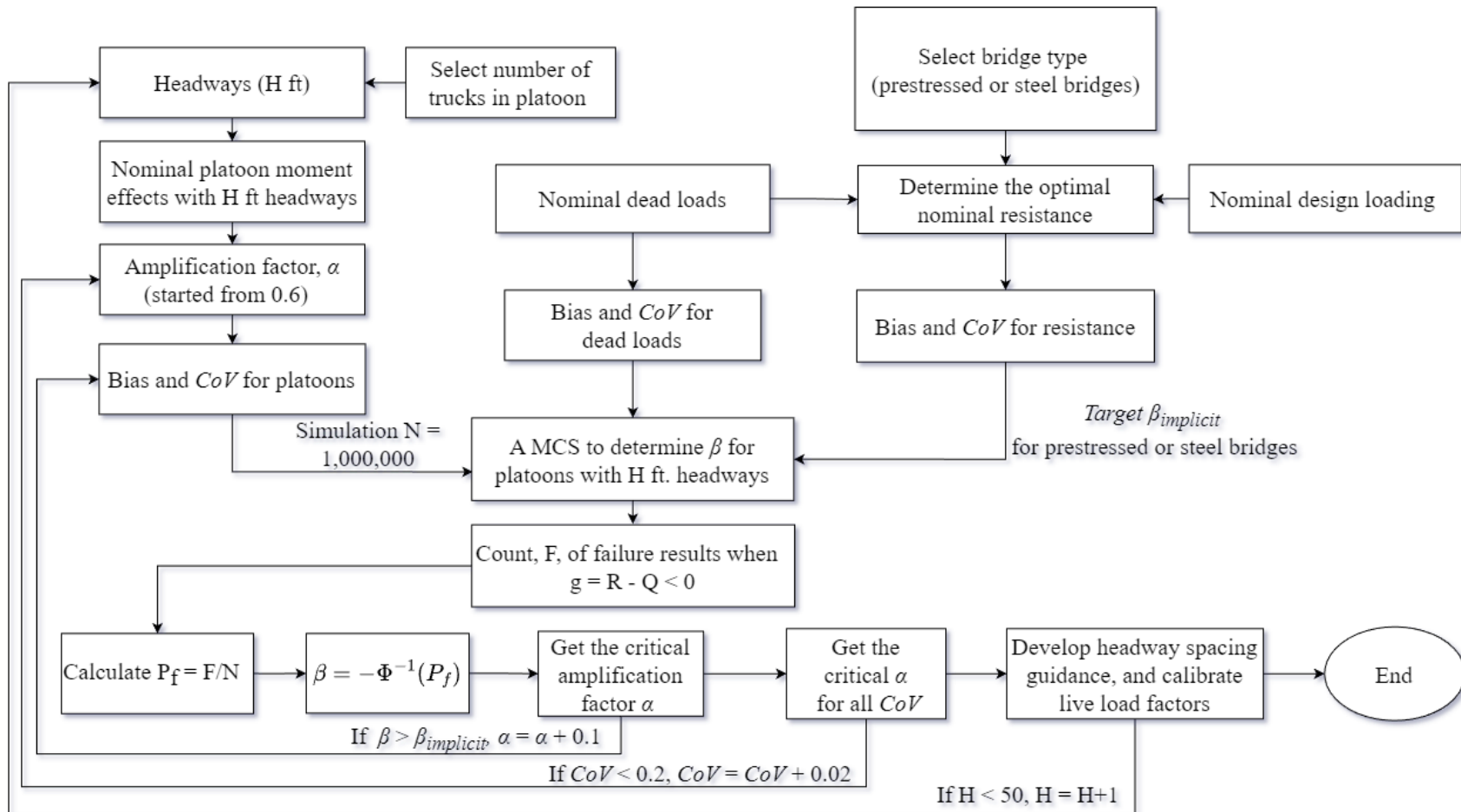


Figure 3.7 Monte Carlo Simulation Flowchart

A flowchart of the MCS procedure is illustrated in Figure 3.7. There are three primary use cases:

- Case I: single lane of platoon loading,
- Case II: two identical platoons operating in adjacent lanes, and
- Case III: one lane of platoon loading operating adjacent to routine traffic.

The procedure for evaluating Service II and Service III is outlined below:

1. Specify bridge characteristics:
 - a) span length,
 - b) simply supported or two-span continuous, and
 - c) steel or prestressed concrete girders.
2. Obtain nominal dead load (top center of the flowchart in Figure 3.7).
3. Determine the nominal design loading (upper right-hand corner of the flowchart).
4. Determine nominal resistance from Equation 3.2 for prestressed concrete girders (Service III) and Equation 3.21 for steel bridges (Service II).
5. Specify platoon configuration (upper left-hand corner of the flowchart):
 - a) truck type, and
 - b) number of trucks in the platoon.
6. Specify headway, H :
 - a) If initializing, set $H = 5$ ft.
 - b) Otherwise, increase H by 1 ft to a maximum of $H = 50$ ft.
7. Determine nominal platoon effects, L_{PL} , for specific bridge and platoon configuration under consideration:

- a) If scenario under consideration is Case I or Case III, use $g = GDF_s / 1.2$, where GDF_s is single lane *LRFD BDS* GDF with an embedded MPF.
 - b) If scenario under consideration is Case II, use $g = GDF_m$, where GDF_m is multi-lane *LRFD BDS* GDF.
8. Determine nominal adjacent lane routine truck effects, L_{adj} , for the specific bridge and platoon configuration under consideration:
- a) If scenario under consideration is Case I or Case II, $L_{adj} = 0$.
 - b) If scenario under consideration is Case III,

$$L_{adj} = \left(\frac{\lambda_{max}}{1.33} \right) * \left(g = \left(GDF_m - \frac{GDF_s}{1.2} \right) \right) * L_n \quad 3.23$$

where L_n is HL-93 design loading, with dynamic amplification, and λ_{max} is the normalized mean of adjacent load (bias) from Tables 17-20 in Steelman et al. (2021). λ_{max} is scaled by 1/1.33 to remove the *LRFD BDS* dynamic amplification that had been applied to WIM data in Barker and Puckett (2016).

9. Amplify nominal static live loads, L_{PL} and L_{adj} , by $(1 + \mu_{IM}) = 1.1$.
10. Set platoon load effect bias and CoV :
- a) If initializing, set platoon load effect $CoV =$ zero.
 - b) Otherwise, increase CoV by 0.02.
11. Specify platoon load effect amplification factor, α :
- a) If initializing, set $\alpha = 0.6$.
 - b) Otherwise, increase α by 0.1.
12. Convert nominal values of platoon load effects to their means and standard deviations.
13. For Case III, dynamic adjacent lane load effect (product of Steps 8 and 9) is a mean value,

L_{adj} . Calculate standard deviation of adjacent lane load effect, where CoV_{adj} corresponds to total CoV in Tables 17-20 in Steelman et al. (2021).

14. Convert component dead load, wearing dead load, and resistance nominal values to means and standard deviations using biases and CoVs provided in Table 3.2 for prestressed concrete girders (Service III) and Table 3.7 for steel bridges (Service II).
15. Generate $N = 1,000,000$ uniformly distributed random values, u , between 0 and 1 for each parameter in all cases. Generate values for L_{adj} if considering Case III.
16. a) If considering Case III, for all cases except negative moments for 90 to 200 ft two-span bridges, calculate corresponding value of L_{adj1} (i.e., extreme Type I random variable).
b) Otherwise, if considering Case III for negative moments for 90 to 200 ft two-span bridges, simulate two adjacent independent loads and calculate corresponding values of L_{adj1} and L_{adj2} (an Extreme Type I random variable).
17. For prestressed concrete girder bridges (Service III), calculate limit state functions for load cases as follows.

a) Case I:

$$g = \left(f_t + \frac{P_{eval}}{A_g} + \frac{P_{eval}e_{nc}}{S_{ncb}} \right) - \left(\frac{(D_{gw} + D_{nc})}{S_{ncb}} + \frac{(D_c + D_w)}{S_{cb}} + \frac{L_{PL}(1+IM)GDF_s}{S_{cb}} \right) \quad 3.24$$

b) Case II:

$$g = \left(f_t + \frac{P_{eval}}{A_g} + \frac{P_{eval}e_{nc}}{S_{ncb}} \right) - \left(\frac{(D_{gw} + D_{nc})}{S_{ncb}} + \frac{(D_c + D_w)}{S_{cb}} + \frac{L_{PL}(1+IM)GDF_m}{S_{cb}} \right) \quad 3.25$$

c) Case III:

$$g = \left(f_t + \frac{P_{eval}}{A_g} + \frac{P_{eval}e_{nc}}{S_{ncb}} \right) - \left(\frac{(D_{gw} + D_{nc})}{S_{ncb}} + \frac{(D_c + D_w)}{S_{cb}} + \frac{L_{PL}(1+IM)GDF_s}{S_{cb}} + \frac{L_{adj}}{S_{cb}} \right) \quad 3.26$$

18. For steel girder bridges (Service II), calculate limit state functions for load cases as follows.

a) Case I:

$$g = 0.95S_{ST}F_{yf} - \frac{S_{ST}}{S_{NC}}(D_{gw} + D_{nc}) - \frac{S_{ST}}{S_{LT}}(D_c + D_w) - L_{PL}(1+IM)GDF_s \quad 3.27$$

b) Case II:

$$g = 0.95S_{ST}F_{yf} - \frac{S_{ST}}{S_{NC}}(D_{gw} + D_{nc}) - \frac{S_{ST}}{S_{LT}}(D_c + D_w) - L_{PL}(1+IM)GDF_m \quad 3.28$$

c) Case III:

- I. for all cases except for negative moments for 90 to 200 ft two-span bridges, calculate corresponding value of L_{adj} (extreme Type I random variable)

$$g = 0.95S_{ST}F_{yf} - \frac{S_{ST}}{S_{NC}}(D_{gw} + D_{nc}) - \frac{S_{ST}}{S_{LT}}(D_c + D_w) - L_{PL}(1+IM)GDF_m - L_{adj} \quad 3.29$$

- II. for negative moments for 90 to 200 ft two-span bridges, simulate two independent adjacent loads and calculate corresponding values of L_{adj1} and L_{adj2} (extreme Type I random variable)

$$g = 0.95S_{ST}F_{yf} - \frac{S_{ST}}{S_{NC}}(D_{gw} + D_{nc}) - \frac{S_{ST}}{S_{LT}}(D_c + D_w) - L_{PL}(1+IM)GDF_m - L_{adj1} - L_{adj2} \quad 3.30$$

19. Count the number of failure cases, F , for which $g_i < 0$.

20. Calculate probability of failure, $P_f = F / N$.

21. Determine reliability index β according to $\beta = -\Phi^{-1}(P_f)$.

22. Compare calculated and target $\beta_{Implicit}$. If calculated $\beta >$ target $\beta_{Implicit}$, return to Step 11.

Otherwise, store the critical value of α and proceed to the next step.

23. If the platoon load effect CoV is less than 0.2, return to Step 10. Otherwise, proceed to the next step.
24. If platoon headway is less than 50 ft, return to Step 6. Otherwise, parametric sweep is complete.
25. Calibrate LL factors and acceptable headway spacing tables.
26. All analyses are complete if no additional truck or bridge configuration variations are required.

3.7 Summary

The effects of platooning have not been evaluated within a probabilistic, reliability-based paradigm for service. Additionally, implications from developing the target implicit reliability $\beta_{Implicit}$, where $\beta_{Implicit}$ refers to designs produced from historical practice, for platooning operations and policies for service have not been fully investigated. This chapter presents information on bridges, trucks, and platoon loading cases considered for MCS used in this study to develop the framework of reliability-based evaluation for service. A general reliability analysis is presented that determines target implicit reliability $\beta_{Implicit}$ for Service II and Service III. After $\beta_{Implicit}$ is determined, load factors can be calibrated, and acceptable headway tables can be developed. In subsequent chapters, descriptions of how LL factors were calibrated, acceptable headways developed, and CoV characterized for platoons are provided. The method for investigating the cracking probability of prestressed concrete bridges was presented in Section 3.4, and the cracking probability results are discussed in Chapter 9.

Chapter 4 Optimal Design and Target Reliability Results

4.1 Overview

This chapter presents optimal design results for steel and prestressed concrete bridges developed from procedures provided in Chapter 3. Target implicit reliability indices for Service III and Service II, which were used to evaluate bridges for platoon loading, are also determined and presented. Finally, evaluations of the effects of parameter uncertainties on reliability indices for Service III and Service II are completed.

4.2 Nominal Live Load Positive Moments

Nominal positive *LL* moments are compared for platoon and HL-93 loadings for simple- and two-span bridges as a function of their span lengths and headways. Nominal positive *LL* moments were determined for a four-truck platoon with adjacent, routine traffic and for two lanes under HL-93 loading. These two loading scenarios and selected headways are shown in Figure 4.1. The platoon model was based on the notional rating load (NRL) as shown in Figure 4.1. The NRL was found to govern positive moment regions as in Steelman et al. (2021). Platoon headways ranged from 10 to 50 ft at increments of 10 ft and span lengths from 60 to 150 ft. According to *LRFD BDS* requirements, HL-93 was considered for one- and two-lane loading. As presented by Yang et al. (2021) and Steelman et al. (2021), the platoon was accompanied by 5,000 ADTT adjacent routine traffic. Adjacent routine traffic was characterized using interstate I-80 WIM data, and more details can be found in Steelman et al. (2021). Multiple presence probabilities for platoons loaded with adjacent routine traffic were adopted from Ghosn et al (2011). *IM* was assumed to be 0.10 for all load cases, the same as its probabilistic mean. For platoons operating alongside routine traffic in the adjacent lane, the GDF was calculated

according to *LRFD BDS* Equation (4.6.2.2.5-1), with additional details found in Yang et al. (2021) and Steelman et al. (2021).

As documented elsewhere in the literature, primary bridges of concern are those with longer span lengths subjected to closely spaced platoons. To help identify controlling load cases, two 3D surfaces were generated for *LL* moments (Figure 4.2a and Figure 4.2b). Figure 4.2 indicates that nominal HL-93 loading often enveloped platoon cases (i.e., produced higher moments), except where platoons operate at small headways of 10 to 20 ft.

Live load moments generated from a platoon at a 10-ft headway with adjacent routine traffic on 150-ft simple-span and two-span bridges were about 21% greater than moments induced by two lanes of HL-93 loading (Figure 4.2a and Figure 4.2b). Published reliability analyses, however, indicated that four-truck platoons with lower uncertainties than typically associated with vehicular *LL* can operate on such bridges and still reach target permit reliability indices for strength (Yang et al., 2021; Steelman et al., 2021). While these results indicate that four-truck platoons can safely traverse bridges for strength based on reliability analyses, the current *LRFD BDS* and *MBE* load factors for Service III and Service II are not reliability-based.

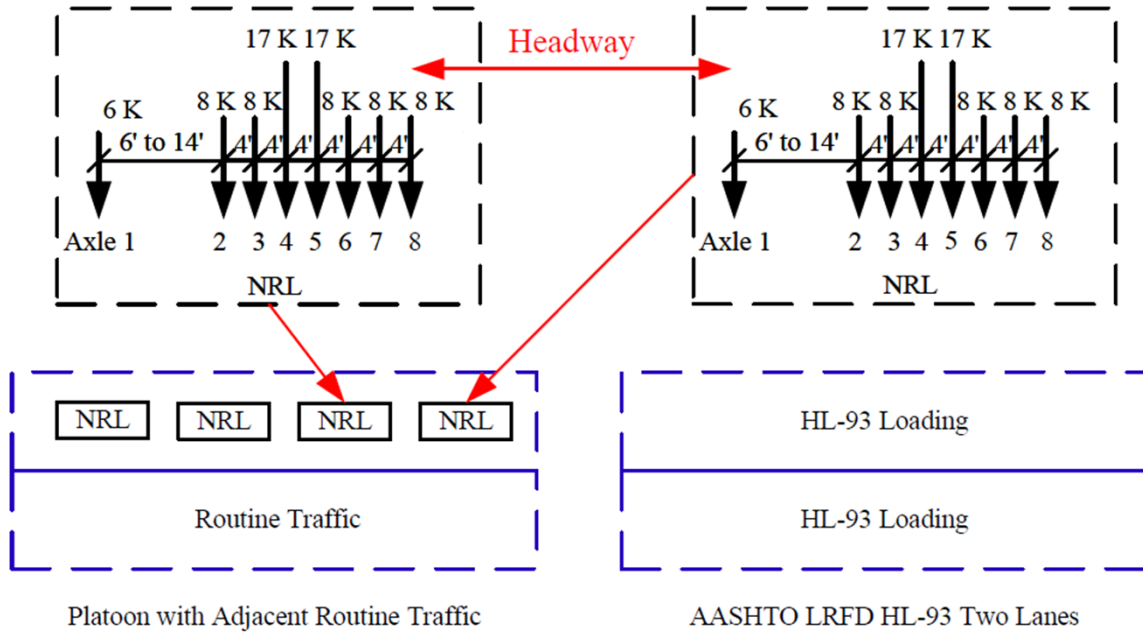
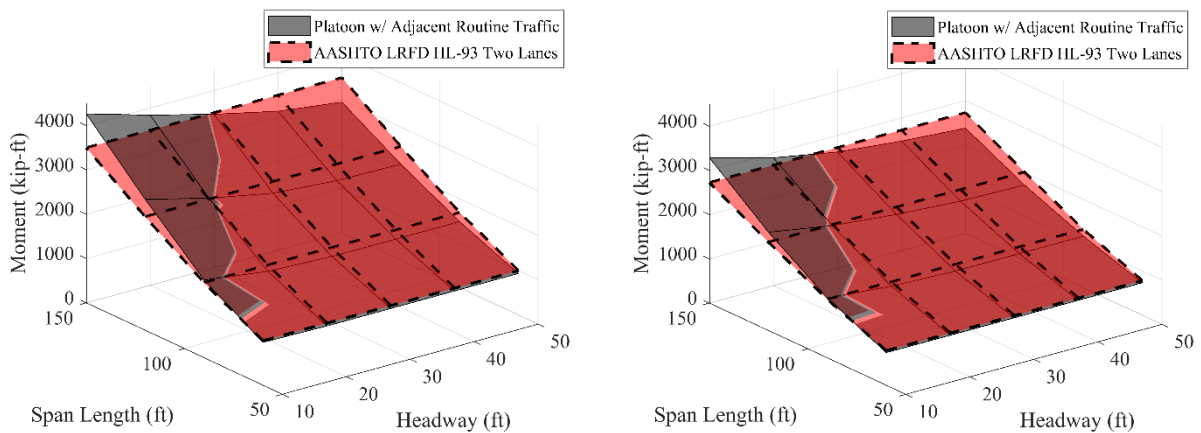


Figure 4.1 Loading Scenarios for Comparison of Nominal LL Moments



(a) Simple-span bridges at midspan

(b) Two-span bridges at 0.4L of end spans

Figure 4.2 LL Moments for Platoons and HL-93 Loadings on Prestressed Girder Bridges

4.3 Service III Optimal Design and Target Reliability Results

For prestressed concrete bridges designed for Service III, this section provides optimal design tensile stresses, prestress losses, elastic gains, effective prestress forces, and resistances due to dead and live loads. Target implicit reliability indices for different bridge design scenarios from Table 3.1 are presented below. This section also discusses uncertainties associated with parameters in the Service III limit state function in Equation 3.11.

The optimal number of strands for each prestress loss method increased with span and decreased as the design tensile stress increased from $\kappa = 0$ to 0.24. *Post-1.0-Gains* predicted the lowest prestress losses, and *Pre-1.0-No-gains* gave the highest prestress losses. The approximate and post-2005 loss methods predicted similar prestress losses for cases using the same design *LL* factor and the same consideration of elastic gains. $\beta_{Implicit}$ results were slightly lower for simple-span bridges than for two-span bridges. Therefore, only simple-span bridge results are presented in this section. Several design cases are excluded from the results for 150-ft bridges because those designs required more than the maximum allowable number of prestressing strands (60 strands). For simplicity, the allowable tensile stress limit with a κ coefficient is represented as $f_t(\kappa)$ (e.g., $0.19\sqrt{f'_c} = f_t(\kappa = 0.19)$). “DET” indicates the use of a deterministic value for the allowable tension stress limit f_t while “VAR” indicates the use of a probabilistically varying value for the modulus of rupture f_r .

4.3.1 Service III Optimal Design Results

In this section, $f_t(\kappa = 0.0948)$ was used to show intermediate calculation results for design and evaluation for Service III, with those results being synthesized through reliability analyses to obtain reliability indices in succeeding sections. Figure 4.3a shows tensile stresses caused by

factored dead and live loads for design and evaluation. Factored f_D values were the same for both design and evaluation. f_{LL+IM} results for evaluation were all based on HL-93 loading with $\gamma_L = 1.0$, while f_{LL+IM} values for design varied. For bridges designed using the $\gamma_L = 0.8$ or pre-2005 loss method, f_{LL+IM} values for design were lower than those designed with Post-1.0-Gains.

Figure 4.3b presents optimal A_{ps} for ft ($\kappa = 0.0948$). For 60-ft bridges, the A_{ps} value was similar for the different loss methods, but A_{ps} varied more across design cases when span lengths increased. A_{ps} values for the *Approx-0.8-Gains* and *Post-0.8-Gains* methods were generally close to each other and smaller than for *Post-1.0-Gains*. Without considering elastic gains, A_{ps} values for 150-ft span bridges designed with approximate and post-2005 loss methods ($\gamma_L = 0.8$) were slightly larger than for *Post-1.0-Gains*. Generally, *Pre-1.0-No-gains* produced larger A_{ps} values than other methods.

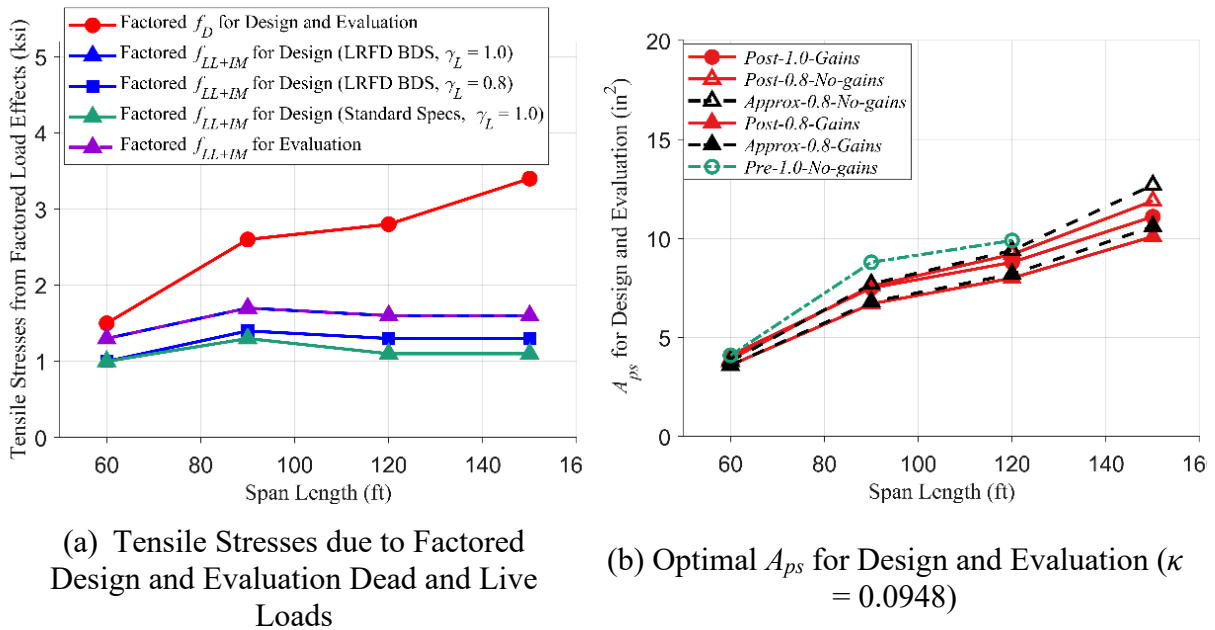


Figure 4.3 Tensile Stresses Due to Factored Dead and Live Loads, and Optimal A_{ps} for f_t ($\kappa = 0.0948$) for Various Design Scenarios

Figure 4.4 presents prestress losses and elastic gains for design and evaluation. *Post-0.8-Gains* generally predicted the lowest Δf_s , and *Pre-1.0-No-gains* the highest Δf_s for design as shown in Figure 4.4a. Δf_s values for *Approx-0.8-Gains* and *Post-0.8-Gains* were generally similar, although the approximate loss method exhibited greater sensitivity to span length. Δf_s generally increased with span length, with changes in girder section size potentially being responsible for slightly reduced Δf_s for the 120-ft bridges. When predicting Δf_s for the studied spans, methods using elastic gains were more consistent than those that excluded them. Because the *Post-1.0-Gains* method was used for evaluation, $\Delta f_{s_{eval}}$ and Δf_s were the same for bridges designed with the *Post-1.0-Gains* method, and $\Delta f_{s_{eval}}$ for evaluation significantly reduced from Δf_s in designs for loss methods without elastic gains (Figure 4.4a and Figure 4.4b). Slight differences between Δf_s and $\Delta f_{s_{eval}}$ for the *Post-0.8-Gains* method were due to slightly different

design configurations resulting from use of different elastic gains for design.

As shown in Figure 4.4c, *Post-1.0-Gains* produced larger elastic gains than the other methods while the trends for the *Post-0.8-Gains* and *Approx-0.8-Gains* methods were similar but lower due to lower γ_L . Elastic gains for evaluation were practically the same for different designs (Figure 4.4d) and contributed to differences between Δf_S and Δf_{Seval} in Figure 4.4a and Figure 4.4b.

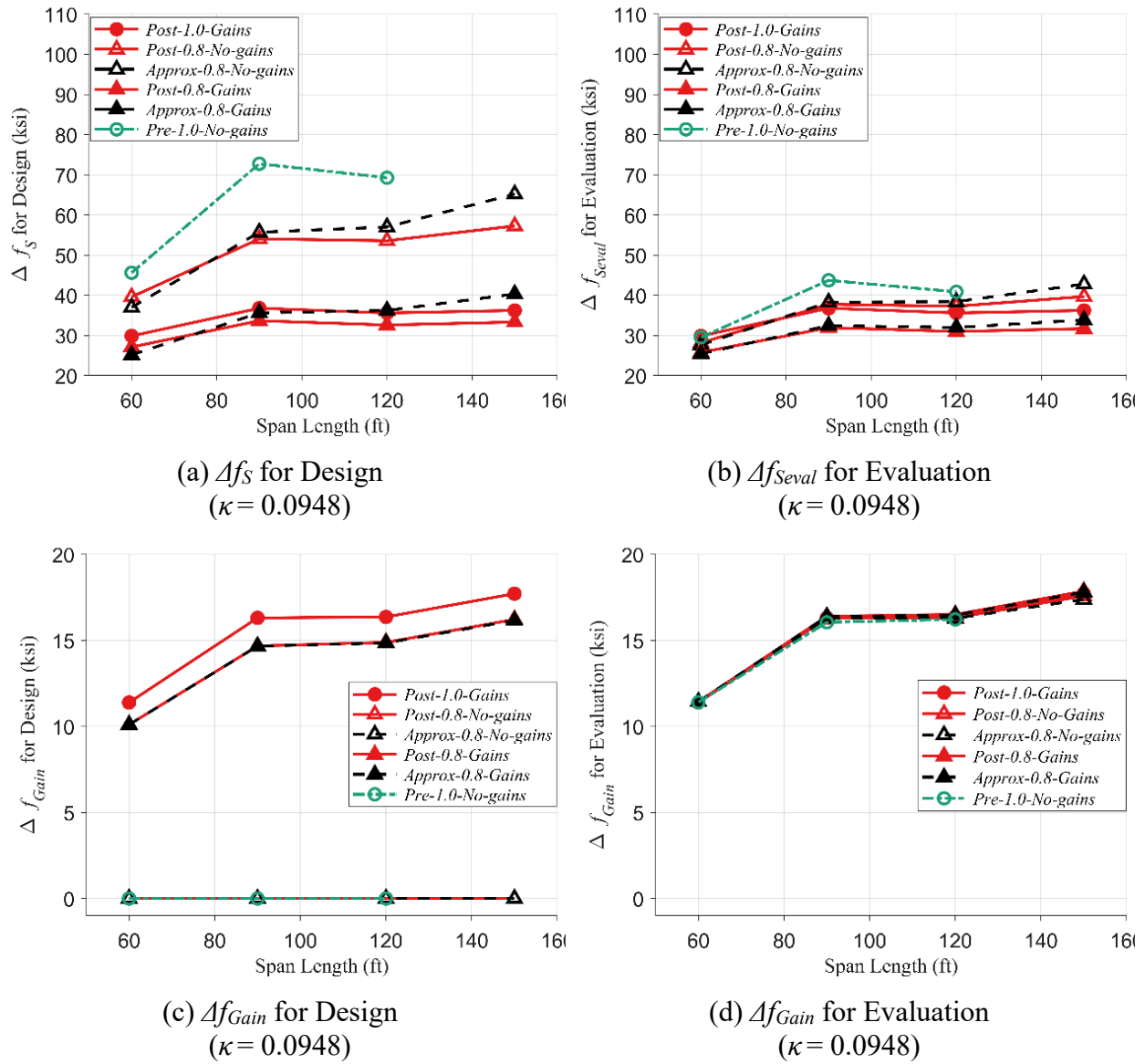


Figure 4.4 Prestress Loss and Elastic Gains for Design and Evaluation at f_i ($\kappa = 0.0948$)

Based on A_{ps} , f_{pi} , Δf_S , and $\Delta f_{S_{eval}}$, effective prestress loss for design and evaluation can be determined using Equations 3.3 and 3.12

$$P_{eval} = A_{ps} (f_{pi} - \Delta f_{S_{eval}}) = A_{ps} (f_{pi} - (\Delta f_{pES} + \Delta f_{pLT} - \Delta f_{GainDL} - \Delta f_{GainLL})) \quad 3.12$$

, with flexural resistances for design and evaluation taken from Equations 3.2 and 3.13. Figure 4.5 presents effective prestress force and flexure resistance for design and evaluation. Figure 4.5a shows that the *Post-1.0-Gains* method had the largest P_e for design. P_e for bridges for all other design scenarios was similar.

As expected, P_{eval} tracks with A_{ps} and was identical for P_e and P_{eval} for the *Post-1.0-Gains* method, and was comparatively largest for bridges designed using *Pre-1.0-No-gains* when that method could be proportioned according to study parameters (Figure 4.5b). P_{eval} values were similar for bridges designed using loss methods including gains and $\gamma_L = 0.8$, and were smaller than those using *Post-1.0-Gains* as shown in Figure 4.5b due to lower A_{ps} provided from the design. Similarly, bridges designed with loss methods neglecting elastic gains and using $\gamma_L = 0.8$ generally produced larger P_{eval} values than *Post-1.0-Gains*. Figure 4.5c and Figure 4.5d present flexural resistances for design and evaluation, respectively. Note that *Post-0.8-No-gains*, *Post-0.8-Gains*, *Approx-0.8-No-gains*, and *Approx-0.8-Gains* methods overlap in Figure 4.5c, exhibiting similar trends for effective prestress force and flexure resistance for design and evaluation. As illustrated in Figure 4.5d and Figure 4.3b, methods requiring a larger A_{ps} led to a larger f_{Reval} . Various influences from the selected loss method, LL factors, and use or neglect of elastic gains produced bridges with differing f_{Reval} values relative to the baseline *Post-1.0-Gains* case, all of which exhibited span length sensitivity. Therefore, marginal differences in reliabilities for other methods relative to *Post-1.0-Gains* vary with span because of the difference of f_{Reval} .

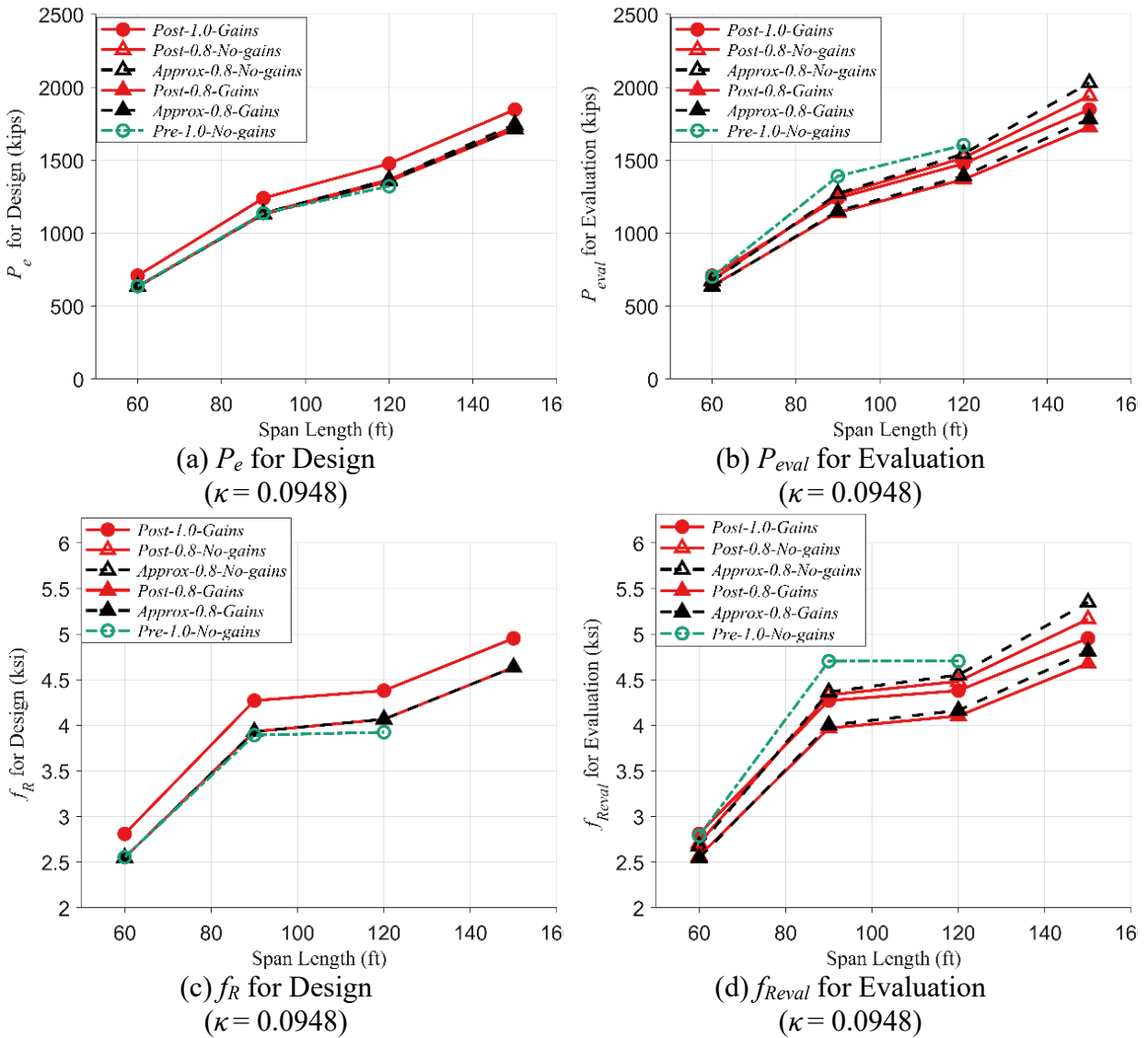


Figure 4.5 Effective Prestress Force and Resistance for Design and Evaluation at f_i ($\kappa = 0.0948$)

4.3.2 Service III Target Reliability Results

MCS was implemented to determine dead load, live load, and resistance according to distributions based on nominal values and statistical parameters described in Sections 3.4.5 through 3.4.7. Figure 4.6a presents resistance, load, and limit state function PDFs for Service III at f_i ($\kappa_{eva} = 0.0948$) for a 120-ft simple-span bridge designed using the *Post-1.0-Gains* method.

The mean resistance was close to the nominal resistance during evaluation from Figure 4.5d, and mean load was greater than mean resistance. The implicit reliability, representing the number of standard deviations between the mean for g and the failure threshold, was -0.61 . A negative value indicated the probability of exceeding the Service III limit state was more than 50%.

Figure 4.6b further examines the PDF for g by depicting the probability that Service III ($f_t (\kappa_{eva} = 0.0948)$) would be exceeded during a bridge's service life. As shown in Figure 4.6b, about 72 out of 100 (72%) 120-ft simple-span bridges with $f_t (\kappa_{eva} = 0.0948)$ were expected to exceed the Service III limit state during their life, despite being optimally proportioned to satisfy Service III design criteria.

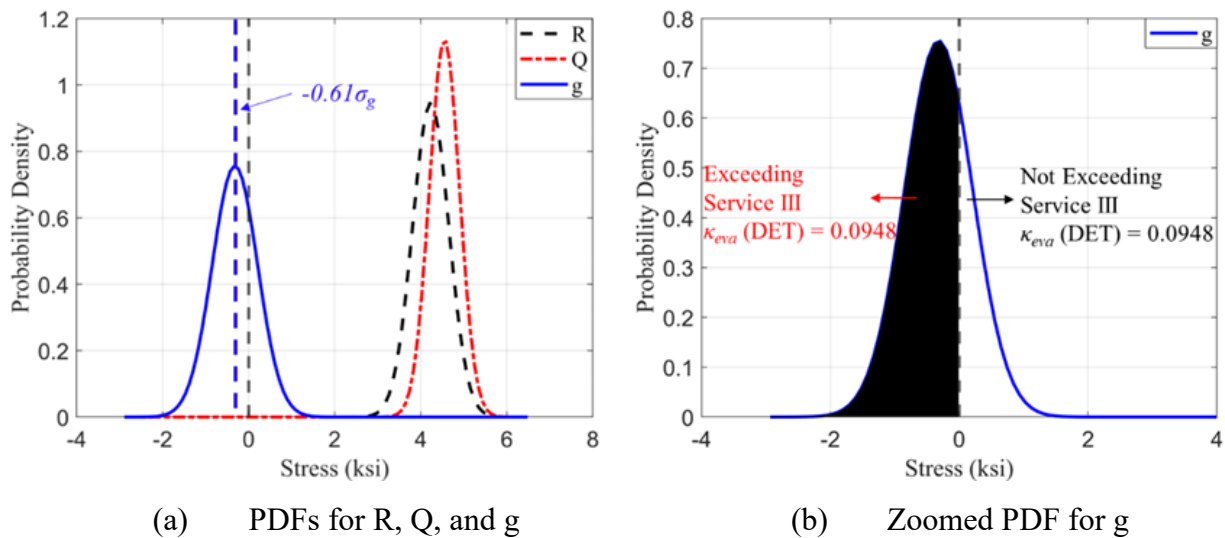


Figure 4.6 Probability Density Functions for Evaluating Service III at $f_t (\kappa = 0.0948)$ for 120-ft Simple-Span Bridges Designed by using *Post-1.0-Gains*

P_{eval} and f_{Reval} values were generally close for *Post-1.0-Gains*, *Post-0.8-No-gains*, and *Approx-0.8-No-gains* for spans between 60 and 120 ft (Figure 4.5b and Figure 4.5d). These three

methods therefore are expected to result in similar $\beta_{Implicit}$. Higher nominal f_{Reval} values lead to higher reliability indices, though f_t and P_{eval} uncertainties also contribute to reliability indices. $\beta_{Implicit}$ and corresponding probabilities of exceeding tension limits for these three loss methods are plotted in Figure 4.7 to Figure 4.9, with key observations presented alongside the figures.

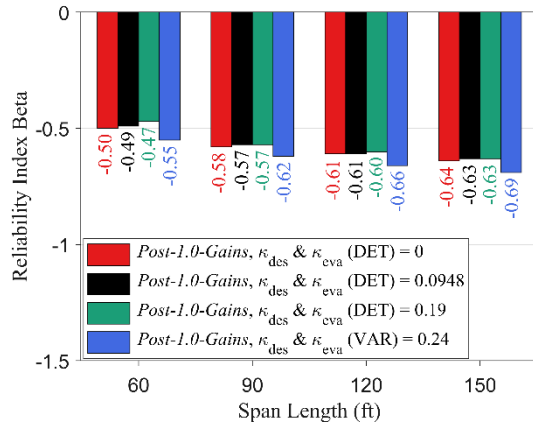
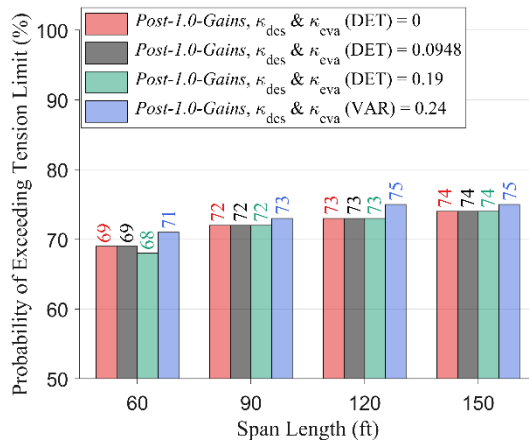
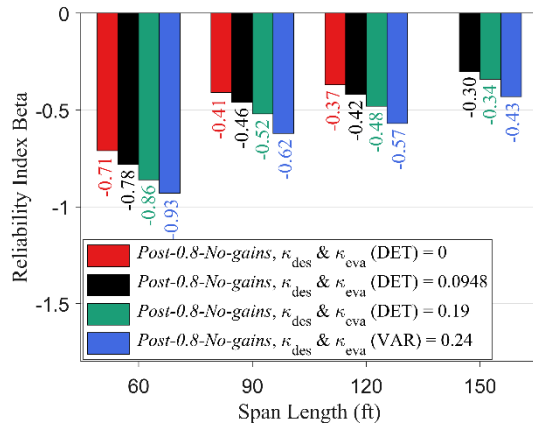
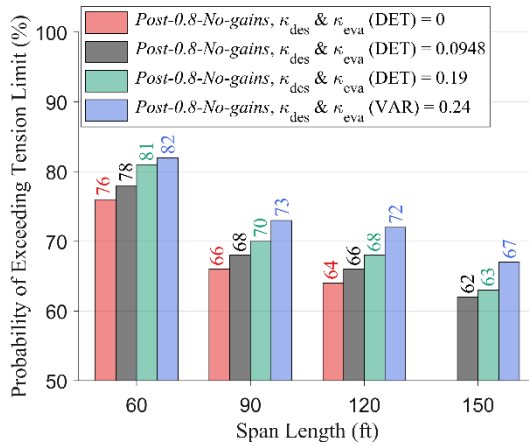
(a) β for *Post-1.0-Gains*(b) Probability of Exceeding Tension Stress Limits for *Post-1.0-Gains*

Figure 4.7 Reliability Index β and Corresponding Probabilities of Exceeding Tension Limits for Simple-span Bridges Designed using *Post-1.0-Gains* Method, Similar Design and Evaluation $f_i(\kappa)$

- Colors denote f_i . $\beta_{implicit}$ was consistently about -0.60 for bridges designed using *Post-1.0-Gains*, was not prominently sensitive to $f_i(\kappa)$, and was slightly sensitive to span length. *Explanation: Referring to Figure 4.5, nominal resistance for design and evaluation are the same. Equation 3.11 leads to relatively close reliability indices for different span lengths and f_i limits, and the slight difference was attributed to the uncertainties of f_i and P_{eval} .*
- Figure 4.7b presents corresponding probabilities of exceeding tension limits. Probabilities were greater than 50% for all cases. Average probability was approximately 73%.
- Considering $f_i(\kappa = 0.0948)$, f_{Reval} for *Post-1.0-Gains* in Figure 4.5d can be used as a reference case since it provided consistent reliability indices for span lengths and f_i .



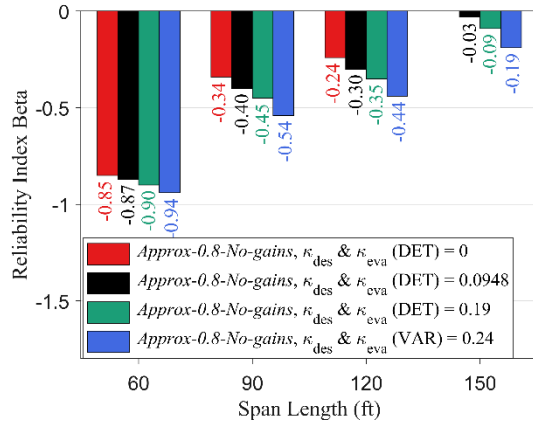
(a) β for *Post-0.8-No-gains*



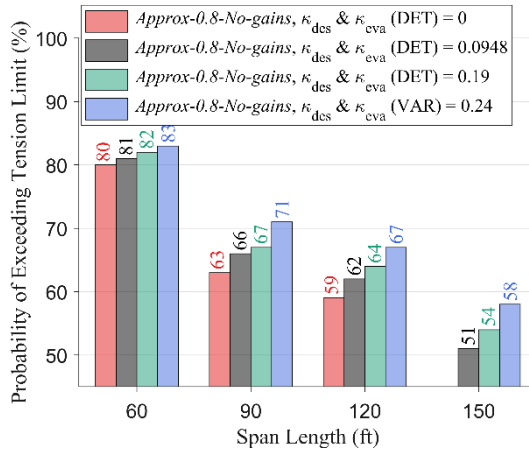
(b) Probability of Exceeding Tension Stress Limits for *Post-0.8-No-gains*

Figure 4.8 Reliability Index $\beta_{Implicit}$ and Corresponding Probabilities of Exceeding Tension Limits for Simple-span Bridges Designed using *Post-0.8-No-gains* Method, Similar Design and Evaluation f_i (κ)

1. Figure 4.8a presents $\beta_{Implicit}$ for bridges designed using *Post-0.8-No-gains*.
2. Figure 4.8a shows $\beta = -0.42$ for a 120-ft bridge designed and evaluated with f_i ($\kappa = 0.0948$); higher than -0.61 in Figure 4.7a. *Explanation: f_{Reval} for the 120-ft bridge designed with *Post-0.8-No-gains* was slightly larger than that for *Post-1.0-Gains*.*
3. $\beta_{Implicit}$ increased with increasing span. *Explanation: The difference between the f_{Reval} for *Post-0.8-No-gains* and *Post-1.0-gains* generally increased as span lengths increased (Figure 4.5d)*
4. Span-by-span comparison between Figure 4.7a and Figure 4.8a reveals inconsistent differences between reliabilities including or neglecting elastic gains and using 1.0 or 0.8 load factor.
5. The average probability of exceeding tension limits was approximately 70% (Figure 4.8b).



(a) β for *Approx-0.8-No-gains*

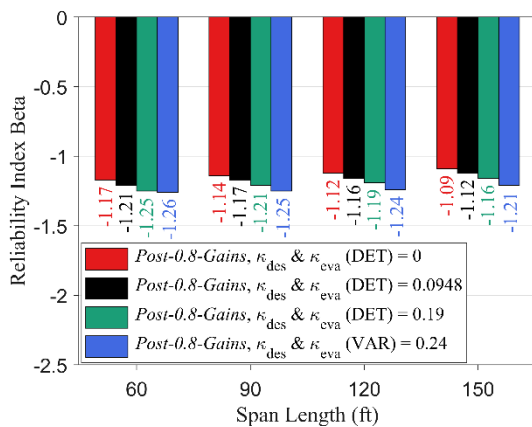


(b) Probability of Exceeding Tension Stress Limits for *Approx-0.8-No-gains*

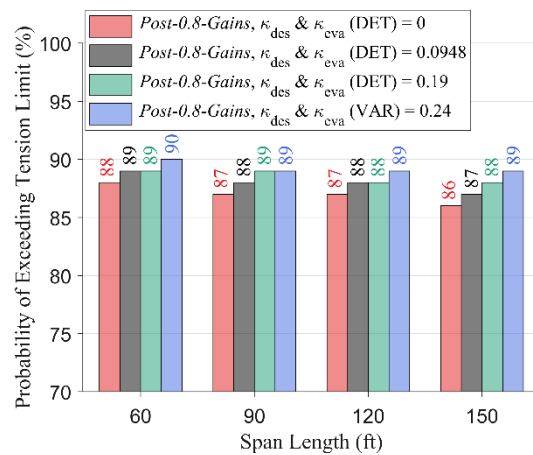
1. Figure 4.9a presents $\beta_{Implicit}$ for bridges designed using *Approx-0.8-No-gains*.
2. Comparing Figure 4.8a to Figure 4.9a, a similar β trend existed as span length increased. Slight differences were attributed to *Approx-0.8-No-gains* producing relatively higher f_{Reval} than *Post-0.8-No-gains* (Figure 4.5d).
3. Like Figure 4.8b, probability of exceeding tension limits decreased as the span length increased (Figure 4.9b).
4. Average probability of exceeding tension limits was approximately 67% (Figure 4.9b)

Figure 4.9 Reliability Index $\beta_{Implicit}$ and Corresponding Probabilities of Exceeding Tension Limits for Simple-span Bridges Designed using *Approx-0.8-No-gains* Method, Similar Design and Evaluation f_i (κ)

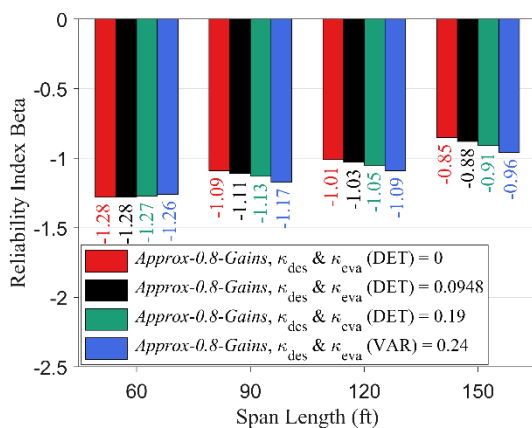
P_{eval} and f_{Reval} values were generally similar for *Post-0.8-Gains* and *Approx-0.8-Gains* but lower than the loss methods depicted in Figure 4.7 to Figure 4.9 (Figure 4.5b and Figure 4.5d). Therefore, these two methods resulted in similar $\beta_{Implicit}$ but lower values than methods presented in Figure 4.7 to Figure 4.9. Figure 4.10 presents $\beta_{Implicit}$ and corresponding probabilities of exceeding tension limits for two design methods with elastic gains and $\gamma_L = 0.8$. Figure 4.10a presents β for bridges designed using *Post-0.8-Gains* and indicates that β was approximately -1.20 and largely insensitive to $f_t(\kappa)$ and span length. Lower reliabilities in Figure 4.10a were expected when compared against those in Figure 4.7a due to a smaller area of prestressing reinforcement resulting from a lower *LL* factor (Figure 4.3b). Figure 4.10b indicates that the average probability of exceeding tension limits was about 88%, higher than 73% shown in Figure 4.7b. Figure 4.10c presents β for bridges designed using *Approx-0.8-Gains*, with β generally close to results in Figure 4.10a, having an average of -1.10, and with slightly more sensitivity to span length. In both cases, elastic gains were considered, and the same design *LL* factor was used. As a result, prestress loss predictions were similar. Figure 4.10d indicates that the average probability of exceeding tension limits was about 86%, which is similar to 88% from Figure 4.10b.



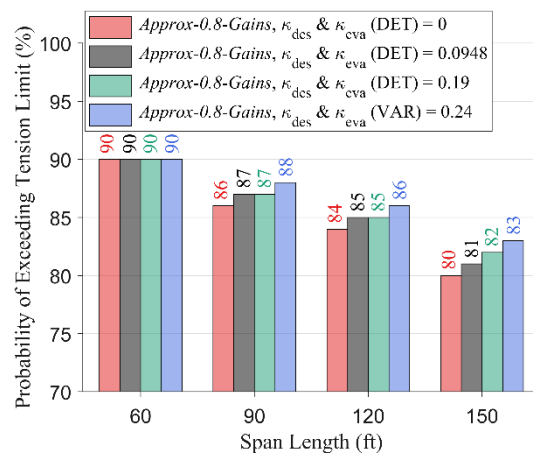
(a) β for *Post-0.8-Gains*



(b) Probability of Exceeding Tension Stress Limits for *Post-0.8-Gains*



(c) β for *Approx-0.8-Gains*



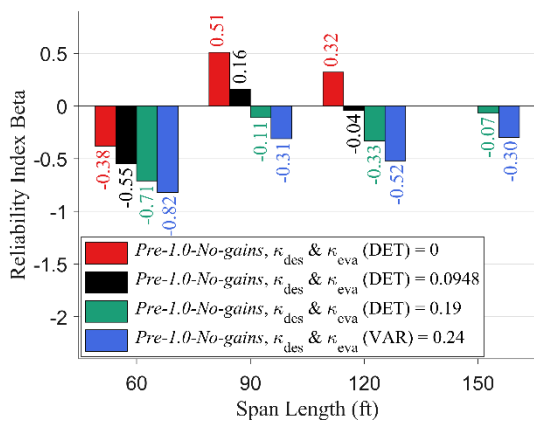
(d) Probability of Exceeding Tension Stress Limits for *Approx-0.8-Gains*

Figure 4.10 Reliability Index $\beta_{Implicit}$ and Corresponding Probabilities of Exceeding Tension Limits for Simple-span Bridges Designed using *Post-0.8-Gains* and *Approx-0.8-Gains* Methods, Similar Design and Evaluation f_t (κ)

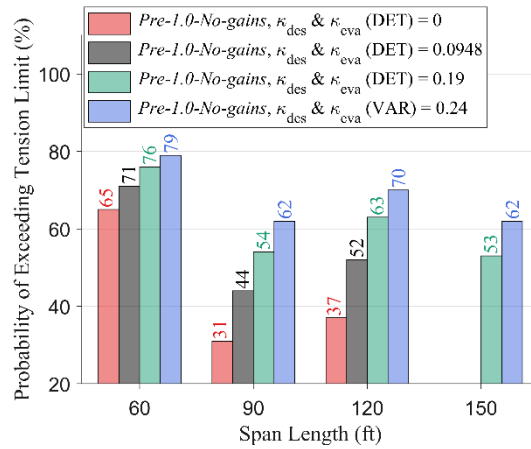
Generally, *Pre-1.0-No-gains* produced higher P_{eval} and f_{Reval} values than the other design loss methods, except for some 60-ft bridge span cases (Figure 4.5b and Figure 4.5d). $\beta_{Implicit}$ for *Pre-1.0-No-gains* was generally higher than that for other methods. Figure 4.11a presents $\beta_{Implicit}$

for *Pre-1.0-No-gains*. Bridges were designed based on the *Standard Specifications* but evaluated using parameters consistent with LRFR. β 's varied as a function of span length and generally increased as span increased, and trends for P_{eval} and f_{Reval} did not consistently match those observed using prestress loss methods from the *LRFD BDS*. Compared to β from other design methods, *Pre-1.0-No-gains* generally provided much higher reliability, except for some 60-ft simple-span *Post-1.0-Gains* cases (Figure 4.7 to Figure 4.11). Figure 4.11b indicates that the average probability of exceeding the tension limit is about 59%, which is noticeably lower than other design methods.

Generally, loss design methods considering elastic gains produced a more consistent β for considered spans (Figure 4.7a, Figure 4.10a, and Figure 4.10c). Bridges designed without considering elastic gain possessed higher β and more pronounced span length sensitivity (Figure 4.8a, Figure 4.9a, and Figure 4.11a) reflecting variation in dead load stresses and the expected result of neglecting associated elastic gain.



(a) β for *Pre-1.0-No-gains*



(b) Probability of Exceeding Tension Stress Limits for *Pre-1.0-No-gains*

Figure 4.11 Reliability Index β and Corresponding Probabilities of Exceeding Tension Limits for Simple-span Bridges Designed using *Pre-1.0-No-gains*, Similar Design and Evaluation $f_t(\kappa)$

In summary, average $\beta_{Implicit}$ for optimally designed Service III bridges was approximately:

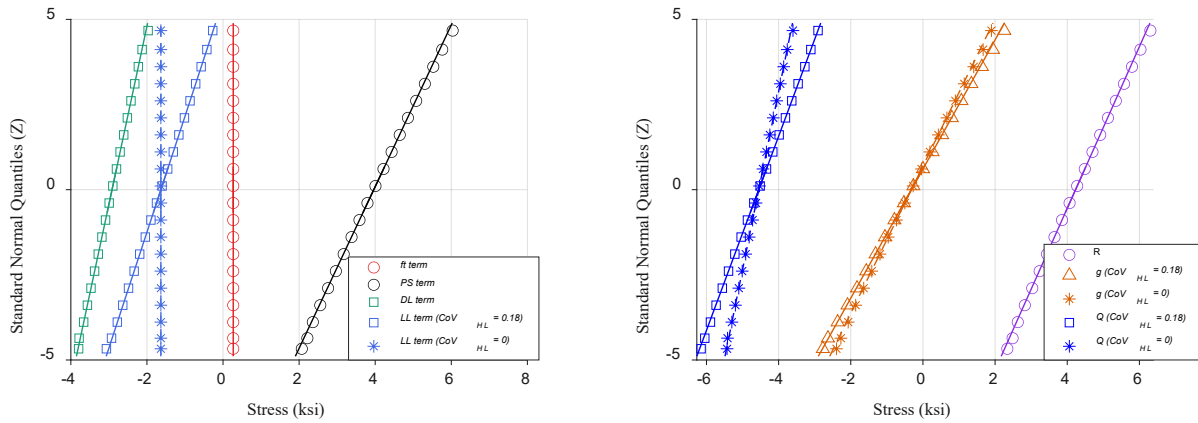
- -0.60 for bridges designed using *Post-1.0-Gains*, *Post-0.8-No-gains*, and *Approx-0.8-No-gains*
- -1.20 for bridges designed using *Post-0.8-Gains* and *Approx-0.8-Gains*

Designs obtained using a recent calibration for Service III (Wassef et al., 2014) corresponded to an implicit reliability of -0.60. There was no published physical evidence that prestressed girders designed using any prestress loss methods with a *LL* factor of 0.8 before 2014 exhibited significant cracking when in service, as stated in *LRFD BDS* C3.4.1. Consequently, this study recommended targeting a relatively conservative $\beta_{Implicit}$ value of -0.60 to evaluate bridges for platoons.

4.3.3 Effects of Parameter Uncertainty on Service III

To evaluate the effect of uncertainty of parameters on reliability analyses, simulated data points for the Service III limit state function (Equation 3.11) are provided in normal probability plots (Figure 4.12a and b) for 120-ft simple-span prestressed concrete bridges designed by *Post-1.0-Gains* with f_t ($\kappa_{des} = 0.0948$) at midspan. Resistance flexural stresses were based on the allowable tensile stress and prestressing terms in Equation 3.11 and are plotted as positive values. The allowable tensile stress ($f_t = 0.0948$) is a deterministic value (Figure 4.12a). In Figure 4.12a, prestressing and dead load terms in Equation 3.11 are plotted in black and green, respectively. HL-93 *CoV*s ($CoV = 0$ and 0.18) are simulated and plotted to evaluate their effects on the reliability index (Figure 4.12a). Figure 4.12a shows that primary sources of uncertainties were live load and prestress loss. The influence of prestress loss uncertainty was comparable to that from the live loads (Figure 4.12a).

Figure 4.12b plots PDFs for the limit state function terms (g , Q , and R) over stress. It can be seen that a change in *CoV* of live load from 0.18 to 0 had a slight effect on the distribution of load effects, but not a significant effect on the distribution of the limit state function, g . Thus, changing the live load *CoV* may not significantly affect the reliability index.



(a) Normal Probably Plot for Terms in Service III Limit State Function

(b) Normal Probably Plot for the Service III Limit State Function

Figure 4.12 Normal Probably Plots for 120-ft Prestressed Concrete Bridges Designed by *Post-1.0-Gains* with $f_t(\kappa_{des} = 0.0948)$

4.4 Service II Optimal Design and Target Reliability Results

This section provides optimal design performance ratios for positive and negative moment regions for steel bridges designed for Strength I and Service II. Positive moment regions are considered when determining the target implicit reliability index for both simple- and two-span bridges. This section also discusses uncertainties associated with Service II limit state function parameters in Equation 3.22.

4.4.1 Service II Optimal Design Results

This section presents performance ratios (Demand/Capacity) for the Strength I and Service II steel bridge designs. Strength I and Service II demands were determined using Equations 3.13 and 3.21, respectively. *LRFD BDS* design specifications used to determine nominal resistance for Strength I and Service II were presented in Section 3.5.3. Optimal design involved varying the bottom flange width to achieve a maximum performance ratio of 1.0 for

Service II and Strength I. Figure 4.13a shows performance ratios for simple-span positive moments, which was governed by Service II at the bottom flange for all spans. It can be seen from Figure 4.13a that Strength I performance ratios were greater than 0.8 for all spans. Figure 4.13b indicates performance ratios were close to 1.0 for both Service II at the bottom flange and strength for two-span positive moment region designs, while the performance ratio for Service II still governed.

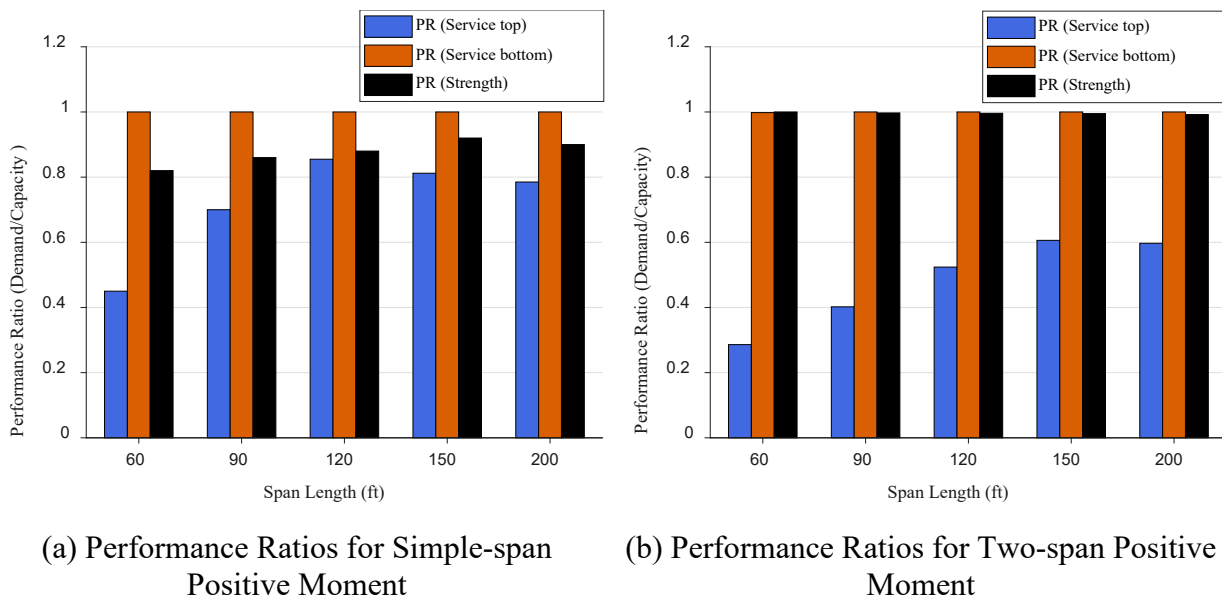


Figure 4.13 Performance Ratios for Simple-, and Two-span Positive Moment at Strength I and Service II

Figure 4.14 indicates that the Strength I controlled the design at two-span negative moment locations rather than Service II. Service II implicit reliability indices for simple- and two-span bridges were determined based on the limit state function as shown in Equation 3.22.

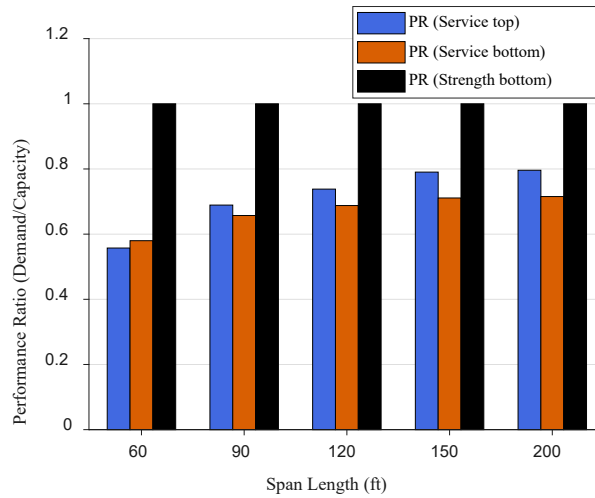


Figure 4.14 Performance Ratios for Two-span Negative Moment at Strength I and Service II

4.4.2 Service II Target Reliability Results

MCS was implemented to determine the dead loads, live loads, and resistances according to previously described nominal values and statistical parameter distributions. Figure 4.15a presents Service II PDFs for a 120-ft simple-span bridge positive moment region. Figure 4.15a shows mean resistance was larger than the mean load. The implicit reliability, representing the number of standard deviations between the mean for g and the failure threshold was 1.48. A positive value indicated that the probability of exceeding the Service II limit state was less than 50%. Figure 4.15b further examines the PDF for g , with about 7 out of 100 (7%) 120-ft simple-span bridge positive moment regions expected to exceed the Service II limit state.

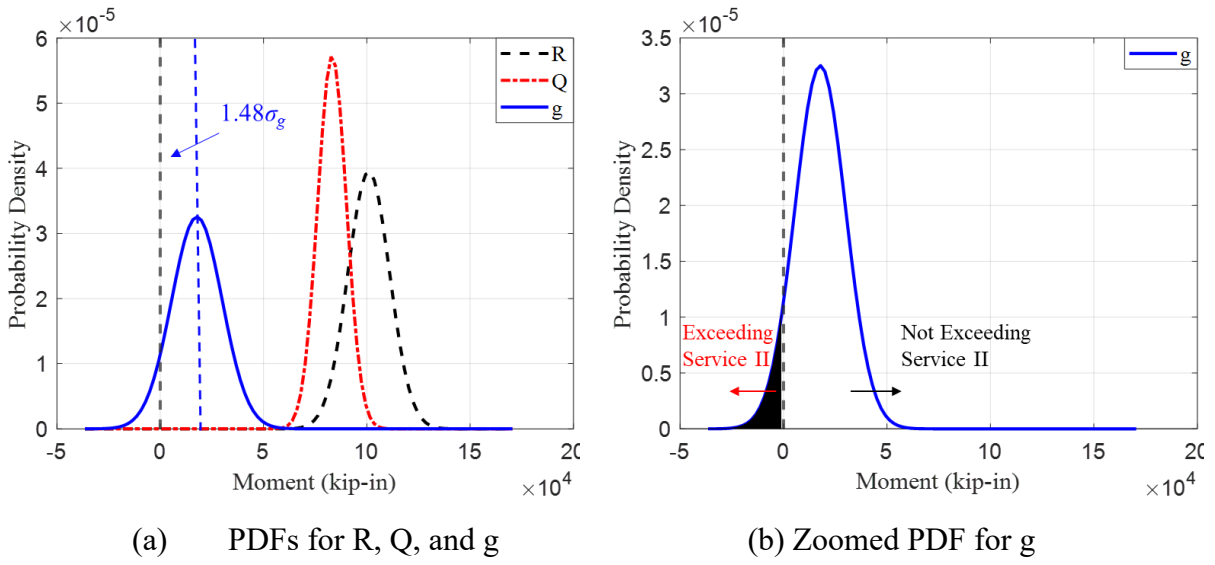
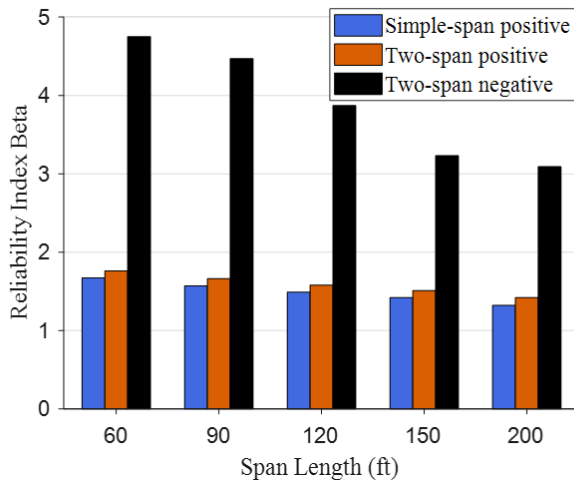
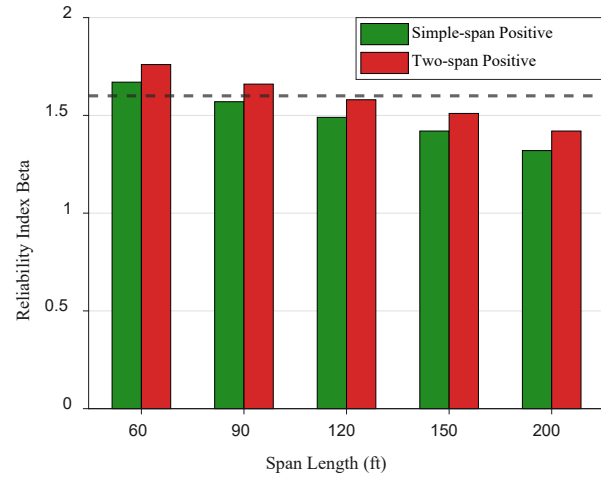


Figure 4.15 Probability Density Functions for Evaluating Service II for 120-ft Simple-Span Bridges Positive Moment Region

The reliability indices for simple- and two-span positive moment regions were generally close to 1.60 (Figure 4.16). As shown in Figure 4.16a, reliability indices were high for the two-span negative moment region (around 4.0) because Strength I governed bridge designs and they were therefore oversized for Service II ($RF > 1.0$) in these regions. Accordingly, this study focused on positive moment regions for simple- and two-span bridges for Service II and recommended a $\beta_{implicit}$ value of 1.60 (Figure 4.16b).



(a) β for Simple- and Two-span Bridges



(b) β for Simple- and Two-span Bridges Positive Moment Regions

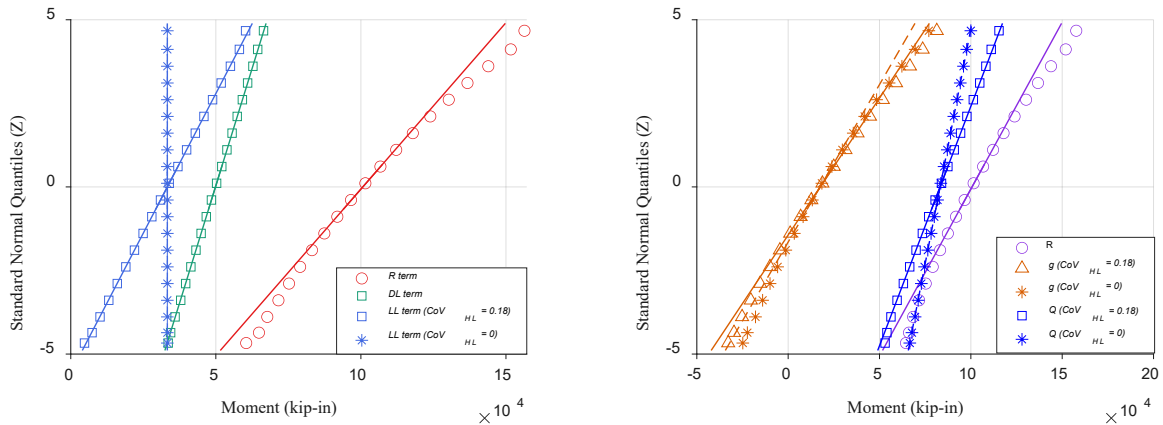
Figure 4.16 Reliability Index β for Simple-span and Two-span Bridges at Service II

4.4.3 Effects of Parameter Uncertainty on Service II

To evaluate the effect of parameter uncertainties on reliability analyses, simulated parameter data points for the Service II limit state function (Equation 3.22) are provided on normal probability plots (Figure 4.17a and b) for a 120-ft simple-span steel bridge midspan moment region, with flexural for Service II in Equation 3.22 plotted as positive values. The resistance follows a lognormal distribution, as illustrated in Figure 4.17a. The dead load flexure moments including the transformed section modulus ratio in Equation 3.22 are plotted in green (Figure 4.17a). HL-93 loading $CoVs$ ($CoV = 0$ and 0.18) are simulated and plotted to evaluate their effects on the reliability index (Figure 4.17a). Figure 4.17a shows that dead loads and resistance are primary sources of uncertainties.

The plot of the limit state function terms (g , Q , and R) in Figure 4.17b shows that a change in LL CoV from 0.18 to 0 will have a slight effect on the distribution of load effects and

the distribution of the limit state function, g . When the $LL\ CoV$ equals zero, fewer data points are below zero than for g with a $CoV = 0.18$ (Figure 4.17b). As a result, it would be expected that reducing $LL\ CoV$ may slightly increase the reliability index (Figure 4.17b).



(a) Normal Probably Plot for Terms in Service II Limit State Function

(b) Normal Probably Plot for the Service II Limit State Function

Figure 4.17 Normal Probably Plots for 120-ft Simple-span Steel Bridges Positive Moment at the Mid

4.5 Summary

For the simulated prestressed concrete bridges, a target implicit reliability index of -0.60 was recommended for Service III platoon load ratings. For the simulated steel bridges, a target implicit reliability index of 1.60 was recommended for Service II platoon load ratings. Changes to $LL\ CoV$ were shown to have a negligible effect on the reliability index for Service III and a slight effect for Service II.

Chapter 5 LRFR Live Load Factor Calibration

5.1 Overview

Live load factors were calibrated for platoon cases with a single-lane loaded, two-lane loaded and fully correlated, and with routine traffic in the lane adjacent to the platoon. Amplification and LL factors are presented for Service II for steel bridges and Service III for prestressed concrete bridges. In addition, LRFR LL factor tables are proposed for platoon permitting.

5.2 Service III Calibration Procedure

As described in the methodology, platoon LL effects were investigated over a range of potential CoV_s . Parameter uncertainties that differed from code calibration assumptions required LL factor calibration to facilitate platoon ratings. It should be noted that LL calibration for bridges designed using *Pre-1.0-No-gains* and HS20-44 loading was not performed because they have a higher $\beta_{Implicit}$ compared to other prestressed concrete design methods and may be oversized, as shown in Section 4.3.2.

Equation 3.1 provided an expression for Service III, where typical LL terms were updated while resistance and dead load terms remained unchanged. Equation 3.1 was rearranged by setting $RF = 1.0$ and isolating LL effects:

$$f_R - (\gamma_D)(f_D) = (\gamma_L)(f_{LL+IM}) \quad 5.1$$

where f_R , f_D , and f_{LL+IM} are given in Equations 3.2 through 3.5. γ_D is the rating dead load factor (equal to 1.0 for Service III). γ_L is the rating LL factor (equal to 0.8 or 1.0 based on MBE Table 6A.4.2.2-2). Setting platoon effects equal to typical design LL effects resulted in:

$$\frac{\gamma_{platoon} \lambda_{platoon} \alpha LL_{platoon} (1 + IM_{platoon}) GDF_{platoon}}{S_{cb}} = \frac{\gamma_L LL_{HL-93} (1 + IM_{HL-93}) GDF_m}{S_{cb}} \quad 5.2$$

Right-hand side subscripts in Equation 5.2 were modified to clarify that those terms were associated with $LRFR$ bases. Isolating the platoon LL factor on one side of the equation gives:

$$\gamma_{platoon} = \frac{\gamma_L LL_{HL-93} (1 + IM_{HL-93}) GDF_m}{\lambda_{platoon} \alpha LL_{platoon} (1 + IM_{platoon}) GDF_{platoon}} \quad 5.3$$

where IM_{HL-93} and GDF_m corresponded to the typical $LRFR$ dynamic impact amplification factor and GDF_m for multiple lanes-loaded, respectively. LL bias for platoons, $\lambda_{platoon}$, was assumed to be 1.0 throughout this research, as was the case in Steelman et al. (2021). The critical amplification factor, α , was applied to the platoon nominal static load effect, $LL_{platoon}$, which was determined using MCS to satisfy a target $\beta_{Implicit} = -0.6$ for Service III. $GDF_{platoon}$ depended on the load case being considered (see Section 3.6 Step 17). $IM_{platoon}$ was a deterministic impact factor value for platoon ratings and was set to 0.33 to ensure consistency with the typical $LRFR$ value used for design.

5.3 Service III Calibration Results

As expected, the two-lane fully-correlated platoon loading scenario was found to be critical. Calibrated LL factors for the single- and two-lane fully-correlated platoon loading scenarios were identical. The same observation was observed in Steelman et al. (2021) because the only difference between a single-lane platoon and a two-lane fully-correlated platoon scenario was using a multi-lane rather than a single-lane GDF. Because the increased load reflected in a multi-lane GDF was offset by a reduced amplification factor, LL factors were not significantly affected. This scenario was less likely to occur in real traffic than for a single-lane platoon with or without routine traffic.

Calibrated LL factors for Service III were slightly higher for simple-span than two-span bridges. Therefore, only simple-span bridge results are presented in this section. Results for the four-truck platoon at a 5-ft headway were based on Post-1.0-Gains designs at f_t ($\kappa = 0.0948$).

All LL factors were calibrated for a 5-ft headway. The exact headway value did not affect LL factor calibration because it only influenced $LL_{platoon}$. When a larger headway was selected, $LL_{platoon}$ decreased from its maximum value, but the MCS produced a correspondingly higher α so that $\mu_{platoon}$ remained at the target β . Results in the following subsections include both α and $\gamma_{platoon}$.

5.3.1 Single-Lane Loaded Service III Results

Table 5.1 shows α factors obtained using MCS for four-truck platoons traversing bridges at a 5-ft headway without adjacent traffic, with the bridges designed using *Post-1.0-Gains* with f_t ($\kappa_{des} = 0.0948$). The CoV ranged from 0 to 0.2 in 0.01 increments, although only 0.04 increments are shown in the table. The target reliability index was $\beta_{Implicit} = -0.6$ for all α factors, as shown in

Section 4.3.2. Amplification factors were greater than 1.0 for *CoV*s between 0 and 0.2, meaning that a four-truck platoon with all trucks at the legal load limit could acceptably travel across bridges within the scope of the study at a 5-ft headway.

Table 5.1 Single-Lane Platoon (Without Adjacent Traffic) Positive Moment Critical Amplification Factor, α

PS Concrete Bridges Span Length (ft)	<i>CoV</i>					
	0.00	0.04	0.08	0.12	0.16	0.20
60	1.9	1.9	1.9	2.0	2.0	2.0
90	1.6	1.6	1.6	1.6	1.6	1.6
120	1.4	1.4	1.4	1.4	1.4	1.4
150	1.3	1.3	1.3	1.3	1.3	1.3
Min	1.3	1.3	1.3	1.3	1.3	1.3
Avg	1.6	1.6	1.6	1.6	1.6	1.6

Corresponding *LL* factors and maximum and average values for each *CoV* are shown in Table 5.2 for selected span lengths. *LL* factors were generally uniform across different span lengths. In general, the calibrated *LL* factor for *Post-1.0-Gains* was about 0.83, which was less than 1.0 in MBE Table 6A.4.2.2-2.

Table 5.2 Single-Lane Platoon (Without Adjacent Traffic) Positive Moment Calibrated LL Factors, γ_{LL}

PS Concrete Bridges Span Length (ft)	CoV					
	0.00	0.04	0.08	0.12	0.16	0.20
60	0.84	0.84	0.84	0.80	0.80	0.80
90	0.83	0.83	0.83	0.83	0.83	0.83
120	0.84	0.84	0.84	0.84	0.84	0.84
150	0.82	0.82	0.82	0.82	0.82	0.82
Max	0.84	0.84	0.84	0.84	0.84	0.84
Avg	0.83	0.83	0.83	0.82	0.82	0.82

5.3.2 Platoon with Routine Traffic in Adjacent Lane Service III Results

The upper bound of 100 platoon crossings per day with a routine traffic ADTT of 5,000 from Steelman et al. (2021) was used for cases when traffic was adjacent to a platoon. Table 5.3 provides α factors obtained using MCS for four-truck platoons at a 5-ft headway with adjacent traffic traversing bridges designed using *Post-1.0-Gains* with $f_i (\kappa_{des} = 0.0948)$. The amplification factors were smaller than for a single-lane platoon without adjacent traffic, as expected.

Amplification factors were greater than or equal to 1.0 for $CoVs$ between 0 and 0.2 for 60- and 90-ft bridges, meaning that a four-truck platoon with all trucks at the legal load limit could acceptably cross 60- and 90-ft bridges within the scope of the study at a 5-ft headway with routine traffic in the adjacent lane. However, amplification factors were lower than 1.0 (red text in Table 5.3) for bridges longer than 90 ft, indicating that platoon headways for these cases need to be increased to meet Service III $\beta_{Implicit}$.

Table 5.4 shows that platoon LL factors for operations in a single lane with routine traffic in the adjacent lane were higher than those without routine traffic shown in Table 5.2. Routine traffic in an adjacent lane was not explicitly included in the rating factor equation, so the platoon

LL effect should be amplified with an increased *LL* factor to reflect adjacent lane loading. *LL* factors were generally uniform across all studied *CoV*s.

Table 5.3 Single-Lane Platoon (With Adjacent Traffic) Positive Moment Critical Amplification Factor, α

PS Concrete Bridges Span Length (ft)	<i>CoV</i>					
	0.00	0.04	0.08	0.12	0.16	0.20
60	1.2	1.2	1.2	1.2	1.3	1.3
90	1.0	1.0	1.0	1.0	1.0	1.0
120	0.8	0.8	0.8	0.8	0.9	0.9
150	0.7	0.7	0.7	0.7	0.8	0.8
Min	0.7	0.7	0.7	0.7	0.8	0.8
Avg	0.9	0.9	0.9	0.9	1.0	1.0

Table 5.4 Single-Lane Platoon (With Adjacent Traffic) Positive Moment Calibrated *LL* Factors, γ_{LL}

PS Concrete Bridges Span Length (ft)	<i>CoV</i>					
	0.00	0.04	0.08	0.12	0.16	0.20
60	1.33	1.33	1.33	1.33	1.23	1.23
90	1.33	1.33	1.33	1.33	1.33	1.33
120	1.46	1.46	1.46	1.46	1.30	1.30
150	1.53	1.53	1.53	1.53	1.34	1.34
Max	1.53	1.53	1.53	1.53	1.34	1.34
Avg	1.41	1.41	1.41	1.41	1.30	1.30

5.4 Service II Calibration Procedure

For Service II, Equation 3.21 provided an expression for optimal inventory level resistance with the *RF* equal to 1.0. Rearranging Equation 3.13 by setting *RF* equal to 1.0 and isolating *LL* effects gave Equation 3.25:

$$f_R - (\gamma_D)(f_D) = (\gamma_L)(f_{LL+IM}) \quad 5.4$$

f_R , f_D , and f_{LL+IM} were given in Equations 3.17 through 3.20. γ_D is the dead load factor (equal to 1.0 for Service II), and γ_L is the rating LL factor (equal to 1.30 for inventory level rating). Setting platoon effects equal to typical design LL effects gave:

$$\frac{\gamma_{platoon} \lambda_{platoon} \alpha LL_{platoon} (1 + IM_{platoon}) GDF_{platoon}}{S_{ST}} = \frac{\gamma_L LL_{HL-93} (1 + IM_{HL-93}) GDF_m}{S_{ST}} \quad 5.5$$

Right-hand side subscripts in Equation 5.5 were modified to clarify that those terms were associated $LRFR$ bases. Isolating the platoon LL factor on one side of the equation gave:

$$\gamma_{platoon} = \frac{\gamma_L LL_{HL-93} (1 + IM_{HL-93}) GDF_m}{\lambda_{platoon} \alpha LL_{platoon} (1 + IM_{platoon}) GDF_{platoon}} \quad 5.6$$

IM_{HL-93} , $IM_{platoon}$, GDF_m , and $\lambda_{platoon}$ for Service II calibration were the same as for Service III. The critical amplification factor, α , was applied to the platoon nominal static load effect, $LL_{platoon}$, and was determined using MCS to meet a target $\beta_{Implicit}$ value of 1.6 for Service II. $GDF_{platoon}$ differed for the load case being considered (see Section 3.6 Step 18).

5.5 Service II Calibration Results

As shown in Section 4.4.1, the negative moment range for two-span bridges was controlled by Strength I and not Service II. Therefore, Service II *LL* calibration focused only on positive moment regions for simple-span and two-span bridges. The calibrated *LL* factors for the single- and two-lane fully-correlated platoon loading scenarios were also the same for Service II. Calibrated *LL* factors for Service II results were slightly higher for simple-span than two-span bridges in the positive moment regions. Therefore, only simple-span bridge results are presented in this section. All *LL* factors were calibrated for a 5-ft headway because the *LL* factors were insensitive to headways, as described in Section 5.3. This section presents results for four-truck platoons at a 5-ft headway for steel bridges.

5.5.1 Single-Lane Loaded Service II Results

Table 5.5 provides α factors obtained using MCS for four-truck platoons at a 5-ft headway crossing steel bridges with no adjacent traffic. All amplification factors were for the target reliability index of $\beta_{Implicit}$ equal to 1.6, as shown in Section 4.4.2. Amplification factors were greater than 1.0 for *CoV*s between 0 and 0.2. Comparing Table 5.5 with Table 5.1, α factors for Service II at steel bridges and Service III at prestressed concrete bridges were generally similar for single-lane platoons without adjacent, routine traffic.

Table 5.5 Single-Lane Platoon (Without Adjacent Traffic) Positive Moment Critical Amplification Factor, α

Steel Bridges Span Length (ft)	<i>CoV</i>					
	0.00	0.04	0.08	0.12	0.16	0.20
60	2.1	2.1	2.1	2.0	2.0	1.9
90	1.7	1.7	1.7	1.7	1.6	1.6
120	1.5	1.5	1.5	1.4	1.4	1.3
150	1.3	1.3	1.3	1.3	1.2	1.2
200	1.2	1.2	1.2	1.2	1.1	1.1
Min	1.2	1.2	1.2	1.2	1.1	1.1
Avg	1.6	1.6	1.6	1.5	1.5	1.4

Table 5.6 presents *LL* calibration factors. The factors increased slightly as *CoV* increased. For the 120-ft bridge example, the mean of the limit state function was greater than zero, as shown in Figure 4.15b. Therefore, as *CoV* decreased (data became less scattered), there were fewer predicted failures. The maximum calibrated *LL* factor for *CoVs* between 0 and 0.08 was 1.11 and was controlled by 200-ft bridges. Increasing the *CoV* to 0.20 increased maximum *LL* factors by 9% to 1.21.

Table 5.6 Single-Lane Platoon (Without Adjacent Traffic) Positive Moment Calibrated *LL* Factors, γ_{LL}

Steel Bridges Span Length (ft)	<i>CoV</i>					
	0.00	0.04	0.08	0.12	0.16	0.20
60	0.99	0.99	0.99	1.04	1.04	1.09
90	1.02	1.02	1.02	1.02	1.08	1.08
120	1.01	1.01	1.01	1.08	1.08	1.17
150	1.07	1.07	1.07	1.07	1.16	1.16
200	1.11	1.11	1.11	1.11	1.21	1.21
Max	1.11	1.11	1.11	1.11	1.21	1.21
Avg	1.04	1.04	1.04	1.06	1.11	1.14

5.5.2 Platoon with Routine Traffic in Adjacent Lane Service II Results

Table 5.7 provides α factors obtained using MCS for four-truck platoons traversing steel bridges at a 5-ft headway with an adjacent traffic ADTT of 5,000. Comparing Table 5.7 with Table 5.3, α factors for Service II at steel bridges and Service III at prestressed concrete bridges were generally close for single-lane platoons with routine traffic. Amplification factors were lower than 1.0 (red text in Table 5.7) for bridges longer than 90 ft, indicating that platoon headways for these cases need to be increased to meet Service II $\beta_{Implicit}$. Table 5.8 shows LL factors for single-lane platoons with routine traffic in the adjacent lane. For spans 90 ft and longer, LL factors were insensitive to changes in CoV . This might have resulted from an increase in the dead-to-live load ratio as the span increased, as well as the presence of routine traffic in another lane. Overall, changes in platoon CoV did not affect most calibrated LL factors for these bridges, particularly not in cases when LL factors were maximum.

Table 5.7 Single-Lane Platoon (With Adjacent Traffic) Positive Moment Critical Amplification Factor, α

Steel Bridges Span Length (ft)	CoV					
	0.00	0.04	0.08	0.12	0.16	0.20
60	1.5	1.5	1.4	1.4	1.4	1.3
90	1.1	1.1	1.1	1.1	1.1	1.1
120	0.9	0.9	0.9	0.9	0.9	0.9
150	0.8	0.8	0.8	0.8	0.8	0.8
200	0.7	0.7	0.7	0.7	0.7	0.7
Min	0.7	0.7	0.7	0.7	0.7	0.7
Avg	1.0	1.0	1.0	1.0	1.0	1.0

Table 5.8 Single-Lane Platoon (With Adjacent Traffic) Positive Moment Calibrated LL Factors, γ_{LL}

Steel Bridges Span Length (ft)	CoV					
	0.00	0.04	0.08	0.12	0.16	0.20
60	1.39	1.39	1.48	1.48	1.48	1.60
90	1.57	1.57	1.57	1.57	1.57	1.57
120	1.69	1.69	1.69	1.69	1.69	1.69
150	1.73	1.73	1.73	1.73	1.73	1.73
200	1.90	1.90	1.90	1.90	1.90	1.90
Max	1.90	1.90	1.90	1.90	1.90	1.90
Avg	1.65	1.65	1.67	1.67	1.67	1.70

5.6 Proposed LRFR Factors

Truck weight amplification factors, α , were evaluated for all considered platoons, headways, superstructure types, and spans. For Service III, LL factors were insensitive to the design tensile stress limit, CoV , headways, span numbers, and number of trucks in a platoon. Only one LRFR LL factor is proposed for use with all LL $CoVs$ from 0 to 0.2. Proposed LRFR LL factors calibrated to a $\beta_{implicit}$ value of -0.6 for different loading scenarios for bridges designed for Service III using the *Post-1.0 Gains* method are shown in Table 5.9. Appendix A contains proposed LL factors for prestressed concrete bridges designed with other methods as outlined in Table 3.1. “Single-trip” in the frequency column denotes only a single platoon crossing is requested in a permit. For Service II, LL factors were also insensitive to span number, headways, and number of trucks. LL factors slightly decreased as CoV decreased (approximately 10% for single-lane platoons loaded without routine traffic and for two-lane platoons). To maintain consistency with the proposed Service III LL factor table, only one LRFR LL factor is conservatively proposed for use with all LL $CoVs$ from 0 to 0.2. Proposed LRFR LL factors calibrated to a target $\beta_{implicit}$ of 1.6 for Service II at steel bridges under different loading scenarios

are shown in Table 5.10. In Appendix A, *LL* factors for a range of *CoV*s are proposed if load rating engineers wish to take advantage of reduced platoon *CoV* for Service II. Factors proposed in Table 5.9 and Table 5.10 were rounded upward from calculated values to the nearest 0.05 increment and enveloped all calculated values.

Table 5.9 Proposed Moment Calibrated *LL* Factors for Service III

Truck platoon	Frequency	Load conditions	DF	ADTT (one direction)	Load factors by <i>COV</i> of total live load
					$COV_{LL} = 0 - 0.20$
Multiple trucks in platoon	single-trip	No other vehicles on the bridge	One lane	N/A	0.85
	single-trip	Two identical platoons loaded on two lanes	Two or more lanes	N/A	0.85
	100 Crossings	Mixed with routine traffic in the adjacent lane	One lane	> 5000	1.55

Table 5.10 Proposed Moment Calibrated *LL* Factors for Service II

Truck platoon	Frequency	Load conditions	DF	ADTT (one direction)	Load factors by <i>COV</i> of total live load
					$COV_{LL} = 0 - 0.20$
Multiple trucks in platoon	single-trip	No other vehicles on the bridge	One lane	N/A	1.15
	single-trip	Two identical platoons loaded on two lanes	Two or more lanes	N/A	1.15
	100 Crossings	Mixed with routine traffic in the adjacent lane	One lane	> 5000	1.90

- a. DF is the *LRFD BDS* approximate GDF, with the multiple presence factor (MPF=1.2) removed for one-lane GDFs.
 b. To use with a different *IM* factor, scale tabulated values by $1.33 / (1 + IM_{desired})$.

5.7 Summary

This section developed and proposed LRFR-calibrated Service III and Service II *LL* factors for positive moments bridge load ratings. If platoon trucks were spaced at a 5-ft headway, a four-truck platoon with all trucks at the legal load limit without routine traffic was shown to be able to acceptably cross all steel and prestressed concrete bridges within the scope of the study. However, if this 5-ft headway platoon may cross bridges with routine traffic, headways would need to be increased for bridges longer than 90 ft in order to meet implicit reliability indices for service. Acceptable spacing guidelines for Service III and Service II are presented and discussed in Chapter 6.

Chapter 6 Serviceable Combinations of Truck Weight and Headway

6.1 Overview

Headway tables for a target $\beta_{Implicit} = -0.6$ for Service III and a target $\beta_{Implicit} = 1.6$ for Service II were determined for four-truck platoons traversing simple- and two-span bridges for single-lane platoons with or without adjacent routine traffic. The headway tables, including different span lengths and amplification factors, are provided so bridge engineers can efficiently evaluate acceptable headway ranges without requiring moving load or reliability analyses. Positive critical midspan moments in simple-span bridges and at $0.4L$ from the interior support for two-span bridges were calculated and used in reliability analyses to establish acceptable platoon headways. Headways required for simple-span bridges are slightly more conservative than those for two-span bridges. Therefore, only simple-span bridge results are presented. General guidelines are provided at the end of the chapter for legal load ($\alpha = 1.0$) platooning scenarios on steel and prestressed concrete *LRFD*-designed girder bridges.

6.2 Prestressed Concrete Bridges Service III

Platoons operating at close headways with weights exceeding legal limits (i.e., “platoon permits”) could potentially induce unacceptably large *LL* effects and result in reliability indices less than the target $\beta = -0.6$. For simple- and two-span bridge positive moment regions, platoon *LL* effects consistently decreased with increasing headway. Therefore, if a desired combination of headway and truck weight is unacceptable, serviceability could be maintained by temporarily increasing headway when the platoon traverses the bridge. For Service III, Chapter 4 and Chapter 5 demonstrate that varying uncertainties, represented using *CoV*, do not significantly change results and, consequently, headway selection guidance. Therefore, results are presented

based on an assumed $CoV = 0.18$ for platoons, which is the same as the HL-93 design load CoV . Results are shown for prestressed concrete bridges designed using *Post-1.0-Gains* with $f_t (\kappa_{des} = 0.0948)$ because this design scenario provided relatively consistent implicit reliability indices as shown in Figure 4.7a and was recently calibrated in Wassef et al. (2014).

For illustrative purposes, a four-truck legal load platoon ($\alpha = 1.0$) single-lane loaded, simple-span bridge was considered as shown in Figure 6.1. The platoon was run in both directions across the bridge, and the critical positive moment at midspan incorporating the single-lane GDF was determined. The critical positive moment was substituted into Equation 3.24 as the nominal platoon load effect (L_{pL}), and then uncertainties for components in Equation 3.24 were combined to determine the reliability index. For each headway spacing from 5 to 50 ft and CoV from 0 to 0.20, α started at 0.6 and was increased by increments of 0.1 until $\beta \leq \beta_{Implicit}$. Then, headway tables for each α and CoV were determined based on the minimum headways that met $\beta \geq \beta_{Implicit}$. Initializing at $\alpha = 0.6$ began the analysis with axle spacings and proportionate axle weights consistent with the NRL, but with all axle weights, and therefore the GVW, scaled to 60% of the typical (legal) vehicle weight.

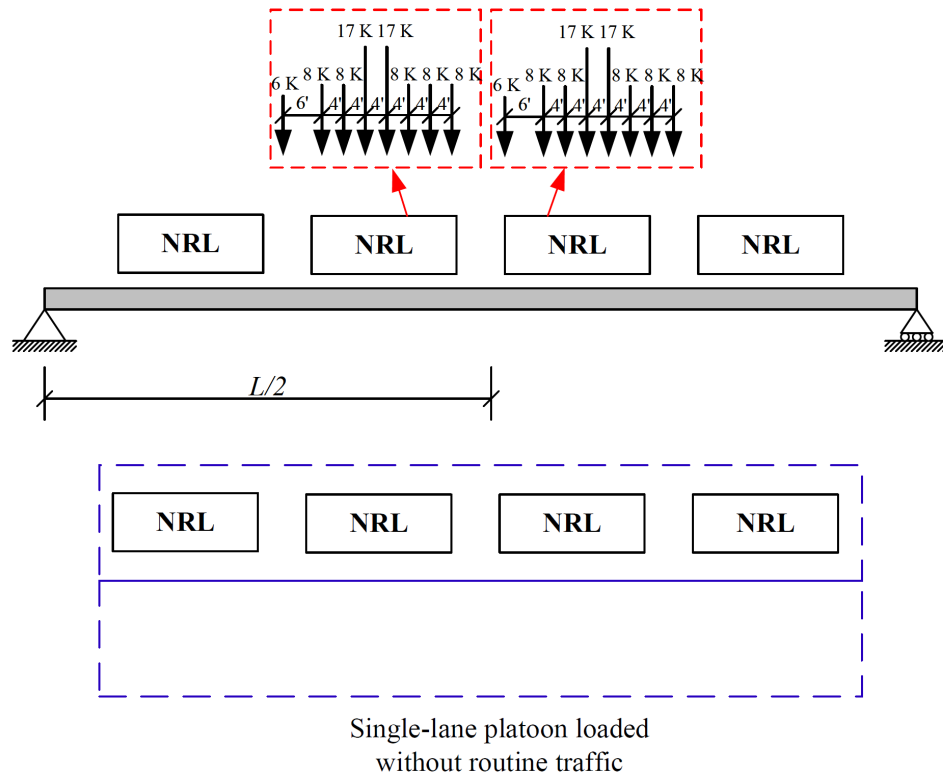


Figure 6.1 Single-lane Loaded Four-truck NRL Platoon without Routine Traffic on a Simple-Span Bridge Scenario for Developing Headway Tables

A four-truck legal load platoon ($\alpha = 1.0$) single-lane loaded with routine traffic in the adjacent lane, simple-span bridge was also considered, as shown in Figure 6.2. The critical positive moment at midspan incorporating the single-lane GDF, with the multiple presence factor of 1.2 being removed, was determined for the four-NRL platoon. As presented by Yang et al. (2021) and Steelman et al. (2021), the platoon was assumed to have 100 crossings per day and was accompanied by 5,000 *ADTT* routine traffic. It was previously demonstrated that these two parameters were insensitive to precise values selected by Steelman et al. (2021). Multiple presence probabilities for platoons loaded with adjacent routine traffic were adopted from Ghosh et al. (2011). Section 3.5.5 in Steelman et al. (2021) provides detailed routine traffic information.

Resulting reliability indices β were calculated based on Equation 3.26. To develop the headway spacing tables, α started at 0.6 and was increased by increments of 0.1 until $\beta \leq \beta_{Implicit}$.

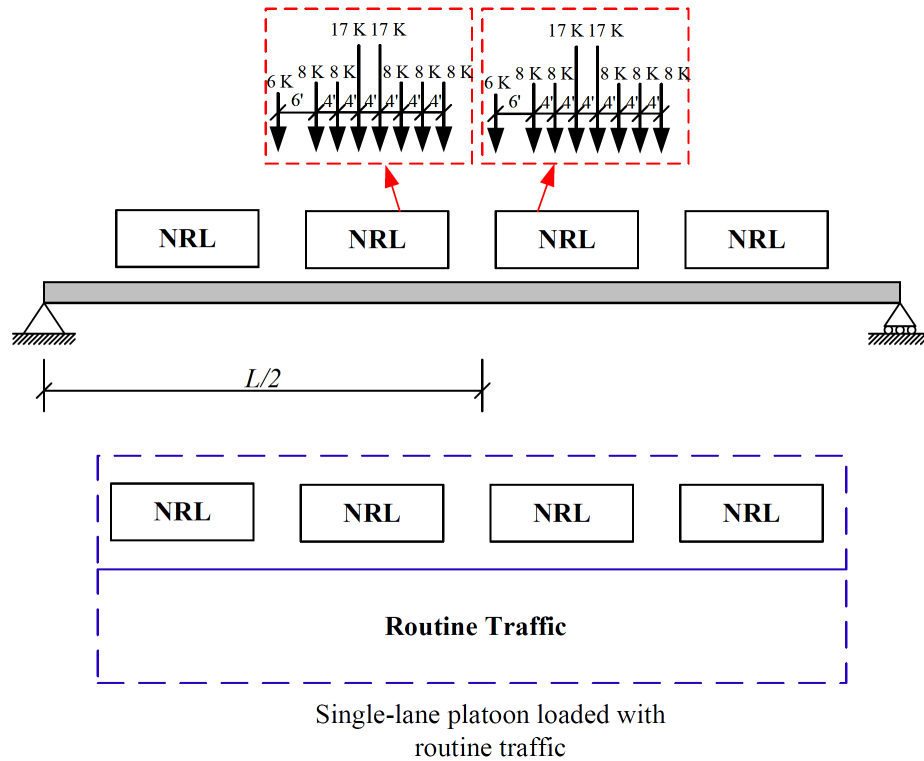


Figure 6.2 Single-lane Loaded Four-truck NRL Platoon with Routine Traffic on a Simple-Span Bridge Scenario for Developing Headway Table

6.2.1 Single-Lane Platoon Without Adjacent Traffic

Table 6.1 shows minimum acceptable headways as a function of span length based on positive moment demands for simple-span bridges carrying a four-truck platoon in one lane assuming a constant $CoV = 0.18$.

Table 6.1 indicates that headways increase with longer span lengths as more axles can simultaneously load the bridge. “Fail” in Table 6.1 indicates that the required headway is greater than 50 ft or that the bridge has reached its limit regardless of headway. The NRL truck length examined in the study was 30 ft as shown in Figure 6.1. As a result, because only a fractional portion of two NRLs at most can load a 60-ft bridge, headway has a relatively small effect on platoon load limits for that span length. The upper bound α that satisfies the target $\beta_{Implicit}$ for all span lengths was 2.3. Maximum α trends upward with increasing span as platoons can use increased headways to reduce load effects. If a platooning route included only longer spans, the upper limit of α increased, up to a maximum of 3.0 with a 49-ft headway for 150-ft spans. When the 50-ft headway governs, typical processes provided in the MBE may allow for heavy truck passage under special permitting conditions, but the truck would no longer be in an aerodynamically efficient platoon.

Table 6.1 also details that, as a platoon operating with $\alpha = 2.3$ travels along a highway and encounters longer bridges, the platoon must increase headways to 15, 17, 25, or 33 ft when crossing 60-, 90-, 120-, or 150-ft simple-span bridges, respectively, to maintain acceptable service operations.

Table 6.1 Acceptable Simple-Span Bridge Platoon Headways (ft) Without Adjacent Routine Traffic ($CoV = 0.18$)

Amplification factor α	L (ft)			
	60	90	120	150
0.6	5	5	5	5
0.7	5	5	5	5
0.8	5	5	5	5
0.9	5	5	5	5
1.0	5	5	5	5
1.1	5	5	5	5
1.2	5	5	5	5
1.3	5	5	5	5
1.4	5	5	5	7
1.5	5	5	6	10
1.6	5	5	9	13
1.7	5	6	12	16
1.8	5	8	14	20
1.9	5	10	17	23
2.0	5	11	19	26
2.1	7	13	21	28
2.2	10	15	23	31
2.3	15	17	25	33
2.4	Fail	20	27	35
2.5	Fail	23	29	37
2.6	Fail	30	31	39
2.7	Fail	Fail	34	41
2.8	Fail	Fail	38	44
2.9	Fail	Fail	Fail	46
3.0	Fail	Fail	Fail	49
3.1	Fail	Fail	Fail	Fail

6.2.2 Single-Lane Platoon, Routine Traffic in Adjacent Lane

The potential presence of heavy trucks in the adjacent lane reduces acceptable operating headways. Table 6.2 shows minimum headways as a function of span length for simple-span bridges carrying a four-truck platoon in one lane, and with routine traffic in an adjacent lane. The table illustrates that a legal load platoon ($\alpha = 1.0$) cannot cross 120- or 150-ft bridges without increasing headways from 5 ft due to the presence of adjacent routine traffic. For example, legal limit platoons ($\alpha = 1.0$) must increase headways from 5 to 10 ft for a 120-ft span, and from 10 ft to 15 ft for a 150-ft span.

The maximum α that satisfied target β implicit with adjusted headways was reduced from 2.3 to 1.4 for platoons with typical LL uncertainty ($CoV = 0.18$) on 60- to 150-ft span bridges (Table 6.1 and Table 6.2). α must be limited to no greater than 0.8 (80% of the legal load weight limit) to ensure acceptably serviceable operations with unrestricted headway spacings as low as 5 ft.

Table 6.2 Acceptable Simple-Span Bridge Platoon Headways (ft) With Adjacent Routine Traffic (100 Crossings, and ADTT = 5000) ($CoV = 0.18$)

Amplification factor α	L (ft)			
	60	90	120	150
0.6	5	5	5	5
0.7	5	5	5	5
0.8	5	5	5	5
0.9	5	5	5	10
1.0	5	5	10	15
1.1	5	7	14	21
1.2	5	10	18	26
1.3	5	13	21	30
1.4	9	16	25	34
1.5	Fail	19	28	38
1.6	Fail	26	32	41
1.7	Fail	Fail	37	45
1.8	Fail	Fail	Fail	Fail

6.3 Steel Bridges Service II

Platoons on steel bridges were evaluated for simple- and two-span bridge positive moment regions for Service II. Reducing LL uncertainties for Service II slightly decreased minimum required headways but not to the same magnitude as for Strength I in Steelman et al. (2021). If the platoon operator wishes to justify reduced uncertainty for platoons to maintain a desired headway, tables for Service II for different platoon $CoVs$ are provided in Appendix B. Results were conservatively based on the assumption that the platoon CoV equaled the CoV for HL-93 design loading.

For Service II the general procedure for developing headway tables was the same as for Service III, except using $\beta_{Implicit} = 1.6$ as shown in Figure 4.16b. A four-truck platoon was used to

determine the load effects for single-lane loaded platoons with or without adjacent traffic.

Reliability analyses were then conducted using Equations 3.27 and 3.29.

6.3.1 Single-Lane Platoon Without Adjacent Traffic

Table 6.3 summarizes the results to show minimum headway variations as a function of span length that ensure acceptable positive moment demands for simple-span bridges carrying only a four-truck platoon in one lane, assuming a constant $CoV = 0.18$. Maximum α generally trends upward with an increasing span as platoons can take advantage of increased headways to reduce load effects except for 200-ft bridges. Platoon vehicles could operate on 200-ft spans at greater separations than 50 ft and with escalating α similar to shorter spans. However, under those conditions, the platoon would need to be evaluated as typical permit vehicles with a special analysis accounting for multiple heavy vehicles simultaneously on the bridge. Because aerodynamic benefits will be negligible in such a case, it was deemed outside the scope of the study.

Table 6.3 shows that a platoon operating with $\alpha = 2.2$ is the maximum that can acceptably operate on all simple-span bridge spans. With $\alpha = 2.2$, as the platoon travels along a highway and encounters longer bridges, platoon trucks must increase headways between trucks to 12, 16, 25, 34 or 47 ft when crossing 60-, 90-, 120-, 150- or 200-ft simple-span bridges, respectively, to maintain safe operations. Maximum α for all spans, achievable by adjusting platoon headways, and acceptable for Service II and Service III is similar, at 2.2 (Table 6.1) and 2.3 (Table 6.3), respectively, for single-lane loaded platoons without routine traffic.

Table 6.3 Acceptable Simple-Span Bridge Platoon Headways (ft) Without Adjacent Routine Traffic ($CoV = 0.18$)

Amplification factor α	L (ft)				
	60	90	120	150	200
0.6	5	5	5	5	5
0.7	5	5	5	5	5
0.8	5	5	5	5	5
0.9	5	5	5	5	5
1.0	5	5	5	5	5
1.1	5	5	5	5	5
1.2	5	5	5	5	6
1.3	5	5	5	6	11
1.4	5	5	5	9	15
1.5	5	5	8	12	19
1.6	5	5	11	16	22
1.7	5	7	14	20	27
1.8	5	9	16	23	32
1.9	5	11	19	26	36
2.0	5	12	21	29	40
2.1	8	14	23	31	44
2.2	12	16	25	34	47
2.3	Fail	19	27	36	50
2.4	Fail	22	29	38	Fail
2.5	Fail	27	32	40	Fail
2.6	Fail	Fail	35	43	Fail
2.7	Fail	Fail	39	45	Fail
2.8	Fail	Fail	Fail	48	Fail
2.9	Fail	Fail	Fail	Fail	Fail

6.3.2 Single-Lane Platoon, Routine Traffic in Adjacent Lane

Table 6.4 shows minimum headways as a function of span length that ensure acceptable positive moment demands for simple-span bridges carrying a four-truck platoon in one lane and routine traffic in an adjacent lane, assuming a constant $CoV = 0.18$. Table 6.4 illustrates that a legal load platoon ($\alpha = 1.0$) cannot cross 120-, 150- or 200-ft bridges without increasing the headways from 5 ft due to the presence of adjacent traffic. For example, at the legal load platoon ($\alpha = 1.0$) level, the headway must increase from 5 to 8 ft for a 120-ft span, from 8 to 15 ft for a 150-ft span, and from 15 to 23 ft for a 200-ft span.

The maximum α that provides target $\beta_{Implicit}$ with adjusted headways is reduced from 2.2 to 1.4 on 60- to 200-ft span bridges (Table 6.3 and Table 6.4). To achieve unrestricted headway spacings (5-50 ft), α must be limited to 0.7 (70% of the legal load weight limit).

Similar to the case without adjacent traffic, maximum α for all spans, achievable by adjusting platoon headways, and acceptable for Service II and Service III is similar, at 1.4 in both Table 6.2 and Table 6.4, for single-lane loaded platoons with routine adjacent traffic.

Table 6.4 Acceptable Simple-Span Bridge Platoon Headways (ft) With Adjacent Routine Traffic (100 Crossings, and ADTT = 5000) ($CoV = 0.18$)

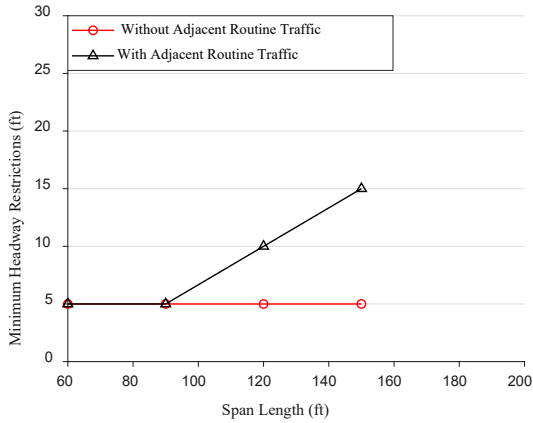
Amplification factor α	L (ft)				
	60	90	120	150	200
0.6	5	5	5	5	5
0.7	5	5	5	5	5
0.8	5	5	5	5	11
0.9	5	5	5	9	18
1.0	5	5	8	15	23
1.1	5	5	13	21	31
1.2	5	8	17	25	38
1.3	5	11	20	30	44
1.4	5	13	23	34	49
1.5	9	16	26	37	Fail
1.6	18	20	30	41	Fail
1.7	Fail	26	34	44	Fail
1.8	Fail	Fail	41	49	Fail
1.9	Fail	Fail	Fail	Fail	Fail

6.4 Preliminary Operational Guidance

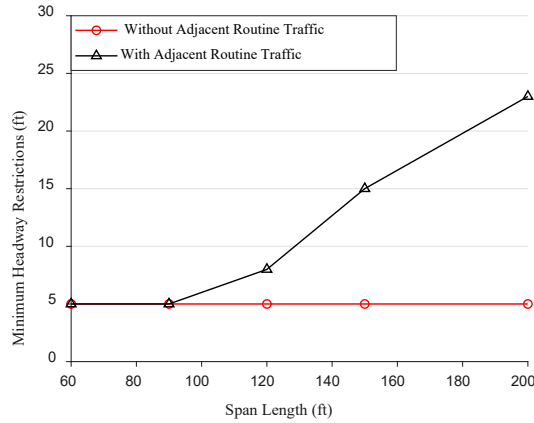
Initial platoon deployments are expected to be limited to trucks operating within the Federal Bridge Formula B (FBF B) legal load limit, corresponding to $\alpha = 1.0$. This section addresses these considerations and enables next steps for operational platoon deployment. Results were based on four-truck platoons, which were the critical positive moment cases for simple- and two-span bridges.

For Service III, at the target $\beta_{Implicit} = -0.6$, a minimum headway of 5 ft is acceptable for bridge spans between 60 and 150 ft (Figure 6.3a) carrying a platoon in a single lane without adjacent routine traffic. With adjacent traffic, the headway would need to increase to 10 ft and 15 ft for 120-ft and 150-ft spans, respectively. For Service II, at the target $\beta_{Implicit} = 1.6$, a minimum headway of 5 ft is similarly acceptable for bridge spans between 60 and 200 ft (Figure 6.3b)

carrying a platoon in a single lane without adjacent routine traffic. With adjacent traffic, the headway would need to increase to 8 ft, 15 ft, and 23 ft for 120-ft, 150-ft, and 200-ft spans, respectively.



(a) Legal load platoon headway restrictions for prestressed bridges



(b) Legal load platoon headway restrictions for steel bridges

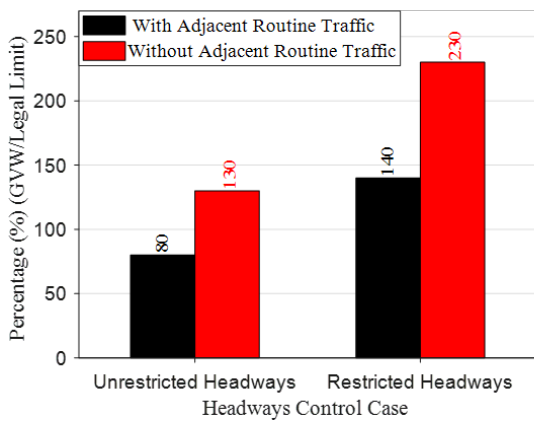
Figure 6.3 Legal Load Platoon Headway Restrictions for Steel and Prestressed Bridges

Figure 6.4 summarizes findings for potential GVW modification percentages relative to an 80-kip legal load limit for the different loading scenarios on prestressed concrete and steel bridges in Sections 6.2 and 6.3. Platoons are presumed to be deployed on interstates initially. However, legal limits on state highway bridges may be higher, and so the results presented in Figure 6.4 would be slightly conservative in that case and headway tables presented in this chapter should be referenced for guidance applicable to $\alpha > 1.0$.

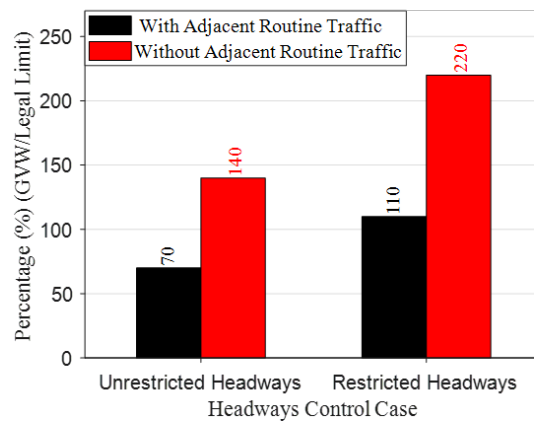
For prestressed concrete bridges, platoons can operate at any headway on all spans and configurations with adjacent routine traffic at 80% of the legal load limit (Table 6.2 and Figure 6.4a). If a platoon can avoid traveling adjacent to routine traffic, it can potentially operate at up

to 130% of the legal load limit (Table 6.1 and Figure 6.4a). Platoons can operate adjacent to routine traffic at up to 140% of the legal load limit by increasing to minimum headways (Table 6.2 and Figure 6.4a). If the platoon can avoid traveling adjacent to routine traffic, it can potentially operate at up to 230% of the legal load limit (Table 6.1 and Figure 6.4a).

For steel bridges, platoons can operate at any headway on all spans and configurations with adjacent routine traffic at 70% of the legal load limit (Table 6.4 and Figure 6.4b). If a platoon can avoid traveling adjacent to routine traffic, it can potentially operate at up to 140% of the legal load limit (Table 6.3 and Figure 6.4b). Platoons can operate adjacent to routine traffic at up to 140% of the legal load limit by increasing to minimum headways (Table 6.4 and Figure 6.4b). If the platoon can avoid traveling adjacent to routine traffic, it can potentially operate at up to 220% of the legal load limit (Table 6.3 and Figure 6.4b).



(a) Headway restrictions for prestressed concrete girder bridges ($\beta_{Implicit} = -0.6$)



(b) Headway restrictions for steel girder bridges ($\beta_{Implicit} = 1.6$)

Figure 6.4 Headway Restrictions for Prestressed Concrete and Steel Girder Bridges ($CoV = 0.18$)

6.5 Summary

This chapter summarized an investigation of acceptable headways as a function of platoon truck weight and bridge span. Critical loading occurs with closely grouped trucks for simple- and two-span bridge positive moment regions, so permitted truck weights can increase with increasing headway.

For Service III, a single-lane platoon can operate at a constant headway of 5 ft on all simple spans up to an α of 1.3, or 130% of the legal load limit. If the platoon operator is willing to adjust headways along the route according to varying bridge spans, truck weights can increase up to 230% of the legal load limit. If the route includes only simple-span bridges spanning at least 90 ft, the load can increase to approximately 260% the legal limit by adjusting headways.

When routine traffic exists in the adjacent lane, a legal load platoon ($\alpha = 1.0$) cannot traverse all the considered spans at a constant headway of 5 ft. The presence of adjacent lane loading lowers the acceptable α by 50% of the legal load limit, from 130% to 80% (Table 6.1 and Table 6.2). If the operator is willing to adjust headways along the route to accommodate varying bridge lengths, truck weights can increase up to 140% of the legal load limit with adjacent lane loading or up to 230% without adjacent loading (Table 6.1 and Table 6.2). If the route includes simple-span bridges spanning at least 90 ft, loads can increase to 160% of the legal limit with adjacent lane loading by adjusting platoon headways or up to 260% without (Table 6.1 and Table 6.2). These readily available overload capacities reflect presumed resistances consistent with LRFD BDS Service III optimal design, which considered two lanes of HL-93 LL, appropriate multiple lane distribution factors, a dynamic load allowance ($IM = 0.33$), which correspond to $\beta_{Implicit} = -0.6$.

For Service II, a single-lane loaded platoon can operate at a constant headway of 5 ft on all simple spans up to an α of 1.1, or 110% of the legal load limit (Table 6.3). If the platoon operator is willing to adjust headways along the route to accommodate varying bridge lengths, truck weights can increase by an additional 110% above the legal load limit, to 220% of the legal load limit (Table 6.3).

When routine traffic exists in the adjacent lane, a legal load platoon ($\alpha = 1.0$) cannot operate at a constant headway of 5 ft to traverse all the considered spans. The presence of adjacent lane loading lowers the acceptable α by 40% of the legal load limit, from 110% to 70% (Table 6.3 and Table 6.4). If the operator is willing to adjust headways along the route to accommodate varying bridge lengths, truck weights can increase up to 140% of the legal load limit with adjacent lane loading versus 220% without (Table 6.3 and Table 6.4).

These readily available overload capacities reflect presumed resistances consistent with LRFD BDS Service II optimal design for positive moment regions, which considered two lanes loaded HL-93 *LL*, appropriate multiple lane distribution factors, a dynamic load allowance ($IM = 0.33$), and which correspond to an implicit reliability index, $\beta_{Implicit} = 1.6$.

Guidance is provided for operational platooning weight limits accounting for Service III and Service II. For Service III, platoons may operate with upper limits from 80% to 230%, depending on whether the lane adjacent to a platoon may be occupied by a routine truck and whether the platooning operator is willing to adjust headways on a bridge-by-bridge basis along the route. For Service II, the upper limits are similar, at 70% to 220%.

Chapter 7 Framework for Aggregating Live Load Uncertainties

7.1 Overview

This chapter proposes a framework for aggregating *LL* uncertainties based on truck weight, dynamic amplification, and girder distribution factors and results of sensitivity analyses to establish total platoon *CoV*s. Using Monte Carlo simulations discussed in Chapter 3, *LL* uncertainties were aggregated based on total platoon *CoV*. To calibrate *LL* factors the total platoon *CoV* was between 0 and 0.2. Steelman et al. (2021) demonstrated that total platoon *CoV* could be calculated based on uncertainties associated with truck weight, dynamic amplification, and girder distribution factors. Calibrated *LL* factors could be selected for Strength I as presented in Steelman et al. (2021) and for Service III and II from Chapter 5 by implementing the developed framework to quantify *LL* uncertainties. It should be noted that in Chapter 5 *LL* factors were shown to not be significantly affected by variations in *LL CoV* for Service III and II.

7.2 Live Load Statistical Model

Recognizing that each *LL* component (weights, dynamic amplification factor, GDF) is uncertain, Steelman et al. (2021) proposed the following equation to determine dynamic *LL*

CoV_{L_GDF+IM} :

$$CoV_{L_GDF+IM} = \frac{\sqrt{(1 + 2\mu_{IM})(A) + \mu_{IM}^2(A + B)}}{(1 + \mu_{IM})} \quad 7.1$$

$$A = (CoV_L^2 + CoV_{GDF}^2 + CoV_{GDF}^2 CoV_L^2) \quad 7.2$$

$$B = (CoV_L^2 CoV_{GDF}^2 CoV_{IM}^2 + CoV_{GDF}^2 CoV_{IM}^2 + CoV_L^2 CoV_{IM}^2 + CoV_{IM}^2) \quad 7.3$$

where μ_{IM} is the mean of the dynamic impact factor; CoV_L is the CoV of static LL ; CoV_{GDF} is the CoV of GDF ; and CoV_{IM} is the CoV of impact factor. As shown in Equations 7.1 to 7.3, the total CoV_{L_GDF+IM} for a platoon would be dependent on CoV_L , CoV_{IM} , μ_{IM} , and CoV_{GDF} .

In this chapter, characterizations of CoV_L , CoV_{IM} , μ_{IM} , and CoV_{GDF} for different scenarios are discussed so that calibrated LL factors and headways can be determined based on CoV_{L_GDF+IM} from Equations 7.1 to 7.3.

7.3 Truck Weight Uncertainty Framework

Truck weight uncertainty can be reduced via direct measurement of axle loads with commercially available sensors, so long as their resolution (i.e., measurement error) is known. Weigh-in-motion (WIM) stations capture, record, and catalog axle spacings, weights, and gross truck weight (GVW) as trucks drive over sensors installed in the roadway. WIM arrays frequently include inductive loops (ILDs) in the roadway. The ILD acts as a presence detector while a pressure sensor measures axle or tire weights (FHWA, 2018).

ASTM E1318-09 (ASTM, 2017) is the primary WIM standard in the United States. Based on the application and functional performance requirements, ASTM E1318-09 categorizes WIM systems into four distinct types:

- Type I and Type II systems: Suitable for traffic data collection purposes, with Type I systems having slightly more stringent performance requirements. Vehicle speed range to meet functional performance requirements is 10 to 80 mph.
- Type III systems: Suitable for screening vehicles suspected of weight limit or load limit violations. Stricter functional performance requirements than Type I and

Type II systems. Vehicle speed range to meet functional performance requirements is 10 to 80 mph.

- Type IV systems: Not approved for use in the United States but intended for use at weight enforcement stations. Vehicle speed range to meet functional performance requirements is 2 to 10 mph.

In accordance with the Nebraska Truck Information Guide (2022), any vehicle operating with an overweight/over-dimensional permit is required to stop at all open scale facilities. If platoons need to be weighed, a Type III WIM system should be used.

ASTM E1318-09 (ASTM, 2017) sets accuracy standards for sensor type, wheel load, axle load, axle-group load, gross vehicle weight, speed, and axle spacing, as shown in Table 7.1. Accuracy is determined by calculating probabilities that individual axle load measurement errors are within prescribed limits. Maximum CoV_L for static truck WIM weights was determined using GVW tolerance. ASTM E1318-09 specifies that Type III systems must achieve $\pm 6\%$ GVW accuracy at a 95% tolerance. As shown in Figure 7.1, based on a normal distribution mean of 1.0 and 6% GVW accuracy with 95% tolerance, the standard deviation was determined to be 0.031. As a result, the CoV_L was calculated as $Std/Mean = 0.031$. Accordingly, the upper bound CoV_L for static truck weight with Type WIM III systems was inferred to be 0.031.

Table 7.1 ASTM 1318E-09 Functional Performance Requirements for WIM Systems
(Reproduced Based on ASTM, 2017)

Function	Tolerance for 95%		
	Type I	Type II	Type III
Wheel Load	±25%		±20%
Axle Load	±20%	±30%	±15%
Axle-Group Load	±15%	±20%	±10%
Gross Vehicle Weight	±10%	±15%	±6%
Speed	±1 mph		
Axle-Spacing and Wheelbase	±0.5 ft		

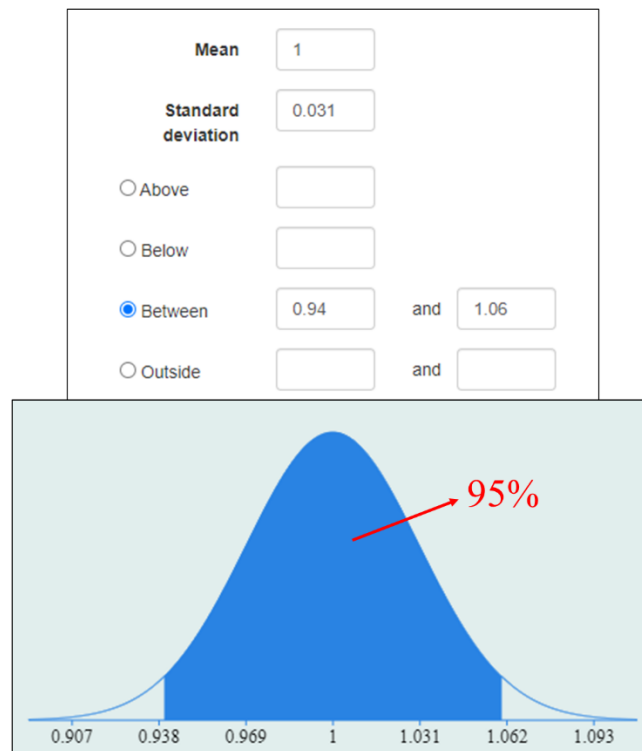


Figure 7.1 Normal Distribution with Mean = 1.0 (95% Compliance)

Trucking companies specify platoon truck axle configurations, number of trucks, gross weight, and headways for a platoon permit. The permitting DOT determines whether trucks in the platoon are legal-load trucks. If so, then CoV_L for static truck weight equals 0.12 from

Kulicki et al. (2007). If a platoon truck exceeds the legal load limit and GVW documentation includes historical WIM data, static weight standard deviation can be calculated directly using Equation 7.4. In Nebraska, if GVW documentation is not available the platoon must stop at all WIM stations according to the Nebraska Truck Information Guide, where WIM sensors are expected to be calibrated and maintained in accordance with ASTM 1318E-09. WIM data records can potentially be used to approximately characterize CoV_L according to Equation 7.4:

$$\sigma = \sqrt{\frac{\sum (x_i - \mu)^2}{N - 1}} \quad 7.4$$

where σ is the standard deviation, x_i is the data set, μ the mean, and N the number of available WIM data records. Figure 7.2 illustrates how CoV_L is determined and used in Equation 7.1 through 7.3.

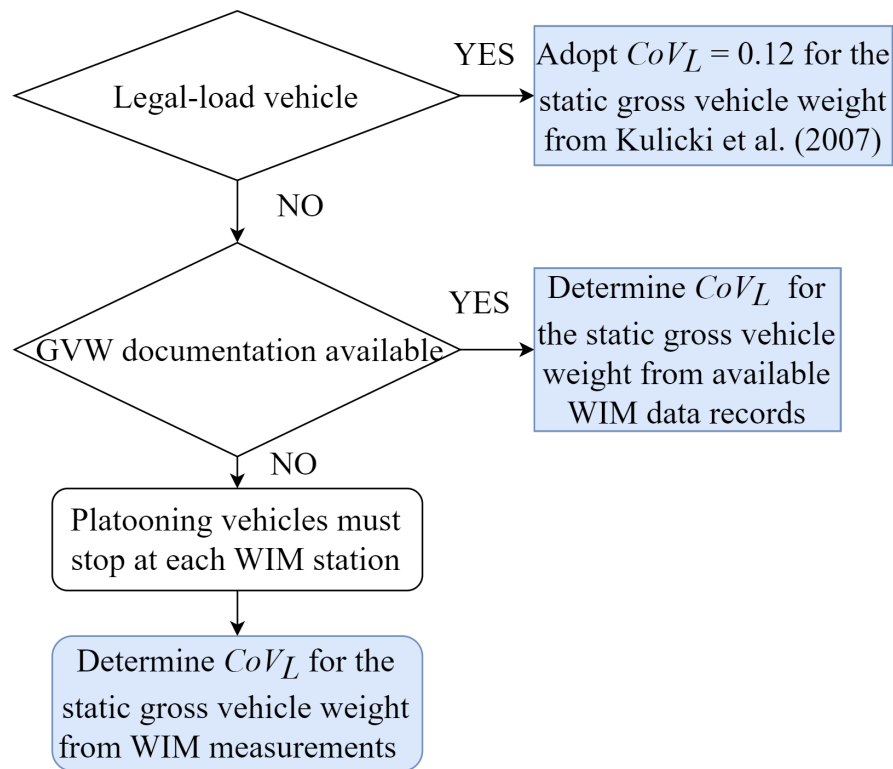


Figure 7.2 Truck Weight Uncertainty Framework

7.4 Dynamic Amplification Uncertainty Framework

Dynamic amplification (i.e., impact factor, IM) should ideally be measured directly from axle load variation using reliable, on-board sensors. Evaluating the dynamic amplification is challenging since vehicle-bridge interaction (VBI) and consequent amplified structural demands are influenced by many parameters, such as bridge dynamic characteristics (mass, stiffness, damping), truck weight, suspension stiffness and damping properties, road roughness, and truck speed. Two predominant methods are currently used to evaluate IMs , with the most reliable being field tests. Analytical studies may provide a less expensive method, but ultimately require experimental validation.

An example of a field test used to assess dynamic amplification was conducted in Ontario during the 1980s based on Billing (1984). The tests covered 27 highway bridges with different construction materials and span lengths, and data were collected for both test trucks and actual traffic. Based on this field-testing program, mean values of IM were found to be approximately 0.05 to 0.10 for prestressed concrete girders and 0.08 to 0.20 for steel girders. Detailed information about procedures for dynamic bridge testing can be found in Paultre et al. (1992), Paultre et al. (1995), as well as Deng et al. (2015).

An analytical study of dynamics typically includes a vehicle model, a bridge model, a road profile model, and a solution for the vehicle-bridge system. Huang and Nowak (1991) simulated dynamic loads on bridges based on truck parameters, including mass, suspension, and tires, as well as the bridge surface. Dynamic amplifications decrease as gross vehicle weights increase, according to Huang and Nowak. Huang and Nowak found that CoV_{IM} varies from 0.40 to 0.70, depending on span length. Detailed information for a rigorous evaluation of bridge dynamics can be found in Deng et al. (2015).

Ling et al. (2022) studied resonance effects of platoons and found that adverse dynamic loading effects can result on existing highway bridges, particularly medium- to long-span bridges with a fundamental frequency below 6.5 Hz. Ling et al. noted that resonance can be attributed to a combination of speed and headway, the number of trucks on the road and road surface conditions. Rigorously performing detailed analyses to evaluate platoon resonance effects is beyond the scope of the present project. Resonant critical truck speeds may be estimated from simple analyses. For example, a two-truck platoon crossing a simple-span bridge is considered in Figure 7.3. Trucks are denoted as $T1$ and $T2$, the distance between them as d , and vehicle speed

v. Assuming the bridge natural frequency is f_1 . The time interval between successive trucks arriving at midspan can be calculated using Equation 7.5. Rearranging provides truck excitation frequency, truck, as shown in Equation 7.6, and resonance will occur when the truck excites a bridge at its natural frequency, f_1 . Finally, critical speeds that may cause resonance are determined according to Equation 7.7.

$$t = \frac{d}{v} \tag{7.5}$$

$$\left[f_{truck} = \frac{v}{d} \right] = f_1 \tag{7.6}$$

$$v_{critical} = (f_{truck} = f_1)d \tag{7.7}$$

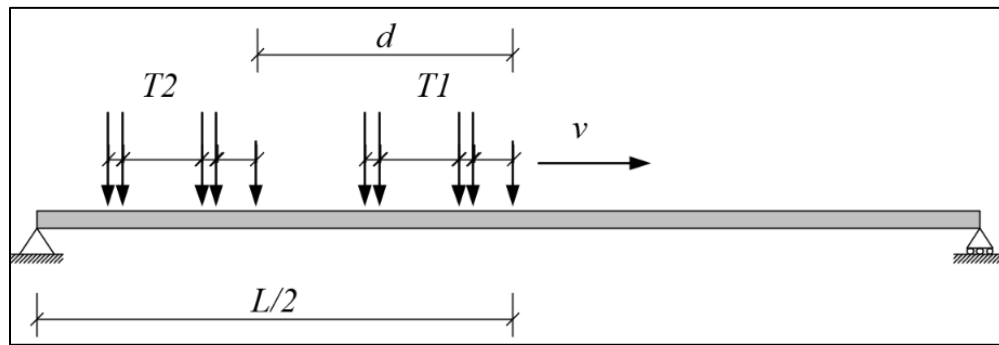


Figure 7.3 Two-truck Platoon on a Simple-span Bridge

A general framework for determining CoV_{IM} and μ_{IM} is presented in Figure 7.4. A trucking company specifies planned platoon truck characteristics, number of trucks, gross weight, and headways. The rating engineer can obtain bridge natural frequencies from free vibrations using a variety of instruments and methods as reported in Linzell et al. (2021) and then determine critical platoon speed for each bridge on the planned route using Equations 7.5

through 7.7 to avoid resonance effects. Bridge natural frequencies can be rigorously determined by conducting FEM modal analyses and/or spectrum analyses of measured accelerations from moving load tests, if available. Alternatively, bridge fundamental frequencies may be estimated using formulations available in literature. Hwang and Nowak (1990) used the following equation in a study related to bridge dynamics:

$$f = 95.4 \times L^{-0.933} \tag{7.8}$$

The equation was extracted from a Swiss report by Cantieni (1983) and reflected measured frequency data for 224 in-service bridges that may or may not be applicable to US or particular states' typical designs. Alternatively, Cantieni also recommended using a classical beam vibration formulation:

$$f = \frac{\pi}{2L^2} \sqrt{\frac{EI}{m}} \tag{7.9}$$

where f is the natural frequency and L is the span length, or conservatively the maximum span length for multi-span continuous bridges, EI is the bending stiffness, and m is the mass per unit length.

In the absence of test data and corresponding calibrated analytical models, a $CoV_{IM} = 0.80$ and $\mu_{IM} = 0.10$ can be directly adopted from Nowak (1999) and Kulicki et al. (2007). Figure 7.4 illustrates how CoV_{IM} and μ_{IM} are determined and used in Equations 7.1 through 7.3. Testing

at a specific bridge, for a specific platoon, and operating at a specific speed, could provide updated *IM* characterization for that single, narrow set of conditions. However, many such tests would be required to update *IM* for a full transit corridor over multiple bridges, each with their own dynamic characteristics and differing responses to even a single platoon configuration and speed. Further research will be necessary to improve characterization for *IM* broadly for a range of platooning operations and including multiple bridges.

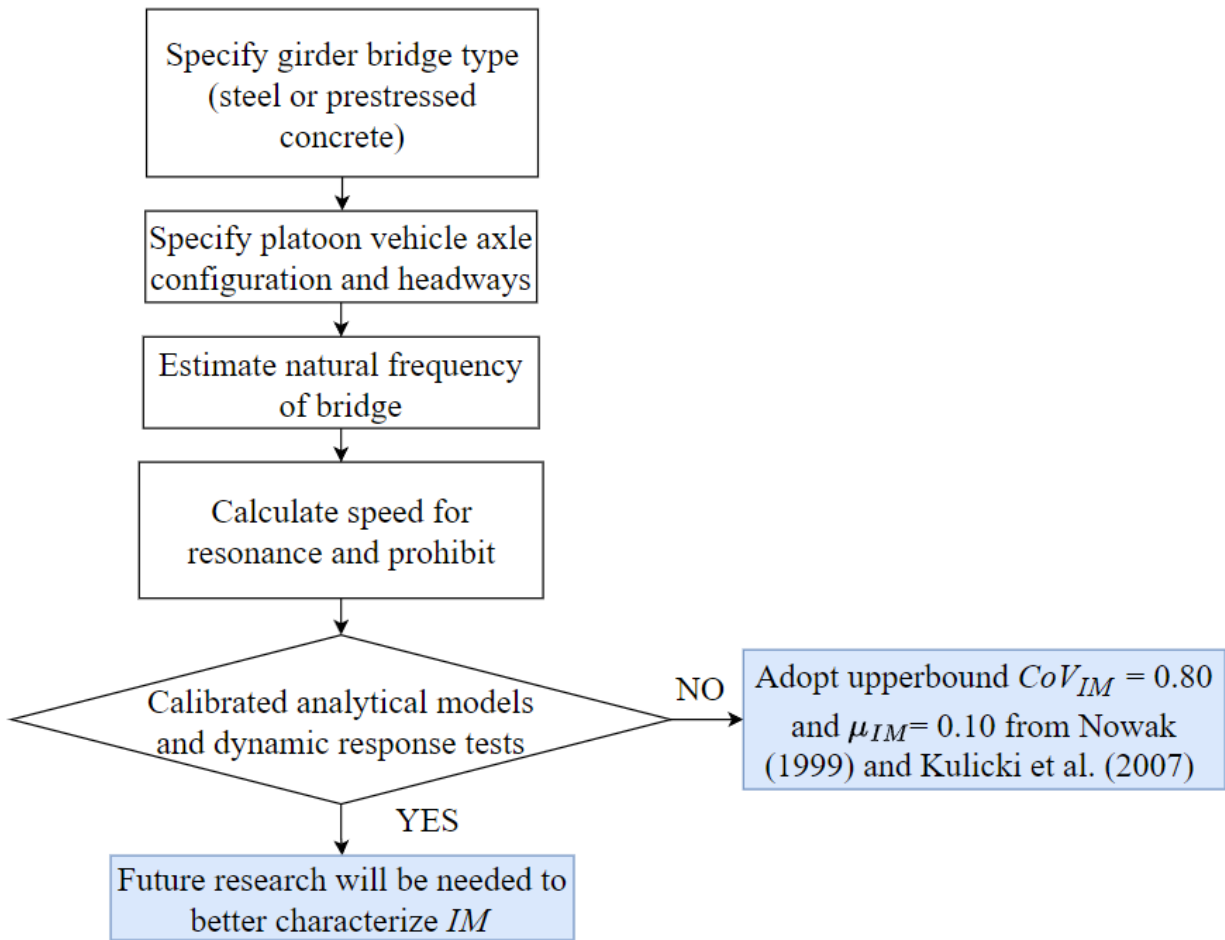


Figure 7.4 Dynamic Allowance Uncertainty Framework

7.5 Girder Distribution Factor Uncertainty Framework

The girder distribution factor (*GDF*) represents the proportionate share of load carried by the most heavily loaded girder, characterized as a decimal number of loaded lanes, and serves to establish moment and shear effects for girder design and evaluation. Analytical methods, finite-element analyses, and field tests have been widely used to simplify the analysis of transverse effects caused by live loads.

Considering the conservative nature of *LRFD BDS GDF* formulas, Puckett et al. (2007) used actual bridges to conduct a rigorous, calibrated finite element method analysis to propose new simplified *GDF* equations. Calibrated *GDF* results were compared to Standard Specification equivalent *GDF* and *LRFD BDS GDF* values for steel and prestressed concrete bridges. *GDF* bias (λ_{GDF}) can be obtained by dividing the field measured *GDF* values by the *LRFD BDS GDF*. Table 7.2 shows that λ_{GDF} ranges from 0.72 to 0.90 for single-lane and multiple-lane loaded cases, indicating that the *LRFD BDS GDF* values are conservative. *GDF* average *CoV* (CoV_{GDF}) is 14%, with a range of 11% to 18%. Note the λ_{GDF} was assumed to be 1.0 for live load calibrations in this project. The rating factor can be modified based on calculated λ_{GDF} in the future.

This study assumed a calibrated finite element analysis (FEM) can be used for platoon rating, with a calculated *GDF* being used to represent actual *GDFs* and with $CoV_{GDF} = 0.08$. This assumption is based on Sivakumar et al. (2011) and Ghosn (2019). A normal probability distribution was assumed for the *GDF* according to Ghosn (2019).

Table 7.2 Comparison of Field-Measured *GDF* to *LRFD BDS GDF* (Reproduced Based on Ghosn, 2019 and Puckett et al., 2007)

		$\lambda_{GDF} = \text{Field results/AASHTO GDF}$			
		Moment		Shear	
Bridge type	Statistic	1 lane	2 or more lanes	1 lane	2 or more lanes
Steel	Average	0.78	0.90	0.72	0.82
	CoV	11%	14%	14%	18%
Prestressed concrete I-girder	Average	0.78	0.90	0.77	0.88
	CoV	12%	13%	11%	16%

It should be noted that CoV_{GDF} for platoons may potentially be adjusted by accounting for transverse truck location on the bridge determined from sensors. Rigorously investigating GDF uncertainty and its sensitivity to various structural characteristics were beyond the scope of the present project.

The general framework for determining CoV_{GDF} and λ_{GDF} is proposed in Figure 7.5. The trucking company specifies platoon truck configurations, the number of trucks, gross truck weights, and headways. In the absence of field tests and calibrated models, there are two typical scenarios for determining the CoV_{GDF} and λ_{GDF} . Option 1 is to directly adopt both CoV_{GDF} and λ_{GDF} as presented in Table 7.2 from Puckett et al. (2007). For Option 2, it is also possible for the rating engineer to use an uncalibrated 3D finite element model (from AASHTOWare™ or other similar software) to determine GDF and λ_{GDF} directly, and to then adopt only CoV_{GDF} from Table 7.2. Future WIM technology might reduce the CoV_{GDF} to zero. According to Gilbert (2022), an upcoming technology called mobile WIM places sensors on vehicles that measure the condition of bridges as they pass over them. Smart trucks may be outfitted with image sensing such as LiDAR or photogrammetry so that the truck's position can be known and potentially guided to minimize critical girder structural demands. Two options exist if load testing and calibrated models are available. If platoon transverse location on the bridge is not known, then the GDF obtained from a calibrated FEM analysis can be directly used as the mean with a $CoV_{GDF} = 0.08$ from Sivakumar et al. (2011) and Ghosn (2019). The CoV_{GDF} could be reduced to zero in the future if a platoon's transverse location is known using mobile WIM technology as discussed in Gilbert (2022). Figure 7.5 illustrates how CoV_{GDF} is determined based on the availability of

calibrated analytical models, field tests, and the future mobile WIM technology. The determined CoV_{GDF} can then be used in Equations 7.1 through 7.3 to determine the total CoV for platoons.

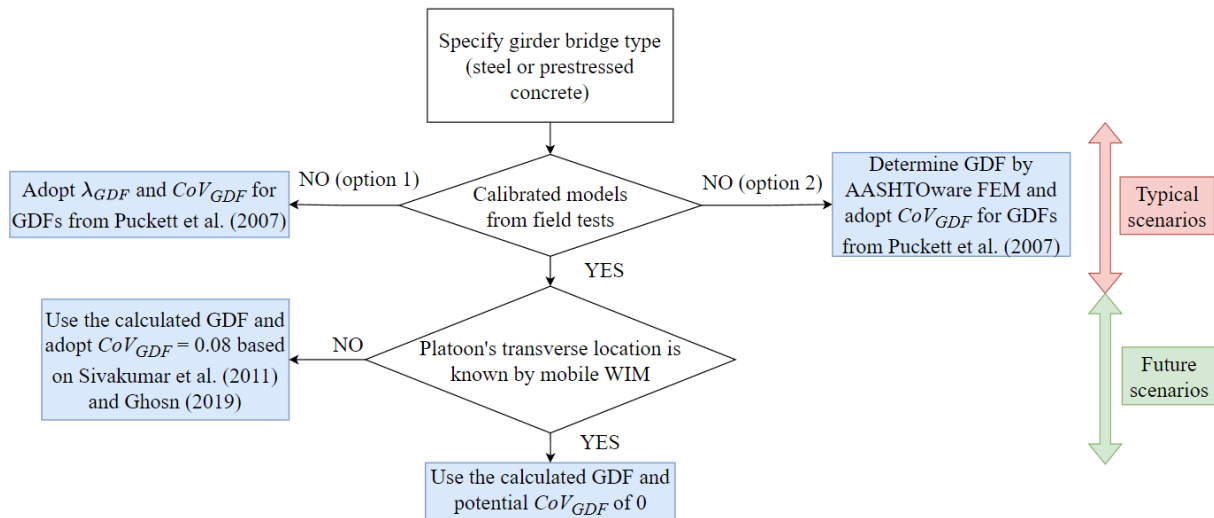


Figure 7.5 Girder Distribution Factor Uncertainty Framework

7.6 Sensitivity Analysis for Platoon Uncertainty

Table 7.3 presents results for various combinations of CoV_L , CoV_{IM} , μ_{IM} , and CoV_{GDF} used in Equations 7.1 through 7.3 to evaluate sensitivity of total platoon LL CoV . For the first scenario, μ_{IM} was assumed to be 0.10 and $CoV_{IM} = 0.80$ without resonance based on Nowak (1999) and Kulicki et al. (2007), and $CoV_{GDF} = 0.12$ from Kulicki et al. (2007). The A , B , and CoV_{L_GDF+IM} were then determined using Equations 7.1 through 7.3. For this scenario, the total $CoV_{L_GDF+IM} = 0.19$. CoV_L , CoV_{IM} and CoV_{GDF} were then independently set to zero to investigate their effects on total CoV_{L_GDF+IM} . For example, CoV_{L_GDF+IM} would reduce to 0.17 if CoV_{IM} was zero. However, if either CoV_L or CoV_{GDF} equaled zero, CoV_{L_GDF+IM} would reduce to 0.14, which indicated that CoV_L and CoV_{GDF} are more influential on total CoV_{L_GDF+IM} than CoV_{IM} .

There was no discernable difference between effects of CoV_L and CoV_{GDF} on total CoV_{L_GDF+IM} (Table 7.2).

Table 7.3 Sensitivity Analysis for Different Terms in Determining Platoon Uncertainty

μ_{IM}	CoV_L	CoV_{IM}	CoV_{GDF}	A	B	CoV_{L_GDF+IM}
0.10	0.12	0.80	0.12	0.03	0.66	0.19
0.10	0.00	0.80	0.12	0.01	0.65	0.14
0.10	0.12	0.00	0.12	0.03	0.00	0.17
0.10	0.12	0.80	0.00	0.01	0.65	0.14
0.10	0.00	0.00	0.12	0.01	0.00	0.12
0.10	0.12	0.00	0.00	0.01	0.00	0.12
0.10	0.00	0.80	0.00	0.00	0.64	0.07
0.10	0.00	0.00	0.00	0.00	0.00	0.00

7.7 Summary

A framework for aggregating LL uncertainties based on truck weight, dynamic amplification, and girder distribution factor was presented. Using the proposed framework, calibrated LL factors may be determined for different $CoVs$ for strength and service. The proposed framework is preliminary and will need to be refined in future research as the availability of WIM data increases and complexity associated with evaluating platoon dynamic allowances and girder distribution factors from field data is addressed. A sensitivity analysis was conducted to evaluate the effects of truck weight, dynamic amplification, and girder distribution factor uncertainties on total platoon uncertainty. Results indicate that uncertainties associated with truck weight and girder distribution factors effects on total platoon CoV are appreciable and identical, while those associated with dynamic amplification are less influential on total platoon CoV .

Chapter 8 Illustrative Examples for Platoon Evaluation

8.1 Overview

This chapter presents four representative steel and prestressed concrete girder bridges from the Nebraska inventory and load rated for strength and service limit states. Evaluations generally followed the LRFR procedure according to the *MBE* (2018). Calibrated strength and service *LL* factors were implemented from Table 2.2, Table 5.9, and Table 5.10. Additionally, this chapter discusses the influence of platoons on fatigue at steel bridge welded cross-frame connection plates and shear studs. A cumulative fatigue damage assessment was conducted for a platoon with 5-ft and 50-ft headways and compared to an AASHTO fatigue truck. Detailed computations for the examples are provided in Appendices C through F.

8.2 Prestressed Concrete Simple-Span Bridge (S080 41653)

Bridge S080 41653 is a 130-ft simple-span, prestressed multi-girder bridge at the I-80 4S Greenwood Interchange in Greenwood, Nebraska (Figure 8.1). The bridge was constructed in 2009 and has three design lanes, and the average daily traffic is 49,240. The rating code in NBI (2022) indicates that the rating method is LRFR.

The example illustrates design and platoon ratings of an interior prestressed concrete girder at midspan (@ 0.5L) for positive moment, at the first critical shear section, and at a location where vertical shear reinforcement spacings change. Elastic gains from dead and live loads were considered. The analysis was based on the gross section properties. Shear resistance was calculated using the simplified and general modified compression field theory (MCFT). Prestress losses were calculated using refined estimates described in LRFD BDS Article 5.9.3.4. HL-93 design and platoon rating factors were computed for Strength I and Service III.

The bridge was rated for Service I, treating the platoon as a permit load case according to the MBE. A brief description of the bridge and resulting ratings are provided below, and Appendix C provides detailed computations.



Figure 8.1 Prestressed Concrete Simple-Span Bridge (S080 41653) (Google Map, 2023)

8.2.1 Bridge Details

The bridge has a 10-degree skew, as shown in Figure 8.2, which was ignored. It is comprised of six NU-1600 girders spaced at 11 ft (Figure 8.3). The average deck thickness is 8 in., and overhangs are 3 ft-10 in. (Figure 8.3). The haunch thickness between the girder's top and the slab's bottom is 1 in. (Figure 8.3). Final and initial girder concrete strengths were 9.5 ksi and 7.5 ksi, respectively. The deck design strength is 4 ksi.

Grade 270 0.6-in low-relaxation strands having a modulus of elasticity of 28,500 ksi were used. The initial stress at transfer (f_{pi}) was assumed to be 0.75, the ultimate tensile strength (f_{pu}) and 52 strands were used, with the strands in 5 layers (Figure 8.4). Bottom concrete cover was 2 in., and distance between prestressing layers was 2 in. Ten strands were harped 52.4 ft from the ends (Figure 8.4). The allowable tensile stress was set to $0.19\sqrt{f'_c}$ (ksi). Participation of mild reinforcing steel in girder cross-sectional resistance was ignored.

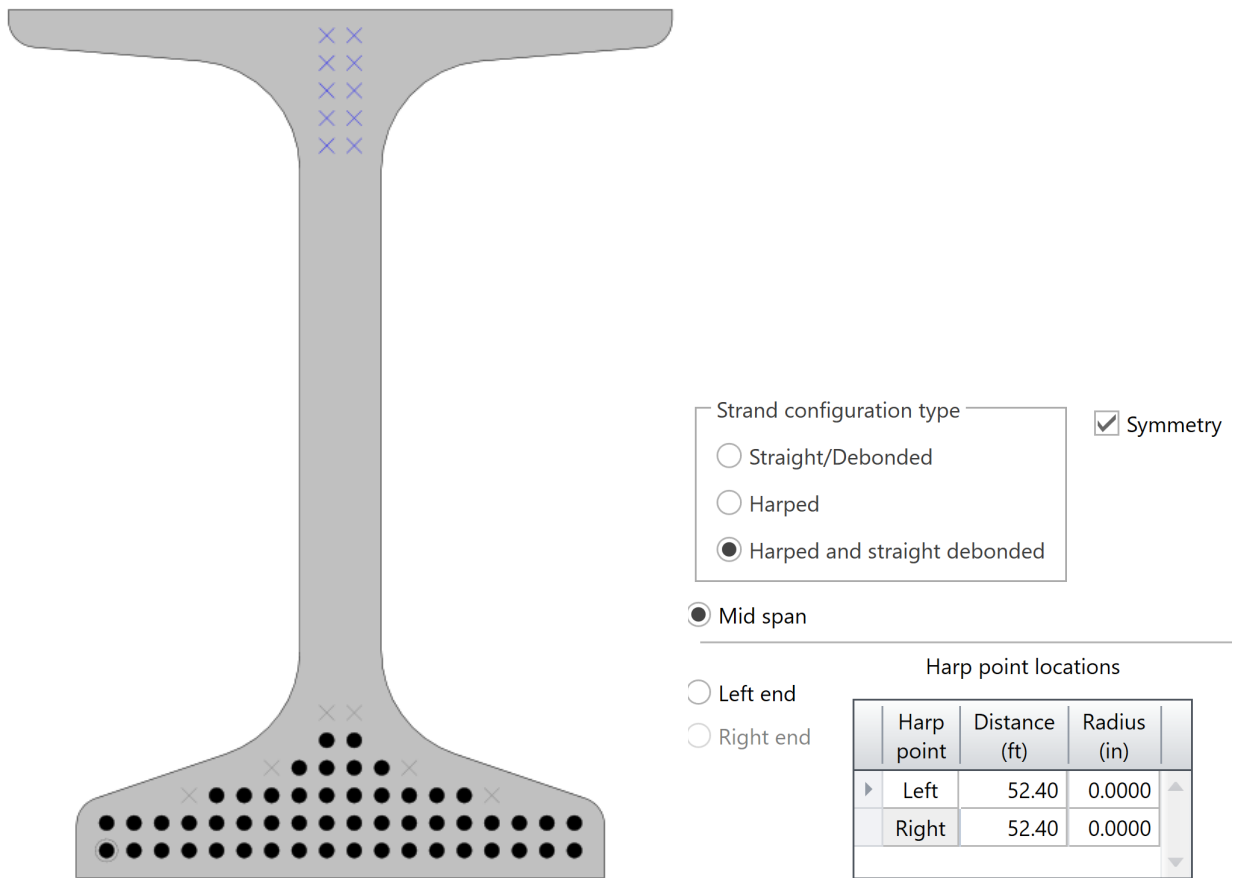


Figure 8.4 Bridge Girder Details for S080 41653 (AASHTOWare™ BrR, 2023)

Wire fabric (70 ksi) was used as shear reinforcement, and the BrR does not readily support this. In BrR and the example computations, shear reinforcement was modeled using 3.1 legs. Similarly, 1.80 legs were used for other locations. Vertical shear reinforcement details and spacings are shown below (Figure 8.5).

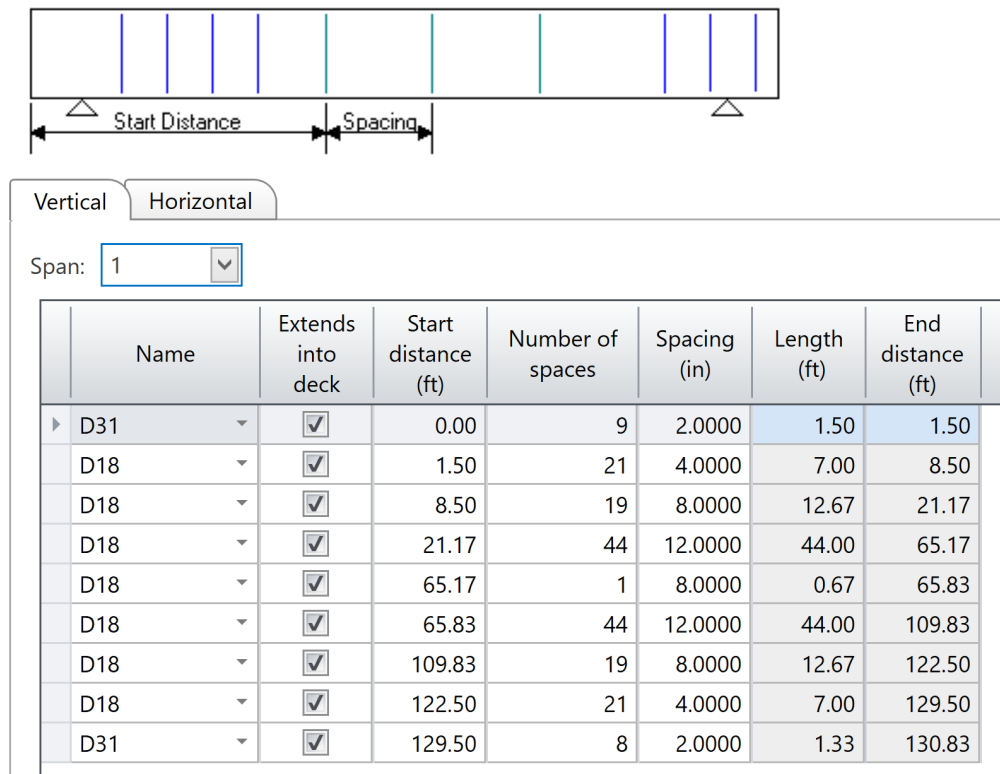


Figure 8.5 Vertical Shear Reinforcement Ranges (AASHTOWare™ BrR, 2023)

8.2.2 Vehicle Details

HL-93 loading, assuming multiple-lanes loaded, was used to determine the GDF based on *LRFD BDS* Table 4.6.2.2.2b-1 for Strength I moment and shear. According to the *LRFD BDS* Article 3.6.2.3, the dynamic load allowance for HL-93 is 33%. The same load model was used for the Service III inventory rating.

The platoon rating was based on a single-lane loaded four-truck (legal load platoon) at a 5-ft headway with routine traffic in the adjacent lane. An upper bound CoV of 0.20 was used. One hundred platoons per day were assumed, and the ADTT for adjacent lanes was 5000. The platoon truck was based on the NRL, see Figure 3.1. The dynamic allowance, IM, was assumed to be 0.33 based on MBE permit load rating. The platoon rating used a single-lane loaded GDF from LRFD BDS Table 4.6.2.2.2b-1 and removed the 1.20 multiple presence factor.

As the strength and service calibrated LL factors for single-lane loaded platoons with routine traffic in the adjacent lane have been implicitly considered ADTT of adjacent lane traffic and platoon crossing per day during calibration, the LL effects of adjacent lane traffic have not been considered separately. The details of the characteristics of adjacent traffic are provided in Steelman et al. (2021).

8.2.3 Moment and Shear Rating Check Locations

Design and platoon ratings were for an interior girder at 0.5L span (65 ft to the centerline of support) for positive moment, at the first critical shear section (5.87 ft to centerline of support), and at one a change in shear reinforcement spacing (8 ft to centerline of support) (see Figure 8.6). The first critical shear point was determined based on the effective shear depth (d_v) per LRFD BDS Article 5.7.2.8, plus the distance from the face of the support to the centerline of the bearing (6 in). A second point of interest where shear reinforcement spacing changed from 4 to 8 in. was also provided (8.5 ft from the beam end) (Figure 8.5).

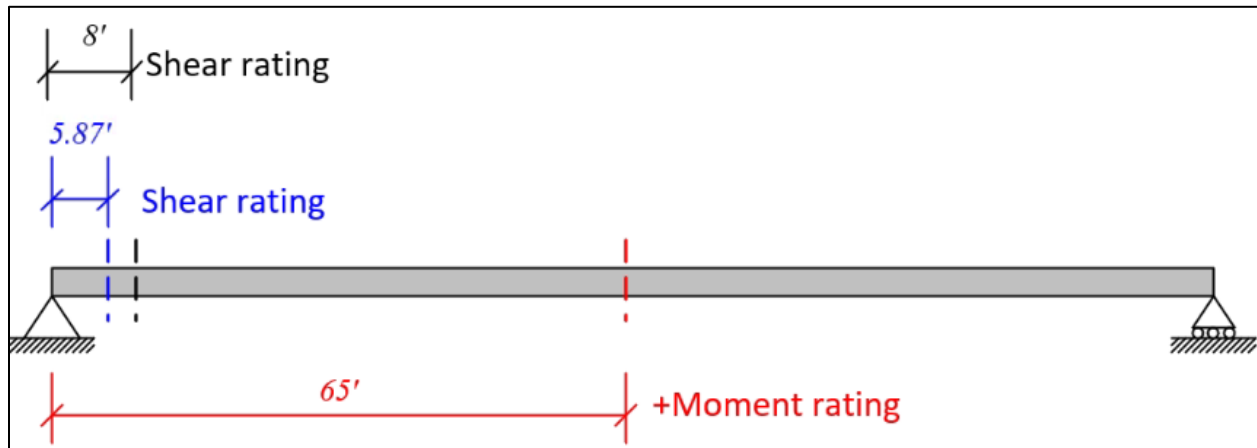


Figure 8.6 Moment and Shear Rating Check Locations

8.2.4 Moment and Shear Rating Check Results

Strength I moment, shear, and Service III moment load factors for design rating were taken from MBE Table 6A.4.2.2-1. For platoons, Strength I moment and shear *LL* factors (target $\beta = 2.5$) were obtained from Table 2.2 (Steelman et al., 2021). Service III moment *LL* factors (target $\beta = -0.6$) for platoons were based on Table 5.9. MBE Article 6A.5.4.2.2b specifies Service I limit state for the permit rating that prestressing steel closest to the extreme tension fiber of the member should not exceed 0.90 of its yield stress. MBE C6A.5.4.2.2b states an alternative method for checking Service I that limits unfactored moments to 75% of the nominal flexural capacity. This rating example used this alternative method, which limits the unfactored moment, to rate platoons for Service I.

As shown in Table 8.1, Service III governed the platoon rating, and shear rating factors for the two checked locations were similar. Table 8.2 shows that all rating factors exceed 1.0, indicating that this bridge can accommodate the design loads and a four-truck (legal load platoon) at a 5-ft headway with traffic in the adjacent lane. See Appendix C for details.

Table 8.1 Rating Factors for Different Limit States

Limit state	Design load rating		Platoon load rating (Strength I $\beta_{target} = 2.5$ and Service III $\beta_{target} = -0.6$)
	Inventory	Operating	
Strength I for Design and platoon load rating			
Flexure (at midspan)	1.656	2.146	2.088
Shear at (5.87 ft to the centerline of support)	1.354	1.755	1.403
Shear at (8 ft to the centerline of support)	1.377	1.785	1.443
Service III			
Flexure (at midspan)	1.427		1.062
Service I			
Flexure (at midspan)			Stress ratio = 1.177

8.3 Prestressed Concrete Continuous Span Bridge

Bridge S080 41465 is a 170-ft (42.5'-85'-42.5') three-span, prestressed multi-girder bridge at the I-80 5N Waverly Interchange in Waverly, Nebraska (Figure 8.7). According to the National Bridge Inventory (NBI) (2022), the bridge was constructed in 2009 with three design lanes, and the average daily traffic is 49,240. The rating code in NBI (2022) indicates that the rating is LRFR.

The example illustrates the design and platoon ratings of an interior prestressed concrete girder at 0.5L of the interior span for positive moment, at the interior support for negative moment, at the first critical shear section, and one of the changes in vertical shear reinforcement spacing. For this example, the interior span was used. The bridge was simple-span for dead load and made continuous for live load. The elastic gains from dead and live loads were considered when calculating prestress loss. The analysis was based on the gross section properties. The shear resistance was calculated using the simplified and general MCFT methods. Prestress losses were calculated using the refined estimates described in LRFD BDS Article 5.9.3.4. Strength I and Service III rating factors for HL-93 inventory and platoon loads were computed. Considering the platoon as a future permit truck, the Service I rating was performed as the permit rating in

MBE (2018). A brief overview of the bridge and resulting ratings is provided below. Appendix D provides the details.



Figure 8.7 Prestressed Concrete Continuous Span Bridge (S080 41465) (Google Map, 2023)

8.3.1 Bridge Details

The bridge has no skew (Figure 8.8). It is comprised of six NU-900 girders spaced at 11 ft (Figure 8.9). The average deck thickness is 8 in., and the overhangs are 3 ft-10 in (Figure 8.9). The haunch thickness is 1 in. (Figure 8.9). Final and initial concrete strengths for the girder are 9 ksi and 7 ksi, respectively. The concrete design strength for the deck is 4 ksi.

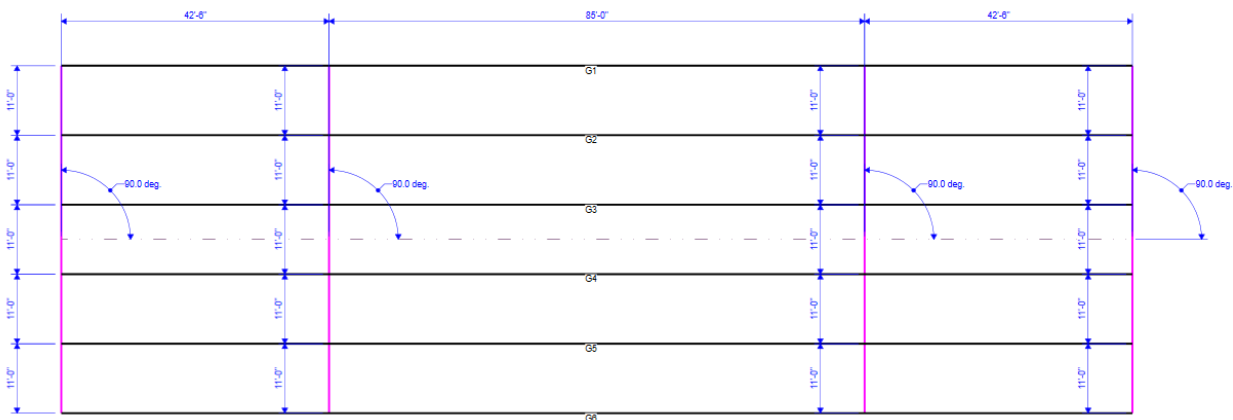


Figure 8.8 Bridge Plan View for S080 41465 (AASHTOWare™ BrR, 2023)

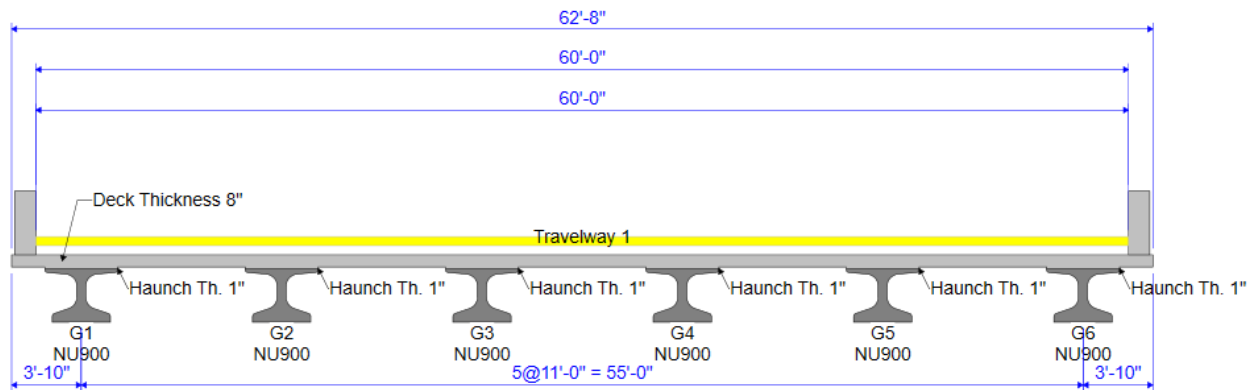


Figure 8.9 Bridge Cross Section for S080 41465 (AASHTOWare™ BrR, 2023)

Grade 270 0.6-in low-relaxation strands having a modulus of elasticity of 28,500 ksi were used. The initial stress at transfer (f_{pi}) was assumed to be 0.75 of the ultimate tensile strength (f_{pu}), and 38 strands were used, with the strands in three layers (Figure 8.10). The bottom concrete cover was 2 in., and the distance between prestressing layers was 2 in. Six strands were harped 33.73 ft from the ends (Figure 8.10). The non-prestressed reinforcement in the beam was considered for the negative moment region. The allowable tensile was set to $0.19\sqrt{f'_c}$ (ksi). Participation of mild reinforcing steel in girder cross-sectional resistance was ignored.

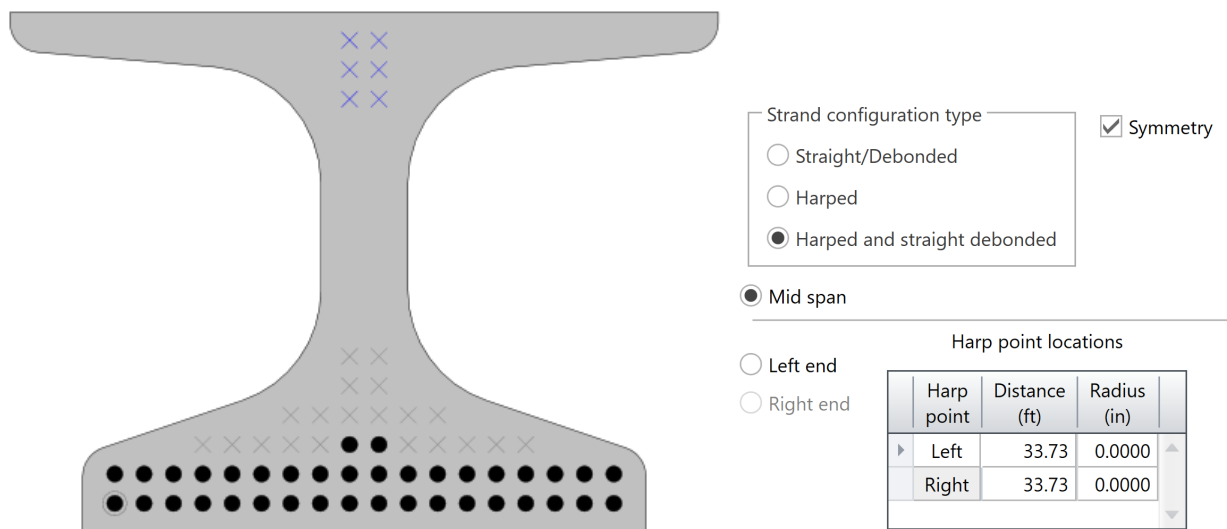


Figure 8.10 Bridge Girder Details for S080 41465 (AASHTOWare™ BrR, 2023)

Shear was checked at two locations. Welded wire fabric (WWF) (70 ksi) was used. At the support ends, the WWF was modeled with 2.8 legs (#4 bars); this was to use BrR that does not directly model WWF. 1.80 legs (#4 bars) were used for other locations (Figure 8.11).

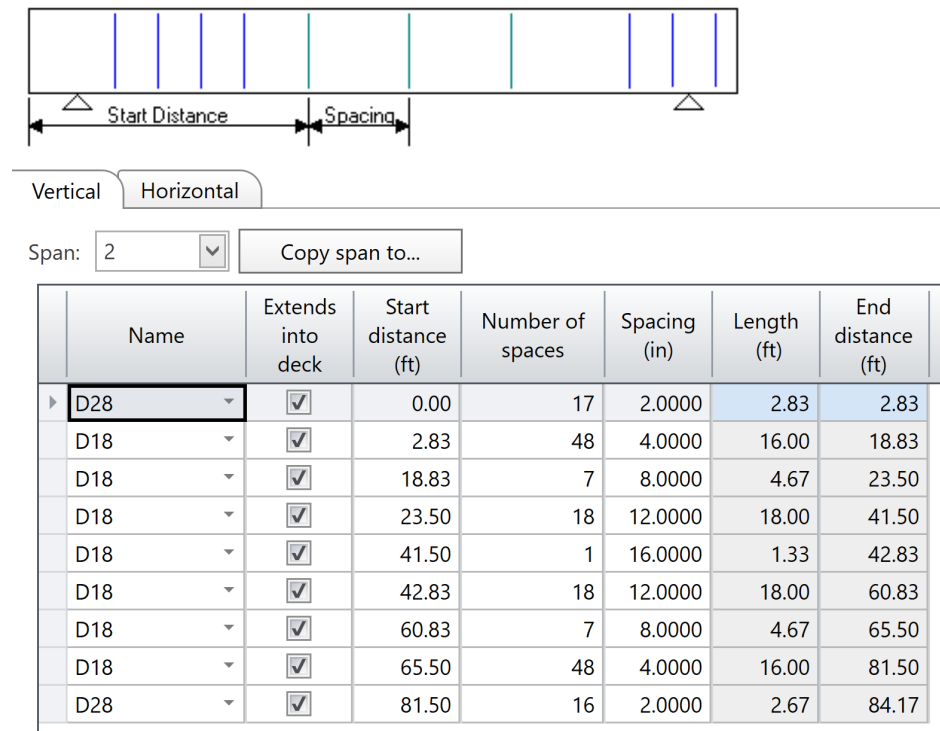


Figure 8.11 Vertical Shear Reinforcement Ranges (AASHTOWare™ BrR, 2023)

8.3.2 Vehicle Details

The HL-93 was used for inventory ratings. The combination includes 90% of the effect of two design trucks having a 14-ft spacing between the 32-kip axles and a minimum headway of 50 ft between the trucks, which were spaced to create maximum loading effects plus 90% of the design lane load.

Platoon characteristics were described previously. Critical negative moments may occur for continuous-span bridges when adjacent spans are loaded. Accordingly, platoons with a 5-ft headway may not result in this example's critical negative moment rating factors, as this example was intended to demonstrate the use of LL factors for platoon permits. The rating engineers can use AASHTOWare™ BrR to evaluate critical LL effects for platoons on a particular bridge.

8.3.3 Moment and Shear Rating Check Locations

Design and platoon ratings were for an interior prestressed concrete girder at $0.5L$ of interior span (85 ft to the centerline of the left beam end support) for positive moment, at the interior support for negative moment, at the first critical shear section (3.93 ft to the centerline of the left interior support), and at one of the changes in vertical shear reinforcement spacing (18.33 ft to the centerline of the left interior support) (Figure 8.12). At the negative moment section, the compression face was the bottom flange. The non-prestressed reinforced concrete section was used when evaluating the interior support negative moment resistance. For example, a shear rating was provided where the spacing changed from 4 to 8 in. (18.33 ft to the centerline of the left interior support) (Figure 8.11). The procedure for checking shear at other locations is similar.

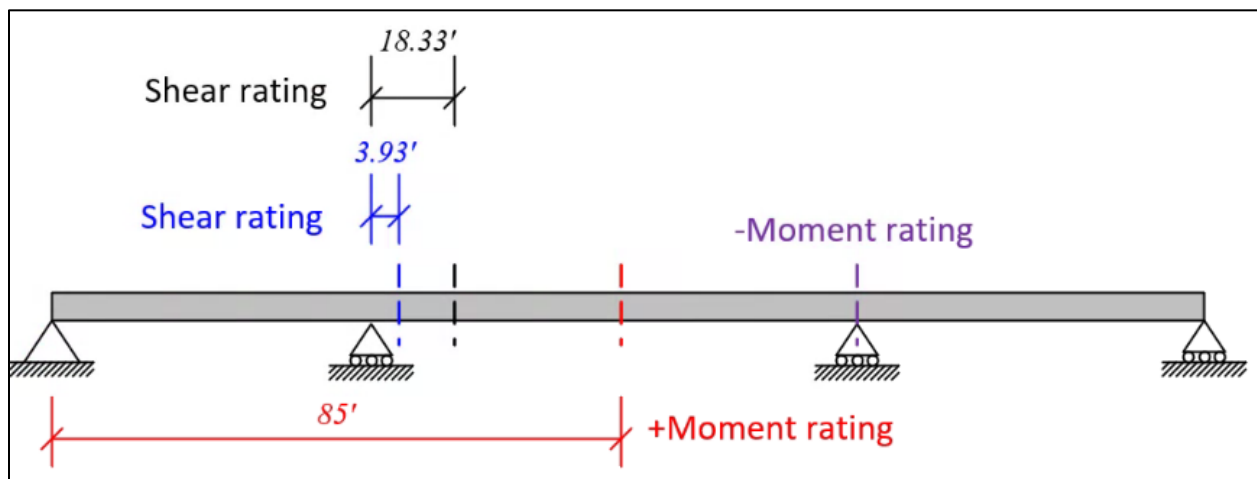


Figure 8.12 Moment and Shear Rating Check Locations

8.3.4 Moment and Shear Rating Check Results

The design and platoon load factors were the same as above. Table 8.2 provides the rating factors for different limit states where all the rating factors were greater than 1.0 for a single-lane loaded four-truck platoon (legal-load platoon) with 5-ft headways mixed with traffic in adjacent lanes.

Table 8.2 Rating Factors for Different Limit States

Limit state	Design load rating		Platoon load rating (Strength I $\beta_{target} = 2.5$ and Service III $\beta_{target} = -0.6$)
	Inventory	Operating	
Strength I for Design and platoon load rating			
Flexure (at the 0.5L of the interior span)	2.562	3.321	4.474
Flexure (at interior supports)	1.922	2.491	2.429
Shear at (3.93 ft to the centerline of interior supports at the interior span side)	1.629	2.111	2.156
Shear at (18.33 ft to the centerline of interior supports at the interior span side)	1.500	1.944	2.271
Service III			
Flexure (at midspan)	2.108		2.171
Service I			
Flexure (at midspan)			Stress ratio = 1.774

8.4 Steel Simple-Span Bridge

Bridge S080 00526 is a 100-ft simple-span, steel welded plate-girder bridge at the I-80 3W Bushnell Interchange in Bushnell, Nebraska, constructed in 1970 (Figure 8.13). The bridge has two design lanes (HS20) and an average daily traffic of 8,115. The bridge was later widened by replacing existing girders and adding a new girder. The original girders were 36 ksi steel, whereas the new girder is ASTM (2021) A709-50W.

The bridge's load factor rating is LFR. However, the LRFR rating method was used here. Steelman et al. (2021) indicated that rating factors for LRFR and LFR differ due to LL components, GDF, impact factors, and resistance effects. A calibrated LFR method that accounts

for the bias of LFR GDFs relative to LRFR GDFs for different limit states is needed (Steelman et al., 2021). It is beyond this project's scope to calibrate *LL* factors for LFR.

The example below illustrates an interior steel girder's design and platoon ratings at the interior span ($0.5L$) for positive moment and at the beam end supports for shear. Rating factors for the Strength I and Service II limit states were provided for HL-93 design and platoon loads. Fatigue I and Fatigue II for the AASHTO fatigue truck and platoons with 5- or 50-ft headways were considered to evaluate the welded cross-frame connection plate at a typical cross-frame location. The fatigue damage ratios for a single crossing of a four-truck platoon with a 5- or 50-ft headway and an AASHTO fatigue truck were determined. This rating example also considered Fatigue I and Fatigue II for shear studs at the beam end, based on AASHTO fatigue truck and platoons with a 5-ft headway. The ratings are provided below. Appendix E provides detailed computations.



Figure 8.13 Steel Welded Plate Girder Simple-Span Bridge (S080 00526) (Google Map, 2023)

8.4.1 Bridge Details

The bridge is straight, as shown in Figure 8.14. It is comprised of six steel plate girders spaced at 8 ft-2in. (Figure 8.15). The average deck thickness is 7.5 in., and overhangs are 2 ft-11

in (Figure 8.15). The interior girder (G2) was rated, and the haunch is 1 in. (Figure 8.15). The yield stress for this girder is 36 ksi, and the concrete strength for the deck is 4 ksi. Two types of girder sections are used for the interior girder G2, as shown in Figure 8.16.

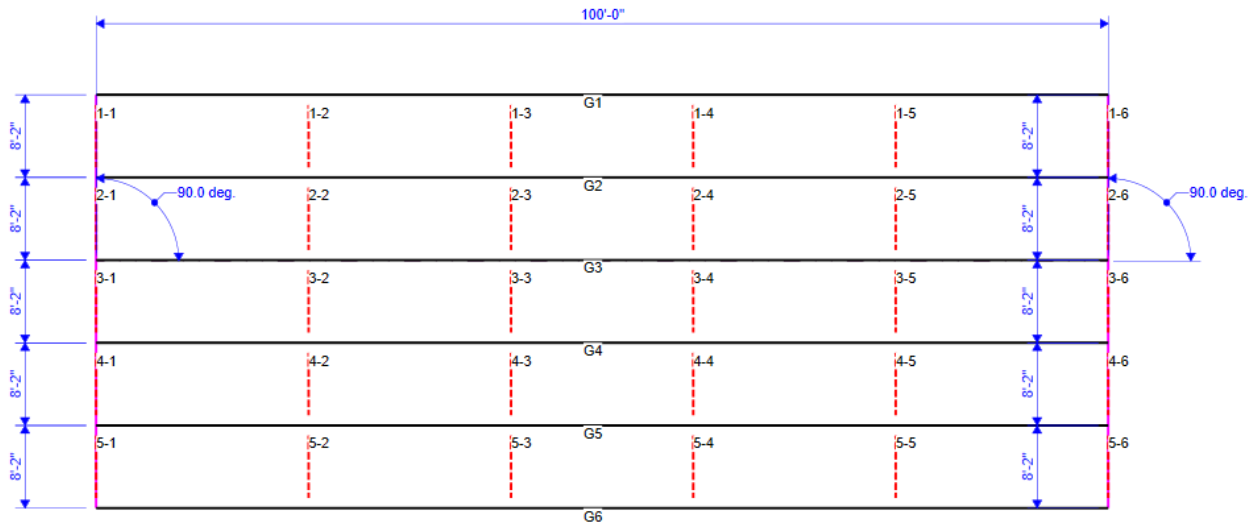


Figure 8.14 Bridge Plan View for S080 00526 (AASHTOWare™ BrR, 2023)

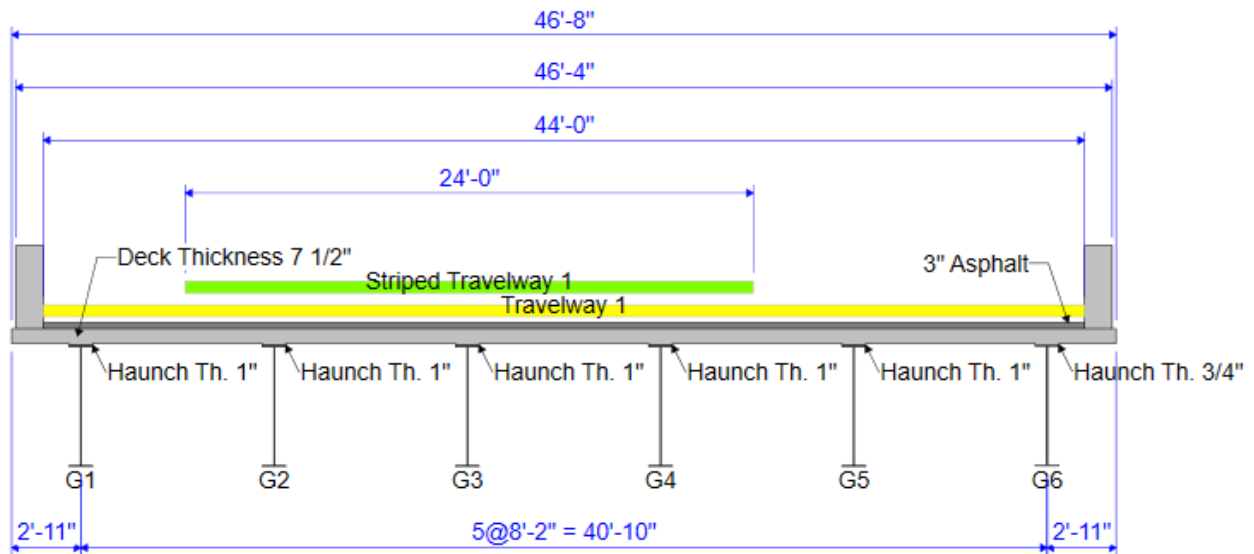


Figure 8.15 Bridge Cross Section for S080 00526 (AASHTOWare™ BrR, 2023)

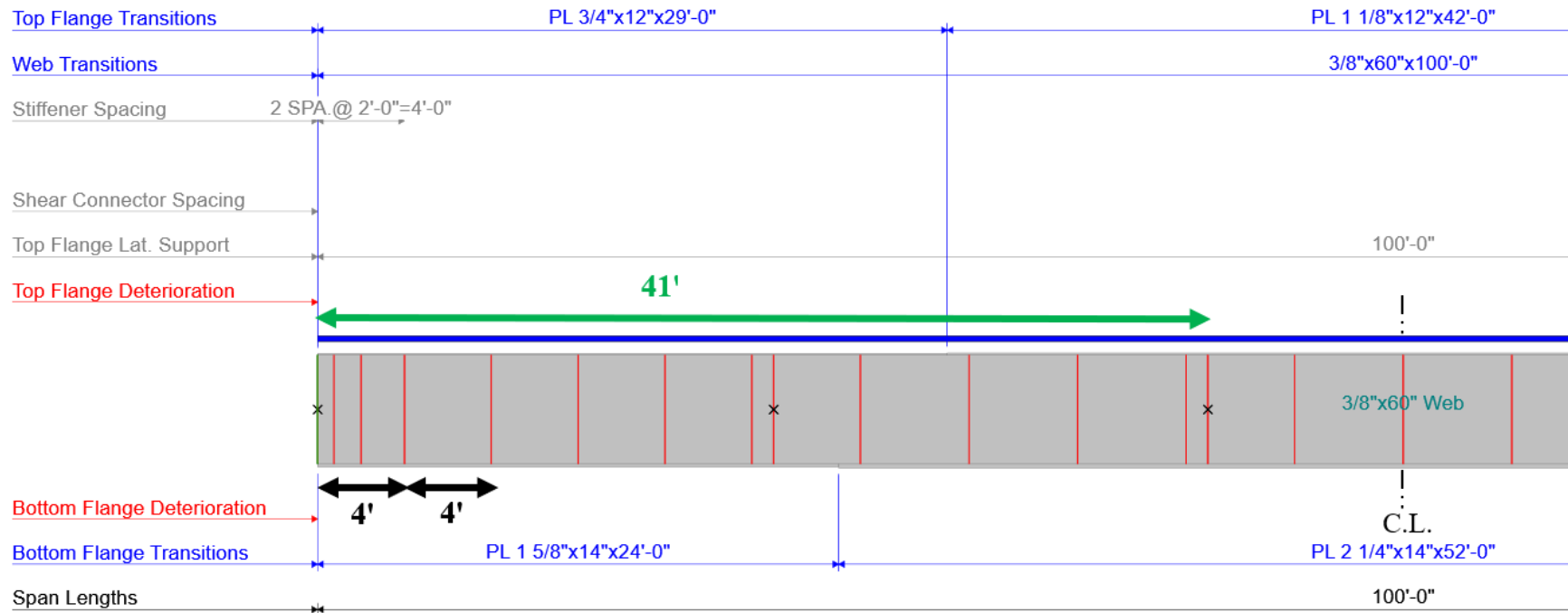


Figure 8.16 Bridge Girder Details for S080 00526 (AASHTOWare™ BrR, 2023)

8.4.2 Vehicle Details

As before, HL-93 was used for the moment and shear inventory ratings for Strength I and Service II. The platoon characteristics were the same as previously outlined.

A single-lane loaded AASHTO fatigue truck with a removed MPF = 1.2 was considered for a Fatigue I and II check at the cross-frame location and the shear stud. As specified in LRFD BDS Article 3.6.1.4, the IM of the fatigue truck is 15%. Fatigue I and II checks were also conducted for a single-lane four-truck (legal-load platoon) with 5-ft headways without routine traffic in the adjacent lane. When evaluating the platoons for fatigue, the IM for platoons of 15% for platoons was assumed to be the same as for the AASHTO fatigue truck. When evaluating the platoons for fatigue, the IM of 15% assumed for platoons was the same as for the AASHTO fatigue truck. Note that a single-lane loaded four-truck platoon (legal-load platoon) with 50-ft headways without routine traffic in the adjacent lane was also evaluated when conducting cumulative fatigue damage assessment.

8.4.3 Fatigue Damage Assessment

As discussed in Section 2.6, a linear accumulative fatigue damage model by Deng and Yan (2018) was used. Cumulative fatigue damage for evaluating the AASHTO fatigue truck and platoons at 5- or 50-ft headways was determined using Equation 2.9. A from Equation 2.9 was determined to be 440,000,000 based on LRFD BDS Table 6.6.1.2.3-1 categories for welded cross-frame connection plates. $ENSC$ in Equation 2.9 for the AASHTO fatigue truck was taken from LRFD BDS Table 6.6.1.2.5-2. An analysis was conducted at cross-frame locations to determine $ENSC$ in Equation 2.6. The number of platoon crossings per day was assumed to be

100 for 75 years. Cumulative fatigue damage (CFD) assessment results are presented in Table 8.3. A CFD of unity indicates 100% utilization or no more service life. The damage ratio was relatively low (0.14 for scenario “a” in Table 8.3), indicating that welded cross-frame connection plates were fine for fatigue.

For one platoon crossing at a 5-ft headway, the damage ratio was 10.759, indicating that a platoon at a 5-ft headway equaled around 11 crossings of an AASHTO fatigue truck (Table 8.3). If platoon headways increased to 50 ft, the damage ratio reduced to 2.368. As expected, increasing headways for the platoon on simple-span bridges could reduce fatigue damage.

Table 8.3 Cumulative Fatigue Damage Assessment

Notation	Scenarios	A	ENSC	Num	CFD
a	Platoon with 5 ft headways for 75 Years	440000000	1.000	2737500	0.140000000
b	Platoon with 50 ft headways for 75 Years	440000000	1.044	2737500	0.031000000
c	Platoon with 5 ft headways for one crossing	440000000	1.000	1	0.000000051
d	Platoon with 50 ft headways for one crossing	440000000	1.044	1	0.000000011
e	AASHTO fatigue truck for one crossing	440000000	1.000	1	0.000000005

Note: fatigue damage ratio (c/e) = 10.759; fatigue damage ratio (d/e) = 2.368; fatigue damage ratio (c/d) = 4.548

Stawska et al. (2022) used the damage ratio to establish a permit vehicle fee model. Their study assumed bridge life was based on cumulative fatigue damage from 75 years of AASHTO fatigue truck crossings. They suggested that it is possible that damage ratios for platoons at different headways could also be used to establish platoon permit fees.

8.4.4 Moment and Shear Rating Check Locations

Design and platoon ratings were calculated for positive moment for an interior steel welded plate girder at 0.5L span (50’ from the centerline of support), and for shear at the beam

end support and four ft from the beam end support (Figure 8.17). The maximum transverse stiffener spacing was four ft, starting at four ft to the end of the beam (Figure 8.16), which was used to conduct interior panel shear rating (Figure 8.17). This example also includes the shear stud fatigue check (Figure 8.17). A welded cross-frame connection plate fatigue at the 41 ft to the end beam support (Figure 8.16 and Figure 8.17) is also included.

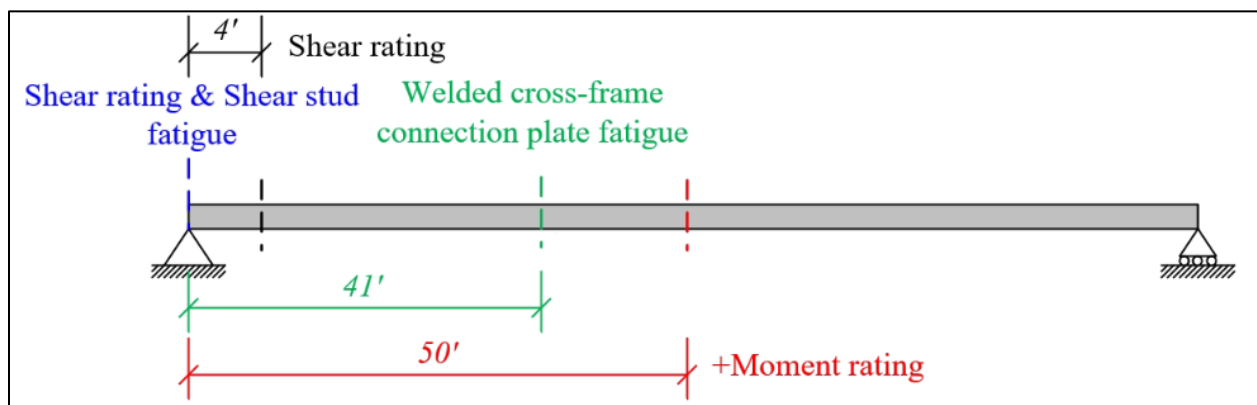


Figure 8.17 Moment and Shear Rating Check Locations

8.4.5 Moment and Shear Rating Check Results

The HL-93 was used for Strength I and Service II rating based on *MBE* Table 6A.4.2.2-1. The platoon's Strength I moment and shear load factors (target $\beta = 2.5$) were based on Table 2.2 reproduced from Steelman et al. (2021). The Service II moment load factors (target $\beta = 1.6$) for the platoon were based on Table 5.10 (see Table 8.4). All the Strength I and Service II rating factors were greater than 1.0 for operating loads and the single-lane loaded four-truck (legal-load platoon) with 5 ft headways mixed with traffic in the adjacent lane.

The Fatigue I and Fatigue II load factors (γ in Equation 2.3) for AASHTO fatigue truck and platoon ratings were based on *MBE* Table 6A.4.2.2-1. The Fatigue I and Fatigue II I rating

factors were calculated based on capacity over demand. The capacity is the $(\Delta F)_n$ in Equation 2.3. The demand is the γ in Equation 2.3 times the LL stress range $(\Delta f_{platoon})$. Fatigue I rating factors for design and platoon loads were all greater than 1.0, see Table 8.5. As a result, the Fatigue I checks of the welded cross-frame connection plate for the design and platoon loads were satisfactory. Therefore, Fatigue II checks for design and platoon loads were not performed at this location.

The Fatigue I and Fatigue II shear stud checks were performed for the AASHTO fatigue truck and platoon loads at the end beam support according to LRFD BDS Article 6.10.10. The shear stud rating factor was calculated based on LRFD BDS Equation 6.10.10.1.2-1 over the actual pitch (see Table 8.6). According to Table 8.6, the shear stud Fatigue I check for a four-truck platoon with 5-ft headway had a rating factor of 0.819, less than 1.0. This result was due to the relatively high shear forces near the beam ends for the platoon. Assuming the platoon had 100 crossings per day for 75 years, the Fatigue II shear stud check passed as the rating factor increased to 1.034. Increasing the platoon headways can satisfy the Fatigue I shear stud check.

Table 8.4 Rating Factors for Strength and Service Limit States

Limit state	Design load rating		Platoon load rating
	Inventory	Operating	(Strength I $\beta_{target} = 2.5$ and Service II $\beta_{target} = 1.6$)
Strength I for design and platoon load rating			
Flexure (at midspan)	1.278	1.656	1.728
Shear (at end)	2.159	2.799	2.386
Shear (at 4 ft)	1.990	2.580	2.242
Service II			
Flexure (at midspan)	1.842	2.395	1.558

Table 8.5 Rating Factors for Fatigue Limit States for Welded Cross-frame Connection Plate

Limit state	AASHTO Fatigue Truck	Four-truck Platoons (5-ft NRL 100 crossings per day)
Fatigue I welded cross-frame connection plate		
Stress (at 41 ft)	2.488	1.127
Fatigue II welded cross-frame connection plate		
Stress (at 41 ft)		

Table 8.6 Rating Factors for Fatigue Limit States for Shear Stud

Limit state	AASHTO Fatigue Truck	Four-truck Platoons (5-ft NRL 100 crossings per day)
Fatigue I shear stud		
Shear (at end)	1.773	0.819
Fatigue II shear stud		
Shear (at end)		1.034

8.5 Steel Continuous Span Bridge

Bridge S080 40375 is a 220-ft (60'-100'-60') three-span, steel rolled beam bridge at the I-80 2W US77 Interchange in Davey, Nebraska (Figure 8.18) constructed in 1960. The bridge has three design lanes (HS25), and the average daily traffic is 48,015. It was widened twice, the first time in 1992 by replacing 1960 girders with ASTM (2021) A709 50 ksi weathering steel rolled beams and a 3.5 ksi slab. During the second widening in 2005, two more girders were added, and the slab strength was increased to 4.0 ksi. The design trucks for these two widenings were HS25. The rating method was load factor rating (LFR). However, the LRFR rating method was used as before for this rating example. The negative moment region design was considered noncomposite, so the deck was assumed to be ineffective at carrying tension for Service II. As a result, the section modulus would be a steel section only for Service II.

Design and platoon ratings for an interior steel girder at 0.5L of the interior span and 0.4L from abutments at end spans for positive moment, at the interior supports for negative moment, and at the beam end supports for shear. Rating factors for the Strength I and Service II limit states were provided for HL-93 design and platoon loads. Fatigue I and Fatigue II for AASHTO fatigue truck and platoons with 5- or 50-ft headways were considered to evaluate a welded cross-frame connection plate at one cross-frame location. The fatigue damage ratio for a single crossing of a four-truck platoon with a 5- or 50-ft headway and an AASHTO fatigue truck was determined. Fatigue I and Fatigue II were considered for shear studs at the beam end, based on AASHTO fatigue truck and platoons with 5- ft headways. Appendix F provides computation.



Figure 8.18 Steel Rolled Beam Three-Span Bridge (S080 40375) (Google Map, 2023)

8.5.1 Bridge Details

The bridge has a 15-degree skew, as shown in Figure 8.19, which was ignored in the example. It is comprised of seven steel girders (Figure 8.20). Girder spacing between G1 and G2 and G2 and G3 is 9 ft, while spacing for other girders is 9 ft -10 in. (Figure 8.20). The average deck thickness is 8 in. (Figure 8.20). The left and right overhangs are 2 ft-8 in. and 2 ft-6 in., respectively (Figure 8.20). This rating example used the interior girder (G4) with 9 ft -10 in. girder spacing (Figure 8.20). The yield stress for this girder is 50 ksi, and the deck concrete

design strength is 4 ksi. Two types of girder sections are used for the G4, as shown in Figure 8.21.

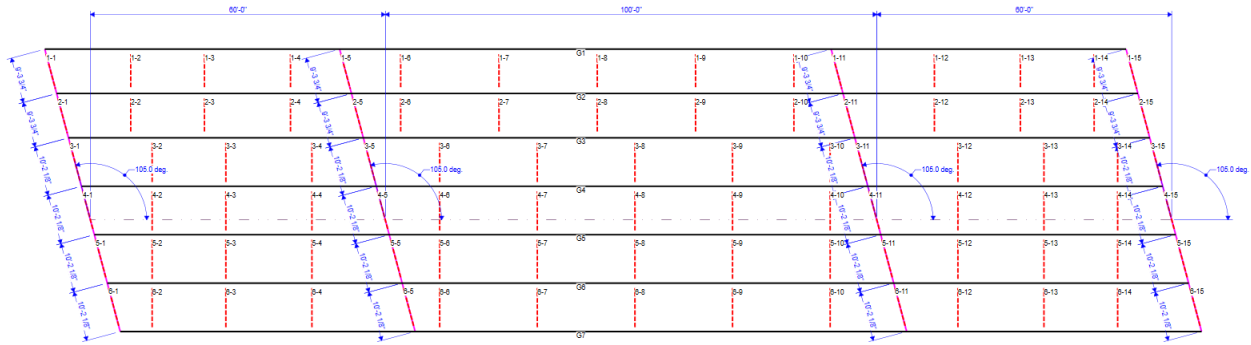


Figure 8.19 Bridge Plan View for S080 40375 (AASHTOWare™ BrR, 2023)

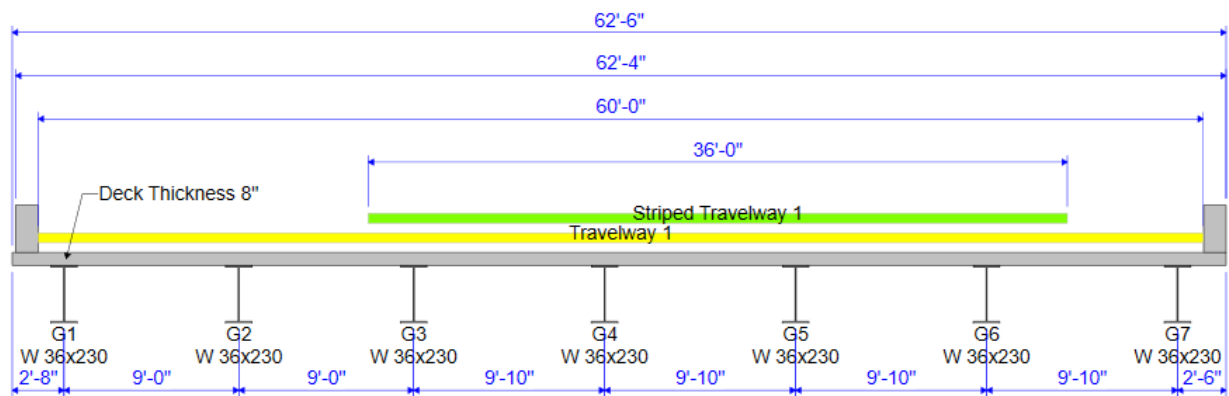


Figure 8.20 Bridge Cross Section for S080 40375 (AASHTOWare™ BrR, 2023)

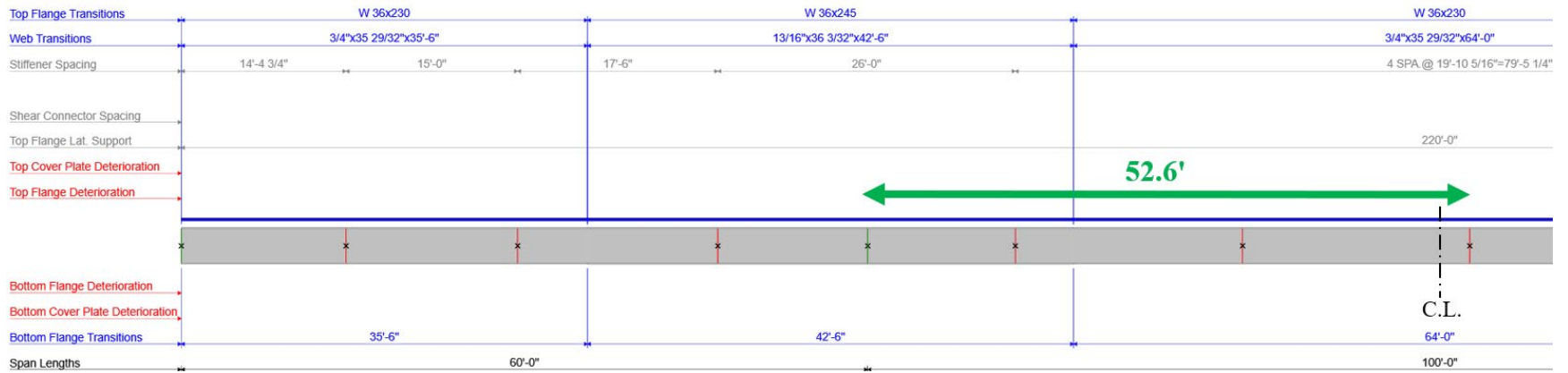


Figure 8.21 Bridge Girder Details for S080 40375 (AASHTOWare™ BrR, 2023)

8.5.2 Vehicle Details

HL-93 was used for Strength I and Service II inventory ratings. Platoon characteristics were considered the same as before.

8.5.3 Fatigue Damage Assessment

As discussed in Section 8.4.3, the linear accumulative fatigue damage model by Deng and Yan (2018) was used, see Table 8.7. The cumulative fatigue damage caused by a platoon traveling at 5- or 50-ft headway with a 100 crossing per day for 75 years was relatively low (0.388 for scenario “a” in Table 8.7).

For one crossing platoon with a 5-ft headway, the fatigue damage ratio was 8.200, which indicated that a running platoon with a 5-ft headway was equal to running around eight crossings for an AASHTO fatigue truck (Table 8.7). If platoon headway increased to 50 ft, the damage ratio relative to the AASHTO fatigue truck was reduced to 2.379 (Table 8.7). Table 8.3 and Table 8.7 demonstrate the damage ratios and cumulative fatigue. Because fatigue damage varied based on the characteristics of the bridge and the platoon, additional research should be prioritized in a future parametric study to understand better fatigue damage caused by platoons on steel bridges demonstrating a variety of CAFs.

Table 8.7 Cumulative Fatigue Damage Assessment

Notation	Scenarios	A	ENSC	Num	CFD
a	Platoon with 5 ft headways for 75 Years	440000000	1.000	2737500	0.388000000
b	Platoon with 50 ft headways for 75 Years	440000000	1.037	2737500	0.113000000
c	Platoon with 5 ft headways for one crossing	440000000	1.000	1	0.000000142
d	Platoon with 50 ft headways for one crossing	440000000	1.037	1	0.000000041
e	AASHTO fatigue truck for one crossing	440000000	1.000	1	0.000000017

Note: fatigue damage ratio (c/e) = 8.200; fatigue damage ratio (d/e) = 2.379; fatigue damage ratio (c/d) = 3.447.

8.5.4 Moment and Shear Rating Check Locations

Typical locations for positive and negative moments, and shear were used (Figure 8.22). The shear stud fatigue check at the end beam support was checked (Figure 8.22). Also, this example investigated a welded cross-frame connection plate fatigue at 52.6 ft from the left interior support (Figure 8.21 and Figure 8.22).

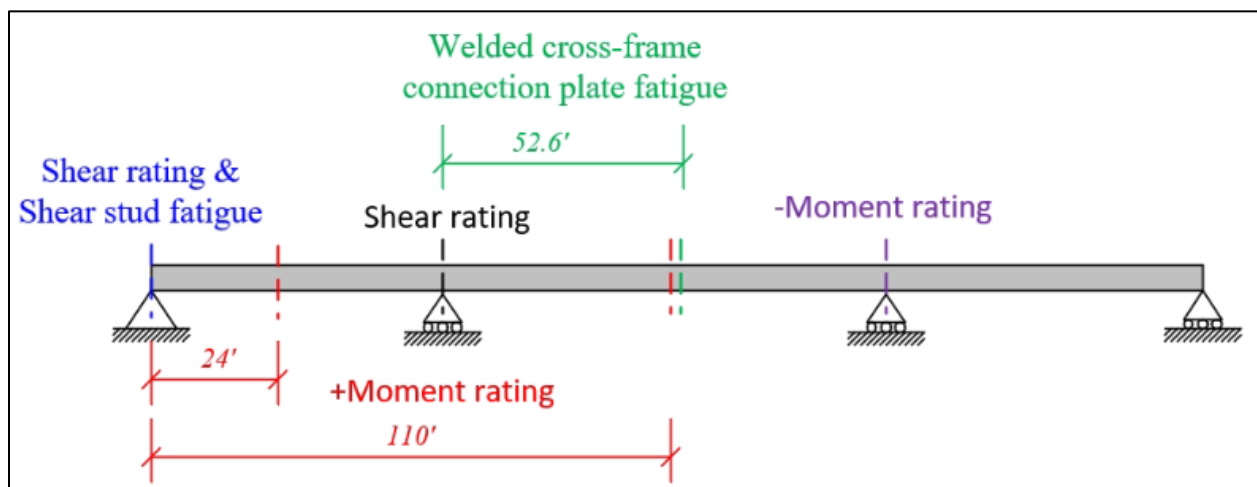


Figure 8.22 Moment and Shear Rating Check Locations

8.5.5 Moment and Shear Rating Check Results

The rating factors are provided in Table 8.8. In Table 8.8, the Service II moment rating for the negative moment region was more critical than the Service II moment rating for the positive moment region. This was due to the conservative assumption that the section modulus was only steel for the negative moment region. As shown in Table 8.8, all the Strength I and Service II rating factors were greater than 1.0. This bridge was safe for operating design loads and the single-lane loaded four-truck (legal-load platoon) with 5-ft headways mixed with traffic in the adjacent lane.

The Fatigue I rating factor was 1.618 (satisfactory) for the design loads of a welded cross-frame connection plate at 52.6 ft to the left interior support (Table 8.9). However, the Fatigue I rating factor for the platoon was smaller than 1.0 (not satisfactory), see Table 8.9. Therefore, the Fatigue II check for the platoon was performed. The Fatigue II rating factor for platoons was greater than 1.0 (satisfactory), see Table 8.9.

Using the same details as above, Table 8.10 shows the shear stud Fatigue I rating for a four-truck platoon with 5-ft headway was 1.324, greater than 1.0. Therefore, the Fatigue II shear stud checks for AASHTO fatigue truck and platoons were not performed.

Table 8.8 Rating Factors for Strength and Service Limit States

Limit state	Design load rating		Platoon load rating (Strength I $\beta_{target} = 2.5$ and Service II $\beta_{target} = 1.6$)
	Inventory	Operating	
Strength I for design and platoon load rating			
Flexure (at 0.4L of the end span)	3.191	4.137	5.860
Flexure (at 0.5L of the interior span)	2.062	2.672	3.243
Flexure (at the interior support)	1.507	1.953	1.864
Shear (at the interior support)	4.427	5.739	6.861
Shear (at the interior support of the interior span side)	3.436	4.454	3.947
Service II			
Flexure (at 0.4L of the end span)	3.444	4.477	3.956
Flexure (at 0.5L of the interior span)	2.125	2.763	2.091
Flexure (at the interior support)	2.076	2.699	1.607

Table 8.9 Rating Factors for Fatigue Limit States for Welded Cross-frame Connection Plate

Limit state	AASHTO Fatigue Truck	Four-truck Platoons (5-ft NRL 100 crossings)
Fatigue I welded cross-frame connection plate		
Stress (at 52.6 ft to the left interior support)	1.618	0.802
Fatigue II welded cross-frame connection plate		
Stress (aat 52.6 ft to the left interior support)		1.713

Table 8.10 Rating Factors for Fatigue Limit States for Shear Stud

Limit state	AASHTO Fatigue Truck	Four-truck Platoons (5-ft NRL 100 crossings per day)
Fatigue I shear stud		
Shear (at the beam end support)	2.134	1.324
Fatigue II shear stud		
Shear (at the beam end support)		

8.6 Summary

This chapter presented rating examples for four typical steel and prestressed concrete girder bridges from the Nebraska inventory. These examples demonstrated how to conduct ratings for design and platoon loads. All calculated strength and service ratings were greater than 1.0.

This chapter also evaluated fatigue of steel bridge shear studs and welded cross-frame connection plates. These rating factors were greater than unity. A preliminary assessment of cumulative fatigue damage was conducted for a 5-ft and 50-ft headways platoon and an AASHTO fatigue truck. The cumulative fatigue damage caused by a platoon at 100 crossings per day over 75 years was relatively low. Additional research is needed to assess the extent to which this finding may be generalizable to a broad population of steel bridges containing various fatigue details at different locations.

Chapter 9 Cracking Reliability and Probability for Prestressed Girder Bridges

9.1 Overview

Based on the reliability analysis procedure presented in Section 3.4 for Service III, implicit reliability indices ($\beta_{implicit}$) were determined in Section 4.3.2. When $\beta_{implicit}$ was negative, optimally designed bridges for service were more than 50% likely to violate tensile stress limits under current design live loads at some point during their service lives. However, exceeding the service limit did not necessarily mean bridges experience flexural cracking in their precompressed tensile zones. As a result, it was of interest to investigate cracking reliability, $\beta_{Cracking}$, against mechanical cracking limits provided by code-compliant bridge designs. $\beta_{Cracking}$ and cracking probabilities for bridge design scenarios from Table 3.1 were determined. Three assumed nominal moduli of rupture were considered. Relationships between assumed nominal moduli of rupture and cracking reliability and probability were also established and presented.

9.2 Service III Cracking Reliability and Probability Results

Figure 9.1a presents PDFs estimating the likelihood of cracking at f_r ($\kappa_{eva} = 0.24$) for a 120 ft simple-span bridge designed using *Post-1.0-Gains*. The bridge was assumed to be designed with f_t ($\kappa = 0.0948$). The corresponding cracking reliability was +0.08, with the shaded area in Figure 9.1b representing cracking cases and results indicated that about 47 out of 100 120-ft simple-span bridges were expected to crack during their service lives.

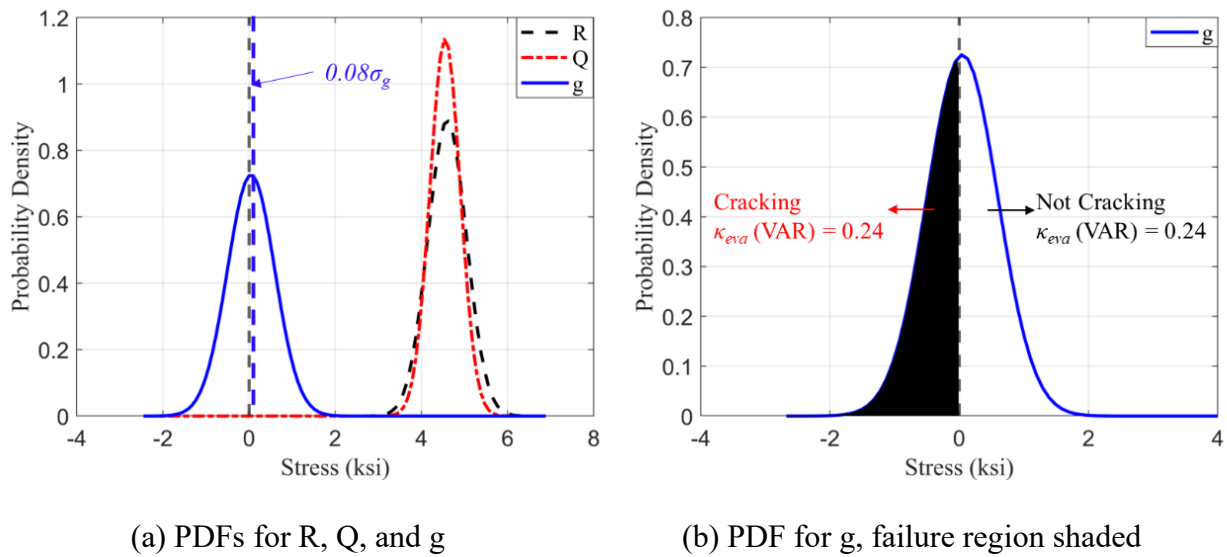


Figure 9.1 Probability Density Functions for evaluating cracking at $f_r (\kappa = 0.24)$ for 120-ft Simple-Span Bridges Designed by using *Post-1.0-Gains*

To further evaluate $\beta_{Cracking}$, bridges designed using a typical $f_i (\kappa = 0.0948)$ were evaluated over a range of $f_r (\kappa)$. Nominal moduli of rupture were assumed equal to $0.24\sqrt{f'_c}$, $0.30\sqrt{f'_c}$, and $0.37\sqrt{f'_c}$ to examine the effect of cracking strength on cracking probability variations.

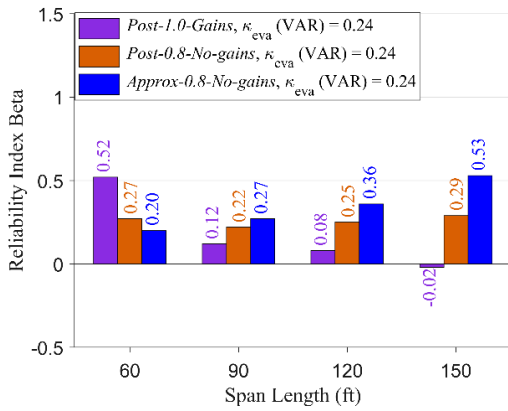
Figure 9.2 presents cracking reliability indices and corresponding cracking probabilities for *Post-1.0-Gains*, *Post-0.8-No-gains*, and *Approx-0.8-No-gains* methods. Figure 9.2a shows $\beta_{Cracking}$ values for simple-span bridges designed using different loss methods with $f_i (\kappa = 0.0948)$ and evaluated for $f_r (\kappa = 0.24)$. Consider a 60-ft simple-span bridge designed using *Post-1.0-Gains* as an example. $\beta_{Cracking}$ for this case equaled 0.52 as indicated by the leftmost purple bar in Figure 9.2a. This result implied that 30 out of 100 optimally designed bridges for Service III were expected to crack during their service lives. As span length increased from 60 to 150 ft, $\beta_{Cracking}$ decreased from 0.52 to -0.02 due to increasing dead-to-live ratios. However, for bridges

designed using *Post-0.8-No-gains* and *Approx-0.8-No-gains*, $\beta_{Cracking}$ slightly increased as span length increased. Figure 9.2b shows that cracking probability (shaded to distinguish from the reliability index) was generally less than or equal to 50% for all three methods. Increasing nominal f_r ($\kappa = 0.24$) to f_r ($\kappa = 0.30$) increased $\beta_{Cracking}$ by about 0.30 on average (Figure 9.2a and Figure 9.2c), with cracking probabilities being reduced by about 11% (Figure 9.2b and Figure 9.2d). Increasing nominal f_r ($\kappa = 0.30$) to f_r ($\kappa = 0.37$), $\beta_{Cracking}$ increased by about 0.32 on average (Figure 9.2c and Figure 9.2e). Changing nominal f_r ($\kappa = 0.24$) to f_r ($\kappa = 0.37$) increased reliability indices by an average of 0.62 and decreased cracking probabilities by an average of 20%.

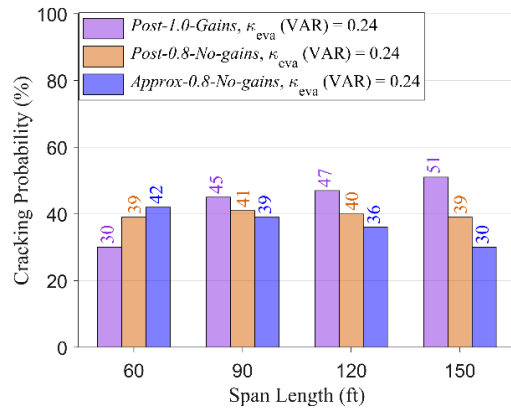
Figure 9.3a shows $\beta_{Cracking}$ values for simple-span bridges designed using *Post-0.8-Gains* and *Approx-0.8-Gains* with f_i ($\kappa = 0.0948$) and evaluated using f_r ($\kappa = 0.24$). $\beta_{Cracking}$ was always negative in Figure 9.3a, and cracking probabilities were close for bridges designed using *Post-0.8-Gains* and *Approx-0.8-Gains*. Increasing nominal f_r ($\kappa = 0.24$) to f_r ($\kappa = 0.37$) increased reliability indices by an average of 0.68, with cracking probabilities decreasing by an average of 26%.

Figure 9.4a shows $\beta_{Cracking}$ values for simple-span bridges designed using *Pre-1.0-No-gains* with f_i ($\kappa = 0.0948$) and evaluated using f_r ($\kappa = 0.24$) to f_r ($\kappa = 0.37$). $\beta_{Cracking}$ was always positive in Figure 9.4a, and was generally higher than $\beta_{Cracking}$ for the same nominal f_r in Figure 9.2 and Figure 9.3. The maximum $\beta_{Cracking}$ was 1.29 for 90-ft simple-span bridges, which implied that 9 out of 100 optimally designed Service III bridges would experience cracking during their service life (Figure 9.4). Increasing nominal f_r ($\kappa = 0.24$) to f_r ($\kappa = 0.37$) increased reliability

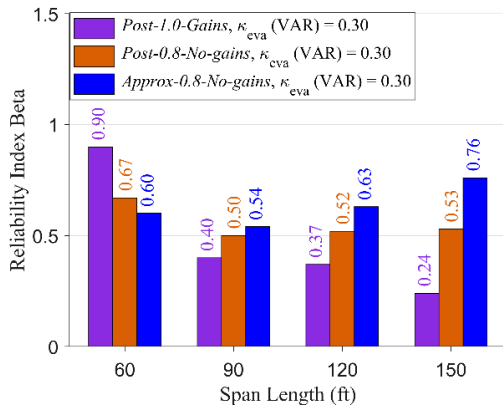
indices by an average of 0.61, with cracking probabilities decreasing by an average of 16% (Figure 9.4).



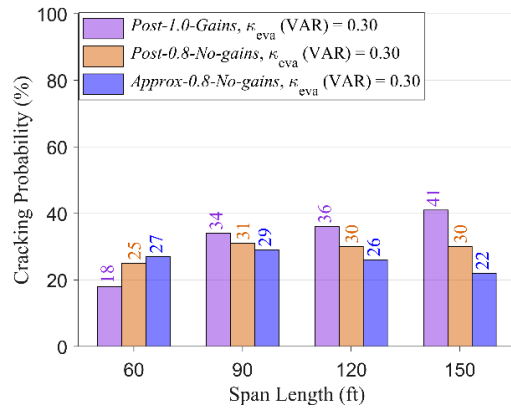
(a) $\beta_{Cracking}$ for $f_r(\kappa = 0.24)$



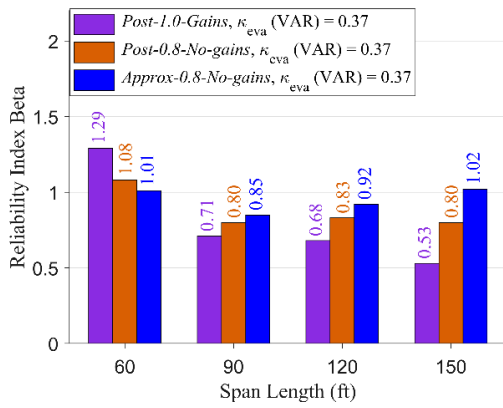
(b) Cracking Probability for $f_r(\kappa = 0.24)$



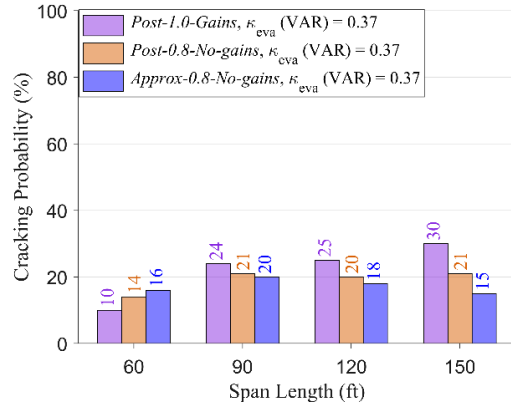
(c) $\beta_{Cracking}$ for $f_r(\kappa = 0.30)$



(d) Cracking Probability for $f_r(\kappa = 0.30)$

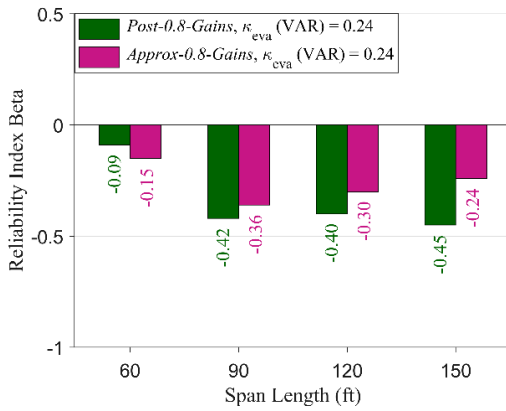


(e) $\beta_{Cracking}$ for $f_r(\kappa = 0.37)$

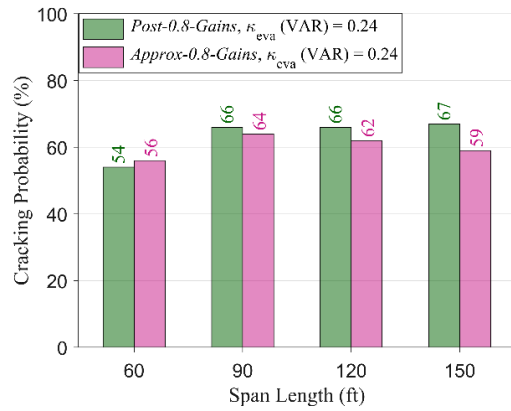


(f) Cracking Probability for $f_r(\kappa = 0.37)$

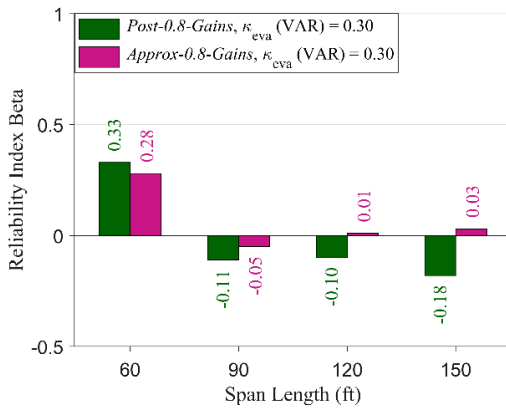
Figure 9.2 $\beta_{Cracking}$ and Cracking Probability for Simple-span Bridges Designed using *Post-1.0-Gains*, *Post-0.8-No-gains*, and *Approx-0.8-No-gains* Methods, Different $f_r(\kappa = 0.24, 0.30, \text{ and } 0.37)$



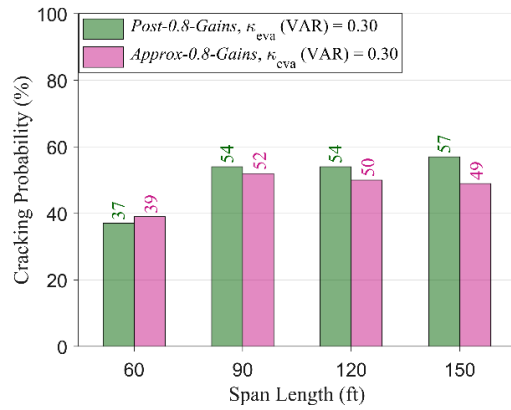
(a) $\beta_{Cracking}$ for $f_r(\kappa = 0.24)$



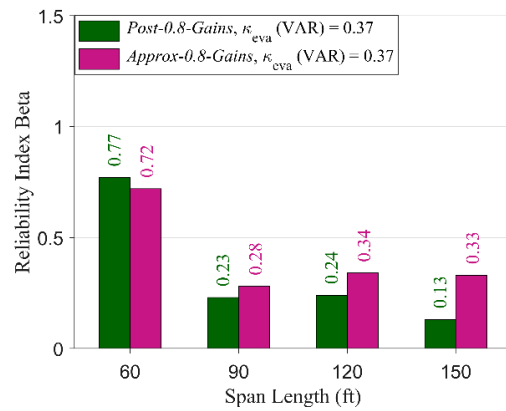
(b) Cracking Probability for $f_r(\kappa = 0.24)$



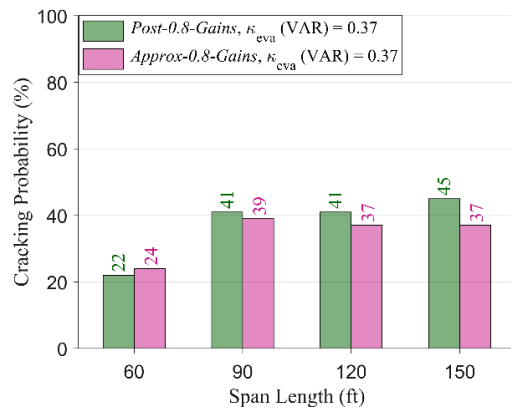
(c) $\beta_{Cracking}$ for $f_r(\kappa = 0.30)$



(d) Cracking Probability for $f_r(\kappa = 0.30)$

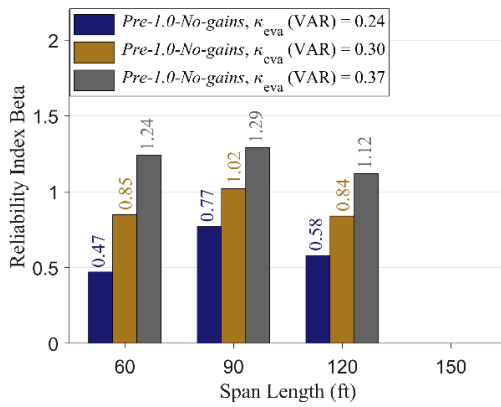


(e) $\beta_{Cracking}$ for $f_r(\kappa = 0.37)$

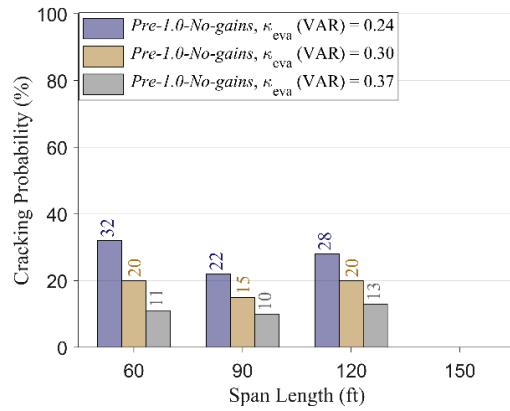


(f) Cracking Probability for $f_r(\kappa = 0.37)$

Figure 9.3 $\beta_{Cracking}$ and Cracking Probability for Simple-span Bridges Designed using *Post-0.8-Gains* and *Approx-0.8-Gains* Methods, Different $f_r(\kappa = 0.24, 0.30, \text{ and } 0.37)$



(a) $\beta_{Cracking}$ for Different f_r



(a) Cracking Probability for Different f_r

Figure 9.4 $\beta_{Cracking}$ and Cracking Probability for Simple-span Bridges Designed using *Pre-1.0-No-gains*, *Post-0.8-No-gains* Method, and *Approx-0.8-No-gains* Methods, Different f_r ($\kappa = 0.24$, 0.30, and 0.37)

Increasing nominal f_r ($\kappa = 0.24$) to f_r ($\kappa = 0.30$) increased $\beta_{Cracking}$ by an average of 0.31, with cracking probabilities decreasing by an average of 11% (Figure 9.2, Figure 9.3, and Figure 9.4). Changing the nominal f_r ($\kappa = 0.24$) to f_r ($\kappa = 0.37$) increased the reliability index by an average of 0.64, with cracking probabilities decreasing by an average of 22%. Given that linear changes in reliabilities and cracking probabilities as a function of nominal rupture moduli were observed for all cases, the $\beta_{Cracking}$ and cracking probability can be preliminarily estimated based on linear interpolation for nominal moduli of rupture between 0.24 and 0.37.

Current optimally designed Service III bridges with f_i ($\kappa = 0.0948$) that were subjected to current design live loads had $\beta_{Cracking}$ between -0.45 and 1.29 for the nominal moduli of rupture range considered herein. Estimated cracking probabilities during their service lives ranged between 10% and 67%, with highest reliabilities and lowest cracking probabilities corresponding to upper-bound rupture moduli, which the *LRFD BDS* notes corresponds to small-depth samples,

that were moist-cured before testing. These results imply that lower reliabilities and higher cracking probabilities were likely representative of many in-service prestressed concrete bridges.

9.3 Summary

This chapter determined cracking reliability indices and probabilities for various designed prestressed concrete bridges optimally designed for Service III. Three different nominal moduli of rupture were considered. As nominal moduli of rupture increased, cracking probabilities decreased. $\beta_{Cracking}$ results indicated that cracking probabilities were between 10% and 67% for code-specified service loads. This implies that optimally designed bridges may crack during their service life, despite the expectation that cracking is avoided by using tensile stress limits less than the modulus of rupture. Also, $\beta_{Cracking}$ and cracking probabilities changed approximately linearly as a function of nominal moduli of rupture. Derived linear relationships can be preliminarily used to estimate the $\beta_{Cracking}$ and cracking probabilities based on the nominal moduli of rupture.

Chapter 10 Summary and Conclusions

10.1 Summary

Platoons can operate in convoys at close headways using currently available and future technology, thereby reducing transportation, and potentially environmental, costs associated with shipping freight. Platoons could, however, subject bridges to greater demands than under normal traffic conditions. Studies have widely examined platoon effects on girder bridges for strength (Steelman et al., 2021). However, reliability-based studies examining platoon effects for service are lacking.

This research developed a Load and Resistance Factor Rating (LRFR) methodology to investigate service limit states using four-truck platoons loading simple- and two-span steel and prestressed girder bridges. A parametric study established headways between platoon trucks that would inform effective platoon operational strategies, considering different girder spacings, span lengths and numbers, truck configurations and numbers, and adjacent lane loading scenarios. Prestressed concrete bridges were conservatively assumed to have an optimal Service III design capacity equal to setting the Manual for Bridge Evaluation rating factor equation to 1.0. Optimal bridge design cases considered three prestress loss methods, two design LL factors, four allowable tensile stress limits, with or without elastic gains. Optimal steel bridge design criteria were defined to achieve a maximum performance ratio (demand/capacity) equal to 1.0 for Service II and Strength I. Monte Carlo Simulations (MCS) were used to determine target implicit reliability indices (β_{Implicit}) of optimally designed prestressed concrete and steel bridges under design HL-93 loading multiple-lane loads from the Load and Resistance Factor Design (LRFD) Bridge Design Specifications (BDS) (2020).

Platoon truck weights were scaled by an amplification factor, α , relative to an 80-kip GVW baseline for parametric headway combinations and CoV_s to determine critical (maximum) safe vehicle weights satisfying target $\beta_{Implicit}$ values. MCS was used to calibrate LL factors associated with target $\beta_{Implicit}$ for Service III and Service II limit states. Calibrated LL factors were then proposed that accounted for studied platoon-loading scenarios and LL CoV_s .

Summary headway guidance was developed for service limit states to illustrate potential safe operational strategies for varying truck weights and platoon uncertainties, with total platoon CoV ranging between 0 and 0.2. Sensitivity analyses were completed to develop frameworks that explicitly aggregated LL uncertainties based on truck weight and dynamic amplification. Girder distribution factors were developed so that rating engineers could reasonably select LL factors and corresponding headways based on their known or assumed uncertainties. Results indicated that uncertainties associated with truck weight and girder distribution factor effects on total platoon CoV were identical while those associated with dynamic amplification were less significant.

Example ratings of four representative steel and prestressed concrete girder bridges from the Nebraska inventory for strength and service were provided. The study also completed a cursory fatigue evaluation of welded cross-frame connection plates and shear studs for the steel bridges loaded by platoons at 5- and 50-ft headways and for an AASHTO fatigue truck.

The likelihood of exceeding Service III limits raised questions regarding appropriateness of current LRFD BDS and MBE methods to evaluate potential frequent heavy loads, such as those from platoons. This led to additional studies investigating $\beta_{Cracking}$ for these optimally designed prestressed concrete bridges.

10.2 Conclusions for Prestressed Concrete Bridges

Key findings for prestressed concrete bridges are:

- $\beta_{Implicit}$ was approximately -0.60 (Service III) when averaged across all considered span lengths for optimally-designed bridges designed using (Section 4.3.2):
 - Post-2005 losses (*LRFD BDS 5.9.3.4*) with elastic gains using $\gamma_L = 1.0$ (*Post-1.0-Gains*),
 - Post-2005 losses (*LRFD BDS 5.9.3.4*) without elastic gains using $\gamma_L = 0.8$ (*Post-0.8-No-gains*), and
 - Approximate losses (*LRFD BDS 5.9.3.3*) without elastic gains using $\gamma_L = 0.8$ (*Approx-0.8-No-gains*).
- $\beta_{Implicit}$ was approximately -1.20 (Service III) when averaged across all considered span lengths for optimally-designed bridges designed using (Section 4.3.2):
 - Post-2005 losses (*LRFD BDS 5.9.3.4*) with elastic gains using $\gamma_L = 0.8$ (*Post-0.8-Gains*), and
 - Approximate losses (*LRFD BDS 5.9.3.3*) with elastic gains using $\gamma_L = 0.8$ (*Approx-0.8-Gains*).
- A target of $\beta_{Implicit} = -0.60$ was recommended for platoons at Service III.
- $\beta_{Implicit}$ of -0.60 and -1.20 implies 73% and 88% probability, respectively, of exceeding the Service III limit during a bridge's service life.
- Changes in total *LL CoV* have negligible effects on reliability indices and calibrated *LL* factors for Service III, with the influence of prestress loss uncertainty on indices being comparable to that for live loads.

- Single-lane loaded legal-load platoons without adjacent traffic can acceptably traverse all examined prestressed concrete bridge configurations at a target Service III $\beta_{Implicit} = -0.6$ (Figure 6.3a).
- Single-lane loaded legal-load platoons with adjacent traffic can acceptably traverse all examined prestressed concrete bridge configurations at a target Service III $\beta_{Implicit} = -0.6$ with headways of at least 15 ft (Figure 6.3a).
- Platoons can operate at any headway on all examined prestressed concrete bridge configurations at 80% of the legal load limit with adjacent routine traffic. If a platoon can avoid traveling adjacent to routine traffic, it can potentially operate at up to 130% of the legal load limit (Figure 6.4a).
- Platoons can operate on all examined prestressed concrete bridge configurations at up to 140% of the legal load limit by controlling headways adjacent to routine traffic. If the platoon can avoid traveling adjacent to routine traffic, it can potentially operate at up to 230% of the legal load limit (Figure 6.4a).
- Bridge cracking probabilities ranged between 10% and 67% for code-specified service loads, which indicates that optimally designed bridges may crack during their service life despite the expectation that cracking is avoided using tensile stress limits less than the modulus of rupture.
- $\beta_{Cracking}$ and cracking probability change approximately linearly as a function of nominal moduli of rupture (between $0.24\sqrt{f'_c}$ and $0.37\sqrt{f'_c}$ (ksi)) and can be preliminarily estimated based on the linear relationship.

10.3 Conclusions for Steel Bridges

Key findings of steel bridges are:

- $\beta_{Implicit}$ was approximately 1.60 (Service II) when averaged across all considered positive moment regions for bridges. Based on the optimally-designed steel bridges in this study, Strength I governed over Service II in the negative moment region (note: C_b was assumed equal to 1 when proportioning optimal designs).
- A target of $\beta_{Implicit} = 1.60$ is recommended for platoons at Service II (Section 4.4.2).
- Changes in total CoV of platoons would have a slight effect on reliability indices and calibrated LL factors for Service II. Reducing the total CoV of platoons would result in lower LL factors and more flexible headway requirements for Service II.
- Single-lane loaded legal-load platoons without adjacent traffic can acceptably traverse all examined steel bridge configurations at a target Service II $\beta_{Implicit} = 1.6$ (Figure 6.3b).
- Single-lane loaded legal-load platoons with adjacent traffic can acceptably traverse all examined steel bridge configurations at a target Service II $\beta_{Implicit} = 1.6$ with headways of at least 23 ft (Figure 6.3b).
- Platoons can operate at any headway on all examined steel bridge configurations at 70% of the legal load limit with adjacent routine traffic. If a platoon can avoid traveling adjacent to routine traffic, it can potentially operate at up to 140% of the legal load limit (Figure 6.4b).
- Platoons can operate on all steel bridge configurations up to 110% of the legal load limit by controlling headways adjacent to routine traffic. If the platoon can avoid traveling

adjacent to routine traffic, it can potentially operate at up to 220% of the legal load limit (Figure 6.4b).

- Single-lane loaded legal-load platoons with adjacent traffic can acceptably traverse two selected representative steel girder bridges from the Nebraska inventory at the target Strength I $\beta = 2.5$ and Service II $\beta_{Implicit} = 1.6$ with headways of five ft.
- For the selected representative steel simple-span bridge, Fatigue I check of a welded cross-frame connection plate and Fatigue II check of the shear stud for single-lane loaded legal-load platoons (five-ft headways) without adjacent traffic are satisfactory. Operating this platoon on this bridge once would result in the same cumulative fatigue damage as running an AASHTO fatigue truck around 11 crossings.
- For the selected representative steel continuous span bridge, Fatigue II check of a welded cross-frame connection plate and Fatigue I check of the shear stud for Single-lane loaded legal-load platoons (five-ft headways) without adjacent traffic are satisfactory. Operating this platoon on the bridge once would result in the same cumulative fatigue damage as running an AASHTO fatigue truck around eight crossings.
- Cumulative fatigue damage for platoons on two selected representative steel girder bridges from the Nebraska inventory of this research varies based on the characteristics of both the bridge and the platoon.
- The cumulative fatigue damage caused by a platoon traveling at a 5- or 50-ft headway with a 100 crossing per day assumption under 75 years is at most 0.388 for two selected representative steel girder bridges from the Nebraska inventory of this research, indicating that this platoon is unlikely to cause significant fatigue problems for welded

connection plates at the cross-frame location. Owners must carefully document the number of platoon crossings for each bridge, as permits issued to multiple operators will compound and accelerate fatigue damage.

10.4 Recommended Future Research

The following topics are proposed for future research:

- Investigating effects of heavy loads, such as those from platoons, on prestressed concrete girder cracking.
- Re-examining service behavior and performance to investigate whether an alternate mechanistic format may be more appropriate for Service III evaluations.
- Improving $\beta_{Implicit}$ estimates through calibration to represent WIM data.
- Developing a calibrated *LFR* method that accounts for bias of *LFR* GDFs relative to *LRFR* GDFs for service limit states.
- Calibrating platoon *LL* factors for Fatigue limit states.
- Studying the potential implications of platoons on fatigue damage for steel bridges.

10.5 Implementation and Technology Transfer

The procedures outlined herein may be implemented in the following workflow for platoon permitting in Nebraska as presented in Figure 10.1 and listed below:

1. Operators provide platoon characteristics and request permit (upper right portion of Figure 10.1).
2. Bridge engineers determine whether platoon is a legal-load platoon.
3. If a legal-load platoon, engineers check whether the platoon:
 - a. Follows headway restrictions from Chapter 6,

- b. Avoids critical truck speed that may cause resonance (Chapter 7), and
- c. Administratively requires a permit (upper left portion of Figure 10.1).

If the platoon meets these requirements, bridge engineers can issue a permit with the information about type of permit, restrictions, time limit, enforcement and might include multistate corridor collaboration (bottom left portion of Figure 10.1). If the platoon does not meet these requirements, a detailed assessment is needed, according to subsequent steps, below.

4. If an overweight platoon meets the following criteria, an administrative permit can be issued:
 - a. Moderate overload (as determined by the owner agency),
 - b. Follows headway restrictions, and
 - c. Does not require continued assessment (if follows *a* and *b*).

If the platoon does not comply with these requirements, a detailed analysis will be required for each bridge the platoon will traverse as outlined below and in the center portion of Figure 10.1:

- a. First characterize platoon *LL* with respect to single or multiple trips, ADTT, adjacent loading, axle weights, axle spacings, and headway controls (center right portion of Figure 10.1).
- b. Use *LL* characteristics to characterize static loads, *GDF*, and *IM* based on proposed framework from Chapter 7 for the platoon route, apply calibrated *LL* factors for strength (Table 2.2) and service (Table 5.9 and Table 5.10).

- c. Input LL and bridge information into AASHTOWare™ Bridge Rating to directly calculate rating factors.
- d. DOT issues permit if rating factor is greater than or equal to 1.0.
- e. DOT refuses to issue permit if rating factor is less than 1.0, or modify platoon characteristics and repeat steps *a* through *c*.

Potential Platoon Permit Workflow Process

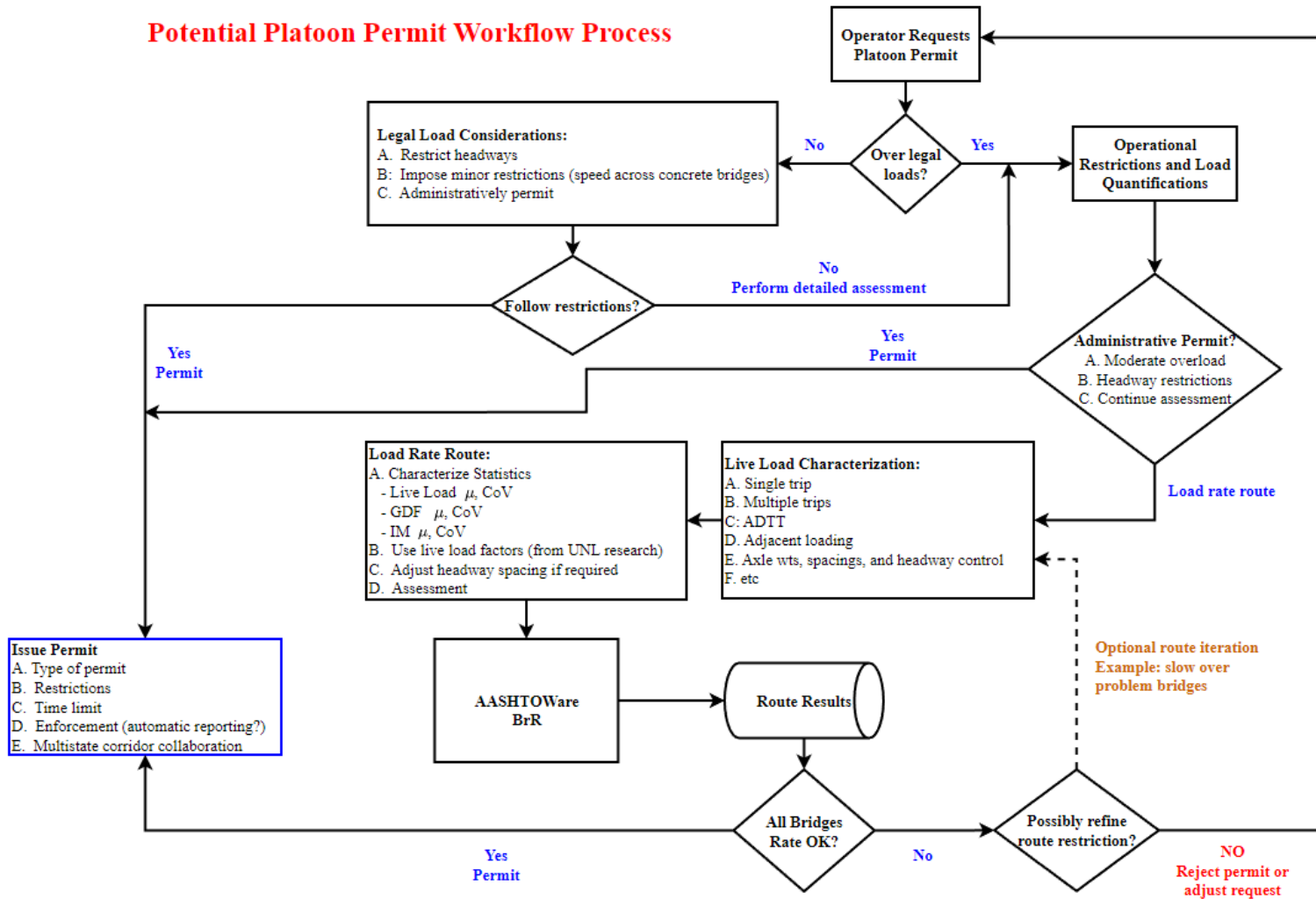


Figure 10.1 Potential Workflow Process for Permitting Platoons on Girder Bridges in Nebraska

References

- American Association of State Highway and Transportation Officials (AASHTO). (1961) *Standard Specification for Highway Bridges*, 8th Ed, Washington, D.C.
- American Association of State Highway and Transportation Officials (AASHTO). (1973) *Standard Specification for Highway Bridges*, 8th Ed, Washington, D.C.
- American Association of State Highway and Transportation Officials (AASHTO). (1996) *Standard Specification for Highway Bridges*, 16th Ed, Washington, D.C.
- American Association of State Highway and Transportation Officials (AASHTO). (2002) *Standard Specification for Highway Bridges*, 17th Ed, Washington, D.C.
- American Association of State Highway and Transportation Officials (AASHTO). (2018). *The Manual for Bridge Evaluation*, 3rd Ed., 2019 and 2020 Interim Revisions, Washington, DC.
- American Association of State Highway and Transportation Officials (AASHTO). (2020). *AASHTO LRFD Bridge Design Specifications*, 9th Ed., Washington, DC
- ASTM. (2017). *Standard Specification for Highway Weigh-In-Motion (WIM) Systems with User Requirements and Test Methods E 1318-09*. 2017 Annual Book of ASTM Standards. Edited by ASTM Committee E17-52 on Traffic Monitoring. ASTM International, USA.
- ASTM. (2021). *Standard Specification for Structural Steel for Bridges*. Under the Jurisdiction of ASTM Committee A01, ASTM International, USA. DOI: 10.1520/A0709_A0709M-21.
- Barker, M., & Puckett, J. (2016). “*Assessment and evaluations of I-80 truck loads and their load effects*” No. FHWA-WY-17/02F). Wyoming. Dept. of Transportation. <https://rosap.ntl.bts.gov/view/dot/32469>
- Barker, M., Goodrich, B. L., Jablin, M. C., & Puckett, J. A. (2020). *Assessment and Evaluations of I-80 Truck Loads and Their Load Effects: Phase 2: Service* (No. WY-20/05F). Wyoming. Department of Transportation. <https://rosap.ntl.bts.gov/view/dot/53888>
- Bibeka, A., Songchitruksa, P., & Zhang, Y. (2021). *Assessing environmental impacts of ad-hoc truck platooning on multilane freeways*. Journal of Intelligent Transportation Systems, 25(3), 281-292. <https://www.tandfonline.com/doi/abs/10.1080/15472450.2019.1608441>
- Billing, J. R. (1984). *Dynamic loading and testing of bridges in Ontario*. Canadian journal of civil engineering, 11(4), 833-843. <https://cdnscepub.com/doi/abs/10.1139/184-101>
- Cantieni, R. (1983). *Dynamic load tests on highway bridges in Switzerland*. Report, 211. https://www.dora.lib4ri.ch/empa/islandora/object/empa%3A16409/datastream/PDF/Cantieni-1983-Dynamic_Load_Tests_on_Highway-%28published_version%29.pdf

- Couto Braguim, T., Lou, P., & Nassif, H. (2021). *Truck platooning to minimize load-induced fatigue in steel girder bridges*. Transportation research record, 2675(4), 146-154. <https://journals.sagepub.com/doi/10.1177/0361198120973657>
- Deng, L., & Yan, W. (2018). *Vehicle weight limits and overload permit checking considering the cumulative fatigue damage of bridges*. Journal of Bridge Engineering, 23(7), 04018045. <https://www.dengteam.com/uploadfile/2019/0126/20190126023548125.pdf>
- Deng, L., Yu, Y., Zou, Q., & Cai, C. S. (2015). *State-of-the-art review of dynamic impact factors of highway bridges*. Journal of Bridge Engineering, 20(5), 04014080. [https://ascelibrary.org/doi/abs/10.1061/\(asce\)be.1943-5592.0000672](https://ascelibrary.org/doi/abs/10.1061/(asce)be.1943-5592.0000672)
- Elshazli, M., Ibrahim, A., Abdel-Rahim, A., & Pacific Northwest Transportation Consortium. (2022). *Impact of Autonomous and Connected Truck Platoons in the Pacific Northwest on Transportation Infrastructure* (No. 2021-S-UI-2). Pacific Northwest Transportation Consortium (PacTrans)(UTC). <https://rosap.ntl.bts.gov/view/dot/64114>
- Federal Highway Administration (FHWA). (2018). *WIM Technology Selection, Data Acquisition Requirements, and Procurement Guide Part 1*. https://www.fhwa.dot.gov/policyinformation/knowledgecenter/wim_guide/
- Federal Highway Administration. (FHWA). (2022). *National Bridge Inventory (NBI)*. <https://www.fhwa.dot.gov/bridge/nbi/ascii2022.cfm>
- Ghosn, M. (2019). *Load Rating for the Fast Act Emergency Vehicles Ev-2 and Ev-3*. National Cooperative Highway Research Program (NCHRP) Project 20-07/Task 410, Transportation Research Board, Washington, DC. http://www.dotd.la.gov/Inside_LaDOTD/Divisions/Engineering/Bridge_Design/Downloads/NCHRP20-07Task410FinalReport_March2019.pdf
- Ghosn, M., Sivakumar, B., & Miao, F. (2011). *Load and resistance factor rating (LRFR) in NYS: volume I final report (No. C-06-13)*. City University of New York. City College. Dept. of Civil Engineering. <https://rosap.ntl.bts.gov/view/dot/24033>
- Gilbert (2022). "How do you measure bridge safety? We'll cross that one when we come to it?" UNSW Newsroom. September 5, 2022. <https://newsroom.unsw.edu.au/news/science-tech/how-do-you-measure-bridge-safety-well-cross-one-when-we-come-it>
- Google. (2023). *The prestressed concrete simple-span bridge at the 4S Greenwood Interchange*. <https://www.google.com/maps/@40.9283261,-96.4490717,3a,90y,198.53h,79.22t/data=!3m6!1e1!3m4!1sUIUQx9om-5PhZf88iKETJw!2e0!7i16384!8i8192>
- Google. (2023). *The prestressed concrete continuous span bridge at the 5N Waverly Interchange*. <https://www.google.com/maps/@40.9138196,->

[96.4800505,3a,75y,343.89h,84.14t/data=!3m6!1e1!3m4!1sOJ7F1BJx7McQ4J8ajQnkrw!2e0!7i16384!8i8192](https://www.google.com/maps/@41.1920908,-103.9544071,3a,75y,343.89h,84.14t/data=!3m6!1e1!3m4!1sOJ7F1BJx7McQ4J8ajQnkrw!2e0!7i16384!8i8192)

Google. (2023). *The steel simple-span bridge at the 43W Bushnell Interchange.*

<https://www.google.com/maps/@41.1920908,-103.9544071,3a,75y,344.17h,76.31t/data=!3m6!1e1!3m4!1sxQTCNsmgAo6aRndotd3rbQ!2e0!7i16384!8i8192>

Google. (2023). *The steel continuous span bridge at the 2W US77 Interchange.*

<https://www.google.com/maps/@40.8888052,-96.678416,3a,90y,149.79h,93.34t/data=!3m6!1e1!3m4!1sxG5fO4Fx7EnYkXXH-bSGHg!2e0!7i16384!8i8192>

Gross, S. P. (1998). *Field performance of prestressed high-performance concrete highway bridges in Texas.* The University of Texas at Austin.

<https://www.proquest.com/openview/ba57c06ed19d80bef5e65caeb7eb1c22/1?pq-origsite=gscholar&cbl=18750&diss=y>

Hanna, K., Morcous, G., & Tadros, M. K. (2010). *Design Aids of NU I-Grinder Bridges.* Nebraska Department of Roads.

<https://digitalcommons.unl.edu/cgi/viewcontent.cgi?article=1079&context=ndor>

Hassan, H., Dessouky, S., Talebpour, A., & Rahim, M. A. (2020). *Investigating the Impacts of Truck Platooning on Transportation Infrastructure in the South-Central Region* (No. 19PITSLSU14). Transportation Consortium of South-Central States.

<https://rosap.nrl.bts.gov/view/dot/56563>

Highway Research Board (1962). *The AASHO Road Test Report 4. HRB Special Report 61D,* HRB, Washington, DC.

Holombo, J., & Tadros, M. (2010). *Recommended LRFD Minimum Flexural Reinforcement Requirements* (No. NCHRP Project 12-80). <https://trid.trb.org/view/914326>

Hwang, E. S., & Nowak, A. S. (1990). *Dynamic analysis of girder bridges.* Transportation Research Record, 1223, 85-92.

<https://onlinepubs.trb.org/Onlinepubs/trr/1989/1223/1223-010.pdf>

Hwang, E.-S., and Nowak, A. S. (1991). "Simulation of dynamic load for bridges." *J. Struct. Eng.*, 10.1061/(ASCE)0733-9445(1991)117:5(1413), 1413–1434

[https://ascelibrary.org/doi/abs/10.1061/\(ASCE\)0733-9445\(1991\)117:5\(1413\)](https://ascelibrary.org/doi/abs/10.1061/(ASCE)0733-9445(1991)117:5(1413))

Keating, P. B., & Fisher, J. W. (1986). *Evaluation of fatigue tests and design criteria on welded details* (No. 286). <https://trid.trb.org/view/276881>

Kulicki, J., Prucz, Z., Clancy, C. M., Mertz, D. R., and Nowak, A. S. (2007). "Updating the calibration report for AASHTO LRFD code." Final Rep. for National Cooperative

- Highway Research Program (NCHRP) 20-7/186, AASHTO, Washington, DC.
[https://onlinepubs.trb.org/onlinepubs/archive/notesdocs/20-07\(186\)_fr.pdf](https://onlinepubs.trb.org/onlinepubs/archive/notesdocs/20-07(186)_fr.pdf)
- Lammert, M. P., Duran, A., Diez, J., Burton, K., & Nicholson, A. (2014). Effect of platooning on fuel consumption of class 8 vehicles over a range of speeds, following distances, and mass (Vol. 7, No. 2). National Renewable Energy Lab.(NREL), Golden, CO.
<https://www.sae.org/publications/technical-papers/content/2014-01-2438/>
- Lammert, M. P., McAuliffe, B., Smith, P., Raeesi, A., Hoffman, M., & Bevly, D. (2020). Impact of lateral alignment on the energy savings of a truck platoon (No. NREL/CP-5400-78216). National Renewable Energy Lab.(NREL), Golden, CO (United States).
<https://www.osti.gov/biblio/1726028>
- Ling, T., Cao, R., Deng, L., He, W., Wu, X., & Zhong, W. (2022). *Dynamic impact of automated truck platooning on highway bridges*. Engineering Structures, 262, 114326.
<https://www.sciencedirect.com/science/article/abs/pii/S014102962200445X>
- Linzell, D., Eftekhar Azam, S., Ardani, S., & Rageh, A. E. (2021). Low-Cost Modal Identification Sensors for Bridge Field Testing.
https://dot.nebraska.gov/media/sxuprtag/m105-low-cost-modal-final-report_06032021.pdf
- McConnell and Zettlemoyer. (2007). *Moment Redistribution and the Service II Limit State*. Delaware Center for Transportation. <https://bpb-us-w2.wpmucdn.com/sites.udel.edu/dist/1/1139/files/2013/10/Rpt.-185-Moment-Redistribution-Service-II-Limit-State-sf44fm.pdf>
- Mertz, D. R. (2000). *Service Limit State Control of Permanent Deflection for Steel Sections in Flexure*. In Advanced Technology in Structural Engineering (pp. 1-5).
[https://ascelibrary.org/doi/abs/10.1061/40492\(2000\)158](https://ascelibrary.org/doi/abs/10.1061/40492(2000)158)
- Mlynarski, M., Wassef, W. G., & Nowak, A. S. (2011). *A comparison of AASHTO bridge load rating methods (Vol. 700)*. Transportation Research Board. Washington, D.C
<https://nap.nationalacademies.org/catalog/22874/a-comparison-of-aashto-bridge-load-rating-methods>
- Moses, F. (2001). “*Calibration of load factors for LFRF bridge evaluation.*” National Cooperative Highway Research Program (NCHRP) Rep. 454, Transportation Research Board, Washington, DC. https://onlinepubs.trb.org/onlinepubs/nchrp/nchrp_rpt_454.pdf
- National Freight Strategic Plan (NFSP) (2020). U.S. Department of Transportation,
https://www.transportation.gov/sites/dot.gov/files/2020-09/NFSP_fullplan_508_0.pdf.
- National Steel Bridge Alliance (NSBA) (2015). *Continuous Span Standards*
<https://www.aisc.org/nsba/design-resources/continuous-span-standards/>

- Nebraska Department of Roads (NDOR). (2016). *Bridge Office Policies and Procedures* (BOPP), Lincoln, NE. <https://dot.nebraska.gov/business-center/bridge/>
- Nebraska Department of Roads (NDOR). (2022). *Nebraska Truck Information Guide*, Lincoln, NE. https://statepatrol.nebraska.gov/sites/default/files/2022-2023_truck_guide_-_web_copy.pdf
- Nowak, A. S. (1999). “*Calibration of LRFD bridge design code.*” National Cooperative Highway Research Program (NCHRP) Rep. 368, Transportation Research Board, Washington, DC. <https://www.trb.org/Publications/Blurbs/164809.aspx>
- Nowak, A. S., & Collins, K. R. (2012). *Reliability of structures*. CRC Press.
- Paultre, P., Chaallal, O., and Proulx, J. (1992). “*Bridge dynamics and dynamic amplification factors—a review of analytical and experimental findings.*” *Can. J. Civ. Eng.*, 19(2), 260–278. <https://cdnsiencepub.com/doi/abs/10.1139/192-032>
- Paultre, P., Proulx, J., & Talbot, M. (1995). *Dynamic testing procedures for highway bridges using traffic loads*. *Journal of structural engineering*, 121(2), 362-376. <https://ascelibrary.org/doi/abs/10.1061/%28ASCE%290733-9445%281995%29121%3A2%28362%29>
- Puckett, J., et al. (2007). *Simplified Live Load Distribution Factor Equations*, NCHRP Report 592, Transportation Research Board, The National Academies, Washington DC.
- Sajid, S., Chouinard, L., Legeron, F., Ude, T., He, E., & Ajrab, J. (2023). *Reliability analysis of bridges for autonomous truck platoons*. *Transportation research record*, 03611981221103235. <https://journals.sagepub.com/doi/full/10.1177/03611981221103235>
- Schilling, C. G. (1984). *Stress cycles for fatigue design of steel bridges*. *Journal of Structural Engineering*, 110(6), 1222-1234. [https://doi.org/10.1061/\(ASCE\)0733-9445\(1984\)110:6\(1222\)](https://doi.org/10.1061/(ASCE)0733-9445(1984)110:6(1222)).
- Siriaksorn, A & Naaman, A. E., (1982). *Reliability of partially prestressed beams at serviceability limit states*. *PCI Journal*, 27(6), 66-85. https://www.pci.org/PCI/Publications/PCI_Journal/Issues/1982/November-December/Reliability_of_Partially_Prestressed_Beams_at_Serviceability_Limit_States.a_spx
- Sivakumar, B., Ghosn, M., and Moses, F. (2011). “*Protocols for collecting and using traffic data in bridge design.*” National Cooperative Highway Research Program (NCHRP) Rep. No. 683, Transportation Research Board, Washington, DC. <https://www.trb.org/Publications/Blurbs/165399.aspx>

- Stallings, J. M., & Yoo, C. H. (1993). *Tests and ratings of short-span steel bridges*. Journal of Structural Engineering, 119(7), 2150-2168. [https://doi.org/10.1061/\(ASCE\)0733-9445\(1993\)119:7\(2150\)](https://doi.org/10.1061/(ASCE)0733-9445(1993)119:7(2150)).
- Stawska, S., Chmielewski, J., Nowak, A. S., & Stallings, M. (2022). *Bridge life consumption by permit vehicles*. Structure and Infrastructure Engineering, 1-13. https://www.tandfonline.com/doi/full/10.1080/15732479.2022.2028859?casa_token=Y50_-HSDzRVwAAAAA%3AhuPLRft3cgcxJT0xOqmDZkgVLHBvPOaTph3p2UMgY8hwXRhlzKzEb1_YgvStdCL-bLJuQYFv-6uAgLM
- Steelman, J. S., Puckett, J. A., Linzell, D. G., & Yang, B. (2021). *Truck Platooning Effects on Girder Bridges (No. SPR-1 (20) M030)*. Nebraska. Department of Transportation. <https://dot.nebraska.gov/media/114516/spr-1-20-m030-truck-platooning-effects-on-girder-bridges-final-report.pdf>
- Tadros et al. (2001), *Prestress losses in pretensioned high-strength concrete bridge girders*, Transportation Research Board, NCHRP Report 496 https://onlinepubs.trb.org/onlinepubs/nchrp/nchrp_rpt_496.pdf
- Texas Department of Transportation (TXDOT). (2021). *Preferred Practices for Steel Bridge Design*, Austin, TX. https://ftp.dot.state.tx.us/pub/txdot-info/library/pubs/bus/bridge/steel_bridge.pdf
- Tohme R, Yarnold M. (2020). “*Steel Bridge Load Rating Impacts Owing to Autonomous Truck Platoons*.” Transportation Research Record: Journal of the Transportation Research Board. 2674(2):57-67. <https://journals.sagepub.com/doi/abs/10.1177/0361198120902435?journalCode=trra>
- Trimble, T. E., Baker, S., Wagner, J., Blano, M., Mallory, B., and Serian, B. (2018) “*Impacts of Connected Vehicles and Automated Vehicles on State and Local Transportation Agencies*.” National Cooperative Highway Research Program (NCHRP) Report 20-102(07) Transportation Research Board, Washington, D.C. <https://apps.trb.org/cmsfeed/TRBNetProjectDisplay.asp?ProjectID=4006>
- Tsugawa, S., Kato, S., & Aoki, K. (2011). *An automated truck platoon for energy saving*. IEEE/RSJ international conference on intelligent robots and systems (pp. 4109-4114). <https://ieeexplore.ieee.org/document/6094549>
- Wassef, W. G., Kulicki, J. M., Nassif, H., Mertz, D., & Nowak, A. S. (2014). *Calibration of AASHTO LRFD concrete bridge design specifications for serviceability*. NCHRP. <https://www.trb.org/Publications/Blurbs/170575.aspx>
- Wassef, W. (2021). *Truck Platooning Impacts on Bridges: Phase I–Structural Safety (No. FHWA-HIF-21-043)*. United States. Department of Transportation. Intelligent

Transportation Systems Joint Program Office (ITS JPO).
<https://rosap.ntl.bts.gov/view/dot/61012>

Yang, B., Steelman, J. S., Puckett, J. A., & Linzell, D. G. (2021). *Safe platooning headways on girder bridges*. Transportation Research Record, 03611981211036379.
<https://doi.org/10.1177/03611981211036379>

Yarnold M T, Weidner J S. (2019). “*Truck Platoon Impacts on Steel Girder Bridges.*” Journal of Bridge Engineering, 24(7). [https://ascelibrary.org/doi/abs/10.1061/\(ASCE\)BE.1943-5592.0001431](https://ascelibrary.org/doi/abs/10.1061/(ASCE)BE.1943-5592.0001431)

Zokaie, T., Osterkamp, T. A., and Imbsen, R. A.(1991). “*Distribution of wheel loads on highway bridges: Final report.*” National Cooperative Highway Research Program.
[https://www.safetylit.org/citations/index.php?fuseaction=citations.viewdetails&citationIds\[\]=citjournalarticle_602578_38](https://www.safetylit.org/citations/index.php?fuseaction=citations.viewdetails&citationIds[]=citjournalarticle_602578_38)

Appendices

Appendix A

This appendix recommended LRFR live load factor tables as described in Section 5.6. For steel bridges at Service II, there is a table for different platoon *LL CoVs*. For prestressed concrete bridges at Service III, there are tables for platoon *LL CoV* up to 0.2. These prestressed concrete bridges are designed using different methods, as shown in Table 3.1.

Appendix A. Recommended LRFR Live Load Factors

- Table A-1 provides the live load factors for various $CoVs$ of platoons.
- Bridge engineers can use Table A-1 to assess the load rating of steel bridges for Service II, considering the total CoV of platoons.
- Table A-2 to Table A-5 present the Service III live load factors for prestressed concrete bridges designed with *Post-0.8-Gains*, *Approx-0.8-Gains*, *Post-0.8-No-gains* and *Approx-0.8-No-gains* methods.
- Note: *Post-0.8-Gains* represents prestress loss method (LRFD BDS 5.9.3.4) with $\gamma_L = 0.8$ and considering elastic gains.
Approx-0.8-Gains represents prestress loss method (LRFD BDS 5.9.3.3) with $\gamma_L = 0.8$ and considering elastic gains.
Post-0.8-No-gains represents prestress loss method (LRFD BDS 5.9.3.3) with $\gamma_L = 0.8$ and without considering elastic gains.
Approx-0.8-No-gains represents prestress loss method (LRFD BDS 5.9.3.3) with $\gamma_L = 0.8$ and without considering elastic gains.

Table A-1. Calibrated Service II Live Load Factors for Steel bridges Considering Changes of CoV ($\beta_{Implicit} = 1.6$)

Truck platoon	Frequency	Load conditions	DF	ADTT (one direction)	Load factors by CoV of total live load					
					$COV_{LL} = 0.00$	$COV_{LL} = 0.04$	$COV_{LL} = 0.08$	$COV_{LL} = 0.12$	$COV_{LL} = 0.16$	$COV_{LL} = 0.20$
Multiple trucks in platoon	single-trip	No other vehicles on the bridge	One lane	N/A	1.15	1.15	1.15	1.15	1.25	1.25
	single-trip	Two identical platoons loaded on two lanes	Two or more lanes	N/A	1.15	1.15	1.15	1.15	1.25	1.25
	100 Crossings	Mixed with routine traffic in the adjacent lane	One lane	> 5000	1.90	1.90	1.90	1.90	1.90	1.90

- DF is the *AASHTO LRFD* approximate GDF, with the multiple presence factor (MPF = 1.2) removed for one-lane GDFs.
- To use with a different IM factor, scale tabulated values by $1.33 / (1 + IM_{desired})$.

Table A-2. Calibrated Service III Live Load Factors for Prestressed Concrete Bridges Using *Post-0.8-Gains* ($\beta_{Implicit} = -0.6$)

Truck platoon	Frequency	Load conditions	DF	ADTT (one direction)	Load factors by <i>COV</i> of total live load
					$COV_{LL} = 0 - 0.20$
Multiple trucks in platoon	single-trip	No other vehicles on the bridge	One lane	N/A	0.90
	single-trip	Two identical platoons loaded on two lanes	Two or more lanes	N/A	0.90
	100 Crossings	Mixed with routine traffic in the adjacent lane	One lane	> 5000	1.75

a. DF is the *AASHTO LRFD* approximate GDF, with the multiple presence factor (MPF = 1.2) removed for one-lane GDFs.

b. To use with a different *IM* factor, scale tabulated values by $1.33 / (1 + IM_{desired})$.

Table A-3. Calibrated Service III Live Load Factors for Prestressed Concrete Bridges Using *Approx-0.8-Gains* ($\beta_{Implicit} = -0.6$)

Truck platoon	Frequency	Load conditions	DF	ADTT (one direction)	Load factors by <i>COV</i> of total live load
					$COV_{LL} = 0 - 0.20$
Multiple trucks in platoon	single-trip	No other vehicles on the bridge	One lane	N/A	0.90
	single-trip	Two identical platoons loaded on two lanes	Two or more lanes	N/A	0.90
	100 Crossings	Mixed with routine traffic in the adjacent lane	One lane	> 5000	1.65

a. DF is the *AASHTO LRFD* approximate GDF, with the multiple presence factor (MPF = 1.2) removed for one-lane GDFs.

b. To use with a different *IM* factor, scale tabulated values by $1.33 / (1 + IM_{desired})$.

Table A-4. Calibrated Service III Live Load Factors for Prestressed Concrete Bridges Using *Post-0.8-No-gains* ($\beta_{Implicit} = -0.6$)

Truck platoon	Frequency	Load conditions	DF	ADTT (one direction)	Load factors by <i>COV</i> of total live load
					$COV_{LL} = 0 - 0.20$
Multiple trucks in platoon	single-trip	No other vehicles on the bridge	One lane	N/A	0.75
	single-trip	Two identical platoons loaded on two lanes	Two or more lanes	N/A	0.75
	100 Crossings	Mixed with routine traffic in the adjacent lane	One lane	> 5000	1.20

a. DF is the *AASHTO LRFD* approximate GDF, with the multiple presence factor (MPF = 1.2) removed for one-lane GDFs.

b. To use with a different *IM* factor, scale tabulated values by $1.33 / (1 + IM_{desired})$.

Table A-5. Calibrated Service III Live Load Factors for Prestressed Concrete Bridges Using *Approx-0.8-No-gains* ($\beta_{Implicit} = -0.6$)

Truck platoon	Frequency	Load conditions	DF	ADTT (one direction)	Load factors by <i>COV</i> of total live load
					$COV_{LL} = 0 - 0.20$
Multiple trucks in platoon	single-trip	No other vehicles on the bridge	One lane	N/A	0.80
	single-trip	Two identical platoons loaded on two lanes	Two or more lanes	N/A	0.80
	100 Crossings	Mixed with routine traffic in the adjacent lane	One lane	> 5000	1.30

a. DF is the *AASHTO LRFD* approximate GDF, with the multiple presence factor (MPF = 1.2) removed for one-lane GDFs.

b. To use with a different *IM* factor, scale tabulated values by $1.33 / (1 + IM_{desired})$.

Appendix B

This appendix contains recommended safe headway spacing tables for different platoon *LL CoVs* for steel bridges at Service II, as described in Section 6.3.

Appendix B. Recommended Safe Headway Tables for Steel Bridges at Service II

- Table B-1 to Table B-10 present the safe headway tables for different *CoV*s of platoons.
- To evaluate steel bridges Service II, bridge engineers can use these tables to establish platoon headway operation headway guidance based on the total *CoV* of platoons.
- “Fail” in these tables indicates that either the required headway is greater than 50 ft or that the bridge has reached its limit regardless of headway.
- For simple-span bridges, the safe headway requirements were slightly more conservative than for two-span bridges. Only simple-span bridge results are presented here.

Table B-1. Positive Moment (+M) Safe Headways, Single-Lane Platoons, 60-ft Steel Bridges

Amplification factor α	<i>CoV</i>					
	0.00	0.04	0.08	0.12	0.16	0.20
0.6	5	5	5	5	5	5
0.7	5	5	5	5	5	5
0.8	5	5	5	5	5	5
0.9	5	5	5	5	5	5
1.0	5	5	5	5	5	5
1.1	5	5	5	5	5	5
1.2	5	5	5	5	5	5
1.3	5	5	5	5	5	5
1.4	5	5	5	5	5	5
1.5	5	5	5	5	5	5
1.6	5	5	5	5	5	5
1.7	5	5	5	5	5	5
1.8	5	5	5	5	5	5
1.9	5	5	5	5	5	5
2.0	5	5	5	5	5	6
2.1	5	5	5	6	7	9
2.2	6	6	7	8	10	14
2.3	8	8	10	12	17	Fail
2.4	11	12	14	Fail	Fail	Fail
2.5	Fail	Fail	Fail	Fail	Fail	Fail

Table B-2. Positive Moment (+M) Safe Headways, Single-Lane Platoons with Adjacent Routine Traffic (100 Crossings, ADTT = 5000), 60-ft Steel Bridges

Amplification factor α	<i>CoV</i>					
	0.00	0.04	0.08	0.12	0.16	0.20
0.6	5	5	5	5	5	5
0.7	5	5	5	5	5	5
0.8	5	5	5	5	5	5
0.9	5	5	5	5	5	5
1.0	5	5	5	5	5	5
1.1	5	5	5	5	5	5
1.2	5	5	5	5	5	5
1.3	5	5	5	5	5	5
1.4	5	5	5	5	5	6
1.5	5	5	6	7	8	10
1.6	9	9	10	12	14	Fail
1.7	15	16	Fail	Fail	Fail	Fail
1.8	Fail	Fail	Fail	Fail	Fail	Fail

Table B-3. Positive Moment (+M) Safe Headways, Single-Lane Platoons, 90-ft Steel Bridges

Amplification factor α	<i>CoV</i>					
	0.00	0.04	0.08	0.12	0.16	0.20
0.6	5	5	5	5	5	5
0.7	5	5	5	5	5	5
0.8	5	5	5	5	5	5
0.9	5	5	5	5	5	5
1.0	5	5	5	5	5	5
1.1	5	5	5	5	5	5
1.2	5	5	5	5	5	5
1.3	5	5	5	5	5	5
1.4	5	5	5	5	5	5
1.5	5	5	5	5	5	5
1.6	5	5	5	5	5	5
1.7	5	5	5	5	6	7
1.8	6	6	7	7	8	9
1.9	8	8	8	9	10	11
2.0	9	10	10	11	12	13
2.1	11	11	12	13	14	15
2.2	13	13	14	15	16	17
2.3	15	15	15	17	18	20
2.4	17	17	18	19	21	24
2.5	19	19	20	22	25	32
2.6	22	22	24	27	Fail	Fail
2.7	26	27	31	Fail	Fail	Fail
2.8	Fail	Fail	Fail	Fail	Fail	Fail

Table B-4. Positive Moment (+M) Safe Headways, Single-Lane Platoons with Adjacent Routine Traffic (100 Crossings, ADTT = 5000), 90-ft Steel Bridges

Amplification factor α	<i>CoV</i>					
	0.00	0.04	0.08	0.12	0.16	0.20
0.6	5	5	5	5	5	5
0.7	5	5	5	5	5	5
0.8	5	5	5	5	5	5
0.9	5	5	5	5	5	5
1.0	5	5	5	5	5	5
1.1	5	5	5	5	5	5
1.2	6	6	6	7	7	8
1.3	8	9	9	9	10	11
1.4	11	11	11	12	13	14
1.5	14	14	14	15	15	17
1.6	16	17	17	18	19	21
1.7	20	20	21	22	25	28
1.8	26	26	28	33	0	Fail
1.9	Fail	Fail	Fail	Fail	Fail	Fail

Table B-5. Positive Moment (+M) Safe Headways, Single-Lane Platoons, 120-ft Steel Bridges

Amplification factor α	CoV					
	0.00	0.04	0.08	0.12	0.16	0.20
0.6	5	5	5	5	5	5
0.7	5	5	5	5	5	5
0.8	5	5	5	5	5	5
0.9	5	5	5	5	5	5
1.0	5	5	5	5	5	5
1.1	5	5	5	5	5	5
1.2	5	5	5	5	5	5
1.3	5	5	5	5	5	5
1.4	5	5	5	5	5	6
1.5	5	5	5	6	7	9
1.6	7	8	8	9	10	12
1.7	10	10	11	12	13	14
1.8	13	13	14	15	16	17
1.9	15	16	16	17	18	19
2.0	18	18	18	19	20	21
2.1	20	20	20	21	22	24
2.2	22	22	22	23	24	26
2.3	24	24	24	25	26	28
2.4	25	26	26	27	29	30
2.5	27	28	28	29	31	33
2.6	29	30	30	32	34	36
2.7	32	32	33	35	38	42
2.8	34	35	36	39	45	Fail
2.9	39	40	42	Fail	Fail	Fail
3.0	Fail	Fail	Fail	Fail	Fail	Fail

Table B-6. Positive Moment (+M) Safe Headways, Single-Lane Platoons with Adjacent Routine Traffic (100 Crossings, ADTT = 5000), 120-ft Steel Bridges

Amplification factor α	<i>CoV</i>					
	0.00	0.04	0.08	0.12	0.16	0.20
0.6	5	5	5	5	5	5
0.7	5	5	5	5	5	5
0.8	5	5	5	5	5	5
0.9	5	5	5	5	5	5
1.0	6	6	6	7	8	9
1.1	10	10	11	12	12	13
1.2	14	14	15	15	16	17
1.3	18	18	18	19	20	21
1.4	21	21	21	22	23	24
1.5	24	24	25	25	26	27
1.6	27	27	28	28	29	30
1.7	30	30	31	32	33	35
1.8	34	34	35	37	39	44
1.9	41	42	44	Fail	Fail	Fail
2.0	Fail	Fail	Fail	Fail	Fail	Fail

Table B-7. Positive Moment (+M) Safe Headways, Single-Lane Platoons, 150-ft Steel Bridges

Amplification factor α	CoV					
	0.00	0.04	0.08	0.12	0.16	0.20
0.6	5	5	5	5	5	5
0.7	5	5	5	5	5	5
0.8	5	5	5	5	5	5
0.9	5	5	5	5	5	5
1.0	5	5	5	5	5	5
1.1	5	5	5	5	5	5
1.2	5	5	5	5	5	5
1.3	5	5	5	5	6	7
1.4	6	7	7	8	9	10
1.5	9	9	10	10	11	13
1.6	12	12	13	14	15	17
1.7	15	16	16	17	19	20
1.8	19	19	20	21	22	24
1.9	22	22	23	24	25	27
2.0	25	25	26	27	28	29
2.1	28	28	28	29	31	32
2.2	30	30	31	32	33	34
2.3	32	32	33	34	35	37
2.4	34	35	35	36	37	39
2.5	37	37	37	38	40	41
2.6	39	39	39	40	42	43
2.7	41	41	42	43	44	46
2.8	43	43	44	45	47	49
2.9	45	45	46	48	Fail	Fail
3.0	48	48	50	Fail	Fail	Fail
3.1	Fail	Fail	Fail	Fail	Fail	Fail

Table B-8. Positive Moment (+M) Safe Headways, Single-Lane Platoons with Adjacent Routine Traffic (100 Crossings, ADTT = 5000), 150-ft Steel Bridges

Amplification factor α	<i>CoV</i>					
	0.00	0.04	0.08	0.12	0.16	0.20
0.6	5	5	5	5	5	5
0.7	5	5	5	5	5	5
0.8	5	5	5	5	5	5
0.9	8	8	8	8	9	10
1.0	12	12	13	13	14	15
1.1	18	18	18	19	20	21
1.2	23	23	23	24	25	26
1.3	27	27	28	28	29	30
1.4	31	31	32	32	33	34
1.5	35	35	35	36	37	38
1.6	38	38	39	39	40	41
1.7	41	41	42	43	44	45
1.8	45	45	45	47	48	50
1.9	50	50	Fail	Fail	Fail	Fail

Table B-9. Positive Moment (+M) Safe Headways, Single-Lane Platoons, 200-ft Steel Bridges

Amplification factor α	<i>CoV</i>					
	0.00	0.04	0.08	0.12	0.16	0.20
0.6	5	5	5	5	5	5
0.7	5	5	5	5	5	5
0.8	5	5	5	5	5	5
0.9	5	5	5	5	5	5
1.0	5	5	5	5	5	5
1.1	5	5	5	5	5	5
1.2	5	5	5	5	6	7
1.3	8	8	8	9	10	12
1.4	12	12	13	14	15	16
1.5	16	16	17	17	19	20
1.6	19	19	20	21	22	23
1.7	22	23	23	24	26	28
1.8	26	27	28	29	31	33
1.9	31	31	32	33	35	37
2.0	35	36	36	38	39	41
2.1	39	39	40	41	43	45
2.2	43	43	44	45	46	48
2.3	46	46	47	48	49	Fail
2.4	49	49	50	Fail	Fail	Fail
2.5	Fail	Fail	Fail	Fail	Fail	Fail

Table B-10. Positive Moment (+M) Safe Headways, Single-Lane Platoons with Adjacent Routine Traffic (100 Crossings, ADTT = 5000), 200-ft Steel Bridges

Amplification factor α	<i>CoV</i>					
	0.00	0.04	0.08	0.12	0.16	0.20
0.6	5	5	5	5	5	5
0.7	5	5	5	5	5	5
0.8	9	9	9	10	11	12
0.9	16	16	16	17	17	18
1.0	21	21	22	22	23	24
1.1	28	28	28	29	30	32
1.2	35	35	36	36	38	39
1.3	41	41	42	43	44	45
1.4	47	47	47	48	49	50
1.5	Fail	Fail	Fail	Fail	Fail	Fail

Appendix C

This appendix contains detailed calculations related to the example prestressed concrete simple-span bridge described in Section 8.2.

Appendix C. LRFR Load Rating Example of a 130' NU1600 Simple-span Prestressed Concrete I-girder Bridge (interior girder)

Note: Bridge S080 41653 is a 130-ft simple-span, prestressed multi-girder bridge at the I-80 4S Greenwood Interchange in Greenwood, Nebraska (Figure 39). The bridge was constructed in 2009 and has three design lanes, and the average daily traffic is 49,240. The rating code in NBI (2022) indicates that the rating method is LRFR.

The example illustrates design and platoon ratings of an interior prestressed concrete girder at midspan (@ 0.5L) for positive moment, at the first critical shear section, and at a location where vertical shear reinforcement spacings changes.

Elastic gains from dead and live loads were considered. The analysis was based on the gross section properties. Shear resistance was calculated using the simplified and general modified compression field theory (MCFT). Prestress losses were calculated using refined estimates described in LRFD BDS Article 5.9.3.4. HL-93 design and platoon rating factors were computed for Strength I and Service III.

Considering the platoon as a future permit truck, the Service I rating for the platoon was performed as the permit rating in MBE (2018).

1. Bridge Data

Span Length $L := 130 \text{ ft}$

Year built 2009

Concrete information

Ultimate strength for deck $f'_{cd} := 4 \text{ ksi}$

Initial strength for deck $f'_{cdi} := 4 \text{ ksi}$

Strength of girder concrete at time of transfer $f'_{ci} := 7.5 \text{ ksi}$

Ultimate strength of girder concrete $f'_c := 9.5 \text{ ksi}$

Unit weight of concrete for determining dead loads $w_c := 155 \text{ pcf}$

Unit weight of concrete for determining deck modulus of elasticity $w_{cd_modulus} := 155 \text{ pcf}$

Unit weight of concrete for determining girder modulus of elasticity $w_{cg_modulus} := 150 \text{ pcf}$

$$E_c = 120,000K_1w_c^{2.0}f_c'^{0.33} \quad (5.4.2.4-1)$$

$$E_c = 33,000K_1w_c^{1.5}\sqrt{f_c'} \quad (C5.4.2.4-2)$$

Modulus of elasticity of concrete girder at time of transfer

$$E_{ci} := 120000 \cdot \left(\frac{w_{cg_modulus}}{pcf \cdot 1000} \right)^{2.0} \cdot \left(\frac{f'_{ci}}{ksi} \right)^{0.33} \cdot ksi = 5249.694 \text{ ksi}$$

Modulus of elasticity of concrete girder at ultimate strength

$$E_c := 120000 \cdot \left(\frac{w_{cg_modulus}}{pcf \cdot 1000} \right)^{2.0} \cdot \left(\frac{f'_c}{ksi} \right)^{0.33} \cdot ksi = 5675.61 \text{ ksi}$$

Modulus of elasticity of deck at final time

$$E_{cd} := 33000 \cdot \left(\frac{w_{cd_modulus}}{pcf \cdot 1000} \right)^{1.5} \cdot \left(\frac{f'_{cd}}{ksi} \right)^{0.5} \cdot ksi = 4027.555 \text{ ksi}$$

Modulus of elasticity of deck at initial

$$E_{cdi} := 33000 \cdot \left(\frac{w_{cd_modulus}}{pcf \cdot 1000} \right)^{1.5} \cdot \left(\frac{f'_{cdi}}{ksi} \right)^{0.5} \cdot ksi = 4027.555 \text{ ksi}$$

Vertical shear reinforcement information

Note: Wire fabric (70 ksi) was used as shear reinforcement, and BrR does not readily support this. In BrR and the example computations, shear reinforcement was modeled using 3.1 legs. Similarly, 1.80 legs were used for other locations. Vertical shear reinforcement details and spacings are shown below.



Vertical Horizontal

Span:

	Name	Extends into deck	Start distance (ft)	Number of spaces	Spacing (in)	Length (ft)	End distance (ft)
▶	D31	<input checked="" type="checkbox"/>	0.00	9	2.0000	1.50	1.50
	D18	<input checked="" type="checkbox"/>	1.50	21	4.0000	7.00	8.50
	D18	<input checked="" type="checkbox"/>	8.50	19	8.0000	12.67	21.17
	D18	<input checked="" type="checkbox"/>	21.17	44	12.0000	44.00	65.17
	D18	<input checked="" type="checkbox"/>	65.17	1	8.0000	0.67	65.83
	D18	<input checked="" type="checkbox"/>	65.83	44	12.0000	44.00	109.83
	D18	<input checked="" type="checkbox"/>	109.83	19	8.0000	12.67	122.50
	D18	<input checked="" type="checkbox"/>	122.50	21	4.0000	7.00	129.50
	D31	<input checked="" type="checkbox"/>	129.50	8	2.0000	1.33	130.83

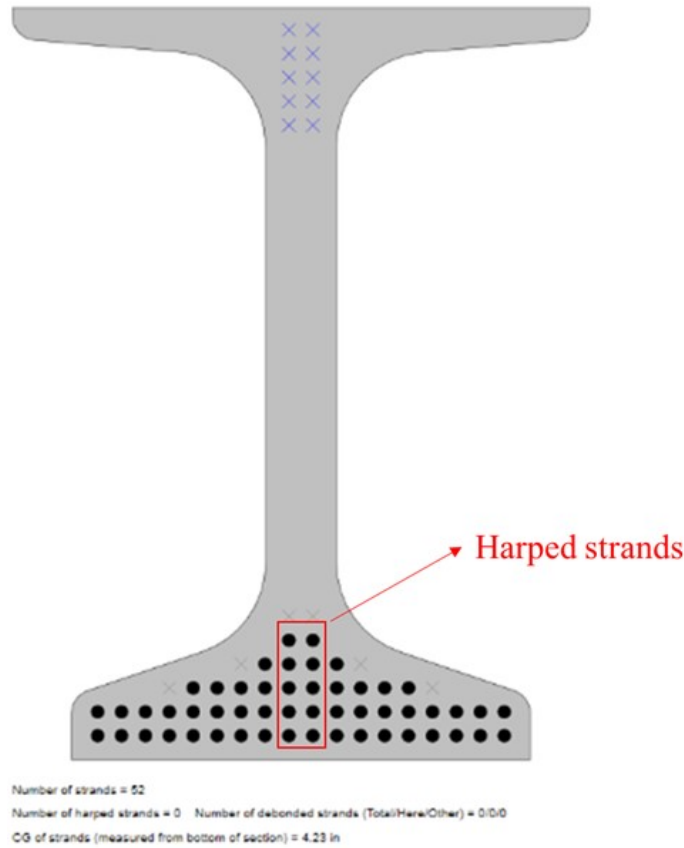
Compression steel

The BrR file does not contain any information about the compression steel.

Other information

1. Skew: 10 degrees.
2. ADT: 49240.

Prestress steel information



Note: 0.6", 270 ksi, low-relaxation strands. There are total 52 prestress strands (10 strands harped).

0.6", low-relaxation strand

$$d_b := 0.6 \text{ in}$$

Area of prestress per strands

$$A_{strand} := 0.217 \text{ in}^2$$

Ultimate strength of prestressed strands

$$f_{pu} := 270 \text{ ksi}$$

Yield stress of prestressed strands

$$f_{py} := 243 \text{ ksi}$$

Prestressed strands stress prior to transfer

$$f_{pi} := 0.75 \cdot f_{pu} = 202.5 \text{ ksi}$$

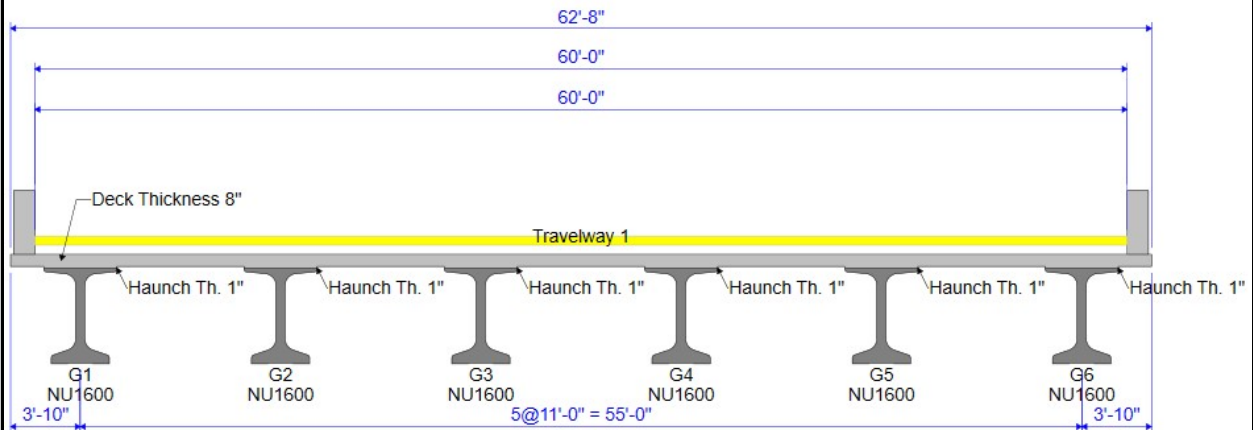
Modulus of elasticity of prestress

$$E_p := 28500 \text{ ksi}$$

Modulus of ratio for deck to girder concrete

$$n_{pd} := \frac{E_{cd}}{E_c} = 0.71$$

2. Bridge Cross Section



Girder spacing (S)

$$S := 11 \text{ ft}$$

Number of girders

$$N_{girder} := 6$$

Overhang

$$overhang := 3.833 \text{ ft}$$

Barrier length

$$L_{barrier} := 0.333 \text{ ft}$$

Total bridge width

$$W_{bridge} := (overhang \cdot 2 + S \cdot (N_{girder} - 1)) = 751.992 \text{ in}$$

Effective width for deck (for interior girders)

$$b_{eff} := S = 132 \text{ in}$$

3. Interior Girder Details

Name:

Description:

Top flange type
 Narrow
 Wide

Dimensions Properties Mild steel Strand grid

Area:	<input type="text" value="812.1589358"/>	in ²	Volume/surface ratio:	<input type="text" value="3.077"/>	in
Nominal load:	<input type="text" value="845.999"/>	lb/ft	Half depth area for pos. flex.:	<input type="text" value="430.298"/>	in ²
Moment of inertia:	<input type="text" value="458893.983"/>	in ⁴	Half depth area for neg. flex.:	<input type="text" value="332.480"/>	in ²
CG from bottom:	<input type="text" value="28.4245"/>	in	St. Venant torsional constant:	<input type="text" value="20894.555"/>	in ⁴
Section modulus, top:	<input type="text" value="13272.244"/>	in ³	<input type="checkbox"/> Use entered section properties		
Section modulus, bot.:	<input type="text" value="16144.290"/>	in ³	Note: see engine related help for analysis engine specific information on the "Use entered section properties" selection.		
Nominal depth:	<input type="text" value="63.0000"/>	in	Note: 150 pcf concrete is assumed to compute the nominal load.		

Girder gross section area

$$A_g := 812 \text{ in}^2$$

Beam height

$$h_{nc} := 63 \text{ in}$$

Top girder width

$$b_{top} := 48.25 \text{ in}$$

Moment of inertia precast girder

$$I_{nc} := 458893 \text{ in}^4$$

Girder centroid to the bottom of fiber

$$y_{ncb} := 28.42 \text{ in}$$

Girder centroid to the top of fiber

$$y_{nct} := h_{nc} - y_{ncb} = 34.58 \text{ in}$$

Non-composite section modulus top

$$S_{top_nc} := \frac{I_{nc}}{h_{nc} - y_{ncb}} = 13270.474 \text{ in}^3$$

Non-composite section modulus bottom

$$S_{bot_nc} := \frac{I_{nc}}{y_{ncb}} = 16146.833 \text{ in}^3$$

Thickness of deck (loads calculations)

$$t_s := 8 \text{ in}$$

Thickness of deck (effective)

$$h_d := 7.5 \text{ in}$$

Section property calculations

Transformed width of deck
(deck concrete to girder concrete)

$$b_{d_tr} := b_{eff} \cdot n_{pd} = 93.671 \text{ in}$$

Cross-section area of deck

$$A_{d_tr} := b_{d_tr} \cdot h_d = 702.529 \text{ in}^2$$

Deck moment of inertia of deck about its centroid

$$I_{d_tr} := \frac{h_d^3 \cdot b_{d_tr}}{12} = 3293.104 \text{ in}^4$$

Height of haunch

$$h_h := 1 \text{ in}$$

Transformed width of haunch

$$b_{h_tr} := b_{top} \cdot n_{pd} = 34.239 \text{ in}$$

Area of haunch

$$A_{h_tr} := b_{h_tr} \cdot h_h = 34.239 \text{ in}^2$$

Haunch moment of inertia of haunch about its centroid

$$I_{h_tr} := \frac{h_h^3 \cdot b_{h_tr}}{12} = 2.853 \text{ in}^4$$

Total height of composite beam

$$h_c := h_h + h_{nc} + h_d = 71.5 \text{ in}$$

Transformed section area
(including deck and haunch)

$$A_c := A_g + A_{d_tr} + A_{h_tr} = 1548.768 \text{ in}^2$$

Center of deck to the bottom of fiber

$$h_{d_center} := \left(h_{nc} + h_h + \frac{h_d}{2} \right) = 67.75 \text{ in}$$

Center of haunch to the bottom of fiber

$$h_{h_center} := \left(h_{nc} + \frac{h_h}{2} \right) = 63.5 \text{ in}$$

Center to the bottom of fiber (composite)

$$y_{cb} := \frac{A_g \cdot y_{ncb} + A_{d_tr} \cdot h_{d_center} + A_{h_tr} \cdot h_{h_center}}{A_c} = 47.036 \text{ in}$$

Moment of inertia (composite)

$$I_c := \left(I_{nc} + A_g \cdot (y_{ncb} - y_{cb})^2 \right) + \left(I_{d_tr} + A_{d_tr} \cdot (h_{d_center} - y_{cb})^2 \right) + \left(I_{h_tr} + A_{h_tr} \cdot (h_{h_center} - y_{cb})^2 \right) = 1054306.916 \text{ in}^4$$

Composite section modulus top beam $S_{top,c} := \frac{I_c}{h_{nc} - y_{cb}} = 66041.996 \text{ in}^3$

Composite section modulus bottom beam $S_{bot,c} := \frac{I_c}{y_{cb}} = 22414.983 \text{ in}^3$

Dead load moment calculations (BrR line-girder analysis)

Non-composite Dead Load DC1 Moment at the mid span $M_{DC1} := 4357.7 \text{ kip} \cdot \text{ft}$

Composite Dead Load DC2 Moment at the mid span $M_{DC2} := 310.5 \text{ kip} \cdot \text{ft}$

Wearing surface load moment at the mid span $M_{DW} := 0 \text{ kip} \cdot \text{ft}$

Note: The dead load effects are directly extracted from BrR.

HL-93 design loading moment calculations (BrR line-girder analysis)

Modular ratio for AASHTO GDFs $n_{GDF} := \frac{E_c}{E_{cd}} = 1.409$

e_g term for AASHTO GDF equations $e_{g,GDF} := y_{nct} + h_h + \frac{h_d}{2} = 39.33 \text{ in}$

K_g term for AASHTO GDF equations $K_g := n_{GDF} \cdot (I_{nc} + A_g \cdot e_{g,GDF}^2) = 2416676.725 \text{ in}^4$

Distribution Factors

One Design Lane Loaded:

$$0.06 + \left(\frac{S}{14}\right)^{0.4} \left(\frac{S}{L}\right)^{0.3} \left(\frac{K_g}{12.0 L t_s^3}\right)^{0.1}$$

Two or More Design Lanes Loaded:

$$0.075 + \left(\frac{S}{9.5}\right)^{0.6} \left(\frac{S}{L}\right)^{0.2} \left(\frac{K_g}{12.0 L t_s^3}\right)^{0.1}$$

Single lane AASHTO moment GDF for interior girders

$$g_{m1} := 0.06 + \left(\frac{S}{14}\right)^{0.4} \cdot \left(\frac{S}{L}\right)^{0.3} \cdot \left(\frac{\frac{K_g}{\text{in}^4}}{\left(12 \cdot \frac{L}{\text{ft}} \cdot \left(\frac{h_d}{\text{in}}\right)^3\right)}\right)^{0.1} = 0.553$$

Multiple lanes AASHTO moment GDF for interior girders

$$g_{m2} := 0.075 + \left(\frac{S}{9.5 \text{ ft}} \right)^{0.6} \cdot \left(\frac{S}{L} \right)^{0.2} \cdot \left(\frac{\frac{K_g}{\text{in}^4}}{\left(12 \cdot \frac{L}{\text{ft}} \cdot \left(\frac{h_d}{\text{in}} \right)^3 \right)} \right)^{0.1} = 0.834$$

Single lane AASHTO shear GDF for interior girders $g_{v1} := 0.36 + \frac{S}{25 \text{ ft}} = 0.8$

Multiple lanes AASHTO shear GDF for interior girders $g_{v2} := 0.20 + \frac{S}{12 \text{ ft}} - \left(\frac{S}{35 \text{ ft}} \right)^2 = 1.018$

Distributed live load moment at the midspan $HL_{93}M_{dist} := 3412.1 \text{ kip} \cdot \text{ft}$
(including $IM = 0.33$ for truck and g_{m2})

Note: The HL-93 loading load effects are directly extracted from BrR.

4. Compute Nominal Flexural Resistance at the Mid Span

$$f_{ps} = f_{pu} \left(1 - k \frac{c}{d_p} \right)$$

$$k = 0.28 \text{ for low-relaxation strands}$$

$$f_{pu} = 270 \text{ ksi}$$

$$d_p = \text{distance from extreme compression fiber to the centroid of the prestressing tendons}$$

Center of PS strands to the bottom girder

$$y_{bar} := 4.23 \text{ in}$$

Distance from extreme compression fiber to the centroid of the prestressing strands

$$d_p := h_{nc} + h_h + h_d - y_{bar} = 67.27 \text{ in}$$

Number of strands

$$N_{ps} := 52$$

Area of total prestress

$$A_{ps} := A_{strand} \cdot N_{ps} = 11.284 \text{ in}^2$$

$$\alpha_1 := 0.85$$

Stress factor of compression block

$$\beta_1 := 0.85$$

0.28 for low-relaxation

$$k := 0.28$$

Distance from neutral axis to the compressive face

$$c := \frac{A_{ps} \cdot f_{pu}}{\alpha_1 \cdot f'_{cd} \cdot \beta_1 \cdot b_{eff} + k \cdot A_{ps} \cdot \frac{f_{pu}}{d_p}} = 7.73 \text{ in}$$

Depth of the equivalent stress block

$$a := \beta_1 \cdot c = 6.57 \text{ in}$$

Note: Because the "a" is smaller than the deck thickness, the rectangular section behavior assumption is valid.

Average stress in prestressing strand, ksi

$$f_{ps} := f_{pu} \cdot \left(1 - k \cdot \frac{c}{d_p} \right) = 261.313 \text{ ksi}$$

Nominal flexural resistance at the mid span

$$M_n := A_{ps} \cdot f_{ps} \cdot \left(d_p - \frac{a}{2} \right) = 15722.487 \text{ kip} \cdot \text{ft}$$

5. Check the Maximum Reinforcement

Note: LRFD BDS Article 5.6.2.1 limits the factor resistance of compression controlled sections. Over-reinforced (compression controlled) sections are limited by this approach. Using similar triangles, the net tensile strain is determined at nominal strength.

Based on an allowable concrete strain of 0.003 and the distance from the extreme concrete compression fiber to the center of gravity of the prestressing strands.

Allowable concrete strain $\varepsilon_c := 0.003$

Net tensile strain $\varepsilon_t := \frac{\varepsilon_c}{c} \cdot (d_p - c) = 0.023$

Note: Because $\varepsilon_t > 0.005$, the section is tension controlled and resistance factor shall be taken as 1.0.

Strength Reduction Factor $\phi := 1.0$

Factored required moment

$$M_u := 1.25 \cdot (M_{DC1} + M_{DC2}) + 1.50 \cdot M_{DW} + 1.75 \cdot (HL_93_M_{dist}) = 11806 \text{ kip} \cdot \text{ft}$$

Demand/capacity ratio for the mid span $DCR_{mid} := \frac{M_u}{\phi \cdot M_n} = 0.751$

6. Compute Prestress Loss according to *LRFD BDS* Article 5.9.3.4 (Gross Section)

Assumed center of PS strands to bottom of fiber $e_{nc} := y_{ncb} - y_{bar} = 24.19 \text{ in}$

Eccentricity (composite at final) $e_c := e_{nc} + y_{cb} - y_{ncb} = 42.806 \text{ in}$

Shape factor (V/S) $V_S_Girder := 3.077$

Average Humidity (Nebraska) $H := 65$

Age of girder concrete at time of transfer (day) $t_i := 1$

Age of girder concrete at time of deck placement $t_d := 30$

Age of girder concrete at time at final time $t_f := 3650$

Permanent load moments at midspan acting on non-composite section (beam) $M_g := 1846.8 \text{ kip} \cdot \text{ft}$

Losses due to elastic shortening $\Delta f_{pES} := \frac{A_{ps} \cdot f_{pi} \cdot (I_{nc} + e_{nc}^2 \cdot A_g) - e_{nc} \cdot M_g \cdot A_g}{A_{ps} \cdot (I_{nc} + e_{nc}^2 \cdot A_g) + \frac{A_g \cdot I_{nc} \cdot E_{ci}}{E_p}} = 21.458 \text{ ksi}$

Stress in strand after elastic shortening $f_{pt1} := f_{pi} - \Delta f_{pES} = 181.042 \text{ ksi}$

Concrete stress at the center of strands due to the prestressing force at transfer and the self weight of the member $f_{cgp} := \frac{f_{pt1} \cdot A_{ps}}{A_g} + \frac{f_{pt1} \cdot A_{ps} \cdot e_{nc}^2}{I_{nc}} - \frac{M_g \cdot e_{nc}}{I_{nc}} = 3.953 \text{ ksi}$

k_s term calculation $k_s := \max(1, (1.45 - 0.13 \cdot V_S_Girder)) = 1.05$

Humidity factor for shrinkage $k_{hs} := 2 - 0.014 \cdot H = 1.09$

Concrete strength factor $k_f := \frac{5 \text{ ksi}}{1 \text{ ksi} + f'_{ci}} = 0.588$

$$k_{td} = \frac{t}{12 \left(\frac{100 - 4 f'_{ci}}{f'_{ci} + 20} \right) + t}$$

Time development factor

Time development factor (initial to deck) $k_{tdd} := \frac{(t_d - t_i)}{12 \cdot \left(\frac{100 \text{ ksi} - 4 \cdot f'_{ci}}{f'_{ci} + 20 \text{ ksi}} \right) + (t_d - t_i)} = 0.487$

Shrinkage strain (initial to deck placement) $\varepsilon_{bid} := k_s \cdot k_{hs} \cdot k_f \cdot k_{tdd} \cdot 0.48 \cdot 10^{-3} = 0$

Transformed section coefficient

$$K_{td} = \frac{1}{1 + \frac{E_p A_{ps}}{E_{ci} A_g} \left(1 + \frac{A_g e^2}{I_g} \right) [1 + 0.7 \psi_b(t_f, t_i)]}$$

(5.9.3.4.2a-2)

Humidity factor for creep

$$k_{hc} := 1.56 - 0.008 \cdot H = 1.04$$

Time development factor (initial to final)

$$k_{tdf} := \frac{(t_f - t_i)}{12 \cdot \left(\frac{100 \text{ ksi} - 4 \cdot f'_{ci}}{f'_{ci} + 20 \text{ ksi}} \right) + (t_f - t_i)} = 0.992$$

Creep coefficients and shrinkage strains (girder)

The creep coefficient may be taken as:

$$\psi(t, t_i) = 1.9 k_s k_{hc} k_f k_{td} t_i^{-0.118} \quad (5.4.2.3.2-1)$$

Creep coefficients (initial to deck placement) $\psi_{td_ti} := 1.9 k_s \cdot k_{hc} \cdot k_f \cdot k_{tdd} \cdot (t_i)^{-0.118} = 0.594$

Creep coefficients (initial to final) $\psi_{tf_ti} := 1.9 k_s \cdot k_{hc} \cdot k_f \cdot k_{tdf} \cdot (t_i)^{-0.118} = 1.21$

Transformed section coefficients (initial to deck)

$$K_{id} := \frac{1}{1 + \frac{E_p}{E_{ci}} \cdot \frac{A_{ps}}{A_g} \cdot \left(1 + \frac{A_g \cdot e_{nc}^2}{I_{nc}} \right)} \cdot (1 + 0.7 \cdot \psi_{tf-ti}) = 0.779$$

Long-term losses prior to deck placement (between transfer and deck placement)

Loss due to girder shrinkage (initial to deck) $\Delta f_{pSR} := \varepsilon_{bid} \cdot E_p \cdot K_{id} = 3.494 \text{ ksi}$

Creep coefficients and shrinkage strains (girder):

The creep coefficient may be taken as:

$$\psi(t, t_i) = 1.9 k_2 k_{hc} k_f k_{td} t_i^{-0.118} \quad (5.4.2.3.2-1)$$

Loss due to girder Creep (initial to deck) $\Delta f_{pCR} := \frac{E_p}{E_{ci}} \cdot f_{cgp} \cdot \psi_{td-ti} \cdot K_{id} = 9.936 \text{ ksi}$

Loss due to relaxation $\Delta f_{pR1} := 1.2 \text{ ksi}$

Total loss before deck placement $\Delta f_{pLTid} := \Delta f_{pSR} + \Delta f_{pCR} + \Delta f_{pR1} = 14.63 \text{ ksi}$

Long-term losses after deck placement

Shrinkage strain (initial to final) $\varepsilon_{bif} := k_s \cdot k_{hs} \cdot k_f \cdot k_{tdf} \cdot 0.48 \cdot 10^{-3} = 0$

The girder concrete shrinkage strain between deck placement and final time is: shrinkage strain (deck to final) $\varepsilon_{bdf} := \varepsilon_{bif} - \varepsilon_{bid} = 0$

Transformed section coefficients (deck to final)

$$K_{df} := \frac{1}{1 + \frac{E_p}{E_{ci}} \cdot \frac{A_{ps}}{A_c} \cdot \left(1 + \frac{A_c \cdot e_c^2}{I_c} \right)} \cdot (1 + 0.7 \cdot \psi_{tf-ti}) = 0.788$$

The prestress loss due to shrinkage of concrete between deck placement and final time is: Shrinkage (deck to final)

$$\Delta f_{pSD} := \varepsilon_{bdf} \cdot E_p \cdot K_{df} = 3.661 \text{ ksi}$$

Loss due to girder Creep (after deck placement)

$$\Delta f_{pCD} = \frac{E_p}{E_{ci}} f_{cgp} [\Psi_b(t_f, t_i) - \Psi_b(t_d, t_i)] K_{df} \quad (5.9.3.4.3b-1)$$

$$+ \frac{E_p}{E_c} \Delta f_{cd} \Psi_b(t_f, t_d) K_{df}$$

Time development factor (deck to final)

$$k_{tdf-d} := \frac{(t_f - t_d)}{12 \cdot \left(\frac{100 \text{ ksi} - 4 \cdot f'_{ci}}{f'_{ci} + 20 \text{ ksi}} \right) + (t_f - t_d)} = 0.992$$

Creep coefficients (deck to final)

$$\psi_{tf-td} := 1.9 k_s \cdot k_{hc} \cdot k_f \cdot k_{tdf-d} \cdot (t_d)^{-0.118} = 0.81$$

Permanent load moments at midspan acting on non-composite section (except beam at transfer) [Haunch + deck]

$$M_{dnc} := 2510.9 \text{ kip} \cdot \text{ft}$$

Permanent load moments at midspan acting on composite section [barrier and wearing]

$$M_{dc} := 310.54 \text{ kip} \cdot \text{ft}$$

Loss in the strands

$$P_{\Delta} := A_{ps} \cdot \Delta f_{pLTid} = 165.089 \text{ kip}$$

Change in concrete stress at centroid of strands due to long-term losses between transfer and deck placement

$$\Delta f_{cd} := - \left(\frac{P_{\Delta}}{A_g} + \frac{P_{\Delta} \cdot e_{nc}^2}{I_{nc}} + \frac{M_{dnc} \cdot e_{nc}}{I_{nc}} + \frac{M_{dc} \cdot e_c}{I_c} \right) = -2.153 \text{ ksi}$$

Losses due to creep between deck placement and final time

$$\Delta f_{pCD} := \frac{E_p}{E_{ci}} \cdot f_{cgp} \cdot (\psi_{tf-ti} - \psi_{td-ti}) \cdot K_{df} + \frac{E_p}{E_c} \cdot \Delta f_{cd} \cdot \psi_{tf-td} \cdot K_{df} = 3.51 \text{ ksi}$$

Loss due to relaxation

$$\Delta f_{pR2} := \Delta f_{pR1} = 1.2 \text{ ksi}$$

Deck material coefficients

It is also necessary to determine some material properties for the deck concrete. Humidity factors (k_{hs} and k_{hc}) are the same as for the beam.

Shape factor for deck estimated (V/S) $VS_d := \frac{h_d \cdot b_{eff}}{(h_d + b_{eff}) \cdot 2 \cdot in} = 3.548$

k_{vs} for deck $k_{sd} := \max(1, (1.45 - 0.13 \cdot VS_d)) = 1$

Concrete strength factor $k_{fd} := \frac{5 \text{ ksi}}{1 \text{ ksi} + f'_{cdi}} = 1$

Time development factor (end of moist to final)

$$k_{tdf_dd} := \frac{(t_f - t_d)}{12 \cdot \left(\frac{100 \text{ ksi} - 4 \cdot f'_{cdi}}{f'_{cdi} + 20 \text{ ksi}} \right) + (t_f - t_d)} = 0.989$$

Shrinkage strain (deck to final) $\epsilon_{ddf} := k_{sd} \cdot k_{hs} \cdot k_{fd} \cdot k_{tdf_d} \cdot 0.48 \cdot 10^{-3} = 0.001$

Creep coefficients (deck to final) $\psi_{d_tf_td} := 1.9 k_{sd} \cdot k_{hc} \cdot k_{fd} \cdot k_{tdf_d} \cdot (t_i)^{-0.118} = 1.959$

Eccentricity of deck with respect to gross composite section $e_d := (h_c - y_{cb}) - \frac{h_d}{2} = 20.714 \text{ in}$

Area of deck concrete $A_d := b_{eff} \cdot h_d = 990 \text{ in}^2$

Change in concrete stress due to deck shrinkage $\Delta f_{cdf} := \frac{(\epsilon_{ddf} \cdot A_d \cdot E_{cd})}{(1 + 0.7 \cdot \psi_{d_tf_td})} \cdot \left(\frac{1}{A_c} - \frac{e_c \cdot e_d}{I_c} \right) = -0.17 \text{ ksi}$

Losses due to shrinkage of deck $\Delta f_{pSS} := \frac{E_p}{E_c} \cdot (-\Delta f_{cdf}) \cdot K_{df} \cdot (1 + 0.7 \cdot \psi_{tf_td}) = 1.056 \text{ ksi}$

Total loss after deck placement $\Delta f_{pLTdf} := \Delta f_{pSD} + \Delta f_{pCD} + \Delta f_{pR2} - \Delta f_{pSS} = 7.314 \text{ ksi}$

Total long-term loss based on refined method $\Delta f_{pLT} := \Delta f_{pLTid} + \Delta f_{pLTdf} = 21.945 \text{ ksi}$

Total loss based on refined method

$$\Delta f_{pLT_without_elastic_gain} := \Delta f_{pES} + \Delta f_{pLTid} + \Delta f_{pLTdf} = 43.403 \text{ ksi}$$

The elastic gain due to deck weight, superimposed dead load, and live load (Service III)

$$elastic_gain_dead := \left(\frac{M_{dnc} \cdot e_{nc}}{I_{nc}} + \frac{M_{dc} \cdot e_c}{I_c} \right) \cdot \frac{E_p}{E_c} = 8.735 \text{ ksi}$$

$$elastic_gain_live := 1.0 \cdot \left(\frac{e_c \cdot HL_{93} M_{dist}}{I_c} \right) \cdot \frac{E_p}{E_c} = 8.348 \text{ ksi}$$

Total loss with elastic gain (dead loads)

$$\Delta f_{p_total_dead_elastic_gain} := \Delta f_{pES} + \Delta f_{pLTid} + \Delta f_{pLTdf} - elastic_gain_dead = 34.667 \text{ ksi}$$

Total loss with elastic gain (live loads)

$$\Delta f_{p_total_live_elastic_gain} := \Delta f_{pES} + \Delta f_{pLTid} + \Delta f_{pLTdf} - elastic_gain_live = 35.055 \text{ ksi}$$

Total loss with elastic gain (dead and live loads)

$$\Delta f_{ps} := \Delta f_{pES} + \Delta f_{pLTid} + \Delta f_{pLTdf} - elastic_gain_dead - elastic_gain_live = 26.32 \text{ ksi}$$

Note: The total loss included both dead and live load elastic gains in this rating example.

Effective stress after loss

$$f_e := f_{pi} - \Delta f_{ps} = 176.18 \text{ ksi}$$

Effective force after loss

$$P_e := A_{ps} \cdot f_e = 1988.02 \text{ kip}$$

Compressive stress due to effective prestress

$$f_{pb} := \frac{P_e}{A_g} + \frac{P_e \cdot e_{nc}}{S_{bot_nc}} = 5.427 \text{ ksi}$$

7. Check the Minimum Reinforcement according to LRFD BDS Article 5.6.3.3

At any section, the amount of prestressed and non-prestressed tensile reinforcement must be adequate to develop a factored flexural resistance, M_r , equal to the lesser of:

- 1.33 times the factored moment required by the applicable strength load combination specified in Table 3.4.1-1;

- $$M_{cr} = \gamma_3 \left[(\gamma_1 f_r + \gamma_2 f_{cpe}) S_c - M_{anc} \left(\frac{S_c}{S_{nc}} - 1 \right) \right]$$
 (5.6.3.3-1)

Design Flexural Strength $M_r := \phi \cdot M_n = 15722.487 \text{ kip} \cdot \text{ft}$

1.33 Factored moment required $M_{u_factored} := 1.33 \cdot M_u = 15702.545 \text{ kip} \cdot \text{ft}$

Modulus of rupture (assume $\lambda = 1.0$) $f_r := 0.24 \cdot \sqrt{\frac{f'_c}{\text{ksi}}} \cdot \text{ksi} = 0.74 \text{ ksi}$
(LRFD BDS 5.4.2.6)

γ_1 = flexural cracking variability factor
= 1.2 for precast segmental structures
= 1.6 for all other concrete structures

γ_2 = prestress variability factor
= 1.1 for bonded tendons
= 1.0 for unbonded tendons

For prestressing steel, γ_3 shall be taken as 1.0.

Cracking moment $\gamma_1 := 1.6 \quad \gamma_2 := 1.1 \quad \gamma_3 := 1.0$

$$M_{cr} := \gamma_3 \cdot \left((\gamma_1 \cdot f_r + \gamma_2 \cdot f_{pb}) \cdot S_{bot_c} - M_{DC1} \cdot \left(\frac{S_{bot_c}}{S_{bot_nc}} - 1 \right) \right) = 11669.245 \text{ kip} \cdot \text{ft}$$

$$check_min_reinforcement := \text{if} (M_r > \min(1.33 M_u, M_{cr}), \text{"OK"}, \text{"NG"}) = \text{"OK"}$$

Note: Therefore, the minimum reinforcement check is good.

8. Compute Nominal Shear Resistance at First Critical Section

Note: The *MBE* Article 6A.5.8 does not require a shear evaluation for design load and legal loads if the bridge shows no visible sign of shear distress. Here the shear calculations are just for illustrative as *MBE* 6A3.8.

Critical location for shear near the supports is determined based on *LRFD BDS* 5.7.3.2. The d_v definition in *LRFD BDS* 5.7.2.8 is given below.

d_v = effective shear depth taken as the distance, measured perpendicular to the neutral axis, between the resultants of the tensile and compressive forces due to flexure; it need not be taken to be less than the greater of $0.9d_e$ or $0.72h$ (in.)

$$f_{ps} = f_{pu} \left(1 - k \frac{c}{d_p} \right)$$

$$k = 0.28 \text{ for low-relaxation strands}$$

$$f_{pu} = 270 \text{ ksi}$$

$$d_p = \text{distance from extreme compression fiber to the centroid of the prestressing tendons}$$

Note: According to BrR file for this bridge, there are 10 harped prestress strands.

$$\text{Number of harped strands} \quad N_{\text{harped}} := 10$$

C.G. of PS straight strands to the bottom girder

$$y_{\text{bar_straight}} := \frac{16 \cdot 2 + 16 \cdot 4 + 8 \cdot 6 + 2 \cdot 8}{42} \cdot \text{in} = 3.81 \text{ in}$$

$$\text{Distance from extreme compression fiber to the centroid of the prestressing tendons} \quad d_{p_straight} := h_{nc} + h_h + h_d - y_{\text{bar_straight}} = 67.69 \text{ in}$$

$$\text{Number of straight strands} \quad N_{\text{ps_straight}} := 42$$

$$\text{Area of total straight strands} \quad A_{\text{ps_straight}} := A_{\text{strand}} \cdot N_{\text{ps_straight}} = 9.114 \text{ in}^2$$

Some of the strands are harped, the effective depth, d_e , varies from point-to-point. However, d_e must be calculated at the critical section in shear which is not yet determined; therefore, for the first iteration, d_e is calculated based on the center of gravity of the straight strand group at the end of the beam, $y_{bar_straight}$.

The corresponding effective depth from the extreme compression fiber to the centroid of the tensile force in the tensile reinforcement (d_e)

$$d_e := h_c - y_{bar_straight} = 67.69 \text{ in}$$

Effective shear depth d_v

$$d_v := \max\left(d_{p_straight} - \frac{a}{2}, 0.9 \cdot d_e, 0.72 \cdot h_c\right) = 64.405 \text{ in}$$

Critical shear location from centerline of bearing
(distance from the face of support to centerline of bearing is 6")

$$d_{critical} := d_v + 6 \text{ in} = 5.87 \text{ ft}$$

Note: The effective depth, d_e , and the position of the critical section in shear may be refined based on the position of the critical section calculated above. However, the difference is small. Therefore, no more refinement is performed in this rating example.

Maximum shear at critical section near supports

Calculated shear loads at the 5.87 ft from the centerline of bearing.

Total distributed shear (including multiple lanes GDF for shear and $IM = 0.33$ for HL-93 truck)

$$V_{distributed_critical} := 124.7 \text{ kip}$$

DC shears (Dnc (non-composite dead loads + Dc (composite dead loads))

$$V_{nc_critical} := 122 \text{ kip}$$

$$V_{c_critical} := 8.7 \text{ kip}$$

$$V_{DC_critical} := V_{nc_critical} + V_{c_critical} = 130.7 \text{ kip}$$

DW shears (DW)

$$V_{DW_critical} := 0 \text{ kip}$$

Compute nominal shear resistance

The nominal shear resistance, V_n , shall be determined as the lesser of both of the following:

$$V_n = V_c + V_s + V_p \quad (5.7.3.3-1)$$

$$V_n = 0.25 f'_c b_v d_v + V_p \quad (5.7.3.3-2)$$

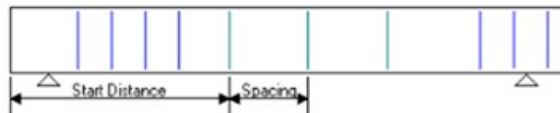
in which:

$$V_c = 0.0316 \beta \lambda \sqrt{f'_c} b_v d_v \quad (5.7.3.3-3)$$

$$V_s = \frac{A_v f_y d_v (\cot \theta + \cot \alpha) \sin \alpha}{s} \lambda_{duct} \quad (5.7.3.3-4)$$

$$\lambda_{duct} = 1 - \delta \left(\frac{\phi_{duct}}{b_w} \right)^2 \quad (5.7.3.3-5)$$

Based on the beam shear reinforcement layout below, the transverse reinforcement provided at 5.87 ft from the bearing centerline is D18 shear reinforcement at 4-in. spacing.



Vertical Horizontal

Span: 1

Name	Extends into deck	Start distance (ft)	Number of spaces	Spacing (in)	Length (ft)	End distance (ft)
D31	<input checked="" type="checkbox"/>	0.00	9	2.0000	1.50	1.50
D18	<input checked="" type="checkbox"/>	1.50	21	4.0000	7.00	8.50
D18	<input checked="" type="checkbox"/>	8.50	19	8.0000	12.67	21.17
D18	<input checked="" type="checkbox"/>	21.17	44	12.0000	44.00	65.17
D18	<input checked="" type="checkbox"/>	65.17	1	8.0000	0.67	65.83
D18	<input checked="" type="checkbox"/>	65.83	44	12.0000	44.00	109.83
D18	<input checked="" type="checkbox"/>	109.83	19	8.0000	12.67	122.50
D18	<input checked="" type="checkbox"/>	122.50	21	4.0000	7.00	129.50
D31	<input checked="" type="checkbox"/>	129.50	8	2.0000	1.33	130.83

Minimum transverse reinforcement (LRFD BDS 5.7.2.5)

C5.7.2.8

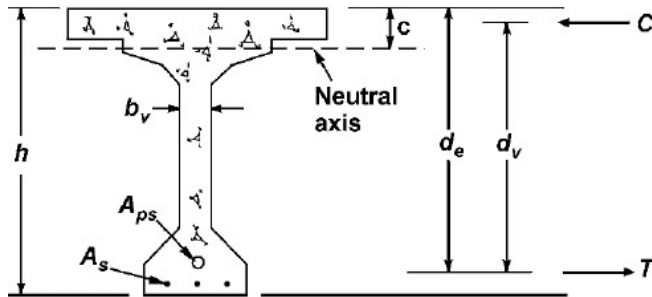


Figure C5.7.2.8-1—Illustration of the Terms b_v and d_v

Effective web width, b_v $b_v := 5.9375 \text{ in}$

Shear reinforcement spacings, s_{shear} $s_{shear} := 4 \text{ in}$

Shear reinforcement yield strength, f_{y_shear} $f_{y_shear} := 70 \text{ ksi}$

Where transverse reinforcement is required as specified in either [Article 5.7.2.3](#) or [Article 5.12.5.3.8c](#), and nonprestressed reinforcement is used to satisfy that requirement, the area of steel shall satisfy:

$$A_v \geq 0.0316 \lambda \sqrt{f'_c} \frac{b_v s}{f_y} \quad (5.7.2.5-1)$$

$$A_v := 0.0316 \cdot (1.0) \cdot \sqrt{\frac{f'_c}{\text{ksi}}} \cdot \text{ksi} \cdot \frac{b_v \cdot s_{shear}}{f_{y_shear}} = 0.033 \text{ in}^2$$

Area provided for the critical section $A_{provided} := 1.8 \cdot 0.2 \text{ in}^2 = 0.36 \text{ in}^2$

`check_min_transverse_reinforcement := if (Aprovided > Av, "OK", "NG") = "OK"`

Determine the V_p

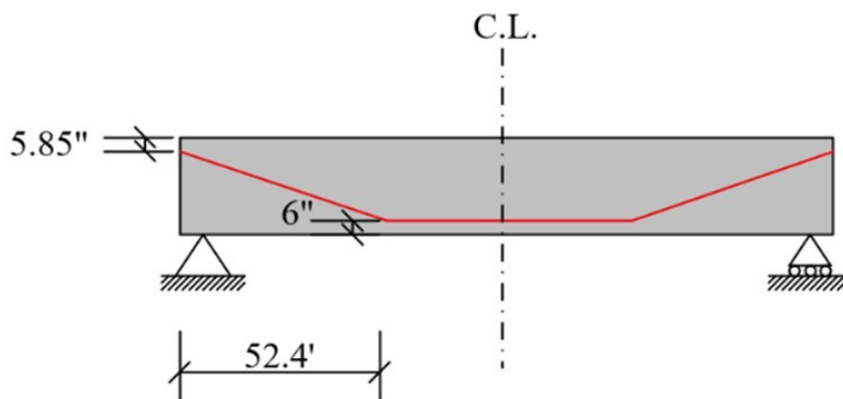
Prestress force per strand without live load gains

$$P_{wo_LG_strand} := (f_{pi} - \Delta f_{p_total_dead_elastic_gain}) \cdot A_{strand} = 36.42 \text{ kip}$$

Top layer of harped strand distance to the top of precast beam

$$d_{harped1} := h_{nc} - 61.15 \text{ in} = 1.85 \text{ in}$$

There are a total of five layers of harped strands and the vertical increment is 2". Each harped strand layer distance to the top of the precast beam can be determined.



The distance between the center of gravity of the 10 harped strands at the end of the beam and the top fiber of the precast beam is:

$$d_{harped_top} := \frac{1.85 \cdot 2 + 3.85 \cdot 2 + 5.85 \cdot 2 + 7.85 \cdot 2 + 9.85 \cdot 2}{10} \cdot \text{in} = 5.85 \text{ in}$$

The distance between the center of gravity of the 10 harped stands at the harp point and the bottom fiber of the beam is:

$$d_{harped_bot} := \frac{2 \cdot 2 + 4 \cdot 2 + 6 \cdot 2 + 8 \cdot 2 + 10 \cdot 2}{10} \cdot \text{in} = 6 \text{ in}$$

$$\psi := \text{atan} \left(\frac{h_{nc} - d_{harped_top} - d_{harped_bot}}{52.4 \text{ ft}} \right) = 4.651 \text{ deg}$$

Component of prestressing force in the direction of the shear force (10 strands harped for this case)

$$V_p := (P_{wo_LG_strand}) \cdot (N_{harped}) \cdot \sin(\psi) = 29.528 \text{ kip}$$

The nominal shear determined by *LRFD BDS* Equation 5.7.3.3-2 $V_{n_equ_1} := 0.25 \cdot f'_c \cdot b_v \cdot d_v + V_p = 937.745 \text{ kip}$

These equations are based on the Modified Compression Field Theory (MCFT) and require the determination of β and θ by detailed analysis. A simplified analysis using $\theta = 45^\circ$ and $\beta = 2.0$ may be utilized for an initial evaluation before resorting to the MCFT, if necessary, for likely improved shear capacity.

C6A.5.8

Simplified approach

Assumed θ_{sim} and β_{sim} based on *MBE C6A.5.8* $\theta_{sim} := 45 \text{ deg}$ $\beta_{sim} := 2.0$

Concrete shear strength $V_c := 0.0316 \beta_{sim} \cdot (1.0) \cdot \sqrt{\frac{f'_c}{ksi}} \cdot ksi \cdot b_v \cdot d_v = 74.491 \text{ kip}$

Steel shear strength $V_s := \frac{A_{provided} \cdot f_{y_shear} \cdot d_v \cdot \cot(\theta_{sim})}{s_{shear}} = 405.754 \text{ kip}$

The nominal shear determined by *LRFD BDS* Equation 5.7.3.3-1 $V_{n_equ_2} := V_c + V_s + V_p = 509.774 \text{ kip}$

The nominal shear determined by *LRFD* Equation 5.7.3.3

$$V_{n_simp} := \min(V_{n_equ_1}, V_{n_equ_2}) = 509.774 \text{ kip}$$

- For shear and torsion in monolithic prestressed concrete sections and prestressed concrete sections with cast-in-place closures or with match cast and epoxied joints having bonded strands or tendons:
 - normal weight concrete..... 0.90
 - lightweight concrete..... 0.90

$$\phi_{ps_shear} := 0.9$$

Factored shear resistance $\phi_{ps_shear} \cdot V_{n_simp} = 458.796 \text{ kip}$

Maximum shear at the critical section (HL-93 inventory loading)

Load	Load Factor γ
<i>DC</i>	1.25
<i>DW</i>	1.50
<i>LL</i>	1.75

Factored shear demand

$$V_u := 1.25 \cdot V_{DC_critical} + 1.5 \cdot V_{DW_critical} + 1.75 \cdot V_{distributed_critical} = 381.6 \text{ kip}$$

$$check_shear_at_the_critical := \text{if}(\phi_{ps_shear} \cdot V_{n_simp} > V_u, \text{"OK"}, \text{"NG"}) = \text{"OK"}$$

Demand/capacity ratio for shear

$$DCR := \frac{V_u}{\phi_{ps_shear} \cdot V_{n_simp}} = 0.832$$

Note: The check was passed for the simplified shear resistance approach. Therefore, the MCFT approach to determine the shear resistance for this critical location was not used.

9. Check the Longitudinal Reinforcement according to LRFD BDS Article 5.7.3.5

Calculated the moment at the 5.87 ft from the centerline of support.

Total distributed moment (including g_{m2} and IM = 0.33 for HL-93 truck)

Total distributed moment $M_{distributed_critical} := 608.4 \text{ kip} \cdot \text{ft}$

DC moment (Dnc (non-composite dead load + Dc (composite dead load))

$$M_{nc_critical} := 751.5 \text{ kip} \cdot \text{ft} \quad M_{c_critical} := 53.6 \text{ kip} \cdot \text{ft}$$

$$M_{DC_critical} := M_{nc_critical} + M_{c_critical} = 805.1 \text{ kip} \cdot \text{ft}$$

DW moment (DW)

$$M_{DW_critical} := 0 \text{ kip} \cdot \text{ft}$$

Maximum moment at the critical section (HL-93 inventory loading)

$$M_{u_critical} := 1.25 \cdot M_{DC_critical} + 1.5 \cdot M_{DW_critical} + 1.75 \cdot M_{distributed_critical} = 2071.075 \text{ kip} \cdot \text{ft}$$

The net force is zero

$$N_u := 0 \text{ kip}$$

The A_s is zero

$$A_s := 0 \text{ in}^2$$

The E_s for non-prestressing longitudinal steel

$$E_s := 29000 \text{ ksi}$$

The f_{po} can be taken as $0.7 f_{pu}$

$$f_{po} := 0.7 \cdot f_{pu} = 189 \text{ ksi}$$

A3.10.3—Check Longitudinal Reinforcement (LRFD Design 5.7.3.5)

Tensile capacity of the longitudinal reinforcement on the flexural tension side of the member shall be proportioned to satisfy LRFD Design Eq. 5.7.3.5-1. “Any lack of full development shall be accounted for.”

$$A_{ps} f_{ps} + A_s f_y \geq \frac{|M_u|}{d_v \phi_f} + 0.5 \frac{N_u}{\phi_c} + \left[\left| \frac{V_u}{\phi_v} - V_p \right| - 0.5 V_s \right] \cot \theta$$

LRFD Design
Eq. 5.7.3.5-1

Calculate minimum required tensile capacity

$$V_{s_req} := \min \left(V_s, \frac{V_u}{\phi_{ps_shear}} \right) = 405.754 \text{ kip}$$

The right side of LRFD BDS Equation 5.7.3.5-1 yields:

$$\frac{\text{abs}(M_{u_critical})}{d_v \cdot \phi_{ps_shear}} + \frac{0.5 \cdot N_u}{\phi_{ps_shear}} + \left(\text{abs} \left(\frac{V_u}{\phi_{ps_shear}} - V_p \right) - 0.5 V_{s_req} \right) \cdot \cot(\theta_{sim}) = 620.353 \text{ kip}$$

Transfer Length:

LRFD Design 5.9.4.3.1

$$\ell_t = 60 \text{ strand diameters}$$

$$\ell_t := 60 \cdot d_b = 36 \text{ in}$$

5.9.4.3.2—Bonded Strand

Pretensioning strand shall be bonded beyond the section required to develop f_{ps} for a development length, ℓ_d , in in., where ℓ_d shall satisfy:

$$\ell_d \geq \kappa \left(f_{ps} - \frac{2}{3} f_{pe} \right) d_b \quad (5.9.4.3.2-1)$$

$\kappa = 1.6$ for pretensioned members with a depth greater than 24.0 in.

$$l_d := 1.6 \cdot \left(\frac{f_{ps} - \frac{2}{3} f_e}{ksi} \right) \cdot d_b = 138.105 \text{ in}$$

- From the point where bonding commences to the end of transfer length:

$$f_{px} = \frac{f_{pe} \ell_{px}}{60 d_b} \quad (5.9.4.3.2-2)$$

- From the end of the transfer length and to the end of the development of the strand:

$$f_{px} = f_{pe} + \frac{\ell_{px} - 60 d_b}{(\ell_d - 60 d_b)} (f_{ps} - f_{pe}) \quad (5.9.4.3.2-3)$$

where:

f_{px} = design stress in pretensioned strand at nominal flexural strength at section of member under consideration (ksi)

ℓ_{px} = distance from free end of pretensioned strand to section of member under consideration (in.)

$$l_{px} := d_v = 64.405 \text{ in}$$

$$f_{px} := f_e + \left(\frac{l_{px} - 60 d_b}{l_d - 60 d_b} \right) \cdot (f_{ps} - f_e) = 199.864 \text{ ksi}$$

Since the transfer length is 36 in. from the end of the beam, the available prestress from the 42 straight strands is a fraction of the effective prestress, f_{px} , in these strands. The 10 harped strands do not contribute to the tensile capacity since they are not on the flexural tension side of the member.

The left side of *LRFD BDS* Equation 5.7.3.5-1 yields:

$$Af := A_{ps_straight} \cdot f_{px} = 1821.562 \text{ kip}$$

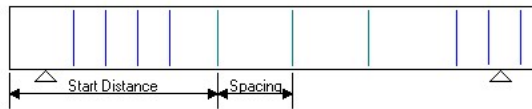
$$check := \text{if} \left(Af > \frac{\text{abs}(M_{u_critical})}{d_v \cdot \phi_{ps_shear}} + \frac{0.5 \cdot N_u}{\phi_{ps_shear}} \downarrow, \text{“OK”}, \text{“NG”} \right) = \text{“OK”}$$

$$+ \left(\text{abs} \left(\frac{V_u}{\phi_{ps_shear}} - V_p \right) - 0.5 V_{s_req} \right) \cdot \cot(\theta_{sim})$$

For this first critical location, the longitudinal reinforcement check is good.

10. Compute Nominal Shear Resistance at Vertical Shear Reinforcement Change

Note: As an example of a calculation, this rating example provided the shear rating at the vertical shear spacing changing from 4" to 8" location (8.5' to the beam end). Since the distance between the beam end and the bearing centerline is 6 in., the distance between the bearing centerline and the location of the spacing change is 8 ft. There is another change in the shear reinforcement spacing at the end of the beam at 21.17 ft, and the quarter point to the centerline of the beam typically also be checked for shear. However, this load rating example did not provide calculations for these two locations. The procedure for checking these two shear locations would generally be similar to that for checking shear at the 8.5' to the beam end in this example.

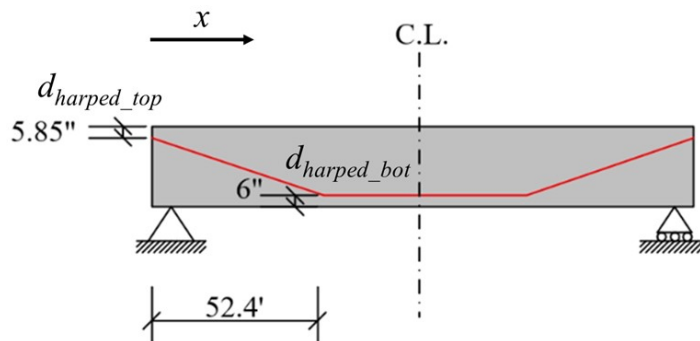


Vertical Horizontal

Span: 1

Name	Extends into deck	Start distance (ft)	Number of spaces	Spacing (in)	Length (ft)	End distance (ft)
D31	<input checked="" type="checkbox"/>	0.00	9	2.0000	1.50	1.50
D18	<input checked="" type="checkbox"/>	1.50	21	4.0000	7.00	8.50
D18	<input checked="" type="checkbox"/>	8.50	19	8.0000	12.67	21.17
D18	<input checked="" type="checkbox"/>	21.17	44	12.0000	44.00	65.17
D18	<input checked="" type="checkbox"/>	65.17	1	8.0000	0.67	65.83
D18	<input checked="" type="checkbox"/>	65.83	44	12.0000	44.00	109.83
D18	<input checked="" type="checkbox"/>	109.83	19	8.0000	12.67	122.50
D18	<input checked="" type="checkbox"/>	122.50	21	4.0000	7.00	129.50
D31	<input checked="" type="checkbox"/>	129.50	8	2.0000	1.33	130.83

$$x_1 := 8.5 \text{ ft}$$



Harped strands distance to the bottom of beam

$$d_{harp_x1} := (h_{nc} - d_{harped_top}) - \frac{(h_{nc} - d_{harped_top}) - (d_{harped_bot})}{52.4 \text{ ft}} \cdot x_1 = 48.853 \text{ in}$$

The distance between the center of gravity of the strands and the bottom of beam at this location is:

$$y_{bar_x1} := \frac{\frac{d_{harp_x1}}{in} \cdot 10 + 2 \cdot 16 + 4 \cdot 16 + 6 \cdot 8 + 8 \cdot 2}{52} \cdot in = 12.472 \text{ in}$$

The corresponding effective depth from the extreme compression fiber to the centroid of the tensile force in the tensile reinforcement (d_{e_x1})

$$d_{e_x1} := h_c - y_{bar_x1} = 59.028 \text{ in}$$

Effective shear depth d_{v_x1}

$$d_{v_x1} := \max\left(d_{e_x1} - \frac{a}{2}, 0.9 \cdot d_{e_x1}, 0.72 \cdot h_c\right) = 55.743 \text{ in}$$

Note: The effective depth, d_{e_x1} , and the position of the critical section in shear are refined based on the position of the critical section calculated above.

Compute maximum shear at shear reinforcement change

Since the beam projection is 6", the distance from this shear reinforcement spacing change location to the bearing centerline is determined.

$$x_{1_centerline} := x_1 - 0.5 \text{ ft} = 8 \text{ ft}$$

Calculated shear at the 8 ft from the bearing centerline

Total distributed shear (including g_{v2} and IM = 0.33 for HL-93 truck)

$$V_{distributed_critical_x1} := 121.8 \text{ kip}$$

DC shears (DC1 + DC2)

$$V_{nc_critical_x1} := 117.6 \text{ kip}$$

$$V_{c_critical_x1} := 8.4 \text{ kip}$$

$$V_{DC_critical_x1} := V_{nc_critical_x1} + V_{c_critical_x1} = 126 \text{ kip}$$

DW shears (DW)

$$V_{DW_critical_x1} := 0 \text{ kip}$$

Shear reinforcement spacings, s_{shear_x1}

$$s_{shear_x1} := 8 \text{ in}$$

$$A_{v_x1} := 0.0316 \cdot (1.0) \cdot \sqrt{\frac{f'_c}{ksi}} \cdot ksi \cdot \frac{b_v \cdot s_{shear_x1}}{f_{y_shear}} = 0.066 \text{ in}^2$$

Area provided for the critical section

$$A_{provided_x1} := 1.8 \cdot 0.20 \text{ in}^2 = 0.36 \text{ in}^2$$

$$check_min_transverse_reinforcement_x := \text{if}(A_{provided_x1} > A_{v_x1}, \text{"OK"}, \text{"NG"}) = \text{"OK"}$$

Simplified approach

The nominal shear determined by *LRFD BDS* Equation 5.7.3.3-2 $V_{n_equ_1_x1} := 0.25 \cdot f'_c \cdot b_v \cdot d_{v_x1} + V_p = 815.595 \text{ kip}$

Concrete shear strength $V_{c_x1} := 0.0316 \beta_{sim} \cdot (1.0) \cdot \sqrt{\frac{f'_c}{ksi}} \cdot ksi \cdot b_v \cdot d_{v_x1} = 64.473 \text{ kip}$

Steel shear strength $V_{s_x1} := \frac{A_{provided_x1} \cdot f_{y_shear} \cdot d_{v_x1} \cdot \cot(\theta_{sim})}{s_{shear_x1}} = 175.591 \text{ kip}$

The nominal shear determined by *LRFD BDS* Equation 5.7.3.3-1 $V_{n_equ_2_x1} := V_{c_x1} + V_{s_x1} + V_p = 269.592 \text{ kip}$

The nominal shear determined by *LRFD BDS* Equation 5.7.3.3 $V_{n_simp_x1} := \min(V_{n_equ_1_x1}, V_{n_equ_2_x1}) = 269.592 \text{ kip}$

Factored shear resistance $\phi_{ps_shear} \cdot V_{n_simp_x1} = 242.633 \text{ kip}$

Maximum factored shear at this section

$$V_{u_x1} := 1.25 \cdot V_{DC_critical_x1} + 1.5 \cdot V_{DW_critical_x1} + 1.75 \cdot V_{distributed_critical_x1} = 370.65 \text{ kip}$$

$$check_shear_at_the_critical_x := \text{if}(\phi_{ps_shear} \cdot V_{n_simp_x1} > V_{u_x1}, \text{"OK"}, \text{"NG"}) = \text{"NG"}$$

Note: The simplified approach is not good. Therefore, the general MCFT method is checked.

Try MCFT General approach (LRFD BDS 5.7.3.4.2)

Shear stress on the concrete $v := \frac{V_{u,x1} - \phi_{ps_shear} \cdot V_p}{\phi_{ps_shear} \cdot b_v \cdot d_{v,x1}} = 1.155 \text{ ksi}$

$$check_using_APPENDIXB5 := \text{if} \left(\frac{v}{f'_c} < 0.25, \text{"OK"}, \text{"NG"} \right) = \text{"OK"}$$

Note: The check for shear stress on the concrete illustrates that the LRFD BDS Appendix B5 can be used to determine resistance. However, Appendix B5 is not used in this example. Instead, this example uses LRFD BDS 5.7.3.4.2, the general MCFT approach to determine shear resistance.

Calculated the moment at 8 ft to the support centerline

Total distributed moment (including g_{m2} and IM = 0.33 for HL-93 truck)

$$M_{distributed_critical_x1} := 814.1 \text{ kip} \cdot \text{ft}$$

DC moments (DC1 + DC2) $M_{nc_critical_x1} := 1006.6 \text{ kip} \cdot \text{ft}$ $M_{c_critical_x1} := 71.7 \text{ kip} \cdot \text{ft}$

$$M_{DC_critical_x1} := M_{nc_critical_x1} + M_{c_critical_x1} = 1078.3 \text{ kip} \cdot \text{ft}$$

DW moment (DW) $M_{DW_critical_x1} := 0 \text{ kip} \cdot \text{ft}$

Maximum moment at this section (HL-93 inventory loading)

$$M_{u_critical_x1} := 1.25 \cdot M_{DC_critical_x1} + 1.5 \cdot M_{DW_critical_x1} \downarrow = 2772.55 \text{ kip} \cdot \text{ft} + 1.75 \cdot M_{distributed_critical_x1}$$

$$\varepsilon_s := \frac{\left(\frac{\text{abs}(M_{u_critical_x1})}{d_{v,x1}} + 0.5 N_u + \text{abs}(V_{u,x1} - V_p) - A_{ps_straight} \cdot f_{po} \right)}{E_s \cdot A_s + E_p \cdot A_{ps_straight}} = -0.003$$

Note: ε_s is less than zero. Use $\varepsilon_s = 0$

$$\varepsilon_s := 0$$

Assume the section contains at least the minimum amount of transverse reinforcement:

$$\beta_{equ} := \frac{4.8}{(1 + 750 \cdot \varepsilon_s)} = 4.8$$

Angle of diagonal compressive stresses is:

$$\theta_{equ} := (29 + 3500 \cdot \varepsilon_s) \text{ deg} = 0.506$$

Concrete shear strength $V_{c_MCFT_x1} := 0.0316 \beta_{equ} \cdot (1.0) \cdot \sqrt{\frac{f'_c}{ksi}} \cdot ksi \cdot b_v \cdot d_{v_x1} = 154.734 \text{ kip}$

Steel shear strength $V_{s_MCFT_x1} := \frac{A_{provided_x1} \cdot f_{y_shear} \cdot d_{v_x1} \cdot \cot(\theta_{equ})}{s_{shear_x1}} = 316.775 \text{ kip}$

The nominal shear determined by $V_{n_MCFT_x1} := V_{c_MCFT_x1} + V_{s_MCFT_x1} + V_p = 501.037 \text{ kip}$
LRFD BDS Equation 5.7.3.3-1

The nominal shear determined by $V_{n_MCFT_x1} := \min(V_{n_equ_1_x1}, V_{n_MCFT_x1}) = 501.037 \text{ kip}$
LRFD BDS Equation 5.7.3.3

Factored shear resistance $\phi_{ps_shear} \cdot V_{n_MCFT_x1} = 450.934 \text{ kip}$

$$check_shear_MCFT := \text{if}(\phi_{ps_shear} \cdot V_{n_MCFT_x1} > V_{u_x1}, \text{"OK"}, \text{"NG"}) = \text{"OK"}$$

Demand/capacity ratio $DCR_{x1} := \frac{V_{u_x1}}{\phi_{ps_shear} \cdot V_{n_MCFT_x1}} = 0.822$

Check the longitudinal reinforcement requirement

Calculate minimum required tensile capacity

$$V_{s_req_x1} := \min\left(V_{s_MCFT_x1}, \frac{V_{u_x1}}{\phi_{ps_shear}}\right) = 316.775 \text{ kip}$$

The right side of *LRFD BDS* Equation 5.7.3.5-1 yields:

$$\frac{\text{abs}(M_{u_critical_x1})}{d_{v_x1} \cdot \phi_{ps_shear}} + \frac{0.5 \cdot N_u}{\phi_{ps_shear}} + \left(\text{abs}\left(\frac{V_{u_x1}}{\phi_{ps_shear}} - V_p\right) - 0.5 V_{s_req_x1}\right) \cdot \cot(\theta_{equ}) = 1067.129 \text{ kip}$$

Determine the f_{px} based on *LRFD BDS* 5.9.4.3.2:

$$l_d := 1.6 \cdot \left(\frac{f_{ps} - \frac{2}{3} f_e}{ksi} \right) \cdot d_b = 138.105 \text{ in} \quad l_{px} := d_{v_{x1}} = 55.743 \text{ in}$$

$$f_{px} := f_e + \left(\frac{l_{px} - 60 \cdot d_b}{l_d - 60 \cdot d_b} \right) \cdot (f_{ps} - f_e) = 192.642 \text{ ksi}$$

Since the transfer length is 36 in. from the end of the beam, the available prestress from the 42 straight strands is a fraction of the effective prestress, f_{px} , in these strands. The center of gravity of 10 harped strands to the bottom of girder is greater than half the height of the composite girder, so they do not contribute to the tensile capacity.

The left side of *LRFD BDS* Equation 5.7.3.5-1 yields:

$$A_{ps_straight} = 9.114 \text{ in}^2$$

$$Af_x := A_{ps_straight} \cdot f_{px} = 1755.738 \text{ kip}$$

$$Check := \text{if} \left(Af_x > \frac{\text{abs}(M_{u_critical_x1})}{d_{v_x1} \cdot \phi_{ps_shear}} + \frac{0.5 \cdot N_u}{\phi_{ps_shear}} \downarrow + \left(\text{abs} \left(\frac{V_{u_x1}}{\phi_{ps_shear}} - V_p \right) - 0.5 V_{s_req_x1} \right) \cdot \cot(\theta_{equ}) \right), \text{“OK”}, \text{“NG”} = \text{“OK”}$$

Note: The longitudinal reinforcement check for this section is good.

11. Load Effects and Resistance Summary

Here is the summary for load effects and bridge resistances.

Load Effects Summary

Load effects (M(kip-ft), and V(kip))	HL-93 Design Loading (with $IM = 0.33$ and multiple lanes GDF)	D_{NC}	D_C	A Four-truck Platoon (5-ft headways) (with $IM = 0.33$ and single lane GDF removed MPF = 1.2)
Moment (at mid)	3412.1	4357.7	310.5	2959.0
Moment (at 5.87 ft)	608.4	751.5	53.6	543.1
Moment (at 8 ft)	814.1	1006.6	71.7	722.6
Shear (at 5.87 ft)	124.7	122.0	8.7	131.6
Shear (at 8 ft)	121.8	117.6	8.4	127.1

Resistance Summary

	Resistance (with ϕ) (M (kip-ft) and V (kip))
Moment (at mid)	15722.5
Shear (at 5.87 ft) (Simplified Approach)	458.8
Shear (at 8 ft) (MCFT Approach)	450.9

12. Load Rating: Design Load Rating for Moment and Shear

$$RF = \frac{(\varphi_c)(\varphi_s)(\varphi)R_n - (\gamma_{DC})(DC) - (\gamma_{DW})(DW)}{(\gamma_L)(LL + IM)}$$

A3.13.2.1a—Inventory Level

Load	Load Factor
DC	1.25
DW	1.50 Overlay thickness was not field measured.
LL	1.75

Parameter information for the equation below.

$$M_n = 15722.487 \text{ kip} \cdot \text{ft}$$

$$g_{m2} = 0.834$$

$$M_{DC1} = 4357.7 \text{ kip} \cdot \text{ft}$$

$$M_{DC2} = 310.5 \text{ kip} \cdot \text{ft}$$

$$M_{DW} = 0 \text{ kip} \cdot \text{ft}$$

Distributed HL-93 moment
(including $IM = 0.33$ for truck and g_{m2})

$$HL_93_M_{dist} := 3412.1 \text{ kip} \cdot \text{ft}$$

Inventory level rating factor

$$RF_{inv} := \frac{(1.0) \cdot M_n - (1.25 \cdot (M_{DC1} + M_{DC2}) + 1.50 \cdot M_{DW})}{1.75 \cdot (HL_93_M_{dist})} = 1.656$$

For Strength I Operating Level only the live load factor changes; therefore the rating factor can be calculated by direct proportions.

Load	Load Factor, γ
DC	1.25
DW	1.50
LL	1.35

Operating level rating factor

$$RF_{ope} := RF_{inv} \cdot \frac{1.75}{1.35} = 2.146$$

The shear rating factors for Design Load Rating are calculated for illustration purposes only. In-service concrete bridges that show no visible signs of shear distress need not be checked for shear during design load or legal load ratings.

6A.5.8

Shear load rating at first critical location (5.87 ft to the centerline of the support)

Parameter information for the equation below.

$$V_{n_simp} = 509.774 \text{ kip}$$

$$g_{v2} = 1.018$$

$$V_{nc_critical} = 122 \text{ kip}$$

$$V_{c_critical} = 8.7 \text{ kip}$$

$$V_{DW_critical} = 0 \text{ kip}$$

Distributed HL-93 shear
(including $IM=0.33$ for truck and g_{v2})

$$V_{distributed_critical} = 124.7 \text{ kip}$$

Inventory level rating factor

$$RF_V := \frac{(0.9) \cdot V_{n_simp} - (1.25 \cdot (V_{nc_critical} + V_{c_critical}) + 1.50 \cdot V_{DW_critical})}{1.75 \cdot (V_{distributed_critical})} = 1.354$$

Operating level rating factor

$$RF_{ope} := RF_V \cdot \frac{1.75}{1.35} = 1.755$$

Shear load rating at location (8 ft to the centerline of the support)

Parameter information for the equation below.

$$V_{n_MCFT_x1} = 501.037 \text{ kip}$$

$$g_{v2} = 1.018$$

$$V_{nc_critical_x1} = 117.6 \text{ kip}$$

$$V_{c_critical_x1} = 8.4 \text{ kip}$$

$$V_{DW_critical_x1} = 0 \text{ kip}$$

Distributed HL-93 shear
(including $IM = 0.33$ for truck and g_{v2})

$$V_{distributed_critical_x1} = 121.8 \text{ kip}$$

Inventory level rating factor

$$RF_{Vx} := \frac{(0.9) \cdot V_{n_MCFT_x1} - (1.25 \cdot (V_{nc_critical_x1} + V_{c_critical_x1}) + 1.50 \cdot V_{DW_critical_x1})}{1.75 \cdot (V_{distributed_critical_x1})} = 1.377$$

Operating level rating factor

$$RF_{ope} := RF_{Vx} \cdot \frac{1.75}{1.35} = 1.785$$

13. Load Rating for Service III Limit State (Inventory Level)

$$RF = \frac{f_R - (\gamma_D)(f_D)}{(\gamma_L)(f_{LL+IM})}$$

Flexural Resistance $f_R = f_{pb} + \text{Allowable tensile stress}$

f_{pb} = Compressive stress due to effective prestress

= 2.550 ksi (from Article A3.7.1.3 of this example)

Allowable tensile stress, ksi

$$f_t := 0.19 \cdot \sqrt{\frac{f'_c}{\text{ksi}}} \cdot \text{ksi} = 0.586 \text{ ksi}$$

Resistance stress

$$f_R := f_{pb} + f_t = 6.012 \text{ ksi}$$

Determine dead load stress at midspan

$$f_{DC} := \frac{\langle M_{DC1} \rangle}{S_{bot_nc}} + \frac{\langle M_{DC2} \rangle}{S_{bot_c}} = 3.405 \text{ ksi}$$

Determine wearing dead load stress at midspan

$$f_{DW} := \frac{\langle M_{DW} \rangle}{S_{bot_c}} = 0 \text{ ksi}$$

Total dead load stress at midspan

$$f_D := f_{DC} + f_{DW} = 3.405 \text{ ksi}$$

Live load stress at midspan

$$f_{LL} := \frac{\langle HL_{93} M_{dist} \rangle}{S_{bot_c}} = 1.827 \text{ ksi}$$

Rating factor for Service III
(Post-1.0-Gains)

$$RF_{ServiceIIIinv} := \frac{f_R - f_D}{1.0 \cdot f_{LL}} = 1.427$$

14. Load Rating for Strength I Limit State Platoon (target beta = 2.5)

4-truck Platoons (NRL with 5 ft headways): single lane platoon mixed with traffic, $CoV = 0.20$ (100 crossings, ADTT = 5000)

Proposed Strength Calibrated LL Factors for the Target $\beta = 2.5$ (Steelman et al., 2021) (Table 2)

Truck Platoon	Frequency	Loading Condition	DF	ADTT (One direction)	Live load factors by CoV of total live load				
					$COV_{LL} = 0$	$COV_{LL} = 0.05$	$COV_{LL} = 0.1$	$COV_{LL} = 0.15$	$COV_{LL} = 0.2$
Multiple Trucks in Platoon	Single-trip	No other vehicles on the bridge	One lane	NA	1.00	1.05	1.10	1.20	1.25
	Single-trip	Two identical platoons loaded on two lanes	Two or more lanes	NA	1.00	1.05	1.10	1.20	1.25
	10 Crossings	Mixed with routine traffic in the adjacent lane	One lane	> 5000	1.35	1.35	1.40	1.45	1.55
				1000	1.35	1.35	1.40	1.45	1.50
				< 100	1.35	1.35	1.40	1.45	1.50
	100 Crossings	Mixed with routine traffic in the adjacent lane	One lane	> 5000	1.35	1.40	1.45	1.50	1.60
				1000	1.35	1.40	1.45	1.45	1.55
				< 100	1.35	1.35	1.45	1.45	1.55

Platoon weight divided by 80 kips
(amplification factor alpha)

$$W_{platoon} := 1.0$$

Assumed IM = 0.33 (same as MBE permit load rating)

$$IM_{surface} := 33\%$$

5 ft headway 4-truck platoon moment at the mid span from the above load effect table:
(with $IM = 0.33$ and single lane moment GDF (g_{m1}) and removed 1.2 multiple presence factor)

$$LL_{platoon} := 2959.0 \text{ kip} \cdot \text{ft}$$

5 ft headway 4-truck platoon moment at the mid span (with amplification factor alpha)

$$LL_{platoon_dis} := W_{platoon} \cdot LL_{platoon} = 2959 \text{ kip} \cdot \text{ft}$$

Platoon calibrated live load factor (the value in the red box as shown above Table)

$$\gamma_{platoon_strength} := 1.60$$

Parameter information for the equation below.

$$M_n = 15722.487 \text{ kip} \cdot \text{ft}$$

$$M_{DC2} = 310.5 \text{ kip} \cdot \text{ft}$$

$$M_{DC1} = 4357.7 \text{ kip} \cdot \text{ft}$$

$$M_{DW} = 0 \text{ kip} \cdot \text{ft}$$

$$RF_{Platoon_flexure} := \frac{(1.0) \cdot M_n - (1.25 \cdot (M_{DC1} + M_{DC2}) + 1.50 \cdot M_{DW})}{\gamma_{platoon_strength} \cdot (LL_{platoon_dis})} = 2.088$$

Shear Rating for 4-truck Platoons (NRL with 5 ft headways): single lane platoon mixed with traffic, $CoV = 0.20$ (100 crossings, ADTT = 5000)

Shear resistance taken from HL-93. Acceptable and conservative as long as M_u and V_u for HL-93 are both $\geq M_u$ and V_u for permit. Must be recalculated if permit values are greater.

Shear load rating at first critical location (5.87 ft to the centerline of the support)

Parameter information for the equation below.

$$V_{n_simp} = 509.774 \text{ kip}$$

$$g_{v1} = 0.8$$

$$V_{nc_critical} = 122 \text{ kip}$$

$$V_{c_critical} = 8.7 \text{ kip}$$

$$V_{DW_critical} = 0 \text{ kip}$$

5 ft headway 4-truck platoon shear at 5.87 ft to the end from the above load effect table: (with $IM = 0.33$ and single lane shear GDF (g_{v1}) and removed 1.2 multiple presence factor)

$$V_{critical_platoon} := 131.6 \text{ kip}$$

5 ft headway 4-truck platoon shear at 5.87 ft to the centerline of support (with amplification factor alpha)

$$V_{critical_platoon_dis} := W_{platoon} \cdot V_{critical_platoon} = 131.6 \text{ kip}$$

$$RF_V := \frac{(0.9) \cdot (V_{n_simp}) - (1.25 \cdot (V_{nc_critical} + V_{c_critical}) + 1.50 \cdot (V_{DW_critical}))}{\gamma_{platoon_strength} \cdot (V_{critical_platoon_dis})} = 1.403$$

Shear load rating at the location (8 ft to the centerline of the support)

Parameter information for the equation below.

$$V_{n_MCFT_x1} = 501.037 \text{ kip}$$

$$g_{v1} = 0.8$$

$$V_{nc_critical_x1} = 117.6 \text{ kip}$$

$$V_{c_critical_x1} = 8.4 \text{ kip}$$

$$V_{DW_critical_x1} = 0 \text{ kip}$$

5 ft headway 4-truck platoon shear at 8 ft to the end from the above load effect table:
(with $IM = 0.33$ and single lane shear GDF (g_{v1}) and removed 1.2 multiple presence factor)

$$V_{critical_platoon_x1} := 127.1 \text{ kip}$$

5 ft headway 4-truck platoon shear at 8 ft to the end (with amplification factor alpha)

$$V_{critical_platoon_dis_x1} := W_{platoon} \cdot V_{critical_platoon_x1} = 127.1 \text{ kip}$$

$$RF_{Vx} := \frac{(0.9) \cdot V_{n_MCFT_x1} - (1.25 \cdot (V_{nc_critical_x1} + V_{c_critical_x1}) + 1.50 \cdot V_{DW_critical_x1})}{\gamma_{platoon_strength} \cdot (V_{critical_platoon_dis_x1})} = 1.443$$

15. Load Rating for Service III Limit State Platoon (target beta = -0.60)

4-truck Platoons (NRL with 5 ft headways): single lane platoon mixed with traffic, $CoV = 0.20$ (100 crossings, ADTT = 5000)

Proposed Service III Calibrated LL Factors for the Target $\beta = -0.6$ (Table 21)

Truck platoon	Frequency	Load conditions	DF	ADTT (one direction)	Load factors by CoV of total live load
					$CoV_{LL} = 0 - 0.20$
Multiple trucks in platoon	single-trip	No other vehicles on the bridge	One lane	N/A	0.85
	single-trip	Two identical platoons loaded on two lanes	Two or more lanes	N/A	0.85
	100 Crossings	Mixed with routine traffic in the adjacent lane	One lane	> 5000	1.55

Platoon calibrated live load factor (the value in the red box as shown above Table)

$$\gamma_{platoon_service} := 1.55$$

Live load stress due to 5 ft headway 4-truck platoon at the mid span (with amplification factor alpha)

$$f_{platoon} := \frac{LL_{platoon_dis}}{S_{bot_c}} = 1.584 \text{ ksi}$$

Parameter information for the equation below.

$$f_R = 6.012 \text{ ksi}$$

$$f_D = 3.405 \text{ ksi}$$

$$S_{bot_c} = 22414.983 \text{ in}^3$$

Rating factor for Service III

$$RF_{ServiceIIIplatoon} := \frac{f_R - f_D}{\gamma_{platoon_service} \cdot f_{platoon}} = 1.062$$

16. Load Rating for Service I Limit State Platoon

A3.13.4.2—Service I Limit State (Optional) (6A.5.4.2.2b)

$$\gamma_L = \gamma_{DC} = \gamma_{DW} = 1.0$$

For concrete members with standard designs and closely clustered tension reinforcement, the Engineer may, as an alternate to limiting the steel stress, choose to limit unfactored moments to 75 percent of nominal flexural capacity. Where computations are performed in terms of

5 ft headway 4-truck platoon moment at the mid span (with $IM = 0.33$ and multiple lanes moment GDF (g_{m2}))

$$LL_{platoon_m} := \frac{LL_{platoon}}{\frac{g_{m1}}{1.20}} \cdot g_{m2} = 5354.595 \text{ kip} \cdot \text{ft}$$

Note: $LL_{platoon}$ includes the $\frac{g_{m1}}{1.20}$ as shown before.

5 ft headway 4-truck platoon moment at the mid span (with amplification factor alpha)

$$LL_{platoon_dis_m} := W_{platoon} \cdot LL_{platoon_m} = 5354.595 \text{ kip} \cdot \text{ft}$$

Parameter information for the equation below.

$$M_n = 15722.487 \text{ kip} \cdot \text{ft}$$

$$M_{DC2} = 310.5 \text{ kip} \cdot \text{ft}$$

$$M_{DC1} = 4357.7 \text{ kip} \cdot \text{ft}$$

$$M_{DW} = 0 \text{ kip} \cdot \text{ft}$$

75% of moment resistance

$$M_{n75} := 0.75 \cdot M_n = 11791.865 \text{ kip} \cdot \text{ft}$$

Moment ratio

$$M_{ratio} := \frac{M_{n75}}{M_{DC1} + M_{DC2} + M_{DW} + LL_{platoon_dis_m}} = 1.177$$

17. Load Rating Summary

Load rating summary table is given below.

Load Rating Summary

Limit state	Design load rating		Platoon load rating (Strength I $\beta_{target} = 2.5$ and Service III $\beta_{target} = -0.6$)
	Inventory	Operating	
Strength I for Design and platoon load rating			
Flexure (at midspan)	1.656	2.146	2.088
Shear at (5.87 ft to the centerline of support)	1.354	1.755	1.403
Shear at (8 ft to the centerline of support)	1.377	1.785	1.443
Service III			
Flexure (at midspan)	1.427		1.062
Service I			
Flexure (at midspan)			Stress ratio = 1.177

Appendix D

This appendix contains detailed calculations related to the example prestressed concrete continuous span bridge described in Section 8.3.

Appendix D. LRFR Load Rating Example of a 170' NU900 Three-span Prestressed Concrete I-Girder Bridge (interior girder)

Note: Bridge S080 41465 is a 170 ft (42.5'-85'-42.5') three-span, prestressed multi-girder bridge at the I-80 5N Waverly Interchange in Waverly, Nebraska (Figure 45). According to the National Bridge Inventory (NBI) (2022), the bridge was constructed in 2009 with three design lanes, and the average daily traffic is 49,240. The rating code in NBI (2022) indicates that the rating is LRFR.

The example illustrates the design and platoon ratings of an interior prestressed concrete girder at 0.5L of the interior span for positive moment, at the interior support for negative moment, at the first critical shear section, and one of the changes in vertical shear reinforcement spacing. For this example, the interior span was used.

The bridge was simple-made continuous, so the dead weight of the beam, the slab, and the haunch act on the non-composite, single-span structure. The elastic gains from dead and live loads were considered when calculating prestress loss. The analysis was based on the gross section properties. The shear resistance was calculated using the simplified and general MCFT methods.

Prestress losses were calculated using the refined estimates described in LRFD BDS Article 5.9.3.4. Strength I and Service III rating factors for HL-93 design and platoon loads are computed. Considering the platoon as a future permit truck, the Service I rating was performed as the permit rating in MBE (2018).

1. Bridge Data

End span length $L_{end} := 42.5 \text{ ft}$

Mid span length $L_{mid} := 85 \text{ ft}$

Year built 2009

Concrete information

Ultimate strength for deck $f'_{cd} := 4 \text{ ksi}$

Initial strength for deck $f'_{cdi} := 4 \text{ ksi}$

Strength of girder concrete at time of transfer $f'_{ci} := 7 \text{ ksi}$

Ultimate strength of girder concrete $f'_c := 9 \text{ ksi}$

Unit weight of concrete for determining dead loads $w_c := 155 \text{ pcf}$

Unit weight of concrete for determining deck modulus of elasticity $w_{cd_modulus} := 155 \text{ pcf}$

Unit weight of concrete for determining girder modulus of elasticity $w_{cg_modulus} := 150 \text{ pcf}$

$$E_c = 120,000K_1w_c^{2.0}f_c'^{0.33} \quad (5.4.2.4-1)$$

$$E_c = 33,000K_1w_c^{1.5}\sqrt{f_c'} \quad (C5.4.2.4-2)$$

Modulus of elasticity of concrete girder at time of transfer

$$E_{ci} := 120000 \cdot \left(\frac{w_{cg_modulus}}{pcf \cdot 1000} \right)^{2.0} \cdot \left(\frac{f'_{ci}}{ksi} \right)^{0.33} \cdot ksi = 5131.521 \text{ ksi}$$

Modulus of elasticity of concrete girder at ultimate strength

$$E_c := 120000 \cdot \left(\frac{w_{cg_modulus}}{pcf \cdot 1000} \right)^{2.0} \cdot \left(\frac{f'_c}{ksi} \right)^{0.33} \cdot ksi = 5575.243 \text{ ksi}$$

Modulus of elasticity of deck at final time

$$E_{cd} := 33000 \cdot \left(\frac{w_{cd_modulus}}{pcf \cdot 1000} \right)^{1.5} \cdot \left(\frac{f'_{cd}}{ksi} \right)^{0.5} \cdot ksi = 4027.555 \text{ ksi}$$

Modulus of elasticity of deck at initial

$$E_{cdi} := 33000 \cdot \left(\frac{w_{cd_modulus}}{pcf \cdot 1000} \right)^{1.5} \cdot \left(\frac{f'_{cdi}}{ksi} \right)^{0.5} \cdot ksi = 4027.555 \text{ ksi}$$

Compression steel

The BrR file does not contain any information about the compression steel.

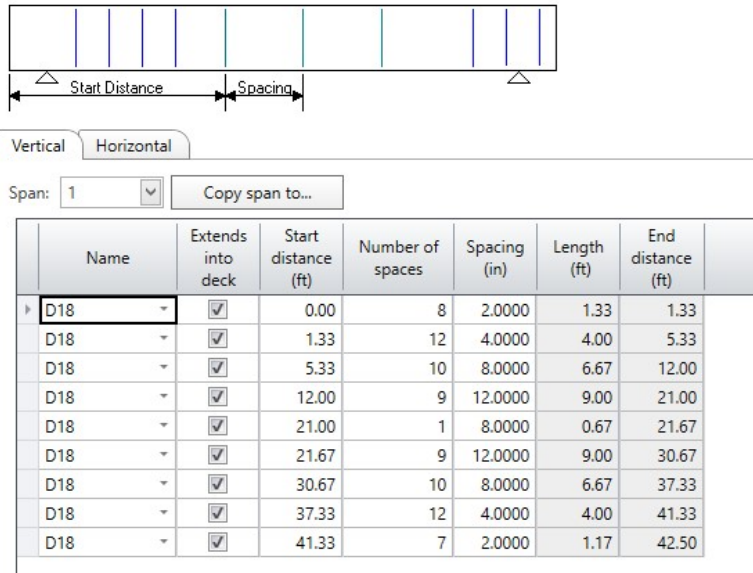
Other information

1. Skew: 0 degrees.
2. ADT: 49240.

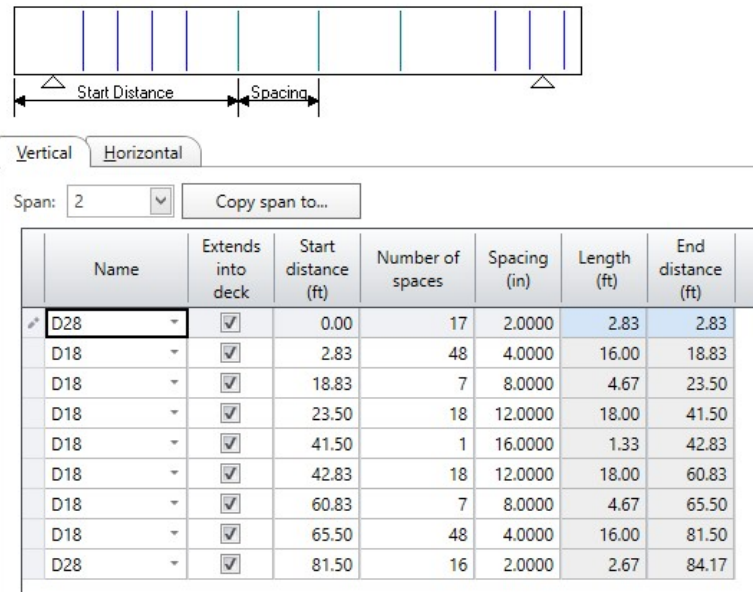
Vertical shear reinforcement information

Note: Shear was checked at two locations at the interior span. Welded wire fabric (WWF) (70 ksi) was used. At the support ends, the WWF was modeled with 2.8 legs (#4 bars). 1.80 legs (#4 bars) were used for other locations.

Span 1 vertical shear reinforcement information



Span 2 vertical shear reinforcement information



Prestress steel information

Span strand layouts are given below for span 1 and 2. Span 3 has the same layout as for span 1.

Span 1 strand layout information

Strand Layout - Span 1

Description type
 P and CGS only Strands in rows

Strand configuration type
 Straight/Debonded
 Harped
 Harped and straight debonded

Symmetry

Mid span

Left end

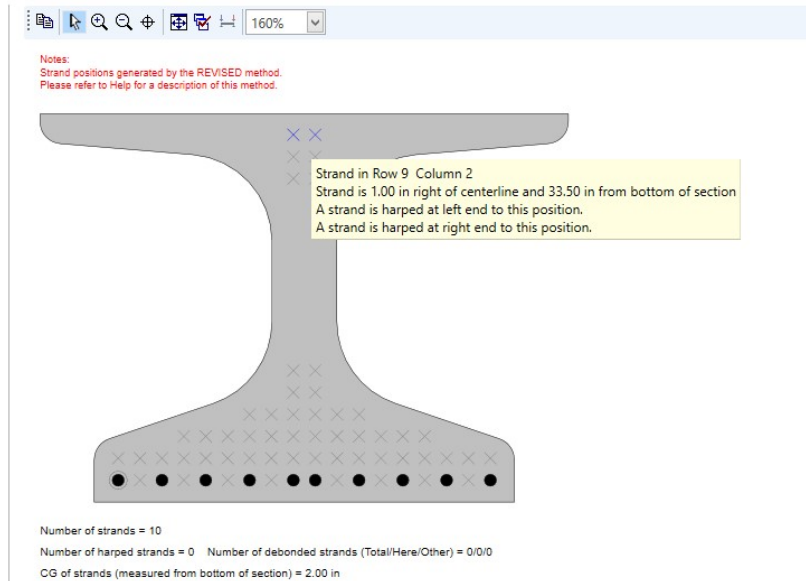
Right end

Harp point locations		
Harp point	Distance (ft)	Radius (in)
Left	17.07	0.0000
Right	17.07	0.0000

Debonding

Section location (in)	Measured and debonded from

New Modify Delete



Span 2 strand layout information

Strand Layout - Span 2

Description type
 P and CGS only Strands in rows

Strand configuration type
 Straight/Debonded
 Harped
 Harped and straight debonded

Symmetry

Mid span

Left end

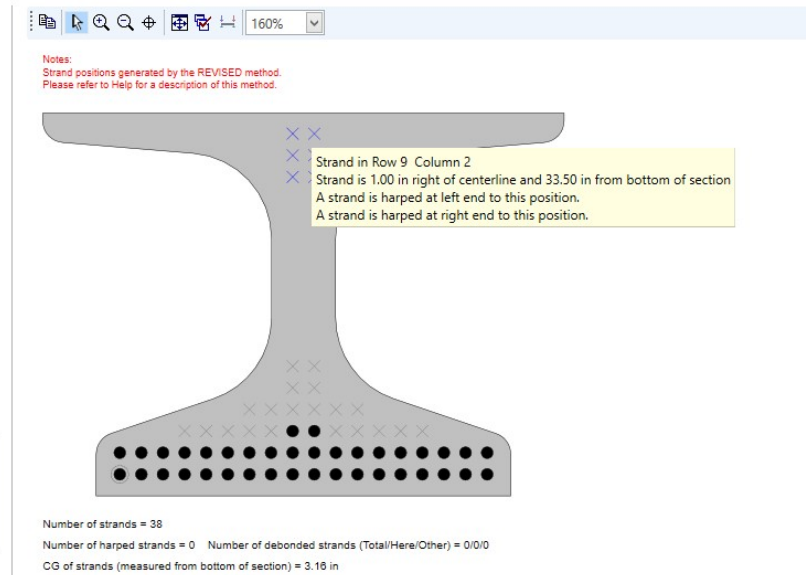
Right end

Harp point locations		
Harp point	Distance (ft)	Radius (in)
Left	33.73	0.0000
Right	33.73	0.0000

Debonding

Section location (in)	Measured and debonded from

New Modify Delete



Note: 0.6", 270 ksi, low-relaxation strands.

Span 1 & 3: There are total 10 prestress strands (2 strands harped).

Span 2: There are total 38 prestress strands (6 strands harped)

This rating example focused on Span 2 (interior span) strand layout.

0.6", low-relaxation strand

$$d_b := 0.6 \text{ in}$$

Area of prestress per strands

$$A_{strand} := 0.217 \text{ in}^2$$

Ultimate strength of prestressed strands

$$f_{pu} := 270 \text{ ksi}$$

Yield stress of prestressed strands

$$f_{py} := 243 \text{ ksi}$$

Prestressed strands stress prior to transfer

$$f_{pi} := 0.75 \cdot f_{pu} = 202.5 \text{ ksi}$$

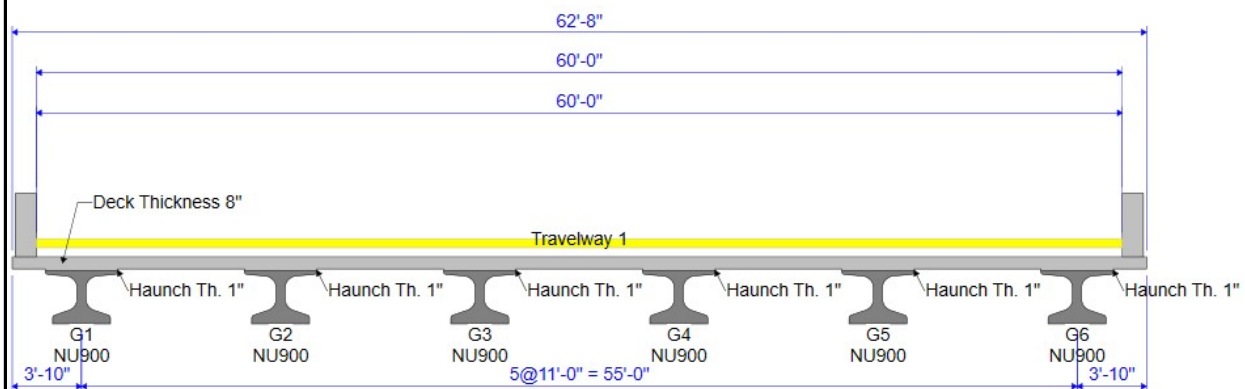
Modulus of elasticity of prestress

$$E_p := 28500 \text{ ksi}$$

Modulus of ratio for deck to girder concrete

$$n_{pd} := \frac{E_{cd}}{E_c} = 0.722$$

2. Bridge Cross Section



Girder spacing (S)

$$S := 11 \text{ ft}$$

Number of girders

$$N_{girder} := 6$$

Overhang

$$overhang := 3.833 \text{ ft}$$

Barrier length

$$L_{barrier} := 0.333 \text{ ft}$$

Total bridge width

$$W_{bridge} := (overhang \cdot 2 + S \cdot (N_{girder} - 1)) = 751.992 \text{ in}$$

Effective width for deck (for interior girders)

$$b_{eff} := S = 132 \text{ in}$$

3. Interior Girder Details

Prestress I Beam _ □ ×

Name:

Description:

Top flange type
 Narrow
 Wide

Area:	<input type="text" value="648.2839358"/>	in ²	Volume/surface ratio:	<input type="text" value="3.105"/>	in
Nominal load:	<input type="text" value="675.296"/>	lb/ft	Half depth area for pos. flex.:	<input type="text" value="357.166"/>	in ²
Moment of inertia:	<input type="text" value="110017.723"/>	in ⁴	Half depth area for neg. flex.:	<input type="text" value="250.543"/>	in ²
CG from bottom:	<input type="text" value="16.1076"/>	in	St. Venant torsional constant:	<input type="text" value="25792.348"/>	in ⁴
Section modulus, top:	<input type="text" value="5702.655"/>	in ³	<input type="checkbox"/> Use entered section properties Note: see engine related help for analysis engine specific information on the "Use entered section properties" selection. Note: 150 pcf concrete is assumed to compute the nominal load.		
Section modulus, bot.:	<input type="text" value="6830.161"/>	in ³	<input type="button" value="Compute"/>		
Nominal depth:	<input type="text" value="35.4000"/>	in			

Girder gross section area

$$A_g := 648.3 \text{ in}^2$$

Beam height

$$h_{nc} := 35.4 \text{ in}$$

Top girder width

$$b_{top} := 48.25 \text{ in}$$

Moment of inertia precast girder

$$I_{nc} := 110017.7 \text{ in}^4$$

Girder centroid to the bottom of fiber

$$y_{ncb} := 16.1 \text{ in}$$

Girder centroid to the top of fiber

$$y_{nct} := h_{nc} - y_{ncb} = 19.3 \text{ in}$$

Non-composite section modulus top

$$S_{top_nc} := \frac{I_{nc}}{h_{nc} - y_{ncb}} = 5700.399 \text{ in}^3$$

Non-composite section modulus bottom

$$S_{bot_nc} := \frac{I_{nc}}{y_{ncb}} = 6833.398 \text{ in}^3$$

Thickness of deck (loads calculations)

$$t_s := 8 \text{ in}$$

Thickness of deck (effective)

$$h_d := 7.5 \text{ in}$$

Section property calculations

Transformed width of deck
(deck concrete to girder concrete)

$$b_{d_tr} := b_{eff} \cdot n_{pd} = 95.357 \text{ in}$$

Cross-section area of deck

$$A_{d_tr} := b_{d_tr} \cdot h_d = 715.176 \text{ in}^2$$

Deck moment of inertia of deck about it centroid

$$I_{d_tr} := \frac{h_d^3 \cdot b_{d_tr}}{12} = 3352.387 \text{ in}^4$$

Height of haunch

$$h_h := 1 \text{ in}$$

Transformed width of haunch

$$b_{h_tr} := b_{top} \cdot n_{pd} = 34.856 \text{ in}$$

Area of haunch

$$A_{h_tr} := b_{h_tr} \cdot h_h = 34.856 \text{ in}^2$$

Haunch moment of inertia of haunch about it centroid

$$I_{h_tr} := \frac{h_h^3 \cdot b_{h_tr}}{12} = 2.905 \text{ in}^4$$

Total height of composite beam

$$h_c := h_h + h_{nc} + h_d = 43.9 \text{ in}$$

Transformed section area
(including deck and haunch)

$$A_c := A_g + A_{d_tr} + A_{h_tr} = 1398.332 \text{ in}^2$$

Center of deck to the bottom of fiber

$$h_{d_center} := \left(h_{nc} + h_h + \frac{h_d}{2} \right) = 40.15 \text{ in}$$

Center of haunch to the bottom of fiber

$$h_{h_center} := \left(h_{nc} + \frac{h_h}{2} \right) = 35.9 \text{ in}$$

Center to the bottom of fiber (composite)

$$y_{cb} := \frac{A_g \cdot y_{ncb} + A_{d_tr} \cdot h_{d_center} + A_{h_tr} \cdot h_{h_center}}{A_c} = 28.894 \text{ in}$$

Moment of inertia (composite)

$$I_c := \left(I_{nc} + A_g \cdot (y_{ncb} - y_{cb})^2 \right) + \left(I_{d_tr} + A_{d_tr} \cdot (h_{d_center} - y_{cb})^2 \right) + \left(I_{h_tr} + A_{h_tr} \cdot (h_{h_center} - y_{cb})^2 \right) = 311812.799 \text{ in}^4$$

Composite section modulus top beam $S_{top_c} := \frac{I_c}{h_{nc} - y_{cb}} = 47926.273 \text{ in}^3$

Composite section modulus bottom beam $S_{bot_c} := \frac{I_c}{y_{cb}} = 10791.645 \text{ in}^3$

Composite section modulus for extreme top fiber of the structural deck slab $S_{top_slab_c} := \frac{1}{n_{pd}} \frac{I_c}{h_c - y_{cb}} = 28763.955 \text{ in}^3$

Dead and live load moments from BrR (interior girders)

Non-composite Dead Load DC1 Moment at the 0.5L of the interior span $M_{DC1_mid} := 1637.5 \text{ kip} \cdot \text{ft}$

Composite Dead Load DC2 Moment at the 0.5L of the interior span $M_{DC2_mid} := 127.6 \text{ kip} \cdot \text{ft}$

Wearing surface load moment at the 0.5L of the interior span $M_{DW_mid} := 0 \text{ kip} \cdot \text{ft}$

HL-93 loading moment at the 0.5L of the interior span (with multiple lanes loaded GDF and IM = 0.33) $HL_93_M_{dist_mid} := 1034 \text{ kip} \cdot \text{ft}$

Note: The HL-93 loading load effects are directly extracted from BrR.

GDF for positive moment region at 0.5L of the interior span (interior girders)

Modular ratio for AASHTO GDFs $n_{GDF} := \frac{E_c}{E_{cd}} = 1.38427479$

e_g term for AASHTO GDF equations $e_{g_GDF} := h_{nc} - y_{ncb} + h_h + \frac{t_s}{2} = 24.3 \text{ in}$

K_g term for AASHTO GDF equations $K_g := n_{GDF} \cdot (I_{nc} + A_g \cdot e_{g_GDF}^2) = 682215 \text{ in}^4$

Distribution Factors

One Design Lane Loaded:

$$0.06 + \left(\frac{S}{14}\right)^{0.4} \left(\frac{S}{L}\right)^{0.3} \left(\frac{K_g}{12.0 L t_s^3}\right)^{0.1}$$

Two or More Design Lanes Loaded:

$$0.075 + \left(\frac{S}{9.5}\right)^{0.6} \left(\frac{S}{L}\right)^{0.2} \left(\frac{K_g}{12.0 L t_s^3}\right)^{0.1}$$

Single lane AASHTO moment GDF for interior girders (0.5L of the interior span)

$$g_{m1_mid} := 0.06 + \left(\frac{S}{14 \text{ ft}}\right)^{0.4} \cdot \left(\frac{S}{L_{mid}}\right)^{0.3} \cdot \left(\frac{\frac{K_g}{\text{in}^4}}{\left(12 \cdot \frac{L_{mid}}{\text{ft}} \cdot \left(\frac{t_s}{\text{in}}\right)^3\right)}\right)^{0.1} = 0.565$$

Multiple lanes AASHTO moment GDF for interior girders (0.5L of the interior span)

$$g_{m2_mid} := 0.075 + \left(\frac{S}{9.5 \text{ ft}}\right)^{0.6} \cdot \left(\frac{S}{L_{mid}}\right)^{0.2} \cdot \left(\frac{\frac{K_g}{\text{in}^4}}{\left(12 \cdot \frac{L_{mid}}{\text{ft}} \cdot \left(\frac{t_s}{\text{in}}\right)^3\right)}\right)^{0.1} = 0.82$$

GDF for negative moment region at the interior supports (interior girders)

Single lane AASHTO moment GDF for interior girders (interior support)

$$L_{inter} := \frac{L_{end} + L_{mid}}{2} = 63.75 \text{ ft}$$

$$g_{m1_inter} := 0.06 + \left(\frac{S}{14 \text{ ft}}\right)^{0.4} \cdot \left(\frac{S}{L_{inter}}\right)^{0.3} \cdot \left(\frac{\frac{K_g}{\text{in}^4}}{\left(12 \cdot \frac{L_{inter}}{\text{ft}} \cdot \left(\frac{t_s}{\text{in}}\right)^3\right)}\right)^{0.1} = 0.627$$

Multiple lanes AASHTO moment GDF for interior girders (interior support)

$$g_{m2_inter} := 0.075 + \left(\frac{S}{9.5 \text{ ft}} \right)^{0.6} \cdot \left(\frac{S}{L_{inter}} \right)^{0.2} \cdot \left(\frac{\frac{K_g}{\text{in}^4}}{\left(12 \cdot \frac{L_{inter}}{\text{ft}} \cdot \left(\frac{t_s}{\text{in}} \right)^3 \right)} \right)^{0.1} = 0.887$$

Single lane AASHTO shear GDF for interior girders

$$g_{v1} := 0.36 + \frac{S}{25 \text{ ft}} = 0.8$$

Multiple lanes AASHTO shear GDF for interior girders

$$g_{v2} := 0.20 + \frac{S}{12 \text{ ft}} - \left(\frac{S}{35 \text{ ft}} \right)^2 = 1.018$$

4. Compute Nominal Flexural Resistance at 0.5L of the Interior Span

$$f_{ps} = f_{pu} \left(1 - k \frac{c}{d_p} \right)$$

$$k = 0.28 \text{ for low-relaxation strands}$$

$$f_{pu} = 270 \text{ ksi}$$

$$d_p = \text{distance from extreme compression fiber to the centroid of the prestressing tendons}$$

Center of PS strands to the bottom girder $y_{bar} := 3.16 \text{ in}$

Distance from extreme compression fiber to the centroid of the prestressing strands $d_p := h_{nc} + h_h + h_d - y_{bar} = 40.74 \text{ in}$

Number of strands $N_{ps} := 38$

Area of total prestress $A_{ps} := A_{strand} \cdot N_{ps} = 8.246 \text{ in}^2$

$$\alpha_1 := 0.85$$

Stress factor of compression block $\beta_1 := 0.85$

0.28 for low-relaxation $k := 0.28$

Distance from neutral axis to the compressive face $c := \frac{A_{ps} \cdot f_{pu}}{\alpha_1 \cdot f'_{cd} \cdot \beta_1 \cdot b_{eff} + k \cdot A_{ps} \cdot \frac{f_{pu}}{d_p}} = 5.611 \text{ in}$

Depth of the equivalent stress block $a := \beta_1 \cdot c = 4.77 \text{ in}$

Note: Because the "a" is smaller than the deck thickness, the rectangular section behavior assumption is valid.

Average stress in prestressing strand, ksi $f_{ps} := f_{pu} \cdot \left(1 - k \cdot \frac{c}{d_p} \right) = 259.587 \text{ ksi}$

Nominal flexural resistance at the interior span $M_n := A_{ps} \cdot f_{ps} \cdot \left(d_p - \frac{a}{2} \right) = 6841.803 \text{ kip} \cdot \text{ft}$

5. Check the Maximum Reinforcement

Note: LRFD BDS Article 5.6.2.1 limits the factor resistance of compression controlled sections. Over-reinforced (compression controlled) sections are limited by this approach. Using similar triangles, the net tensile strain is determined at nominal strength.

Based on an allowable concrete strain of 0.003 and the distance from the extreme concrete compression fiber to the center of gravity of the prestressing strands.

Allowable concrete strain $\varepsilon_c := 0.003$

Net tensile strain $\varepsilon_t := \frac{\varepsilon_c}{c} \cdot (d_p - c) = 0.019$

Note: Because $\varepsilon_t > 0.005$, the section is tension controlled and resistance factor shall be taken as 1.0.

Strength Reduction Factor $\phi := 1.0$

Factored required moment

$$M_{u_mid} := 1.25 \cdot (M_{DC1_mid} + M_{DC2_mid}) + 1.50 \cdot M_{DW_mid} \downarrow = 4016 \text{ kip} \cdot \text{ft} \\ + 1.75 \cdot (HL_93_M_{dist_mid})$$

Demand/capacity ratio for the 0.5L of the interior span

$$DCR_{mid} := \frac{M_{u_mid}}{\phi \cdot M_n} = 0.587$$

6. Compute Prestress Loss according to *LRFD BDS* Article 5.9.3.4 (Gross Section)

Assumed center of PS strands to bottom of fiber $e_{nc} := y_{ncb} - y_{bar} = 12.94 \text{ in}$

Eccentricity (composite at final) $e_c := e_{nc} + y_{cb} - y_{ncb} = 25.734 \text{ in}$

Shape factor (V/S) $V_S_Girder := 3.1052$

Average Humidity (Nebraska) $H := 65$

Age of girder concrete at time of transfer (day) $t_i := 1$

Age of girder concrete at time of deck placement $t_d := 30$

Age of girder concrete at time at final time $t_f := 3650$

Permanent load moments at midspan acting on non-composite section (beam) $M_g := 605.7 \text{ kip} \cdot \text{ft}$

Losses due to elastic shortening $\Delta f_{pES} := \frac{A_{ps} \cdot f_{pi} \cdot (I_{nc} + e_{nc}^2 \cdot A_g) - e_{nc} \cdot M_g \cdot A_g}{A_{ps} \cdot (I_{nc} + e_{nc}^2 \cdot A_g) + \frac{A_g \cdot I_{nc} \cdot E_{ci}}{E_p}} = 20.759 \text{ ksi}$

Stress in strand after elastic shortening $f_{pt1} := f_{pi} - \Delta f_{pES} = 181.741 \text{ ksi}$

Concrete stress at the center of strands due to the prestressing force at transfer and the self weight of the member $f_{cgp} := \frac{f_{pt1} \cdot A_{ps}}{A_g} + \frac{f_{pt1} \cdot A_{ps} \cdot e_{nc}^2}{I_{nc}} - \frac{M_g \cdot e_{nc}}{I_{nc}} = 3.738 \text{ ksi}$

k_s term calculation $k_s := \max(1, (1.45 - 0.13 \cdot V_S_Girder)) = 1.046$

Humidity factor for shrinkage $k_{hs} := 2 - 0.014 \cdot H = 1.09$

Concrete strength factor $k_f := \frac{5 \text{ ksi}}{1 \text{ ksi} + f'_{ci}} = 0.625$

$$k_{td} = \frac{t}{12 \left(\frac{100 - 4 f'_{ci}}{f'_{ci} + 20} \right) + t}$$

Time development factor

Time development factor (initial to deck) $k_{tdd} := \frac{(t_d - t_i)}{12 \cdot \left(\frac{100 \text{ ksi} - 4 \cdot f'_{ci}}{f'_{ci} + 20 \text{ ksi}} \right) + (t_d - t_i)} = 0.475$

Shrinkage strain (initial to deck placement) $\varepsilon_{bid} := k_s \cdot k_{hs} \cdot k_f \cdot k_{tdd} \cdot 0.48 \cdot 10^{-3} = 0$

Transformed section coefficient

$$K_{td} = \frac{1}{1 + \frac{E_p A_{ps}}{E_{ci} A_g} \left(1 + \frac{A_g e^2}{I_g} \right) [1 + 0.7 \psi_b(t_f, t_i)]}$$

(5.9.3.4.2a-2)

Humidity factor for creep

$$k_{hc} := 1.56 - 0.008 \cdot H = 1.04$$

Time development factor (initial to final)

$$k_{tdf} := \frac{(t_f - t_i)}{12 \cdot \left(\frac{100 \text{ ksi} - 4 \cdot f'_{ci}}{f'_{ci} + 20 \text{ ksi}} \right) + (t_f - t_i)} = 0.991$$

Creep coefficients and shrinkage strains (girder)

The creep coefficient may be taken as:

$$\psi(t, t_i) = 1.9 k_s k_{hc} k_f k_{td} t_i^{-0.118} \quad (5.4.2.3.2-1)$$

Creep coefficients (initial to deck placement) $\psi_{td_ti} := 1.9 k_s \cdot k_{hc} \cdot k_f \cdot k_{tdd} \cdot (t_i)^{-0.118} = 0.614$

Creep coefficients (initial to final) $\psi_{tf_ti} := 1.9 k_s \cdot k_{hc} \cdot k_f \cdot k_{tdf} \cdot (t_i)^{-0.118} = 1.281$

Transformed section coefficients (initial to deck)

$$K_{id} := \frac{1}{1 + \frac{E_p}{E_{ci}} \cdot \frac{A_{ps}}{A_g} \cdot \left(1 + \frac{A_g \cdot e_{nc}^2}{I_{nc}}\right)} \cdot (1 + 0.7 \cdot \psi_{tf-ti}) = 0.79$$

Long-term losses prior to deck placement (between transfer and deck placement)

Loss due to girder shrinkage (initial to deck) $\Delta f_{pSR} := \varepsilon_{bid} \cdot E_p \cdot K_{id} = 3.661 \text{ ksi}$

Creep coefficients and shrinkage strains (girder):

The creep coefficient may be taken as:

$$\psi(t, t_i) = 1.9 k_2 k_{hc} k_f k_{td} t_i^{-0.118} \quad (5.4.2.3.2-1)$$

Loss due to girder Creep (initial to deck) $\Delta f_{pCR} := \frac{E_p}{E_{ci}} \cdot f_{cgp} \cdot \psi_{td-ti} \cdot K_{id} = 10.072 \text{ ksi}$

Loss due to relaxation $\Delta f_{pR1} := 1.2 \text{ ksi}$

Total loss before deck placement $\Delta f_{pLTid} := \Delta f_{pSR} + \Delta f_{pCR} + \Delta f_{pR1} = 14.933 \text{ ksi}$

Long-term losses after deck placement

Shrinkage strain (initial to final) $\varepsilon_{bif} := k_s \cdot k_{hs} \cdot k_f \cdot k_{tdf} \cdot 0.48 \cdot 10^{-3} = 0$

The girder concrete shrinkage strain between deck placement and final time is: shrinkage strain (deck to final) $\varepsilon_{bdf} := \varepsilon_{bif} - \varepsilon_{bid} = 0$

Transformed section coefficients (deck to final)

$$K_{df} := \frac{1}{1 + \frac{E_p}{E_{ci}} \cdot \frac{A_{ps}}{A_c} \cdot \left(1 + \frac{A_c \cdot e_c^2}{I_c}\right)} \cdot (1 + 0.7 \cdot \psi_{tf-ti}) = 0.802$$

The prestress loss due to shrinkage of concrete between deck placement and final time is: Shrinkage (deck to final)

$$\Delta f_{pSD} := \varepsilon_{bdf} \cdot E_p \cdot K_{df} = 4.035 \text{ ksi}$$

Loss due to girder Creep (after deck placement)

$$\Delta f_{pCD} = \frac{E_p}{E_{ci}} f_{cgp} [\Psi_b(t_f, t_i) - \Psi_b(t_d, t_i)] K_{df} \quad (5.9.3.4.3b-1)$$

$$+ \frac{E_p}{E_c} \Delta f_{cd} \Psi_b(t_f, t_d) K_{df}$$

Time development factor (deck to final)

$$k_{tdf_d} := \frac{(t_f - t_d)}{12 \cdot \left(\frac{100 \text{ ksi} - 4 \cdot f'_{ci}}{f'_{ci} + 20 \text{ ksi}} \right) + (t_f - t_d)} = 0.991$$

Creep coefficients (deck to final)

$$\psi_{tf_{td}} := 1.9 k_s \cdot k_{nc} \cdot k_f \cdot k_{tdf_d} \cdot (t_d)^{-0.118} = 0.857$$

Permanent load moments at midspan acting on non-composite section (except beam at transfer) [Haunch + deck]

$$M_{dnc} := 1031.8 \text{ kip} \cdot \text{ft}$$

Permanent load moments at midspan acting on composite section [barrier and wearing]

$$M_{dc} := M_{DC2_{mid}} = 127.6 \text{ kip} \cdot \text{ft}$$

Loss in the strands

$$P_{\Delta} := A_{ps} \cdot \Delta f_{pLTid} = 123.136 \text{ kip}$$

Change in concrete stress at centroid of strands due to long-term losses between transfer and deck placement

$$\Delta f_{cd} := - \left(\frac{P_{\Delta}}{A_g} + \frac{P_{\Delta} \cdot e_{nc}^2}{I_{nc}} + \frac{M_{dnc} \cdot e_{nc}}{I_{nc}} + \frac{M_{dc} \cdot e_c}{I_c} \right) = -1.96 \text{ ksi}$$

Losses due to creep between deck placement and final time

$$\Delta f_{pCD} := \frac{E_p}{E_{ci}} \cdot f_{cgp} \cdot (\psi_{tf_{ti}} - \psi_{td_{ti}}) \cdot K_{df} + \frac{E_p}{E_c} \cdot \Delta f_{cd} \cdot \psi_{tf_{td}} \cdot K_{df} = 4.209 \text{ ksi}$$

Loss due to relaxation

$$\Delta f_{pR2} := \Delta f_{pR1} = 1.2 \text{ ksi}$$

Deck material coefficients

It is also necessary to determine some material properties for the deck concrete. Humidity factors (k_{hs} and k_{hc}) will be the same as for the beam.

Shape factor for deck estimated (V/S) $VS_d := \frac{h_d \cdot b_{eff}}{(h_d + b_{eff}) \cdot 2 \cdot in} = 3.548$

k_{vs} for deck $k_{sd} := \max(1, (1.45 - 0.13 \cdot VS_d)) = 1$

Concrete strength factor $k_{fd} := \frac{5 \text{ ksi}}{1 \text{ ksi} + f'_{cdi}} = 1$

Time development factor (end of moist to final)

$$k_{tdf_dd} := \frac{(t_f - t_d)}{12 \cdot \left(\frac{100 \text{ ksi} - 4 \cdot f'_{cdi}}{f'_{cdi} + 20 \text{ ksi}} \right) + (t_f - t_d)} = 0.989$$

Shrinkage strain (deck to final) $\epsilon_{ddf} := k_{sd} \cdot k_{hs} \cdot k_{fd} \cdot k_{tdf_d} \cdot 0.48 \cdot 10^{-3} = 0.001$

Creep coefficients (deck to final) $\psi_{d_tf_td} := 1.9 \cdot k_{sd} \cdot k_{hc} \cdot k_{fd} \cdot k_{tdf_d} \cdot (t_i)^{-0.118} = 1.959$

Eccentricity of deck with respect to gross composite section $e_d := (h_c - y_{cb}) - \frac{h_d}{2} = 11.256 \text{ in}$

Area of deck concrete $A_d := b_{eff} \cdot h_d = 990 \text{ in}^2$

Change in concrete stress due to deck shrinkage $\Delta f_{cdf} := \frac{(\epsilon_{ddf} \cdot A_d \cdot E_{cd})}{(1 + 0.7 \cdot \psi_{d_tf_td})} \cdot \left(\frac{1}{A_c} - \frac{e_c \cdot e_d}{I_c} \right) = -0.186 \text{ ksi}$

Losses due to shrinkage of deck $\Delta f_{pSS} := \frac{E_p}{E_c} \cdot (-\Delta f_{cdf}) \cdot K_{df} \cdot (1 + 0.7 \cdot \psi_{tf_td}) = 1.224 \text{ ksi}$

Total loss after deck placement $\Delta f_{pLTdf} := \Delta f_{pSD} + \Delta f_{pCD} + \Delta f_{pR2} - \Delta f_{pSS} = 8.221 \text{ ksi}$

Total long-term loss based on refined method $\Delta f_{pLT} := \Delta f_{pLTid} + \Delta f_{pLTdf} = 23.154 \text{ ksi}$

Total loss $\Delta f_{pLT_without_elastic_gain} := \Delta f_{pES} + \Delta f_{pLTid} + \Delta f_{pLTdf} = 43.913 \text{ ksi}$

The elastic gain due to deck weight, superimposed dead load, and live load (Service III)

$$elastic_gain_dead := \left(\frac{M_{dnc} \cdot e_{nc}}{I_{nc}} + \frac{M_{dc} \cdot e_c}{I_c} \right) \cdot \frac{E_p}{E_c} = 8.09 \text{ ksi}$$

$$elastic_gain_live := 1.0 \cdot \left(\frac{e_c \cdot HL_{93} M_{dist_mid}}{I_c} \right) \cdot \frac{E_p}{E_c} = 5.235 \text{ ksi}$$

Total loss with elastic gain (dead loads)

$$\Delta f_{p_total_dead_elastic_gain} := \Delta f_{pES} + \Delta f_{pLTid} + \Delta f_{pLTdf} - elastic_gain_dead = 35.822 \text{ ksi}$$

Total loss with elastic gain (live loads)

$$\Delta f_{p_total_live_elastic_gain} := \Delta f_{pES} + \Delta f_{pLTid} + \Delta f_{pLTdf} - elastic_gain_live = 38.678 \text{ ksi}$$

Total loss with elastic gain (dead and live loads)

$$\Delta f_{ps} := \Delta f_{pES} + \Delta f_{pLTid} + \Delta f_{pLTdf} - elastic_gain_dead - elastic_gain_live = 30.587 \text{ ksi}$$

Note: The total loss included both dead and live load elastic gains in this rating example.

Effective stress after loss

$$f_e := f_{pi} - \Delta f_{ps} = 171.913 \text{ ksi}$$

Effective force after loss

$$P_e := A_{ps} \cdot f_e = 1417.591 \text{ kip}$$

Compressive stress due to effective prestress

$$f_{pb} := \frac{P_e}{A_g} + \frac{P_e \cdot e_{nc}}{S_{bot_nc}} = 4.871 \text{ ksi}$$

7. Check the Minimum Reinforcement according to LRFD BDS Article 5.6.3.3

At any section, the amount of prestressed and non-prestressed tensile reinforcement must be adequate to develop a factored flexural resistance, M_r , equal to the lesser of:

- 1.33 times the factored moment required by the applicable strength load combination specified in Table 3.4.1-1;

- $$M_{cr} = \gamma_3 \left[(\gamma_1 f_r + \gamma_2 f_{cpe}) S_c - M_{anc} \left(\frac{S_c}{S_{nc}} - 1 \right) \right]$$
 (5.6.3.3-1)

Design Flexural Strength

$$M_r := \phi \cdot M_n = 6841.803 \text{ kip} \cdot \text{ft}$$

1.33 Factored moment required

$$M_{u_factored} := 1.33 \cdot M_{u_mid} = 5341.114 \text{ kip} \cdot \text{ft}$$

Modulus of rupture (assume $\lambda = 1.0$)
(LRFD BDS 5.4.2.6)

$$f_r := 0.24 \cdot \sqrt{\frac{f'_c}{\text{ksi}}} \cdot \text{ksi} = 0.72 \text{ ksi}$$

γ_1 = flexural cracking variability factor
= 1.2 for precast segmental structures
= 1.6 for all other concrete structures

γ_2 = prestress variability factor
= 1.1 for bonded tendons
= 1.0 for unbonded tendons

For prestressing steel, γ_3 shall be taken as 1.0.

Cracking moment

$$\gamma_1 := 1.6 \quad \gamma_2 := 1.1 \quad \gamma_3 := 1.0$$

$$M_{cr} := \gamma_3 \cdot \left((\gamma_1 \cdot f_r + \gamma_2 \cdot f_{pb}) \cdot S_{bot_c} - M_{DC1_mid} \cdot \left(\frac{S_{bot_c}}{S_{bot_nc}} - 1 \right) \right) = 4906.07 \text{ kip} \cdot \text{ft}$$

$$check_min_reinforcement := \text{if}(M_r > \min(1.33 M_{u_mid}, M_{cr}), \text{"OK"}, \text{"NG"}) = \text{"OK"}$$

Note: Therefore, the minimum reinforcement check is good.

Negative moment region Strength I

Note: M_u is determined firstly for the negative moment region. For this simple made continuous bridge, the self weight of the beam and the weight of the slab and haunch act on the noncomposite, simple-span structure, while the weight of barriers and live loads with impact act on the composite, continuous structure.

Dead and live load moments from BrR (interior support)

Non-composite Dead Load DC1 Moment at the interior support

$$M_{DC1_inter} := 0 \text{ kip} \cdot \text{ft}$$

Composite Dead Load DC2 Moment at the interior support

$$M_{DC2_inter} := -74.7 \text{ kip} \cdot \text{ft}$$

Wearing surface load moment at the interior support

$$M_{DW_inter} := 0 \text{ kip} \cdot \text{ft}$$

HL-93 loading moment at the interior support (with multiple lanes GDF and IM = 0.33 for truck)

$$HL_93_M_{dist_inter} := -1006.1 \text{ kip} \cdot \text{ft}$$

Non-prestressing flexural reinforcement information at the interior support (in BrR)

Flexural Reinforcement	
As	Dist. From Bottom
(in ²)	(in)
2.20	41.40
3.41	37.40
6.60	41.40
8.69	37.40

Centroid of non-prestressed reinforcement to the bottom of beam

$$d_{inter} := \frac{8.8 \text{ in}^2 \cdot 41.4 \text{ in} + 12.1 \text{ in}^2 \cdot 37.4 \text{ in}}{8.69 \text{ in}^2 + 12.1 \text{ in}^2} = 39.291 \text{ in}$$

Notes:

1. At the negative moment section, the compression face is the bottom flange of the beam.
2. This section is a nonprestressed reinforced concrete section, thus ϕ is 0.9 for flexure.

The compression face is the bottom flange of the beam

$$b_{bot} := 38.375 \text{ in}$$

Total non-prestressed flexure reinforcement

$$A_s := 12.1 \text{ in}^2 + 8.69 \text{ in}^2 = 20.79 \text{ in}^2$$

Non-prestressed flexure yield stress

$$f_y := 60 \text{ ksi}$$

Depth of the equivalent stress block

$$a_{inter} := \frac{A_s \cdot f_y}{0.85 b_{bot} \cdot f'_c} = 4.249 \text{ in}$$

Note: This value is smaller than the flange thickness of 5.3125 in. The rectangular section behavior assumption is valid.

Nominal flexural resistance (include the negative sign)

$$M_{n_inter} := -A_s \cdot f_y \cdot \left(d_{inter} - \frac{a_{inter}}{2} \right) = -3863.454 \text{ kip} \cdot \text{ft}$$

ϕ Factor for nonprestressed section

$$\phi_{nonps} := 0.9$$

$$\phi_{nonps} \cdot M_{n_inter} = -3477.108 \text{ kip} \cdot \text{ft}$$

Factored required moment

$$M_{u_inter} := 1.25 \cdot (M_{DC1_inter} + M_{DC2_inter}) + 1.50 \cdot M_{DW_inter} \downarrow + 1.75 \cdot (HL_93_M_{dist_inter}) = -1854 \text{ kip} \cdot \text{ft}$$

Demand/capacity ratio

$$DCR_{mid} := \frac{M_{u_inter}}{\phi_{nonps} \cdot M_{n_inter}} = 0.533$$

Negative moment region minimum reinforcement check (LRFD BDS Article 5.6.3.3)

Note: This cross section is located in the region over the piers. Section is analyzed as a reinforced concrete section. At this section, the amount of non-prestressed tensile reinforcement must be adequate to develop a factored flexural resistance.

Design Flexural Strength $M_{r_inter} := \phi_{nonps} \cdot M_{n_inter} = -3477.108 \text{ kip} \cdot \text{ft}$

1.33 Factored moment required $M_{u_factored_inter} := 1.33 \cdot M_{u_inter} = -2465.887 \text{ kip} \cdot \text{ft}$

Modulus of rupture based on the deck
(assume $\lambda = 1.0$) (LRFD BDS 5.4.2.6) $f_{r_inter} := 0.24 \cdot \sqrt{\frac{f'_{cd}}{\text{ksi}}} \cdot \text{ksi} = 0.48 \text{ ksi}$

γ_3 = ratio of specified minimum yield strength
to ultimate tensile strength of the
nonprestressed reinforcement
= 0.67 for **AASHTO M 31** (ASTM A615),
Grade 60 reinforcement

Cracking moment $\gamma_1 := 1.6$ $\gamma_2 := 1.1$ $\gamma_3 := 0.67$

Composite section modulus for extreme top fiber
of the structural deck slab $S_{top_slab_c} = 28763.955 \text{ in}^3$

Cracking moment (apply negative sign here) (Note: For reinforced concrete members $S_c = S_{nc}$, and without f_{cpe})

$$M_{cr_inter} := -\gamma_3 \cdot (\gamma_1 \cdot f_{r_inter} \cdot S_{top_slab_c}) = -1233.398 \text{ kip} \cdot \text{ft}$$

$check := \text{if}(\text{abs}(M_{r_inter}) > \text{abs}(\min(1.33 M_{u_inter}, M_{cr_inter})), \text{"OK"}, \text{"NG"}) = \text{"OK"}$

Note: Therefore, the minimum reinforcement check is satisfied.

8. Compute Nominal Shear Resistance at First Critical Section

Note: The area and spacing of shear reinforcement must be determined at regular intervals along the entire length of the beam. In this rating example, transverse shear design procedures are demonstrated below by determining these values for the critical section near the interior supports at the interior span.

The d_v definition in *LRFD BDS* 5.7.2.8 is given below.

d_v = effective shear depth taken as the distance, measured perpendicular to the neutral axis, between the resultants of the tensile and compressive forces due to flexure; it need not be taken to be less than the greater of $0.9d_e$ or $0.72h$ (in.)

$$f_{ps} = f_{pu} \left(1 - k \frac{c}{d_p} \right)$$

$$k = 0.28 \text{ for low-relaxation strands}$$

$$f_{pu} = 270 \text{ ksi}$$

$$d_p = \text{distance from extreme compression fiber to the centroid of the prestressing tendons}$$

Note: d_e is calculated considering the nonprestressed reinforcement in the slab as the main reinforcement and neglecting the prestressing strand. This is because this section lies in the negative moment zone.

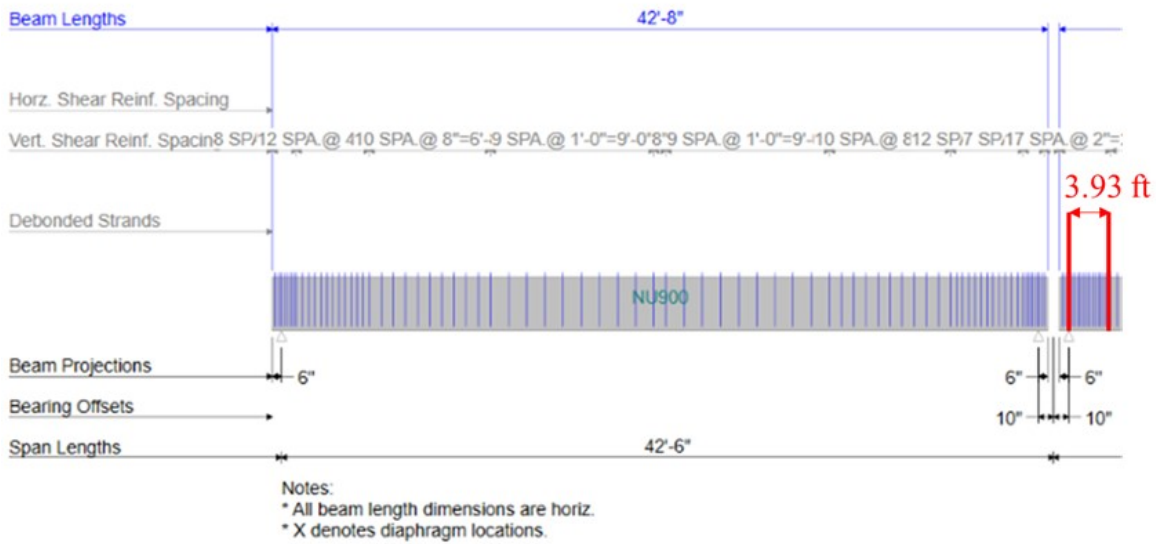
The corresponding effective depth from the extreme compression fiber to the centroid of the tensile force in the tensile reinforcement (d_{e_inter})

$$d_{e_inter} := d_{inter} = 39.291 \text{ in}$$

$$\text{Effective shear depth } d_v = \max \left(d_{e_inter} - \frac{a_{inter}}{2}, 0.9 \cdot d_{e_inter}, 0.72 \cdot h_c \right) = 37.166 \text{ in}$$

Critical shear location from centerline of bearing
(distance from the face of support to centerline of bearing is 10")

$$d_{critical} := d_v + 10 \text{ in} = 3.93 \text{ ft}$$



Compute the factored shear force and bending moment at the critical section for shear, according to Strength I load combination

Calculated shear loads at the 3.93 ft from the centerline of bearing.

Total distributed shear (HL-93 loading with multiple lanes GDF and IM = 0.33)

$$V_{distributed_critical} := 111.6 \text{ kip}$$

DC shears (Dnc (non-composite dead loads + Dc (barrier loads))

$$V_{nc_critical} := 72.8 \text{ kip}$$

$$V_{c_critical} := 5.7 \text{ kip}$$

DW shears (DW)

$$V_{DW_critical} := 0 \text{ kip}$$

Total distributed moment (HL-93 loading with multiple lanes GDF and IM = 0.33)

$$M_{distributed_critical} := -729.7 \text{ kip} \cdot \text{ft}$$

DC moment (Dnc (non-composite dead load + Dc (barrier loads))

$$M_{nc_critical} := 234.4 \text{ kip} \cdot \text{ft}$$

$$M_{c_critical} := -51.3 \text{ kip} \cdot \text{ft}$$

DW moment (DW)

$$M_{DW_critical} := 0 \text{ kip} \cdot \text{ft}$$

Compute nominal shear resistance

The nominal shear resistance, V_n , shall be determined as the lesser of both of the following:

$$V_n = V_c + V_s + V_p \quad (5.7.3.3-1)$$

$$V_n = 0.25 f'_c b_v d_v + V_p \quad (5.7.3.3-2)$$

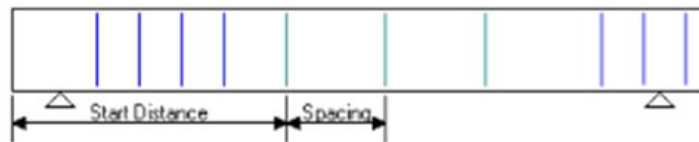
in which:

$$V_c = 0.0316 \beta \lambda \sqrt{f'_c} b_v d_v \quad (5.7.3.3-3)$$

$$V_s = \frac{A_v f_y d_v (\cot \theta + \cot \alpha) \sin \alpha}{s} \lambda_{duct} \quad (5.7.3.3-4)$$

$$\lambda_{duct} = 1 - \delta \left(\frac{\phi_{duct}}{b_w} \right)^2 \quad (5.7.3.3-5)$$

Based on the beam shear reinforcement layout below, the transverse reinforcement provided at 3.93 ft from the bearing centerline is D18 shear reinforcement at 4-in. spacing.



Vertical Horizontal

Span: 2 Copy span to...

Name	Extends into deck	Start distance (ft)	Number of spaces	Spacing (in)	Length (ft)	End distance (ft)
D28	<input checked="" type="checkbox"/>	0.00	17	2.0000	2.83	2.83
D18	<input checked="" type="checkbox"/>	2.83	48	4.0000	16.00	18.83
D18	<input checked="" type="checkbox"/>	18.83	7	8.0000	4.67	23.50
D18	<input checked="" type="checkbox"/>	23.50	18	12.0000	18.00	41.50
D18	<input checked="" type="checkbox"/>	41.50	1	16.0000	1.33	42.83
D18	<input checked="" type="checkbox"/>	42.83	18	12.0000	18.00	60.83
D18	<input checked="" type="checkbox"/>	60.83	7	8.0000	4.67	65.50
D18	<input checked="" type="checkbox"/>	65.50	48	4.0000	16.00	81.50
D28	<input checked="" type="checkbox"/>	81.50	16	2.0000	2.67	84.17

Minimum transverse reinforcement (LRFD BDS 5.7.2.5)

Effective web width, b_v $b_v := 5.9375 \text{ in}$

Shear reinforcement spacings, s_{shear} $s_{shear} := 4 \text{ in}$

Shear reinforcement yield strength, f_{y_shear} $f_{y_shear} := 70 \text{ ksi}$

Where transverse reinforcement is required as specified in either Article 5.7.2.3 or Article 5.12.5.3.8c, and nonprestressed reinforcement is used to satisfy that requirement, the area of steel shall satisfy:

$$A_v \geq 0.0316 \lambda \sqrt{f'_c} \frac{b_v s}{f_y} \quad (5.7.2.5-1)$$

$$A_v := 0.0316 \cdot (1.0) \cdot \sqrt{\frac{f'_c}{\text{ksi}}} \cdot \text{ksi} \cdot \frac{b_v \cdot s_{shear}}{f_{y_shear}} = 0.032 \text{ in}^2$$

Area provided for the critical section $A_{provided} := 1.8 \cdot 0.2 \text{ in}^2 = 0.36 \text{ in}^2$

$check_min_transverse_reinforcement := \text{if}(A_{provided} > A_v, \text{"OK"}, \text{"NG"}) = \text{"OK"}$

Determine the V_p

n type
CGS only Strands in rows

figuration type Symmetry

it/Debonded

and straight debonded

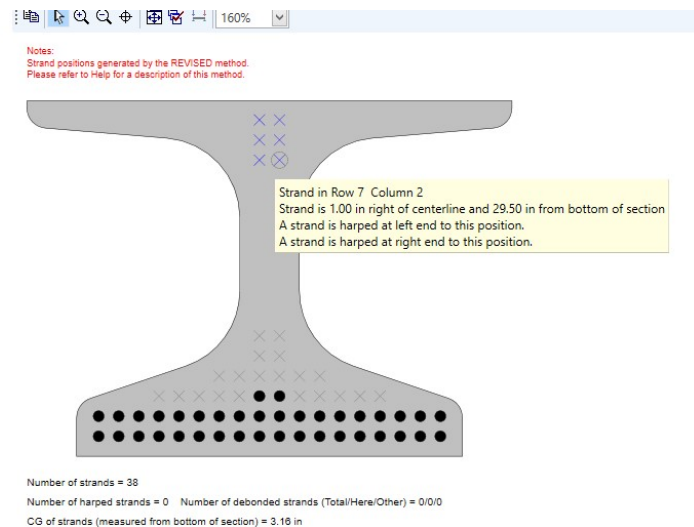
Harp point locations

Harp point	Distance (ft)	Radius (in)
Left	33.73	0.0000
Right	33.73	0.0000

Debonding

Section location (in)	Measured and debonded from

New Modify Delete



Number of harped strands

$$N_{harped} := 6$$

Harped strands point location to the bearing

$$L_{harped} := 33.73 \text{ ft}$$

Prestress force per strand without live load gains

$$P_{wo_LG_strand} := (f_{pi} - \Delta f_{p_total_dead_elastic_gain}) \cdot A_{strand} = 36.169 \text{ kip}$$

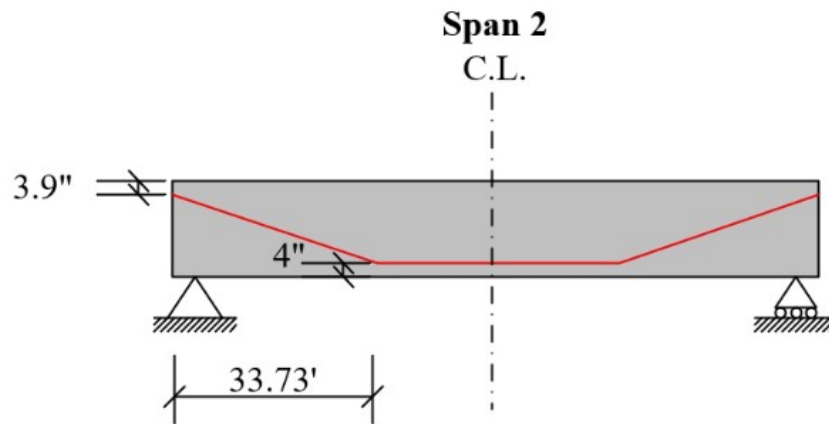
Top layer of harped strand distance to the bottom of precast beam

$$h_{harped_bot1} := 33.5 \text{ in}$$

Top layer of harped strand distance to the top of beam (33.5" to the bottom of beam in BrR)

$$d_{harped1} := h_{nc} - h_{harped_bot1} = 1.9 \text{ in}$$

There are a total of 3 layers of harped strands and the vertical increment is 2". Each harped strand layer distance to the top of the precast beam can be determined.



The distance between the center of gravity of the 6 harped strands at the end of the beam and the top fiber of the precast beam is:

$$d_{harped_top} := \frac{1.9 \cdot 2 + 3.9 \cdot 2 + 5.9 \cdot 2}{6} \cdot \text{in} = 3.9 \text{ in}$$

The distance between the center of gravity of the 6 harped stands at the harp point and the bottom fiber of the beam is:

$$d_{harped_bot} := \frac{2 \cdot 2 + 4 \cdot 2 + 6 \cdot 2}{6} \cdot \text{in} = 4 \text{ in}$$

$$\psi := \text{atan} \left(\frac{h_{nc} - d_{harped_top} - d_{harped_bot}}{L_{harped}} \right) = 3.887 \text{ deg}$$

Component of prestressing force in the direction of the shear force (6 strands harped)

$$V_p := (P_{wo_LG_strand}) \cdot (N_{harped}) \cdot \sin(\psi) = 14.71 \text{ kip}$$

The nominal shear determined by LRFD
Equation 5.7.3.3-2

$$V_{n_equ_1} := 0.25 \cdot f'_c \cdot b_v \cdot d_v + V_p = 511.231 \text{ kip}$$

These equations are based on the Modified Compression Field Theory (MCFT) and require the determination of β and θ by detailed analysis. A simplified analysis using $\theta = 45^\circ$ and $\beta = 2.0$ may be utilized for an initial evaluation before resorting to the MCFT, if necessary, for likely improved shear capacity.

C6A.5.8

Simplified approach

Concrete θ_{sim} and β_{sim}

$$\theta_{sim} := 45 \text{ deg} \quad \beta_{sim} := 2.0$$

Concrete shear strength

$$V_c := 0.0316 \beta_{sim} \cdot (1.0) \cdot \sqrt{\frac{f'_c}{ksi}} \cdot ksi \cdot b_v \cdot d_v = 41.84 \text{ kip}$$

Steel shear strength

$$V_s := \frac{A_{provided} \cdot f_{y_shear} \cdot d_v \cdot \cot(\theta_{sim})}{s_{shear}} = 234.149 \text{ kip}$$

The nominal shear determined by
LRFD BDS Equation 5.7.3.3-1

$$V_{n_equ_2} := V_c + V_s + V_p = 290.699 \text{ kip}$$

The nominal shear determined by LRFD BDS Equation 5.7.3.3

$$V_{n_simp} := \min(V_{n_equ_1}, V_{n_equ_2}) = 290.699 \text{ kip}$$

- For shear and torsion in monolithic prestressed concrete sections and prestressed concrete sections with cast-in-place closures or with match cast and epoxied joints having bonded strands or tendons:

normal weight concrete.....	0.90
lightweight concrete.....	0.90

$$\phi_{ps_shear} := 0.9$$

Factored shear resistance

$$\phi_{ps_shear} \cdot V_{n_simp} = 261.629 \text{ kip}$$

Strength I load factors

Load	Load Factor γ
<i>DC</i>	1.25
<i>DW</i>	1.50
<i>LL</i>	1.75

Maximum shear at the critical section (HL-93 inventory loading)

$$V_{u_critical} := 1.25 \cdot (V_{nc_critical} + V_{nc_critical}) + 1.5 \cdot V_{DW_critical} + 1.75 \cdot V_{distributed_critical} = 377.3 \text{ kip}$$

$$Check_shear_at_the_critical := \text{if}(\phi_{ps_shear} \cdot V_{n_simp} > V_{u_critical}, \text{"OK"}, \text{"NG"}) = \text{"NG"}$$

Note: The check was not good for the simplified shear resistance approach. Therefore, the MCFT approach to determine the shear resistance for this critical location was used.

Try MCFT General approach (LRFD BDS 5.7.3.4.2)

Shear stress on the concrete

$$v := \frac{V_{u_critical} - \phi_{ps_shear} \cdot V_p}{\phi_{ps_shear} \cdot b_v \cdot d_v} = 1.833 \text{ ksi}$$

$$check_using_APPENDIXB5 := \text{if}\left(\frac{v}{f'_c} < 0.25, \text{"OK"}, \text{"NG"}\right) = \text{"OK"}$$

As noted above, this example uses LRFD BDS 5.7.3.4.2, the general MCFT approach to determine shear resistance.

The net force is zero

$$N_u := 0 \text{ kip}$$

The A_s is provided before

$$A_s = 20.79 \text{ in}^2$$

The E_s for non-prestressing longitudinal steel

$$E_s := 29000 \text{ ksi}$$

The f_{po} can be taken as $0.7 f_{pu}$

$$f_{po} := 0.7 \cdot f_{pu} = 189 \text{ ksi}$$

Note: A_{ps} area of prestressing strands on the flexural tension side of the member. For this case, the harped strand area was used.

$$A_{ps_harped} := N_{harped} \cdot A_{strand} = 1.302 \text{ in}^2$$

In Eqs. 5.7.3.4.2-1 through 5.7.3.4.2-3, ϵ_s is the net longitudinal tensile strain in the section at the centroid of the tension reinforcement as shown in Figures 5.7.3.4.2-1 and 5.7.3.4.2-2. In lieu of more involved procedures, ϵ_s may be determined by Eq. 5.7.3.4.2-4:

$$\epsilon_s = \frac{\left(\frac{|M_u|}{d_v} + 0.5N_u + |V_u - V_p| - A_{ps}f_{po} \right)}{E_s A_s + E_p A_{ps}} \quad (5.7.3.4.2-4)$$

Maximum moment at this section (HL-93 inventory loading)

$$M_{u_critical} := 1.25 \cdot (M_{nc_critical} + M_{c_critical}) + 1.5 \cdot M_{DW_critical} + 1.75 \cdot M_{distributed_critical} = -1048.1 \text{ kip} \cdot \text{ft}$$

$$\epsilon_s := \frac{\left(\frac{\text{abs}(M_{u_critical})}{d_v} + 0.5 N_u + \text{abs}(V_{u_critical} - V_p) - A_{ps_harped} \cdot f_{po} \right)}{E_s \cdot A_s + E_p \cdot A_{ps_harped}} = 7.108 \cdot 10^{-4}$$

Assume the section contains at least the minimum amount of transverse reinforcement:

$$\beta_{equ} := \frac{4.8}{(1 + 750 \cdot \epsilon_s)} = 3.131$$

Angle of diagonal compressive stresses is:

$$\theta_{equ} := (29 + 3500 \cdot \epsilon_s) \text{ deg} = 0.55 \quad \cot(\theta_{equ}) = 1.633$$

Concrete shear strength $V_{c_MCFT} := 0.0316 \beta_{equ} \cdot (1.0) \cdot \sqrt{\frac{f'_c}{\text{ksi}}} \cdot \text{ksi} \cdot b_v \cdot d_v = 65.499 \text{ kip}$

Steel shear strength $V_{s_MCFT} := \frac{A_{provided} \cdot f_{y_shear} \cdot d_v \cdot \cot(\theta_{equ})}{s_{shear}} = 382.28 \text{ kip}$

The nominal shear determined by $V_{n_MCFT} := V_{c_MCFT} + V_{s_MCFT} + V_p = 462.489 \text{ kip}$
LRFD BDS Equation 5.7.3.3-1

The nominal shear determined by $V_{n_MCFT} := \min(V_{n_equ_1}, V_{n_MCFT}) = 462.489 \text{ kip}$
LRFD BDS Equation 5.7.3.3

Factored shear resistance $\phi_{ps_shear} \cdot V_{n_MCFT} = 416.24 \text{ kip}$

$check_shear_at_the_critical := \text{if}(\phi_{ps_shear} \cdot V_{n_MCFT} > V_{u_critical}, \text{"OK"}, \text{"NG"}) = \text{"OK"}$

Demand/capacity ratio $DCR_{x2} := \frac{V_{u_critical}}{\phi_{ps_shear} \cdot V_{n_MCFT}} = 0.906$

9. Check the Longitudinal Reinforcement according to *LRFD BDS 5.7.3.5*

A3.10.3—Check Longitudinal Reinforcement (LRFD Design 5.7.3.5)

Tensile capacity of the longitudinal reinforcement on the flexural tension side of the member shall be proportioned to satisfy LRFD Design Eq. 5.7.3.5-1. “Any lack of full development shall be accounted for.”

$$A_{ps}f_{ps} + A_s f_y \geq \frac{|M_u|}{d_v \phi_f} + 0.5 \frac{N_u}{\phi_c} + \left[\left| \frac{V_u}{\phi_v} - V_p \right| - 0.5 V_s \right] \cot \theta$$

LRFD Design
Eq. 5.7.3.5-1

Calculate minimum required tensile capacity

$$V_{s_req} := \min \left(V_s, \frac{V_{u_critical}}{\phi_{ps_shear}} \right) = 234.149 \text{ kip}$$

The right side of *LRFD BDS* Equation 5.7.3.5-1 yields:

$$\frac{\text{abs}(M_{u_critical})}{d_v \cdot \phi_{ps_shear}} + \frac{0.5 \cdot N_u}{\phi_{ps_shear}} + \left(\text{abs} \left(\frac{V_{u_critical}}{\phi_{ps_shear}} - V_p \right) - 0.5 V_{s_req} \right) \cdot \cot(\theta_{sim}) = 663.44 \text{ kip}$$

Transfer Length:

LRFD Design 5.9.4.3.1

$\ell_t = 60$ strand diameters

$$\ell_t := 60 \cdot d_b = 36 \text{ in}$$

5.9.4.3.2—Bonded Strand

Pretensioning strand shall be bonded beyond the section required to develop f_{ps} for a development length, ℓ_d , in in., where ℓ_d shall satisfy:

$$\ell_d \geq \kappa \left(f_{ps} - \frac{2}{3} f_{pe} \right) d_b \quad (5.9.4.3.2-1)$$

$\kappa = 1.6$ for pretensioned members with a depth greater than 24.0 in.

$$\ell_d := 1.6 \cdot \left(\frac{f_{ps} - \frac{2}{3} f_e}{\text{ksi}} \right) \cdot d_b = 139.18 \text{ in}$$

- From the point where bonding commences to the end of transfer length:

$$f_{px} = \frac{f_{pe} \ell_{px}}{60d_b} \quad (5.9.4.3.2-2)$$

- From the end of the transfer length and to the end of the development of the strand:

$$f_{px} = f_{pe} + \frac{\ell_{px} - 60d_b}{(\ell_d - 60d_b)} (f_{ps} - f_{pe}) \quad (5.9.4.3.2-3)$$

where:

f_{px} = design stress in pretensioned strand at nominal flexural strength at section of member under consideration (ksi)

ℓ_{px} = distance from free end of pretensioned strand to section of member under consideration (in.)

$$l_{px} := d_v = 37.166 \text{ in}$$

$$f_{px} := f_e + \left(\frac{l_{px} - 60 d_b}{l_d - 60 \cdot d_b} \right) \cdot (f_{ps} - f_e) = 172.904 \text{ ksi}$$

Since the transfer length is 36 in. from the end of the beam, the available prestress from the 6 harped strands is a fraction of the effective prestress, f_{px} , in these strands. The 6 harped strands contribute to the tensile capacity since they are on the flexural tension side of the member.

The left side of *LRFD BDS* Equation 5.7.3.5-1 yields:

$$A_{ps_harped} \cdot f_{px} = 225.121 \text{ kip}$$

$$\text{check} := \text{if} \left(\begin{array}{l} A_{ps_harped} \cdot f_{px} \downarrow > \frac{\text{abs}(M_{u_critical})}{d_v \cdot \phi_{ps_shear}} + \frac{0.5 \cdot N_u \downarrow}{\phi_{ps_shear}} \quad , \text{“Y”}, \text{“N”} \\ + A_s \cdot f_y \quad + \left(\text{abs} \left(\frac{V_{u_critical}}{\phi_{ps_shear}} - V_p \right) - 0.5 V_{s_req} \right) \cdot \cot(\theta_{sim}) \end{array} \right) = \text{“Y”}$$

Note: For this first critical location, the longitudinal reinforcement check is good.

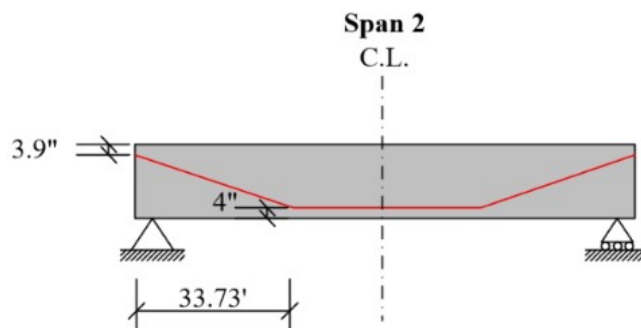
9. Compute Nominal Shear Resistance at Vertical Shear Reinforcement Change

Note: As an example of a calculation, this rating example provided the shear rating at the vertical shear spacing changing from 4" to 8" location (18.33' to the centerline of the left interior support). The procedure for checking shear at other locations would generally be similar to that for checking shear at the 18.33' to the centerline of the left interior support. The procedure for checking other shear locations would generally be similar to that for checking shear at the 18.33' to the interior support end in this example.

$$x_1 := 18.83 \text{ ft}$$



Vertical		Horizontal				
Span: 2		Copy span to...				
Name	Extends into deck	Start distance (ft)	Number of spaces	Spacing (in)	Length (ft)	End distance (ft)
D28	<input checked="" type="checkbox"/>	0.00	17	2.0000	2.83	2.83
D18	<input checked="" type="checkbox"/>	2.83	48	4.0000	16.00	18.83
D18	<input checked="" type="checkbox"/>	18.83	7	8.0000	4.67	23.50
D18	<input checked="" type="checkbox"/>	23.50	18	12.0000	18.00	41.50
D18	<input checked="" type="checkbox"/>	41.50	1	16.0000	1.33	42.83
D18	<input checked="" type="checkbox"/>	42.83	18	12.0000	18.00	60.83
D18	<input checked="" type="checkbox"/>	60.83	7	8.0000	4.67	65.50
D18	<input checked="" type="checkbox"/>	65.50	48	4.0000	16.00	81.50
D28	<input checked="" type="checkbox"/>	81.50	16	2.0000	2.67	84.17



Harped strands distance to the bottom of beam

$$d_{harped_x1} := (h_{nc} - d_{harped_top}) - \frac{(h_{nc} - d_{harped_top}) - (d_{harped_bot})}{33.73 \text{ ft}} \cdot x_1 = 16.148 \text{ in}$$

The distance between the center of gravity of the strands and the bottom of beam at this location is:

$$y_{bar_x1} := \frac{\frac{d_{harp_x1}}{in} \cdot 6 + 2 \cdot 16 + 4 \cdot 16}{38} \cdot in = 5.076 \text{ in}$$

The corresponding effective depth from the extreme compression fiber to the centroid of the tensile force in the tensile reinforcement (d_{e_x1})

$$d_{e_x1} := h_c - y_{bar_x1} = 38.824 \text{ in}$$

Effective shear depth d_{v_x1} $d_{v_x1} := \max\left(d_{e_x1} - \frac{a}{2}, 0.9 \cdot d_{e_x1}, 0.72 \cdot h_c\right) = 36.439 \text{ in}$

Compute maximum shear at shear reinforcement change

Since the beam projection is 6", the distance from this shear reinforcement spacing change location to the bearing centerline is determined.

$$x_{1_centerline} := x_1 - 6 \text{ in} = 18.33 \text{ ft}$$

Calculated shear at the 18.33 ft from the bearing centerline.

Total distributed shear (including g_{v2} and IM = 0.33 for HL-93 truck)

$$V_{distributed_critical_x1} := 86.4 \text{ kip}$$

DC shears (DC1 + DC2)

$$V_{nc_critical_x1} := 45.6 \text{ kip}$$

$$V_{c_critical_x1} := 3.55 \text{ kip}$$

$$V_{DC_critical_x1} := V_{nc_critical_x1} + V_{c_critical_x1} = 49.15 \text{ kip}$$

DW shears (DW)

$$V_{DW_critical_x1} := 0 \text{ kip}$$

Shear reinforcement spacings, s_{shear_x1}

$$s_{shear_x1} := 8 \text{ in}$$

$$A_{v_x1} := 0.0316 \cdot (1.0) \cdot \sqrt{\frac{f'_c}{ksi}} \cdot ksi \cdot \frac{b_v \cdot s_{shear_x1}}{f_{y_shear}} = 0.064 \text{ in}^2$$

Area provided for the critical section

$$A_{provided_x1} := 1.8 \cdot 0.20 \text{ in}^2 = 0.36 \text{ in}^2$$

$$check_min_transverse_reinforcement_x := \text{if}(A_{provided_x1} > A_{v_x1}, \text{"OK"}, \text{"NG"}) = \text{"OK"}$$

Simplified approach

The nominal shear determined by *LRFD BDS* Equation 5.7.3.3-2 $V_{n_equ_1_x1} := 0.25 \cdot f'_c \cdot b_v \cdot d_{v_x1} + V_p = 501.516 \text{ kip}$

Concrete shear strength $V_{c_x1} := 0.0316 \beta_{sim} \cdot (1.0) \cdot \sqrt{\frac{f'_c}{ksi}} \cdot ksi \cdot b_v \cdot d_{v_x1} = 41.021 \text{ kip}$

Steel shear strength $V_{s_x1} := \frac{A_{provided_x1} \cdot f_{y_shear} \cdot d_{v_x1} \cdot \cot(\theta_{sim})}{s_{shear_x1}} = 114.784 \text{ kip}$

The nominal shear determined by *LRFD BDS* Equation 5.7.3.3-1 $V_{n_equ_2_x1} := V_{c_x1} + V_{s_x1} + V_p = 170.516 \text{ kip}$

The nominal shear determined by *LRFD BDS* Equation 5.7.3.3 $V_{n_simp_x1} := \min(V_{n_equ_1_x1}, V_{n_equ_2_x1}) = 170.516 \text{ kip}$

Factored shear resistance $\phi_{ps_shear} \cdot V_{n_simp_x1} = 153.464 \text{ kip}$

Maximum shear at this section (HL-93 inventory loading)

$$V_{u_x1} := 1.25 \cdot V_{DC_critical_x1} + 1.5 \cdot V_{DW_critical_x1} + 1.75 \cdot V_{distributed_critical_x1} = 212.638 \text{ kip}$$

$$check_shear_at_the_critical_x := \text{if}(\phi_{ps_shear} \cdot V_{n_simp_x1} > V_{u_x1}, \text{"OK"}, \text{"NG"}) = \text{"NG"}$$

Note: The simplified approach is not good. Therefore, the general MCFT method is checked.

Try MCFT General approach (LRFD BDS 5.7.3.4.2)

Shear stress on the concrete
$$v := \frac{V_{u,x1} - \phi_{ps_shear} \cdot V_p}{\phi_{ps_shear} \cdot b_v \cdot d_{v,x1}} = 1.024 \text{ ksi}$$

$$\text{check_using_APPENDIXB5} := \text{if} \left(\frac{v}{f'_c} < 0.25, \text{"OK"}, \text{"NG"} \right) = \text{"OK"}$$

The check for shear stress on the concrete illustrates that the *LRFD BDS* Appendix B5 can be used to determine resistance. However, Appendix B5 is not used in this example. Instead, this example uses *LRFD BDS* 5.7.3.4.2, the general MCFT approach to determine shear resistance.

Calculated moment at 18.33 ft to the support centerline.

Total distributed moment (including g_{m2} and IM = 0.33 for HL-93 truck)

$$M_{distributed_critical_x1} := 495.5 \text{ kip} \cdot \text{ft}$$

DC moments (DC1 + DC2)
$$M_{nc_critical_x1} := 1086.5 \text{ kip} \cdot \text{ft} \quad M_{c_critical_x1} := 15.1 \text{ kip} \cdot \text{ft}$$

$$M_{DC_critical_x1} := M_{nc_critical_x1} + M_{c_critical_x1} = 1101.6 \text{ kip} \cdot \text{ft}$$

DW moment (DW)
$$M_{DW_critical_x1} := 0 \text{ kip} \cdot \text{ft}$$

Maximum moment at this section (HL-93 inventory loading)

$$M_{u_critical_x1} := 1.25 \cdot M_{DC_critical_x1} + 1.5 \cdot M_{DW_critical_x1} \downarrow = 2244.125 \text{ kip} \cdot \text{ft} + 1.75 \cdot M_{distributed_critical_x1}$$

Note: Total A_{ps} was used to calculate ϵ_s because the distance between the center of gravity of the strands and the bottom of the beam is on the tension side.

$$\epsilon_s := \frac{\left(\frac{\text{abs}(M_{u_critical_x1})}{d_{v,x1}} + 0.5 N_u + \text{abs}(V_{u,x1} - V_p) - A_{ps} \cdot f_{po} \right)}{E_s \cdot A_s + E_p \cdot A_{ps}} = -7.418 \cdot 10^{-4}$$

Note: ϵ_s is less than zero. Use $\epsilon_s = 0$

$$\epsilon_s := 0$$

Assume the section contains at least the minimum amount of transverse reinforcement:

$$\beta_{equ} := \frac{4.8}{(1 + 750 \cdot \epsilon_s)} = 4.8$$

Angle of diagonal compressive stresses is:

$$\theta_{equ} := (29 + 3500 \cdot \epsilon_s) \text{ deg} = 0.506$$

Concrete shear strength $V_{c_MCFT_x1} := 0.0316 \beta_{equ} \cdot (1.0) \cdot \sqrt{\frac{f'_c}{ksi}} \cdot ksi \cdot b_v \cdot d_{v_x1} = 98.452 \text{ kip}$

Steel shear strength $V_{s_MCFT_x1} := \frac{A_{provided_x1} \cdot f_{y_shear} \cdot d_{v_x1} \cdot \cot(\theta_{equ})}{s_{shear_x1}} = 207.075 \text{ kip}$

The nominal shear determined by $V_{n_MCFT_x1} := V_{c_MCFT_x1} + V_{s_MCFT_x1} + V_p = 320.237 \text{ kip}$
LRFD BDS Equation 5.7.3.3-1

The nominal shear determined by $V_{n_MCFT_x1} := \min(V_{n_equ_1_x1}, V_{n_MCFT_x1}) = 320.237 \text{ kip}$
LRFD BDS Equation 5.7.3.3

Factored shear resistance $\phi_{ps_shear} \cdot V_{n_MCFT_x1} = 288.213 \text{ kip}$

$$check_shear_MCFT := \text{if}(\phi_{ps_shear} \cdot V_{n_MCFT_x1} > V_{u_x1}, \text{“OK”}, \text{“NG”}) = \text{“OK”}$$

Demand/capacity ratio $DCR_{x1} := \frac{V_{u_x1}}{\phi_{ps_shear} \cdot V_{n_MCFT_x1}} = 0.738$

Check the longitudinal reinforcement requirement

Calculate minimum required tensile capacity

$$V_{s_req_x1} := \min \left(V_{s_MCFT_x1}, \frac{V_{u_x1}}{\phi_{ps_shear}} \right) = 207.075 \text{ kip}$$

The right side of *LRFD BDS* Equation 5.7.3.5-1 yields:

$$\frac{\text{abs}(M_{u_critical_x1})}{d_{v_x1} \cdot \phi_{ps_shear}} + \frac{0.5 \cdot N_u}{\phi_{ps_shear}} + \left(\text{abs} \left(\frac{V_{u_x1}}{\phi_{ps_shear}} - V_p \right) - 0.5 V_{s_req_x1} \right) \cdot \cot(\theta_{equ}) = 1034.045 \text{ kip}$$

$$l_d := 1.6 \cdot \left(\frac{f_{ps} - \frac{2}{3} f_e}{ksi} \right) \cdot d_b = 139.18 \text{ in} \quad l_{px} := d_{v_x1} = 36.439 \text{ in}$$

$$f_{px} := f_e + \left(\frac{l_{px} - 60 d_b}{l_d - 60 d_b} \right) \cdot (f_{ps} - f_e) = 172.286 \text{ ksi}$$

Since the transfer length is 36 in. from the end of the beam, the available prestress from the 38 strands is a fraction of the effective prestress, f_{px} , in these strands. The center of gravity of 6 harped strands to the bottom of girder is smaller than half the height of the composite girder, so they do contribute to the tensile capacity.

The left side of *LRFD BDS* Equation 5.7.3.5-1 yields:

$$Af_x := A_{ps} \cdot f_{px} = 1420.669 \text{ kip}$$

$$\text{Check} := \text{if} \left(Af_x > \frac{\text{abs}(M_{u_critical_x1})}{d_{v_x1} \cdot \phi_{ps_shear}} + \frac{0.5 \cdot N_u}{\phi_{ps_shear}} + \left(\text{abs} \left(\frac{V_{u_x1}}{\phi_{ps_shear}} - V_p \right) - 0.5 V_{s_req_x1} \right) \cdot \cot(\theta_{equ}) \right), \text{“OK”}, \text{“NG”} = \text{“OK”}$$

The longitudinal reinforcement check for this section is good.

10. Load Effects and Resistance Summary

Here is the summary for load effects and bridge resistances.

Load Effects Summary

Load effects (M(kip-ft), and V(kip))	HL-93 Design Loading (with $IM = 0.33$ and multiple lanes GDF)	DNC	DC	Four-truck Platoons (5-ft NRL) (with $IM = 0.33$ and single lane GDF removed MPF = 1.2)
Moment (at 0.5L of the interior span)	1034.0	1637.5	127.6	647.6
Moment (at interior supports)	-1006.1	0.0	-74.7	-870.6
Moment (at 3.93 ft)	-729.7	234.4	-51.3	-613.8
Moment (at 18.33 ft)	495.5	1086.5	15.1	281.6
Shear (at 3.93 ft)	111.6	72.8	5.7	92.2
Shear (at 18.33 ft)	86.4	45.6	3.6	62.4

Resistance Summary

	Resistance (with ϕ) (M (kip-ft) and V (kip))
Moment (at 0.5L of the interior span)	6841.8
Moment (at interior supports)	-3477.1
Shear (at 3.93 ft) (MCFT Approach)	416.2
Shear (at 18.33 ft) (MCFT Approach)	288.2

11. Load Rating: Design Load Rating for Moment and Shear

$$RF = \frac{(\phi_c)(\phi_s)(\phi)R_n - (\gamma_{DC})(DC) - (\gamma_{DW})(DW)}{(\gamma_L)(LL + IM)}$$

A3.13.2.1a—Inventory Level

Load	Load Factor
DC	1.25
DW	1.50 Overlay thickness was not field measured.
LL	1.75

Moment load rating at the 0.5L of the mid span

Parameter information for the equation below.

$$M_n = 6841.803 \text{ kip} \cdot \text{ft}$$

$$g_{m2_mid} = 0.82$$

$$M_{DC1_mid} = 1637.5 \text{ kip} \cdot \text{ft}$$

$$M_{DC2_mid} = 127.6 \text{ kip} \cdot \text{ft}$$

$$M_{DW_mid} = 0 \text{ kip} \cdot \text{ft}$$

Distributed HL-93 moment
(including $IM = 0.33$ for truck and g_{m2_mid})

$$HL_93_M_{dist_mid} = 1034 \text{ kip} \cdot \text{ft}$$

Inventory level rating factor

$$RF_{inv} := \frac{(1.0) \cdot M_n - (1.25 \cdot (M_{DC1_mid} + M_{DC2_mid}) + 1.50 \cdot M_{DW_mid})}{1.75 \cdot (HL_93_M_{dist_mid})} = 2.562$$

For Strength I Operating Level only the live load factor changes; therefore the rating factor can be calculated by direct proportions.

Load	Load Factor, γ
DC	1.25
DW	1.50
LL	1.35

Operating level rating factor

$$RF_{ope} := RF_{inv} \cdot \frac{1.75}{1.35} = 3.321$$

Moment load rating at the interior supports

Parameter information for the equation below.

$$M_{n_inter} = -3863.454 \text{ kip} \cdot \text{ft}$$

$$g_{m2_inter} = 0.887$$

$$M_{DC1_inter} = 0 \text{ kip} \cdot \text{ft}$$

$$M_{DC2_inter} = -74.7 \text{ kip} \cdot \text{ft}$$

$$M_{DW_inter} = 0 \text{ kip} \cdot \text{ft}$$

Distributed HL-93 moment
(including $IM=0.33$ for truck and g_{m2_inter})

$$HL_93_M_{dist_inter} = -1006.1 \text{ kip} \cdot \text{ft}$$

Inventory level rating factor

$$RF_{inv} := \frac{(0.9) \cdot \text{abs}(M_{n_inter}) - \text{abs}(1.25 \cdot (M_{DC1_inter} + M_{DC2_inter}) + 1.50 \cdot M_{DW_inter})}{1.75 \cdot \text{abs}(HL_93_M_{dist_inter})} = 1.922$$

For Strength I Operating Level only the live load factor changes; therefore the rating factor can be calculated by direct proportions.

Load	Load Factor, γ
DC	1.25
DW	1.50
LL	1.35

Operating level rating factor

$$RF_{ope} := RF_{inv} \cdot \frac{1.75}{1.35} = 2.491$$

The shear rating factors for Design Load Rating are calculated for illustration purposes only. In-service concrete bridges that show no visible signs of shear distress need not be checked for shear during design load or legal load ratings.

6A.5.8

Shear load rating at first critical location (3.93 ft to the centerline of the support)

Parameter information for the equation below.

$$V_{n_MCFT} = 462.489 \text{ kip}$$

$$g_{v2} = 1.018$$

$$V_{nc_critical} = 72.8 \text{ kip}$$

$$V_{c_critical} = 5.7 \text{ kip}$$

$$V_{DW_critical} = 0 \text{ kip}$$

Distributed HL-93 shear
(including $IM = 0.33$ for truck and g_{v2})

$$V_{distributed_critical} = 111.6 \text{ kip}$$

Inventory level rating factor

$$RF_V := \frac{(0.9) \cdot V_{n_MCFT} - (1.25 \cdot (V_{nc_critical} + V_{c_critical}) + 1.50 \cdot V_{DW_critical})}{1.75 \cdot (V_{distributed_critical})} = 1.629$$

Operating level rating factor

$$RF_{ope} := RF_V \cdot \frac{1.75}{1.35} = 2.111$$

Shear load rating at location (18.33 ft to the centerline of the support)

Parameter information for the equation below.

$$V_{n_MCFT_x1} = 320.237 \text{ kip}$$

$$g_{v2} = 1.018$$

$$V_{nc_critical_x1} = 45.6 \text{ kip}$$

$$V_{c_critical_x1} = 3.55 \text{ kip}$$

$$V_{DW_critical_x1} = 0 \text{ kip}$$

Distributed HL-93 shear
(including $IM = 0.33$ for truck and g_{v2})

$$V_{distributed_critical_x1} = 86.4 \text{ kip}$$

Inventory level rating factor

$$RF_{Vx} := \frac{(0.9) \cdot V_{n_MCFT_x1} - (1.25 \cdot (V_{nc_critical_x1} + V_{c_critical_x1}) + 1.50 \cdot V_{DW_critical_x1})}{1.75 \cdot (V_{distributed_critical_x1})} = 1.5$$

Operating level rating factor

$$RF_{ope} := RF_{Vx} \cdot \frac{1.75}{1.35} = 1.944$$

12. Load Rating for Service III Limit State (Inventory Level)

$$RF = \frac{f_R - (\gamma_D)(f_D)}{(\gamma_L)(f_{LL+IM})}$$

Flexural Resistance $f_R = f_{pb} + \text{Allowable tensile stress}$

f_{pb} = Compressive stress due to effective prestress

= 2.550 ksi (from Article A3.7.1.3 of this example)

Allowable tensile stress, ksi

$$f_t := 0.19 \cdot \sqrt{\frac{f'_c}{\text{ksi}}} \cdot \text{ksi} = 0.57 \text{ ksi}$$

Resistance stress

$$f_R := f_{pb} + f_t = 5.441 \text{ ksi}$$

Determine dead load stress at 0.5L of midspan

$$f_{DC} := \frac{\langle M_{DC1_mid} \rangle}{S_{bot_nc}} + \frac{\langle M_{DC2_mid} \rangle}{S_{bot_c}} = 3.017 \text{ ksi}$$

Determine wearing dead load stress at 0.5L of mid span

$$f_{DW} := \frac{\langle M_{DW_mid} \rangle}{S_{bot_c}} = 0 \text{ ksi}$$

Total dead load stress at 0.5L of midspan

$$f_D := f_{DC} + f_{DW} = 3.017 \text{ ksi}$$

Live load stress at 0.5L of midspan

$$f_{LL} := \frac{\langle HL_{93} M_{dist_mid} \rangle}{S_{bot_c}} = 1.15 \text{ ksi}$$

Rating factor for Service III
(Post-1.0-Gains)

$$RF_{ServiceIIIinv} := \frac{f_R - f_D}{1.0 \cdot f_{LL}} = 2.108$$

13. Load Rating for Strength I Limit State Platoon (target beta = 2.5)

4-truck Platoons (NRL with 5 ft headways): single lane platoon mixed with traffic, $CoV = 0.20$ (100 crossings, ADTT = 5000)

Moment load rating at the 0.5L of the interior span

Proposed Strength Calibrated LL Factors for the Target $\beta = 2.5$ (Steelman et al., 2021) (Table 2)

Truck Platoon	Frequency	Loading Condition	DF	ADTT (One direction)	Live load factors by CoV of total live load				
					$CoV_{LL} = 0$	$CoV_{LL} = 0.05$	$CoV_{LL} = 0.1$	$CoV_{LL} = 0.15$	$CoV_{LL} = 0.2$
Multiple Trucks in Platoon	Single-trip	No other vehicles on the bridge	One lane	NA	1.00	1.05	1.10	1.20	1.25
	Single-trip	Two identical platoons loaded on two lanes	Two or more lanes	NA	1.00	1.05	1.10	1.20	1.25
	10 Crossings	Mixed with routine traffic in the adjacent lane	One lane	> 5000	1.35	1.35	1.40	1.45	1.55
				1000	1.35	1.35	1.40	1.45	1.50
				< 100	1.35	1.35	1.40	1.45	1.50
	100 Crossings	Mixed with routine traffic in the adjacent lane	One lane	> 5000	1.35	1.40	1.45	1.50	1.60
				1000	1.35	1.40	1.45	1.45	1.55
				< 100	1.35	1.35	1.45	1.45	1.55

Platoon weight divided by 80 kips
(amplification factor alpha)

$$W_{platoon} := 1.0$$

Assumed IM = 0.33 (same as MBE permit load rating)

$$IM_{surface} := 33\%$$

5 ft headway 4-truck platoon moment at the 0.5L of the interior span from the above load effect table: ($IM = 0.33$ and single lane moment GDF (g_{m1_mid}) and removed 1.2 multiple presence factor)

$$LL_{platoon} := 647.6 \text{ kip} \cdot \text{ft}$$

5 ft headway 4-truck platoon moment at the 0.5L of the interior span (with amplification factor alpha)

$$LL_{platoon_dis} := W_{platoon} \cdot LL_{platoon} = 647.6 \text{ kip} \cdot \text{ft}$$

Platoon calibrated live load factor (the value in the red box as shown above Table)

$$\gamma_{platoon_strength} := 1.60$$

Parameter information for the equation below.

$$M_n = 6841.803 \text{ kip} \cdot \text{ft}$$

$$M_{DC2_mid} = 127.6 \text{ kip} \cdot \text{ft}$$

$$M_{DC1_mid} = 1637.5 \text{ kip} \cdot \text{ft}$$

$$M_{DW_mid} = 0 \text{ kip} \cdot \text{ft}$$

Rating Factor

$$RF_{Platoon_flexure} := \frac{(1.0) \cdot M_n - (1.25 \cdot (M_{DC1_mid} + M_{DC2_mid}) + 1.50 \cdot M_{DW_mid})}{\gamma_{platoon_strength} \cdot (LL_{platoon_dis})} = 4.474$$

Moment load rating at the interior supports

5 ft headway 4-truck platoon moment at the interior support from the above load effect table: (with $IM = 0.33$ and single lane moment GDF (g_{m1_inter}) and removed 1.2 multiple presence factor)

$$LL_{platoon_inter} := -870.6 \text{ kip} \cdot \text{ft}$$

5 ft headway 4-truck platoon moment at the interior support (with amplification factor alpha)

$$LL_{platoon_inter_dis} := W_{platoon} \cdot LL_{platoon_inter} = -870.6 \text{ kip} \cdot \text{ft}$$

Parameter information for the equation below.

$$M_{n_inter} = -3863.454 \text{ kip} \cdot \text{ft}$$

$$M_{DC2_inter} = -74.7 \text{ kip} \cdot \text{ft}$$

$$M_{DC1_inter} = 0 \text{ kip} \cdot \text{ft}$$

$$M_{DW_inter} = 0 \text{ kip} \cdot \text{ft}$$

Rating Factor

$$RF_{Pl_i} := \frac{(0.9) \cdot \text{abs}(M_{n_inter}) - \text{abs}(1.25 \cdot (M_{DC1_inter} + M_{DC2_inter}) + 1.50 \cdot M_{DW_inter})}{\gamma_{platoon_strength} \cdot \text{abs}(LL_{platoon_inter_dis})} = 2.429$$

Shear Rating for 4-truck Platoons (NRL with 5 ft headways): single lane platoon mixed with traffic, $CoV = 0.20$ (100 crossings, ADTT = 5000)

Shear resistance taken from HL-93. Acceptable and conservative as long as M_u and V_u for HL-93 are both $\geq M_u$ and V_u for permit. Must be recalculated if permit values are greater.

Shear load rating at first critical location (3.93 ft to the centerline of the support)

Parameter information for the equation below.

$$V_{n_MCFT} = 462.489 \text{ kip}$$

$$g_{v1} = 0.8$$

$$V_{nc_critical} = 72.8 \text{ kip}$$

$$V_{c_critical} = 5.7 \text{ kip}$$

$$V_{DW_critical} = 0 \text{ kip}$$

5 ft headway 4-truck platoon shear at 3.93 ft to the interior support from the above load effect table: (with $IM = 0.33$ and single lane shear GDF (g_{v1}) and removed 1.2 multiple presence factor)

$$V_{critical_platoon} := 92.2 \text{ kip}$$

5 ft headway 4-truck platoon shear at 3.93 ft to the interior support (with amplification factor alpha)

$$V_{critical_platoon_dis} := W_{platoon} \cdot V_{critical_platoon} = 92.2 \text{ kip}$$

Rating Factor

$$RF_V := \frac{(0.9) \cdot (V_{n_MCFT}) - (1.25 \cdot (V_{nc_critical} + V_{c_critical}) + 1.50 \cdot (V_{DW_critical}))}{\gamma_{platoon_strength} \cdot (V_{critical_platoon_dis})} = 2.156$$

Shear load rating at the location (18.33 ft to the centerline of the support)

Parameter information for the equation below.

$$V_{n_MCFT_x1} = 320.237 \text{ kip}$$

$$g_{v1} = 0.8$$

$$V_{nc_critical_x1} = 45.6 \text{ kip}$$

$$V_{c_critical_x1} = 3.55 \text{ kip}$$

$$V_{DW_critical_x1} = 0 \text{ kip}$$

5 ft headway 4-truck platoon shear at 18.33 ft to the end from the above load effect table:
(with $IM = 0.33$ and single lane shear GDF (g_{v1}) and removed 1.2 multiple presence factor)

$$V_{critical_platoon_x1} := 62.4 \text{ kip}$$

5 ft headway 4-truck platoon shear at 18.33 ft to the end (with amplification factor alpha)

$$V_{critical_platoon_dis_x1} := W_{platoon} \cdot V_{critical_platoon_x1} = 62.4 \text{ kip}$$

Rating Factor

$$RF_{Vx} := \frac{(0.9) \cdot V_{n_MCFT_x1} - (1.25 \cdot (V_{nc_critical_x1} + V_{c_critical_x1}) + 1.50 \cdot V_{DW_critical_x1})}{\gamma_{platoon_strength} \cdot (V_{critical_platoon_dis_x1})} = 2.271$$

14. Load Rating for Service III Limit State Platoon (target beta = -0.60)

4-truck Platoons (NRL with 5 ft headways): single lane platoon mixed with traffic, $CoV = 0.20$ (100 crossings, ADTT = 5000)

Proposed Service III Calibrated LL Factors for the Target $\beta = -0.6$ (Table 21)

Truck platoon	Frequency	Load conditions	DF	ADTT (one direction)	Load factors by CoV of total live load
					$CoV_{LL} = 0 - 0.20$
Multiple trucks in platoon	single-trip	No other vehicles on the bridge	One lane	N/A	0.85
	single-trip	Two identical platoons loaded on two lanes	Two or more lanes	N/A	0.85
	100 Crossings	Mixed with routine traffic in the adjacent lane	One lane	> 5000	1.55

Platoon calibrated live load factor (the value in the red box as shown above Table)

$$\gamma_{platoon_service} := 1.55$$

Live load stress due to 5 ft headway 4-truck platoon at the 0.5L of the interior span (with amplification factor alpha)

$$f_{platoon} := \frac{LL_{platoon_dis}}{S_{bot_c}} = 0.72 \text{ ksi}$$

Parameter information for the equation below.

$$f_R = 5.441 \text{ ksi}$$

$$f_D = 3.017 \text{ ksi}$$

$$S_{bot_c} = 10791.645 \text{ in}^3$$

Rating factor for Service III

$$RF_{ServiceIIIplatoon} := \frac{f_R - f_D}{\gamma_{platoon_service} \cdot f_{platoon}} = 2.171$$

15. Load Rating for Service I Limit State Platoon

A3.13.4.2—Service I Limit State (Optional) (6A.5.4.2.2b)

$$\gamma_L = \gamma_{DC} = \gamma_{DW} = 1.0$$

For concrete members with standard designs and closely clustered tension reinforcement, the Engineer may, as an alternate to limiting the steel stress, choose to limit unfactored moments to 75 percent of nominal flexural capacity. Where computations are performed in terms of

5 ft headway 4-truck platoon moment at the 0.5L of the interior span (with $IM = 0.33$ and multiple lanes moment GDF (g_{m2}))

$$LL_{platoon_m} := \frac{LL_{platoon}}{\frac{g_{m1_mid}}{1.20}} \cdot g_{m2_mid} = 1127.935 \text{ kip} \cdot \text{ft}$$

5 ft headway 4-truck platoon moment at the mid span (with amplification factor alpha)

$$LL_{platoon_dis_m} := W_{platoon} \cdot LL_{platoon_m} = 1127.935 \text{ kip} \cdot \text{ft}$$

Parameter information for the equation below.

$$M_n = 6841.803 \text{ kip} \cdot \text{ft} \quad M_{DC2_mid} = 127.6 \text{ kip} \cdot \text{ft} \quad M_{DC1_mid} = 1637.5 \text{ kip} \cdot \text{ft}$$

$$M_{DW_mid} = 0 \text{ kip} \cdot \text{ft}$$

75% of moment resistance

$$M_{n75} := 0.75 \cdot M_n = 5131.352 \text{ kip} \cdot \text{ft}$$

Moment ratio

$$M_{ratio} := \frac{M_{n75}}{M_{DC1_mid} + M_{DC2_mid} + M_{DW_mid} + LL_{platoon_dis_m}} = 1.774$$

16. Load Rating Summary

Load rating summary table is given below.

Limit state	Design load rating		Platoon load rating (Strength I $\beta_{target} = 2.5$ and Service III $\beta_{target} = -0.6$)
	Inventory	Operating	
Strength I for Design and platoon load rating			
Flexure (at the 0.5L of the interior span)	2.562	3.321	4.474
Flexure (at interior supports)	1.922	2.491	2.429
Shear at (3.93 ft to the centerline of interior supports at the interior span side)	1.629	2.111	2.156
Shear at (18.33 ft to the centerline of interior supports at the interior span side)	1.500	1.944	2.271
Service III			
Flexure (at midspan)	2.108		2.171
Service I			
Flexure (at midspan)			Stress ratio = 1.774

Appendix E

This appendix contains detailed calculations related to the example steel simple-span bridge described in Section 8.4.

Appendix E. LRFR Load Rating Example of a 100' Simple-span Welded Plate Girder Bridge (interior girder)

Note: Bridge S080 00526 is a 100-ft simple-span, steel welded plate girder bridge at the I-80 3W Bushnell Interchange in Bushnell, Nebraska, constructed in 1970 (Figure 51). Bridge has two design lanes (HS20) and average daily traffic of 8,115. The bridge was later widened by replacing existing girders and adding a new girder. The original girders were 36 ksi steel, whereas the new girder is ASTM (2021) A709-50W.

The bridge's load factor rating is LFR. However, the LRFR rating method was used here. Steelman et al. (2021) indicate that rating factors for LRFR and LFR differ due to LL components, GDF, impact factors, and resistance effects. A calibrated LFR method that accounts for the bias of LFR GDFs relative to LRFR GDFs for different limit states is needed in future research (Steeleman et al., 2021). It is beyond this project's scope to thoroughly calibrate the LL factors for LFR.

The example below illustrates an interior steel girder's design and platoon ratings at the interior span (0.5L) for positive moment and at the beam end supports for shear. Rating factors for the Strength I and Service II limit states were provided for HL-93 design and platoon loads. Fatigue I and Fatigue II for the AASHTO fatigue truck and platoons with 5- or 50-ft headways were considered to evaluate the welded cross-frame connection plate at a typical cross-frame location.

The fatigue damage ratios for a single crossing of a four-truck platoon with a 5- or 50-ft headway and an AASHTO fatigue truck were determined. This rating example also considered Fatigue I and Fatigue II for shear studs at the beam end, based on AASHTO fatigue truck and platoons with a 5-ft headway.

1. Bridge Data

Span length	$L := 100 \text{ ft}$			
Year built	1970			
Material	Steel yield stress (homogenous section)			
$F_y := 36 \text{ ksi}$	$F_{yc} := 36 \text{ ksi}$	$F_{yf} := 36 \text{ ksi}$	$F_{yt} := 36 \text{ ksi}$	$F_{yw} := 36 \text{ ksi}$

F_y : girder yield stress, F_{yc} : compression flange yield stress, F_{yf} : flange yield stress, F_{yt} : tension flange yield stress, and F_{yw} is the web yield stress

Other information

1. Skew: 0 degrees.
2. ADT: 8115.

Concrete information

Unit weight of concrete for determining dead loads

$$w_c := 155 \text{ pcf}$$

Unit weight of concrete for determining deck modulus of elasticity

$$w_{cd_modulus} := 155 \text{ pcf}$$

Unit weight of concrete for determining girder modulus of elasticity

$$w_{cg_modulus} := 150 \text{ pcf}$$

Ultimate strength for deck

$$f'_{cd} := 4 \text{ ksi}$$

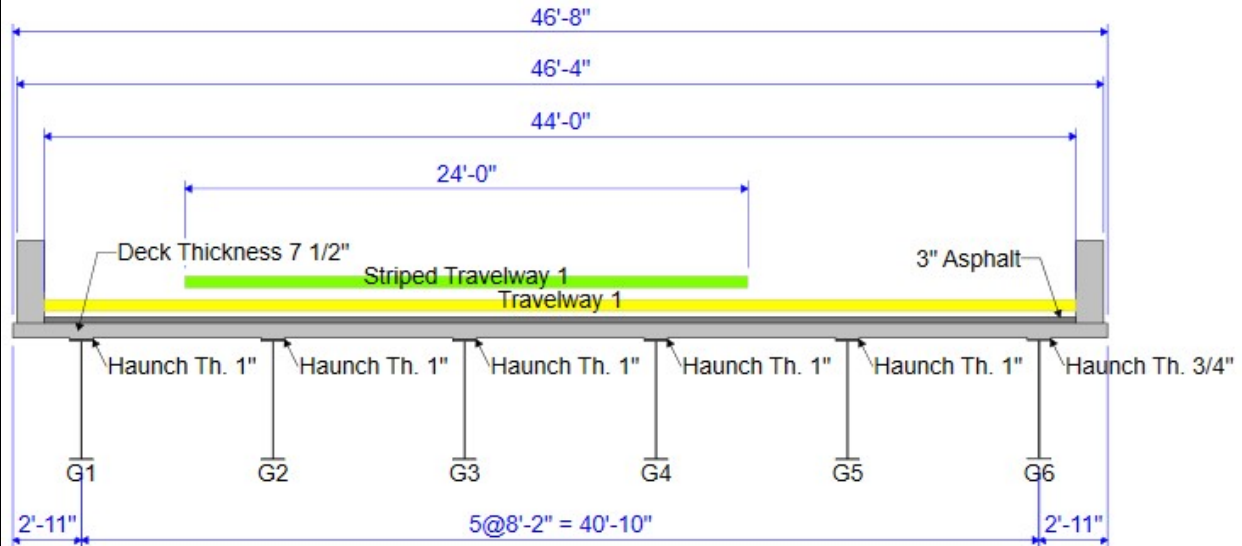
$$E_c = 33,000 K_1 w_c^{1.5} \sqrt{f'_c} \quad (\text{C5.4.2.4-2})$$

Modulus of elasticity of deck at final time

$$E_{cd} := 33000 \cdot \left(\frac{w_{cd_modulus}}{\text{pcf} \cdot 1000} \right)^{1.5} \cdot \left(\frac{f'_{cd}}{\text{ksi}} \right)^{0.5} \cdot \text{ksi} = 4027.56 \text{ ksi}$$

2. Bridge Cross Section

S080 00526L
 100.0 ft simple span welded PL girder - 2018 Including Rehab
 I80 / Stream
 3/4/2023



Steel modulus of elasticity

$$E := 29000 \text{ ksi}$$

Girder spacing (S)

$$S := 98 \text{ in} = 8.167 \text{ ft}$$

Number of girders

$$N_{girder} := 6$$

Overhang

$$overhang := 35 \text{ in} = 2.917 \text{ ft}$$

Total bridge width

$$W_{bridge} := (overhang \cdot 2 + S \cdot (N_{girder} - 1)) = 560 \text{ in}$$

b_{eff} for deck (for interior girders)

$$b_{eff_int} := S = 98 \text{ in}$$

Thickness of deck (loads calculations)

$$t_s := 7.5 \text{ in}$$

Thickness of deck (effective)

$$h_d := 7.0 \text{ in}$$

Haunch thickness (shown in the BrR analysis)

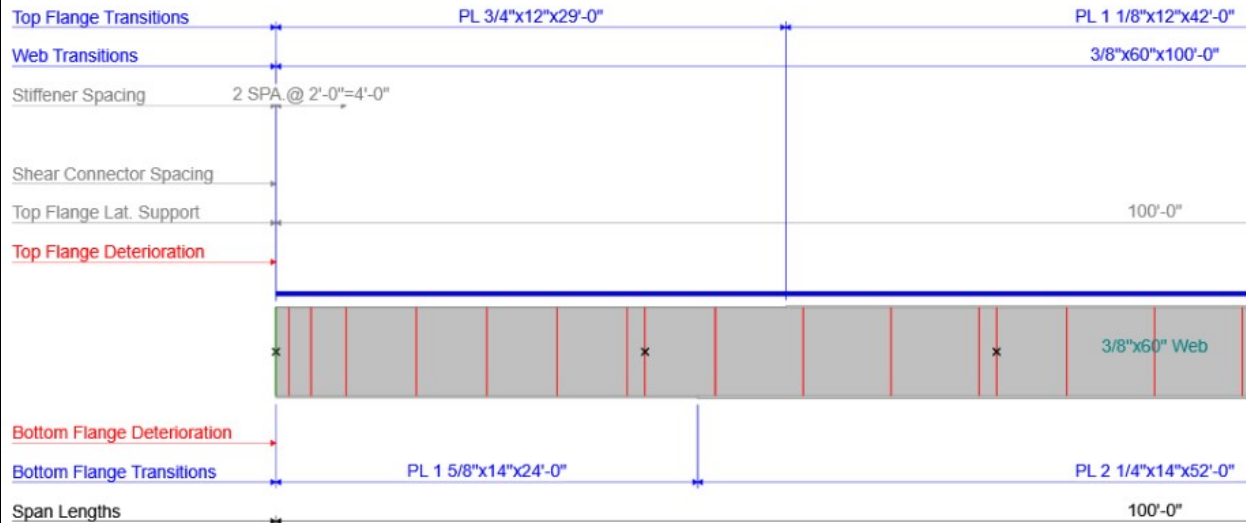
$$h_h := 1 \text{ in}$$

Modulus of ratio for the steel to deck

$$n := \frac{E}{E_{cd}} = 7.2$$

3. Girder Section

S080 00526L
 100.0 ft simple span welded PL girder - 2018 Including Rehab - G2
 I80 / Stream
 3/4/2023



Girder dimensions at the mid span

Web thickness	$t_w := \frac{3}{8} \text{ in} = 0.375 \text{ in}$
Top flange width	$b_{tf} := 12 \text{ in}$
Bottom flange width	$b_{bf} := 14 \text{ in}$
Compression flange (top flange) thickness	$t_{tf} := 1.125 \text{ in}$
Tension flange (bottom flange) thickness	$t_{bf} := 2.25 \text{ in}$
Web Depth	$D := 60 \text{ in}$
Total height of the composite section	$D_t := t_{tf} + D + t_{bf} + h_h + t_s = 71.875 \text{ in}$
Total height of the non-composite section	$D_{girder} := t_{tf} + D + t_{bf} = 63.375 \text{ in}$

Section property calculations

Top flange section area	$A_{tf} := b_{tf} \cdot t_{tf} = 13.5 \text{ in}^2$
Web section area	$A_{web} := t_w \cdot D = 22.5 \text{ in}^2$
Bot flange section area	$A_{bf} := b_{bf} \cdot t_{bf} = 31.5 \text{ in}^2$
Girder section area	$A_{girder} := A_{tf} + A_{web} + A_{bf} = 67.5 \text{ in}^2$
Top flange center to the datum	$y_{tf} := t_{bf} + D + \frac{t_{tf}}{2} = 62.813 \text{ in}$
Web center to the datum	$y_{web} := t_{bf} + \frac{D}{2} = 32.25 \text{ in}$
Bot flange center to the datum	$y_{bf} := \frac{t_{bf}}{2} = 1.125 \text{ in}$
Ay for the tension flange	$A_{y_{tf}} := A_{tf} \cdot y_{tf} = 847.969 \text{ in}^3$
Ay for the web	$A_{y_{web}} := A_{web} \cdot y_{web} = 725.625 \text{ in}^3$
Ay for the bottom flange	$A_{y_{bf}} := A_{bf} \cdot y_{bf} = 35.438 \text{ in}^3$
Ay for the girder	$A_{y_{girder}} := A_{y_{tf}} + A_{y_{web}} + A_{y_{bf}} = 1609.031 \text{ in}^3$
centroid y_b to the datum	$y_{girder_b} := \frac{A_{y_{girder}}}{A_{girder}} = 23.838 \text{ in}$
Moment of inertia for the top flange	$I_{o_{tf}} := \frac{b_{tf} \cdot t_{tf}^3}{12} = 1.42 \text{ in}^4$
Moment of inertia for the web	$I_{o_{web}} := \frac{t_w \cdot D^3}{12} = 6750 \text{ in}^4$
Moment of inertia for the bottom flange	$I_{o_{bf}} := \frac{b_{bf} \cdot t_{bf}^3}{12} = 13.29 \text{ in}^4$
Moment of inertia (girder only)	
	$I_{girder} := I_{o_{tf}} + A_{tf} \cdot (y_{tf} - y_{girder_b})^2 + I_{o_{bf}} + A_{bf} \cdot (y_{bf} - y_{girder_b})^2 + I_{o_{web}} + A_{web} \cdot (y_{web} - y_{girder_b})^2 = 45113.74 \text{ in}^4$

Short term section properties (n)

Area of slab $A_{slab_st} := \frac{b_{eff_int} \cdot t_s}{n} = 102.078 \text{ in}^2$

Center of slab to the datum $y_{slab} := D_{girder} + h_h + \frac{t_s}{2} = 68.125 \text{ in}$

Moment of inertia for the slab (short term) $I_{o_slab_st} := \frac{\frac{b_{eff_int}}{n} \cdot t_s^3}{12} = 478.49 \text{ in}^4$

A_y for the slab (short term) $A_{y_slab_st} := A_{slab_st} \cdot y_{slab} = 6954.042 \text{ in}^3$

centroid y_{b_st} to the datum $y_{b_st} := \frac{A_{y_girder} + A_{y_slab_st}}{A_{girder} + A_{slab_st}} = 50.496 \text{ in}$

Moment of inertia (short term)

$$I_{st} := I_{girder} + A_{girder} \cdot (y_{girder_b} - y_{b_st})^2 + I_{o_slab_st} + A_{slab_st} \cdot (y_{slab} - y_{b_st})^2 = 125286.71 \text{ in}^4$$

Long term section properties (3n)

Area of slab $A_{slab_lt} := \frac{b_{eff_int} \cdot t_s}{3 n} = 34.026 \text{ in}^2$

Moment of inertia for the slab (long term) $I_{o_slab_lt} := \frac{\frac{b_{eff_int}}{3 n} \cdot t_s^3}{12} = 159.5 \text{ in}^4$

A_y for the slab (long term) $A_{y_slab_lt} := A_{slab_lt} \cdot y_{slab} = 2318.014 \text{ in}^3$

centroid y_{b_lt} to the datum $y_{b_lt} := \frac{A_{y_girder} + A_{y_slab_lt}}{A_{girder} + A_{slab_lt}} = 38.68 \text{ in}$

Moment of inertia (long term)

$$I_{lt} := I_{girder} + A_{girder} \cdot (y_{girder_b} - y_{b_lt})^2 + I_{o_slab_lt} + A_{slab_lt} \cdot (y_{slab} - y_{b_lt})^2 = 89644.2 \text{ in}^4$$

Summary of section properties

Section modulus for the bottom of the girder (Steel only) $S_{bx} := \frac{I_{girder}}{y_{girder_b}} = 1892.553 \text{ in}^3$

Section modulus for the top of the girder (Steel only) $S_{tx} := \frac{I_{girder}}{D_{girder} - y_{girder_b}} = 1141.037 \text{ in}^3$

Section modulus for the bottom of the girder (short term) $S_{b_st} := \frac{I_{st}}{y_{b_st}} = 2481.099 \text{ in}^3$

Section modulus for the top of the girder (short term) $S_{t_st} := \frac{I_{st}}{D_{girder} - y_{b_st}} = 9728.335 \text{ in}^3$

Section modulus for the bottom of the girder (long term) $S_{b_lt} := \frac{I_{lt}}{y_{b_lt}} = 2317.571 \text{ in}^3$

Section modulus for the top of the girder (long term) $S_{t_lt} := \frac{I_{lt}}{D_{girder} - y_{b_lt}} = 3630.089 \text{ in}^3$

Dead load moment and shear calculations

Unfactored DC1 moment at the mid span $M_{dc1} := 1324.6 \text{ kip} \cdot \text{ft}$

Unfactored DC2 moment at the mid span $M_{dc2} := 268.8 \text{ kip} \cdot \text{ft}$

Unfactored DW moment at the mid span $M_{dw} := 332.3 \text{ kip} \cdot \text{ft}$

Unfactored DC1 shear at the beam end $V_{dc1} := 52.2 \text{ kip}$

Unfactored DC2 shear at the beam end $V_{dc2} := 10.8 \text{ kip}$

Unfactored DW shear at the beam end $V_{dw} := 13.3 \text{ kip}$

Live load demand calculation (GDF and HL-93 nominal loadings)

Modular ratio for AASHTO GDFs $n_{GDF} := \frac{E}{E_{cd}} = 7.20039821$

e_g term for AASHTO GDF equations $e_{g_GDF} := D_{girder} - y_{girder_b} + h_h + \frac{h_d}{2} = 44.0375 \text{ in}$

K_g term for AASHTO GDF equations $K_g := n_{GDF} \cdot (I_{girder} + A_{girder} \cdot e_{g_GDF}^2) = 1267390 \text{ in}^4$

Distribution Factors

One Design Lane Loaded:

$$0.06 + \left(\frac{S}{14}\right)^{0.4} \left(\frac{S}{L}\right)^{0.3} \left(\frac{K_g}{12.0 L t_s^3}\right)^{0.1}$$

Two or More Design Lanes Loaded:

$$0.075 + \left(\frac{S}{9.5}\right)^{0.6} \left(\frac{S}{L}\right)^{0.2} \left(\frac{K_g}{12.0 L t_s^3}\right)^{0.1}$$

Single lane AASHTO moment GDF for interior girders

$$g_{m1} := 0.06 + \left(\frac{S}{14 \text{ ft}}\right)^{0.4} \cdot \left(\frac{S}{L}\right)^{0.3} \cdot \left(\frac{\frac{K_g}{\text{in}^4}}{\left(12 \cdot \frac{L}{\text{ft}} \cdot \left(\frac{h_d}{\text{in}}\right)^3\right)}\right)^{0.1} = 0.485$$

Multiple lanes AASHTO moment GDF for interior girders

$$g_{m2} := 0.075 + \left(\frac{S}{9.5}\right)^{0.6} \cdot \left(\frac{S}{L}\right)^{0.2} \cdot \left(\frac{\frac{K_g}{\text{in}^4}}{\left(12 \cdot \frac{L}{\text{ft}} \cdot \left(\frac{h_d}{\text{in}}\right)^3\right)}\right)^{0.1} = 0.694$$

Single lane AASHTO shear GDF for interior girders $g_{v1} := 0.36 + \frac{S}{25 \text{ ft}} = 0.687$

Multiple lanes AASHTO shear GDF
for interior girders

$$g_{v2} := 0.20 + \frac{S}{12 \text{ ft}} - \left(\frac{S}{35 \text{ ft}} \right)^2 = 0.826$$

HL-93 loading moment with multiple lanes
GDF and IM = 0.33 at the mid span

$$HL_{93}M_{dist} := 1958.8 \text{ kip} \cdot \text{ft}$$

HL-93 loading shear with multiple lanes
GDF and IM = 0.33 at the beam end

$$HL_{93}V_{dist} := 98.2 \text{ kip}$$

4. Article 6.10.2 Proportional Limits Check

Web check (6.10.2.1.1-1)

$$check := \text{if} \left(\frac{D}{t_w} \leq 150, \text{"OK"}, \text{"No"} \right) = \text{"No"}$$

Bottom Flange check (6.10.2.2-1)

$$check := \text{if} \left(\frac{b_{bf}}{2 t_{bf}} \leq 12, \text{"OK"}, \text{"No"} \right) = \text{"OK"}$$

Top Flange check (6.10.2.2-1)

$$check := \text{if} \left(\frac{b_{tf}}{2 t_{tf}} \leq 12, \text{"OK"}, \text{"No"} \right) = \text{"OK"}$$

Bottom Flange check (6.10.2.2-2)

$$check := \text{if} \left(b_{bf} \geq \frac{D}{6}, \text{"OK"}, \text{"No"} \right) = \text{"OK"}$$

Top Flange check (6.10.2.2-2)

$$check := \text{if} \left(b_{tf} \geq \frac{D}{6}, \text{"OK"}, \text{"No"} \right) = \text{"OK"}$$

Bottom Flange check (6.10.2.2-3)

$$check := \text{if} (t_{bf} \geq 1.1 \cdot t_w, \text{"OK"}, \text{"No"}) = \text{"OK"}$$

Top Flange check (6.10.2.2-3)

$$check := \text{if} (t_{tf} \geq 1.1 \cdot t_w, \text{"OK"}, \text{"No"}) = \text{"OK"}$$

Moment of inertia of the compression flange about the vehicle axis (6.10.2.2-4)

$$I_{yc} := \frac{t_{tf} \cdot b_{tf}^3}{12} = 162 \text{ in}^4$$

Moment of inertia of the tension flange about the vehicle axis (6.10.2.2-4)

$$I_{yt} := \frac{t_{bf} \cdot b_{bf}^3}{12} = 514.5 \text{ in}^4$$

Flange check (6.10.2.2-4)

$$check := \text{if} \left(0.1 \leq \frac{I_{yc}}{I_{yt}} \leq 10, \text{"OK"}, \text{"No"} \right) = \text{"OK"}$$

Note: For this case, D/t_w is 160. Therefore, the webs without longitudinal stiffeners failed the check in 6.10.2.1.1. That is because the bridge was not designed by LRFD.

5. Service II Checks (LRFBD BDS Article 6.10.4.2.2)

Note: This design checks the Service II limit state first and the Strength I limit state will be checked later. For the bottom of the steel flange, the lateral flange stress (f_l) is ignored.

Hybrid factor R_h $R_h := 1.0$

Lateral flange stress (assume to be 0) $f_l := 0$

Flange stress upper limit for the Service II $f_{ServiceII} := 0.95 \cdot R_h \cdot F_{yf} = 34.2 \text{ ksi}$

Check the top steel flange stress due to the Service II loads (6.10.4.2.1)

For the top steel flange of composite sections:

$$f_f \leq 0.95 R_h F_{yf} \quad (6.10.4.2.2-1)$$

Top flange stress due to Service II loads without the consideration of lateral flange bending (ksi) (Service II load factors) (Compression)

$$f_{tf} := \frac{1.0 M_{dc1}}{S_{tx}} + \frac{1.0 (M_{dc2} + M_{dw})}{S_{t_{lt}}} + \frac{1.3 HL_{93} M_{dist}}{S_{t_{st}}} = 19.059 \text{ ksi}$$

$$check := \text{if}(f_{tf} \leq f_{ServiceII}, \text{"OK"}, \text{"No"}) = \text{"OK"}$$

Check the bottom steel flange stress due to the Service II loads (6.10.4.2.1)

For the bottom steel flange of composite sections:

$$f_f + \frac{f_\ell}{2} \leq 0.95R_h F_{yf} \quad (6.10.4.2.2-2)$$

Bottom flange stress due to Service II loads without the consideration of lateral flange bending (ksi) (Service II load factors) (Tension)

$$f_{bf} := \frac{1.0 M_{dc1}}{S_{bx}} + \frac{1.0 (M_{dc2} + M_{dw})}{S_{b_{lt}}} + \frac{1.3 HL_{93} M_{dist}}{S_{b_{st}}} = 23.83 \text{ ksi}$$

$$\text{check} := \text{if } (f_{bf} \leq f_{ServiceII}, \text{“OK”}, \text{“No”}) = \text{“OK”}$$

Note: Since the web does not meet the requirement of Article 6.10.2.1.1, the compression flange stress should also satisfy LRFD BDS Equation 6.10.4.2.2-4.

$$f_c \leq F_{crw} \quad (6.10.4.2.2-4)$$

where:

f_c = compression flange stress at the section under consideration due to the Service II loads calculated without consideration of flange lateral bending (ksi)

F_{crw} = nominal bend-buckling resistance for webs with or without longitudinal stiffeners, as applicable, determined as specified in [Article 6.10.1.9](#) (ksi)

The nominal bend-buckling resistance shall be taken as:

$$F_{crw} = \frac{0.9Ek}{\left(\frac{D}{t_w}\right)^2} \quad (6.10.1.9.1-1)$$

but not to exceed the smaller of $R_h F_{yc}$ and $F_{yw}/0.7$

in which:

k = bend-buckling coefficient

$$= \frac{9}{(D_c / D)^2} \quad (6.10.1.9.1-2)$$

D6.3.1—In the Elastic Range (D_c)

For composite sections in positive flexure, the depth of the web in compression in the elastic range, D_c , shall be the depth over which the algebraic sum of the factored stresses in the steel, long-term composite and short-term composite sections from the dead and live loads, plus impact, is compressive.

In lieu of computing D_c at sections in positive flexure from stress diagrams, the following equation may be used:

$$D_c = \left(\frac{-f_c}{|f_c| + f_t} \right) d - t_{fc} \geq 0 \quad (\text{D6.3.1-1})$$

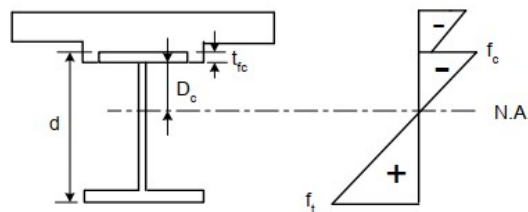


Figure D6.3.1-1—Computation of D_c at Sections in Positive Flexure

Depth of web in compression
(top flange in compression)

$$D_c := \left(\frac{f_{tf}}{f_{tf} + f_{bf}} \right) \cdot D_{girder} - t_{tf} = 27.039 \text{ in}$$

Bend-buckling coefficient

$$k := \frac{9}{\left(\frac{D_c}{D} \right)^2} = 44.316$$

Nominal bend-buckling resistance for webs
(LRFD BDS Equation 6.10.1.9.1-2)

$$F_{crw_equ} := \frac{0.9 \cdot E \cdot k}{\left(\frac{D}{t_w} \right)^2} = 45.182 \text{ ksi}$$

Nominal bend-buckling resistance for webs

$$F_{crw} := \min \left(F_{crw_equ}, R_h \cdot F_{yc}, \frac{F_{yw}}{0.7} \right) = 36 \text{ ksi}$$

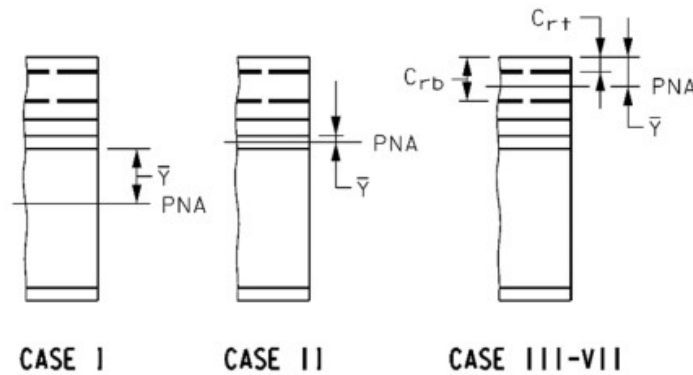
$$\text{check} := \text{if } (f_{tf} \leq F_{crw}, \text{“OK”}, \text{“No”}) = \text{“OK”}$$

6. Moment Strength I Checks (LRFD BDS Article 6.10.7)

First, use LRFD BDS Table D6.1-1 to determine the M_p for this positive bending case. The reinforcements are not considered. Therefore, only three cases of PNA are considered in the slab, top flange, and web.

Table D6.1-1—Calculation of \bar{Y} and M_p for Sections in Positive Flexure

Case	PNA	Condition	\bar{Y} and M_p
I	In Web	$P_t + P_w \geq P_c + P_s + P_{rb} + P_r$	$\bar{Y} = \left(\frac{D}{2}\right) \left[\frac{P_t - P_c - P_s - P_r - P_{rb}}{P_w} + 1 \right]$ $M_p = \frac{P_w}{2D} \left[\bar{Y}^2 + (D - \bar{Y})^2 \right] + [P_t d_t + P_r d_r + P_{rb} d_{rb} + P_c d_c + P_s d_s]$
II	In Top Flange	$P_t + P_w + P_c \geq P_s + P_{rb} + P_r$	$\bar{Y} = \left(\frac{t_c}{2}\right) \left[\frac{P_w + P_t - P_s - P_r - P_{rb}}{P_c} + 1 \right]$ $M_p = \frac{P_c}{2t_c} \left[\bar{Y}^2 + (t_c - \bar{Y})^2 \right] + [P_t d_t + P_r d_r + P_{rb} d_{rb} + P_w d_w + P_s d_s]$
III	Concrete Deck, Below P_{rb}	$P_t + P_w + P_c \geq \left(\frac{c_{rb}}{t_s}\right) P_s + P_{rb} + P_r$	$\bar{Y} = (t_s) \left[\frac{P_c + P_w + P_t - P_r - P_{rb}}{P_s} \right]$ $M_p = \left(\frac{\bar{Y}^2 P_s}{2t_s}\right) + [P_r d_r + P_{rb} d_{rb} + P_c d_c + P_w d_w + P_t d_t]$



Compression flange thickness used in equations

$$t_c := t_{tf}$$

Tension flange thickness used in equations

$$t_t := t_{bf}$$

Plastic force in the web used to compute M_p

$$P_w := F_{yw} \cdot D \cdot t_w = 810 \text{ kip}$$

Plastic force in the compression flange used to compute M_p

$$P_c := F_{yc} \cdot b_{tf} \cdot t_{tf} = 486 \text{ kip}$$

Plastic force in the tension flange used to compute M_p

$$P_t := F_{yt} \cdot b_{bf} \cdot t_{bf} = 1134 \text{ kip}$$

Plastic force in the concrete deck used to compute M_p

$$P_s := 0.85 \cdot f'_{cd} \cdot b_{eff_int} \cdot t_s = 2499 \text{ kip}$$

Check the PNA is in the web, top flange or concrete deck

$$Case := \begin{cases} \text{if } P_t + P_w \geq P_c + P_s \\ \quad \text{return 1} \\ \text{also if } P_t + P_w + P_c \geq P_s \\ \quad \text{return 2} \\ \text{else} \\ \quad 3 \end{cases} = 3$$

Note: Case 1 for PNA in the web, Case 2 for PNA in the top flange, and Case 3 for PNA in the concrete deck.

Y_{bar} in the above figure for the specific case

$$Y_{bar} := \begin{cases} \text{if } Case = 1 \\ \quad \left(\frac{D}{2} \cdot \left(\frac{(P_t - P_c - P_s)}{P_w} + 1 \right) \right) \\ \text{also if } Case = 2 \\ \quad \left(\frac{t_c}{2} \cdot \left(\frac{(P_w + P_t - P_s)}{P_c} + 1 \right) \right) \\ \text{else} \\ \quad t_s \cdot \frac{(P_c + P_w + P_t)}{P_s} \end{cases} = 7.293 \text{ in}$$

d_t is the distance from PNA to the center of the tension flange

$$d_t := \begin{cases} \text{if } Case = 1 \\ \quad \left(\frac{t_t}{2} + D - Y_{bar} \right) \\ \text{also if } Case = 2 \\ \quad \left(\frac{t_t}{2} + D + t_c - Y_{bar} \right) \\ \text{else} \\ \quad t_s + h_h + t_t + D + \frac{t_c}{2} - Y_{bar} \end{cases} = 64.02 \text{ in}$$

d_c is the distance from PNA to the center of the compression flange

$$d_c := \begin{cases} \text{if } Case = 1 & \\ \left\| Y_{bar} + \frac{t_c}{2} \right\| & \\ \text{also if } Case = 2 & \\ \left\| 0 \text{ in} \right\| & \\ \text{else} & \\ \left\| t_s + h_h + \frac{t_c}{2} - Y_{bar} \right\| & \end{cases} = 1.77 \text{ in}$$

d_w is the distance from PNA to the center of the web

$$d_w := \begin{cases} \text{if } Case = 1 & \\ \left\| 0 \text{ in} \right\| & \\ \text{also if } Case = 2 & \\ \left\| \frac{D}{2} + t_c - Y_{bar} \right\| & \\ \text{else} & \\ \left\| t_s + h_h + t_c + \frac{D}{2} - Y_{bar} \right\| & \end{cases} = 32.332 \text{ in}$$

d_s is the distance from PNA to the center of the concrete slab

$$d_s := \begin{cases} \text{if } Case = 1 & \\ \left\| \frac{t_s}{2} + h_h + t_c + Y_{bar} \right\| & \\ \text{also if } Case = 2 & \\ \left\| \frac{t_s}{2} + h_h + Y_{bar} \right\| & \\ \text{else} & \\ \left\| 0 \text{ in} \right\| & \end{cases} = 0 \text{ in}$$

D_p is the distance from PNA to the top of the concrete slab

$$D_p := \begin{cases} \text{if } Case = 1 & \\ \quad \left\| \begin{array}{l} t_s + h_h + t_c + Y_{bar} \\ \text{also if } Case = 2 \\ \quad \left\| \begin{array}{l} t_s + h_h + Y_{bar} \\ \text{else} \\ \quad \left\| Y_{bar} \end{array} \right. \end{array} \right. & \end{cases} = 7.293 \text{ in}$$

D_{cp} is the distance of the web in the compression according to the PNA

$$D_{cp} := \begin{cases} \text{if } Case = 1 & \\ \quad \left\| \begin{array}{l} Y_{bar} \\ \text{also if } Case = 2 \\ \quad \left\| \begin{array}{l} 0 \text{ in} \\ \text{else} \\ \quad \left\| 0 \text{ in} \end{array} \right. \end{array} \right. & \end{cases} = 0 \text{ in}$$

M_p is the plastic moment

$$M_p := \begin{cases} \text{if } Case = 1 & \\ \quad \left\| \begin{array}{l} \frac{P_w}{2 D} (Y_{bar}^2 + (D - Y_{bar})^2) + (P_s \cdot d_s + P_c \cdot d_c + P_t \cdot d_t) \\ \text{also if } Case = 2 \\ \quad \left\| \begin{array}{l} \frac{P_w}{2 t_c} (Y_{bar}^2 + (t_c - Y_{bar})^2) + (P_s \cdot d_s + P_w \cdot d_w + P_t \cdot d_t) \\ \text{else} \\ \quad \left\| \begin{array}{l} \frac{Y_{bar}^2 P_s}{2 t_s} + (P_c \cdot d_c + P_w \cdot d_w + P_t \cdot d_t) \end{array} \right. \end{array} \right. & \end{cases} = 9042.342 \text{ kip} \cdot \text{ft}$$

Calculate the yield moment M_y of the composite section using the equations provided in *LRFD BDS* Appendix D6 (Article D6.2.2). Essentially, M_y is taken as the sum of the factored moments at the strength limit state applied separately to the steel, long-term, and short-term composite sections to cause first yield in either steel flange. Flange lateral bending is to be disregarded in the calculation. The Strength I load factors are used here.

Symbolically, the procedure is:

- 1) Solve for M_{AD} from the equation:

$$F_y = \frac{M_{D1}}{S_{NC}} + \frac{M_{D2}}{S_{LT}} + \frac{M_{AD}}{S_{ST}} \quad (\text{D6.2.2-1})$$

- 2) Then calculate:

$$M_y = M_{D1} + M_{D2} + M_{AD} \quad (\text{D6.2.2-2})$$

M_{D1} , M_{D2} , and M_{AD} are the factored moments at the strength limit state applied separately to the steel, long-term, and short-term composite sections. M_y is taken as the value calculated for the tension (bottom) flange (control for simple-span positive moment case).

$$M_{D1} := 1.25 M_{dc1} = 1655.75 \text{ kip} \cdot \text{ft}$$

$$M_{D2} := 1.25 M_{dc2} + 1.50 M_{dw} = 834.45 \text{ kip} \cdot \text{ft}$$

$$M_{AD} := F_y \cdot S_{b_st} - \left(\frac{S_{b_st}}{S_{bx}} \right) M_{D1} - \left(\frac{S_{b_st}}{S_{b_lt}} \right) M_{D2} = 4379.313 \text{ kip} \cdot \text{ft}$$

$$M_y := M_{D1} + M_{D2} + M_{AD} = 6869.513 \text{ kip} \cdot \text{ft}$$

Nominal Flexural Resistance

First, check if the section is compact or non-compact (*LFRD BDS* Article 6.10.6.2.2). Note that the section is 36 ksi but the web fails *LFRD BDS* Article 6.10.2.1.1 as mentioned above. Therefore, the section is not compact.

- The specified minimum yield strengths of the flanges do not exceed 70.0 ksi,
- The web satisfies the requirement of Article 6.10.2.1.1, and
- The section satisfies the web slenderness limit:

$$\frac{2D_{cp}}{t_w} \leq 3.76 \sqrt{\frac{E}{F_{yc}}} \quad (6.10.6.2.2-1)$$

Check ductility according to *LFRD BDS* Equation 6.10.7.3-1

Compact and noncompact sections shall satisfy:

$$D_p \leq 0.42 D_t \quad (6.10.7.3-1)$$

where:

D_p = distance from the top of the concrete deck to the neutral axis of the composite section at the plastic moment (in.)

D_t = total depth of the composite section (in.)

$$check := \text{if}(D_p \leq 0.42 D_t, \text{"OK"}, \text{"NO"}) = \text{"OK"}$$

6.10.7.2—Noncompact Sections

$$F_{nc} = R_b R_h F_{yc} \quad (6.10.7.2.2-1)$$

6.10.7.2.1—General

At the strength limit state, the compression flange shall satisfy:

$$f_{bu} \leq \phi_f F_{nc} \quad (6.10.7.2.1-1)$$

where:

ϕ_f = resistance factor for flexure specified in [Article 6.5.4.2](#)

f_{bu} = flange stress calculated without consideration of flange lateral bending determined as specified in [Article 6.10.1.6](#) (ksi)

F_{nc} = nominal flexural resistance of the compression-flange determined as specified in [Article 6.10.7.2.2](#) (ksi)

The tension flange shall satisfy:

$$f_{bt} + \frac{1}{3} f_{\ell} \leq \phi_f F_{nt} \quad (6.10.7.2.1-2)$$

where:

f_{ℓ} = flange lateral bending stress determined as specified in [Article 6.10.1.6](#) (ksi)

F_{nt} = nominal flexural resistance of the tension flange determined as specified in [Article 6.10.7.2.2](#) (ksi)

where:

R_b = web load-shedding factor determined as specified in [Article 6.10.1.10.2](#)

R_h = hybrid factor determined as specified in [Article 6.10.1.10.1](#)

The nominal flexural resistance of the tension flange shall be taken as:

$$F_{nt} = R_h F_{yt} \quad (6.10.7.2.2-2)$$

- the web satisfies:

$$\frac{2D_c}{t_w} \leq \lambda_{rw} \quad (6.10.1.10.2-1)$$

then, R_b shall be taken equal to 1.0.

Slenderness ratio for web

$$\lambda := \frac{2 \cdot D_c}{t_w} = 144.208$$

Ratio a_{wc} for the compression flange

$$a_{wc} := \frac{2 \cdot D_c \cdot t_w}{b_{bf} \cdot t_{bf}} = 0.644$$

Slenderness ratio limit for non-compact web

$$\lambda_{rw} := \max \left(4.6 \cdot \sqrt{\frac{E}{F_{yc}}}, \min \left(\left(3.1 + \frac{5}{a_{wc}} \right) \cdot \sqrt{\frac{E}{F_{yc}}}, 5.7 \cdot \sqrt{\frac{E}{F_{yc}}} \right) \right) = 161.779$$

$$\text{check} := \text{if} \left(\frac{2 \cdot D_c}{t_w} \leq \lambda_{rw}, \text{“OK”}, \text{“NO”} \right) = \text{“OK”}$$

Web load-shedding factor

$$R_b := 1$$

$$F_{nc} = R_b R_h F_{yc} \quad (6.10.7.2.2-1)$$

where:

R_b = web load-shedding factor determined as specified in [Article 6.10.1.10.2](#)

R_h = hybrid factor determined as specified in [Article 6.10.1.10.1](#)

The nominal flexural resistance of the tension flange shall be taken as:

$$F_{nt} = R_h F_{yt} \quad (6.10.7.2.2-2)$$

Nominal compression flange flexure strength $F_{nc} := R_b \cdot R_h \cdot F_{yc} = 36 \text{ ksi}$

Nominal tension flange flexure strength $F_{nt} := R_h \cdot F_{yt} = 36 \text{ ksi}$

For design checks where the flexural resistance is based on lateral-torsional buckling:

- The stress f_{bu} shall be determined as the largest value of the compressive stress throughout the unbraced length in the flange under consideration, calculated without consideration of flange lateral bending.
- The moment M_u shall be determined as the largest value of the major-axis bending moment throughout the unbraced length causing compression in the flange under consideration.

Factored moment (Strength I)

$$M_u := 1.25 \cdot (M_{dc1} + M_{dc2}) + 1.50 M_{dw} + 1.75 \cdot HL_93_M_{dist} = 5918.1 \text{ kip} \cdot \text{ft}$$

The bottom flange stress (tension)

$$f_{bot_bu} := \frac{1.25 \cdot M_{dc1}}{S_{bx}} + \frac{1.25 \cdot M_{dc2} + 1.50 M_{dw}}{S_{b_lt}} + \frac{1.75 \cdot HL_93_M_{dist}}{S_{b_st}} = 31.398 \text{ ksi}$$

$$check := \text{if} (f_{bot_bu} \leq F_{nt}, \text{"OK"}, \text{"NO"}) = \text{"OK"}$$

The top flange stress (Compression)

$$f_{top_bu} := \frac{1.25 \cdot M_{dc1}}{S_{tx}} + \frac{1.25 \cdot M_{dc2} + 1.50 M_{dw}}{S_{t_lt}} + \frac{1.75 \cdot HL_93 \cdot M_{dist}}{S_{t_st}} = 24.4 \text{ ksi}$$

$$check := \text{if} (f_{top_bu} \leq F_{nc}, \text{"OK"}, \text{"NO"}) = \text{"OK"}$$

$$F_{nc} = R_b R_h F_{yc} \quad (6.10.7.2.2-1)$$

where:

R_b = web load-shedding factor determined as specified in [Article 6.10.1.10.2](#)

R_h = hybrid factor determined as specified in [Article 6.10.1.10.1](#)

The nominal flexural resistance of the tension flange shall be taken as:

$$F_{nt} = R_h F_{yt} \quad (6.10.7.2.2-2)$$

Summary of performance ratios

Performance ratio for the top flange (Service II)

$$PR_{ServiceII_top} := \frac{f_{tf}}{f_{ServiceII}} = 0.557$$

Performance ratio for the bottom flange (Service II)

$$PR_{ServiceII_bottom} := \frac{f_{bf}}{f_{ServiceII}} = 0.697$$

Performance ratio for the top flange (Strength I)

$$PR_{StrengthI_top} := \frac{f_{top_bu}}{F_{nc}} = 0.678$$

Performance ratio for the bottom flange (Strength I)

$$PR_{StrengthI_bottom} := \frac{f_{bot_bu}}{F_{nt}} = 0.872$$

7. Shear Strength I Check at the Beam End and Maximum Stiffener Spacing Location (LRFD BDS Article 6.10.9)

6.10.9.1—General

At the strength limit state, straight and curved web panels shall satisfy:

$$V_u \leq \phi_v V_n \tag{6.10.9.1-1}$$

where:

ϕ_v = resistance factor for shear specified in [Article 6.5.4.2](#)

V_n = nominal shear resistance determined as specified in [Articles 6.10.9.2](#) and [6.10.9.3](#) for unstiffened and stiffened webs, respectively (kip)

V_u = factored shear in the web at the section under consideration (kip)

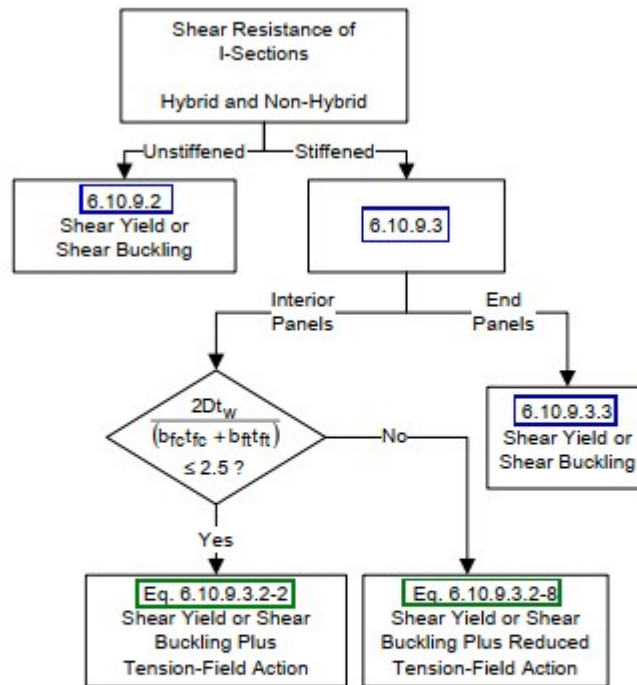


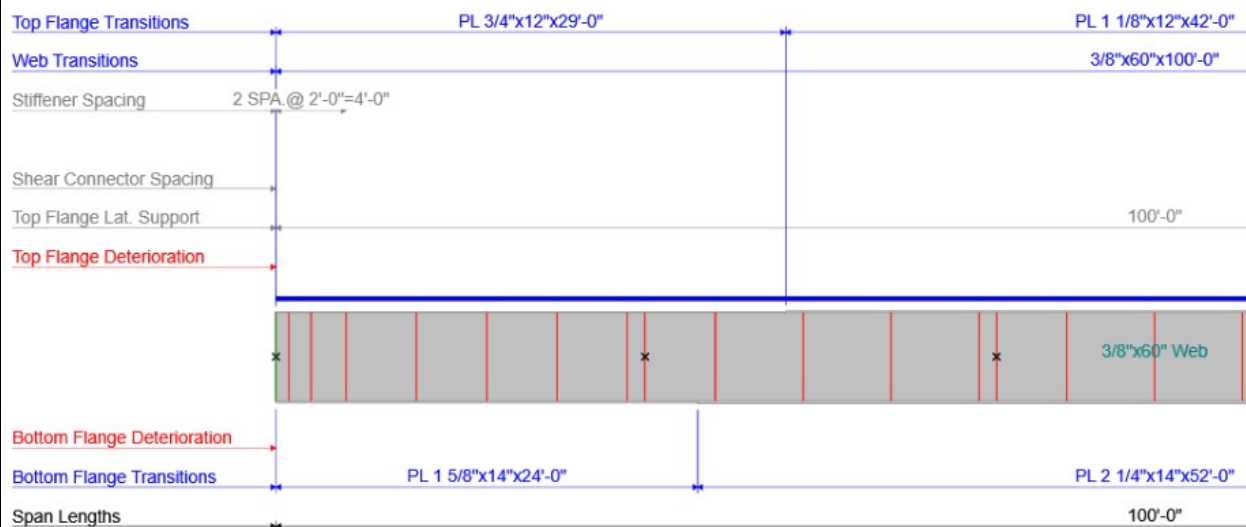
Figure C6.10.9.1-1—Flowchart for Shear Design of I-Sections

Beam end location

Web Panel: End Panel; Transversely Stiffened: Yes; Longitudinally Stiffened : No

Transverse stiffener spacing (in.) $d_o := 9 \text{ in}$

S080 00526L
 100.0 ft simple span welded PL girder - 2018 Including Rehab - G2
 I80 / Stream
 3/4/2023



Girder dimensions at the beam end

- Web thickness $t_w := \frac{3}{8} \text{ in} = 0.375 \text{ in}$
- Top flange width $b_{tf} := 12 \text{ in}$
- Bottom flange width $b_{bf} := 14 \text{ in}$
- Compression flange (top flange) thickness $t_{tf} := 0.75 \text{ in}$
- Tension flange (bottom flange) thickness $t_{bf} := 1.625 \text{ in}$
- Web Depth $D := 60 \text{ in}$

End web panels of nonhybrid and hybrid I-shaped members:

- With or without one or more longitudinal stiffeners and with a transverse stiffener spacing not exceeding $1.5D$

check := if ($d_o \leq 1.5 D$, “Stiffened”, “Unstiffened”) = “Stiffened”

6.10.9.3.3—End Panels

The nominal shear resistance of a stiffened web end panel shall be taken as:

$$V_n = V_{cr} = CV_p \quad (6.10.9.3.3-1)$$

in which:

$$V_p = 0.58 F_{yw} D t_w \quad (6.10.9.3.3-2)$$

where:

- C = ratio of the shear-buckling resistance to the shear yield strength determined by [Eqs. 6.10.9.3.2-4](#), [6.10.9.3.2-5](#), or [6.10.9.3.2-6](#) as applicable
- V_{cr} = shear-yielding or shear-buckling resistance (kip)
- V_p = plastic shear force (kip)

The ratio, C , shall be determined as specified below:

- If $\frac{D}{t_w} \leq 1.12 \sqrt{\frac{Ek}{F_{yw}}}$, then:

$$C = 1.0 \quad (6.10.9.3.2-4)$$

- If $1.12 \sqrt{\frac{Ek}{F_{yw}}} < \frac{D}{t_w} \leq 1.40 \sqrt{\frac{Ek}{F_{yw}}}$, then:

$$C = \frac{1.12}{\frac{D}{t_w}} \sqrt{\frac{Ek}{F_{yw}}} \quad (6.10.9.3.2-5)$$

- If $\frac{D}{t_w} > 1.40 \sqrt{\frac{Ek}{F_{yw}}}$, then:

$$C = \frac{1.57}{\left(\frac{D}{t_w}\right)^2} \left(\frac{Ek}{F_{yw}}\right) \quad (6.10.9.3.2-6)$$

in which:

k = shear-buckling coefficient

$$= 5 + \frac{5}{\left(\frac{d_o}{D}\right)^2} \quad (6.10.9.3.2-7)$$

Otherwise, the nominal shear resistance shall be taken as follows:

$$V_n = V_p \left[C + \frac{0.87(1-C)}{\left(\sqrt{1 + \left(\frac{d_o}{D}\right)^2} + \frac{d_o}{D}\right)} \right] \quad (6.10.9.3.2-8)$$

Shear-buckling coefficient

$$k := 5 + \frac{5}{\left(\frac{d_o}{D}\right)^2} = 227.222$$

$\frac{D}{t_w}$ ratio

$$\frac{D}{t_w} = 160$$

Ratio of the shear-buckling
resistance to the shear yield strength

$$C := \begin{cases} \frac{D}{t_w} \leq 1.12 \cdot \sqrt{\frac{E \cdot k}{F_{yw}}} & = 1 \\ 1 \\ \text{also if } 1.12 \cdot \sqrt{\frac{E \cdot k}{F_{yw}}} \leq \frac{D}{t_w} \leq 1.40 \cdot \sqrt{\frac{E \cdot k}{F_{yw}}} \\ \frac{1.12}{\frac{D}{t_w}} \cdot \sqrt{\frac{E \cdot k}{F_{yw}}} \\ \text{else} \\ \frac{1.57}{\left(\frac{D}{t_w}\right)^2} \cdot \frac{E \cdot k}{F_{yw}} \end{cases}$$

Plastic shear force

$$V_p := 0.58 \cdot F_{yw} \cdot D \cdot t_w = 469.8 \text{ kip}$$

Nominal shear resistance for the web panel

$$V_n := C \cdot V_p$$

Phi factor for steel bridge shear

$$\phi := 1.0$$

Factored shear resistance

$$\phi \cdot V_n = 469.8 \text{ kip}$$

$$V_u := 1.25 \cdot (V_{dc1} + V_{dc2}) + 1.5 \cdot V_{dw} + 1.75 \cdot HL_{93} V_{dist} = 270.55 \text{ kip}$$

$$check_shear_at_the_critical := \text{if}(\phi \cdot V_n > V_u, \text{"OK"}, \text{"NG"}) = \text{"OK"}$$

Demand/capacity ratio for shear

$$DCR := \frac{V_u}{\phi \cdot V_n} = 0.576$$

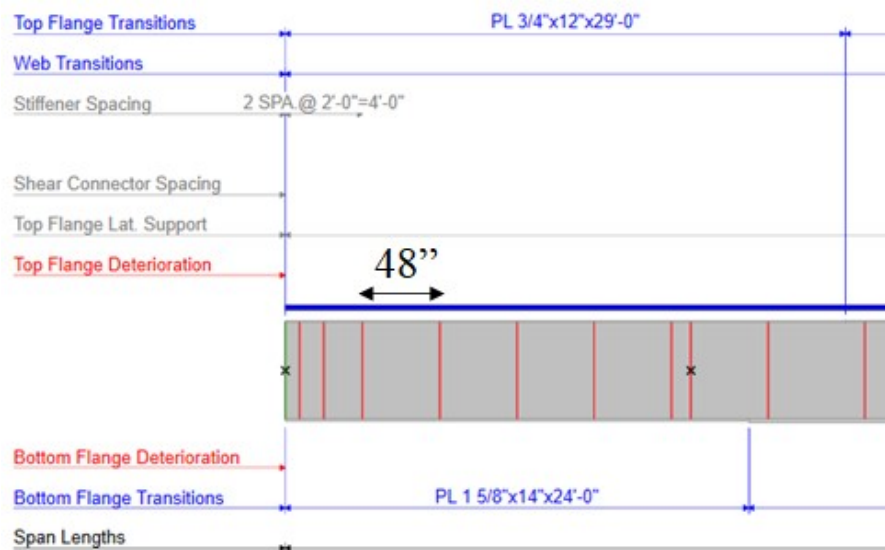
The maximum transverse stiffener spacing location

Interior web panels of nonhybrid and hybrid I-shaped members:

- without a longitudinal stiffener and with a transverse stiffener spacing not exceeding $3D$, or
- with one or more longitudinal stiffeners and with a transverse stiffener spacing not exceeding $2D$

Girder dimensions at the maximum transverse stiffener spacing location

The beam section is the same as for the above end panel shear evaluation. The maximum transverse stiffener spacing, starting at 4 ft to the end of the beam, is 48".



- Notes:
- * All flange length dimensions are horiz. (length along flange may differ).
 - * Transverse stiffener pairs shown in red.
 - * Single transverse stiffener shown in blue.
 - * Bearing stiffeners shown in green.
 - * Dimensioning starts and ends at CL bearings.
 - * X denotes cross frame locations.

Web Panel: Interior Panel; Transversely Stiffened: Yes; Longitudinally Stiffened : No

Transverse stiffener spacing (in.) $d_o := 48 \text{ in}$

$check := \text{if } (d_o \leq 3 D, \text{“Stiffened”}, \text{“Unstiffened”}) = \text{“Stiffened”}$

6.10.9.3.2—Interior Panels

The nominal shear resistance of an interior web panel complying with the provisions of Article 6.10.9.1, and with the section along the entire panel proportioned such that:

$$\frac{2Dt_w}{(b_{fc}t_{fc} + b_{ft}t_{ft})} \leq 2.5 \quad (6.10.9.3.2-1)$$

shall be taken as:

$$V_n = V_p \left[C + \frac{0.87(1-C)}{\sqrt{1 + \left(\frac{d_o}{D}\right)^2}} \right] \quad (6.10.9.3.2-2)$$

in which:

$$V_p = 0.58 F_{yw} D t_w \quad (6.10.9.3.2-3)$$

Shear-buckling coefficient

$$k := 5 + \frac{5}{\left(\frac{d_o}{D}\right)^2} = 12.813$$

$\frac{D}{t_w}$ ratio

$$\frac{D}{t_w} = 160$$

Ratio of the shear-buckling resistance to the shear yield strength

$$C := \begin{cases} \text{if } \frac{D}{t_w} \leq 1.12 \cdot \sqrt{\frac{E \cdot k}{F_{yw}}} & = 0.633 \\ \parallel 1 \\ \text{also if } 1.12 \cdot \sqrt{\frac{E \cdot k}{F_{yw}}} \leq \frac{D}{t_w} \leq 1.40 \cdot \sqrt{\frac{E \cdot k}{F_{yw}}} & \\ \parallel \frac{1.12}{\frac{D}{t_w}} \cdot \sqrt{\frac{E \cdot k}{F_{yw}}} & \\ \parallel \text{else} & \\ \parallel \frac{1.57}{\left(\frac{D}{t_w}\right)^2} \cdot \frac{E \cdot k}{F_{yw}} & \end{cases}$$

Check *LFRD BDS* Equation 6.10.9.3.2-1

$$\frac{2 D \cdot t_w}{(b_{bf} \cdot t_{bf} + b_{tf} \cdot t_{tf})} = 1.417$$

$$\text{check} := \text{if} \left(\frac{2 D \cdot t_w}{(b_{bf} \cdot t_{bf} + b_{tf} \cdot t_{tf})} \leq 2.5, \text{“OK”}, \text{“NO”} \right) = \text{“OK”}$$

Plastic shear force

$$V_{p@4ft} := 0.58 \cdot F_{yw} \cdot D \cdot t_w = 469.8 \text{ kip}$$

Nominal shear resistance for the web panel

$$V_{n@4ft} := V_{p@4ft} \cdot \left(C + \frac{0.87 \cdot (1 - C)}{\sqrt{1 + \left(\frac{d_o}{D} \right)^2}} \right) = 414.512 \text{ kip}$$

ϕ factor for steel bridge shear

$$\phi := 1.0$$

Factored shear resistance

$$\phi \cdot V_{n@4ft} = 414.512 \text{ kip}$$

Shear loads at the 4 ft to the end of the beam

$$V_{dc1@4ft} := 48.2 \text{ kip}$$

$$V_{dc2@4ft} := 9.9 \text{ kip}$$

$$V_{dw@4ft} := 12.2 \text{ kip}$$

HL-93 shear at 4 ft to the end of beam (including multiple lanes GDF for shear and IM=0.33)

$$HL_93_V_{dist@4ft} := 92.9 \text{ kip}$$

Factored shear demand at 4 ft to the end of beam

$$V_{u@4ft} := 1.25 \cdot (V_{dc1@4ft} + V_{dc2@4ft}) + 1.5 \cdot V_{dw@4ft} + 1.75 \cdot HL_93_V_{dist@4ft} = 253.5 \text{ kip}$$

$$\text{check_shear_at_the_critical} := \text{if} (\phi \cdot V_{n@4ft} > V_{u@4ft}, \text{“OK”}, \text{“NG”}) = \text{“OK”}$$

Demand/capacity ratio for shear

$$DCR := \frac{V_{u@4ft}}{\phi \cdot V_{n@4ft}} = 0.612$$

8. Load Effects and Resistance Summary

Here is the summary for load effects and bridge resistances.

Load Effects Summary

Load effects (M(kip-ft), and V(kip))	HL-93 Design Loading (with $IM = 0.33$ and GDF_m)	DNC	DC	DW
Moment (at mid)	1958.8	1324.6	268.8	332.3
Moment (at 41 ft)	1914.9	1281.7	260.0	321.5
Shear (at end)	98.2	52.2	10.8	13.3
Shear (at 4 ft)	92.9	48.2	9.9	12.2

Load effects (M(kip-ft), and V(kip))	AASHTO Fatigue Truck (with $IM = 0.15$ and $GDF_s / 1.2$)	Four-truck Platoons (5-ft NRL) (with $IM = 0.33$ and $GDF_s / 1.2$)	Four-truck Platoons (50-ft NRL) (with $IM = 0.33$ and $GDF_s / 1.2$)
Moment (at mid)	588.0	1584.4	934.0
Moment (at 41 ft)	596.4	1522.7	906.1
Shear (at end)	38.8	97.2	57.0
Shear (at 4 ft)	36.9	90.2	52.8

Resistance Summary

	Resistance (with ϕ) (F_n (ksi) and V (kip))
Strength I Flexural Stress (at mid)	36
Strength I Shear (at end)	469.8
Strength I Shear (at 4 ft)	414.5
Service II Flexural Stress (at mid)	34

Note: The bending (flexural) resistances are written in terms of stress because the section is not compact.

9. Load Rating: Design Load Rating for Moment and Shear

$$RF = \frac{(\varphi_c)(\varphi_s)(\varphi)R_n - (\gamma_{DC})(DC) - (\gamma_{DW})(DW)}{(\gamma_L)(LL + IM)}$$

A3.13.2.1a—Inventory Level

Load	Load Factor
DC	1.25
DW	1.50 Overlay thickness was not field measured.
LL	1.75

Moment load rating at the mid (inventory and operating level)

Parameter information for the equation below.

$$F_{nt} = 36 \text{ ksi}$$

$$g_{m2} = 0.694$$

$$M_{dc1} = 1324.6 \text{ kip} \cdot \text{ft}$$

$$M_{dc2} = 268.8 \text{ kip} \cdot \text{ft}$$

$$M_{dw} = 332.3 \text{ kip} \cdot \text{ft}$$

$$HL_{93}M_{dist} = 1958.8 \text{ kip} \cdot \text{ft}$$

$$S_{bx} = 1892.553 \text{ in}^3$$

$$S_{b_{st}} = 2481.099 \text{ in}^3$$

$$S_{b_{lt}} = 2317.571 \text{ in}^3$$

RF for the inventory level

$$RF_{inv} := \frac{(1.0) \cdot F_{nt} - \left(1.25 \cdot \left(\frac{M_{dc1}}{S_{bx}} + \frac{M_{dc2}}{S_{b_{lt}}} \right) + 1.50 \cdot \frac{M_{dw}}{S_{b_{lt}}} \right)}{1.75 \cdot \left(\frac{HL_{93}M_{dist}}{S_{b_{st}}} \right)} = 1.278$$

For Strength I Operating Level only the live load factor changes; therefore the rating factor can be calculated by direct proportions.

Load	Load Factor, γ
DC	1.25
DW	1.50
LL	1.35

RF for the operating level

$$RF_{ope} := RF_{inv} \cdot \frac{1.75}{1.35} = 1.656$$

Shear load rating at the beam end (inventory and operating level)

Parameter information for the equation below.

$$V_n = 469.8 \text{ kip}$$

$$g_{v2} = 0.826$$

$$V_{dc1} = 52.2 \text{ kip}$$

$$V_{dc2} = 10.8 \text{ kip}$$

$$V_{dw} = 13.3 \text{ kip}$$

$$HL_{93}V_{dist} = 98.2 \text{ kip}$$

RF for the inventory level

$$RF_{invV} := \frac{(1.0) \cdot V_n - (1.25 \cdot (V_{dc1} + V_{dc2}) + 1.50 \cdot V_{dw})}{1.75 \cdot (HL_{93}V_{dist})} = 2.159$$

RF for the operating level

$$RF_{opeV} := RF_{invV} \cdot \frac{1.75}{1.35} = 2.799$$

Shear load rating at the 4 ft from the support (inventory and operating level)

Parameter information for the equation below.

$$V_{n@4ft} = 414.512 \text{ kip}$$

$$g_{v2} = 0.826$$

$$V_{dc1@4ft} = 48.2 \text{ kip}$$

$$V_{dc2@4ft} = 9.9 \text{ kip}$$

$$V_{dw@4ft} = 12.2 \text{ kip}$$

$$HL_{93}V_{dist@4ft} = 92.9 \text{ kip}$$

RF for the inventory level

$$RF_{invV@4ft} := \frac{(1.0) \cdot V_{n@4ft} - (1.25 \cdot (V_{dc1@4ft} + V_{dc2@4ft}) + 1.50 \cdot V_{dw@4ft})}{1.75 \cdot (HL_{93}V_{dist@4ft})} = 1.99$$

RF for the operating level

$$RF_{opeV@4ft} := RF_{invV@4ft} \cdot \frac{1.75}{1.35} = 2.58$$

10. Load Rating for Service II Limit State

For Service Limit States, $C = f_R$

6A.4.2.1

$$RF = \frac{f_R - (\gamma_D)(f_D)}{(\gamma_L)(f_{LL+IM})}$$

$$\gamma_D = \gamma_{DC} = \gamma_{DW} = 1.0$$

Table 6A.4.2.2-1

$$\gamma_L = 1.3 \text{ for Inventory}$$

$$= 1.0 \text{ for Operating}$$

Resistance stress

$$f_R := 0.95 \cdot R_h \cdot F_{yf} = 34.2 \text{ ksi}$$

Determine dead load stress at midspan

$$f_{DC} := \frac{M_{dc1}}{S_{bx}} + \frac{M_{dc2}}{S_{b_{lt}}} = 9.791 \text{ ksi}$$

Determine wearing dead load stress at midspan

$$f_{DW} := \frac{M_{dw}}{S_{b_{lt}}} = 1.721 \text{ ksi}$$

Total dead load stress at midspan

$$f_D := f_{DC} + f_{DW} = 11.511 \text{ ksi}$$

Live load stress at midspan

$$f_{LL} := \frac{(HL_{93} M_{dist})}{S_{b_{st}}} = 9.474 \text{ ksi}$$

Rating factor for Service II
(inventory level)

$$RF_{ServiceIIinv} := \frac{f_R - f_D}{1.30 \cdot f_{LL}} = 1.842$$

Rating factor for Service II
(operating level)

$$RF_{ServiceIIopr} := \frac{f_R - f_D}{1.00 \cdot f_{LL}} = 2.395$$

11. Load Rating for Strength I Limit State Platoon (target beta = 2.5)

4-truck Platoons (NRL with 5 ft headways): single lane platoon mixed with traffic, $CoV = 0.20$ (100 crossings, ADTT = 5000)

Proposed Strength Calibrated LL Factors for the Target $\beta = 2.5$ (Steelman et al., 2021) (Table 2)

Truck Platoon	Frequency	Loading Condition	DF	ADTT (One direction)	Live load factors by CoV of total live load				
					$CoV_{LL} = 0$	$CoV_{LL} = 0.05$	$CoV_{LL} = 0.1$	$CoV_{LL} = 0.15$	$CoV_{LL} = 0.2$
Multiple Trucks in Platoon	Single-trip	No other vehicles on the bridge	One lane	NA	1.00	1.05	1.10	1.20	1.25
	Single-trip	Two identical platoons loaded on two lanes	Two or more lanes	NA	1.00	1.05	1.10	1.20	1.25
	10 Crossings	Mixed with routine traffic in the adjacent lane	One lane	> 5000	1.35	1.35	1.40	1.45	1.55
				1000	1.35	1.35	1.40	1.45	1.50
				< 100	1.35	1.35	1.40	1.45	1.50
	100 Crossings	Mixed with routine traffic in the adjacent lane	One lane	> 5000	1.35	1.40	1.45	1.50	1.60
				1000	1.35	1.40	1.45	1.45	1.55
				< 100	1.35	1.35	1.45	1.45	1.55

Platoon weight divided by 80 kips
(amplification factor alpha)

$$W_{platoon} := 1.0$$

Assumed $IM = 0.33$ (same as MBE permit load rating)

$$IM_{surface} := 33\%$$

5 ft headway 4-truck platoon moment at the mid span from the above load effect table:
(with $IM = 0.33$ and single lane moment GDF (g_{m1}) and removed 1.2 multiple presence factor)

$$LL_{platoon} := 1584.4 \text{ kip} \cdot \text{ft}$$

5 ft headway 4-truck platoon moment at the mid span (with amplification factor alpha)

$$LL_{platoon_dis} := W_{platoon} \cdot LL_{platoon} = 1584.4 \text{ kip} \cdot \text{ft}$$

Platoon calibrated live load factor (the value
in the red box as shown above Table)

$$\gamma_{platoon_strength} := 1.60$$

Parameter information for the equation below.

$$F_{nt} = 36 \text{ ksi}$$

$$g_{m1} = 0.485$$

$$M_{dc1} = 1324.6 \text{ kip} \cdot \text{ft}$$

$$M_{dc2} = 268.8 \text{ kip} \cdot \text{ft}$$

$$M_{dw} = 332.3 \text{ kip} \cdot \text{ft}$$

$$S_{bx} = 1892.553 \text{ in}^3$$

$$S_{b_{st}} = 2481.099 \text{ in}^3$$

$$S_{b_{lt}} = 2317.571 \text{ in}^3$$

$$RF_{Platoon_flexure} := \frac{(1.0) \cdot F_{nt} - \left(1.25 \cdot \left(\frac{M_{dc1}}{S_{bx}} + \frac{M_{dc2}}{S_{b_{lt}}} \right) + 1.50 \cdot \frac{M_{dw}}{S_{b_{lt}}} \right)}{\frac{\gamma_{platoon_strength} \cdot (LL_{platoon_dis})}{S_{b_{st}}}} = 1.728$$

Shear Rating for 4-truck Platoons (NRL with 5 ft headways): single lane platoon mixed with traffic, $CoV = 0.20$ (100 crossings, ADTT = 5000)

Shear load rating at the beam end

Parameter information for the equation below.

$$V_n = 469.8 \text{ kip} \qquad g_{v1} = 0.687$$

$$V_{dc1} = 52.2 \text{ kip} \qquad V_{dw} = 13.3 \text{ kip} \qquad V_{dc2} = 10.8 \text{ kip}$$

$$\text{Shear of platoon loads at the beam end} \qquad V_{PL_end} := 125.4 \text{ kip}$$

5 ft headway 4-truck platoon shear at the end beam from the above load effect table: (with $IM = 0.33$ and single lane shear GDF (g_{v1}) and removed 1.2 multiple presence factor)

$$V_{PL_end} := 97.2 \text{ kip}$$

5 ft headway 4-truck platoon shear at the end beam (with amplification factor alpha)

$$V_{PL_end_dis} := W_{platoon} \cdot V_{PL_end} = 97.2 \text{ kip}$$

$$RF_{PLLV@beam_end} := \frac{(1.0) \cdot V_n - (1.25 \cdot (V_{dc1} + V_{dc2}) + 1.50 \cdot V_{dw})}{\gamma_{platoon_strength} \cdot (V_{PL_end_dis})} = 2.386$$

Shear load rating at the 4 ft to the support

Parameter information for the equation below.

$$V_{n@4ft} = 414.512 \text{ kip} \qquad V_{dc1@4ft} = 48.2 \text{ kip} \qquad V_{dw@4ft} = 12.2 \text{ kip} \qquad V_{dc2@4ft} = 9.9 \text{ kip}$$

5 ft headway 4-truck platoon shear at the 4 ft to the support from the above load effect table: (with $IM = 0.33$ and single lane shear GDF (g_{v1}) and removed 1.2 multiple presence factor)

$$V_{PL@4ft} := 90.2 \text{ kip}$$

5 ft headway 4-truck platoon shear at the 4 ft to the support (with amplification factor alpha)

$$V_{PL@4ft_dis} := W_{platoon} \cdot V_{PL@4ft} = 90.2 \text{ kip}$$

$$RF_{PLLV@4ft} := \frac{(1.0) \cdot (1.0) \cdot (1.0) \cdot V_{n@4ft} - (1.25 \cdot (V_{dc1@4ft} + V_{dc2@4ft}) + 1.50 \cdot V_{dw@4ft})}{\gamma_{platoon_strength} \cdot (V_{PL@4ft_dis})} = 2.242$$

12. Load Rating for Service II Limit State Platoon (target beta = 1.60)

4-truck Platoons (NRL with 5 ft headways): single lane platoon mixed with traffic, $CoV = 0.20$ (100 crossings, ADTT = 5000)

Proposed Service II Calibrated LL Factors for the Target $\beta = 1.6$ (Table 22)

Truck platoon	Frequency	Load conditions	DF	ADTT (one direction)	Load factors by CoV of total live load
					$COV_{LL} = 0 - 0.20$
Multiple trucks in platoon	single-trip	No other vehicles on the bridge	One lane	N/A	1.15
	single-trip	Two identical platoons loaded on two lanes	Two or more lanes	N/A	1.15
	100 Crossings	Mixed with routine traffic in the adjacent lane	One lane	> 5000	1.90

Platoon calibrated live load factor (the value in the red box as shown above Table)

$$\gamma_{platoon_service} := 1.90$$

Live load stress at midspan

$$f_{platoon} := \frac{(LL_{platoon_dis})}{S_{b_st}} = 7.663 \text{ ksi}$$

Parameter information for the equation below.

$$f_R = 34.2 \text{ ksi}$$

$$f_D = 11.511 \text{ ksi}$$

$$S_{b_st} = 2481.099 \text{ in}^3$$

Rating factor for Service II

$$RF_{ServiceIIplatoon_Inv} := \frac{f_R - f_D}{\gamma_{platoon_service} \cdot f_{platoon}} = 1.558$$

13. Load Rating Summary

Load rating summary table is given below.

Limit state	Design load rating		Platoon load rating
	Inventory	Operating	(Strength I $\beta_{target} = 2.5$ and Service II $\beta_{target} = 1.6$)
Strength I for design and platoon load rating			
Flexure (at midspan)	1.278	1.656	1.728
Shear (at end)	2.159	2.799	2.386
Shear (at 4 ft)	1.990	2.580	2.242
Service II			
Flexure (at midspan)	1.842	2.395	1.558

14. Fatigue Check for AASHTO Fatigue Truck

ADT information from NBI database is given below. This example investigates a welded cross-frame connection plate fatigue at the 41 ft (cross-frame location) to the end of supports (near the critical positive moment location).

ADT $ADT := 8115$

Percentage of truck in ADT $P_{truck} := 60\%$

ADTT $ADTT := ADT \cdot P_{truck} = 4869$

Multiple presence factor for two design lanes (AASHTO *LRFD BDS* Table 3.6.1.4.2-1) $m_p := 0.85$

ADTT (single lane) $ADTT_{SL} := ADTT \cdot m_p = 4139$

Table 6.6.1.2.3-1 (cont.)—Detail Categories for Load-Induced Fatigue

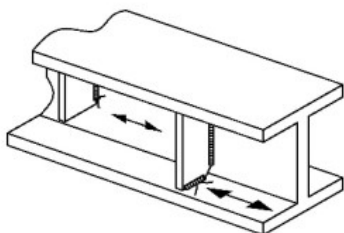
Section 4—Welded Stiffener Connections					
4.1 Base metal at the toe of transverse stiffener-to-flange fillet welds and transverse stiffener-to-web fillet welds. (Note: includes similar welds on bearing stiffeners and connection plates). Base metal adjacent to bearing stiffener-to-flange fillet welds or groove welds.	C'	44×10^8	12	Initiating from the geometrical discontinuity at the toe of the fillet weld extending into the base metal	

Table 6.6.1.2.3-2—75-year ($ADTT$)_{SL} Equivalent to Infinite Life

Detail Category	75-year ($ADTT$) _{SL} Equivalent to Infinite Life (trucks per day)
A	690
B	1120
B'	1350
C	1680
C'	975
D	2450
E	4615
E'	8485

ADTT (single lane threshold)

$$ADTT_{th} := 975$$

$$check := \text{if}(ADTT_{SL} > ADTT_{th}, \text{"Infinite"}, \text{"Finite"}) = \text{"Infinite"}$$

First, check the infinite life for this case. The constant amplitude fatigue limit for C' is 12 ksi as shown in *LRFD BDS* Table 6.6.1.2.5-3.

Table 6.6.1.2.5-3—Constant-Amplitude Fatigue Thresholds

Detail Category	Threshold (ksi)
A	24.0
B	16.0
B'	12.0
C	10.0
C'	12.0
D	7.0
E	4.5
E'	2.6
ASTM F3125/F3125M, Grades A325 and F1852 Bolts in Axial Tension	31.0
ASTM F3125/F3125M, Grades A490 and F2280 Bolts in Axial Tension	38.0

Constant amplitude fatigue thresholds for C'

$$\Delta F_{n_fatigueI} := 12 \text{ ksi}$$

centroid y_{b_st} to the datum

$$y_{b_st} = 50.496 \text{ in}$$

bottom flange thickness

$$t_{bf_mid} := 2.25 \text{ in}$$

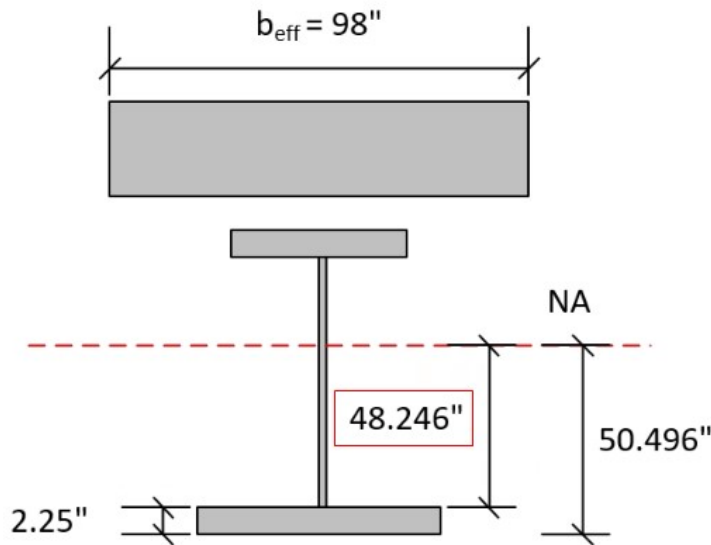
Determine the connection plate to the short-term NA

$$d_{connection_plate} := y_{b_st} - t_{bf_mid} = 48.246 \text{ in}$$

Moment of inertia (short-term)

$$I_{st} = 125286.706 \text{ in}^4$$

Also, the NA and appropriate dimensions are shown below.



6.6.1.2.2—Design Criteria

For load-induced fatigue considerations, each detail shall satisfy:

$$\gamma(\Delta f) \leq (\Delta F)_n \quad (6.6.1.2.2-1)$$

where:

- γ = load factor specified in [Table 3.4.1-1](#) for the fatigue load combination
- (Δf) = force effect, live load stress range due to the passage of the fatigue load as specified in [Article 3.6.1.4](#) (ksi)
- $(\Delta F)_n$ = nominal fatigue resistance as specified in [Article 6.6.1.2.5](#) (ksi)

Therefore, the stress range at the top of the bottom flange is found as follows:

AASHTO Fatigue truck moment at 41 ft (with GDFs/1.2 and IM = 0.15)

$$M_{\text{AASHTO}_Fat} := 596.4 \text{ kip} \cdot \text{ft}$$

Load factor for Fatigue I

$$\gamma_{fatigueI} := 1.75$$

Live load stress range based on AASHTO fatigue truck including $IM = 0.15$

$$\Delta f_{fatigue} := \frac{(M_{AASHTO_Fat}) \cdot d_{connection_plate}}{I_{st}} = 2.756 \text{ ksi}$$

$$check_fatigueI := \text{if} (\gamma_{fatigueI} \cdot \Delta f_{fatigue} \leq \Delta F_{n_fatigueI}, \text{"OK"}, \text{"NG"}) = \text{"OK"}$$

Demand/capacity ratio for fatigue

$$DCR := \frac{\gamma_{fatigueI} \cdot \Delta f_{fatigue}}{\Delta F_{n_fatigueI}} = 0.402$$

Rating factors (inverse of the DCR)

$$RF := \frac{1}{DCR} = 2.488$$

Note: The Fatigue I check for AASHTO fatigue truck check passes.

15. Fatigue Check for Platoons

For this example, check the fatigue based on a 4 NRL platoon with 5 ft headway spacing.

- For the Fatigue II load combination and finite life:

$$(\Delta F)_n = \left(\frac{A}{N} \right)^{\frac{1}{3}} \quad (6.6.1.2.5-2)$$

in which:

$$N = (365)(75)n(ADTT)_{SL} \quad (6.6.1.2.5-3)$$

where:

A = constant taken from [Table 6.6.1.2.5-1](#) (ksi³)

n = number of stress range cycles per truck passage taken from [Table 6.6.1.2.5-2](#)

$(ADTT)_{SL}$ = single-lane $ADTT$ as specified in [Article 3.6.1.4](#)

$(\Delta F)_{TH}$ = constant-amplitude fatigue threshold taken from [Table 6.6.1.2.5-3](#) (ksi)

Table 6.6.1.2.5-1—Detail Category Constant, A

Detail Category	Constant, A (ksi ³)
A	250.0×10^8
B	120.0×10^8
B'	61.0×10^8
C	44.0×10^8
C'	44.0×10^8
D	22.0×10^8
E	11.0×10^8
E'	3.9×10^8
ASTM F3125/F3125M, Grades A325 and F1852 Bolts in Axial Tension	17.1×10^8
ASTM F3125/F3125M, Grades A490 and F2280 Bolts in Axial Tension	31.5×10^8

Fatigue Check for Platoons with 5 ft headways

MBE Fatigue check for permit is not provided. In this example, firstly use the infinite life to check this platoon case. The constant amplitude fatigue limit for C' is 12 ksi as shown in *LRFD BDS* Table 6.6.1.2.5-3.

Therefore, the stress range at the top of the bottom flange is found as follows:

Moment from live load analysis (4 NRL platoon with 5ft at 41 ft (cross-frame location) with GDFs/1.2 and assumed the IM = 0.15 as the same for AASHTO Fatigue Truck)

$$M_{platoon_5ft} := 1522.7 \text{ kip} \cdot \text{ft} \cdot \frac{(1 + 0.15)}{(1 + 0.33)} = 1316.62 \text{ kip} \cdot \text{ft}$$

Note the platoon was calculated with IM = 0.33 in the BrR for this rating example

Live load stress range based on the platoon including IM = 0.15 (assume IM = 0.15 same as for AASHTO fatigue load)

$$\Delta f_{platoon_5ft} := \frac{(M_{platoon_5ft}) \cdot d_{connection_plate}}{I_{st}} = 6.084 \text{ ksi}$$

Platoon load factor for Fatigue I (assume the same as for AASHTO fatigue load)

$$\gamma_{fatigueI_platoon} := 1.75$$

$$check_fatigueI_PL := \text{if} (\gamma_{fatigueI_platoon} \cdot \Delta f_{platoon_5ft} \leq \Delta F_{n_fatigueI}, \text{"OK"}, \text{"NG"}) = \text{"OK"}$$

Demand/capacity ratio for platoon fatigue I

$$DCR := \frac{\gamma_{fatigueI_platoon} \cdot \Delta f_{platoon_5ft}}{\Delta F_{n_fatigueI}} = 0.887$$

Rating factors (inverse of the DCR)

$$RF := \frac{1}{DCR} = 1.127$$

Note: The Fatigue I check for a four-truck platoon with 5 ft headway passes.

Fatigue I and Fatigue II welded cross-frame connection plate check summary

Limit state	AASHTO Fatigue Truck	Four-truck Platoons (5-ft NRL 100 crossings per day)
<i>Fatigue I welded cross-frame connection plate</i>		
Stress (at 41 ft)	2.488	1.127
<i>Fatigue II welded cross-frame connection plate</i>		
Stress (at 41 ft)		

Note: The Fatigue I and Fatigue II l rating factors were calculated based on capacity over demand in terms of the stress.

16. Fatigue Damage Assessment for 5 ft and 50 ft Platoons and AASHTO Fatigue Truck

Fatigue damage for platoons with 5 ft headway

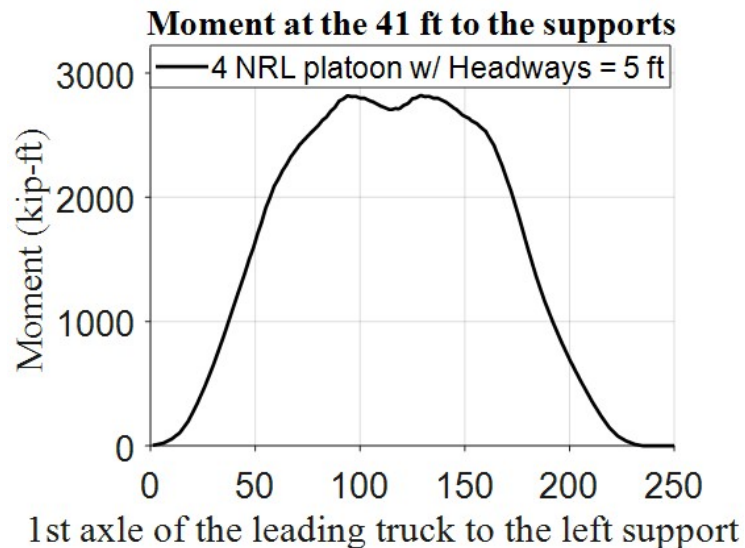
Constant A for C' case

$$A := 44 \cdot 10^8$$

number of stress range cycles per 4 NRL platoon with 5 ft headways (refer to the bottom figure)

$$ENSC_{platoon_5ft} := 1$$

The moment for each step (time-dependent) was plotted using SAP2000 for the 41 ft to the beam end (cross-frame location) of the bridge. Note the platoon effects were plotted without IM and with GDF = 1.0. For the analysis below, GDF/1.2 and IM = 0.15 were assumed.



Assume platoon 100 crossings per day (single lane loaded without routine traffic)

$$Num_{SL_platoon_5ft} := 100$$

Available N (number of crossings) for this platoon truck

$$N_{platoon_5ft} := \frac{A}{\left(\frac{\Delta f_{platoon_5ft}}{ksi}\right)^3} = 19536456$$

Accumulative fatigue damage for 75 year platoon with 5 ft headways

$$CFD_{platoon_5ft} := \frac{Num_{SL_platoon_5ft} \cdot ENSC_{platoon_5ft} \cdot \left(\frac{\Delta f_{platoon_5ft}}{ksi}\right)^3 \cdot 365 \cdot 75}{A} = 0.14$$

Fatigue damage for platoons with 50 ft headway

The stress range at the top of the bottom flange is found as follows:

Moment from live load analysis (4 NRL platoon with 50 ft headways at the cross-frame location) (GDFs/1.2 and assumed the IM = 0.15 as the same for AASHTO Fatigue Truck)

$$M_{platoon_50ft} := 906.1 \text{ kip} \cdot \text{ft} \cdot \frac{(1 + 0.15)}{(1 + 0.33)} = 783.47 \text{ kip} \cdot \text{ft}$$

Note the platoon was calculated with IM = 0.33 in the BrR for this rating example

Live load stress range for this platoon including IM = 0.15 (assume IM = 0.15 same as for AASHTO fatigue load)

$$\Delta f_{platoon_50ft} := \frac{(M_{platoon_50ft}) \cdot d_{connection_plate}}{I_{st}} = 3.62 \text{ ksi}$$

Number of stress range cycles per 4 NRL platoon with 50 ft headways (refer to the below figure)

Equivalent Number of Stress Cycles (ENSC) (Schilling, 1984)

$$ENSC = N_m + \left(\frac{S_{r1}}{S_{rp}}\right)^m + \left(\frac{S_{r2}}{S_{rp}}\right)^m + \dots + \left(\frac{S_{ri}}{S_{rp}}\right)^m$$

Where:

m = the slope constant of the S-N curve,

N_m = the number of maximum stress range caused by individual truck passage;

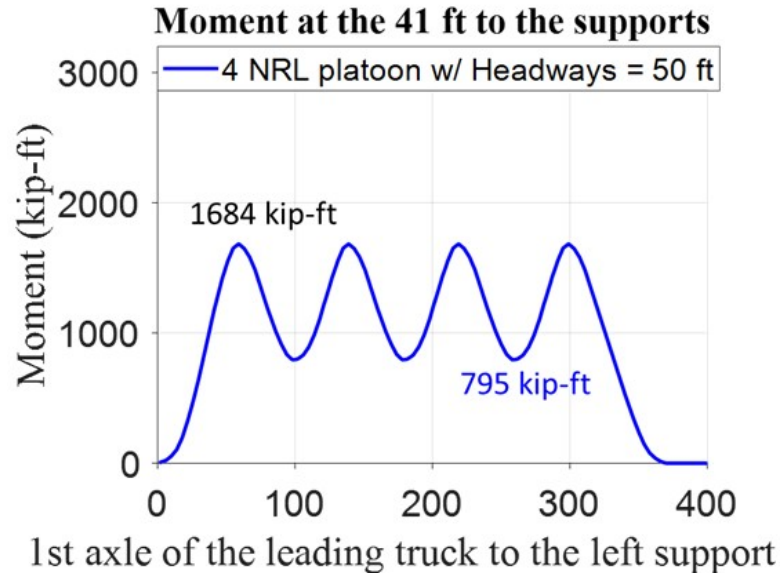
S_{ri} = higher-order stress range; and

S_{rp} = maximum stress range

❖ A complex stress cycle can be broken down into a primary cycle and one or more higher order cycles

❖ Higher-order cycles are secondary reversals of the primary cycle

The moment for each step (time-dependent) was plotted using SAP2000 for the cross-frame location of the bridge. Note the platoon effects were plotted without IM and with GDF = 1.0. For the analysis below, GDF/1.2 and IM =0.15 were assumed.



$$ENSC_{platoon_{50ft}} := 1 + \left((1 + 0.15) \frac{g_{m1}}{1.2} \cdot \left(\frac{1684 \text{ kip} \cdot \text{ft} - 795 \text{ kip} \cdot \text{ft}}{1684 \text{ kip} \cdot \text{ft}} \right) \right)^3 \cdot 3 = 1.044$$

Assume platoon 100 crossings per day
(single lane loaded without routine traffic)

$$Num_{SL_{platoon_{50ft}}} := 100$$

Available N (number of crossings) for
this platoon truck

$$N_{platoon_{50ft}} := \frac{A}{\left(\frac{\Delta f_{platoon_{50ft}}}{ksi} \right)^3} = 92717227$$

Accumulative fatigue damage for 75 year platoon with 50 ft headways

$$CFD_{platoon_{50ft}} := \frac{Num_{SL_{platoon_{50ft}}} \cdot ENSC_{platoon_{50ft}} \cdot \left(\frac{\Delta f_{platoon_{50ft}}}{ksi} \right)^3 \cdot 365 \cdot 75}{A} = 0.031$$

Fatigue damage ratios for AASHTO fatigue truck and platoons

Table 6.6.1.2.5-2—Cycles per Truck Passage, n

Longitudinal Members	
Simple Span Girders	1.0
Continuous Girders:	
1) near interior support	1.5
2) elsewhere	1.0
Cantilever Girders	5.0
Orthotropic Deck Plate Connections Subjected to Wheel Load Cycling	5.0
Trusses	1.0
Transverse Members	
Spacing > 20.0 ft	1.0
Spacing ≤ 20.0 ft	2.0

$$ENSC_{fatigue} := 1$$

Fatigue damage for one crossing for AASHTO fatigue truck

$$FD_{fatigue} := \frac{1 \cdot ENSC_{fatigue} \cdot \left(\frac{\Delta f_{fatigue}}{ksi} \right)^3}{A} = 4.758 \cdot 10^{-9}$$

Fatigue damage for a crossing for a 4-truck platoon with 5 ft headways

$$FD_{platoon_5ft} := \frac{1 \cdot ENSC_{platoon_5ft} \cdot \left(\frac{\Delta f_{platoon_5ft}}{ksi} \right)^3}{A} = 5.119 \cdot 10^{-8}$$

Fatigue damage for a crossing for a 4-truck platoon with 50 ft headways

$$FD_{platoon_50ft} := \frac{1 \cdot ENSC_{platoon_50ft} \cdot \left(\frac{\Delta f_{platoon_50ft}}{ksi} \right)^3}{A} = 1.126 \cdot 10^{-8}$$

Fatigue Damage Ratio for a single crossing for a 4 Truck Platoon with a 5 ft headway to the AASHTO fatigue truck

$$FD_{ratio_platoon_5ft_fatigue} := \frac{FD_{platoon_5ft}}{FD_{fatigue}} = 10.759$$

Fatigue Damage Ratio for a single crossing for a 4 Truck Platoon with a 50 ft headway to the AASHTO fatigue truck

$$FD_{ratio_platoon_50ft_fatigue} := \frac{FD_{platoon_50ft}}{FD_{fatigue}} = 2.368$$

Fatigue Damage Ratio for a single crossing for a 4 Truck Platoon with a 5 ft headway to the 50 ft headway truck platoon

$$FD_{ratio_platoon_5ft_50ft} := \frac{FD_{platoon_5ft}}{FD_{platoon_50ft}} = 4.544$$

Cumulative fatigue damage assessment summary

Notation	Scenarios	A	ENSC	Num	CFD
a	Platoon with 5 ft headways for 75 Years	440000000	1.000	2737500	0.140000000
b	Platoon with 50 ft headways for 75 Years	440000000	1.044	2737500	0.031000000
c	Platoon with 5 ft headways for one crossing	440000000	1.000	1	0.000000051
d	Platoon with 50 ft headwaysfor one crossing	440000000	1.044	1	0.000000011
e	AASHTO fatigue truck for one crossing	440000000	1.000	1	0.000000005

Fatigue damage ratios:

1. fatigue damage ratio (c/e) = 10.759 ;
2. fatigue damage ratio (d/e) = 2.368;
3. fatigue damage ratio (c/d) = 4.544.

17. Fatigue Check for Shear Studs

The shear stud information is given in the bridge drawings, and this example checks the fatigue of shear stud according to AASHTO LRFD Article 6.10.10. The end beam support shear was used to check the shear stud fatigue.

The pitch, p , of shear connectors shall satisfy:

$$p \leq \frac{nZ_r}{V_{sr}} \quad (6.10.10.1.2-1)$$

in which:

V_{sr} = horizontal fatigue shear range per unit length (kip/in.)

$$= \sqrt{(V_{fat})^2 + (F_{fat})^2} \quad (6.10.10.1.2-2)$$

V_{fat} = longitudinal fatigue shear range per unit length (kip/in.)

$$= \frac{V_f Q}{I} \quad (6.10.10.1.2-3)$$

F_{fat} = radial fatigue shear range per unit length (kip/in.) taken as the larger of either:

$$F_{fat1} = \frac{A_{bot} \sigma_{fg} \ell}{wR} \quad (6.10.10.1.2-4)$$

or:

$$F_{fat2} = \frac{F_{rc}}{w} \quad (6.10.10.1.2-5)$$

where:

σ_{fg} = range of longitudinal fatigue stress in the bottom flange without consideration of flange lateral bending (ksi)

A_{bot} = area of the bottom flange (in.²)

F_{rc} = net range of cross-frame or diaphragm force at the top flange (kip)

I = moment of inertia of the short-term composite section (in.⁴)

ℓ = distance between brace points (ft)

n = number of shear connectors in a cross section

p = pitch of shear connectors along the longitudinal axis (in.)

Q = first moment of the transformed short-term area of the concrete deck about the neutral axis of the short-term composite section (in.³)

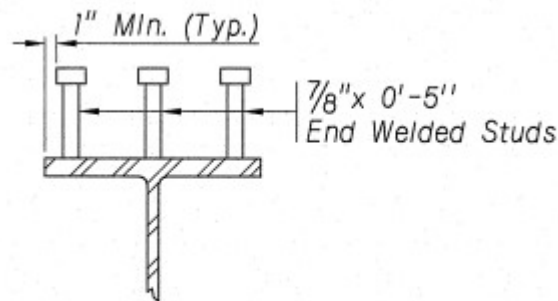
R = minimum girder radius within the panel (ft)

V_f = vertical shear force range under the applicable fatigue load combination specified in [Table 3.4.1-1](#) with the fatigue live load taken as specified in [Article 3.6.1.4](#) (kip)

w = effective length of deck (in.) taken as 48.0 in., except at end supports where w may be taken as 24.0 in.

Z_r = shear fatigue resistance of an individual shear connector determined as specified in [Article 6.10.10.2](#) (kip)

Shear Connectors, 10l Spa. @ 1'-0" = 100'-0"



SHEAR CONNECTOR DETAIL

Number of studs per row (n_{studs})

$$n_{studs} := 3$$

Pitch length (inch)

$$p := 12 \text{ in}$$

Shear stud diameter (inch)

$$d := \frac{7}{8} \text{ in}$$

The horizontal shear range is taken as the vector sum of the longitudinal and radial fatigue shear ranges. For this straight girder bridge, the radial fatigue shear range is zero.

6.10.10.2—Fatigue Resistance

The fatigue shear resistance of an individual stud shear connector, Z_r , shall be taken as:

For stud-type shear connectors:

- Where the projected 75-year single lane Average Daily Truck Traffic ($ADTT$)_{SL} is greater than or equal to 1090 trucks per day, the Fatigue I load combination shall be used and the fatigue shear resistance for infinite life shall be taken as:

$$Z_r = 5.5 d^2 \quad (6.10.10.2-1)$$

- Otherwise, the Fatigue II load combination shall be used and the fatigue shear resistance for finite life shall be taken as:

$$Z_r = \alpha d^2 \quad (6.10.10.2-2)$$

in which:

$$\alpha = 34.5 - 4.28 \log N \quad (6.10.10.2-3)$$

$ADTT$ (single lane threshold 6.10.10.2)

$$ADTT_{th_stud} := 1090$$

$check := \text{if} (ADTT_{SL} > ADTT_{th_stud}, \text{“Fatigue I”}, \text{“Fatigue II”}) = \text{“Fatigue I”}$

Fatigue I Shear Stud Check

Fatigue shear resistance per stud $Z_r := 5.5 \cdot \left(\frac{d}{\text{in}}\right)^2 \cdot \text{kip} = 4.211 \text{ kip}$

Shear stud fatigue check at the end of girder (use the girder section close to the end)

Girder dimensions at the girder end

Web thickness $t_w := \frac{3}{8} \text{ in} = 0.375 \text{ in}$

Top flange width $b_{tf} := 12 \text{ in}$

Bottom flange width $b_{bf} := 14 \text{ in}$

Compression flange (top flange) thickness $t_{tf} := 0.75 \text{ in}$

Tension flange (bottom flange) thickness $t_{bf} := 1.625 \text{ in}$

Web Depth $D := 60 \text{ in}$

Total height of the composite section $D_t := t_{tf} + D + t_{bf} + h_h + t_s = 71.875 \text{ in}$

Total height of the non-composite section $D_{girder} := t_{tf} + D + t_{bf} = 62.375 \text{ in}$

Section property calculations

Top flange section area $A_{tf} := b_{tf} \cdot t_{tf} = 9 \text{ in}^2$

Web section area $A_{web} := t_w \cdot D = 22.5 \text{ in}^2$

Bot flange section area $A_{bf} := b_{bf} \cdot t_{bf} = 22.75 \text{ in}^2$

Girder section area $A_{girder} := A_{tf} + A_{web} + A_{bf} = 54.25 \text{ in}^2$

Top flange center to the datum $y_{tf} := t_{bf} + D + \frac{t_{tf}}{2} = 62 \text{ in}$

Web center to the datum $y_{web} := t_{bf} + \frac{D}{2} = 31.625 \text{ in}$

Bot flange center to the datum $y_{bf} := \frac{t_{bf}}{2} = 0.813 \text{ in}$

Ay for the tension flange $A_{y_{tf}} := A_{tf} \cdot y_{tf} = 558 \text{ in}^3$

Ay for the web $A_{y_{web}} := A_{web} \cdot y_{web} = 711.563 \text{ in}^3$

Ay for the bottom flange

$$A_{y_bf} := A_{bf} \cdot y_{bf} = 18.484 \text{ in}^3$$

Ay for the girder

$$A_{y_girder} := A_{y_tf} + A_{y_web} + A_{y_bf} = 1288.047 \text{ in}^3$$

centroid y_b to the datum

$$y_{girder_b} := \frac{A_{y_girder}}{A_{girder}} = 23.743 \text{ in}$$

Moment of inertia for the top flange

$$I_{o_tf} := \frac{b_{tf} \cdot t_{tf}^3}{12} = 0.42 \text{ in}^4$$

Moment of inertia for the web

$$I_{o_web} := \frac{t_w \cdot D^3}{12} = 6750 \text{ in}^4$$

Moment of inertia for the bottom flange

$$I_{o_bf} := \frac{b_{bf} \cdot t_{bf}^3}{12} = 5.01 \text{ in}^4$$

Moment of inertia (girder only)

$$I_{girder} := I_{o_tf} + A_{tf} \cdot (y_{tf} - y_{girder_b})^2 + I_{o_bf} + A_{bf} \cdot (y_{bf} - y_{girder_b})^2 + I_{o_web} + A_{web} \cdot (y_{web} - y_{girder_b})^2 = 33287.77 \text{ in}^4$$

Short term section properties (n)

Area of slab

$$A_{slab_st} := \frac{b_{eff_int} \cdot t_s}{n} = 102.078 \text{ in}^2$$

Center of slab to the datum

$$y_{slab} := D_{girder} + h_h + \frac{t_s}{2} = 67.125 \text{ in}$$

Moment of inertia for the slab (short term)

$$I_{o_slab_st} := \frac{\frac{b_{eff_int}}{n} \cdot t_s^3}{12} = 478.49 \text{ in}^4$$

Ay for the slab (short term)

$$A_{y_slab_st} := A_{slab_st} \cdot y_{slab} = 6851.965 \text{ in}^3$$

centroid y_{b_st} to the datum

$$y_{b_st} := \frac{A_{y_girder} + A_{y_slab_st}}{A_{girder} + A_{slab_st}} = 52.07 \text{ in}$$

Moment of inertia (short term)

$$I_{st} := I_{girder} + A_{girder} \cdot (y_{girder_b} - y_{b_st})^2 + I_{o_slab_st} + A_{slab_st} \cdot (y_{slab} - y_{b_st})^2 = 100434.32 \text{ in}^4$$

First moment of the transformed short-term area of the concrete deck about the neutral axis of short-term section (in³)

$$Q := A_{slab_st} \cdot (y_{slab} - y_{b_st}) = 1536.761 \text{ in}^3$$

Shear Stud Fatigue Check for AASHTO Fatigue Truck

Shear force at the end of girder including $IM = 0.15$ and $GDF = \frac{g_{v1}}{1.2}$ (AASHTO Fatigue Truck)

$$V_{fatigue} := 38.8 \text{ kip}$$

AASHTO Fatigue Truck V_f including $IM = 0.15$ and $GDF = \frac{g_{v1}}{1.2}$

$$V_f := V_{fatigue} = 38.8 \text{ kip}$$

Longitudinal fatigue shear range per unit length (kip/in.)

$$V_{fat} := \frac{V_f \cdot Q}{I_{st}} = 0.594 \frac{\text{kip}}{\text{in}}$$

Horizontal fatigue shear range per unit length (kip/in.) (without F_{fat} for this case)

$$V_{sr} := V_{fat} = 0.594 \frac{\text{kip}}{\text{in}}$$

Pitch requirement (Equation 6.10.10.1.2-1)

$$p_{req} := \frac{n_{studs} \cdot Z_r}{V_{sr}} = 21.279 \text{ in}$$

$$check := \text{if}(p_{req} > p, \text{"OK"}, \text{"NO"}) = \text{"OK"}$$

The shear stud fatigue check for AASHTO fatigue truck is good at the end of the girder.

Fatigue I shear stud load rating for AASHTO fatigue truck (w.r.t spacing)

$$RF_{stud_fatigue} := \frac{p_{req}}{p} = 1.773$$

Shear Stud Fatigue Check for Platoon with 5 ft Headways

Shear force at the end of girder (4 NRL platoon with 5 ft headways including $IM = 0.15$ and GDFs/1.2)

$$V_{platoon} := 97.2 \text{ kip} \cdot \frac{(1 + 0.15)}{(1 + 0.33)} = 84.045 \text{ kip}$$

Note the platoon was calculated with $IM = 0.33$ in the BrR for this rating example

4 NRL platoon V_f including $IM = 0.15$ and GDFs/1.2

$$V_f := V_{platoon} = 84.045 \text{ kip}$$

Longitudinal fatigue shear range per unit length (kip/in.)

$$V_{fat} := \frac{V_f \cdot Q}{I_{st}} = 1.286 \frac{\text{kip}}{\text{in}}$$

Horizontal fatigue shear range per unit length (kip/in.) (without F_{fat} for this case)

$$V_{sr} := V_{fat} = 1.286 \frac{\text{kip}}{\text{in}}$$

Pitch requirement (Equation 6.10.10.1.2-1)

$$p_{req} := \frac{n_{studs} \cdot Z_r}{V_{sr}} = 9.823 \text{ in}$$

$$check := \text{if}(p_{req} > p, \text{"OK"}, \text{"NO"}) = \text{"NO"}$$

Fatigue I shear stud load rating for platoons (w.r.t spacing)

$$RF_{stud_platoon} := \frac{p_{req}}{p} = 0.819$$

The shear stud fatigue I check for a 4 NRL platoon with 5 ft headway is not good at the end of the girder. Note that the shear force for the platoon near the girder ends is high, the pitch does not meet the Fatigue I requirement. Next, the Fatigue II shear stud check for this platoon case is given.

Fatigue II Shear Stud Check

- Otherwise, the Fatigue II load combination shall be used and the fatigue shear resistance for finite life shall be taken as:

$$Z_r = \alpha d^2 \quad (6.10.10.2-2)$$

in which:

$$\alpha = 34.5 - 4.28 \log N \quad (6.10.10.2-3)$$

$$N = (365)(75)n(ADTT)_{sl} \quad (6.6.1.2.5-3)$$

Assume platoon (4 NRL with 5 ft headways)
100 crossings per day (single lane loaded)

$$ADTT_{sl_platoon_5ft} := 100$$

N (number of crossings) for
this platoon truck

$$N := 365 \cdot 75 \cdot ENSC_{platoon_5ft} \cdot ADTT_{sl_platoon_5ft} = 2737500$$

$$\alpha_{stud} := 34.5 - 4.28 \log(N) = 6.948$$

Fatigue II shear resistance per stud

$$Z_r := \alpha_{stud} \cdot \left(\frac{d}{in} \right)^2 \cdot kip = 5.32 \text{ kip}$$

Pitch requirement (Equation 6.10.10.1.2-1)

$$p_{req} := \frac{n_{studs} \cdot Z_r}{V_{sr}} = 12.41 \text{ in}$$

$$check := \text{if}(p_{req} > p, \text{"OK"}, \text{"NO"}) = \text{"OK"}$$

Fatigue II shear stud load rating for platoons
(w.r.t spacing)

$$RF_{stud_platoon} := \frac{p_{req}}{p} = 1.034$$

The Fatigue II shear stud check for this platoon case is good.

18. Shear Stud Fatigue Load Rating Summary

Shear stud fatigue load rating summary table is given below.

Limit state	AASHTO Fatigue Truck	Four-truck Platoons (5-ft NRL 100 crossings per day)
Fatigue I shear stud		
Shear (at end)	1.773	0.819
Fatigue II shear stud		
Shear (at end)		1.034

Note: The shear stud load rating factor was calculated based on LRFD BDS Equation 6.10.10.1.2-1 over the actual pitch.

Appendix F

This appendix contains detailed calculations related to the example steel continuous span bridge described in Section 8.5.

Appendix F. LRFR Load Rating Example of a Three-span Rolled Beam Bridge (interior girder)

Note: Bridge S080 40375 is a 220-ft (60'-100'-60') three-span, steel rolled beam bridge at the I-80 2W US77 Interchange in Davey, Nebraska (Figure 56) constructed in 1960. The bridge has three design lanes (HS25), and the average daily traffic is 48,015. It was widened twice, the first time in 1992 by replacing 1960 girders with ASTM (2021) A709 50 ksi weathering steel rolled beams and a 3.5 ksi slab. During the second widening in 2005, two more similar girders were added, and the slab strength was increased to 4.0 ksi. The design trucks for these two widenings were HS25. The rating method is load factor rating (LFR). However, the LRFR rating method was used as before for this rating example. The negative moment region design was considered noncomposite, so the deck was ineffective at carrying tension for Service II. As a result, the section modulus would be a steel section only for Service II.

Design and platoon ratings for an interior steel girder at 0.5L of the interior span and 0.4L from abutments at end spans for positive moment, at the interior supports for negative moment, and at the beam end supports for shear. Rating factors for the Strength I and Service II limit states were provided for HL-93 design and platoon loads.

Fatigue I and Fatigue II for AASHTO fatigue truck and platoons with 5- or 50-ft headways were considered to evaluate a welded cross-frame connection plate at one cross-frame location. The fatigue damage ratio for a single crossing of a four-truck platoon with a 5- or 50-ft headway and an AASHTO fatigue truck was determined. Fatigue I and Fatigue II were considered for shear studs at the beam end, based on AASHTO fatigue truck and platoons with 5- ft headways.

1. Bridge Data

End span length $L_{end} := 60 \text{ ft}$

Middle span length $L_{mid} := 100 \text{ ft}$

Material Steel yield stress (homogenous section)

$F_y := 50 \text{ ksi}$ $F_{yc} := 50 \text{ ksi}$ $F_{yf} := 50 \text{ ksi}$ $F_{yt} := 50 \text{ ksi}$ $F_{yw} := 50 \text{ ksi}$

F_y : girder yield stress, F_{yc} : compression flange yield stress, F_{yf} : flange yield stress, F_{yt} : tension flange yield stress, and F_{yw} is the web yield stress

Other information

1. Skew: 15 degrees.
2. ADT: 48,015.

Concrete information

Unit weight of concrete for determining dead loads

$$w_c := 155 \text{ pcf}$$

Unit weight of concrete for determining deck modulus of elasticity

$$w_{cd_modulus} := 155 \text{ pcf}$$

Unit weight of concrete for determining girder modulus of elasticity

$$w_{cg_modulus} := 150 \text{ pcf}$$

Ultimate strength for deck

$$f'_{cd} := 3.5 \text{ ksi}$$

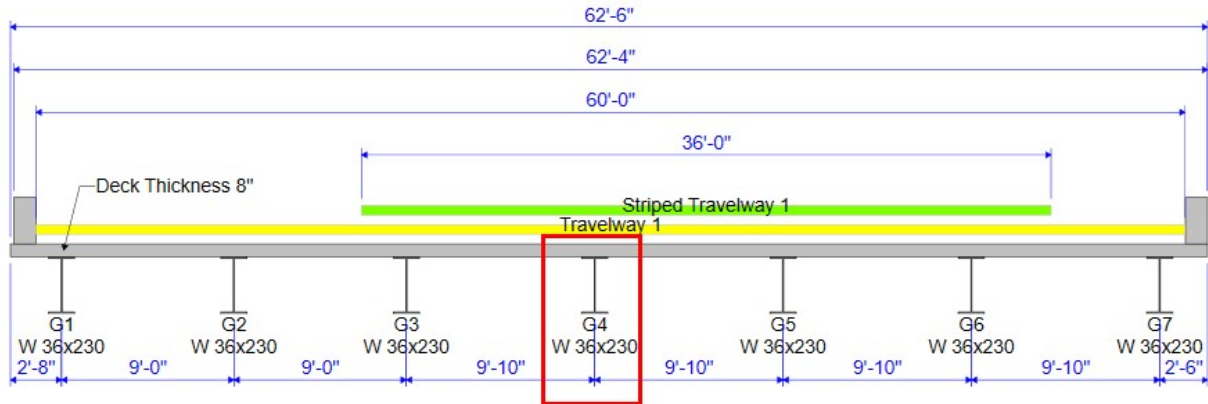
$$E_c = 33,000 K_1 w_c^{1.5} \sqrt{f'_c} \quad (\text{C5.4.2.4-2})$$

Modulus of elasticity of deck at final time

$$E_{cd} := 33000 \cdot \left(\frac{w_{cd_modulus}}{\text{pcf} \cdot 1000} \right)^{1.5} \cdot \left(\frac{f'_{cd}}{\text{ksi}} \right)^{0.5} \cdot \text{ksi} = 3767.43 \text{ ksi}$$

2. Bridge Cross Section

S080 40375L
 3 span rolled beam steel girder continuous - 2018 Exist Cond
 180 / Little Salt Creek
 3/15/2023



Steel modulus of elasticity

$$E := 29000 \text{ ksi}$$

Girder spacing (S)

$$S := 118 \text{ in} = 9.833 \text{ ft}$$

Number of girders

$$N_{girder} := 7$$

Left overhang

$$overhang_L := 32 \text{ in} = 2.667 \text{ ft}$$

Right overhang

$$overhang_R := 30 \text{ in} = 2.5 \text{ ft}$$

Total bridge width

$$W_{bridge} := (overhang_L + overhang_R + S \cdot (N_{girder} - 1)) = 770 \text{ in}$$

b_{eff} for deck (for interior girders)

$$b_{eff_int} := S = 118 \text{ in}$$

Thickness of deck (effective)

$$t_s := 7.5 \text{ in}$$

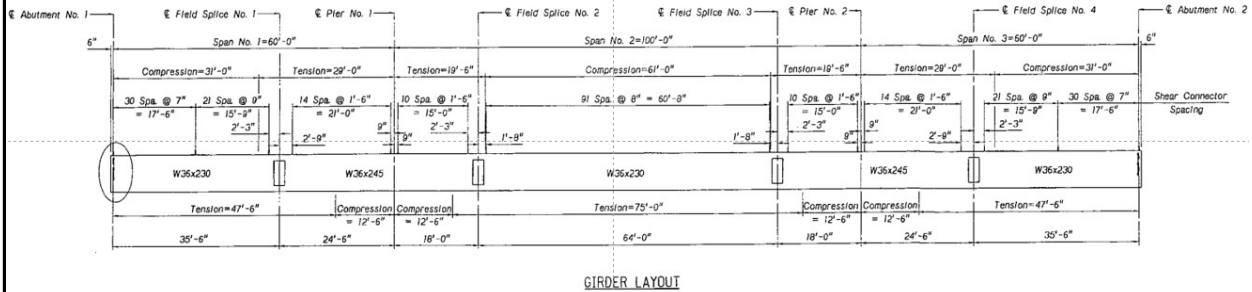
Haunch thickness

$$h_h := 0 \text{ in}$$

Modulus of ratio for the steel to deck

$$n := \frac{E}{E_{cd}} = 7.6975$$

3. Girder Section



GIRDER LAYOUT

Girder dimensions W 36x230

Web thickness	$t_w := 0.76 \text{ in}$
Top flange width	$b_{tf} := 16.47 \text{ in}$
Bottom flange width	$b_{bf} := 16.47 \text{ in}$
Top flange thickness	$t_{tf} := 1.26 \text{ in}$
Bottom flange thickness	$t_{bf} := 1.26 \text{ in}$
Web Depth	$D := 33.38 \text{ in}$
Total height of the composite section	$D_t := t_{tf} + D + t_{bf} + h_h + t_s = 43.4 \text{ in}$
Total height of the non-composite section	$D_{girder} := t_{tf} + D + t_{bf} = 35.9 \text{ in}$

Section property calculations

centroid y_b to the datum	$y_{girder_b} := 17.95 \text{ in}$
Moment of inertia (girder only)	$I_{girder} := 15000 \text{ in}^4$
Section modulus for the bottom of the girder (Steel only)	$S_{bx} := 837 \text{ in}^3$
Section modulus for the top of the girder (Steel only)	$S_{tx} := 837 \text{ in}^3$
Girder section area	$A_{girder} := 67.6 \text{ in}^2$
A_y for the girder	$A_{y_girder} := A_{girder} \cdot y_{girder_b} = 1213.42 \text{ in}^3$

Positive Flexure

Short term section properties (n)

Area of slab $A_{slab_st} := \frac{b_{eff_int} \cdot t_s}{n} = 114.972 \text{ in}^2$

Center of slab to the datum $y_{slab} := D_{girder} + h_h + \frac{t_s}{2} = 39.65 \text{ in}$

Moment of inertia for the slab (short term) $I_{o_slab_st} := \frac{b_{eff_int} \cdot t_s^3}{12} = 538.93 \text{ in}^4$

A_y for the slab (short term) $A_{y_slab_st} := A_{slab_st} \cdot y_{slab} = 4558.626 \text{ in}^3$

centroid y_{b_st} to the datum $y_{b_st} := \frac{A_{y_girder} + A_{y_slab_st}}{A_{girder} + A_{slab_st}} = 31.615 \text{ in}$

Moment of inertia (short term)

$$I_{st} := I_{girder} + A_{girder} \cdot (y_{girder_b} - y_{b_st})^2 + I_{o_slab_st} + A_{slab_st} \cdot (y_{slab} - y_{b_st})^2 = 35584.74 \text{ in}^4$$

Section modulus for the bottom of the girder (short term) $S_{b_st} := \frac{I_{st}}{y_{b_st}} = 1125.557 \text{ in}^3$

Section modulus for the top of the girder (short term) $S_{t_st} := \frac{I_{st}}{D_{girder} - y_{b_st}} = 8304.949 \text{ in}^3$

Long term section properties (3n)

Area of slab

$$A_{slab_lt} := \frac{b_{eff_int} \cdot t_s}{3 n} = 38.324 \text{ in}^2$$

Moment of inertia for the slab
(long term)

$$I_{o_slab_lt} := \frac{\frac{b_{eff_int}}{3 n} \cdot t_s^3}{12} = 179.64 \text{ in}^4$$

A_y for the slab (long term)

$$A_{y_slab_lt} := A_{slab_lt} \cdot y_{slab} = 1519.542 \text{ in}^3$$

centroid y_{b_lt} to the datum

$$y_{b_lt} := \frac{A_{y_girder} + A_{y_slab_lt}}{A_{girder} + A_{slab_lt}} = 25.801 \text{ in}$$

Moment of inertia (long term)

$$I_{lt} := I_{girder} + A_{girder} \cdot (y_{girder_b} - y_{b_lt})^2 + I_{o_slab_lt} + A_{slab_lt} \cdot (y_{slab} - y_{b_lt})^2 = 26696.71 \text{ in}^4$$

Section modulus for the bottom of the girder (long term)

$$S_{b_lt} := \frac{I_{lt}}{y_{b_lt}} = 1034.708 \text{ in}^3$$

Section modulus for the top of the girder (long term)

$$S_{t_lt} := \frac{I_{lt}}{D_{girder} - y_{b_lt}} = 2643.549 \text{ in}^3$$

Negative Flexure

Ignore Long. Reinf. in Negative Moment Capacity Control Option: No.

Therefore, the section properties for the negative flexure are based on steel girder only for Strength I.

Girder dimensions W 36x245

Haunch thickness	$h_{h2} := h_h$
Thickness of deck (effective)	$t_{s2} := t_s$
Effective slab width	$b_{eff_int2} := 118 \text{ in}$
Web thickness	$t_{w2} := 0.80 \text{ in}$
Top flange width	$b_{tf2} := 16.51 \text{ in}$
Bottom flange width	$b_{bf2} := 16.51 \text{ in}$
Top flange thickness	$t_{tf2} := 1.35 \text{ in}$
Bottom flange thickness	$t_{bf2} := 1.35 \text{ in}$
Web Depth	$D_2 := 33.38 \text{ in}$
Total height of the composite section	$D_{t2} := t_{tf2} + D_2 + t_{bf2} + h_{h2} + t_{s2} = 43.58 \text{ in}$
Total height of the non-composite section	$D_{girder2} := t_{tf2} + D_2 + t_{bf2} = 36.08 \text{ in}$

Section property calculations

centroid y_b to the datum	$y_{girder_b2} := 18.04 \text{ in}$
Moment of inertia (girder only)	$I_{girder2} := 16100 \text{ in}^4$
Section modulus for the bottom of the girder (Steel only)	$S_{bx2} := 895 \text{ in}^3$
Section modulus for the top of the girder (Steel only)	$S_{tx2} := 895 \text{ in}^3$
Girder section area	$A_{girder2} := 72.1 \text{ in}^2$
A_y for the girder	$A_{y_girder2} := A_{girder2} \cdot y_{girder_b2} = 1300.684 \text{ in}^3$

Positive Flexure

Short term section properties (n)

Area of slab $A_{slab_st2} := \frac{b_{eff_int2} \cdot t_{s2}}{n} = 114.972 \text{ in}^2$

Center of slab to the datum $y_{slab2} := D_{girder2} + h_{h2} + \frac{t_{s2}}{2} = 39.83 \text{ in}$

Moment of inertia for the slab (short term) $I_{o_slab_st2} := \frac{b_{eff_int2} \cdot t_{s2}^3}{12} = 538.93 \text{ in}^4$

A_y for the slab (short term) $A_{y_slab_st2} := A_{slab_st2} \cdot y_{slab2} = 4579.321 \text{ in}^3$

centroid y_{b_st} to the datum $y_{b_st2} := \frac{A_{y_girder2} + A_{y_slab_st2}}{A_{girder2} + A_{slab_st2}} = 31.432 \text{ in}$

Moment of inertia (short term)

$$I_{st2} := I_{girder2} + A_{girder2} \cdot (y_{girder_b2} - y_{b_st2})^2 + I_{o_slab_st2} + A_{slab_st2} \cdot (y_{slab2} - y_{b_st2})^2 = 37678.29 \text{ in}^4$$

Section modulus for the bottom of the girder (short term) $S_{b_st2} := \frac{I_{st2}}{y_{b_st2}} = 1198.73 \text{ in}^3$

Section modulus for the top of the girder (short term) $S_{t_st2} := \frac{I_{st2}}{D_{girder2} - y_{b_st2}} = 7655.65 \text{ in}^3$

Long term section properties (3n)

Area of slab

$$A_{slab_lt2} := \frac{b_{eff_int2} \cdot t_{s2}}{3 n} = 38.324 \text{ in}^2$$

Moment of inertia for the slab
(long term)

$$I_{o_slab_lt2} := \frac{\frac{b_{eff_int2}}{3 n} \cdot t_{s2}^3}{12} = 179.64 \text{ in}^4$$

A_y for the slab (long term)

$$A_{y_slab_lt2} := A_{slab_lt2} \cdot y_{slab2} = 1526.44 \text{ in}^3$$

centroid y_{b_lt} to the datum

$$y_{b_lt2} := \frac{A_{y_girder2} + A_{y_slab_lt2}}{A_{girder2} + A_{slab_lt2}} = 25.602 \text{ in}$$

Moment of inertia (long term)

$$I_{lt2} := I_{girder2} + A_{girder2} \cdot (y_{girder_b2} - y_{b_lt2})^2 + I_{o_slab_lt2} + A_{slab_lt2} \cdot (y_{slab2} - y_{b_lt2})^2 = 28160.73 \text{ in}^4$$

Section modulus for the bottom of the girder (long term)

$$S_{b_lt2} := \frac{I_{lt2}}{y_{b_lt2}} = 1099.922 \text{ in}^3$$

Section modulus for the top of the girder (long term)

$$S_{t_lt2} := \frac{I_{lt2}}{D_{girder2} - y_{b_lt2}} = 2687.726 \text{ in}^3$$

Negative Flexure

Ignore Long. Reinf. in Negative Moment Capacity Control Option: No.

Therefore, the section properties for the negative flexure are based on steel girder only for Strength I.

Dead load moment and shear effects from BrR file (interior girder)

Unfactored DC1 moment at the end span 0.4L $M_{dc1_end} := 175.8 \text{ kip} \cdot \text{ft}$

Unfactored DC2 moment at the end span 0.4L $M_{dc2_end} := 13.6 \text{ kip} \cdot \text{ft}$

Unfactored DW moment at the end span 0.4L $M_{dw_end} := 0 \text{ kip} \cdot \text{ft}$

Unfactored DC1 moment at the interior span 0.5L $M_{dc1_mid} := 648.9 \text{ kip} \cdot \text{ft}$

Unfactored DC2 moment at the interior span 0.5L $M_{dc2_mid} := 47.4 \text{ kip} \cdot \text{ft}$

Unfactored DW moment at the interior span 0.5L $M_{dw_mid} := 0 \text{ kip} \cdot \text{ft}$

Unfactored DC1 moment at the interior support $M_{dc1_inter} := -933.7 \text{ kip} \cdot \text{ft}$

Unfactored DC2 moment at the interior support $M_{dc2_inter} := -50.8 \text{ kip} \cdot \text{ft}$

Unfactored DW moment at the interior support $M_{dw_inter} := 0 \text{ kip} \cdot \text{ft}$

Unfactored DC1 shear at the interior support $V_{dc1_inter} := 63.4 \text{ kip}$

Unfactored DC2 shear at the interior support $V_{dc2_inter} := 3.9 \text{ kip}$

Unfactored DW shear at the interior support $V_{dw_inter} := 0 \text{ kip}$

Unfactored DC1 shear at the end support $V_{dc1_end} := 22.4 \text{ kip}$

Unfactored DC2 shear at the end support $V_{dc2_end} := 1.5 \text{ kip}$

Unfactored DW shear at the end support $V_{dw_end} := 0 \text{ kip}$

GDF calculations for positive moment regions (W 36x230) (interior girder)

Modular ratio for AASHTO GDFs $n_{GDF} := \frac{E}{E_{cd}} = 7.69754947$

e_g term for AASHTO GDF equations $e_{g_GDF} := D_{girder} - y_{girder_b} + h_h + \frac{t_s}{2} = 21.7 \text{ in}$

K_g term for AASHTO GDF equations $K_g := n_{GDF} \cdot (I_{girder} + A_{girder} \cdot e_{g_GDF}^2) = 360493 \text{ in}^4$

Distribution Factors

One Design Lane Loaded:

$$0.06 + \left(\frac{S}{14}\right)^{0.4} \left(\frac{S}{L}\right)^{0.3} \left(\frac{K_g}{12.0 L t_s^3}\right)^{0.1}$$

Two or More Design Lanes Loaded:

$$0.075 + \left(\frac{S}{9.5}\right)^{0.6} \left(\frac{S}{L}\right)^{0.2} \left(\frac{K_g}{12.0 L t_s^3}\right)^{0.1}$$

Single lane AASHTO moment GDF for interior girders (0.4L of the end span)

$$g_{m1_end} := 0.06 + \left(\frac{S}{14 \text{ ft}}\right)^{0.4} \cdot \left(\frac{S}{L_{end}}\right)^{0.3} \cdot \left(\frac{\frac{K_g}{\text{in}^4}}{\left(12 \cdot \frac{L_{end}}{\text{ft}} \cdot \left(\frac{t_s}{\text{in}}\right)^3\right)}\right)^{0.1} = 0.573$$

Multiple lanes AASHTO moment GDF for interior girders (0.4L of the end span)

$$g_{m2_end} := 0.075 + \left(\frac{S}{9.5 \text{ ft}}\right)^{0.6} \cdot \left(\frac{S}{L_{end}}\right)^{0.2} \cdot \left(\frac{\frac{K_g}{\text{in}^4}}{\left(12 \cdot \frac{L_{end}}{\text{ft}} \cdot \left(\frac{t_s}{\text{in}}\right)^3\right)}\right)^{0.1} = 0.798$$

Single lane AASHTO moment GDF for interior girders (0.5L of the interior span)

$$g_{m1_mid} := 0.06 + \left(\frac{S}{14 \text{ ft}} \right)^{0.4} \cdot \left(\frac{S}{L_{mid}} \right)^{0.3} \cdot \left(\frac{\frac{K_g}{\text{in}^4}}{\left(12 \cdot \frac{L_{mid}}{\text{ft}} \cdot \left(\frac{t_s}{\text{in}} \right)^3 \right)} \right)^{0.1} = 0.478$$

Multiple lanes AASHTO moment GDF for interior girders (0.5L of the interior span)

$$g_{m2_mid} := 0.075 + \left(\frac{S}{9.5 \text{ ft}} \right)^{0.6} \cdot \left(\frac{S}{L_{mid}} \right)^{0.2} \cdot \left(\frac{\frac{K_g}{\text{in}^4}}{\left(12 \cdot \frac{L_{mid}}{\text{ft}} \cdot \left(\frac{t_s}{\text{in}} \right)^3 \right)} \right)^{0.1} = 0.696$$

GDF calculations for negative moment region (W 36x245) (interior girder)

e_g term for AASHTO GDF equations $e_{g_GDF2} := D_{girder2} - y_{girder_b2} + h_{h2} + \frac{t_{s2}}{2} = 21.79 \text{ in}$

K_g term for AASHTO GDF $K_{g2} := n_{GDF} \cdot \left(I_{girder2} + A_{girder2} \cdot e_{g_GDF2}^2 \right) = 387444 \text{ in}^4$

Single lane AASHTO moment GDF for interior girders (interior support)

$$L_{inter} := \frac{L_{end} + L_{mid}}{2} = 80 \text{ ft}$$

$$g_{m1_inter} := 0.06 + \left(\frac{S}{14 \text{ ft}} \right)^{0.4} \cdot \left(\frac{S}{L_{inter}} \right)^{0.3} \cdot \left(\frac{\frac{K_{g2}}{\text{in}^4}}{\left(12 \cdot \frac{L_{inter}}{\text{ft}} \cdot \left(\frac{t_{s2}}{\text{in}} \right)^3 \right)} \right)^{0.1} = 0.521$$

Multiple lanes AASHTO moment GDF for interior girders (interior support)

$$g_{m2_inter} := 0.075 + \left(\frac{S}{9.5 \text{ ft}} \right)^{0.6} \cdot \left(\frac{S}{L_{inter}} \right)^{0.2} \cdot \left(\frac{\frac{K_{g2}}{\text{in}^4}}{\left(12 \cdot \frac{L_{inter}}{\text{ft}} \cdot \left(\frac{t_{s2}}{\text{in}} \right)^3 \right)} \right)^{0.1} = 0.743$$

GDF calculations for shear (interior girder)

Single lane AASHTO shear GDF for interior girders $g_{v1} := 0.36 + \frac{S}{25 \text{ ft}} = 0.753$

Multiple lanes AASHTO shear GDF for interior girders $g_{v2} := 0.20 + \frac{S}{12 \text{ ft}} - \left(\frac{S}{35 \text{ ft}} \right)^2 = 0.941$

HL-93 positive moment at the end span (at 0.4L) (including IM=0.33 and AASHTO GDF for multiple lanes)

$HL_93_M_{dist_end} := 939.11 \text{ kip} \cdot \text{ft}$

HL-93 positive moment at the interior span (at 0.5L) (including IM=0.33 and AASHTO GDF for multiple lanes)

$HL_93_M_{dist_mid} := 1278 \text{ kip} \cdot \text{ft}$

HL-93 negative moment at the interior support (including IM=0.33 and AASHTO GDF for multiple lanes)

$HL_93_M_{dist_inter} := -947.7 \text{ kip} \cdot \text{ft}$

HL-93 shear at the mid span side of piers (including IM=0.33 and AASHTO GDF for multiple lanes)

$HL_93_V_{dist_inter} := 114.8 \text{ kip}$

HL-93 shear at the end beam support (including IM=0.33 and AASHTO GDF for multiple lanes)

$HL_93_V_{dist_end} := 91.1 \text{ kip}$

4. Article 6.10.2 Proportional Limits Check

Article 6.10.2 check for W 36x230

Web check (6.10.2.1.1-1)

$$check := \text{if} \left(\frac{D}{t_w} \leq 150, \text{"OK"}, \text{"No"} \right) = \text{"OK"}$$

Bottom Flange check (6.10.2.2-1)

$$check := \text{if} \left(\frac{b_{bf}}{2 t_{bf}} \leq 12, \text{"OK"}, \text{"No"} \right) = \text{"OK"}$$

Top Flange check (6.10.2.2-1)

$$check := \text{if} \left(\frac{b_{tf}}{2 t_{tf}} \leq 12, \text{"OK"}, \text{"No"} \right) = \text{"OK"}$$

Bottom Flange check (6.10.2.2-2)

$$check := \text{if} \left(b_{bf} \geq \frac{D}{6}, \text{"OK"}, \text{"No"} \right) = \text{"OK"}$$

Top Flange check (6.10.2.2-2)

$$check := \text{if} \left(b_{tf} \geq \frac{D}{6}, \text{"OK"}, \text{"No"} \right) = \text{"OK"}$$

Bottom Flange check (6.10.2.2-3)

$$check := \text{if} \left(t_{bf} \geq 1.1 \cdot t_w, \text{"OK"}, \text{"No"} \right) = \text{"OK"}$$

Top Flange check (6.10.2.2-3)

$$check := \text{if} \left(t_{tf} \geq 1.1 \cdot t_w, \text{"OK"}, \text{"No"} \right) = \text{"OK"}$$

Moment of inertia of the compression flange about the vehicle axis (6.10.2.2-4)

$$I_{yc} := \frac{t_{tf} \cdot b_{tf}^3}{12} = 469.105 \text{ in}^4$$

Moment of inertia of the tension flange about the vehicle axis (6.10.2.2-4)

$$I_{yt} := \frac{t_{bf} \cdot b_{bf}^3}{12} = 469.105 \text{ in}^4$$

Flange check (6.10.2.2-4)

$$check := \text{if} \left(0.1 \leq \frac{I_{yc}}{I_{yt}} \leq 10, \text{"OK"}, \text{"No"} \right) = \text{"OK"}$$

Note: The Article 6.10.2 check for W 36x230 is good. WF shapes are typically compact. The checks here for completeness.

Article 6.10.2 check for W 36x245

Web check (6.10.2.1.1-1)

$$\text{check} := \text{if} \left(\frac{D_2}{t_{w2}} \leq 150, \text{"OK"}, \text{"No"} \right) = \text{"OK"}$$

Bottom Flange check (6.10.2.2-1)

$$\text{check} := \text{if} \left(\frac{b_{bf2}}{2 t_{bf2}} \leq 12, \text{"OK"}, \text{"No"} \right) = \text{"OK"}$$

Top Flange check (6.10.2.2-1)

$$\text{check} := \text{if} \left(\frac{b_{tf}}{2 t_{tf2}} \leq 12, \text{"OK"}, \text{"No"} \right) = \text{"OK"}$$

Bottom Flange check (6.10.2.2-2)

$$\text{check} := \text{if} \left(b_{bf2} \geq \frac{D_2}{6}, \text{"OK"}, \text{"No"} \right) = \text{"OK"}$$

Top Flange check (6.10.2.2-2)

$$\text{check} := \text{if} \left(b_{tf2} \geq \frac{D}{6}, \text{"OK"}, \text{"No"} \right) = \text{"OK"}$$

Bottom Flange check (6.10.2.2-3)

$$\text{check} := \text{if} (t_{bf2} \geq 1.1 \cdot t_{w2}, \text{"OK"}, \text{"No"}) = \text{"OK"}$$

Top Flange check (6.10.2.2-3)

$$\text{check} := \text{if} (t_{tf2} \geq 1.1 \cdot t_{w2}, \text{"OK"}, \text{"No"}) = \text{"OK"}$$

Moment of inertia of the compression flange about the vehicle axis (6.10.2.2-4)

$$I_{yc} := \frac{t_{tf2} \cdot b_{tf2}^3}{12} = 506.283 \text{ in}^4$$

Moment of inertia of the tension flange about the vehicle axis (6.10.2.2-4)

$$I_{yt} := \frac{t_{bf2} \cdot b_{bf2}^3}{12} = 506.283 \text{ in}^4$$

Flange check (6.10.2.2-4)

$$\text{check} := \text{if} \left(0.1 \leq \frac{I_{yc}}{I_{yt}} \leq 10, \text{"OK"}, \text{"No"} \right) = \text{"OK"}$$

Note: The Article 6.10.2 check for W 36x245 is good.

5. Service II Checks (Article 6.10.4.2.2)

Note: This Service II check was performed for the positive moment at the 0.4L of the end span, and 0.5L of the interior span, and the negative moment region at the interior support.

Service II check at the end span (at 0.4L)

Note: The lateral flange stress (f_l) is ignored. The beam section is W36x230 at this location.

Hybrid factor R_h $R_h := 1.0$

Lateral flange stress (assume to be 0) $f_l := 0$

Flange stress upper limit for the Service II $f_{ServiceII} := 0.95 \cdot R_h \cdot F_{yf} = 47.5 \text{ ksi}$

Check the top steel flange stress due to the Service II loads (6.10.4.2.1)

For the top steel flange of composite sections:

$$f_f \leq 0.95 R_h F_{yf} \quad (6.10.4.2.2-1)$$

Top flange stress due to Service II loads without the consideration of lateral flange bending (ksi) (Service II load factors) (compression)

$$f_{tf} := \frac{1.0 M_{dc1_end}}{S_{tx}} + \frac{1.0 (M_{dc2_end} + M_{dw_end})}{S_{t_lt}} + \frac{1.3 HL_93_M_{dist_end}}{S_{t_st}} = 4.346 \text{ ksi}$$

$$check := \text{if}(f_{tf} \leq f_{ServiceII}, \text{"OK"}, \text{"No"}) = \text{"OK"}$$

Check the bottom steel flange stress due to the Service II loads (6.10.4.2.1)

For the bottom steel flange of composite sections:

$$f_f + \frac{f_\ell}{2} \leq 0.95R_h F_{yf} \quad (6.10.4.2.2-2)$$

Bottom flange stress due to Service II loads without the consideration of lateral flange bending (ksi) (Service II load factors) (tension)

$$f_{bf} := \frac{1.0 M_{dc1_end}}{S_{bx}} + \frac{1.0 (M_{dc2_end} + M_{dw_end})}{S_{b_lt}} + \frac{1.3 HL_93_M_{dist_end}}{S_{b_st}} = 15.69 \text{ ksi}$$

$$check := \text{if}(f_{bf} \leq f_{ServiceII}, \text{"OK"}, \text{"No"}) = \text{"OK"}$$

Note: Since the web does meet the requirement of Article 6.10.2.1.1, LRFD BDS Equation 6.10.4.2.2-4 is not checked.

Performance ratio for the top flange (Service II)

$$PR_{ServiceII_top} := \frac{f_{tf}}{f_{ServiceII}} = 0.091$$

Performance ratio for the bottom flange (Service II)

$$PR_{ServiceII_bottom} := \frac{f_{bf}}{f_{ServiceII}} = 0.33$$

Service II check at the interior span (at 0.5L)

Note: The lateral flange stress is ignored. The beam section is W36x230 at this location.

Top flange stress due to Service II loads without the consideration of lateral flange bending (ksi) (Service II load factors) (compression)

$$f_{tf} := \frac{1.0 M_{dc1_mid}}{S_{tx}} + \frac{1.0 (M_{dc2_mid} + M_{dw_mid})}{S_{t_lt}} + \frac{1.3 HL_93 M_{dist_mid}}{S_{t_st}} = 11.919 \text{ ksi}$$

$$check := \text{if}(f_{tf} \leq f_{ServiceII}, \text{"OK"}, \text{"No"}) = \text{"OK"}$$

Bottom flange stress due to Service II loads without the consideration of lateral flange bending (ksi) (Service II load factors) (tension)

$$f_{bf} := \frac{1.0 M_{dc1_mid}}{S_{bx}} + \frac{1.0 (M_{dc2_mid} + M_{dw_mid})}{S_{b_lt}} + \frac{1.3 HL_93 M_{dist_mid}}{S_{b_st}} = 27.57 \text{ ksi}$$

$$check := \text{if}(f_{bf} \leq f_{ServiceII}, \text{"OK"}, \text{"No"}) = \text{"OK"}$$

Performance ratio for the top flange (Service II)

$$PR_{ServiceII_top} := \frac{f_{tf}}{f_{ServiceII}} = 0.251$$

Performance ratio for the bottom flange (Service II)

$$PR_{ServiceII_bottom} := \frac{f_{bf}}{f_{ServiceII}} = 0.58$$

Service II check at the interior support

Note: The lateral flange stress is ignored. The beam section is W36x245 at this location. This design of the bridge was assumed to be noncomposite for the negative moment region. The section modulus for short and long term are the same as for only steel section modulus.

Top flange stress due to Service II loads without the consideration of lateral flange bending (ksi) (Service II load factors) (tension)

$$f_{tf} := -1 \left(\frac{1.0 M_{dc1_inter}}{S_{tx2}} + \frac{1.0 (M_{dc2_inter} + M_{dw_inter})}{S_{tx2}} + \frac{1.3 HL_93 M_{dist_inter}}{S_{tx2}} \right) = 29.72 \text{ ksi}$$

Note: To make the stress positive, applied the negative sign

$$check := \text{if} (\text{abs} (f_{tf}) \leq f_{ServiceII}, \text{"OK"}, \text{"No"}) = \text{"OK"}$$

Bottom flange stress due to Service II loads without the consideration of lateral flange bending (ksi) (Service II load factors) (compression)

$$f_{bf} := -1 \left(\frac{1.0 M_{dc1_inter}}{S_{bx2}} + \frac{1.0 (M_{dc2_inter} + M_{dw_inter})}{S_{bx2}} + \frac{1.3 HL_93 M_{dist_inter}}{S_{bx2}} \right) = 29.72 \text{ ksi}$$

Note: To make the stress positive, applied the negative sign

$$check := \text{if} (\text{abs} (f_{bf}) \leq f_{ServiceII}, \text{"OK"}, \text{"No"}) = \text{"OK"}$$

Performance ratio for the top flange (Service II)

$$PR_{ServiceII_top} := \frac{\text{abs} (f_{tf})}{f_{ServiceII}} = 0.626$$

Performance ratio for the bottom flange (Service II)

$$PR_{ServiceII_bottom} := \frac{\text{abs} (f_{bf})}{f_{ServiceII}} = 0.626$$

Note: The compression flange for the composite negative region should also pass the following Equation 6.10.4.2.2-4 check.

$$f_c \leq F_{crw} \quad (6.10.4.2.2-4)$$

where:

f_c = compression flange stress at the section under consideration due to the Service II loads calculated without consideration of flange lateral bending (ksi)

F_{crw} = nominal bend-buckling resistance for webs with or without longitudinal stiffeners, as applicable, determined as specified in [Article 6.10.1.9](#) (ksi)

The nominal bend-buckling resistance shall be taken as:

$$F_{crw} = \frac{0.9Ek}{\left(\frac{D}{t_w}\right)^2} \quad (6.10.1.9.1-1)$$

but not to exceed the smaller of $R_h F_{yc}$ and $F_{yw}/0.7$

in which:

k = bend-buckling coefficient

$$= \frac{9}{(D_c/D)^2} \quad (6.10.1.9.1-2)$$

For composite sections in negative flexure, D_c shall be computed for the section consisting of the steel girder plus the longitudinal reinforcement with the exception of the following. For composite sections in negative flexure at the service limit state where the concrete deck is considered effective in tension for computing flexural stresses on the composite section due to Load Combination Service II, D_c shall be computed from [Eq. D6.3.1-1](#).

Depth of web in compression (top flange in tension)

$$D_{c2} := \left(\frac{f_{bf}}{f_{tf} + f_{bf}}\right) \cdot D_{girder2} - t_{tf2} = 16.69 \text{ in}$$

Bend-buckling coefficient

$$k := \frac{9}{\left(\frac{D_{c2}}{D}\right)^2} = 36$$

Nominal bend-buckling resistance for webs (LRFD BDS 6.10.1.9.1-2)

$$F_{crw_equ} := \frac{0.9 \cdot E \cdot k}{\left(\frac{D_2}{t_{w2}}\right)^2} = 539.697 \text{ ksi}$$

Nominal bend-buckling resistance for webs

$$F_{crw} := \min\left(F_{crw_equ}, R_h \cdot F_{yc}, \frac{F_{yw}}{0.7}\right) = 50 \text{ ksi}$$

$$\text{check} := \text{if}(\text{abs}(f_{bf}) \leq F_{crw}, \text{"OK"}, \text{"No"}) = \text{"OK"}$$

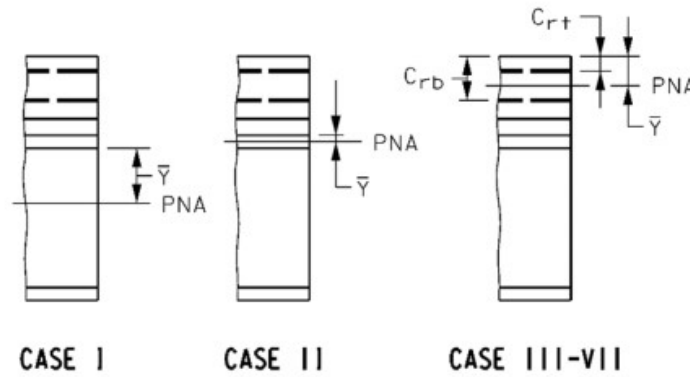
6. Moment Strength I Checks (LRFD BDS Article 6.10.7)

Strength I check at the end span (at 0.4L)

First, use LRFD BDS Table D6.1-1 to determine the M_p for this positive bending case. The reinforcements are not considered. Therefore, only three cases of PNA are considered in the slab, top flange, and web.

Table D6.1-1—Calculation of \bar{Y} and M_p for Sections in Positive Flexure

Case	PNA	Condition	\bar{Y} and M_p
I	In Web	$P_t + P_w \geq P_c + P_s + P_{rb} + P_r$	$\bar{Y} = \left(\frac{D}{2}\right) \left[\frac{P_t - P_c - P_s - P_r - P_{rb}}{P_w} + 1 \right]$ $M_p = \frac{P_w}{2D} [\bar{Y}^2 + (D - \bar{Y})^2] + [P_s d_s + P_r d_r + P_{rb} d_{rb} + P_c d_c + P_t d_t]$
II	In Top Flange	$P_t + P_w + P_c \geq P_s + P_{rb} + P_r$	$\bar{Y} = \left(\frac{t_c}{2}\right) \left[\frac{P_w + P_t - P_s - P_r - P_{rb}}{P_c} + 1 \right]$ $M_p = \frac{P_c}{2t_c} [\bar{Y}^2 + (t_c - \bar{Y})^2] + [P_s d_s + P_r d_r + P_{rb} d_{rb} + P_w d_w + P_t d_t]$
III	Concrete Deck, Below P_{rb}	$P_t + P_w + P_c \geq \left(\frac{c_{rb}}{t_s}\right) P_s + P_{rb} + P_r$	$\bar{Y} = (t_s) \left[\frac{P_c + P_w + P_t - P_r - P_{rb}}{P_s} \right]$ $M_p = \left(\frac{\bar{Y}^2 P_s}{2t_s}\right) + [P_r d_r + P_{rb} d_{rb} + P_c d_c + P_w d_w + P_t d_t]$



Compression flange thickness used in equations

$$t_c := t_{tf}$$

Tension flange thickness used in equations

$$t_t := t_{bf}$$

Plastic force in the web

$$P_w := F_{yw} \cdot D \cdot t_w = 1268.44 \text{ kip}$$

Plastic force in the compression flange

$$P_c := F_{yc} \cdot b_{tf} \cdot t_{tf} = 1037.61 \text{ kip}$$

Plastic force in the tension flange

$$P_t := F_{yt} \cdot b_{bf} \cdot t_{bf} = 1037.61 \text{ kip}$$

Plastic force in the concrete deck

$$P_s := 0.85 \cdot f'_{cd} \cdot b_{eff_int} \cdot t_s = 2632.875 \text{ kip}$$

Check the PNA is in the web, top flange or concrete deck

$$Case := \begin{cases} \text{if } P_t + P_w \geq P_c + P_s & = 2 \\ \quad \text{return 1} \\ \text{also if } P_t + P_w + P_c \geq P_s & \\ \quad \text{return 2} \\ \text{else} & \\ \quad 3 & \end{cases}$$

Note: Case 1 for PNA in the web, Case 2 for PNA in the top flange, and Case 3 for PNA in the concrete deck.

Y_{bar} in the above figure for the specific case

$$Y_{bar} := \begin{cases} \text{if } Case = 1 & = 0.432 \text{ in} \\ \quad \left| \frac{D}{2} \cdot \left(\frac{(P_t - P_c - P_s)}{P_w} + 1 \right) \right. \\ \text{also if } Case = 2 & \\ \quad \left| \frac{t_c}{2} \cdot \left(\frac{(P_w + P_t - P_s)}{P_c} + 1 \right) \right. \\ \text{else} & \\ \quad \left| t_s \cdot \frac{(P_c + P_w + P_t)}{P_s} \right. \end{cases}$$

d_t is the distance from PNA to the center of the tension flange

$$d_t := \begin{cases} \text{if } Case = 1 & = 34.838 \text{ in} \\ \quad \left| \frac{t_t}{2} + D - Y_{bar} \right. \\ \text{also if } Case = 2 & \\ \quad \left| \frac{t_t}{2} + D + t_c - Y_{bar} \right. \\ \text{else} & \\ \quad \left| t_s + h_h + t_t + D + \frac{t_c}{2} - Y_{bar} \right. \end{cases}$$

d_c is the distance from PNA to the center of the compression flange

$$d_c := \begin{cases} \text{if } Case = 1 & = 0 \text{ in} \\ \left\| Y_{bar} + \frac{t_c}{2} \right. \\ \text{also if } Case = 2 \\ \left\| 0 \text{ in} \right. \\ \text{else} \\ \left\| t_s + h_h + \frac{t_c}{2} - Y_{bar} \right. \end{cases}$$

d_w is the distance from PNA to the center of the web

$$d_w := \begin{cases} \text{if } Case = 1 & = 17.518 \text{ in} \\ \left\| 0 \text{ in} \right. \\ \text{also if } Case = 2 \\ \left\| \frac{D}{2} + t_c - Y_{bar} \right. \\ \text{else} \\ \left\| t_s + h_h + t_c + \frac{D}{2} - Y_{bar} \right. \end{cases}$$

d_s is the distance from PNA to the center of the concrete slab

$$d_s := \begin{cases} \text{if } Case = 1 & = 4.182 \text{ in} \\ \left\| \frac{t_s}{2} + h_h + t_c + Y_{bar} \right. \\ \text{also if } Case = 2 \\ \left\| \frac{t_s}{2} + h_h + Y_{bar} \right. \\ \text{else} \\ \left\| 0 \text{ in} \right. \end{cases}$$

D_p is the distance from PNA to the top of the concrete slab

$$D_p := \begin{cases} \text{if } Case = 1 & \\ \quad \left\| \begin{array}{l} t_s + h_h + t_c + Y_{bar} \\ \text{also if } Case = 2 \\ \quad \left\| \begin{array}{l} t_s + h_h + Y_{bar} \\ \text{else} \\ \quad \left\| Y_{bar} \end{array} \right. \end{array} \right. & \end{cases} = 7.932 \text{ in}$$

D_{cp} is the distance of the web in the compression according to the PNA

$$D_{cp} := \begin{cases} \text{if } Case = 1 & \\ \quad \left\| \begin{array}{l} Y_{bar} \\ \text{also if } Case = 2 \\ \quad \left\| \begin{array}{l} 0 \text{ in} \\ \text{else} \\ \quad \left\| 0 \text{ in} \end{array} \right. \end{array} \right. & \end{cases} = 0 \text{ in}$$

M_p is the plastic moment

$$M_p := \begin{cases} \text{if } Case = 1 & \\ \quad \left\| \begin{array}{l} \frac{P_w}{2 D} (Y_{bar}^2 + (D - Y_{bar})^2) + (P_s \cdot d_s + P_c \cdot d_c + P_t \cdot d_t) \\ \text{also if } Case = 2 \\ \quad \left\| \begin{array}{l} \frac{P_w}{2 t_c} (Y_{bar}^2 + (t_c - Y_{bar})^2) + (P_s \cdot d_s + P_w \cdot d_w + P_t \cdot d_t) \\ \text{else} \\ \quad \left\| \frac{Y_{bar}^2 P_s}{2 t_s} + (P_c \cdot d_c + P_w \cdot d_w + P_t \cdot d_t) \end{array} \right. \end{array} \right. & \end{cases} = 5818.211 \text{ kip} \cdot \text{ft}$$

Calculate the yield moment M_y of the composite section using the equations provided in Appendix D6 (Article D6.2.2). Flange lateral bending is to be disregarded in the calculation. The Strength I load factors are used here.

Symbolically, the procedure is:

- 1) Solve for M_{AD} from the equation:

$$F_{\mathcal{N}} = \frac{M_{D1}}{S_{NC}} + \frac{M_{D2}}{S_{LT}} + \frac{M_{AD}}{S_{ST}} \quad (\text{D6.2.2-1})$$

- 2) Then calculate:

$$M_y = M_{D1} + M_{D2} + M_{AD} \quad (\text{D6.2.2-2})$$

M_{D1} , M_{D2} , and M_{AD} are the factored moments at the strength limit state applied separately to the steel, long-term, and short-term composite sections. M_y is taken as the value calculated for the tension (bottom) flange for the positive moment region.

$$M_{D1_end} := 1.25 M_{dc1_end} = 219.75 \text{ kip} \cdot \text{ft}$$

$$M_{D2_end} := 1.25 M_{dc2_end} + 1.50 M_{dw_end} = 17 \text{ kip} \cdot \text{ft}$$

$$M_{AD_end} := F_y \cdot S_{b_st} - \left(\frac{S_{b_st}}{S_{bx}} \right) M_{D1_end} - \left(\frac{S_{b_st}}{S_{b_lt}} \right) M_{D2_end} = 4375.818 \text{ kip} \cdot \text{ft}$$

$$M_{y_end} := M_{D1_end} + M_{D2_end} + M_{AD_end} = 4612.568 \text{ kip} \cdot \text{ft}$$

Nominal Flexural Resistance

Firstly, check if the section is compact or non-compact (Article 6.10.6.2.2). Note the F_y is 50 ksi and the web satisfies *LRFD BDS* Article 6.10.2.1.1 as mentioned before. Therefore, only need to check the third requirement :

- The specified minimum yield strengths of the flanges do not exceed 70.0 ksi,
- The web satisfies the requirement of Article 6.10.2.1.1, and
- The section satisfies the web slenderness limit:

$$\frac{2D_{cp}}{t_w} \leq 3.76 \sqrt{\frac{E}{F_{yc}}} \quad (6.10.6.2.2-1)$$

$$check := \text{if} \left(\frac{2 D_{cp}}{t_w} \leq 3.76 \sqrt{\frac{E}{F_{yc}}}, \text{“Compact”}, \text{“Non-compact”} \right) = \text{“Compact”}$$

Check ductility according to *LRFD BDS* 6.10.7.3-1

Compact and noncompact sections shall satisfy:

$$D_p \leq 0.42 D_t \quad (6.10.7.3-1)$$

where:

D_p = distance from the top of the concrete deck to the neutral axis of the composite section at the plastic moment (in.)

D_t = total depth of the composite section (in.)

$$check := \text{if} (D_p \leq 0.42 D_t, \text{“OK”}, \text{“NO”}) = \text{“OK”}$$

According to the provisions of *LRFD BDS* Article 6.10.7.1.2, the nominal flexural resistance of compact composite sections in positive flexure is determined as follows:

If $D_p \leq 0.1D_t$, then:

$$M_n = M_p \quad \text{Eq. (6.10.7.1.2-1)}$$

Otherwise:
$$M_n = M_p \left(1.07 - 0.7 \frac{D_p}{D_t} \right) \quad \text{Eq. (6.10.7.1.2-2)}$$

$$M_n := \begin{cases} \text{if } D_p \leq 0.1 D_t \\ \quad \left\| \begin{array}{l} M_p \\ \text{else} \\ M_p \cdot \left(1.07 - 0.7 \cdot \frac{D_p}{D_t} \right) \end{array} \right\| \end{cases} = 65774.05 \text{ kip} \cdot \text{in}$$

In a continuous span, the nominal flexural resistance of the section shall satisfy:

$$M_n \leq 1.3 R_h M_y \quad (6.10.7.1.2-3)$$

where:

M_n = nominal flexural resistance determined from [Eq. 6.10.7.1.2-1](#) or [6.10.7.1.2-2](#), as applicable (kip-in.)

M_y = yield moment determined as specified in [Article D6.2](#) (kip-in.)

R_h = hybrid factor determined as specified in [Article 6.10.1.10.1](#)

unless:

- the span under consideration and all adjacent interior-pier sections satisfy the requirements of [Article B6.2](#),

and:

- the appropriate value of θ_{RL} from [Article B6.6.2](#) exceeds 0.009 radians at all adjacent interior-pier sections,

However, in a continuous span, the nominal flexural resistance of the section is also limited to the following check.

This example conservatively assumed insufficient stiffness and ductility of adjacent pier sections, and it does not meet the exception in 6.10.7.1.2-3.

$$M_{n_end} := \min(M_n, 1.3 R_h \cdot M_{y_end}) = 5481.171 \text{ kip} \cdot \text{ft}$$

Then determine the M_u . Note the f_l is 0 and ϕ_f is 1.0.

$$M_u + \frac{1}{3} f_l S_{xt} \leq \phi_f M_n \quad (6.10.7.1.1-1)$$

Factored moment (Strength I)

$$M_{u_end} := 1.25 \cdot (M_{dc1_end} + M_{dc2_end}) + 1.50 M_{dw_end} + 1.75 \cdot HL_{93} M_{dist_end} = 1880.193 \text{ kip} \cdot \text{ft}$$

$$\text{check} := \text{if}(M_{u_end} \leq 1.0 M_{n_end}, \text{"OK"}, \text{"NO"}) = \text{"OK"}$$

Performance ratio for the bottom flange (Strength I)

$$PR_{StrengthI} := \frac{M_{u_end}}{1.0 M_{n_end}} = 0.343$$

Strength I check at the interior span (at 0.5L)

The girder section is also W36x230. Therefore, the M_P is the same as for the end span at 0.4L as above calculations. Calculations can be found above. Calculate the yield moment of the composite section using the equations provided in Appendix D6 (Article D6.2.2). Flange lateral bending is to be disregarded in the calculation. The Strength I load factors are used here.

Symbolically, the procedure is:

- 1) Solve for M_{AD} from the equation:

$$F_M = \frac{M_{D1}}{S_{NC}} + \frac{M_{D2}}{S_{LT}} + \frac{M_{AD}}{S_{ST}} \quad (\text{D6.2.2-1})$$

- 2) Then calculate:

$$M_y = M_{D1} + M_{D2} + M_{AD} \quad (\text{D6.2.2-2})$$

M_{D1} , M_{D2} , and M_{AD} are the factored moments at the strength limit state applied separately to the steel, long-term, and short-term composite sections. M_y is taken as the value calculated for the tension (bottom) flange for the positive moment region.

$$M_{D1_mid} := 1.25 M_{dc1_mid} = 811.125 \text{ kip} \cdot \text{ft}$$

$$M_{D2_mid} := 1.25 M_{dc2_mid} + 1.50 M_{dw_mid} = 59.25 \text{ kip} \cdot \text{ft}$$

$$M_{AD_mid} := F_y \cdot S_{b_st} - \left(\frac{S_{b_st}}{S_{bx}} \right) M_{D1_mid} - \left(\frac{S_{b_st}}{S_{b_lt}} \right) M_{D2_mid} = 3534.606 \text{ kip} \cdot \text{ft}$$

$$M_{y_mid} := M_{D1_mid} + M_{D2_mid} + M_{AD_mid} = 4404.981 \text{ kip} \cdot \text{ft}$$

Nominal Flexural Resistance

As mentioned before, the W36x230 section is compact according to *LRFD BDS* Article 6.10.6.2.2. Also, this section passes the ductility check according to Equation 6.10.7.3-1. These two check details can be found above.

According to the provisions of *LRFD BDS* Article 6.10.7.1.2, the nominal flexural resistance of compact composite sections in positive flexure is determined as follows:

If $D_p \leq 0.1D_t$, then:

$$M_n = M_p \quad \text{Eq. (6.10.7.1.2-1)}$$

$$\text{Otherwise: } M_n = M_p \left(1.07 - 0.7 \frac{D_p}{D_t} \right) \quad \text{Eq. (6.10.7.1.2-2)}$$

$$M_n := \left\| \begin{array}{l} \text{if } D_p \leq 0.1 D_t \\ \quad \left\| M_p \right\| \\ \text{else} \\ \quad \left\| M_p \cdot \left(1.07 - 0.7 \cdot \frac{D_p}{D_t} \right) \right\| \end{array} \right\| = 65774.05 \text{ kip} \cdot \text{in}$$

In a continuous span, the nominal flexural resistance of the section shall satisfy:

$$M_n \leq 1.3 R_h M_y \quad (6.10.7.1.2-3)$$

where:

M_n = nominal flexural resistance determined from Eq. 6.10.7.1.2-1 or 6.10.7.1.2-2, as applicable (kip-in.)

M_y = yield moment determined as specified in Article D6.2 (kip-in.)

R_h = hybrid factor determined as specified in Article 6.10.1.10.1

The nominal flexural resistance of the section also considered the *LRFD BDS* Equation 6.10.7.1.2-3 as above.

$$M_{n_mid} := \min(M_n, 1.3 R_h \cdot M_{y_mid}) = 5481.171 \text{ kip} \cdot \text{ft}$$

Then determine the M_u . Note the f_l is 0 and ϕ_f is 1.0.

$$M_u + \frac{1}{3} f_\ell S_{xt} \leq \phi_f M_n \quad (6.10.7.1.1-1)$$

Factored moment (Strength I)

$$M_{u_mid} := 1.25 \cdot (M_{dc1_mid} + M_{dc2_mid}) + 1.50 M_{dw_mid} + 1.75 \cdot HL_93_M_{dist_mid} = 3106.88 \text{ kip} \cdot \text{ft}$$

$$check := \text{if} (M_{u_mid} \leq 1.0 M_{n_mid}, \text{"OK"}, \text{"NO"}) = \text{"OK"}$$

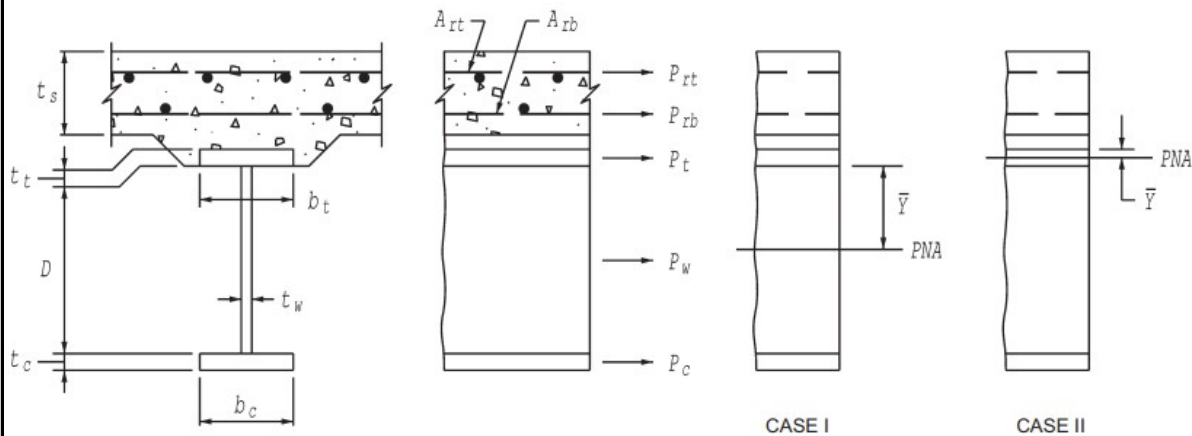
Performance ratio for the bottom flange (Strength I)

$$PR_{StrengthI} := \frac{M_{u_mid}}{1.0 M_{n_mid}} = 0.567$$

Strength I check at the interior support

Use Table D6.1-2 to determine the Y_{bar} and M_p for this negative flexure case. The negative moment region is considered as the noncomposite section for this example. The reinforcements are not considered. Two cases of PNA are considered either in the top flange or web.

Case	PNA	Condition	\bar{Y} and M_p
I	In Web	$P_c + P_w \geq P_t + P_{rb} + P_{rt}$	$\bar{Y} = \left(\frac{D}{2}\right) \left[\frac{P_c - P_t - P_{rt} - P_{rb}}{P_w} + 1 \right]$ $M_p = \frac{P_w}{2D} \left[\bar{Y}^2 + (D - \bar{Y})^2 \right] + [P_{rt}d_{rt} + P_{rb}d_{rb} + P_t d_t + P_c d_c]$
II	In Top Flange	$P_c + P_w + P_t \geq P_{rb} + P_{rt}$	$\bar{Y} = \left(\frac{t}{2}\right) \left[\frac{P_w + P_c - P_{rt} - P_{rb}}{P_t} + 1 \right]$ $M_p = \frac{P_t}{2t} \left[\bar{Y}^2 + (t - \bar{Y})^2 \right] + [P_{rt}d_{rt} + P_{rb}d_{rb} + P_w d_w + P_c d_c]$



Plastic force in the web used to compute the M_p

$$P_w := F_{yw} \cdot D_2 \cdot t_{w2} = 1335.2 \text{ kip}$$

Plastic force in the compression flange used to compute M_p

$$P_c := F_{yc} \cdot b_{bf2} \cdot t_{bf2} = 1114.425 \text{ kip}$$

Plastic force in the tension flange used to compute M_p

$$P_t := F_{yt} \cdot b_{tf2} \cdot t_{tf2} = 1114.425 \text{ kip}$$

Plastic force in the top layer reinforcement

$$P_{rt} := 0 \text{ kip}$$

Plastic force in the bottom layer reinforcement

$$P_{rb} := 0 \text{ kip}$$

Cover for the bottom layer reinforcement

$$Cover_{bot} := 0 \text{ in}$$

Cover for the top layer reinforcement

$$Cover_{top} := 0 \text{ in}$$

Check the PNA is in the web or top flange

$$\boxed{\text{Case}} := \left\| \begin{array}{l} \text{if } P_c + P_w \geq P_t + P_{rb} + P_{rt} \\ \quad \left\| \begin{array}{l} \text{return 1} \\ \text{else} \\ \quad \left\| \text{return 2} \end{array} \right. \\ \end{array} \right. \right\| = 1$$

Note: Case 1 for PNA in the web and Case 2 for PNA in the top flange.

Y_{bar} in the above figure for the specific case

$$\boxed{Y_{bar}} := \left\| \begin{array}{l} \text{if Case} = 1 \\ \quad \left\| \frac{D_2}{2} \cdot \left(\frac{(P_c - P_t - P_{rb} - P_{rt})}{P_w} + 1 \right) \right. \\ \quad \text{else} \\ \quad \left\| \frac{t_{tf2}}{2} \cdot \left(\frac{(P_c + P_w - P_{rb} - P_{rt})}{P_t} + 1 \right) \right. \\ \end{array} \right\| = 16.69 \text{ in}$$

d_t is the distance from PNA to the center of the tension flange

$$\boxed{d_t} := \left\| \begin{array}{l} \text{if Case} = 1 \\ \quad \left\| \frac{t_{tf2}}{2} + Y_{bar} \right. \\ \quad \text{else} \\ \quad \left\| 0 \text{ in} \right. \\ \end{array} \right\| = 17.365 \text{ in}$$

d_c is the distance from PNA to the center of the compression flange

$$\boxed{d_c} := \left\| \begin{array}{l} \text{if Case} = 1 \\ \quad \left\| D_2 - Y_{bar} + \frac{t_{bf2}}{2} \right. \\ \quad \text{else} \\ \quad \left\| t_{tf2} - Y_{bar} + D_2 + \frac{t_{bf2}}{2} \right. \\ \end{array} \right\| = 17.365 \text{ in}$$

d_w is the distance from PNA to the center of the web

$$d_w := \begin{cases} \text{if } Case = 1 & = 0 \text{ in} \\ \parallel & \\ 0 \text{ in} & \\ \text{else} & \\ \parallel & \\ t_{tf2} - Y_{bar} + \frac{D_2}{2} & \end{cases}$$

d_{rb} is the distance from the PNA to the center of the bottom layer reinforcement

$$d_{rb} := \begin{cases} \text{if } Case = 1 & = 18.04 \text{ in} \\ \parallel & \\ t_{tf2} + h_{h2} + Y_{bar} + Cover_{bot} & \\ \text{else} & \\ \parallel & \\ h_{h2} + Y_{bar} + Cover_{bot} & \end{cases}$$

d_{rt} is the distance from the PNA to the center of the top layer reinforcement

$$d_{rt} := \begin{cases} \text{if } Case = 1 & = 25.54 \text{ in} \\ \parallel & \\ t_{tf2} + h_{h2} + Y_{bar} + t_{s2} - Cover_{top} & \\ \text{else} & \\ \parallel & \\ h_{h2} + Y_{bar} + t_{s2} - Cover_{top} & \end{cases}$$

D_{cp} is the distance of the web in the compression according to the PNA

$$D_{cp2} := \begin{cases} \text{if } Case = 1 & = 16.69 \text{ in} \\ \parallel & \\ D_2 - Y_{bar} & \\ \text{else} & \\ \parallel & \\ D_2 & \end{cases}$$

M_p is the plastic moment

$$M_{p2} := \begin{cases} \text{if } Case = 1 & = 4153.85 \text{ kip} \cdot \text{ft} \\ \parallel & \\ \frac{P_w}{2 D_2} (Y_{bar}^2 + (D_2 - Y_{bar})^2) + (P_{rt} \cdot d_{rt} + P_{rb} \cdot d_{rb} + P_c \cdot d_c + P_t \cdot d_t) & \\ \text{else} & \\ \parallel & \\ \frac{P_t}{2 D_2} (Y_{bar}^2 + (t_{tf2} - Y_{bar})^2) + (P_{rt} \cdot d_{rt} + P_{rb} \cdot d_{rb} + P_c \cdot d_c + P_w \cdot d_w) & \end{cases}$$

The plastic moment (include the negative sign)

$$M_{p2} := -1 \cdot M_{p2} = -4153.852 \text{ kip} \cdot \text{ft}$$

Note: In this load rating example, the reinforcement were not considered for the negative region. Also only the steel section is considered for resisting short-term and long-term loads. Therefore, the M_y for bottom flange and top flange is the same for this case.

Symbolically, the procedure is:

- 1) Solve for M_{AD} from the equation:

$$F_y = \frac{M_{D1}}{S_{NC}} + \frac{M_{D2}}{S_{LT}} + \frac{M_{AD}}{S_{ST}} \quad (\text{D6.2.2-1})$$

- 2) Then calculate:

$$M_y = M_{D1} + M_{D2} + M_{AD} \quad (\text{D6.2.2-2})$$

Yield moment for the bottom of the steel M_{y_bot}

$$M_{D1_inter} := 1.25 M_{dc1_inter} = -1167.125 \text{ kip} \cdot \text{ft}$$

$$M_{D2_inter} := 1.25 M_{dc2_inter} + 1.50 M_{dw_inter} = -63.5 \text{ kip} \cdot \text{ft}$$

$$M_{AD_bot_inter} := F_y \cdot S_{bx2} - \left(\frac{S_{bx2}}{S_{bx2}} \right) M_{D1_inter} - \left(\frac{S_{bx2}}{S_{bx2}} \right) M_{D2_inter} = 4959.792 \text{ kip} \cdot \text{ft}$$

$$M_{y_bot_inter} := M_{D1_inter} + M_{D2_inter} + M_{AD_bot_inter} = 3729.167 \text{ kip} \cdot \text{ft}$$

Nominal Flexural Resistance

Firstly, check the web compactness according to *LRFD BDS* 6.10.6.2.3-1. The flange yield stress F_y is 50 ksi, therefore, only check the other two requirements as below. This load rating example cannot use the Appendix A6 since the diaphragms are not parallel to supports.

Sections in straight bridges whose supports are normal or skewed not more than 20 degrees from normal, and with intermediate diaphragms or cross-frames placed in contiguous lines parallel to the supports may be proportioned according to the provisions for compact or noncompact web sections specified in [Appendix A6](#). For these sections:

Otherwise, the section shall be proportioned according to provisions specified in [Article 6.10.8](#).

Note: Therefore, this load rating example uses [Article 6.10.8](#).

Flange local buckling check

Top flange continuously laterally supported for this bridge. Then check the compression flange local buckling according to *LRFD BDS* 6.10.8.2.2-3 & 4.

$$\begin{aligned}\lambda_f &= \text{slenderness ratio for the compression flange} \\ &= \frac{b_{fc}}{2t_{fc}} \quad (6.10.8.2.2-3)\end{aligned}$$

$$\begin{aligned}\lambda_{pf} &= \text{limiting slenderness ratio for a compact flange} \\ &= 0.38 \sqrt{\frac{E}{F_{yc}}} \quad (6.10.8.2.2-4)\end{aligned}$$

$$\begin{aligned}\lambda_{nf} &= \text{limiting slenderness ratio for a noncompact flange} \\ &= 0.56 \sqrt{\frac{E}{F_{yr}}} \quad (6.10.8.2.2-5)\end{aligned}$$

$$\text{Slenderness ratio for the compression flange} \quad \lambda_f := \frac{b_{bf2}}{2 t_{bf2}} = 6.115$$

$$\text{Limiting slenderness ratio for a compact flange} \quad \lambda_{pf} := 0.38 \cdot \sqrt{\frac{E}{F_{yc}}} = 9.152$$

check := if ($\lambda_f \leq \lambda_{pf}$, “Compact flange”, “Non-compact flange”) = “Compact flange”

The local buckling resistance of the compression flange shall be taken as:

- If $\lambda_f \leq \lambda_{pf}$, then:

$$F_{nc} = R_b R_h F_{yc} \quad (6.10.8.2.2-1)$$

- Otherwise:

$$F_{nc} = \left[1 - \left(1 - \frac{F_{yr}}{R_h F_{yc}} \right) \left(\frac{\lambda_f - \lambda_{pf}}{\lambda_{rf} - \lambda_{pf}} \right) \right] R_b R_h F_{yc} \quad (6.10.8.2.2-2)$$

Determine the R_b according to Article 6.10.1.10.2 which is used to calculate FLB resistance.

Slenderness ratio for web

$$\lambda := \frac{2 \cdot D_{c2}}{t_w} = 43.921$$

Ratio a_{wc} for the compression flange

$$a_{wc} := \frac{2 \cdot D_{c2} \cdot t_{w2}}{b_{bf2} \cdot t_{bf2}} = 1.198$$

λ_{rw} = limiting slenderness ratio for a noncompact web, expressed in terms of $2D_c/t_w$, calculated as follows:

- for longitudinally-stiffened sections:

$$= \left(\frac{2D_c}{D} \right) \lambda_{rwD} \quad (6.10.1.10.2-4)$$

- for all other cases:

$$4.6 \sqrt{\frac{E}{F_{yc}}} \leq \lambda_{rw} = \left(3.1 + \frac{5.0}{a_{wc}} \right) \sqrt{\frac{E}{F_{yc}}} \leq 5.7 \sqrt{\frac{E}{F_{yc}}} \quad (6.10.1.10.2-5)$$

Slenderness ratio limit for non-compact web

$$\lambda_{rw} := \max \left(4.6 \cdot \sqrt{\frac{E}{F_{yc}}}, \min \left(\left(3.1 + \frac{5}{a_{wc}} \right) \cdot \sqrt{\frac{E}{F_{yc}}}, 5.7 \cdot \sqrt{\frac{E}{F_{yc}}} \right) \right) = 137.274$$

Web check (6.10.6.2.3-1)

$$\text{check} := \text{if} (\lambda \leq \lambda_{rw}, \text{“OK”}, \text{“NO”}) = \text{“OK”}$$

- the web satisfies:

$$\frac{2D_c}{t_w} \leq \lambda_{rw} \quad (6.10.1.10.2-1)$$

then, R_b shall be taken equal to 1.0.

Web load-shedding
factor

$$R_b := 1$$

Local buckling resistance (compact flange)

$$F_{nc_FLB} := R_b \cdot R_h \cdot F_{yc} = 50 \text{ ksi}$$

Lateral flange buckling check

Then check the compression flange lateral torsion buckling according to *LRFD BDS* 6.10.8.2.3-9 & 4 to determine the braced length compactness. The unbraced length for the bottom flange is 157.20" for this bridge.

L_b = unbraced length (in.)
 L_p = limiting unbraced length to achieve the nominal flexural resistance of $R_b R_h F_{yc}$ under uniform bending (in.)

$$= 1.0 r_t \sqrt{\frac{E}{F_{yc}}} \quad (6.10.8.2.3-4)$$

r_t = effective radius of gyration for lateral-torsional buckling (in.)

$$= \frac{b_{fc}}{\sqrt{12 \left(1 + \frac{1}{3} \frac{D_c t_w}{b_{fc} t_{fc}} \right)}} \quad (6.10.8.2.3-9)$$

L_r = limiting unbraced length to achieve the onset of nominal yielding in either flange under uniform bending with consideration of compression flange residual stress effects (in.)

$$= \pi r_t \sqrt{\frac{E}{F_{yr}}} \quad (6.10.8.2.3-5)$$

Effective radius of gyration for LTB (in.) $r_t := \frac{b_{bf2}}{\sqrt{12 \left(1 + \frac{1}{3} \frac{D_{c2} \cdot t_{w2}}{b_{bf2} \cdot t_{bf2}} \right)}} = 4.351 \text{ in}$

Unbraced length (based on the BrR file) $L_b := 157.2 \text{ in}$

Limiting braced length to achieve the nominal flexure resistance $R_b \cdot R_h \cdot F_{yc}$ under uniform bending (in.) $L_p := 1.0 \cdot r_t \cdot \sqrt{\frac{E}{F_{yc}}} = 104.794 \text{ in}$

F_{yr} = compression flange stress at the onset of nominal yielding within the cross section, including residual stress effects, but not including compression flange lateral bending, taken as the smaller of $0.7F_{yc}$ and F_{yw} , but not less than $0.5F_{yc}$

Compression flange stress at the onset of nominal yielding within the cross-section $F_{yr} := \max(0.5 F_{yc}, \min(0.7 F_{yc}, F_{yw})) = 35 \text{ ksi}$

Limiting braced length to achieve the onset of nominal yielding considering the compression flange residual stress effects (in.)

$$L_r := \pi \cdot r_t \cdot \sqrt{\frac{E}{F_{yr}}} = 393.494 \text{ in}$$

<p><i>Compactness</i> := if $L_b \leq L_p$ return “Compact unbraced” also if $L_p \leq L_b \leq L_r$ return “Non–compact unbraced” else return “Slender unbraced”</p>	<p>= “Non–compact unbraced”</p>
---	---------------------------------

This design moment gradient modifier C_b is 1.896 based on the BrR file.

Moment gradient modifier

$$C_b := 1.896$$

- If $L_b \leq L_p$, then:

$$F_{nc} = R_b R_h F_{yc} \tag{6.10.8.2.3-1}$$

- If $L_p < L_b \leq L_r$, then:

$$F_{nc} = C_b \left[1 - \left(1 - \frac{F_{yr}}{R_h F_{yc}} \right) \left(\frac{L_b - L_p}{L_r - L_p} \right) \right] R_b R_h F_{yc} \leq R_b R_h F_{yc} \tag{6.10.8.2.3-2}$$

- If $L_b > L_r$, then:

$$F_{nc} = F_{cr} \leq R_b R_h F_{yc} \tag{6.10.8.2.3-3}$$

Lateral torsional resistance (non-compact unbraced length)

$$F_{nc_LTB} := \min \left(C_b \cdot \left(1 - \left(1 - \frac{F_{yr}}{R_h \cdot F_{yc}} \right) \cdot \left(\frac{L_b - L_p}{L_r - L_p} \right) \right) \cdot R_b \cdot R_h \cdot F_{yc}, R_b \cdot R_h \cdot F_{yc} \right) = 50 \text{ ksi}$$

The smaller value of the calculated FLB and LTB resistances will be considered as the nominal compression flange flexure resistance as shown below.

$$F_{nc} := \min (F_{nc_FLB}, F_{nc_LTB}) = 50 \text{ ksi}$$

At the strength limit state, the following requirement shall be satisfied:

$$f_{bu} + \frac{1}{3} f_t \leq \phi_f F_{nc} \quad (6.10.8.1.1-1)$$

The strength I bottom flange stress (compression).

For design checks where the flexural resistance is based on lateral-torsional buckling:

- The stress f_{bu} shall be determined as the largest value of the compressive stress throughout the unbraced length in the flange under consideration, calculated without consideration of flange lateral bending.

$$f_{bu_b} := -1 \left(\frac{1.25 \cdot M_{dc1_inter}}{S_{bx2}} + \frac{1.25 \cdot M_{dc2_inter} + 1.50 M_{dw_inter}}{S_{bx2}} \downarrow + \frac{1.75 \cdot HL_93_M_{dist_inter}}{S_{bx2}} \right) = 38.74 \text{ ksi}$$

Note: To make the stress positive, applied the negative sign

$$check := \text{if} (\text{abs}(f_{bu_b}) \leq F_{nc}, \text{"OK"}, \text{"NO"}) = \text{"OK"}$$

Strength I bottom flange performance ratio

$$PR_{StrengthI_bottom} := \frac{\text{abs}(f_{bu_b})}{F_{nc}} = 0.775$$

The continuously braced for the tension flange, and check the strength for the tension flange.

The strength I top flange stress (tension)

At the strength limit state, the following requirement shall be satisfied:

$$f_{bu} \leq \phi_f R_h F_{yf} \quad (6.10.8.1.3-1)$$

$$F_{nt} := R_h \cdot F_{yf} = 50 \text{ ksi}$$

$$f_{bu,t} := -1 \left(\frac{1.25 \cdot M_{dc1_inter}}{S_{tx2}} + \frac{1.25 \cdot M_{dc2_inter} + 1.50 M_{dw_inter}}{S_{tx2}} + \frac{1.75 \cdot HL_93_M_{dist_inter}}{S_{tx2}} \right) = 38.74 \text{ ksi}$$

Note: To make the stress positive, applied the negative sign

$$check := \text{if}(f_{bu,t} \leq F_{nt}, \text{"OK"}, \text{"NO"}) = \text{"OK"}$$

Strength I top flange performance ratio

$$PR_{StrengthI_top} := \frac{\text{abs}(f_{bu,t})}{F_{nt}} = 0.775$$

7. Shear Strength I Check at the end beam support (end panel) and interior support location at the interior span side (interior panel) (LRFD BDS Article 6.10.9)

6.10.9.1—General

At the strength limit state, straight and curved web panels shall satisfy:

$$V_u \leq \phi_v V_n \tag{6.10.9.1-1}$$

where:

ϕ_v = resistance factor for shear specified in [Article 6.5.4.2](#)

V_n = nominal shear resistance determined as specified in [Articles 6.10.9.2](#) and [6.10.9.3](#) for unstiffened and stiffened webs, respectively (kip)

V_u = factored shear in the web at the section under consideration (kip)

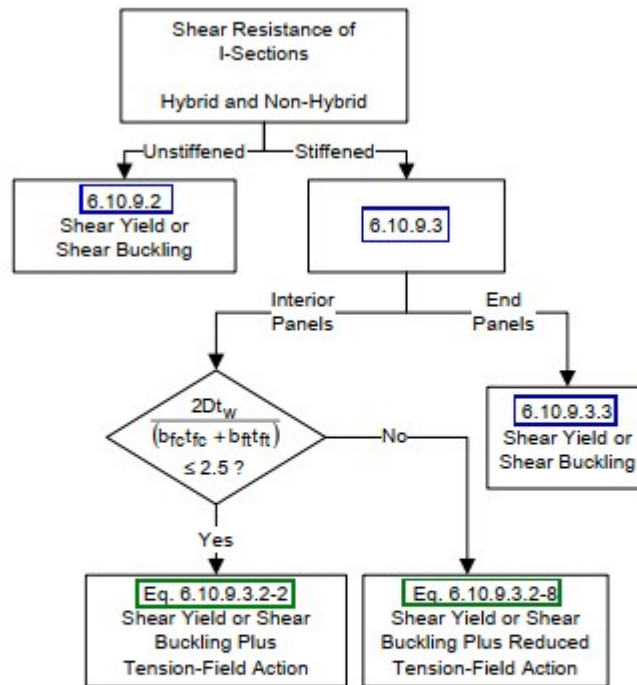


Figure C6.10.9.1-1—Flowchart for Shear Design of I-Sections

End beam support location

Web Panel: End Panel; Transversely Stiffened: Yes; Longitudinally Stiffened : No

Transverse stiffener spacing (in.) $d_o := 172.8 \text{ in}$

End web panels of nonhybrid and hybrid I-shaped members:

- With or without one or more longitudinal stiffeners and with a transverse stiffener spacing not exceeding $1.5D$

$check := \text{if}(d_o \leq 1.5 D, \text{“Stiffened”}, \text{“Unstiffened”}) = \text{“Unstiffened”}$

6.10.9.3.3—End Panels

The nominal shear resistance of a stiffened web end panel shall be taken as:

$$V_n = V_{cr} = C V_p \tag{6.10.9.3.3-1}$$

in which:

$$V_p = 0.58 F_{yw} D t_w \tag{6.10.9.3.3-2}$$

where:

C = ratio of the shear-buckling resistance to the shear yield strength determined by Eqs. 6.10.9.3.2-4, 6.10.9.3.2-5, or 6.10.9.3.2-6 as applicable

V_{cr} = shear-yielding or shear-buckling resistance (kip)

V_p = plastic shear force (kip)

The ratio, C , shall be determined as specified below:

- If $\frac{D}{t_w} \leq 1.12 \sqrt{\frac{Ek}{F_{yw}}}$, then:

$$C = 1.0 \tag{6.10.9.3.2-4}$$

- If $1.12 \sqrt{\frac{Ek}{F_{yw}}} < \frac{D}{t_w} \leq 1.40 \sqrt{\frac{Ek}{F_{yw}}}$, then:

$$C = \frac{1.12}{\frac{D}{t_w}} \sqrt{\frac{Ek}{F_{yw}}} \quad (6.10.9.3.2-5)$$

- If $\frac{D}{t_w} > 1.40 \sqrt{\frac{Ek}{F_{yw}}}$, then:

$$C = \frac{1.57}{\left(\frac{D}{t_w}\right)^2} \left(\frac{Ek}{F_{yw}}\right) \quad (6.10.9.3.2-6)$$

in which:

$$\begin{aligned} k &= \text{shear-buckling coefficient} \\ &= 5 + \frac{5}{\left(\frac{d_o}{D}\right)^2} \end{aligned} \quad (6.10.9.3.2-7)$$

Otherwise, the nominal shear resistance shall be taken as follows:

$$V_n = V_p \left[C + \frac{0.87(1-C)}{\left(\sqrt{1 + \left(\frac{d_o}{D}\right)^2} + \frac{d_o}{D}\right)} \right] \quad (6.10.9.3.2-8)$$

Shear-buckling coefficient

$$k := 5 + \frac{5}{\left(\frac{d_o}{D}\right)^2} = 5.187$$

$\frac{D}{t_w}$ ratio

$$\frac{D}{t_w} = 43.921$$

Ratio of the shear-buckling
resistance to the shear yield strength

$$C := \begin{cases} \frac{D}{t_w} \leq 1.12 \cdot \sqrt{\frac{E \cdot k}{F_{yw}}} & = 1 \\ 1 \\ \text{also if } 1.12 \cdot \sqrt{\frac{E \cdot k}{F_{yw}}} \leq \frac{D}{t_w} \leq 1.40 \cdot \sqrt{\frac{E \cdot k}{F_{yw}}} \\ \frac{1.12}{\frac{D}{t_w}} \cdot \sqrt{\frac{E \cdot k}{F_{yw}}} \\ \text{else} \\ \frac{1.57}{\left(\frac{D}{t_w}\right)^2} \cdot \frac{E \cdot k}{F_{yw}} \end{cases}$$

Plastic shear force

$$V_p := 0.58 \cdot F_{yw} \cdot D \cdot t_w = 735.695 \text{ kip}$$

Nominal shear resistance for the web panel

$$V_{n_end} := C \cdot V_p$$

Phi factor for steel bridge shear

$$\phi := 1.0$$

Factored shear resistance

$$\phi \cdot V_{n_end} = 735.7 \text{ kip}$$

$$V_{u_end} := 1.25 \cdot (V_{dc1_end} + V_{dc2_end}) + 1.5 \cdot V_{dw_end} + 1.75 \cdot HL_{93} V_{dist_end} = 189.3 \text{ kip}$$

$$check_shear_at_the_critical := \text{if}(\phi \cdot V_{n_end} > V_{u_end}, \text{"OK"}, \text{"NG"}) = \text{"OK"}$$

Demand/capacity ratio for shear

$$DCR := \frac{V_{u_end}}{\phi \cdot V_{n_end}} = 0.257$$

Interior support location

Web Panel: Interior Panel; Transversely Stiffened: Yes; Longitudinally Stiffened : No

Transverse stiffener spacing (in.) $d_o := 157.2 \text{ in}$

Interior web panels of nonhybrid and hybrid I-shaped members:

- without a longitudinal stiffener and with a transverse stiffener spacing not exceeding $3D$, or
- with one or more longitudinal stiffeners and with a transverse stiffener spacing not exceeding $2D$

$check := \text{if}(d_o \leq 3 D, \text{“Stiffened”}, \text{“Unstiffened”}) = \text{“Unstiffened”}$

6.10.9.2—Nominal Resistance of Unstiffened Webs

The nominal shear resistance of unstiffened webs shall be taken as the shear-yielding or shear-buckling resistance as follows:

$$V_n = V_{cr} = C V_p \tag{6.10.9.2-1}$$

in which:

$$V_p = 0.58 F_{yw} D t_w \tag{6.10.9.2-2}$$

where:

- C = ratio of the shear-buckling resistance to the shear yield strength determined by [Eqs. 6.10.9.3.2-4](#), [6.10.9.3.2-5](#) or [6.10.9.3.2-6](#) as applicable, with the shear-buckling coefficient, k , taken equal to 5.0
- V_{cr} = shear-yielding or shear-buckling resistance (kip)
- V_n = nominal shear resistance (kip)
- V_p = plastic shear force (kip)

The ratio, C , shall be determined as specified below:

- If $\frac{D}{t_w} \leq 1.12 \sqrt{\frac{Ek}{F_{yw}}}$, then:

$$C = 1.0 \quad (6.10.9.3.2-4)$$

- If $1.12 \sqrt{\frac{Ek}{F_{yw}}} < \frac{D}{t_w} \leq 1.40 \sqrt{\frac{Ek}{F_{yw}}}$, then:

$$C = \frac{1.12}{\frac{D}{t_w}} \sqrt{\frac{Ek}{F_{yw}}} \quad (6.10.9.3.2-5)$$

- If $\frac{D}{t_w} > 1.40 \sqrt{\frac{Ek}{F_{yw}}}$, then:

$$C = \frac{1.57}{\left(\frac{D}{t_w}\right)^2} \left(\frac{Ek}{F_{yw}}\right) \quad (6.10.9.3.2-6)$$

Shear-buckling coefficient
(C.6.10.9.2 for unstiffened web)

$$k := 5$$

$\frac{D}{t_w}$ ratio

$$\frac{D_2}{t_{w2}} = 41.725$$

Ratio of the shear-buckling
resistance to the shear yield strength

$$C := \begin{cases} \text{if } \frac{D_2}{t_{w2}} \leq 1.12 \cdot \sqrt{\frac{E \cdot k}{F_{yw}}} & = 1 \\ \parallel 1 \\ \text{also if } 1.12 \cdot \sqrt{\frac{E \cdot k}{F_{yw}}} \leq \frac{D_2}{t_{w2}} \leq 1.40 \cdot \sqrt{\frac{E \cdot k}{F_{yw}}} & \\ \parallel \frac{1.12}{\frac{D_2}{t_{w2}}} \cdot \sqrt{\frac{E \cdot k}{F_{yw}}} & \\ \parallel \frac{D_2}{t_{w2}} & \\ \text{else} & \\ \parallel \frac{1.57}{\left(\frac{D_2}{t_{w2}}\right)^2} \cdot \frac{E \cdot k}{F_{yw}} & \end{cases}$$

Plastic shear force

$$V_{p_inter} := 0.58 \cdot F_{yw} \cdot D \cdot t_{w2} = 774.4 \text{ kip}$$

Nominal shear resistance

$$V_{n_inter} := C \cdot V_{p_inter} = 774.4 \text{ kip}$$

Phi factor for steel bridge shear

$$\phi := 1.0$$

Factored shear resistance

$$\phi \cdot V_{n_inter} = 774.42 \text{ kip}$$

Factored shear demand at the interior support on the mid span side

$$V_{u_inter} := 1.25 \cdot (V_{dc1_inter} + V_{dc2_inter}) + 1.5 \cdot V_{dw_inter} + 1.75 \cdot HL_{93} V_{dist_inter} = 285.025 \text{ kip}$$

$$check_shear_at_the_critical := \text{if} (\phi \cdot V_{n_inter} > V_{u_inter}, \text{"OK"}, \text{"NG"}) = \text{"OK"}$$

Demand/capacity ratio for shear

$$DCR := \frac{V_{u_inter}}{\phi \cdot V_{n_inter}} = 0.368$$

8. Load Effects and Resistance Summary

Here is the summary for load effects and bridge resistances.

Load Effects Summary

Load effects (M(kip-ft), and V(kip))	HL-93 Design Loading (with $IM = 0.33$ and GDF_m)	DNC	DC
Moment (at 0.4L of the end span)	939.1	175.8	13.6
Moment (at 0.5L of the interior span)	1278.0	648.9	47.4
Positive Moment (at 52.4 ft to the left interior support of the interior span side)	1278.1	645.6	47.2
Negative Moment (at 52.4 ft to the left interior support of the interior span side)	-140.9		
Moment (at the interior support)	-947.7	-933.7	-50.8
Shear (at the beam end support)	91.1	22.4	1.5
Shear (at the interior support of the interior span side)	114.8	63.4	3.9

Load effects (M(kip-ft), and V(kip))	AASHTO Fatigue Truck (with $IM = 0.15$ and $GDF_s / 1.2$)	Four-truck Platoons (5-ft NRL) (with $IM = 0.33$ and $GDF_s / 1.2$)	Four-truck Platoons (50-ft NRL) (with $IM = 0.33$ and $GDF_s / 1.2$)
Moment (at 0.4L of the end span)	283.1	559.3	510.9
Moment (at 0.5L of the interior span)	376.0	888.7	570.8
Positive Moment (at 52.4 ft to the left interior support of the interior span side)	380.2	889.4	572.2
Negative Moment (at 52.4 ft to the left interior support of the interior span side)	-33.8	-76.1	-59.3
Moment (at the interior support)	-247.8	-837.9	-482.3
Shear (at the beam end support)	34.5	64.3	49.3
Shear (at the interior support of the interior span side)	43.3	109.3	63.0

Resistance Summary

	Resistance (with ϕ) (M (kip-ft) and V (kip))
Strength I Moment (at 0.4L of the end span)	5481.2
Strength I Moment (at 0.5L of the interior span)	5481.2
Strength I Shear (at the beam end support)	735.7
Strength I Shear (at the interior support of the interior span side)	774.4

	Resistance (with ϕ) F_n (ksi)
Strength I Flexural Stress (at the interior support)	50.0
Service II Flexural Stress (at 0.4L of the end span)	47.5
Service II Flexural Stress (at 0.5L of the interior span)	47.5
Service II Flexural Stress (at the interior support)	47.5

9. Load Rating: Design Load Rating for Moment and Shear

$$RF = \frac{(\varphi_c)(\varphi_s)(\varphi)R_n - (\gamma_{DC})(DC) - (\gamma_{DW})(DW)}{(\gamma_L)(LL + IM)}$$

A3.13.2.1a—Inventory Level

Load	Load Factor
DC	1.25
DW	1.50 Overlay thickness was not field measured.
LL	1.75

Moment load rating at the 0.4L of end span (inventory and operating level)

Parameter information for the equation below.

$$M_{n_end} = 5481.171 \text{ kip} \cdot \text{ft}$$

$$g_{m2_end} = 0.798$$

$$M_{dc1_end} = 175.8 \text{ kip} \cdot \text{ft}$$

$$M_{dc2_end} = 13.6 \text{ kip} \cdot \text{ft}$$

$$M_{dw_end} = 0 \text{ kip} \cdot \text{ft}$$

$$HL_{93}M_{dist_end} = 939.1 \text{ kip} \cdot \text{ft}$$

Rating factor at the inventory level

$$RF_{inv_end} := \frac{(1.0) \cdot M_{n_end} - 1.25 \cdot (M_{dc1_end} + M_{dc2_end}) - 1.50 \cdot M_{dw_end}}{1.75 \cdot (HL_{93}M_{dist_end})} = 3.191$$

Rating factor at the operating level

For Strength I Operating Level only the live load factor changes; therefore the rating factor can be calculated by direct proportions.

Load	Load Factor, γ
DC	1.25
DW	1.50
LL	1.35

$$RF_{ope_end} := RF_{inv_end} \cdot \frac{1.75}{1.35} = 4.137$$

Moment load rating at the 0.5L of the interior span (inventory and operating level)

Parameter information for the equation below.

$$M_{n_mid} = 5481.171 \text{ kip} \cdot \text{ft}$$

$$g_{m2_mid} = 0.696$$

$$M_{dc1_mid} = 648.9 \text{ kip} \cdot \text{ft}$$

$$M_{dc2_mid} = 47.4 \text{ kip} \cdot \text{ft}$$

$$M_{dw_mid} = 0 \text{ kip} \cdot \text{ft}$$

$$HL_93_M_{dist_mid} = 1278 \text{ kip} \cdot \text{ft}$$

Rating factor at the inventory level

$$RF_{inv_mid} := \frac{(1.0) \cdot M_{n_mid} - 1.25 \cdot (M_{dc1_mid} + M_{dc2_mid}) - 1.50 \cdot M_{dw_mid}}{1.75 \cdot (HL_93_M_{dist_mid})} = 2.062$$

Rating factor at the operating level

$$RF_{ope_mid} := RF_{inv_mid} \cdot \frac{1.75}{1.35} = 2.672$$

Moment load rating at the interior support (inventory and operating level)

Parameter information for the equation below. The bottom flange is rated here.

$$F_{nc} = 50 \text{ ksi}$$

$$g_{m2_inter} = 0.743$$

$$M_{dc1_inter} = -933.7 \text{ kip} \cdot \text{ft}$$

$$M_{dc2_inter} = -50.8 \text{ kip} \cdot \text{ft}$$

$$M_{dw_inter} = 0 \text{ kip} \cdot \text{ft}$$

$$HL_93_M_{dist_inter} = -947.7 \text{ kip} \cdot \text{ft}$$

$$S_{bx2} = 895 \text{ in}^3$$

Rating factor at the inventory level

$$RF_{inv_inter} := \frac{(1.0) \cdot F_{nc} - 1.25 \cdot \text{abs} \left(\frac{M_{dc1_inter}}{S_{bx2}} + \frac{M_{dc2_inter}}{S_{bx2}} \right) - 1.50 \cdot \text{abs} \left(\frac{M_{dw_inter}}{S_{bx2}} \right)}{1.75 \cdot \text{abs} \left(\frac{HL_93_M_{dist_inter}}{S_{bx2}} \right)} = 1.507$$

Rating factor at the operating level

$$RF_{ope_inter} := RF_{inv_inter} \cdot \frac{1.75}{1.35} = 1.953$$

Shear load rating at the beam end support (inventory and operating level)

Parameter information for the equation below.

$$V_{n_end} = 735.695 \text{ kip}$$

$$g_{v2} = 0.941$$

$$V_{dc1_end} = 22.4 \text{ kip}$$

$$V_{dc2_end} = 1.5 \text{ kip}$$

$$V_{dw_end} = 0 \text{ kip}$$

$$HL_93_V_{dist_end} = 91.1 \text{ kip}$$

Rating factor at the inventory level

$$RF_{invV} := \frac{(1.0) \cdot V_{n_end} - 1.25 \cdot (V_{dc1_end} + V_{dc2_end}) - 1.50 \cdot V_{dw_end}}{1.75 \cdot (HL_93_V_{dist_end})} = 4.427$$

Rating factor at the operating level

$$RF_{opeV} := RF_{invV} \cdot \frac{1.75}{1.35} = 5.739$$

Shear load rating at the interior support of the interior span side (inventory and operating level)

Parameter information for the equation below.

$$V_{n_inter} = 774.416 \text{ kip}$$

$$g_{v2} = 0.941$$

$$V_{dc1_inter} = 63.4 \text{ kip}$$

$$V_{dc2_inter} = 3.9 \text{ kip}$$

$$V_{dw_inter} = 0 \text{ kip}$$

$$HL_93_V_{dist_inter} = 114.8 \text{ kip}$$

Rating factor at the inventory level

$$RF_{invV} := \frac{(1.0) \cdot V_{n_inter} - 1.25 \cdot (V_{dc1_inter} + V_{dc2_inter}) - 1.50 \cdot V_{dw_inter}}{1.75 \cdot (HL_93_V_{dist_inter})} = 3.436$$

Rating factor at the operating level

$$RF_{opeV} := RF_{invV} \cdot \frac{1.75}{1.35} = 4.454$$

10. Load Rating for Service II Limit State

For Service Limit States, $C = f_R$

6A.4.2.1

$$RF = \frac{f_R - (\gamma_D)(f_D)}{(\gamma_L)(f_{LL+IM})}$$

$$\gamma_D = \gamma_{DC} = \gamma_{DW} = 1.0$$

Table 6A.4.2.2-1

$$\gamma_L = 1.3 \text{ for Inventory}$$

$$= 1.0 \text{ for Operating}$$

Service II moment rating at the 0.4L of end span (inventory and operating level)

Resistance stress

$$f_R := 0.95 \cdot R_h \cdot F_{yf} = 47.5 \text{ ksi}$$

Determine dead load stress at 0.4L of end span

$$f_{DC} := \frac{M_{dc1_end}}{S_{bx}} + \frac{M_{dc2_end}}{S_{b_lt}} = 2.678 \text{ ksi}$$

Determine wearing dead load stress at 0.4L of end span $f_{DW} := \frac{M_{dw_end}}{S_{b_lt}} = 0 \text{ ksi}$

Total dead load stress at 0.4L of end span

$$f_D := f_{DC} + f_{DW} = 2.678 \text{ ksi}$$

Live load stress at 0.4L of end span

$$f_{LL} := \frac{(HL_{93} M_{dist_end})}{S_{b_st}} = 10.012 \text{ ksi}$$

Rating factor for Service II
(inventory level)

$$RF_{ServiceIIinv} := \frac{f_R - f_D}{1.30 \cdot f_{LL}} = 3.444$$

Rating factor for Service II
(operating level)

$$RF_{ServiceIIopr} := \frac{f_R - f_D}{1.00 \cdot f_{LL}} = 4.477$$

Service II moment rating at the 0.5L of mid span (inventory and operating level)

Resistance stress

$$f_R := 0.95 \cdot R_h \cdot F_{yf} = 47.5 \text{ ksi}$$

Determine dead load stress at 0.5L of the interior span

$$f_{DC} := \frac{M_{dc1_mid}}{S_{bx}} + \frac{M_{dc2_mid}}{S_{b_lt}} = 9.853 \text{ ksi}$$

Determine wearing dead load stress at 0.5L of the interior span

$$f_{DW} := \frac{M_{dw_mid}}{S_{b_lt}} = 0 \text{ ksi}$$

Total dead load stress at 0.5L of the interior span

$$f_D := f_{DC} + f_{DW} = 9.853 \text{ ksi}$$

Live load stress at 0.5L of the interior span

$$f_{LL} := \frac{(HL_{93} M_{dist_mid})}{S_{b_st}} = 13.625 \text{ ksi}$$

Rating factor for Service II (inventory level)

$$RF_{ServiceIIinv} := \frac{f_R - f_D}{1.30 \cdot f_{LL}} = 2.125$$

Rating factor for Service II (operating level)

$$RF_{ServiceIIopr} := \frac{f_R - f_D}{1.00 \cdot f_{LL}} = 2.763$$

Service II moment rating at the interior support (inventory and operating level)

Resistance stress

$$f_R := 0.95 \cdot R_h \cdot F_{yf} = 47.5 \text{ ksi}$$

Determine dead load stress at the interior support

$$f_{DC} := \frac{M_{dc1_inter}}{S_{bx2}} + \frac{M_{dc2_inter}}{S_{bx2}} = -13.2 \text{ ksi}$$

Determine wearing dead load stress at the interior support

$$f_{DW} := \frac{M_{dw_inter}}{S_{bx2}} = 0 \text{ ksi}$$

Total dead load stress at the interior support

$$f_D := f_{DC} + f_{DW} = -13.2 \text{ ksi}$$

Live load stress at the interior support

$$f_{LL} := \frac{\langle HL_{93} M_{dist_inter} \rangle}{S_{bx2}} = -12.707 \text{ ksi}$$

Rating factor for Service II
(inventory level)

$$RF_{ServiceIIinv} := \frac{f_R - \text{abs}(f_D)}{1.30 \cdot \text{abs}(f_{LL})} = 2.076$$

Rating factor for Service II
(operating level)

$$RF_{ServiceIIopr} := \frac{f_R - \text{abs}(f_D)}{1.00 \cdot \text{abs}(f_{LL})} = 2.699$$

11. Load Rating for Strength I Limit State Platoon (target beta = 2.5)

4-truck Platoons (NRL with 5 ft headways): single lane platoon mixed with traffic, $CoV = 0.20$ (100 crossings, ADTT = 5000)

Proposed Strength Calibrated LL Factors for the Target $\beta = 2.5$ (Steelman et al., 2021) (Table 2)

Truck Platoon	Frequency	Loading Condition	DF	ADTT (One direction)	Live load factors by CoV of total live load				
					$CoV_{LL} = 0$	$CoV_{LL} = 0.05$	$CoV_{LL} = 0.1$	$CoV_{LL} = 0.15$	$CoV_{LL} = 0.2$
Multiple Trucks in Platoon	Single-trip	No other vehicles on the bridge	One lane	NA	1.00	1.05	1.10	1.20	1.25
	Single-trip	Two identical platoons loaded on two lanes	Two or more lanes	NA	1.00	1.05	1.10	1.20	1.25
	10 Crossings	Mixed with routine traffic in the adjacent lane	One lane	> 5000	1.35	1.35	1.40	1.45	1.55
				1000	1.35	1.35	1.40	1.45	1.50
				< 100	1.35	1.35	1.40	1.45	1.50
	100 Crossings	Mixed with routine traffic in the adjacent lane	One lane	> 5000	1.35	1.40	1.45	1.50	1.60
				1000	1.35	1.40	1.45	1.45	1.55
				< 100	1.35	1.35	1.45	1.45	1.55

Moment load rating at the 0.4L of end span

Platoon weight divided by 80 kips
(amplification factor alpha)

$$W_{platoon} := 1.0$$

Assumed $IM = 0.33$ (same as MBE permit load rating)

$$IM_{surface} := 33\%$$

5 ft headway 4-truck platoon moment at the 0.4L of end span from the above load effect table:
(with $IM = 0.33$ and single lane moment GDF (g_{m1}) and removed 1.2 multiple presence factor)

$$LL_{platoon_legal_end} := 559.3 \text{ kip} \cdot \text{ft}$$

5 ft headway 4-truck platoon moment at the 0.4L of end span (with amplification factor alpha)

$$LL_{platoon_legal_end} := W_{platoon} \cdot LL_{platoon_legal_end} = 559.3 \text{ kip} \cdot \text{ft}$$

Platoon calibrated live load factor (the value in the red box as shown above Table)

$$\gamma_{platoon_strength} := 1.60$$

Parameter information for the equation below.

$$M_{n_end} = 5481.171 \text{ kip} \cdot \text{ft}$$

$$g_{m1_end} = 0.573$$

$$M_{dc1_end} = 175.8 \text{ kip} \cdot \text{ft}$$

$$M_{dc2_end} = 13.6 \text{ kip} \cdot \text{ft}$$

$$M_{dw_end} = 0 \text{ kip} \cdot \text{ft}$$

$$LL_{platoon_legal_end} = 559.3 \text{ kip} \cdot \text{ft}$$

$$RF_{PL_end} := \frac{(1.0) \cdot M_{n_end} - 1.25 \cdot (M_{dc1_end} + M_{dc2_end}) - 1.50 \cdot M_{dw_end}}{\gamma_{platoon_strength} \cdot (LL_{platoon_legal_end})} = 5.86$$

Moment load rating at the 0.5L of the interior span

5 ft headway 4-truck platoon moment at the 0.5L of the interior span from the above load effect table: (with $IM = 0.33$ and single lane moment GDF (g_{m1}) and removed 1.2 multiple presence factor)

$$LL_{platoon_legal_mid} := 888.7 \text{ kip} \cdot \text{ft}$$

5 ft headway 4-truck platoon moment at the mid span (with amplification factor alpha)

$$LL_{platoon_legal_mid} := W_{platoon} \cdot LL_{platoon_legal_mid} = 888.7 \text{ kip} \cdot \text{ft}$$

Parameter information for the equation below.

$$M_{n_mid} = 5481.171 \text{ kip} \cdot \text{ft}$$

$$g_{m1_mid} = 0.478$$

$$M_{dc1_mid} = 648.9 \text{ kip} \cdot \text{ft}$$

$$M_{dc2_mid} = 47.4 \text{ kip} \cdot \text{ft}$$

$$M_{dw_mid} = 0 \text{ kip} \cdot \text{ft}$$

$$LL_{platoon_legal_mid} = 888.7 \text{ kip} \cdot \text{ft}$$

$$RF_{PL_mid} := \frac{(1.0) \cdot M_{n_mid} - 1.25 \cdot (M_{dc1_mid} + M_{dc2_mid}) - 1.50 \cdot M_{dw_mid}}{\gamma_{platoon_strength} \cdot (LL_{platoon_legal_mid})} = 3.243$$

Moment load rating at the interior support

5 ft headway 4-truck platoon moment at the interior support from the above load effect table:
(with $IM = 0.33$ and single lane moment GDF (g_{m1}) and removed 1.2 multiple presence factor)

$$LL_{platoon_legal_inter} := -837.9 \text{ kip} \cdot \text{ft}$$

5 ft headway 4-truck platoon moment at the interior support (with amplification factor alpha)

$$LL_{platoon_legal_inter} := W_{platoon} \cdot LL_{platoon_legal_inter} = -837.9 \text{ kip} \cdot \text{ft}$$

Parameter information for the equation below. The bottom flange is rated here.

$$F_{nc} = 50 \text{ ksi}$$

$$g_{m2_inter} = 0.743$$

$$M_{dc1_inter} = -933.7 \text{ kip} \cdot \text{ft}$$

$$M_{dc2_inter} = -50.8 \text{ kip} \cdot \text{ft}$$

$$M_{dw_inter} = 0 \text{ kip} \cdot \text{ft}$$

$$LL_{platoon_legal_inter} = -837.9 \text{ kip} \cdot \text{ft}$$

$$S_{bx2} = 895 \text{ in}^3$$

$$RF_{PL_inter} := \frac{(1.0) \cdot F_{nc} - 1.25 \cdot \text{abs} \left(\frac{M_{dc1_inter}}{S_{bx2}} + \frac{M_{dc2_inter}}{S_{bx2}} \right) - 1.50 \cdot \text{abs} \left(\frac{M_{dw_inter}}{S_{bx2}} \right)}{\gamma_{platoon_strength} \cdot \text{abs} \left(\frac{LL_{platoon_legal_inter}}{S_{bx2}} \right)} = 1.864$$

Shear Rating for 4-truck Platoons (NRL with 5 ft headways): single lane platoon mixed with traffic, $CoV = 0.20$ (100 crossings, ADTT = 5000)

5 ft headway 4-truck platoon shear at the beam end support from the above load effect table: (with $IM = 0.33$ and single lane moment GDF (g_{v1}) and removed 1.2 multiple presence factor)

$$V_{PL_legal_end} := 64.3 \text{ kip}$$

5 ft headway 4-truck platoon shear at the beam end support (with amplification factor alpha)

$$V_{PL_legal_end} := W_{platoon} \cdot V_{PL_legal_end} = 64.3 \text{ kip}$$

Shear load rating for the beam end support

Parameter information for the equation below.

$$V_{n_end} = 735.695 \text{ kip}$$

$$g_{v1} = 0.753$$

$$V_{dc1_end} = 22.4 \text{ kip}$$

$$V_{dw_end} = 0 \text{ kip}$$

$$V_{dc2_end} = 1.5 \text{ kip}$$

$$RF_{PLv} := \frac{(1.0) \cdot V_{n_end} - 1.25 \cdot (V_{dc1_end} + V_{dc2_end}) - 1.50 \cdot V_{dw_end}}{\gamma_{platoon_strength} \cdot (V_{PL_legal_end})} = 6.861$$

5 ft headway 4-truck platoon shear at the interior support from the above load effect table: (with $IM = 0.33$ and single lane moment GDF (g_{v1}) and removed 1.2 multiple presence factor)

$$V_{PL_legal_inter} := 109.3 \text{ kip}$$

5 ft headway 4-truck platoon shear at the interior support (with amplification factor alpha)

$$V_{PL_legal_inter} := W_{platoon} \cdot V_{PL_legal_inter} = 109.3 \text{ kip}$$

Shear load rating for the interior support

Parameter information for the equation below.

$$V_{n_inter} = 774.416 \text{ kip}$$

$$g_{v1} = 0.753$$

$$V_{dc1_inter} = 63.4 \text{ kip}$$

$$V_{dw_inter} = 0 \text{ kip}$$

$$V_{dc2_inter} = 3.9 \text{ kip}$$

$$RF_{PLv} := \frac{(1.0) \cdot V_{n_inter} - 1.25 \cdot (V_{dc1_inter} + V_{dc2_inter}) - 1.50 \cdot V_{dw_inter}}{\gamma_{platoon_strength} \cdot (V_{PL_legal_inter})} = 3.947$$

12. Load Rating for Service II Limit State Platoon (target beta = 1.60)

4-truck Platoons (NRL with 5 ft headways): single lane platoon mixed with traffic, $CoV = 0.20$ (100 crossings, ADTT = 5000)

Proposed Service II Calibrated LL Factors for the Target $\beta = 1.6$ (Table 22)

Truck platoon	Frequency	Load conditions	DF	ADTT (one direction)	Load factors by CoV of total live load
					$COV_{LL} = 0 - 0.20$
Multiple trucks in platoon	single-trip	No other vehicles on the bridge	One lane	N/A	1.15
	single-trip	Two identical platoons loaded on two lanes	Two or more lanes	N/A	1.15
	100 Crossings	Mixed with routine traffic in the adjacent lane	One lane	> 5000	1.90

Platoon calibrated live load factor (the value in the red box as shown above Table)

$$\gamma_{platoon_service} := 1.90$$

Service II moment load rating at the 0.4L of end span

Live load stress at the 0.4L of the end span for the platoon

$$f_{platoon_end} := \frac{\langle LL_{platoon_legal_end} \rangle}{S_{b_st}} = 5.963 \text{ ksi}$$

Parameter information for the equation below.

$$f_{DC} := \frac{M_{dc1_end}}{S_{bx}} + \frac{M_{dc2_end}}{S_{b_lt}} = 2.678 \text{ ksi} \quad f_{DW} := \frac{M_{dw_end}}{S_{b_lt}} = 0 \text{ ksi} \quad f_D := f_{DC} + f_{DW} = 2.678 \text{ ksi}$$

$$f_R = 47.5 \text{ ksi}$$

Rating factor for Service II

$$RF_{PL_SVII_end} := \frac{f_R - f_D}{\gamma_{platoon_service} \cdot \frac{\langle LL_{platoon_legal_end} \rangle}{S_{b_st}}} = 3.956$$

Service II moment load rating at the 0.5L of the interior span

Live load stress at the 0.5L of the interior span for the platoon

$$f_{platoon_mid} := \frac{(LL_{platoon_legal_mid})}{S_{b_st}} = 9.475 \text{ ksi}$$

Parameter information for the equation below.

$$f_{DC} := \frac{M_{dc1_mid}}{S_{bx}} + \frac{M_{dc2_mid}}{S_{b_lt}} = 9.853 \text{ ksi} \quad f_{DW} := \frac{M_{dw_mid}}{S_{b_lt}} = 0 \text{ ksi} \quad f_D := f_{DC} + f_{DW} = 9.853 \text{ ksi}$$

$$f_R = 47.5 \text{ ksi}$$

Rating factor for Service II

$$RF_{PL_SVII_mid} := \frac{f_R - f_D}{\gamma_{platoon_service} \cdot \frac{(LL_{platoon_legal_mid})}{S_{b_st}}} = 2.091$$

Service II moment load rating at the interior support (apply live load factors calibrated based on positive moment regions)

Live load stress at the interior support for the platoon

$$f_{platoon_inter} := \frac{(LL_{platoon_legal_inter})}{S_{bx2}} = -11.234 \text{ ksi}$$

Parameter information for the equation below.

$$f_{DC} := \frac{M_{dc1_inter}}{S_{bx2}} + \frac{M_{dc2_inter}}{S_{bx2}} = -13.2 \text{ ksi} \quad f_{DW} := \frac{M_{dw_inter}}{S_{bx2}} = 0 \text{ ksi}$$

$$f_D := f_{DC} + f_{DW} = -13.2 \text{ ksi} \quad f_R = 47.5 \text{ ksi}$$

Rating factor for Service II

$$RF_{PL_SVII_inter} := \frac{f_R - \text{abs}(f_D)}{\gamma_{platoon_service} \cdot \frac{\text{abs}(LL_{platoon_legal_inter})}{S_{bx2}}} = 1.607$$

13. Load Rating Summary

Load rating summary table is given below.

Limit state	Design load rating		Platoon load rating
	Inventory	Operating	(Strength I $\beta_{target} = 2.5$ and Service II $\beta_{target} = 1.6$)
Strength I for design and platoon load rating			
Flexure (at 0.4L of the end span)	3.191	4.137	5.860
Flexure (at 0.5L of the interior span)	2.062	2.672	3.243
Flexure (at the interior support)	1.507	1.953	1.864
Shear (at the interior support)	4.427	5.739	6.861
Shear (at the interior support of the interior span side)	3.436	4.454	3.947
Service II			
Flexure (at 0.4L of the end span)	3.444	4.477	3.956
Flexure (at 0.5L of the interior span)	2.125	2.763	2.091
Flexure (at the interior support)	2.076	2.699	1.607

14. Fatigue Check for AASHTO Fatigue Truck

ADT information from NBI database is given below. This example investigates a welded cross-frame connection plate fatigue at the 52.6 ft (cross-frame location) to the interior support at the mid span (near the critical positive moment at the mid span).

ADT	$ADT := 48015$
Percentage of truck in ADT	$P_{truck} := 17\%$
ADTT	$ADTT := ADT \cdot P_{truck} = 8162.55$
Multiple presence factor for three design lanes (AASHTO Table 3.6.1.4.2-1)	$m_p := 0.80$
ADTT (single lane)	$ADTT_{SL} := ADTT \cdot m_p = 6530$

Table 6.6.1.2.3-1 (cont.)—Detail Categories for Load-Induced Fatigue

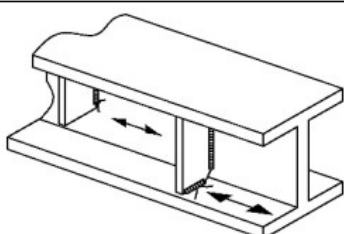
Section 4—Welded Stiffener Connections					
4.1 Base metal at the toe of transverse stiffener-to-flange fillet welds and transverse stiffener-to-web fillet welds. (Note: includes similar welds on bearing stiffeners and connection plates). Base metal adjacent to bearing stiffener-to-flange fillet welds or groove welds.	C'	44×10^8	12	Initiating from the geometrical discontinuity at the toe of the fillet weld extending into the base metal	

Table 6.6.1.2.3-2—75-year ($ADTT$)_{SL} Equivalent to Infinite Life

Detail Category	75-year ($ADTT$) _{SL} Equivalent to Infinite Life (trucks per day)
A	690
B	1120
B'	1350
C	1680
C'	975
D	2450
E	4615
E'	8485

ADTT (single lane threshold)

$$ADTT_{th} := 975$$

$$check := \text{if}(ADTT_{SL} > ADTT_{th}, \text{"Infinite"}, \text{"Finite"}) = \text{"Infinite"}$$

First, check the infinite life for this case. The constant amplitude fatigue limit for C' is 12 ksi as shown in Table 6.6.1.2.5-3.

Table 6.6.1.2.5-3—Constant-Amplitude Fatigue Thresholds

Detail Category	Threshold (ksi)
A	24.0
B	16.0
B'	12.0
C	10.0
C'	12.0
D	7.0
E	4.5
E'	2.6
ASTM F3125/F3125M, Grades A325 and F1852 Bolts in Axial Tension	31.0
ASTM F3125/F3125M, Grades A490 and F2280 Bolts in Axial Tension	38.0

Constant amplitude fatigue thresholds for C'

$$\Delta F_{n_fatigueI} := 12 \text{ ksi}$$

centroid y_{b_st} to the datum

$$y_{b_st} = 31.615 \text{ in}$$

bottom flange thickness

$$t_{bf} = 1.26 \text{ in}$$

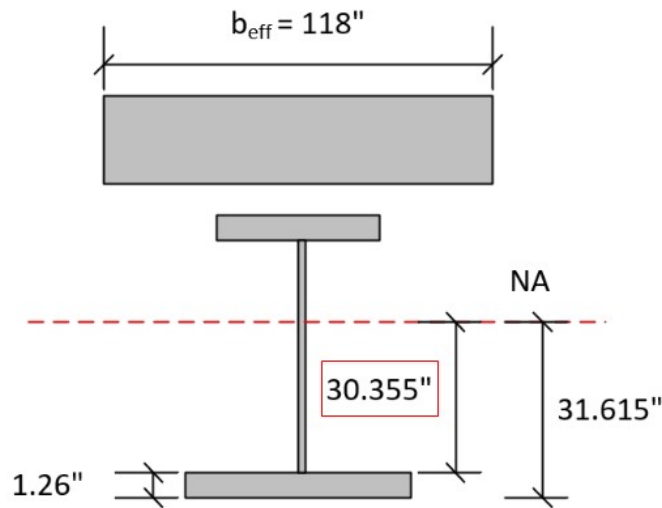
Determine the connection plate to the short-term NA

$$d_{plate} := y_{b_st} - t_{bf} = 30.355 \text{ in}$$

Moment of inertia (short-term)

$$I_{st} = 35584.739 \text{ in}^4$$

Also, the NA and appropriate dimensions are shown below.



6.6.1.2.2—Design Criteria

For load-induced fatigue considerations, each detail shall satisfy:

$$\gamma(\Delta f) \leq (\Delta F)_n \quad (6.6.1.2.2-1)$$

where:

- γ = load factor specified in [Table 3.4.1-1](#) for the fatigue load combination
- (Δf) = force effect, live load stress range due to the passage of the fatigue load as specified in [Article 3.6.1.4](#) (ksi)
- $(\Delta F)_n$ = nominal fatigue resistance as specified in [Article 6.6.1.2.5](#) (ksi)

Therefore, the stress range at the top of the bottom flange is found as follows:

Moment from live load analysis (AASHTO Fatigue truck at 52.6 ft cross-frame location with $GDF = \frac{g_{m1_mid}}{1.2}$ and including $IM = 0.15$)

$$M_{AASHTO_Fat} := 380.2 \text{ kip} \cdot \text{ft}$$

Negative Moment from live load analysis (AASHTO Fatigue truck at 52.6 ft cross-frame location with $GDF = \frac{g_{m1_mid}}{1.2}$ and including $IM = 0.15$)

$$M_{AASHTO_Fat_neg} := -33.8 \text{ kip} \cdot \text{ft}$$

Load factor for Fatigue I from LRFD Table 3.4.1-1 $\gamma_{fatigueI} := 1.75$

Live load stress range for AASHTO fatigue truck including $IM = 0.15$

$$\Delta f_{fatigue} := \frac{(M_{AASHTO_Fat} + \text{abs}(M_{AASHTO_Fat_neg})) \cdot d_{plate}}{I_{st}} = 4.238 \text{ ksi}$$

$$check_fatigueI := \text{if}(\gamma_{fatigueI} \cdot \Delta f_{fatigue} \leq \Delta F_{n_fatigueI}, \text{"OK"}, \text{"NG"}) = \text{"OK"}$$

Demand/capacity ratio for fatigue

$$DCR := \frac{\gamma_{fatigueI} \cdot \Delta f_{fatigue}}{\Delta F_{n_fatigueI}} = 0.618$$

Rating factor for fatigue

$$RF := \frac{1}{DCR} = 1.618$$

Note: The Fatigue I check for AASHTO fatigue truck check passes.

15. Fatigue Check for Platoons with 5 ft and 50 ft headways

For this example, evaluate the fatigue for a 4 NRL platoon with 5 ft and 50 ft headway spacing.

- For the Fatigue II load combination and finite life:

$$(\Delta F)_n = \left(\frac{A}{N}\right)^{\frac{1}{3}} \quad (6.6.1.2.5-2)$$

in which:

$$N = (365)(75)n(ADTT)_{sl} \quad (6.6.1.2.5-3)$$

where:

A = constant taken from [Table 6.6.1.2.5-1](#) (ksi³)

n = number of stress range cycles per truck passage taken from [Table 6.6.1.2.5-2](#)

$(ADTT)_{sl}$ = single-lane $ADTT$ as specified in [Article 3.6.1.4](#)

$(\Delta F)_{TH}$ = constant-amplitude fatigue threshold taken from [Table 6.6.1.2.5-3](#) (ksi)

Table 6.6.1.2.5-1—Detail Category Constant, A

Detail Category	Constant, A (ksi ³)
A	250.0×10^8
B	120.0×10^8
B'	61.0×10^8
C	44.0×10^8
C'	44.0×10^8
D	22.0×10^8
E	11.0×10^8
E'	3.9×10^8
ASTM F3125/F3125M, Grades A325 and F1852 Bolts in Axial Tension	17.1×10^8
ASTM F3125/F3125M, Grades A490 and F2280 Bolts in Axial Tension	31.5×10^8

Fatigue Check for Platoons with 5 ft

MBE Fatigue check for permit is not provided. In this example, firstly use the infinite life for checking this platoon case. The constant amplitude fatigue limit for C' is 12 ksi as shown in Table 6.6.1.2.5-3.

Therefore, the stress range at the top of the bottom flange is found as follows:

Positive Moment from live load analysis (4 NRL platoon with 5ft at 52.6 ft cross-frame location with $GDF = \frac{g_{m1_mid}}{1.2}$ and assumed the IM = 0.15 as the same for AASHTO Fatigue Truck)

$$M_{platoon_5ft_pos} := 889.4 \text{ kip} \cdot \text{ft} \cdot \frac{(1 + 0.15)}{(1 + 0.33)} = 769.03 \text{ kip} \cdot \text{ft}$$

Negative Moment from live load analysis

(4 NRL platoon with 5ft at 52.6 ft cross-frame location with $GDF = \frac{g_{m1_mid}}{1.2}$ and assumed the IM = 0.15 as the same for AASHTO Fatigue Truck)

$$M_{platoon_5ft_neg} := -76.1 \text{ kip} \cdot \text{ft} \cdot \frac{(1 + 0.15)}{(1 + 0.33)} = -65.801 \text{ kip} \cdot \text{ft}$$

Note the platoon was calculated with IM = 0.33 in the BrR for this rating example

Live load stress range for the platoon including IM = 0.15 (assume IM = 0.15 same as for AASHTO fatigue load)

$$\Delta f_{platoon_5ft} := \frac{(M_{platoon_5ft_pos} + \text{abs}(M_{platoon_5ft_neg})) \cdot d_{plate}}{I_{st}} = 8.5 \text{ ksi}$$

Platoon load factor for Fatigue I from LRFD Table 3.4.1-1 (assume the same as for AASHTO fatigue load)

$$\gamma_{fatigueI_platoon} := 1.75$$

$$check_fatigueI_PL := \text{if}(\gamma_{fatigueI_platoon} \cdot \Delta f_{platoon_5ft} \leq \Delta F_{n_fatigueI}, \text{"OK"}, \text{"NG"}) = \text{"NG"}$$

Demand/capacity ratio for platoon fatigue I

$$DCR := \frac{\gamma_{fatigueI_platoon} \cdot \Delta f_{platoon_5ft}}{\Delta F_{n_fatigueI}} = 1.246$$

Rating factor for fatigue

$$RF := \frac{1}{DCR} = 0.802$$

Note: The Fatigue I check for a four-truck platoon with 5 ft headway fails.

Fatigue II Check for Platoons with 5 ft headways

- For the Fatigue II load combination and finite life:

$$(\Delta F)_n = \left(\frac{A}{N}\right)^{\frac{1}{3}} \quad (6.6.1.2.5-2)$$

in which:

$$N = (365)(75)n(ADTT)_{sl} \quad (6.6.1.2.5-3)$$

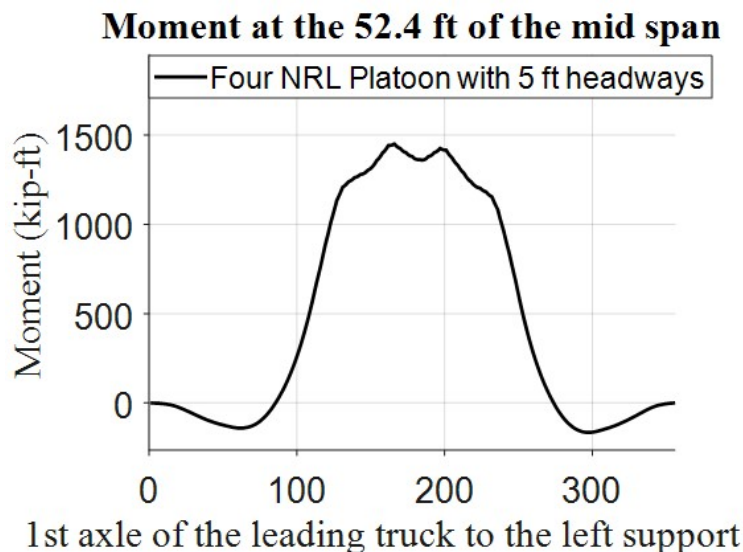
Constant A for C' case

$$A := 44 \cdot 10^8$$

number of stress range cycles per 4 NRL platoon with 5 ft headways (refer to the bottom figure)

$$ENSC_{platoon_5ft} := 1$$

The moment for each step (time-dependent) was plotted using SAP2000 for the 52.6 ft to the interior support at the mid span (cross-frame location) of the bridge. Note the platoon effects were plotted without IM and with GDF = 1.0. For the analysis below, GDF/1.2 and IM = 0.15 were assumed.



Assume platoon (4 NRL with 5 ft headways)
100 crossings per day (single lane loaded)

$$ADTT_{sl_platoon_5ft} := 100$$

N (number of crossings) for this platoon truck $N := 365 \cdot 75 \cdot ENSC_{platoon_5ft} \cdot ADTT_{sl_platoon_5ft} = 2737500$

Fatigue II strength $\Delta F_{n_fatigueII} := \left(\frac{A}{N}\right)^{\frac{1}{3}} \cdot ksi = 11.714 \text{ ksi}$

Platoon load factor for Fatigue II from LRFD Table 3.4.1-1 (assume the same as for AASHTO fatigue load) $\gamma_{fatigueII_platoon} := 0.8$

$check_fatigueI_PL := \text{if} (\gamma_{fatigueII_platoon} \cdot \Delta f_{platoon_5ft} \leq \Delta F_{n_fatigueI}, \text{“OK”}, \text{“NG”}) = \text{“OK”}$

Demand/capacity ratio for platoon fatigue II $DCR := \frac{\gamma_{fatigueII_platoon} \cdot \Delta f_{platoon_5ft}}{\Delta F_{n_fatigueII}} = 0.584$

Rating factor for fatigue $RF := \frac{1}{DCR} = 1.713$

Note: The Fatigue II check for a four-truck platoon with 5 ft headway passes.

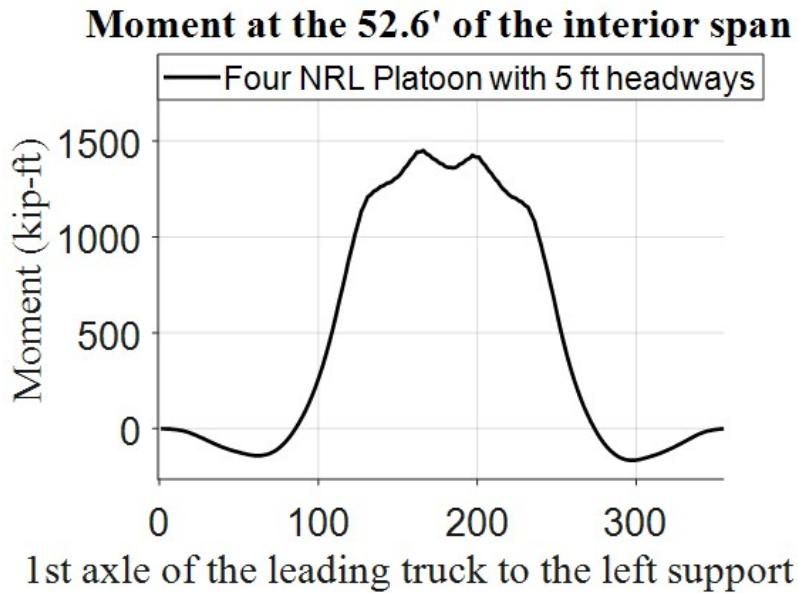
Fatigue I and Fatigue II welded cross-frame connection plate check summary

Limit state	AASHTO Fatigue Truck	Four-truck Platoons (5-ft NRL 100 crossings)
Fatigue I welded cross-frame connection plate		
Stress (at 52.6 ft to the left interior support)	1.618	0.802
Fatigue II welded cross-frame connection plate		
Stress (aat 52.6 ft to the left interior support)		1.713

Note: The Fatigue I and Fatigue II l rating factors were calculated based on capacity over demand in terms of the stress.

16. Fatigue Damage Assessment for 5 ft and 50 ft Platoons and AASHTO Fatigue Truck

Fatigue damage for platoons with 5 ft headway



Assume platoon 100 crossings per day
(single lane loaded without routine traffic)

$$Num_{SL_platoon_5ft} := 100$$

Available N (number of crossings) for
this platoon truck

$$N_{platoon_5ft} := \frac{A}{\left(\frac{\Delta f_{platoon_5ft}}{ksi}\right)^3} = 7050241$$

Accumulative fatigue damage for 75
year platoon with 5 ft headways

$$CFD_{platoon_5ft} := \frac{Num_{SL_platoon_5ft} \cdot ENSC_{platoon_5ft} \cdot \left(\frac{\Delta f_{platoon_5ft}}{ksi}\right)^3 \cdot 365 \cdot 75}{A} = 0.388$$

Fatigue damage for platoons with 50 ft headway

The stress range at the top of the bottom flange is found as follows:

Positive Moment from live load analysis (4 NRL platoon with 50 ft headways at the cross-frame location (GDFs/1.2 and assumed the IM = 0.15 as the same for AASHTO Fatigue Truck)

$$M_{platoon_50ft_pos} := 572.2 \text{ kip} \cdot \text{ft} \cdot \frac{(1 + 0.15)}{(1 + 0.33)} = 494.759 \text{ kip} \cdot \text{ft}$$

Negative Moment from live load analysis (4 NRL platoon with 50 ft headways at the cross-frame location (GDFs/1.2 and assumed the IM = 0.15 as the same for AASHTO Fatigue Truck)

$$M_{platoon_50ft_neg} := -59.3 \text{ kip} \cdot \text{ft} \cdot \frac{(1 + 0.15)}{(1 + 0.33)} = -51.274 \text{ kip} \cdot \text{ft}$$

Live load stress range for the platoon including $IM = 0.15$ (assume $IM = 0.15$ same as for AASHTO fatigue load)

$$\Delta f_{platoon_50ft} := \frac{(M_{platoon_50ft_pos} - M_{platoon_50ft_neg}) \cdot d_{plate}}{I_{st}} = 5.589 \text{ ksi}$$

Number of stress range cycles per 4 NRL platoon with 50 ft headways (refer to the below figure)

Equivalent Number of Stress Cycles (ENSC) (Schilling, 1984)

$$ENSC = N_m + \left(\frac{S_{r1}}{S_{rp}}\right)^m + \left(\frac{S_{r2}}{S_{rp}}\right)^m + \dots + \left(\frac{S_{ri}}{S_{rp}}\right)^m$$

Where:

m = the slope constant of the S-N curve,

N_m = the number of maximum stress range caused by individual truck passage;

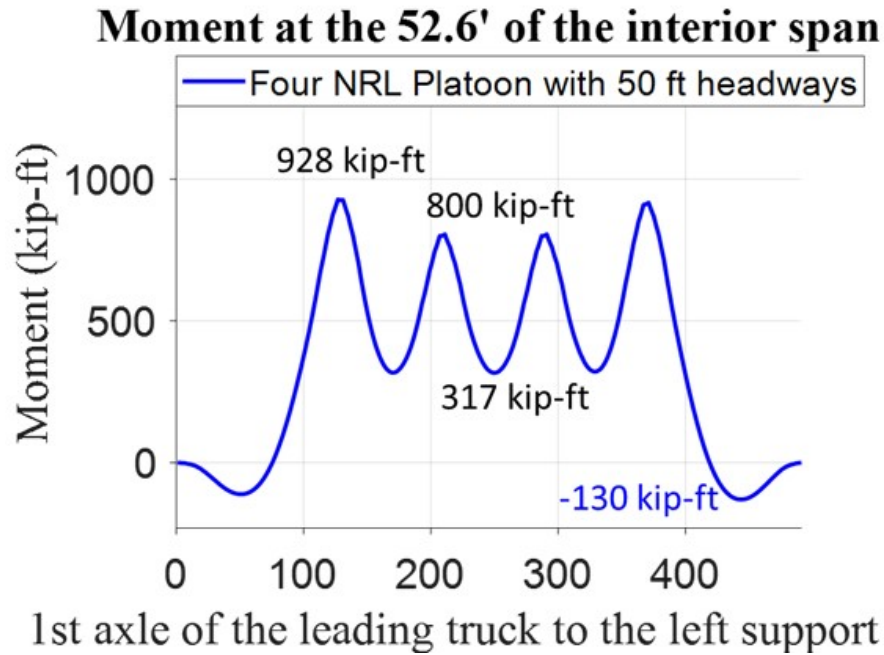
S_{ri} = higher-order stress range; and

S_{rp} = maximum stress range

❖ A complex stress cycle can be broken down into a primary cycle and one or more higher order cycles

❖ Higher-order cycles are secondary reversals of the primary cycle

The moment for each step (time-dependent) was plotted using SAP2000 for the cross-frame location of the bridge. Note the platoon were effects were plotted without IM and with GDF = 1.0. For the analysis below, GDF/1.2 and IM =0.15 were assumed.



$$ENSC_{platoon_50ft} := 1 + \left((1 + 0.15) \frac{g_{m1_mid}}{1.2} \cdot \frac{800 \text{ kip} \cdot \text{ft} - 317 \text{ kip} \cdot \text{ft}}{928 \text{ kip} \cdot \text{ft} - (-130 \text{ kip} \cdot \text{ft})} \right)^3 \cdot 2 \downarrow = 1.037$$

$$+ \left((1 + 0.15) \frac{g_{m1_mid}}{1.2} \cdot \frac{928 \text{ kip} \cdot \text{ft} - 317 \text{ kip} \cdot \text{ft}}{928 \text{ kip} \cdot \text{ft} - (-130 \text{ kip} \cdot \text{ft})} \right)^3 \cdot 1$$

Assume platoon 100 crossings per day
(single lane loaded without routine traffic)

$$Num_{SL_platoon_50ft} := 100$$

Available N (number of crossings) for
this platoon truck

$$N_{platoon_50ft} := \frac{A}{\left(\frac{\Delta f_{platoon_50ft}}{ksi} \right)^3} = 25196531$$

Accumulative fatigue damage for 75 year platoon with 50 ft headways

$$CFD_{platoon_50ft} := \frac{Num_{SL_platoon_50ft} \cdot ENSC_{platoon_50ft} \cdot \left(\frac{\Delta f_{platoon_50ft}}{ksi} \right)^3 \cdot 365 \cdot 75}{A} = 0.113$$

Fatigue damage ratios for AASHTO fatigue truck and platoons

Table 6.6.1.2.5-2—Cycles per Truck Passage, n

Longitudinal Members	
Simple Span Girders	1.0
Continuous Girders:	
1) near interior support	1.5
2) elsewhere	1.0
Cantilever Girders	5.0
Orthotropic Deck Plate Connections Subjected to Wheel Load Cycling	5.0
Trusses	1.0
Transverse Members	
Spacing > 20.0 ft	1.0
Spacing ≤ 20.0 ft	2.0

$$ENSC_{fatigue} := 1$$

Fatigue damage for one crossing for AASHTO fatigue truck

$$FD_{fatigue} := \frac{1 \cdot ENSC_{fatigue} \cdot \left(\frac{\Delta f_{fatigue}}{ksi} \right)^3}{A} = 1.73 \cdot 10^{-8}$$

Fatigue damage for a crossing for a 4-truck platoon with 5 ft headways

$$FD_{platoon_5ft} := \frac{1 \cdot ENSC_{platoon_5ft} \cdot \left(\frac{\Delta f_{platoon_5ft}}{ksi} \right)^3}{A} = 1.418 \cdot 10^{-7}$$

Fatigue damage for a crossing for a 4-truck platoon with 50 ft headways

$$FD_{platoon_50ft} := \frac{1 \cdot ENSC_{platoon_50ft} \cdot \left(\frac{\Delta f_{platoon_50ft}}{ksi} \right)^3}{A} = 4.115 \cdot 10^{-8}$$

Fatigue Damage Ratio for a single crossing for a 4 Truck Platoon with a 5 ft headway to the AASHTO fatigue truck

$$FD_{ratio_platoon_5ft_fatigue} := \frac{FD_{platoon_5ft}}{FD_{fatigue}} = 8.2$$

Fatigue Damage Ratio for a single crossing for a 4 Truck Platoon with a 50 ft headway to the AASHTO fatigue truck

$$FD_{ratio_platoon_50ft_fatigue} := \frac{FD_{platoon_50ft}}{FD_{fatigue}} = 2.379$$

Fatigue Damage Ratio for a single crossing for a 4 Truck Platoon with a 5 ft headway to the 50 ft headway truck platoon

$$FD_{ratio_platoon_5ft_50ft} := \frac{FD_{platoon_5ft}}{FD_{platoon_50ft}} = 3.447$$

Cumulative fatigue damage assessment summary

Notation	Scenarios	A	ENSC	Num	CFD
a	Platoon with 5 ft headways for 75 Years	440000000	1.000	2737500	0.388000000
b	Platoon with 50 ft headways for 75 Years	440000000	1.037	2737500	0.113000000
c	Platoon with 5 ft headways for one crossing	440000000	1.000	1	0.000000142
d	Platoon with 50 ft headwaysfor one crossing	440000000	1.037	1	0.000000041
e	AASHTO fatigue truck for one crossing	440000000	1.000	1	0.000000017

Fatigue damage ratios:

1. fatigue damage ratio (c/e) = 8.199;
2. fatigue damage ratio (d/e) = 2.379;
3. fatigue damage ratio (c/d) = 3.446.

17. Fatigue Check for Shear Studs

The shear stud information is given in the bridge drawings, and this example checks the fatigue of shear stud according to AASHTO LRFD Article 6.10.10. The end beam support shear was used to check the shear stud fatigue.

The pitch, p , of shear connectors shall satisfy:

$$p \leq \frac{nZ_r}{V_{sr}} \quad (6.10.10.1.2-1)$$

in which:

V_{sr} = horizontal fatigue shear range per unit length (kip/in.)

$$= \sqrt{(V_{far})^2 + (F_{far})^2} \quad (6.10.10.1.2-2)$$

V_{far} = longitudinal fatigue shear range per unit length (kip/in.)

$$= \frac{V_f Q}{I} \quad (6.10.10.1.2-3)$$

F_{far} = radial fatigue shear range per unit length (kip/in.) taken as the larger of either:

$$F_{far1} = \frac{A_{bot} \sigma_{fkg} \ell}{wR} \quad (6.10.10.1.2-4)$$

or:

$$F_{far2} = \frac{F_{rc}}{w} \quad (6.10.10.1.2-5)$$

where:

σ_{fkg} = range of longitudinal fatigue stress in the bottom flange without consideration of flange lateral bending (ksi)

A_{bot} = area of the bottom flange (in.²)

F_{rc} = net range of cross-frame or diaphragm force at the top flange (kip)

I = moment of inertia of the short-term composite section (in.⁴)

ℓ = distance between brace points (ft)

n = number of shear connectors in a cross section

p = pitch of shear connectors along the longitudinal axis (in.)

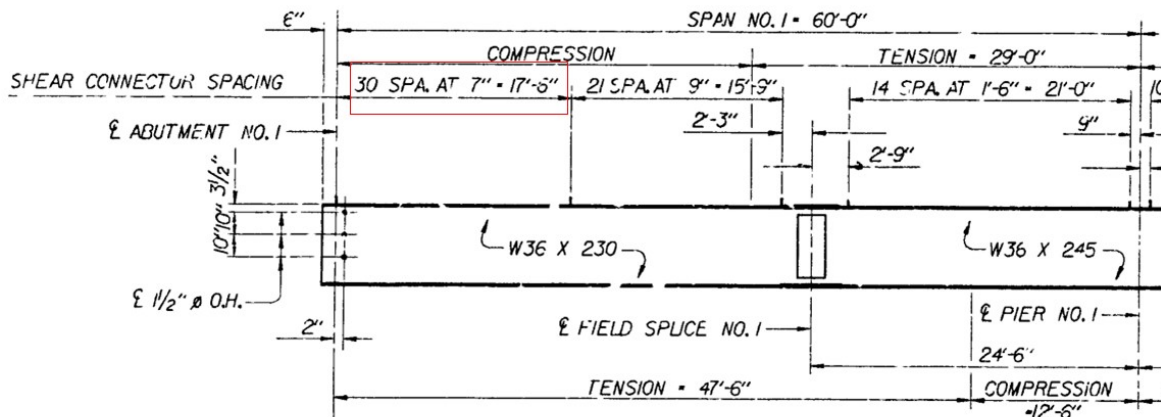
Q = first moment of the transformed short-term area of the concrete deck about the neutral axis of the short-term composite section (in.³)

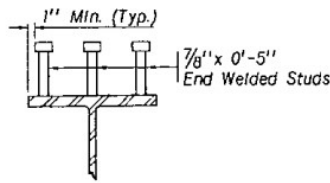
R = minimum girder radius within the panel (ft)

V_f = vertical shear force range under the applicable fatigue load combination specified in [Table 3.4.1-1](#) with the fatigue live load taken as specified in [Article 3.6.1.4](#) (kip)

w = effective length of deck (in.) taken as 48.0 in., except at end supports where w may be taken as 24.0 in.

Z_r = shear fatigue resistance of an individual shear connector determined as specified in [Article 6.10.10.2](#) (kip)





SHEAR CONNECTOR DETAIL

Number of studs per row (n_{studs}) $n_{studs} := 3$

Pitch length (inch) $p := 7 \text{ in}$

Shear stud diameter (inch) $d := \frac{7}{8} \text{ in}$

The horizontal shear range is taken as the vector sum of the longitudinal and radial fatigue shear ranges. For this slightly skewed girder bridge, the radial fatigue shear range is zero.

6.10.10.2—Fatigue Resistance

The fatigue shear resistance of an individual stud shear connector, Z_r , shall be taken as:

For stud-type shear connectors:

- Where the projected 75-year single lane Average Daily Truck Traffic ($ADTT$)_{SL} is greater than or equal to 1090 trucks per day, the Fatigue I load combination shall be used and the fatigue shear resistance for infinite life shall be taken as:

$$Z_r = 5.5 d^2 \quad (6.10.10.2-1)$$

- Otherwise, the Fatigue II load combination shall be used and the fatigue shear resistance for finite life shall be taken as:

$$Z_r = \alpha d^2 \quad (6.10.10.2-2)$$

in which:

$$\alpha = 34.5 - 4.28 \log N \quad (6.10.10.2-3)$$

ADTT (single lane threshold 6.10.10.2)

$$ADTT_{th_stud} := 1090$$

$$check := \text{if}(ADTT_{SL} > ADTT_{th_stud}, \text{"Fatigue I"}, \text{"Fatigue II"}) = \text{"Fatigue I"}$$

Fatigue I Shear Stud Check

Fatigue shear resistance per stud

$$Z_r := 5.5 \cdot \left(\frac{d}{in}\right)^2 \cdot kip = 4.211 \text{ kip}$$

First moment of the transformed short-term area of the concrete deck about the neutral axis of short-term section (in³)

$$Q := A_{slab_st} \cdot (y_{slab} - y_{b_st}) = 923.77 \text{ in}^3$$

Shear Stud Fatigue Check for AASHTO Fatigue Truck

Shear force at the interior support (AASHTO Fatigue Truck) with GDF = $\frac{g_{v1}}{1.2}$ and IM = 0.15

$$V_{fatigue} := 34.5 \text{ kip}$$

AASHTO Fatigue Truck V_f including IM = 0.15 and GDF

$$V_f := V_{fatigue} = 34.5 \text{ kip}$$

Longitudinal fatigue shear range per unit length (kip/in.)

$$V_{fat} := \frac{V_f \cdot Q}{I_{st2}} = 0.846 \frac{kip}{in}$$

Horizontal fatigue shear range per unit length (kip/in.) (without F_{fat} for this case)

$$V_{sr} := V_{fat} = 0.846 \frac{kip}{in}$$

Pitch requirement (Equation 6.10.10.1.2-1)

$$p_{req} := \frac{n_{studs} \cdot Z_r}{V_{sr}} = 14.935 \text{ in}$$

$$check := \text{if}(p_{req} > p, \text{"OK"}, \text{"NO"}) = \text{"OK"}$$

Fatigue I shear stud load rating for AASHTO fatigue truck (w.r.t spacing)

$$RF_{stud_fatigue} := \frac{p_{req}}{p} = 2.134$$

The shear stud fatigue check for AASHTO fatigue truck is good.

Shear Stud Fatigue Check for Platoon with 5 ft Headways

Shear force at the interior support (platoon with 5 ft headways) with $GDF = \frac{g_{v1}}{1.2}$ and $IM = 0.15$

$$V_{pl@5ft} := V_{PL_{legal_end}} \cdot \frac{(1 + 0.15)}{(1 + 0.33)} = 55.598 \text{ kip}$$

Platoon with 5 ft headways V_f including $IM = 0.15$ and $GDF = \frac{g_{v1}}{1.2}$

$$V_f := V_{pl@5ft} = 55.598 \text{ kip}$$

Longitudinal fatigue shear range per unit length (kip/in.)

$$V_{pl@5ft} := \frac{V_f \cdot Q}{I_{st2}} = 1.363 \frac{\text{kip}}{\text{in}}$$

Horizontal fatigue shear range per unit length (kip/in.) (without F_{fat} for this case)

$$V_{sr} := V_{pl@5ft} = 1.363 \frac{\text{kip}}{\text{in}}$$

Pitch requirement (Equation 6.10.10.1.2-1)

$$p_{req} := \frac{n_{studs} \cdot Z_r}{V_{sr}} = 9.268 \text{ in}$$

$$check := \text{if}(p_{req} > p, \text{"OK"}, \text{"NO"}) = \text{"OK"}$$

Fatigue I shear stud load rating for platoons (w.r.t spacing)

$$RF_{stud_platoon} := \frac{p_{req}}{p} = 1.324$$

The shear stud fatigue I check for platoon with 5 ft headways is good.

18. Shear Stud Fatigue Load Rating Summary

Shear stud fatigue load rating summary table is given below.

Limit state	AASHTO Fatigue Truck	Four-truck Platoons (5-ft NRL 100 crossings per day)
Fatigue I shear stud		
Shear (at the beam end support)	2.134	1.324
Fatigue II shear stud		
Shear (at the beam end support)		

Note: The shear stud load rating factor was calculated based on LRFD BDS Equation 6.10.10.1.2-1 over the actual pitch.

Appendix G

This appendix provides detailed BrR implementations for future platoon load ratings on steel and prestressed concrete bridges.

Appendix G. BrR Platoon Load Rating Implementations

- The load rating example below is based on the simple-span prestressed concrete bridge (S080 41653).
- This appendix includes both the current and future BrR platoon load rating implementations.

BrR Platoon Rating Implementations

UNIVERSITY OF
Nebraska
Lincoln

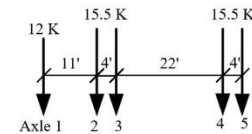
➤ The following slides will describe the implementation of platoon rating based on Phase I and Phase II



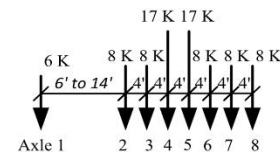
Prestressed concrete bridges (S080 41653)

Example Load rating case

- Four-truck Platoons (NRL and Type 3S2 with 5 ft headways)
- Single lane platoon mixed with adjacent routine traffic
- 100 platoon crossings per day and adjacent lane ADTT = 5000
- Amplification factor (α) = 1.0
- $CoV = 0.20$



AASHTO Type 3S2 (74 kips GVW)



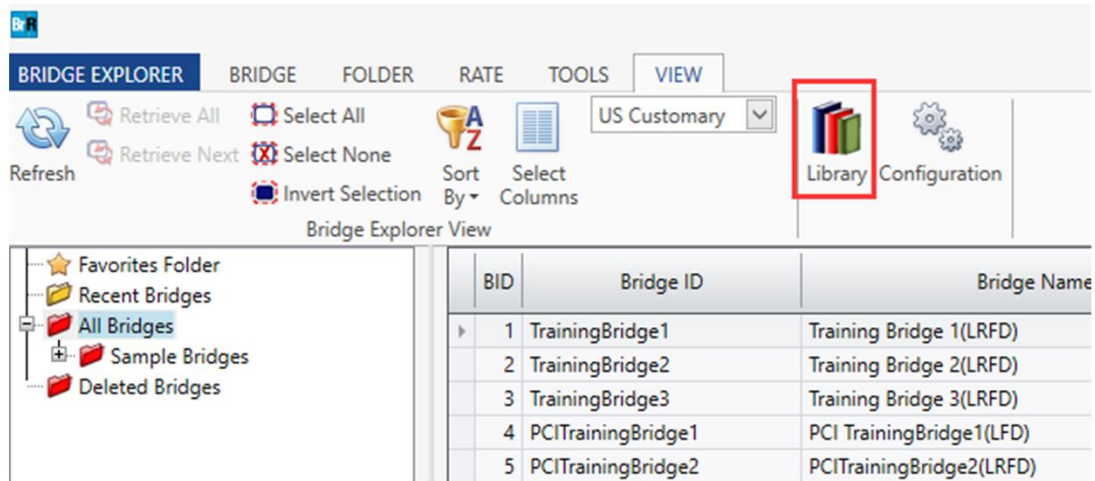
AASHTO NRL (80 kips GVW)

Step 1 Define the Truck Platoon

Step 1 Define the truck platoon configurations

- Permit requester specifies number of vehicles in platoon, axle weights, and headways, which can either be a special or standard vehicle type
- NDOT rating engineer determines critical load effects by specifying the minimum/maximum headways or evaluates load effects for particular headways

Step 1 Define the Truck Platoon



➤ Open the BrR library

Step 1 Define the Truck Platoon

Vehicle: Standard Gauge: 2-NRL Platoon (5 to 50 ft headways) X

Name: 2-NRL Platoon (5 to 50 ft headways)
Description: Two-NRL Platoon with 5 to 50 ft headways

Store units as: US SI

Library: Standard Agency defined User defined

Notional vehicle

Rating: LRFD ASD/LFD LRRR

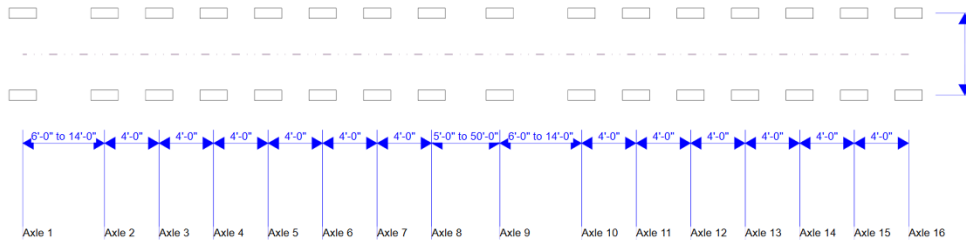
Design: LRFD ASD/LFD

Axle no.	Axle load (kip)	Gage dist. (ft)	Wheel contact width (in)	Axle spacing (ft)	
				Minimum	Maximum
1	6.00	6.00			
2	8.00	6.00		6.00	14.00
3	8.00	6.00		4.00	4.00
4	17.00	6.00		4.00	4.00
5	17.00	6.00		4.00	4.00
6	8.00	6.00		4.00	4.00
7	8.00	6.00		4.00	4.00
8	8.00	6.00		4.00	4.00
9	6.00	6.00		5.00	50.00
10	8.00	6.00		6.00	14.00
11	8.00	6.00		4.00	4.00

Totals: 160.0 kip 65.00 126.00

2-NRL Platoon (5 to 50 ft headways)
Vehicle Plan
5/25/2023 6:16:41 PM

New Duplicate Delete



➤ Suggest copying axle details from Excel and pasting into BrR

Step 1 Define the Truck Platoon

Library	Units	Name	Description
Agency...	US Customary	4-NRL Platoon (5 ft headways)	Four-NRL Platoon with 5 ft headways
Agency...	US Customary	4-NRL Platoon (50 ft headways)	Four-NRL Platoon with 50 ft headways
Agency...	US Customary	3-NRL Platoon (5 to 50 ft headwa...	Three-NRL Platoon with 5 to 50 ft headways
Agency...	US Customary	3-NRL Platoon (5 ft headways)	Three-NRL Platoon with 5 ft headways
Agency...	US Customary	3-NRL Platoon (50 ft headways)	Three-NRL Platoon with 50 ft headways
Agency...	US Customary	2-NRL Platoon (5 to 50 ft headwa...	Two-NRL Platoon with 5 to 50 ft headways
Agency...	US Customary	2-NRL Platoon (5 ft headways)	Two-NRL Platoon with 5 ft headways
Agency...	US Customary	2-NRL Platoon (50 ft headways)	Two-NRL Platoon with 50 ft headways
Agency...	US Customary	4-Type3-3 Platoon (5 to 50 ft hea...	4-Type3-3 Platoon with 5 to 50 ft headways
Agency...	US Customary	4-Type3-3 Platoon (5 ft headways)	4-Type3-3 Platoon with 5 ft headways
Agency...	US Customary	4-Type3-3 Platoon (50 ft headways)	4-Type3-3 Platoon with 50 ft headways
Agency...	US Customary	3-Type3-3 Platoon (5 to 50 ft hea...	3-Type3-3 Platoon with 5 to 50 ft headways
Agency...	US Customary	3-Type3-3 Platoon (5 ft headways)	3-Type3-3 Platoon with 5 ft headways
Agency...	US Customary	3-Type3-3 Platoon (50 ft headways)	3-Type3-3 Platoon with 50 ft headways
Agency...	US Customary	2-Type3-3 Platoon (5 to 50 ft hea...	2-Type3-3 Platoon with 5 to 50 ft headways
Agency...	US Customary	2-Type3-3 Platoon (5 ft headways)	2-Type3-3 Platoon with 5 ft headways
Agency...	US Customary	2-Type3-3 Platoon (50 ft headways)	2-Type3-3 Platoon with 50 ft headways
Agency...	US Customary	4-NJTAType3S2 Platoon (5 to 50 ft)	4-NJTAType3S2 Platoon with 5 to 50 ft headways
Agency...	US Customary	4-NJTAType3S2 Platoon (5 ft)	4-NJTAType3S2 Platoon with 5 ft headways
Agency...	US Customary	4-NJTAType3S2 Platoon (50 ft)	4-NJTAType3S2 Platoon with 50 ft headways
Agency...	US Customary	3-NJTAType3S2 Platoon (5 ft)	3-NJTAType3S2 Platoon with 5 ft headways
Agency...	US Customary	3-NJTAType3S2 Platoon (5 to 50 ft)	3-NJTAType3S2 Platoon with 5 to 50 ft headways
Agency...	US Customary	3-NJTAType3S2 Platoon (50 ft)	3-NJTAType3S2 Platoon with 50 ft headways
Agency...	US Customary	2-NJTAType3S2 Platoon (5 to 50 ft)	2-NJTAType3S2 Platoon with 5 to 50 ft headways
Agency...	US Customary	2-NJTAType3S2 Platoon (5 ft)	2-NJTAType3S2 Platoon with 5 ft headways
Agency...	US Customary	2-NJTAType3S2 Platoon (50 ft)	2-NJTAType3S2 Platoon with 50 ft headways
Agency...	US Customary	4-Class 9 Platoon (5 to 50 ft)	4-Class 9 Platoon with 5 to 50 ft headways
Agency...	US Customary	4-Class 9 Platoon (5 ft)	4-Class 9 Platoon with 5 ft headways
Agency...	US Customary	4-Class 9 Platoon (50 ft)	4-Class 9 Platoon with 50 ft headways
Agency...	US Customary	3-Class 9 Platoon (5 to 50 ft)	3-Class 9 Platoon with 5 to 50 ft headways
Agency...	US Customary	3-Class 9 Platoon (5 ft)	3-Class 9 Platoon with 5 ft headways
Agency...	US Customary	3-Class 9 Platoon (50ft)	3-Class 9 Platoon with 50 ft headways
Agency...	US Customary	2-Class 9 Platoon (5 to 50 ft)	2-Class 9 Platoon with 5 to 50 ft headways
Agency...	US Customary	2-Class 9 Platoon (5 ft)	2-Class 9 Platoon with 5 ft headways

- **“Truck platoon database.brlx”** has been created. The file can be modified for other headways
- Includes 2- to 4-truck platoons (FHWA class 9, NJTA type 3S2, NRL, and Type 3-3) with varying headways from **5 to 50 ft**
- Includes 2- to 4-truck platoons (FHWA class 9, NJTA type 3S2, NRL, and Type 3-3) with **5 ft or 50 ft** headways

Step 2 Define platoon live load factors

From Phase I UNL/NDOT Research

Table 2. Proposed Calibrated LL Factors for the Target $\beta = 2.5$ (Steelman et al., 2021)

Truck Platoon	Frequency	Loading Condition	DF	ADTT (One direction)	Live load factors by CoV of total live load				
					$COV_{LL} = 0$	$COV_{LL} = 0.05$	$COV_{LL} = 0.1$	$COV_{LL} = 0.15$	$COV_{LL} = 0.2$
Multiple Trucks in Platoon	Single-trip	No other vehicles on the bridge	One lane	N/A	1.00	1.05	1.10	1.20	1.25
	Single-trip	Two identical platoons loaded on two lanes	Two or more lanes	N/A	1.00	1.05	1.10	1.20	1.25
	10 Crossings	Mixed with routine traffic in the adjacent lane	One lane	> 5000	1.35	1.35	1.40	1.45	1.55
				1000	1.35	1.35	1.40	1.45	1.50
				< 100	1.35	1.35	1.40	1.45	1.50
	100 Crossings	Mixed with routine traffic in the adjacent lane	One lane	> 5000	1.35	1.40	1.45	1.50	1.60
				1000	1.35	1.40	1.45	1.45	1.55
				< 100	1.35	1.35	1.45	1.45	1.55

a. DF is the *LRFD BDS* approximate GDF, with the multiple presence factor (MPF=1.2) removed for one-lane GDFs.

b. To use with a different IM factor, scale tabulated values by $1.33 / (1 + IM_{desired})$.

Step 2 Define platoon live load factors

Library	Name	Description
Standard	2003 AASHTO LRFR Specifications	2003 AASHTO LRFR Specifications, including 2005 Int...
Standard	2008 AASHTO LRFR Specifications	2008 AASHTO LRFR Specifications, including 2010 In...
Standard	2011 AASHTO LRFR Specifications	2011 AASHTO LRFR Specifications
Standard	2013 Interims AASHTO LRFR Culv...	Includes only the culvert factors as approved by the T...
Standard	2011 (2013 Interim) AASHTO LRFR...	AASHTO Manual for Bridge Evaluation, 2nd Edition, L...
Standard	2011 (2014 Interim) AASHTO LRFR...	AASHTO Manual for Bridge Evaluation, 2nd Edition, L...
Standard	2011 (2015 Interim) AASHTO LRFR...	AASHTO Manual for Bridge Evaluation, 2nd Edition, L...
Standard	2011 (2016 Interim) AASHTO LRFR...	AASHTO Manual for Bridge Evaluation, 2nd Edition, L...
Standard	2018 AASHTO LRFR Specifications	AASHTO Manual for Bridge Evaluation, 3rd Edition 20...
Standard	2018 (2020 Interim) AASHTO LRFR...	AASHTO Manual for Bridge Evaluation, 3rd Edition, in...
Standard	2018 (2022 Interim) AASHTO LRFR...	AASHTO Manual for Bridge Evaluation, 3rd Edition, in...
Agency...	Platoon (single lane, two lanes lo...	The live load factors of single lane loaded platoon wi...
Agency...	Platoon (single lane loaded w/ adj...	The live load factors of single lane loaded platoon wi...

- Click LRFR in the library
- Copy the latest MBE specification and modify the LLFs for Strength and Service to obtain the two platoon load rating specifications:
 1. Platoon loaded with adjacent traffic
 2. Single-Lane Loaded Platoon without Adjacent Traffic or Two-Lane Loaded Platoon
- Select the permit check box for Strength I and enter a live load factor of 1.60 for the single lane loaded with adjacent traffic

Limit state	Dead load		Design load		Legal load	Permit load	Vehicle			
	DC	DW	Inventory	Operating			Inv	Op	Legal	Permit
STRENGTH I	1.250	1.500	1.750	1.350	Table...	1.600	<input checked="" type="checkbox"/>	<input checked="" type="checkbox"/>	<input checked="" type="checkbox"/>	<input checked="" type="checkbox"/>
STRENGTH II	1.250	1.500					<input type="checkbox"/>	<input type="checkbox"/>	<input type="checkbox"/>	<input checked="" type="checkbox"/>
SERVICE I	1.000	1.000					<input type="checkbox"/>	<input type="checkbox"/>	<input type="checkbox"/>	<input checked="" type="checkbox"/>
SERVICE III	1.000	1.000	Table 6...		1.000	1.550	<input checked="" type="checkbox"/>	<input type="checkbox"/>	<input checked="" type="checkbox"/>	<input checked="" type="checkbox"/>

Step 2 Define platoon live load factors

From Phase II UNL/NDOT Research

Table 5.9 Proposed Moment Calibrated *LL* Factors for Service III

Truck platoon	Frequency	Load conditions	DF	ADTT (one direction)	Load factors by <i>COV</i> of total live load
					$COV_{LL} = 0 - 0.20$
Multiple trucks in platoon	single-trip	No other vehicles on the bridge	One lane	N/A	0.85
	single-trip	Two identical platoons loaded on two lanes	Two or more lanes	N/A	0.85
	100 Crossings	Mixed with routine traffic in the adjacent lane	One lane	> 5000	1.55

Table 5.10 Proposed Moment Calibrated *LL* Factors for Service II

Truck platoon	Frequency	Load conditions	DF	ADTT (one direction)	Load factors by <i>COV</i> of total live load
					$COV_{LL} = 0 - 0.20$
Multiple trucks in platoon	single-trip	No other vehicles on the bridge	One lane	N/A	1.15
	single-trip	Two identical platoons loaded on two lanes	Two or more lanes	N/A	1.15
	100 Crossings	Mixed with routine traffic in the adjacent lane	One lane	> 5000	1.90

a. DF is the *LRFD BDS* approximate GDF, with the multiple presence factor (MPF=1.2) removed for one-lane GDFs.

b. To use with a different *IM* factor, scale tabulated values by $1.33 / (1 + IM_{desired})$.

Step 2 Define platoon live load factors

Factors: LRFR: Platoon (single lane loaded w/ adjacent) x

Name: Platoon (single lane loaded w/ adjac)

Description: The live load factors of single lane loaded platoon with adjacent lane traffic (CoV of platoon = 0.2)

Load factors | Legal loads | Permit loads | Concrete | Steel | Wood | Aluminum | Buried structures | Specifications

Bridge type: Prestressed | Post-tension secondary effects: 1.000

Limit state	Dead load		Design load		Legal load	Permit load	Vehicle			
	DC	DW	Inventory LL	Operating LL			LL	Inv	Op	Legal
STRENGTH I	1.250	1.500	1.750	1.350	Table...	1.600	<input checked="" type="checkbox"/>	<input checked="" type="checkbox"/>	<input checked="" type="checkbox"/>	<input checked="" type="checkbox"/>
STRENGTH II	1.250	1.500			Table...		<input type="checkbox"/>	<input type="checkbox"/>	<input type="checkbox"/>	<input checked="" type="checkbox"/>
SERVICE I	1.000	1.000				1.000	<input type="checkbox"/>	<input type="checkbox"/>	<input type="checkbox"/>	<input checked="" type="checkbox"/>
SERVICE III	1.000	1.000	Table 6...		1.000	1.550	<input checked="" type="checkbox"/>	<input type="checkbox"/>	<input checked="" type="checkbox"/>	<input checked="" type="checkbox"/>

Factors: LRFR: Platoon (single lane loaded w/ adjacent) x

Name: Platoon (single lane loaded w/ adjac)

Description: The live load factors of single lane loaded platoon with adjacent lane traffic (CoV of platoon = 0.2)

Load factors | Legal loads | Permit loads | Concrete | Steel | Wood | Aluminum | Buried structures | Specifications

Bridge type: Steel

Limit state	Dead load		Design load		Legal load	Permit load	Vehicle			
	DC	DW	Inventory LL	Operating LL			LL	Inv	Op	Legal
STRENGTH I	1.250	1.500	1.750	1.350	Table...	1.600	<input checked="" type="checkbox"/>	<input checked="" type="checkbox"/>	<input checked="" type="checkbox"/>	<input checked="" type="checkbox"/>
STRENGTH II	1.250	1.500			Table...		<input type="checkbox"/>	<input type="checkbox"/>	<input type="checkbox"/>	<input checked="" type="checkbox"/>
SERVICE II	1.000	1.000	1.300	1.000	1.300	1.900	<input checked="" type="checkbox"/>	<input checked="" type="checkbox"/>	<input checked="" type="checkbox"/>	<input checked="" type="checkbox"/>
FATIGUE	0.000	0.000	0.800				<input checked="" type="checkbox"/>	<input type="checkbox"/>	<input type="checkbox"/>	<input type="checkbox"/>

➤ Select the permit check box for Service III and enter a live load factor of 1.55 for single lane loaded with adjacent traffic

➤ “Platoon Load Rating Specifications.brlx” has been created with Strength I, Service II, and Service III live load factors for load rating platoons

Step 3 Select bridge

Step 3 Select bridge for platoon rating evaluation

Example prestressed concrete bridge:

BID	Bridge ID	Bridge Name	District	County	Facility	Location	Route	Feature Intersected	Mile/Km Post (mi)	Owner	Maintainer	Admin Area	Length (ft)	Year Built
32	S080 41653L	130' Simple Span PS NU1600	District 1		I80	4S GREENWOOD	I80	DEE CREEK	416.53	State Highway Agency	State Highway Agency	Unknown	130.000	2009

Step 4 Add additional points of interest

The screenshot shows the Bridge Workspace software interface. The main window is titled 'Bridge Workspace - S080 41653L'. The 'ANALYSIS' tab is active, and the 'DESIGN/RATE' sub-tab is selected. The 'Point of Interest' dialog box is open, showing the following settings:

- Distance from leftmost support: 5.87 ft or Span: Span 1 Fraction: 0.045154 Side: Left Right
- Shear: Override schedule % Shear: 100.000 % Shear distance: in
- Vertical shear reinf. and Horiz shear reinf. sections with fields for Material, Bar size, # of legs, Area, Inclination, and Spacing.
- LRFD section with fields for Computation method, Six, Beta, and Theta.
- LFD section with Ignore shear.
- LRFR section with Ignore design & legal load shear, Ignore permit load shear, and Consider permit load tensile steel stress.

The 'OK' and 'Apply' buttons are highlighted with red boxes. In the left-hand tree, the 'Points of Interest' folder is also highlighted with a red box.

➤ Optional: Add additional points of interest

Step 5 Assign live load factors

- For this example, select a single lane loaded platoon with adjacent routine traffic

Member Alternative Description

Member alternative: Interior

Description Specs Factors Engine Import Control options

Analysis method type	Analysis module	Selection type	Spec version	Factors
ASD	AASHTO ASD	System Default	MBE 3rd 2022i, Std 17th	N/A
LFD	AASHTO LFD	System Default	MBE 3rd 2022i, Std 17th	2002 AASHTO Std. Specifications
LRFD	AASHTO LRFD	System Default	LRFD 9th	2020 AASHTO LRFD Specifications
LRFR	AASHTO LRFR	Override	MBE 3rd 2022i, LRFD 9th	Platoon (single lane loaded w/ adjacent)

OK Apply Cancel

Step 6 Analysis details settings

The screenshot displays a software workspace with a tree view on the left and a 'Member Alternative Description' dialog box on the right. The tree view shows a project named 'S080 41653L' with various components and definitions. The 'MEMBERS' section is expanded, showing 'Interior (E) (C)' selected. The dialog box has tabs for 'Description', 'Specs', 'Factors', 'Engine', 'Import', and 'Control options', with 'Control options' selected. The dialog is divided into three sections: 'LRFD', 'LFR', and 'LFD'. Each section contains a list of analysis options with checkboxes and radio buttons. The 'LRFD' section includes options for 'Points of interest' (all checked), 'Shear computation method' (radio buttons for 'Ignore', 'General procedure', 'General procedure - Appendix B5', 'Simplified procedure', 'Simplified procedure - Vci, Vcw'), and 'Loss & stress calculations' (radio buttons for 'Use gross section properties', 'Use transformed section properties'). The 'LFR' section includes 'Points of interest' (all checked), 'Multi-span analysis' (radio buttons for 'Continuous', 'Continuous and simple'), and 'Distribution factor application method' (radio buttons for 'By axle', 'By PCI'). The 'LFD' section includes 'Points of interest' (all checked), 'Distribution factor application method' (radio buttons for 'By axle', 'By PCI'), and 'Consider moment redistribution' (checkbox). At the bottom of the dialog are 'OK', 'Apply', and 'Cancel' buttons.

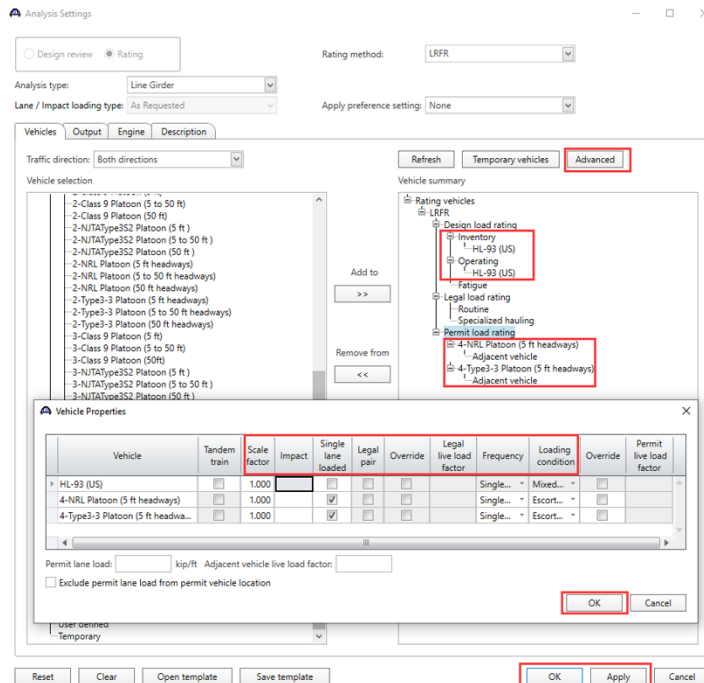
➤ Modify analysis settings, such as the shear load rating method, if necessary

Step 7 LRFR analysis settings

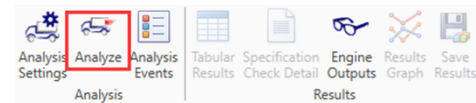
The screenshot displays the Bridge Workspace software interface. The 'Analysis Settings' dialog box is open, showing the 'Rating' method selected. The 'Rating method' dropdown is set to 'LRFR'. The 'Analysis type' is 'Line Girder'. The 'Lane / Impact loading type' is 'As Requested'. The 'Vehicles' list includes various truck and platoon types. The 'Rating vehicles' list shows the selected LRFR rating method and its sub-categories.

- Click “Analysis settings”
- Select LRFR rating method

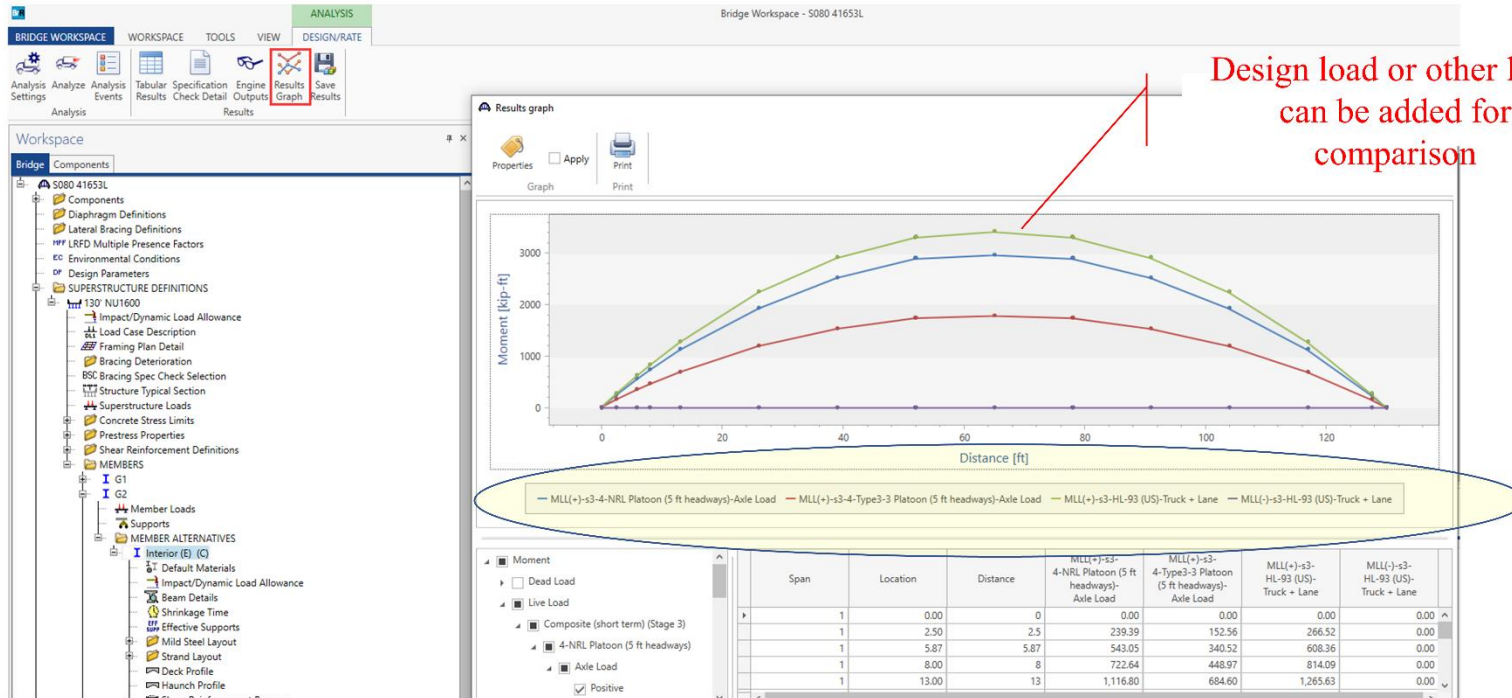
Step 7 LRFR analysis settings



- Optional: Include design loads for comparison.
- Click the “Advanced” button to change scale factor, impact, load condition, and frequency.
- Note that “**Impact**” is a scale factor for *IM*. The default is 0.33. There is no need to enter a value. If the desired *IM* is 0.2, then the impact should be changed to $0.2/0.33 = 0.606$.
- **Scale Factor** is the amplification factor (α) used to amplify the total weight of the platoon (here $\alpha = 1.0$).
- Select "Single lane loaded with escort on adjacent lane" for both single lane loaded platoon with / without adjacent lane cases. Calibrated live load factors **implicitly** account for the effects of adjacent traffic, if applicable.
- Click OK and apply
- Run the analysis



Step 8 LRFR analysis results



➤ The “Results Graph” can be used to plot the effects of dead and live loads

Step 8 LRFR analysis results

The screenshot displays the BRIDGE WORKSPACE interface. The left sidebar shows a project tree with 'Interior (E) (C)' selected. The main window is titled 'Specification Checks for Interior - 26 of 892'. It features a 'Specification filter' on the left and a table of results on the right. The table has columns for 'Specification reference', 'Limit State', 'Flex. Sense', and 'Pass/Fail'. A red box highlights the 'Interior' section in the filter and the corresponding rows in the table.

Specification reference	Limit State	Flex. Sense	Pass/Fail
✓ 5.4.2.1 Compressive Strength		N/A	Passed
✓ 5.4.2.5 Poisson's Ratio		N/A	General Comp.
✓ 5.4.2.6 Modulus of Rupture		N/A	General Comp.
✓ 5.4.2.8 Concrete Density Modification Factor		N/A	General Comp.
NA 5.5.3.2 Reinforcing Bars and Welded Wire Reinforcement		N/A	Not Required
✓ 5.5.4.2 PS Strength Limit State - Resistance Factors		N/A	General Comp.
✓ 5.6.2.2 Rectangular Stress Distribution		N/A	General Comp.
✓ 5.6.3.2 PS Flexural Resistance (Prestressed Concrete)		N/A	Passed
✓ 5.6.3.3 Minimum Reinforcement		N/A	Passed
✓ 5.7.2.5 Minimum Transverse Reinforcement		N/A	Passed
✓ 5.7.2.6 Maximum Spacing of Transverse Reinforcement		N/A	Passed
✓ 5.7.3.3 Nominal Shear Resistance		N/A	Passed
✓ 5.7.3.4 Procedures for Determining Shear Resistance		N/A	General Comp.
✓ 5.7.3.5 Longitudinal Reinforcement		N/A	Passed
✓ 5.7.4 Interface Shear Transfer		N/A	Passed
✓ 5.7.4.2 Minimum Area of Interface Shear Reinforcement		N/A	Passed
✓ 5.9.2.3.2a Compressive Stresses		N/A	Passed
✓ 5.9.2.3.2b Tensile Stresses		N/A	Passed
✓ 5.9.4.3.2 Bonded Strand		N/A	General Comp.
✓ 6A.4.2.1 Design Load Rating Prestress Service III Tensile Stress		N/A	Passed
✓ 6A.4.2.1 General Load Rating Equation - Concrete Flexure		N/A	Passed
✓ 6A.4.2.1 General Load Rating Equation - Concrete Shear		N/A	Passed
■ Computation of V_p		N/A	General Comp.
■ Cracked_Moment_of_Inertia Section Property Calculations		N/A	General Comp.
■ PS_Basic_Properties Calculation		N/A	General Comp.
■ PS_Gross_Composite_Section_Properties PS Gross Composite Section		N/A	General Comp.

➤ "Specification Check Detail" provides detailed calculations for the platoon load rating

Step 8 LRFR analysis results

Workspace

Report type: LRFR analysis output

Report

Overall summary
 Reactions
 Moment summary
 Shear summary
 Detailed rating results
 Diaphragm forces

Report by Action: Flexure Concrete Stresses Shear Critical

Detailed Rating Results
Interior
4-NRL Platoon (5 ft headways)
Axle Load
Impact: As Requested
Lane: As Requested

Span 1

Location	Permit Rating	Permit Load Rating
(ft)	Factor	(Ton)
0.00	0.0	15840.00
0.00	0.0	15840.00
2.50	1.9	3527.84
2.50	1.9	3536.69

➤ "Report Tool" provides a summary and detailed platoon load rating results (click the generate button)

Future Platoon Rating Implementations

Current Limitations: the following email was provided by an expert in AASHTOWare Bridge Task Force

With that said, I think I understand what you're trying to do here with the Analysis Settings and General Preferences. Unfortunately, the General Preferences can't be used currently to change the spec version or factors, just the analysis module. You asked in Figure 6 about changing the LRFR methods. The Analysis Module is not selecting the LRFR method, but instead, the analysis engine. Currently, this is what you would use to select a different engine if there was another one available (such as BRASS LRFR).

Member Alternative Description

Member alternative:

Description Specs Factors Engine Import Control options

Analysis method type	Analysis module	Selection type	Spec version	Factors
ASD	AASHTO ASD	System Default	MBE 3rd 2020i, Std 17th	N/A
LFD	AASHTO LFD	System Default	MBE 3rd 2020i, Std 17th	2002 AASHTO Std. Specifications
LRFD	AASHTO LRFD	System Default	LRFD 9th	2020 AASHTO LRFD Specifications
LRFR	AASHTO LRFR	Override	MBE 3rd 2020i, LRFD 9th	<ul style="list-style-type: none">platoon2018 (2020 Interim) AASHTO LRFR Spec.platoon-- Copy from library --

- *Unfortunately*, for now, NDOT bridge load rating engineers may have to copy the BrR bridge files and place them in a separate folder to avoid confusion with load ratings for other permitted vehicles.
- This is not good practice, but may be the best available option until AASHTOWare BrR is modified for platoon load rating in the future

Future Platoon Rating Implementations UNIVERSITY OF Nebraska Lincoln

AASHTOWare Bridge Rating

BRIDGE EXPLORER BRIDGE FOLDER RATE TOOLS VIEW

Rate Update Ratings Rating Results Recent Rating Results Manage Analysis Events Open Route Routing Precomputed Data Load Rating Tool

BID	Bridge ID	Bridge Name	District	County	Facility	Location	Route	Feature Intersected	Mile/Km Post (m)	Owner	Maintainer	Admin Area	Length (ft)	Year Built
36	S080 00526L	100.0 ft simple span welded PL girder	District 5		180	3W Bushnell Inte	80	Stream	5.26	State Highway Agency	State Highway Agency	Unknown	100.000	1970
34	S080 14033R	3 simple spans prestressed Type 3 144 ft	District 6		180	5 W Paxton Inte	80	South Platte R. Cana	140.33	State Highway Agency	State Highway Agency	Unknown	144.000	1968
38	S080 18181R	299 ft 3 span continuous welded plate steel bridge	District 6	111 Suffolk	180	3 E North Platte	80	Tri County Canal	181.81	State Highway Agency	State Highway Agency	Unknown	299.000	1964
37	S080 28566	4 span steel welded plate girder continuous	District 4		L10C GIBBON	GIBBON INTRCH	180			State Highway Agency	State Highway Agency	Unknown	252.000	1963
35	S080 31446L	11-70'-0 Spans PS Concrete Girder Bridge	District 4		180	4W GRAND ISL	180	S CH PLATTE RIVER	314.46	State Highway Agency	State Highway Agency	Unknown	770.000	1965
33	S080 41465L	170' 3-Span Continuous PS NU900	District 1		180	5N WAVERLY IN	180	CAMP CREEK	414.65	State Highway Agency	State Highway Agency	Unknown	170.000	2009
32	S080 41653L	130' Simple Span PS NU1600	District 1		180	4S GREENWOOD	180	DEE CREEK	416.53	State Highway Agency	State Highway Agency	Unknown	130.000	2009

- Click “Rate” to change analysis settings
- **No** need to modify the original BrR files (**best practice**)
- BrR will permit to have different load rating events, for: Standard permits, **platoons**, other types. This will require changes by programming. (Automatic if MBE, service units if not)
- Click the “Ok” to run analysis for a route of bridges
- Automate similar to *Superload* (option)

Future Platoon Rating Implementations UNIVERSITY OF Nebraska Lincoln

AASHTOWare Bridge Rating

BRIDGE EXPLORER BRIDGE FOLDER RATE TOOLS VIEW

New Open Import Batch Find Copy Paste Copy To Remove From Delete

Bridge Manage

- ★ Favorites Folder
- Recent Bridges
- All Bridges
- Sample Bridges
 - AISI LRFD Example Bridges
 - Concrete Example Bridges
 - 1-80 bridges operating platoons**
 - Steel Example Bridges
 - Timber Example Bridges
- Deleted Bridges

BID	Bridge ID	Bridge Name	District	County	Facility	Location	Route	Feature Intersected	Mile/Km Post (mi)	Owner	Maintainer	Admin Area	Length (ft)	Year Built
36	S080 00526L	100.0 ft simple span welded PL girder	District 5		I80	3W Bushnell Int	80	Stream	5.26	State Highway Agency	State Highway Agency	Unknown	100.000	1970
34	S080 14033R	3 simple spans prestressed Type 3 144 ft	District 6		I 80	5 W Paxton Int	80	South Platte R. Cana	140.33	State Highway Agency	State Highway Agency	Unknown	144.000	1968
38	S080 18181R	299 ft 3 span continuous welded plate steel bridge	District 6	111 Suffolk	I 80	3 E North Platte	80	Tri County Canal	181.81	State Highway Agency	State Highway Agency	Unknown	299.000	1964
37	S080 28566	4 span steel welded plate girder continuous	District 4		L10C GIBBON	GIBBON INTRCH	I80			State Highway Agency	State Highway Agency	Unknown	252.000	1963
35	S080 31446L	11-70'-0 Spans PS Concrete Girder Bridge	District 4		I80	4W GRAND ISLA	I80	S CH PLATTE RIVER	314.46	State Highway Agency	State Highway Agency	Unknown	770.000	1965
33	S080 41465L	170' 3-Span Continuous PS NU900	District 1		I80	5N WAVERLY IN	I80	CAMP CREEK	414.65	State Highway Agency	State Highway Agency	Unknown	170.000	2009
32	S080 41653L	130' Simple Span PS NU1600	District 1		I80	4S GREENWOOD	I80	DEE CREEK	416.53	State Highway Agency	State Highway Agency	Unknown	130.000	2009

Place Routes in folder using *links* to not duplicate the base bridge definitions

